Regioselective Allylic Alkene Amination by Photo-Aerobic Selenium-π-Acid Multicatalysis

Dissertation
zur Erlangung des Doktorgrades der Naturwissenschaften (Dr. rer. nat.)
der Fakultät für Chemie und Pharmazie
der Universität Regensburg

vorgelegt von
Theresa Appleson
aus München

im Jahr 2025

Promotionsgesuch eingereicht am: 09.12.2025
Die Arbeit wurde angeleitet von: Prof Dr. Alexander Breder

Promotionsausschuss:
Vorsitzender: Prof. Dr. Patrick Nürnberger
1. Gutachter: Prof. Dr. Alexander Breder
2. Gutachterin: Prof. Dr. Julia Rehbein
3. Prüfer: Prof. Dr. Frank-Michael Matysik

Contents

Acknowledgements

First, I would like to express my sincere gratitude to my doctoral advisor, Prof. Dr. Alexander Breder. Thank you for providing the funding and the opportunity to pursue this work in your group. I am very grateful for the valuable discussions, your guidance, and that I had the chance to learn from you over the years.

Next, I would like to thank my examination committee — Prof. Dr. Julia Rehbein, Prof. Dr. Frank-Michael Matysik, and Prof. Dr. Patrick Nürnberger — for their time, their expertise, and the opportunity to defend my work in front of them.

My heartfelt thanks go to Anja for her reliable work in the Breder group's administration. Thank you for handling every request with such care and trustworthiness.

I am very grateful to Michaela for the wonderful time we shared in the laboratory. Your dedication and meticulous work keep the group running, and I truly appreciate everything I learned from you.

I would also like to thank my students Jana, Ludwig, and Ben for their committed support in my projects.

My sincere thanks go to all my colleagues in the Breder group — Caro, Anna, Christopher, Ludwig, Poorva, Berni, Markus, Edu, Dani, Kilian, Sebi, Tao, Georg, Sooyoung and Lisa, the secret Breder group member. Thank you for welcoming me so quickly into the group, especially as someone new to the University of Regensburg. I am grateful for the after-work evenings, the chaotic and fun carnival tuesdays, the many cooking nights, and the wonderful company during our trips to Brazil and Japan. Thank you for your constant willingness to listen, for your friendship, and for all the moments that made these years so memorable. Without you, this journey would not have been half as enjoyable.

A special thank-you goes to Tao and Sebi for the excellent collaboration on our joint projects. Tao, I am particularly grateful for everything I was able to learn from you and for the thoughtful discussions and exchange of ideas.

My deepest thanks also go to my lab companions — Poorva, Berni, and Markus. I will always remember our time together, from the absurd Spotify Weekly playlists to the late-afternoon Finch sessions that helped us push through the day.

I would also like to thank Poorva and Christopher for carefully proofreading this thesis. Your time, attention to detail, and support are truly appreciated.

I would like to thank Lisa, Chris, Julia, Tobi, Nico, Marcel and Lea for the inter-group communication that made getting to know the university and the other research groups so much easier, and that enriched everyday academic life in countless ways.
My friends in Munich deserve special thanks for offering distraction, support, and a welcome escape from the daily routine of laboratory work. Thank you, Tuan, for the many cooking nights, and thank you, Ben, for the long phone calls — whether to exchange ideas, talk about projects, or simply to vent.
My heartfelt thanks go to my family, my parents and my brother, who have supported me unconditionally throughout my life, my studies, and this PhD journey. I would not be where I am today without you.
Finally, I want to express my deepest gratitude to my best friend and partner, Michi. Thank you for always being there for me, for believing in me unfailingly, and for supporting me in every possible way.

List of Abbreviations

Ac	acetyl
Ar	aryl
APCI	atmospheric pressure chemical ionisation
Boc	*tert*-butyloxycarbonyl
BQ	benzoquinone
Bu	butyl
Bn	benzyl
Bz	benzoyl
COSY	correlation spectroscopy
(R)-CSA	((1R,4S)-7,7-dimethyl-2-oxobicyclo[2.2.1]heptan-1-yl)methanesulfonic acid
(S)-CSA	((1S,4R)-7,7-dimethyl-2-oxobicyclo[2.2.1]heptan-1-yl)methanesulfonic acid
Cy	cyclohexyl
DCC	*N*,*N*'-dicyclohexylcarbodiimide
DCE	1,2-dichloroethane
DCM	1,2-dichloromethane
DCN	1,4-dicyanonaphtalene
DEAD	diethyl (*E*)-diazene-1,2-dicarboxylate
DIPEA	*N*,*N*-diisopropylethylamine
DMA	*N*,*N*-dimethylacetamide
DMAP	4-(*N*,*N*-dimethylamino)pyridin
DMB	1,4-dimethoxybenzene
DMP	Dess-Martin periodinane
DMSO	dimethyl sulfoxide
EDAC	1-Ethyl-3-(3-dimethylaminopropyl)carbodiimid
ee	enantiomeric excess
EI	electron ionisation
equiv.	equivalent(s)
E	redox potential

ESI	electrospray ionisation
Et	ethyl
Et_2O	diethyl ether
EtOAc	ethyl acetate
EtOH	ethanol
EWG	electron withdrawing group
Fc	ferrocene
h	hour(s)
HAT	H-atom transfer
HFIP	1,1,1,3,3,3-Hexafluoropropan-2-ol
HMBC	heteronuclear multiple bond correlation
HRMS	high resolution mass spectrometry
HSQC	heteronuclear single quantum coherence
Hz	hertz [1/s]
IR	infrared
ISC	intersystem crossing
J	coupling constant (NMR)
LG	leaving group
m.p.	melting point
M	molarity ($mol \cdot L^{-1}$)
MA	maleic anhydride
Me	methyl
MeOH	methanol
Mes	mesitylene, 1,3,5-trimethylbenzene
min	minute(s)
MS	mass spectrometry or molecular sieves
NHE	normal hydrogen electrode
NMR	nuclear magnetic resonance
NOESY	nuclear overhauser effect spectroscopy
NaBArF	sodium tetrakis[3,5-bis(trifluoromethyl)phenyl]borate
NTf_2	bis(trifluoromethanesulfonyl)azanide
o	ortho
p	para
PC	photocatalyst
PE	petroleum ether
Ph	phenyl

PhBQ	2-phenyl-*p*-benzoquinone
PhCl	chlorobenzene
φ	quantum yield
ppm	parts per million
qNMR	quantitative nuclear magnetic resonance
R_f	retardation factor
r.t.	room temperature
r.r.	regioselective ratio
rpm	revolutions per minute
SET	single electron transfer
SCE	saturated calomel electrode
TAP	trisanisylpyrylium
TAPT	trisanisylpyrylium tetrafluoroborate
TBS	*tert*-butyldimethylsilyl
*t*Bu	*tert*-butyl
TEMPO	2,2,6,6-Tetramethylpiperidinyloxyl
Tf	triflyl, trifluoromethanesulfonyl
TFA	trifluoroacetic acid
THF	tetrahydrofuran
THP	tetrahydropyran
TLC	thin layer chromatography
TMB	1,3,5-trimethoxybenzene
TMBE	*tert*-butyl methyl ether
TMOF	trimethyl orthoformate
TMSCl	trimethylsilyl chloride
TPPT	2,4,6-triphenylpyrylium tetrafluoroborate
TCE	trichloroethylene
(R)-TRIP	(2r,4R,11cS)-4-hydroxy-2,6-bis(2,4,6-triisopropylphenyl)dinaphtho[2,1-d:1',2'-f][1,3,2]dioxaphosphepine 4-oxide
(S)-TRIP	(2s,4R,11bS)-4-hydroxy-2,6-bis(2,4,6-triisopropylphenyl)dinaphtho[2,1-d:1',2'-f][1,3,2]dioxaphosphepine 4-oxide
Ts	tosyl, *p*-toluenesulfonyl
UV	ultraviolet

1 Theoretical Background

For chemists, amines are among the most prominent structural motifs that are encountered on a daily basis. Already during the general studies at university, amines are introduced as multifunctional reagents in chemical transformations, mainly utilised as bases, nucleophiles, ligands, and catalysts.[1] As substrates, amines are indispensable for incorporating amine functionalities and C–N bonds during the synthesis of desired structures. This is of high value, as the amine motif is found in the molecular architecture of a majority of natural products, bioactive compounds, approved drugs, and drug candidates.[1–6] In 2022 and 2023, over 87% of the top 200 small molecule drugs ranked by retail sales were structures comprising amine moieties, such as free amines (-NH_2) and *N*-heterocycles.[3,6] Hence, the availability of a grand library of chemical reactions for the formation of C–N bonds – so-called aminations – can be a valuable toolkit for the synthesis of medicinally and industrially crucial materials.[7] In this context, allylic amines are of special interest since their double bond is an effective handle for further reduction, oxidation, or functionalisation.[8] Possible functionalities derived from allylic amines include α- and β-amino acids,[9–12] alkaloids,[13,14] and carbohydrate derivatives.[15] As a result, research into finding new ways to synthesise allylic amines is of high interest, with the goal of simpler and accessible strategies, as well as extending the scope of accessible structural motifs. There are several ways to form allylic amines (**1**). 1,2-, 1,3-dienes and alkynes for example can be elegantly transformed to allylic amines in a hydroamination reaction.[16,17] Another straightforward strategy is the direct coupling of an amine with an alkene possessing an isolated double bond. For this, several methods have been developed, allowing the use of various amine precursors and/or the chemical groups attached to or near the double bond. They can be divided into three groups: i) reductive amination from substrates such as aldehydes or ketones (**2**), ii) redox-neutral amination from functionalised alkenes (**3**), and iii) oxidative amination from simple alkenes (**4**) (Scheme 1.1).

Reductive aminations, in general, involve the reaction of a carbonyl compound and ammonia, a primary or a secondary amine. A suitable hydride donor reduces the formed imine or iminium ion intermediate to afford the desired amine product.[18, 19] When α,β-unsaturated carbonyls **2** are subjected to reductive amination conditions, the respective allylic amine (**1**) is formed.[20–23] The choice of a highly chemoselective hydrogenating system is of high importance in this transformation, as the C=C double bond – besides the imine/iminium ion C=N – can also be subjected to reduction.[24,25] Redox-neutral aminating processes can be realised *via* the allylic substitution of functionalised alkenes **3**. Their potential was manifested in the extensive development of methodologies for the transformation of (allylic) alcohols, such as the Overman rearrangement

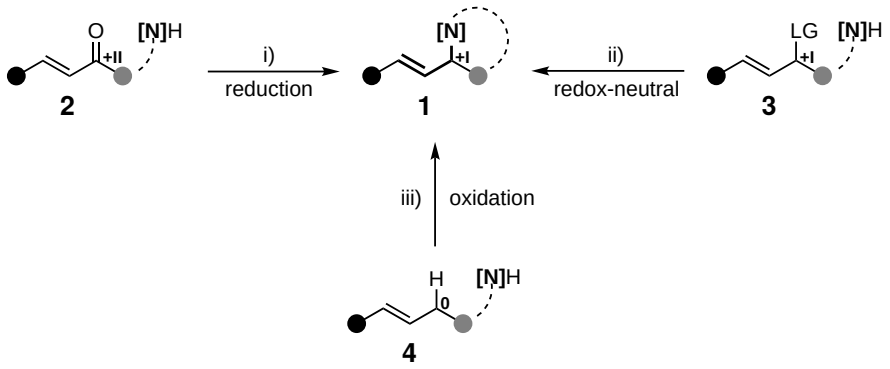

Scheme 1.1: Methods for the direct formation of *N*-allylic amine **1** by coupling of alkenes **2**–**4** with an amine source **[N]**H. LG = leaving group.

and MITSUNOBU reaction or (allylic) halides, as in the GABRIEL synthesis, to give their respective allylic amines in perfect regioselectivity.[8] Expanding the possibilities, Tsuji and Trost discovered that allyl-Pd^{II} complexes – derived from an allylic functionalised alkene **3** and a Pd^0-species – are highly reactive towards nucleophiles.[8,13,26,27] This development enabled for the redox-neutral reaction of functionalised alkenes **3** such as acetates,[13,28] carbonates,[8,13] phosphates[29] or chlorides[29,30] towards allylic amines **1**. The further development of the Tsuji-Trost reaction towards an asymmetric protocol by employing various engineered chiral ligands enabled the reliable formation of enantioenriched allylic functionalised alkenes.[9,27,31–35] Since then, a variety of transition metals besides Pd[8,13,28,35–37] have been reported to catalyse the allylic substitution reaction with amine-nucleophiles, such as Ir,[29,38–42] Rh,[43] and Mo.[44,45] The transition metal-mediated redox-neutral allylic aminations showed promising results for styrenes as well as terminal and symmetrical internal alkenes, but the regiocontrol in asymmetrically substituted, internal alkenes remains challenging.[29,46]

In addition to reductive elimination and allylic substitution reactions, allylic amines **1** can also be obtained *via* oxidative processes. The application of oxidants facilitates the coupling of non-functionalised alkenes **4** with amines to form allylic amines **1** through an oxidative process. This hugely broadens the substrate availability for the direct allylic amination with amines and alkenes and provides alternative pathway with high atom economy to the reductive and redox-neutral amination described above. The availability of various oxidants gives this reaction a further advantage, with oxygen from the air being a cheap, readily available and ecological friendly example. The named features led to the development of an assortment of pathways for the oxidative allylic amination, which will be discussed further in the following chapters.

1.1 Strategies for the Oxidative *N*-Allylation of Amines

The direct oxidative *N*-allylation of amines has been subject to numerous methodological investigations and is still of high interest for further development. In this reaction class, the desired

allylic amine (**1**) is accessed from simple alkenes by intra- or intermolecular coupling with an amine source (**[N]**H) facilitated by an oxidant. Depending on the reaction conditions and applied substrates, **1** is formed either by (formal) N-insertion into the C-H σ-bond of the alkene, keeping the double bond fixed in 1,2-position (Scheme 1.2, path a) or by a π-bond forming process which leads to transposition of the double bond from 2,3-position to 1,2-position (Scheme 1.2, path b). Hence, in theory, the same allylic amine **1** can be accessed from different alkenes by varying reaction mechanisms and modes of activation, which will be disclosed in further chapters. And vice versa, one may access different allylic amines **1** from the same alkene starting material. The regioselective outcome can be influenced by finetuning the reaction conditions, the applied additives and catalysts, and/or the constitution of the applied substrates. As an example, in the case of olefins bearing a remote amine group as the internal amine source, the regioselectivity of the intramolecular allylic amination is, among others, influenced by the size of the ring that can be possibly formed in the product. This offers a first point of control of the regioselective outcome in an intramolecular process.

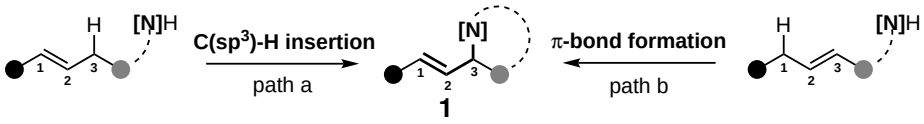

Scheme 1.2: Oxidative allylic introduction of N-moieties into alkenes. **[N]**H = amine source.

To overcome the activation barrier of the oxidative transformation, both the amine and alkene can undergo in-situ activation. N-activation in the synthesis of (allylic) amines *via* the in-situ formation of *N*-centred radicals[47,48] or (metal-)nitrenes[49,50] is an own topic out of the scope of this thesis and is covered by the cited literature.[51] In this introduction, a special focus is set on strategies to activate the C-fragment, leading to the formation of allylic amines. Both possible strategies will be discussed, one focusing on the method activating the allylic C-H σ-bond and the other one focusing on activating the olefinic π-bond to facilitate the oxidative coupling of simple non-functionalised alkenes with amines to give allylic amines (Figure 1.1).

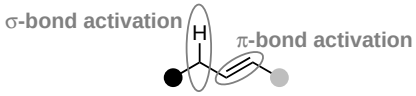

Figure 1.1: Strategies to activate the olefinic substrates for the allylic amination.

To-date achievements will be displayed in addition to substrate specifications and individual and sometimes intrinsic regioselective challenges, as both strategies can lead to formal C-H insertion or π-bond formation.

1.1.1 σ-Bond Activation

Regarding the current literature, σ-Bond activation for the oxidative allylic amination of non-functionalised alkenes is mainly facilitated by transition metal catalysis, with Pd being the most important metal.[52] Mechanistically, the transformation involves the coordination of a Pd^{II}-species to alkene substrate **5**, giving **6** (Scheme 1.3).[34,53,54] The Pd^{II}-species functions as an electrophilic promoter of a heterolytic, allylic C-H cleavage event, which omits the need for preactivated alkenes required in Pd^0 substitution reactions.[55] The coordination activates the allylic C-H bond towards abstraction, leading to the formation of η^3-complex **7**. Nucleophilic substitution and reductive elimination releases Pd^0 and affords the final product **9**. The reoxidation of the released Pd^0-species to Pd^{II} requires at least stoichiometric amounts of the oxidant to utilise catalytic amounts of Pd. The oxidant must also be selective enough to oxidise only a Pd^0-species without affecting the olefin or amine present. Enantiomeric induction could be achieved by the usage of chiral ligands.[34]

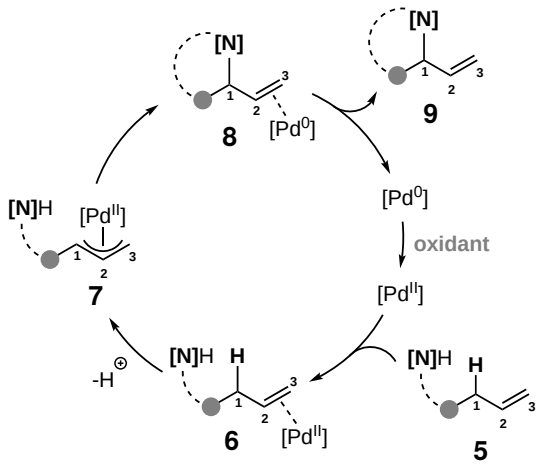

Scheme 1.3: Proposed mechanism of the Pd^{II}-mediated intramolecular oxidative allylic C-H amination of alkenes. L = ligand.[34,52–54]

When internal olefins **10** are applied in the Pd^{II}-mediated oxidative allylic amination, two protons can be subject in the C-H abstraction event, affording two different η^3-complexes (Scheme 1.4). The following nucleophilic substitution with an N-nucleophile can proceed on either end of the allyl-complex (positions 2/4 or 1/3), resulting in the theoretical formation of four regioisomers.

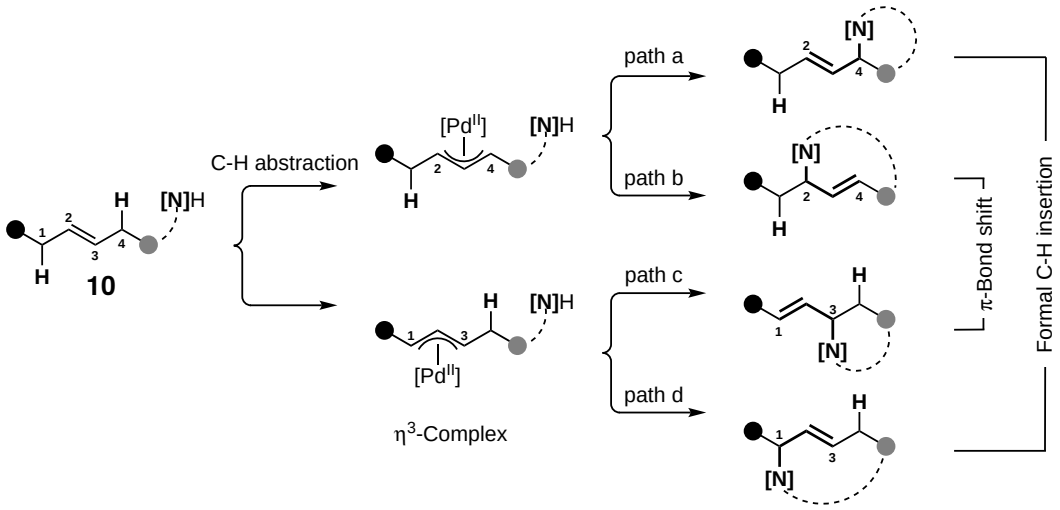

Scheme 1.4: Possible products from the allylic amination *via* metal-catalysed σ-bond activation of internal double bonds. **[N]**H = amine source.

Especially for the depicted internal olefins **10**, regioselective control poses significant challenges and is even fortified by Pd^{II} suffering from inefficient coordination to internal alkenes.[56] Additionally, the formed intermediates in the reaction are inclined to isomerisation of the double bond to an often more stabilised terminal or conjugated position by β-H elimination and Pd-chain walking, resulting in a product mixture.[57–59] Another challenge is posed with the experience that aliphatic and basic amines show extremely tight coordination to Pd^{II} and, therefore, inhibit coordination to the alkene, limiting the scope of the applicable amines in the reaction.[56,60]

Regarding this background, several strategies were developed, addressing the named regioselective issues of introducing the amine moiety during Pd-catalysed oxidative allylic aminations. The majority of developed methods, both intra- and intermolecular, involve the allylic amination of terminal olefins, while the conversion of internal alkenes leads to poor yields and a mixture of products.[52,61–64] Employing a terminal olefin excludes a second allylic H to be abstracted, leaving only two regioisomers as the possible outcome compared to four with internal olefins.

As shown in 2009 by Liu and coworkers, the formed product ring size in the Pd^{II}-mediated intramolecular oxidative allylic C-H amination of alkenes **11** can be influenced by adjustment of the reaction conditions (Equation 1.1).[64] The formation of five-membered lactam **12** was achieved with 10 mol% $Pd(OAc)_2$ and 10 mol% of a Cr^{III} co-catalyst in *N*,*N*-dimethylacetamide (DMA) and O_2 as the oxidant. A proportion of less than 3% of the seven-membered lactam isomer **13** was detected in the crude reaction mixture *via* GC analysis.

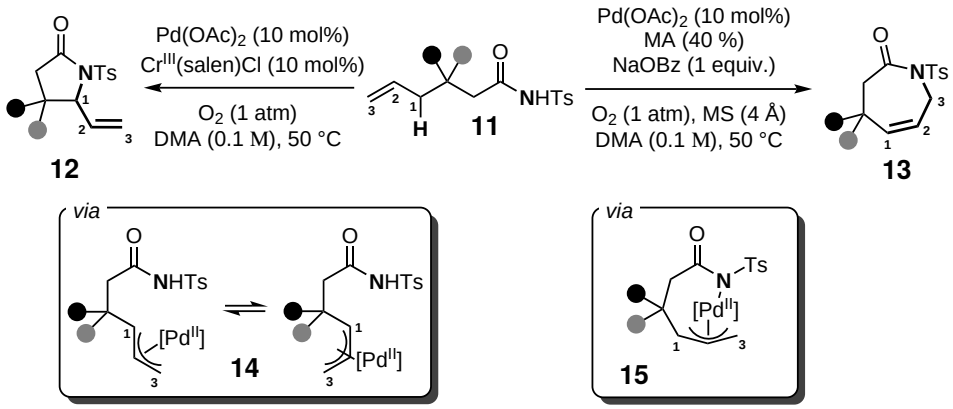

(1.1)

Interestingly, the group found that 1 equiv. of the BRØNSTED-base NaOBz could shift the reaction outcome towards the formation of seven-membered lactam **13** and a 18% proportion of five-membered isomer **12** in the crude product mixture. The addition of 40% maleic anhydride (MA), acting as a π-acid ligand and proposed to aid nucleophilic substitution at the η^3-complex and 4 Å molecular sieves (MS) further improved the product yield of **13** and the regioselective ratio.

The regioselective outcome is proposed to result from an equilibrium between intermediates **14** and **15**. A nucleophilic intramolecular attack in **14** in *exo*-fashion leads to the predominant formation of five-membered lactam **12**. LIU and coworkers argue that BRØNSTED-base NaOBz is able to promote the Pd-N bond formation, which has been shown in previous reports,[64–66] shifting the equilibrium towards intermediate **15**. This promotes the nucleophilic attack in *endo*-fashion, resulting in the formation of seven-membered lactame **13**. The example shows how simple, easily accessible additives can influence the regioselectivity of the Pd-catalysed intramolecular oxidative allylic amination.

The intramolecular allylic amination has made huge advances, with the ring size that is formed in the product generally being the driving force for regioselectivity.[52,64] In comparison, intermolecular variants are less studied and pose more challenges in regioselective control.[52]

Seminal Pd^{II}-catalysed intermolecular oxidative allylic amination reactions were reported independently by the groups of WHITE[62] and LIU[63] in 2008, who further developed their intramolecular protocols towards intermolecular ones. WHITE and coworkers found that a bis-sulfoxide/$Pd(OAc)_2$ catalyst, which was previously reported to successfully catalyse the intramolecular allylic C-H amination,[61] and the intermolecular allylic oxidation,[67,68] in combination with a Cr^{III}-catalyst finally facilitates the intermolecular allylic C-H amination of terminal olefins **16** with an excess of *N*-tosyl carbamate nucleophiles (Equation 1.2). The in-situ formed η^3-Pd^{II} intermediate is proposed to be activated towards nucleophilic attack by the π-acidic ligand benzoquinone (BQ) and the Cr^{III} LEWIS-acid cocatalyst, affording complex **18**.[55,69] This enables the final nucleophilic attack of the *N*-nucleophile at the lesser hindered terminal carbon, leading to linear products **17**.

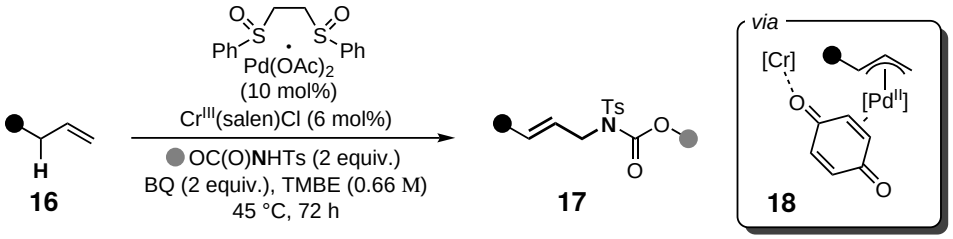

(1.2)

While several methods for the Pd^{II}-catalysed allylic amination were developed for transforming terminal olefins, employing internal olefins remains challenging. The reason for this is not only due to the higher degree of possible functionalisation sites in comparison to terminal olefins but also due to lower coordination of the Pd^{II}-species to the sterically more demanding internal alkene.[56] In addition, internal alkenes are also reported to undergo undesired isomerisation, which lowers the regioselective control even further.[56,57,59]

In to-date reports, the transition metal-catalysed intermolecular oxidative allylic amination of internal olefins is realised by sustaining or forming a conjugated double bond (Scheme 1.5, b). Here, the driving force for the (re-)formation of a conjugated π-system leads to a regioselective outcome of one major product and has been reported with Rh^{III}-[70,71] and Ir^{III}-catalysts[71,72] and follows the same mechanism as Pd^{II}-species.

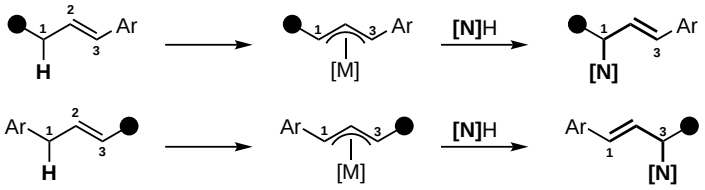

Scheme 1.5: Substrates and product scope of the metal-catalysed allylic amination *via* σ-bond activation, involving conjugated internal alkenes. **[N]**H = amine source.

Allylic Amination *via* Photoinduced C-H Abstraction.

Traditional methods suffered from low coordination of the Pd^{II}-species to internal double bonds, making their transformation hard to accomplish. Only recently, the challenge of transforming internal non-conjugated double bonds towards allylic amines *via* oxidative allylic amination was overcome by exploiting the energy of light in contrast to traditional thermal pathways.[56] Gevorgyan and coworkers reported an innovative method for the Pd-catalysed allylic amination of internal olefins **19**, enabled by photoinduced C-H abstraction.[56] This was made possible through a light-induced Pd(0/I/II) evolution during the reaction, which, in contrast to the common Pd(II/0) transformation, enables the application of basic aliphatic amines and internal (non-) conjugated olefins (Equation 1.3).

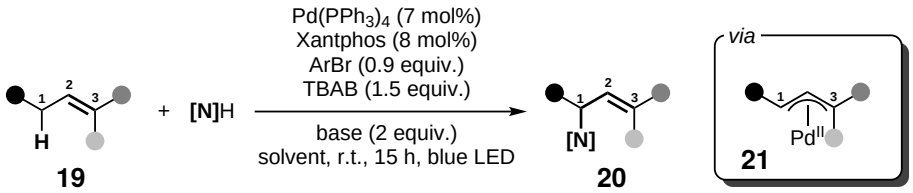

(1.3)

Key to the reaction is the light-induced electron transfer from Pd^0 (here $Pd(PPh_3)_4$) onto an aryl-bromide (ArBr)-species, functioning as the oxidant.[73] The resulting Ar-radical can abstract an allylic H of the alkene compound **19**, facilitating a second oxidation *via* H-atom transfer (HAT). The so-formed allyl-radical **22** coordinates to the previously formed Pd^I-species, presenting the third involved oxidation step and leading to the formation of reactive η^3-Pd^{II}-complex **21** (Scheme 1.6). Nucleophilic substitution follows, affording the desired *N*-allylic amines **20** under the reformation of Pd in its original redox state, closing the catalytic cycle.[56]

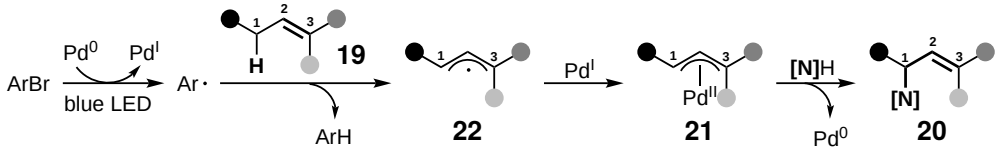

Scheme 1.6: Proposed mechanism of the Pd-catalysed allylic amination of non-conjugated, internal olefins, reported by GEVORGYAN and coworkers.[56] **[N]**H = aliphatic amine.

In contrast to the previously reported Pd^{II}-catalysed allylic aminations, here, the H-abstraction is not facilitated by the Pd-catalyst but by an in-situ formed aryl radical, which enables the utilisation of Pd^0-species. This itself results in the ability to apply basic amines as substrates, which were incompatible with Pd^{II}-catalysts as they would strongly bind and, with this, deactivate their catalytic ability.[56] The high regioselectivity is driven by electronic effects *via* the (re)formation of a conjugated double bond or, in the case of simple aliphatic alkenes, by sterical effects *via* the substitution at the least hindered position (Figure 1.2). Compounds **20a** and **20b** both show preferential amination at the lesser hindered terminal carbon over the tertiary or secondary position. In the case of the only reported 1,2-disubstituted aliphatic alkene **20c**, regioselective control is achieved by the sterically demanding, remote ^{t}Bu-group, blocking one site for nucleophilic attack.

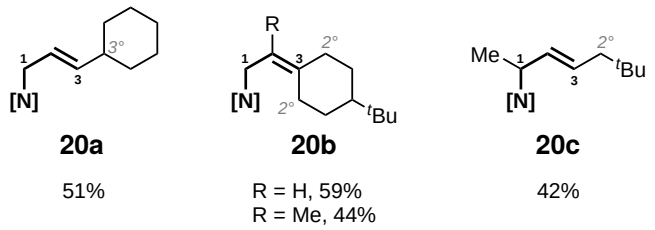

Figure 1.2: Regioselective outcome of the allylic amination of aliphatic internal olefins by GEVORGYAN and coworkers.[56] **[N]** = amine.

In Summary, σ-bond activation has shown to be a valuable tool for the allylic amine-functionalisation of alkenes. Predominantly terminal alkenes and internal, conjugated alkenes showed high regioselectivity in their product-forming reactions. Internal, non-functionalised alkenes were shown to be difficult substrates, as their coordination to the transition metal-catalyst is sterically more hindered, which leads to a slower reaction and allows undesired side reactions. Additionally, the regioselective outcome depends only on the alkene-substituents, making the differentiation very difficult. Only a few examples have been reported where remote directing groups were able to influence this outcome. This shows that further development is required to improve the regioselective outcome in the allylic amination of simple non-functionalised internal alkenes, especially 1,2-difunctionalised alkenes.

1.1.2 π-bond activation

Another way to activate an alkene moiety **23** for the oxidative allylic amination is *via* π-bond activation, giving access to two possible allylic isomers **24** and **25** by nucleophilic attack on either olefinic carbon (Scheme 2.5).

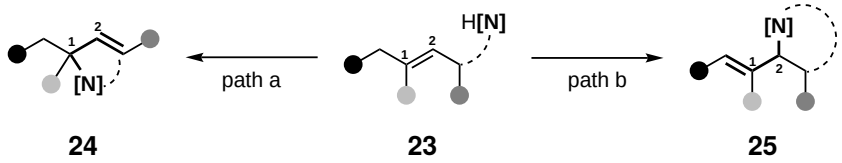

Scheme 1.7: Regioselective outcome of the allylic amination of internal olefins *via* π-bond activation. **[N]**H = amine source.

In the intramolecular variant, the selectivity is, among others, influenced by the size of the ring formed in the product. This leads to the build-up of allylic amines, accompanied by a π-bond shift, affording an endogenous double bond included in the formed ring system (**24**) or an exogenous double bond forming outside of the ring system (**25**). Steric and electronic properties of the alkene substrate can further influence the selectivity in intramolecular as well as intermolecular allylic amination reactions. This is especially noteworthy if asymmetrically substituted alkenes, such as mono-, 1,1-di- and trisubstituted alkenes, are employed and a differentiation in MARKOVNIKOV (**24**) vs. *anti*-MARKOVNIKOV selectiviy (**25**) can be observed. Comparable to methods involving σ-bond

activation, 1,2-disubstituted (aliphatic) alkenes also present a challenging class of substrates for the regioselective formation of allylic amines enabled by π-bond activation. In this case, this is due to the difficulty in distinguishing the chemical, steric, and electronic surroundings of the olefinic carbons.

Over the last decades, several successful strategies involving π-bond activation of olefins for the allylic functionalisation with amines were established, which will be discussed in the following sections.

Pd-Catalysed aza-Wacker Reaction

As discussed in Subsection 1.1.1, transition metal catalysts are known to enable the transformation of alkenes and amines towards allylic amines through a C-H activation–reductive elimination sequence (cf. Scheme 1.3). A further reported pathway for Pd-catalysed allylic aminations is presented by a Wacker-type amination reaction following a π-bond activation pathway (Scheme 1.8). Here, the coordination of Pd^{II} to the double bond is followed by an aminopalladation pathway, affording intermediate **28**. Subsequent β-hydride elimination affords either the allylic or vinylic amine product **29** accompanied by the release of Pd^0. Oxidation reintroduces Pd^{II} into the catalytic cycle.

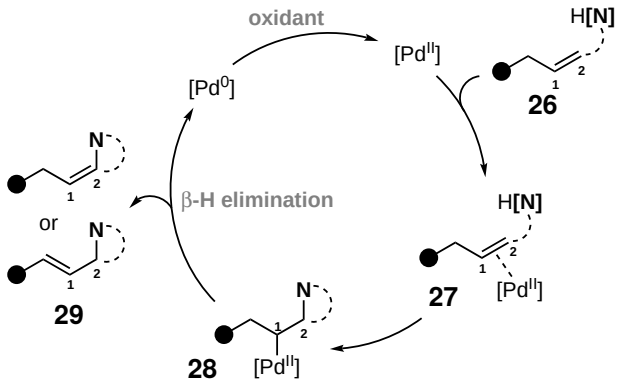

Scheme 1.8: Mechanism for the Pd^{II} catalysed aza-Wacker reaction.[74]

Utilising the same substrate, the outcome of this π-bond activation method may be different from the σ-bond activation method discussed above as the different reactive intermediates derived from the alkene substrate are of varied nature and offer distinct sites of attack for the nucleophile, which can be specific to the mode of activation. This broadens the variety of products that may be formed depending on the reaction conditions, but distinguishing the two mechanisms is not always easy or even possible.[75,76]

An example of a good differentiation was given by Broggini and coworkers in 2004, reporting on a base-dependent divergent cyclisation of *N*-allyl-anthranilamides **30** with 10 mol% of $Pd^{II}(OAc)_2$ (Scheme 1.9).[77]

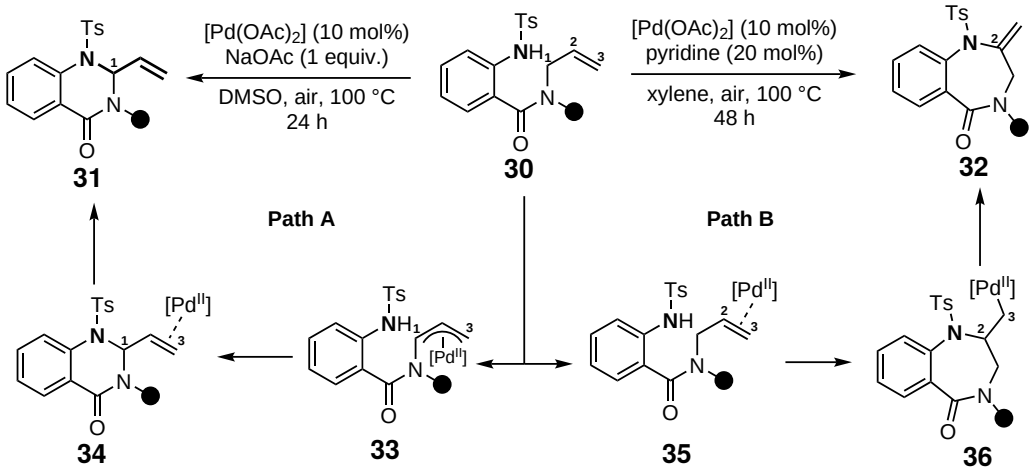

Scheme 1.9: Proposed mechanism for the Pd^{II} catalysed regiodivergent cyclisation of *N*-allyl-anthranilamides **30** according to Broggini.[77] Path A: C-H abstraction–reductive elimination sequence (σ-bond activation). Path B: aza-Wacker reaction involving a nucleopalladation–β-H elimination sequence (π-Bond activation).

Two major products were formed depending on the reaction conditions, reportedly following two condition-dependent mechanisms. When NaOAc was applied in a polar solvent, six-membered heterocycles 2-vinyl-quinazolin-4-ones **31** were isolated as the major products (Scheme 1.9, Path A). The strongly basic conditions are proposed to support the direct allylic C-H cleavage, forming η^3-allyl-Pd complex **33** *via* σ-bond activation. Intramolecular nucleophilic substitution by the tosylamide at C1 of the allyl-complex afforded allylic amine **31**. On the other hand, seven-membered heterocycles 2-methylene-1,4-benzodiazepin-5-ones **32** were formed when pyridine in a non-polar solvent was employed in the reaction (Scheme 1.9, Path B). This transformation is proposed to proceed through π-bond activation by the Pd^{II} species (**35**), facilitating nucleophilic attack at C2, which is inaccessible from allyl-complex **33**. With this step, aminopalladation intermediate **36** is formed. Subsequent β-hydride elimination classifies this conversion as an aza-Wacker reaction, forming vinylic amine **32**. The highly selective outcome is proposed to result from the preferential formation of the lesser strained seven-membered vinylic amine heterocycle in Markovnikov selectivity, compared to its eight-membered allylic isomer formed from nucleophilic attack at C3. During both pathways, the formed Pd^0 is reoxidised to its catalytically active Pd^{II}-species by oxygen from the air.[77]

Several entities such as the formed ring size in the product,[77] additives,[77] and ligand size,[78] can influence the regioselectivity in the intramolecular aza-Wacker cyclisation, and several methods for the regiocontrolled transformation towards allylic amines have been reported.[78–84] Intermolecular variants mainly cover terminal olefins[85,86] and alkenols,[83,84] affording the corresponding amino-aldehydes. Markovnikov products are mostly favoured in intermolecular nucleopalladation reactions of terminal alkenes, adding the nucleophile to the more substituted carbon of the olefin due to favourable electrostatic and orbital interactions between the nucleophile and the more

substituted sp^2-carbon.[83,86–90]

Despite further studies on the intermolecular aza-WACKER reaction, the regioselective transformation of internal alkenes proved challenging, and the first reports included symmetric, cyclic examples, where regioselectivity was not addressed.[91,92] In a seminal report, SASAI, TAKENAKA, and their coworkers showed that internal alkenes **40** afforded allylic amines **41** when applying a Pd/spiro bis(isoxazoline) (SPRIX) catalytic system (Equation 1.4).[93]

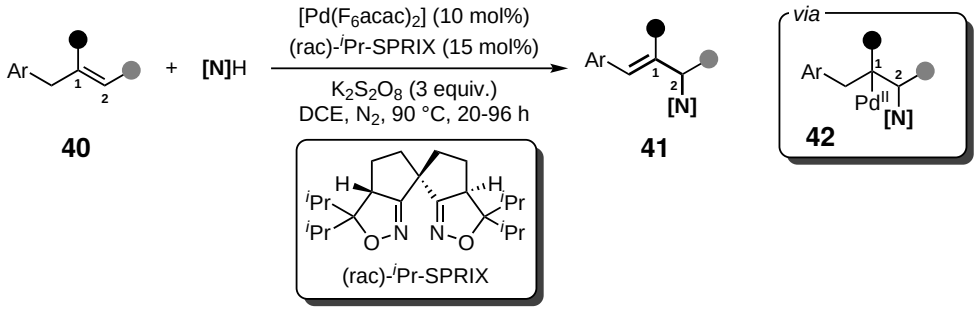

(1.4)

Through the low σ-donating ability of SPRIX compared to other, frequently used ligands, such as OAc, the intrinsic LEWIS acidity of the Pd is preserved and found effective for activating internal C-C double bonds.[82,94] Employing both symmetrically and asymmetrically substituted internal alkenes, the reaction is proposed to follow an aminopalladation–β-hydride elimination sequence with $K_2S_2O_8$ as the terminal oxidant to regenerate the Pd^{II} species. A high regioselective outcome is driven by the build-up of conjugated allylic amines **41**, preferred over their vinylic isomers, from homoallylaromats **40**. When an aliphatic cyclohexane derivative was applied, no reaction was observed, highlighting the necessity of an aromatic substituent in the homoallylic position for this transformation, which could be crucial for the formation as well as for stabilising the aminopalladation intermediate **42**. This indicates that the coordination of Pd and the nucleophilic attack are both reversible, and the β-H elimination represents the rate-limiting step. Without adding base, the β-H in the aminopalladated intermediate must be labile enough for successful elimination. Trisubstituted alkenes follow an *anti*-MARKOVNIKOV pathway, which overrides the driving force towards a conjugation to the aromatic system and leads to the successful formation of one non-conjugated allylic amine **41b**, albeit in lower yields compared to the conjugated regioisomer **41a** (Scheme 1.10).

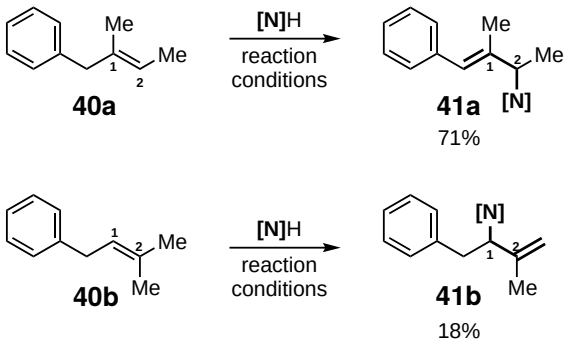

Scheme 1.10: Regioselective outcome in the intermolecular allylic amination of trisubstituted alkenes reported by SASAI.[93]

In summary, the aza-WACKER reaction has shown to be a valuable tool for the build-up of allylic amines and offers a pathway towards a different regioselective outcome compared to the σ-bond activation pathway. Both intra- and intermolecular variants show a preferred restoration of the double bond in a terminal position or in conjugation to a pre-existing π-system, demanding further investigations to broaden the substrate scope and accessible allylic amines. Especially alkenes with longer carbon chains are subject to metal shifts/Pd-chain walking mechanisms through the carbon chains, reducing regioselective control and applicability.[84–86,93]
In the so-called aza-WACKER-reaction, the ring size outcome again may influence the regioselectivity in intramolecular variants, and steric[78] and electronic effects can play a role in the selective outcome in both intra- and intermolecular reactions. Additionally, the stability of the formed aminopalladation-intermediate plays a role in the product formation.[93]

Photocatalysis

Besides thermal energy, the absorption of energy from light can promote chemical reactions. This is made possible, for example, by a catalyst, which is able to absorb the photon's energy to access an electronically excited state. Activation of non-absorbing substrates and reformation of the catalyst's ground state renders this mode photocatalytic. In the case of photoredox catalysis, the excited state photocatalyst can accelerate chemical processes *via* single electron transfer (SET) events, either acting as an oxidant or reductant.[95] Even under mild conditions, such as low-energy light for excitation and ambient temperature, a low amount of highly reactive radical species could be generated.[95–97] In contrast, common radical generation strategies often require hazardous radical initiators, toxic reagents, high temperatures, and/or ultraviolet (UV)-light irradiation to generate high amounts of radicals.[95] To meet specific needs, the redox properties of a photoredox catalyst may be tuned by altering the central metal of the catalyst (Ru, Ir, W, etc.) or tailoring the substitution patterns on the ligands and the organic framework. This led to the development of a wide array of novel synthetic methodologies, including reports on the formation of allylic amines.[95]
Photoredox catalysts show high potential as reactants in the allylic functionalisation of olefins due to their ability to activate π-bonds towards radical ions. 1,2,2-trisubstituted olefins could

almost not be transformed to allylic amines by traditional thermal Pd catalysis due to low coordination of the transition metal to the internal double bond combined with a missing driving force for the β-hydride elimination.[56,93] In contrast, Yoon and coworkers were able to transform 1,2,2-trisubstituted olefinic tosylamides **43** in high to perfect *anti*-Markovnikov regioselectivity towards non-conjugated, terminal allylic amines **44** *via* a photocatalytic protocol (Equation 1.5).[98] The intramolecular photocatalytic transformation is enabled by 2.5 mol% of acridinium salt photocatalyst **45** and 2 equiv. of Cu^{II} 2-ethylhexanoate ($Cu(EH)_2$), serving as the oxidant.

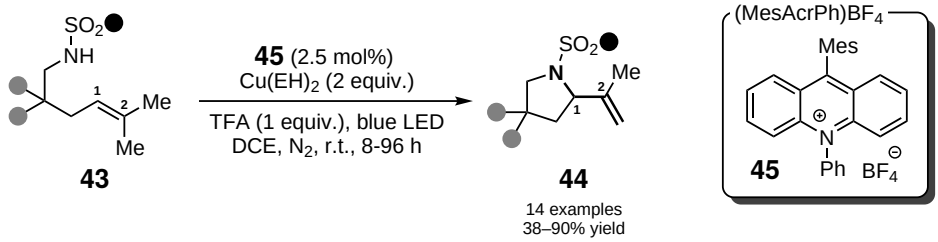

(1.5)

Regarding the mechanism, the group proposes that blue light irradiation (hν) is absorbed by photocatalyst **45** and the so-formed excited state **45*** can undergo a single electron transfer (SET)-event with the applied olefinic tosylamides **43**, affording radical cation **51** (Scheme 1.11). Subsequent intramolecular nucleophilic attack affords radical **52**, which, upon oxidation with Cu^{II}, produces the desired allylic amine **44**. The reduced Cu^{I} then reoxidises radical photocatalyst **46**, closing the catalytic cycle. This interesting $Cu^{II}/Cu^{I}/Cu^{0}$-sequence enables the dual functionality of the Cu-species to both serve as the oxidant in the final oxidative elimination step towards the product and the terminal oxidant to regenerate photocatalyst **45**.

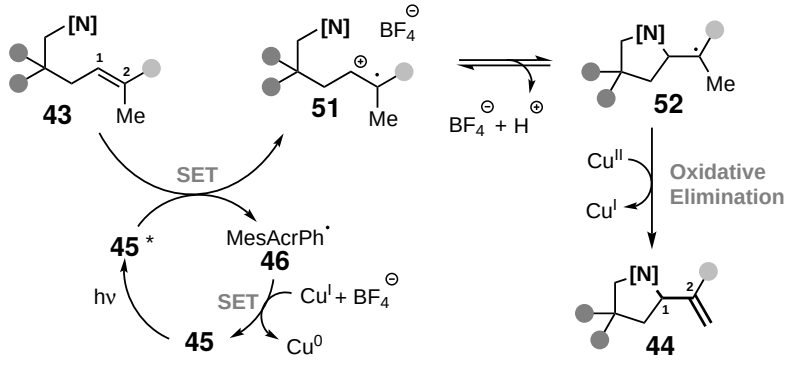

Scheme 1.11: Mechanistic proposal for the photocatalytic intermolecular allylic amination of 1,1,2-trisubstituted alkenes **43** according to Yoon and coworkers.[98]

Key to the high regioselective control is the in-situ formation of radical-cation species **51** (Scheme 1.11), in which the radical is more stabilised at the higher substituted carbon. Subse-

quent nucleophilic attack consequently follows at the lesser substituted carbon, leading to *anti*-Markovnikov products **44**, enabling a high regioselective control in 1,2,2-triubstituted alkenes. 14 examples were reported, showing flexibility towards various sulfonamide nucleophiles and tethers. Additionally, two examples of alkene modifications were shown: The application of a 1,1,2-trisubstituted alkene led to a six-membered heterocycle formation and a regioisomeric product mixture with an exocyclic and endocyclic double bond in a 4:1 ratio (**47**). Endocyclic product formation was observed when a tetrahydropyran was employed. Due to its symmetry, elimination into either direction of the ring leads to the desired product (Scheme 1.12, Substance **48**). 1,1-disubstituted styrenes **49** were formed in perfect regioselectivity. Even sterically demanding tetrasubstituted alkenes can react under photocatalytic conditions (Scheme 1.12, substance **50**), which was challenging with traditional Pd^{II} catalytic systems. Even though the reported methodology shows high abilities in some substrate classes compared to the Pd^{II}-catalysed oxidative amination variants, the transformation of terminal and 1,2-disubstituted olefins was no subject in this publication.

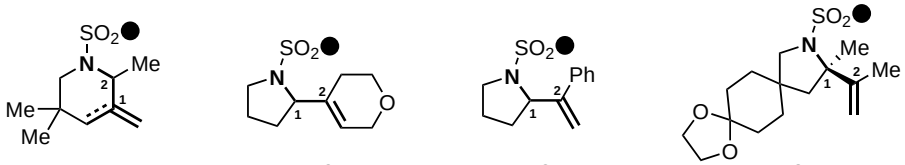

Scheme 1.12: Substrate variation in the photocatalytic allylic amination by Yoon et al.[98]

The extension of the photocatalytic oxidative allylic amination protocol to an intermolecular variant with a broad range of linear alkenes was accomplished in 2023 by Cai, Lei, and their coworkers.[99] Applying a Co^{III}-species together with acridinium salt photocatalyst **55** enables the transformation of cyclic and multiple linear alkenes **53** *via* their radical cation with azoles **[N]**H towards their respective allylic azoles **54** (Scheme 1.13).

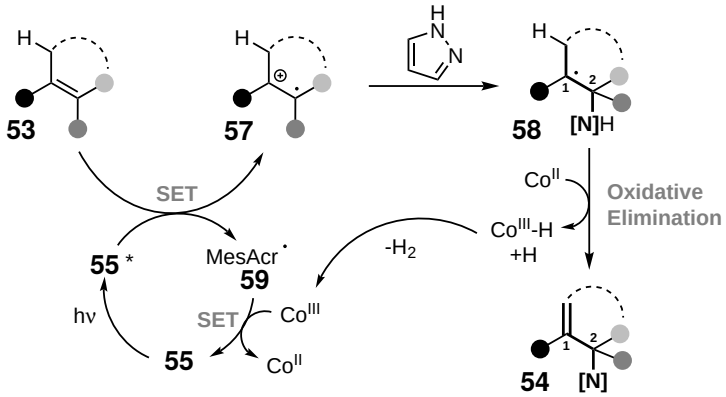

Scheme 1.13: Mechanistic proposal for the photocatalytic intermolecular allylic amination of **53** according to Cai, Lei and their coworkers.[99]

Similar to the mechanism reported by Yoon (cf. Scheme 1.11), Co^{III} is proposed to engage in two oxidation events. In this case, Co^{III} is proposed to serve as the oxidant to regenerate photocatalyst **55** and, in a second step, serve as the reductant in a radical-polar crossover event *via* H-atom transfer (HAT), facilitating the final product formation. This $Co^{III}/Co^{II}/Co^{III}$-H sequence enables the regeneration and, with this, the catalytic usage of Co^{III} from Co^{III}-H with available protons, releasing H_2 in a hydrogen-evolution mechanism.

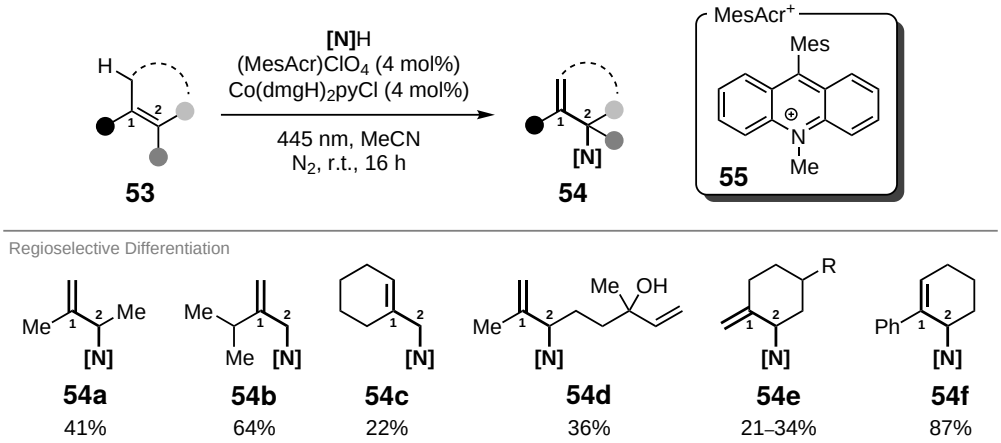

Scheme 1.14: Photocatalytic intermolecular allylic amination of alkenes **53** with azoles **[N]**H reported by Lei, Cai and co workers.[99] Isolated yields given.

In nonsymmetrically substituted alkenes, the reported method shows high regioselectivity towards *anti*-Markovnikov products. 1,1-disubstituted (**53b**, **53c**) and trisubstituted alkenes (**53a**, **53d**-**53f**) afforded either internal cyclic (**54c**, **54f**) or terminal (**54a**, **54b**, **54d**, **54e**) allylic amines.

The reported photocatalytic methods show great ability to transform asymmetrically substituted linear (1,1-disubstitituted, trisubstituted) and cyclic alkenes to their corresponding allylic amines in high regioselectivity. The outcome is driven by the stabilisation of the in-situ formed radical cations and sterical hindrance in allylic radicals. Even though this method is highly successful in the named substrates, the regioselectivity in 1,2-disubstituted linear alkenes remains challenging to accomplish, as the sterical and electronic differentiation is limited due to a similar surrounding at the olefinic carbons. This may be the reason why no 1,2-disubstituted substrates were reported in the photocatalytic transformation towards allylic amines.
The thermal synthetic methods presented so far proceed *via* closed-shell, sometimes ionic intermediates. Meaning that the orbitals are either fully filled or empty. Photocatalytic methods proceed *via* a different mode of activation, forming reactive radical species that present open-shell intermediates during a transformation. This difference promotes different reaction pathways and might lead to different regioselectivity.

Selenium-π-Acid Catalysis

The regioselective challenges encountered by transition metal-catalysed allylic amination reactions, such as poor coordination to internal alkenes of the catalysts or a few examples of 1,2-disubstituted alkenes as substrates, may be overcome by Lewis-acidic selenium species. Chalcogenium (Ch = S, Se) ions exhibit an exceptional reactivity towards π-bonds, which is proposed to result from a donation–back-donation manifold, very similar to the transition metal activation of alkenes (**60**) (Scheme 1.15). The interaction is suggested to establish between the olefinic π-orbital and the σ*-orbital of the chalcogen catalyst as well as a back-donation from the chalcogen lone pairs to the olefinic π* orbital (Scheme 1.15, left).[100,101] Subsequently, these interactions result in the formation of the corresponding iranium ion **61**, representing a covalent activation of the double bond, in contrast to the non-covalent transition-metal-induced activation. These orbital considerations account for the high carbophilicity and high chemoselectivity in a following nucleophilic attack facilitated by partially positive charges at the former olefinic carbons.

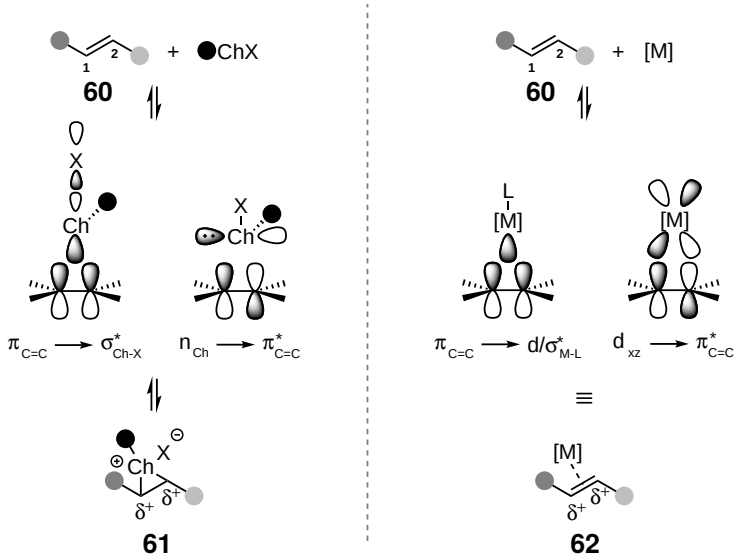

Scheme 1.15: Comparison of π-bond activation principles *via* chalocogen π-acids (left) to transition metal π-acids (right).[100–102]

The initially formed seleniranium ion intermediate **61** can be rapidly opened in the presence of a nucleophile to afford two different regioisomers, **64a** or **64b**. In asymmetrically substituted alkenes such as primary, 1,1-disubstituted, or 1,1,2-trisubstituted alkenes, the ring-opening step usually follows the thermodynamically favored Markovnikov regioselectivity. The method shows similarity to the formation of nucleopalladation intermediate by Pd-catalysed (aza-)Wacker reaction (cf. Subsection 1.1.2) albeit in complementary regioselectivity to the metal-base method, which prefers the *anti*-Markovnikov isomer.

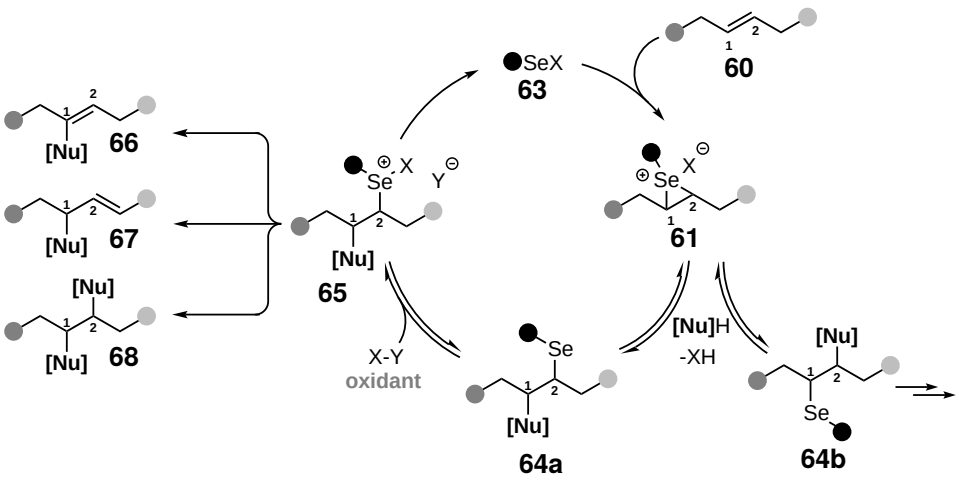

Scheme 1.16: Typical reaction mechanism and possible regioselective outcome of the nuclephilic functionalisation of alkenes *via* selenium-π-acid catalysis. Nu = nucleophile or X^-.[103,104]

Oxidation of the selenofunctionalised intermediates **64** to **65** gives way to three deselenylation pathways, which lead to the corresponding vinylic (**66**), allylic (**67**), or disubstituted (**68**) compound.[104] The properties of the oxidant used, as well as the resulting endogenous nucleophiles, a nucleophlic species derived from the oxidant or chalcogen electrophile, play a crucial role in determining the range of carbon-heteroatom bonds (with heteroatoms being nitrogen, oxygen, or halogen) that can be created through selenium-pi-acid catalysis.[100] The last elimination step is typically irreversible and is often identified as the rate-limiting step. Controlling the position of nucleophilic attack and the following deprotonation and, with this, the overall regioselective outcome proved challenging in seminal works by SHARPLESS, who afforded unselective chlorination mixtures.[104–106] Over the last decades, several strategies have been developed to control regioselectivity in this highly potential reaction, which has been successfully applied in the vinylic-,[107–112] allylic-[104,113–121] and difunctionalisation[122–126] of olefins such as halogenations, esterifications, and etherifications. Conventional approaches for the alkene halofunctionalisations primarily utilise *N*-haloimides and -amides as both the terminal oxidants and sources of halogen. These reagents are effective in transforming diaryldiselanes into the corresponding arylselenyl halides (Scheme 1.16, structure **63**, X = halide, black sphere = aryl). The halide anion functions as an endogenous nucleophile, aiding the conversion of the seleniranium intermediate **61** into adduct **64** (Nu = X^-). Meanwhile, the imide or amide counterion Y serves as an inherent base, which, upon the reaction of intermediate **64** with the halogenating agent, triggers the dehydrodeselenenylation of intermediate **65**. Consequently, this series of reactions produces allylic **66** and vinylic **67** halides.[100] Compared to previous transition metal-catalysed allylic aminations, selenium does not undergo reversible β-hydride elimination and, consequently, product isomerisation. As a result, selenium-π-acids **63** were recently introduced as mechanistically complementary catalysts for aza-WACKER reactions (Scheme 1.16, Nu = Nitrogen-source) in a range of selective inter- and intramolecular allylic and vinylic alkene aminations, some of which were partially not suitable for Pd or Cu catalysis.[100,107,110,112,120,127–132]

The Se-π-acid catalysed allylic functionalisation with N-nucleophiles was first reported by BREDER and coworkers in 2013 with the intermolecular coupling of unactivated alkenes **69** (Scheme 1.17). Key to the successful transformation was the determination of *N*-fluorobenzenesulfonimide (NFSI) as the suitable oxidant, functioning as both the terminal oxidant and the endogenous nucleophile, a nucleophilic species derived from the oxidant or chalcogen electrophile.[129] The design of a selenium-π-acid catalysed allylic amination was based on a mechanistic approach to alter the reactivity profile of *N*-heteroatomic imides. In this setup, the nitrogen group functions as the endogenous nucleophile (Scheme 1.16, $X^-/Nu = NR_2$), while the N-heteroatomic group (Y) acts as the intrinsic base. Following this design framework, BREDER and coworkers discovered that NFSI met all the necessary mechanistic requirements.[100]

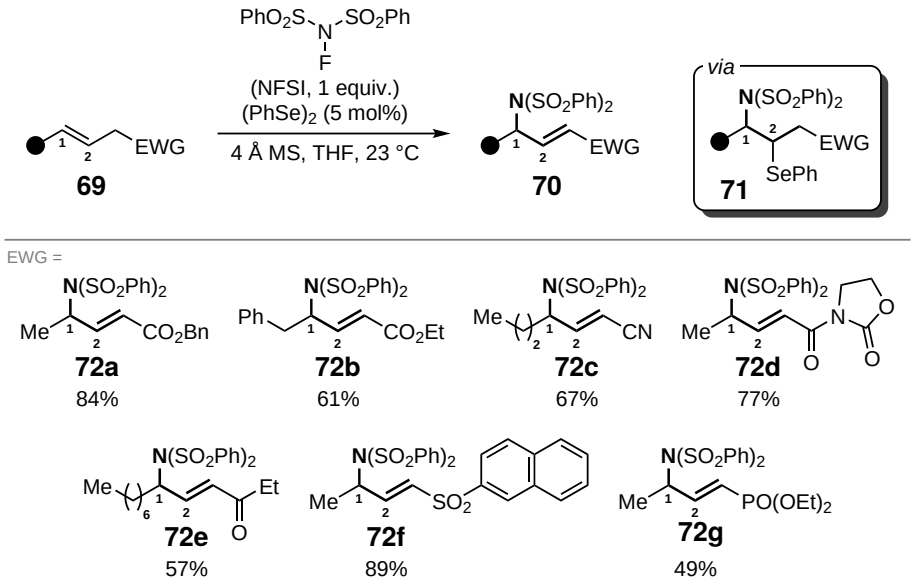

Scheme 1.17: Se-π-acid catalysed allylic amination of alkenes **69** to allylic amines **70** reported by BREDER and co workers.[129] Isolated yields given. NFSI = *N*-fluorobenzenesulfonimide, EWG = electron withdrawing group.

The strategic implementation of electron-withdrawing groups (EWG) enhances the acidity of adjacent protons and, with this, facilitates their deprotonation accompanied by the driving force of the formation of a conjugated system with the EWG in the product.[104] This virtue enables the transformation of 1,2-disubstituted alkenes, which were previously hardly convertible with metal-catalysed methods, while demonstrating excellent tolerance for a range of functional groups, including esters, nitriles, imides, ketones, sulfones, and phosphonates, and showing remarkable selectivity for the allylic C-N bond motif (Scheme 1.17).[100]

A similar strategy to control regioselectivity *via* neighboring group effect was developed later by WANG in 2022 and coworkers by the employment of olefins with an *N*-methyliminodiacetic acid (MIDA) boronate substituent **73**, which was known to exploit a directing effect in metal-catalysed functionalisation of alkenes (Scheme 1.18).[104] As the key to the regioselective control, they name

the neighboring stabilisation of adjacent negative charges by the boron-moiety through accepting electron density, facilitating deprotonation in the α-position and directing the regioselective formation of the respective α,β-unsaturated boronates **70**.

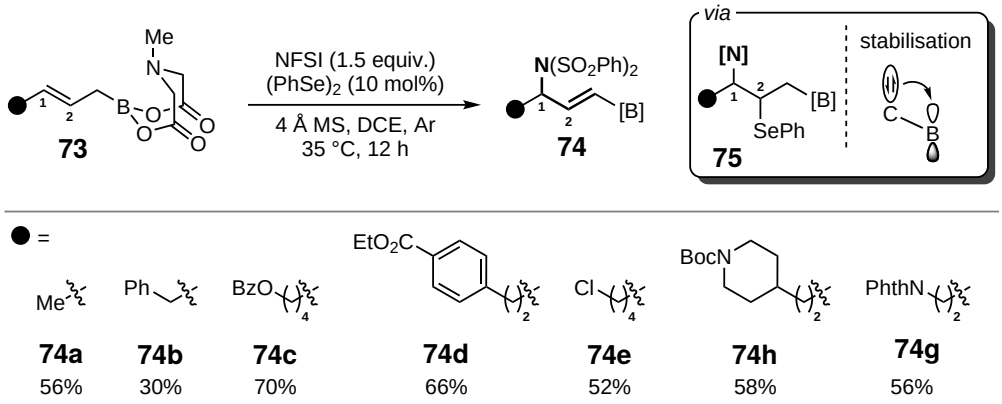

Scheme 1.18: Se-π-acid catalysed allylic amination of alkenes **73** to allylic amines **74** reported by WANG and co workers.[104] Isolated yields given. NFSI = *N*-fluorobenzenesulfonimide, Boc = *tert*-butyloxycarbonyl, NPhth = phtalimide.

Both intermolecular methods resulted in the creation of a diverse range of multifunctional building blocks with remarkable regioselectivity, while maintaining the olefin (and boron) functionalities as essential tools for additional chemical modifications.[104,129] Despite these successes, the ability to employ exogenous nucleophiles not derived from the oxidant or selenium electrophile was still desired. This was met first by independent reports of BREDER[107] and ZHAO[109] in 2015, who developed an intramolecular vinylic amination towards indoles. Here, the intramolecular nucleophile could outcompete the endogenous nucleophile derived from oxidant NFSI, now serving only as the terminal oxidant.

In a further development, ZHAO and coworkers were able to substitute NFSI as the terminal oxidant in an intramolecular transformation towards five-, six- and seven-membered *N*-heterocycles, firstly accessing allylic amines with exogenous nucleophiles (Equation 1.6).[120] Common oxidants used in selenium-catalysed alkene reactions, like $PhI(OAc)_2$, $PhI(OCOCF_3)_2$, and $(NH_4)_2S_2O_8$, did not work at all in the related intramolecular allylic cycloetherification. However, *N*-fluorinated oxidants were effective for both cycloetherification and the related allylic amination reactions. The best results came from using *N*-fluoropyridinium triflate (FP-OTf) as the oxidant, a well-compatiable agent in selenium catalysed transformations as shown by DENMARK and coworkers in their work on dichlorinations.[122]

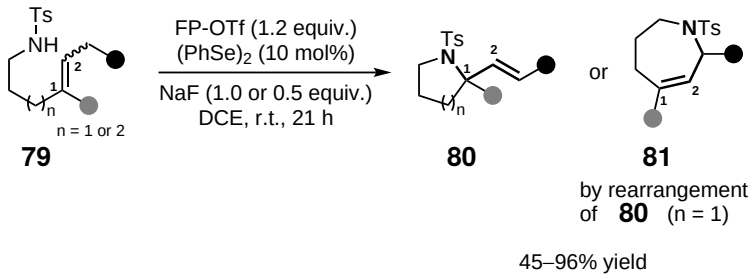

(1.6)

The mechanism is proposed to proceed analogous to the generalised scheme discussed above (Scheme 1.16).[100] Oxidative activation of $(PhSe)_2$ forms π-acidic species **82**, which enables the building of seleniraniumion **83** with olefinic sulfonamide **79** (Scheme 1.19). The subsequent intramolecular nucleophilic attack follows MARKOVNIKOV-selectivity, complementary to the photocatalytic variant, affording intermediate **84** with high regioselectivity. The second oxidation by Pf-OTf enables the release of the desired product **80** and brings back **82** into the catalytic cycle. Using base NaF as an absorbent of the formed HF drives the reaction to high yields. Due to the free rotation of intermediate **84**, the application of *E*/*Z* mixtures **79** selectively affords *E*-products. Five and six-membered exocyclic products **80** are formed in excellent regioselectivity in this formal 5- and 6-exo-trig cyclisation reaction. Seven-membered endocyclic azepine derivatives **81** resulted from subsequent rearrangement of the respective five-membered heterocycles **80** (n = 1) when using 0.5 equiv. instead of 1.0 equiv. of NaF, facilitated by HF remaining in this case.

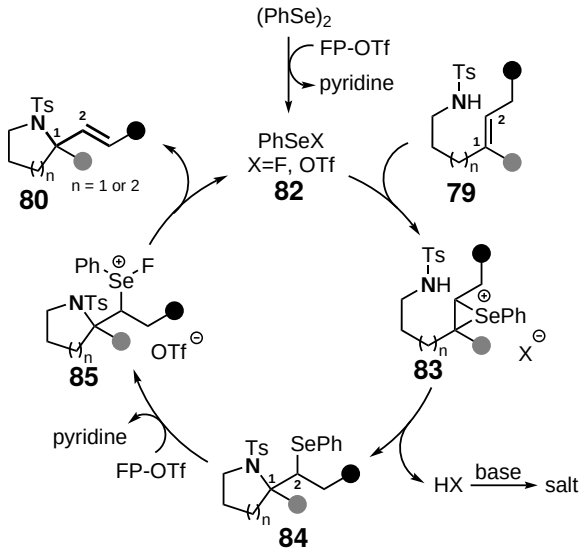

Scheme 1.19: Proposed mechanism of the selenium-π-acid catalysed intramolecular allylic amination of olefinic sulfonamides **79** reported by ZHAO and coworkers.[120]

Remarkably, the transformation of a 1,2-disubstituted alkene without a directing group was reported,

affording six-membered **80** (n = 2) without detecting the corresponding seven-membered isomer. This high regioselectivity probably results from a preferential 6-exo-tet reaction forming six-membered *exo*-product **80** over a 7-endo-tet reaction forming the seven-membered *endo*-isomer **81** according to BALDWIN's rules (Scheme 1.20).[133–135] This marks the ring-forming process as the regioselective driving force.

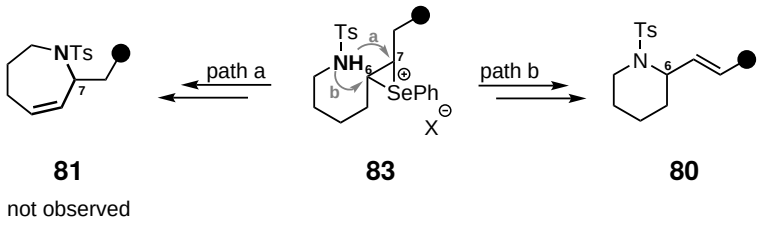

Scheme 1.20: Regioselectivity in the cyclisation reaction of **83**.

The previous reports laid the basis for an unprecedented selenium-π-acid promoted construction of allylic bridged *N*-heterocycles, which are prevalent in nature but generally challenging to synthesise due to their ring strain.[136] YAO, LIN, and coworkers reported the synthesis of bicyclic 2-azabicyclo[2.2.1]heptenes **77** from cyclopentenes **76** in 58–96% yields, facilitated by 1.2 equiv. NFSI as the terminal oxidant and 1.0 equiv. $NaHCO_3$ as the BRØNSTED-base additive (Equation 1.7). Larger ring sizes, such as cyclohexenes and cycloheptenes, were also successfully transformed in this protocol.

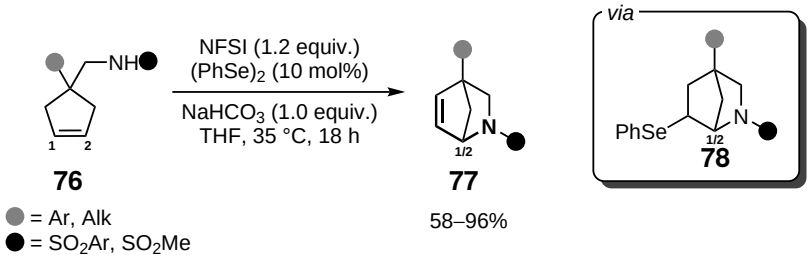

(1.7)

As shown, selenium in the form of a π-acid exhibits high potential towards the inter- and intramolecular allylic and vinylic functionalisation of alkenes as it is extremely carbophilic towards the C-C double bond and does not interact with other additives such as bases and LEWIS-acids. Notable aspects of these syntheses include excellent regiocontrol, typically mild reaction conditions, ease of operation in selenium-catalysed alkene oxidations, and an impressive tolerance for various functional groups.[100] The reported examples of the Se-π-acid catalysis so far were able to readily transform internal alkenes, which were previously challenging to access with traditional Pd-catalysis due to steric hindrance leading to insufficient catalyst coordination and isomerisation issues. In addition, first attempts showed great results in the challenging functionalisation of 1,2-disubstituted alkenes, even though the olefinic carbons are hard to distinguish from one

another. For this, a remote directing group or a preferential cyclisation process enabled for a high regioselective control. In summary, several strategies were developed to control the regioselective outcome of the selenium-π-acid catalysed allylic amination of internal olefins. Many methods that use intermolecular reactions rely on the terminal oxidant to perform two main tasks: accepting electrons indirectly derived from the alkene and providing the nucleophile that will be added to the carbon structure of the olefin. Because of this, in order to expand the scope to incorporate external nucleophiles, finding suitable oxidants that do not form strong endogenous nucleophiles is crucial.[100]

1.2 Photoredox Se-π Acid Dual Catalysis

Resulting from their ongoing investigations and interest in the functionalisation of alkenes, BREDER and coworkers identified a photocatalyst/O_2 from air oxidation system to be able to perform selenium-π-acid catalysed allylic introductions of exogenous nucleophiles under mild reaction conditions and high functional group tolerance. The developed concept relayed on seminal reports by PANDEY and coworkers, who disclosed the ability of photocatalyst 1,4-dicyanonaphthalene (DCN) to mediate the oxidative cleavage of diphenyl diselenide (Se-Se).[137–139] In the following years, further photocatalyst were reported for the successful cleavage of the Se-Se bond,[130,140–144] and even sole irradiation by 455 nm blue light[145] was reported to promote the cleavage. In these reports, the so-formed active cationic Se-species could then add to alkenes, forming the desired selenofunctionalisation products with exogenous nucleophiles. In a separate approach, the successful photoinduced cleavage of selenides (C-Se) was reported in the 1990s by PANDEY and coworkers[146–149] and led to substitution products. The high potential of an elimination mechanism after photoinduced cleavage of the C-Se bond towards functionalised alkenes still remained open. Based on these results, BREDER and coworkers argued that a cooperative system consisting of a photocatalyst with a redox potential higher than that of a diaryldiselenide and a potential selenofunctionalised intermediate might be able to facilitate selenium-π-acid mediated allylic functionalisation of alkenes.[150] Following intensive investigations, it was proposed that a cooperative dual catalytic mechanism performs allylic functionalisation with oxygen from the air as the cheap terminal oxidant and photocatalyst 2,4,6-tris(4-methoxyphenyl)pyrylium tetrafluoroborate **86** as the mild oxidant to catalytically cleave the Se-Se and Se-C bond. Extensive mechanistic investigations were performed to propose the following underlying photoredox/Se-π-acid dual catalytic mechanism in the intramolecular allylic lactonisation (Scheme 1.21).[128,151] During their investigations, they found that the redox potential of the excited state of **86** (E^* = +1.74 V vs. SCE in MeCN)[150,152,153] is sufficiently high and suitable to oxidise $(PhSe)_2$ (E = +1.35 V vs. SCE in MeCN)[128,154] and the formed selenofunctionalised intermediate (e.g. lactonisation: E = +1.55 V vs. SCE[128]) without the oxidation of the present olefin or nucleophile, enabling the selenium-π-acid catalysed allylic and vinylic functionalisation of alkenes.

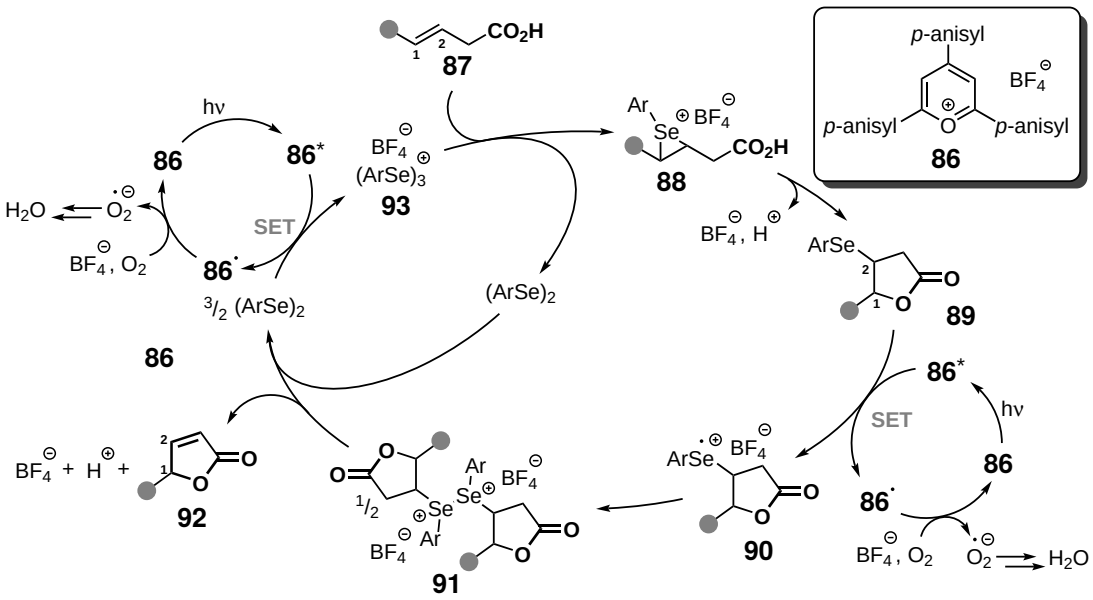

Scheme 1.21: Mechanistic proposal of the intramolecular allylic lactonisation *via* a photoredox/Se-π-acid dual catalytic system.[151]

An arylselenide species $(PhSe)_2$ undergoes a SET event with the excited state photocatalyst **86*** to afford a radical cation, which readily oligomerises to its cationic species **93**. Other arylselenium oligomeric species were detected during chemical and electrochemical analytical investigations, which are proposed to engage in minor reaction pathways and partially lead to the desired product formation. The selenocationic species then reacts with olefin **87** towards selenofunctionalised intermediate **89** *via* intramolecular cyclisation of the previously formed seleniraniumion **88**. The redoxpotential of the applied photocatalyst allows for the second photoinitiated oxidation process (SET), which is followed by a dimerisation of the so-formed radical cation **90** to **91**, which facilitates the release of the desired product **92** and the reformation of arylselenium, closing the catalytic cycle. The reduced photocatalyst **86**$^{\cdot}$ is oxidised by O_2, affording pyrylium ion **86** to reenter the catalytic regime and superoxide $O_2{}^{-}$, which transforms to H_2O as the final byproduct.[151]
The milder oxidative conditions finally enable the application of various exogenous nucleophiles and the method has successfully been applied to the allylic functionalisation of alkenes, including inter-[150] and intramolecular esterification,[151] inter- and intramolecular etherification,[155] phosphatation,[156] and the synthesis of cyclic carbonates[157] (Scheme 1.22). These reactions show remarkable functional group tolerance due to the high carbophilicity of the selenium (cf. Subsection 1.1.2),[100,101] allowing for the supportive usage of additives such as Lewis-acids and/or Brønsted-bases.[155–157] Besides the successful transformation of terminal and symmetric internal alkenes, asymmetrically 1,2-disubstituted alkenes were readily transformed in high regioselectivity, which has been proven hard to accomplish with established methods. The high carbophilicity of the selenium-π-acid enables a high transformation of internal alkenes compared to the Pd-variants. The regioselectivity in the reported examples is driven by the preferential formation of a heterocy-

cle or remote EWG leading to an acidic bias of the adjacent protons for preferential elimination towards a conjugated π-system. Because of the high affinity of the selenium-π-acid due to the above-mentioned orbital interaction (cf. Subsection 1.1.2) that is not possible with other LEWIS-basic groups such as carbonyls, amines, halogens, and alcohol, the method is especially exceptionally of functional groups (Scheme 1.22).

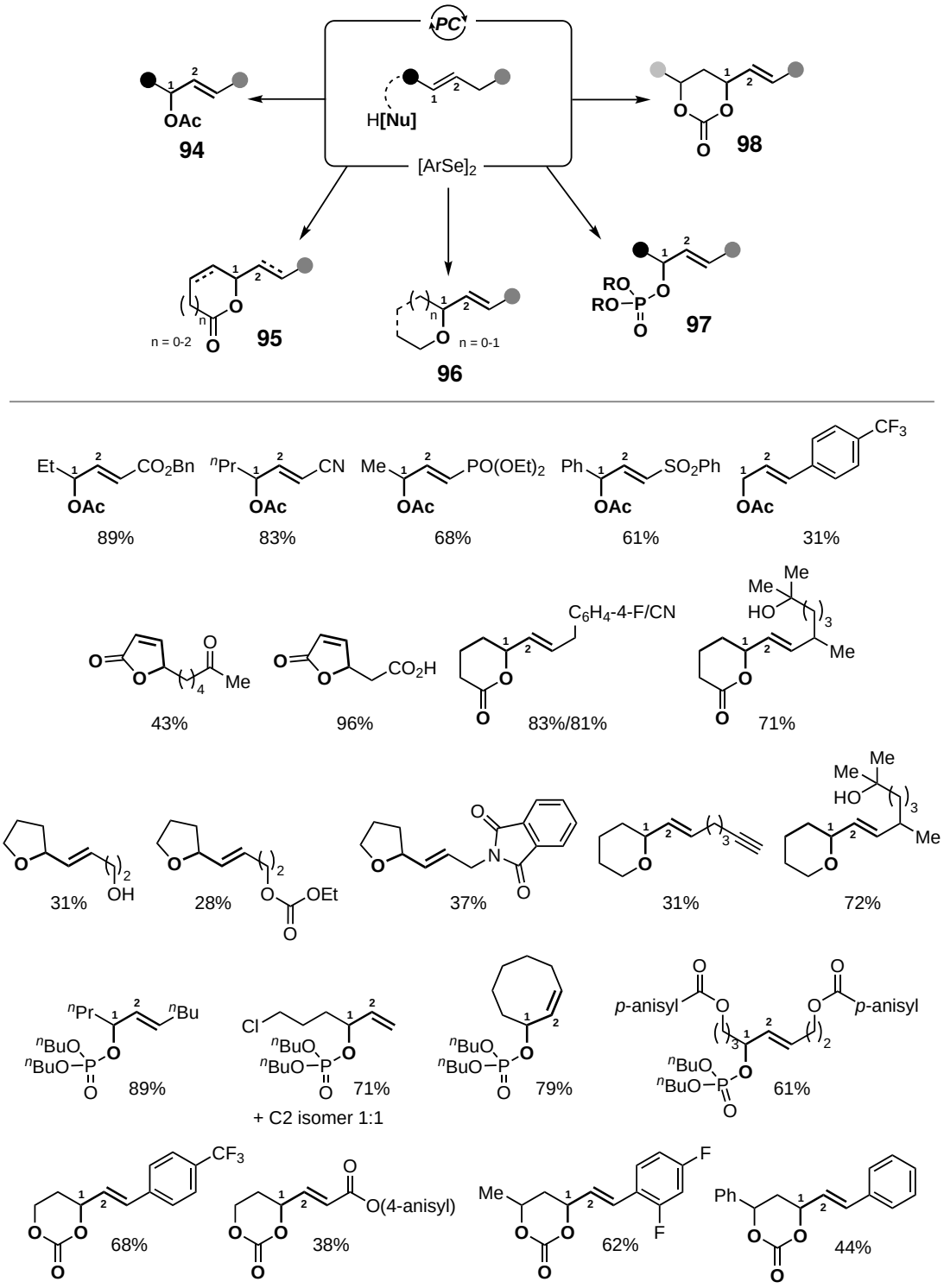

Scheme 1.22: Product scope of the photoredox/Se-π-acid dual catalytic allylic functionalisation reported by Breder.[150,151,155–157] Isolated yields given. PC = photocatalyst, Nu = nucleophile.

In 2023, Liu and coworkers applied a photocatalyst–selenium-π-acid dual catalytic system to transform alkynes **100** (Scheme 1.23).[144] Enabled by MesAcrMeBF$_4$ **102** (E^*_{red} > +2.0 V vs. SCE

in MeCN)[158–160] and $(PhSe)_2$, *N*-propargylamines **101** were readily formed through a proposed selenofunctionalisation–elimination process, enabled by oxygen-incorporation from in-situ formed singlet-oxygen ($^1O_2$) by quenching of the triplet state photocatalyst by triplet oxygen.

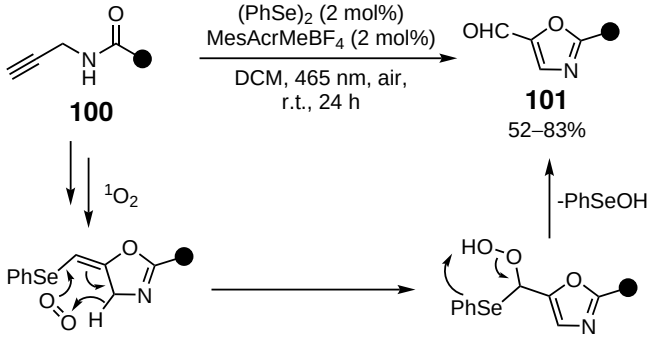

Scheme 1.23: Synthesis of *N*-propargylamines **101** reported by Liu and coworkers.[144]

The reported methods show the high applicability of the photoredox–selenium π-acid dual catalytic system for the oxidative incorporation of oxygen-nucleophiles into alkenes and alkynes. While these are undoubtedly valuable transformations, expanding the scope to N-nucleophiles to form allylic amines would be highly desirable and useful for the broad synthetic community. Such a method would represent a new, complementary transformation towards allylic amines possibly overcoming the regioselectivity issues known for traditional catalytic systems, as described before, by utilising the inherent regioselective control of Se-π-acid catalysis in the intermolecular allylic amination of alkenes with exogenous nucleophiles.

Overall, several methods for the regioselective oxidative allylic amination of alkenes have been developed. Hereby, intermolecular variants have been shown to be more challenging, e.g., due to lower regioselective control and/or competing reactions, and are less reported than intramolecular transformations. Traditional Pd-catalysed methods mainly cover terminal alkenes and non-basic amines. 1,2-disubstituted alkenes could be transformed by Se-πacid catalysis, but a suitable oxidative system for the intermolecular amination with external nucleophiles, not derived from the oxidant or catalyst, is still to be developed. Photocatalysts proved to be enabling oxidants in the Se-π-acid catalysed allylic functionalisation and will be investigated towards amines in the course of this thesis.

2 Objectives

The focus during this thesis was laid on the development of highly regioselective controlled inter- and intramolecular allylic amination reactions. As disclosed in Chapter 1 the oxidative allylic amination proved to be a valuable tool for the transformation of alkenes with amines with a high atom economy being one of the advantages. Even though several synthetic methods were developed, with metal-based protocols being the most prominent, they are often in need of specific substrates or suffer from isomerisation resulting in a reduced regioselective outcome.[52,57–59,61–64] As a metal-free example, selenium-π-acid catalysis showed high ability to control regioselectivity in allylic functionalisations and nitrogen nucleophiles were readily introduced into the allylic position, albeit the reported intermolecular protocols are still limited to the usage of endogenous nucleophiles, such as *N*-fluorobenzenesulfonimide (NFSI), which acts both as the oxidant and the nucleophile.[100,107,110,112,120,128–132] In this context, it is argued that the selenium/photoredox dual catalytic system developed by Breder and coworkers offers a highly promising system for the regioselective intra- and intermolecular allylic amination including exogenous nucleophiles.
Reports by Breder et al., following the selenium/photoredox dual catalytic functionalisation of alkenes, included oxygen nucleophiles such as carbonic acids,[150,151] alcohols,[155] phosphates[156] and carbonates.[157] As a result, it was discussed whether nitrogen compounds could also function as nucleophiles in this dual catalytic method and with this could finally include exogenous N-nucleophiles that are not derived from the oxidant in the selenium-π-acid transformation. Both intra- and intermolecular transformations were to be investigatiedin in this work with a diarlydiselenide $(ArSe)_2$ in combination with a suitable photocatalyst (PC) and in some cases a beneficial additive (Equation 2.1).

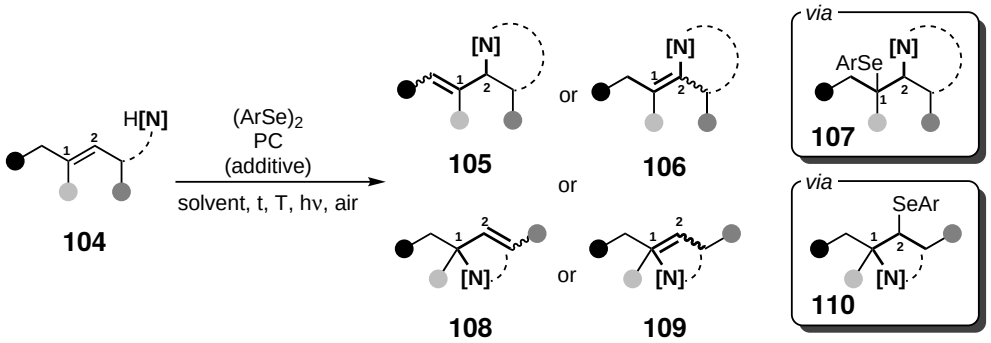

(2.1)

The regioselective outcome of the transformation is to be investigated. Several regioisomers are

possible to form: The ring formation may occur, affording an internal (**108** and **109**) or external double bond (**105** and **106**). Previous reports on the selenium-π-acid allylic amination showed that the ring formation follows BALDWIN's rules.[120,133–135] Further, the synthesis may lead to MARKOVNIKOV products **108** and **109** or *anti*-MARKOVNIKOV products **105** and **106**, which is to investigated for the selenium/photoredox dual catalytic system. Elimination in the final step may afford the vinylic regioisomers **106** and **109** in competition with the respective allylic isomer, which was observed for cyclic substrates in the intermolecular se-π-acid catalysed amniation with NFSI.[129] Also, the *E* or *Z* product may be formed due to a fully sp^3 hybridised intermediate (**107** and **110**). Previous similar reports predominantly reported the *E*-isomer to be the only isolated product, even when a *Z*-configured alkene was employed as the substrate.[150,151,155–157]
Eventually, the development of an enantioselective variant by employing a chiral selenium catalyst or a photocatalyst with a chiral counter anion shall be investigated both for the intra- and intermolecular variant.

3 Results And Discussion

3.1 Intramolecular Allylic Amination with Sulfonamides

Parts of the following investigatory results were published in 2024 in *ChemSusChem* (e202301518).[127]

The successful application of the developed Se-π-acid/photoredox dual catalytic system towards the allylic functionalisation of olefins for the build-up of new C-O bonds with a variety of nucleophiles[150,151,155,156] led to speculations whether N-nucleophiles could serve under these reaction conditions as well as the approved O-nucleophiles, and whether a regioselective outcome can be achieved.

During his experimental work in the Breder group, Dr. S. Graf investigated suitable reaction conditions for the intramolecular Se-π-acid/photoredox dual catalytic allylic amination of olefinic tosylamides **111** (Equation 3.1). Optimisation screening identified 5 mol% of photocatalyst (PC) 2,4,6-tris(4-methoxyphenyl)pyrylium tetrafluoroborate (**86**) and 10 mol% of diselenide $(PhSe)_2$ as the most productive catalyst loading.[127] 10 mol% of $(4\text{-ClPhS})_2$ co-catalyst was added to some substrates. The exact role played by the disulfide in the reaction will be discussed in a later section.

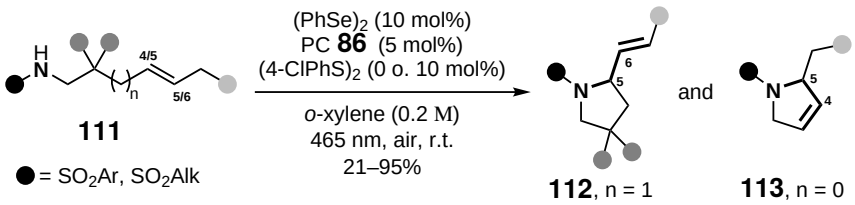

(3.1)

Variation in solvent, ranging from nonpolar to polar, showed that more polar solvents consistently led to lower product yields, with DMSO and MeCN as the reaction media without any product formation. This observation is in stark contrast to previous investigations in the Breder group.[150,151,155] As **86** exhibits low solubility in nonpolar solvents, resulting in a very low concentration of the excited state photoredox catalyst present under reaction conditions, this previously led to significantly diminished product yields in less polar solvents compared to solvents with a higher polarity. In contrast, *o*-xylene (0.1 M) gave the best reaction outcome in the present transformation. The application of basic additives such as Na_2HPO_4 and KF, which positively influenced previously reported similar transformations,[155,156] did not show an increase in product yield in

this intramolecular allylic amination, which could result from a low solubility in the used solvent. The subsequent control experiments highlighted the required presence of both catalysts, air, and irradiation at 465 nm for a successful product formation.
Under these reaction conditions, the transformation exhibited substrate-specific regioselectivity with the formation of five-membered heterocycles (**112**, **113**) (Equation 3.1). The formal 5-*exo*-trig products (**112**) were formed from 5,6-unsaturated tosylamides (n = 1), and the cyclisation of 4,5-unsaturated tosylamides (n = 0) afforded formal 5-*endo*-trig products 3-pyrrolines (**113**). Notably, according to rules established by BALDWIN,[133,161] 5-*endo*-trig reactions are disfavoured compared to the competing 4-*exo*-trig pathways, which would afford 4-membered heterocycles with an exogenous double bond. The application of selenium-π-acid catalysis enables the hybridisation change of the former sp^2-olefin to an sp^3 hybridised seleniranium ion. The following intramolecular nucleophilic attack in δ-position actually follows a favourable 5-*exo*-tet pathway, comparable to an epoxide-opening, leading to the formal 5-*endo*-trig product after subsequent reformation of the double bond.[135] This offers an unprecedented pathway towards the formation of 3-pyrrolines from olefinic sulfonamides. The applicability of the developed method with high functional group tolerance was demonstrated on various olefinic sulfonamides with isolated yields of up to 95% and an average yield of 50% (median = 55%) and 60% (median = 55%) for **112** and **113**, respectively.

3.1.1 Susbtrate Synthesis

The scope of the intramolecular allylic amination with olefinic sulfonamides was further investigated in relation to the formation of piperidines and azepanes. For this, the corresponding olefinic sulfonamides were synthesised.
In earlier studies, the WITTIG reaction proved to be an attractive pathway for the fast and easy build-up of a variety of internal olefins[151,155] and was therefore proposed in the course of this study for the construction of 6,7-unsaturated sulfonamides **120**. In order to obtain WITTIG-salt **117**, 5-aminopentan-1-ol **114** was brominated *via* nucleophilic substitution (S_N2) under acidic conditions by addition into aq. HBr (Scheme 3.1, a).[162] The so-formed substitution product **115** was then tosylated by deprotonation with NEt_3 and the addition of 1 equiv. of TsCl, affording **116** in 58% yield over two steps. During the second step, adding sufficient quantities of NEt_3 was crucial, as it was neutralised by residual amounts of HBr. Finally, subsequent substitution with PPh_3 afforded WITTIG-salt **117** in 68% yield, accumulating an overall yield of 39% over three steps.
In order to raise the step economy of the WITTIG salt formation, an alternative pathway was proposed. Referring to reports on the formation of WITTIG salts with a tosylate counterion[163,164] instead of a bromide, a two-step route was conducted. 5-aminopentan-1-ol was directly tosylated with 2 equiv. of TsCl, protecting both the amine and alcohol moieties, which afforded **118** in 66% yield. The unchanged procedure for the substitution with PPh_3 led to the desired product **119** in 59% yield. In summary, this two-step pathway resulted in the same overall yield from **114** to

WITTIG-salt **119** of 39%, as the three-step synthesis to **117**, but in one step less and under avoidance of the time-consuming removal of excess HBr after the bromination reaction.

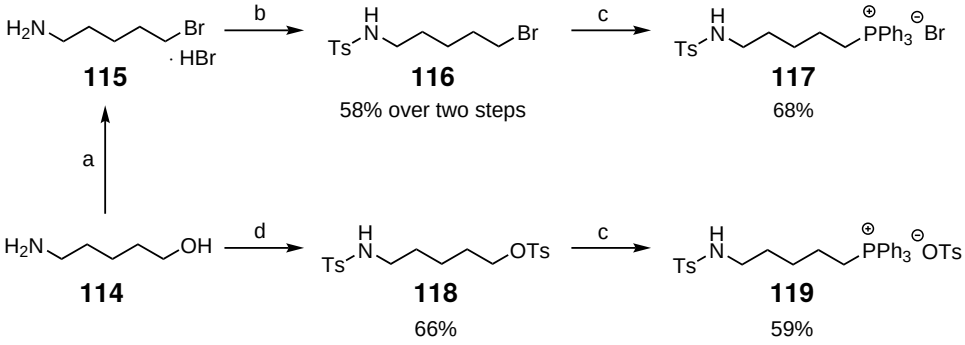

Scheme 3.1: Synthetic pathway towards the construction of wittig salts **117** and **119** from **114**. Reaction conditions: a) HBr (aq.), reflux, 3h. b) NEt_3, TsCl (1 equiv.), DCM, 0 °C to r.t., 19 h. c) PPh_3, MeCN, reflux. d) NEt_3, TsCl (2 equiv.), DCM, 0 °C to r.t., 47 h.

With the suitable WITTIG-salts in hand, the following WITTIG reactions afforded the desired olefinic tosylamides **120** by addition of the respective aldehyde **121** to WITTIG salt **117** or **119** in dry THF with KO^{t}Bu as the base (Table 3.1).

Table 3.1: WITTIG Reaction Towards the Synthesis of Olefinic Tosylamides **120**.[127]

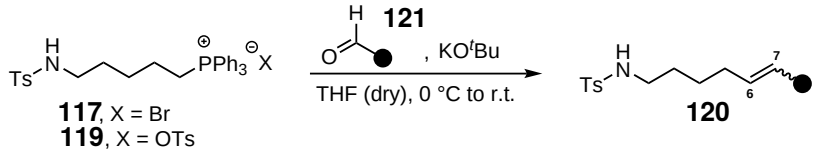

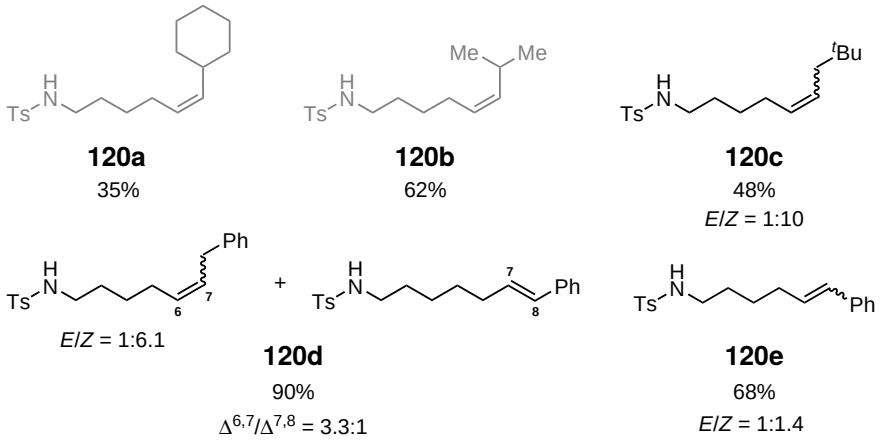

Reaction conditions: **117** or **119** (2.0 equiv.), aldehyde **121** (2.00–5.00 mmol, 1.0 equiv.), KO^{t}Bu (4.0 equiv.), stirred until full conversion was confirmed *via* TLC. Grayed Substrates were Synthesised by Dr. S. GRAF.

Branched products **120a** and **120b** were synthesised by Dr. S. GRAF and isolated in their *Z*-configuration, the expected major isomer resulting from an unstabilised ylide intermediate.[19] This stereoselectivity is also confirmed with bulky *tert*-butyl substituent in compound **120c**, which was afforded with an *E*/*Z* ratio of 1:10. NMR analysis shows two singlet signals below 1 ppm for the *tert*-butyl moiety, indicating the presence of two stereoisomers. Due to signal overlap, a coupling constant could not be distinguished for either compound. Regarding previous results and the reaction mechanism proceeding *via* an unstabilised ylide, the *Z*-isomer is proposed to be the primary compound present in the product mixture. When employing 2-phenylacetaldehyde (**121d**), two constitutional isomers were formed. The desired 6,7-unsaturated sulfonamide was built as the major isomer with an *E*/*Z* ratio of 1:6.1, which could be distinguished by ^{1}H- and NOESY NMR analysis (Figure 3.1). Here, signal proton **a** would only show a coupling with proton **b** in the *Z*-configured product, which is the case for the signal with higher intensity. Additionally, a significant amount of the conjugated styrylic isomer was formed in pure *E*-configuration, which could be formed in situ by double bond isomerisation.

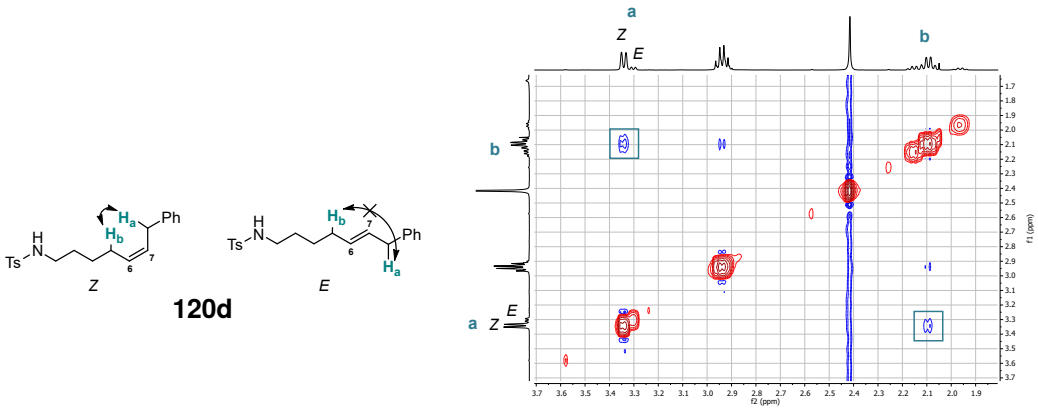

Figure 3.1: NOESY-Coupling expected for product **120d** and NOESY NMR experiment of **120d**.

Finally, the desired styrylic sulfonamide **120e** was also readily formed during the reaction conditions with benzaldehyde. Here, the *E*/*Z* ratio was more balanced than in the previous substrates.

3.1.2 Cyclisation Reactions

The olefinic sulfonamides **120** were then subjected to the Se-π-acid/photoredox dual catalytic conditions previously optimised by Dr. S. GRAF, which successfully afforded piperidines **122** (Table 3.2).

Table 3.2: Substrate Scope of the Se-π-acid/Photoredox Dual Catalytic Intramolecular Allylic Amination of Olefinic Tosylamides **120** towards Piperidines **122** conducted by Dr. S. GRAF.[127]

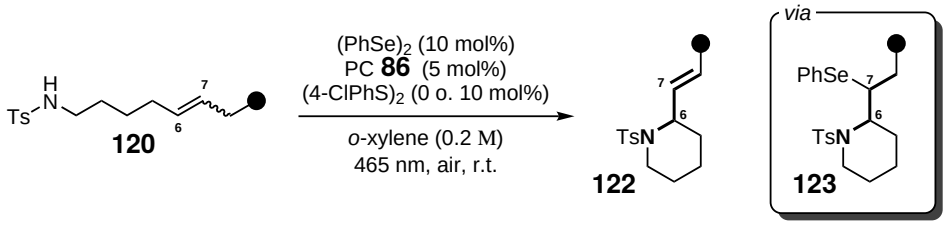

122a	**122b**	**122c**	**122d**	**122f**
46% (38%)[a]	79% (42%)[a,b,c]	58% (48%)[a]	17% (13%)[a,b,d]	79% (64%)
	$\Delta^{6,7}/\Delta^{7,8}$=1:1.8		*E*/*Z* = 15:1	

Reactions were performed with 0.5 mmol of **120** for 4–96 h. [a] Addition of (4-ClPhS)$_2$ (10 mol%). [b] Addition of 2-nitrobenzaldehyde (25 mol%). [c] Second addition of (PhSe)$_2$ (10 mol%) after 11 h. [d] **120d** (372 µmol). NMR yields were determined with 1,3,5-trimethoxybenzene (TMB) as the internal standard. Isolated yields in parentheses.

Both predominantly *Z*-configured aliphatic and aromatic olefinic tosylamides afforded the desired products **122** preferentially in the thermodynamically favoured *E*-configuration, made possible by the sp^3 hybridised selenofunctionalised intermediate **123** in the underlying mechanism.[127,151] Notably, the formation of six-membered heterocyclic piperidines (formal 6-*exo*-trig) was always preferred over the competing formation of seven-membered azepanes (formal 7-*endo*-trig). To investigate this tendency further, substrate **120e**, which only offers the possibility of allylic azepane formation and no allylic piperidine formation, was applied to cyclisation conditions by Dr. S. GRAF (Equation 3.2).[165] Interestingly, the formation of allylic azepane **125** was not observed. Instead, a mixture of vinylic azepane **124** and pyrrolidine **112a** could be isolated, which was confirmed *via* NMR and MS analysis.

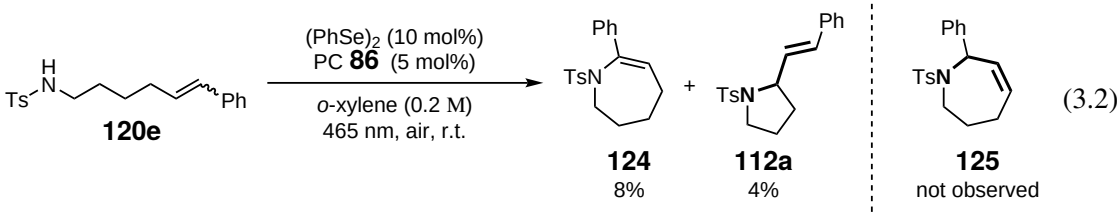

(3.2)

The mechanistic proposal was disclosed by Dr. S. GRAF, who argued that both observed products are formed *via* seleniranium intermediate **126** (Scheme 3.2).[165] 7-*Endo*-tet cyclisation[133–135] followed by oxidation (Scheme 3.2, path **A**) enables the elimination of the selenoaryl species preferentially with the benzylic proton (see **127**), leading to the formation of vinylic azepane **124**. **112a** was proposed to be obtained by a 5-*exo*-trig cyclisation of a previously formed allylselane **128**, undergoing an S_N2'-reaction (Scheme 3.2, path **B**). The latter reaction pathway was already discussed by the BREDER group in previous similar investigations.[165,166]

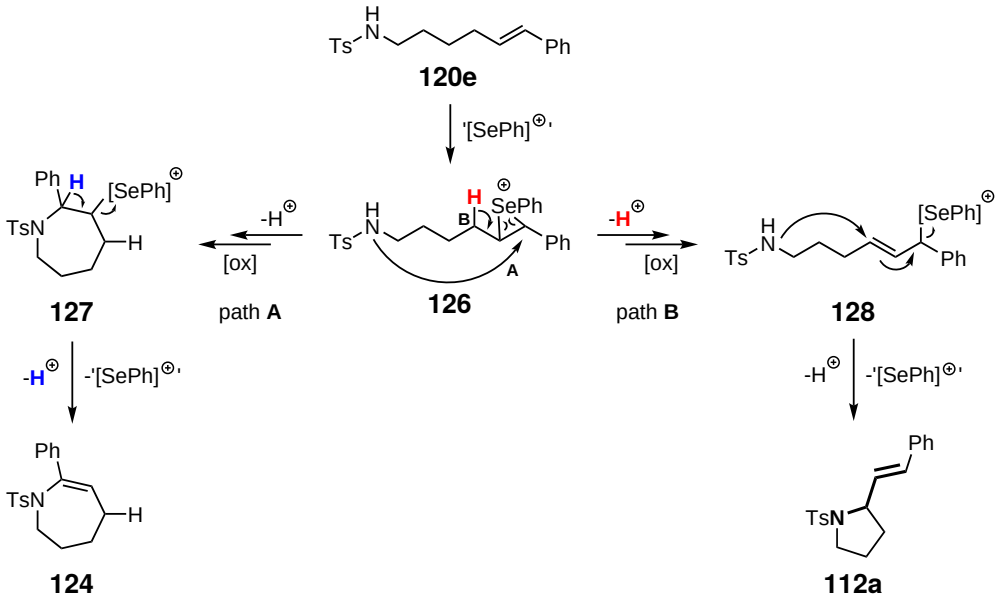

Scheme 3.2: Mechanistic proposal for the formation of **124** and **112a** from **120e**.[165]

3.1.3 Mechanistic Investigation

During the photoaerobic selenium-π-acid catalysed intramolecular amination, various substrates showed a significant increase in product yield when co-catalyst $(4\text{-ClPhS})_2$ was added to the reaction mixture. In the following section, the role of disulfide $(4\text{-ClPhS})_2$ in the reaction mechanism is investigated.

To elucidate the underlying mechanism, quenching experiments of photocatalyst **86** were conducted (Figure 3.2). The quenching properties of catalysts $(PhSe)_2$ and $(4\text{-ClPhS})_2$, and intermediate **129a** were investigated in a STERN-VOLMER Analysis. For this, the emission of **86** (I) combined with varying concentrations of the respective quencher (c_q) was measured. Including the resulting values I and the value for the emission of sole **86** (I_0) into the STERN-VOLMER-equation (Equation 3.3) afforded STERN-VOLMER-constants K_{SV} of the quenchers. These were obtained from the slopes of plotting $\frac{I_0}{I} - 1$ against c_q and are detailed in Table 3.3. For the experimental procedure, see Subsection 5.4.2.

$$\frac{I_0}{I} - 1 = K_{SV} \cdot c_q \tag{3.3}$$

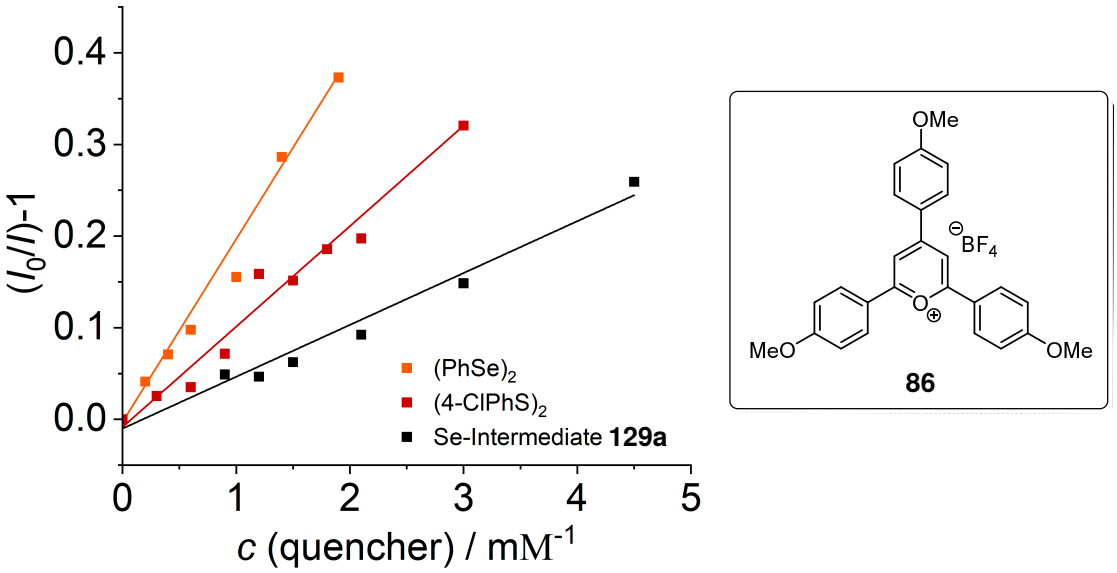

Figure 3.2: STERN-VOLMER quenching of photocatalyst **86** with quenchers $(PhSe)_2$, $4\text{-}ClPhS)_2$ and **129a**.

The results show that out of the three tested quenchers, $(PhSe)_2$ exhibits the highest quenching ability of the excited state photocatalyst **86** with K_{SV} = 200±26.5 M^{-1}. $(4\text{-}ClPhS)_2$ and **129a** both showed lower quenching ability with K_{SV} = 110±23.1 M^{-1} and K_{SV} = 56.6±17.1 M^{-1}, respectively (Table 3.3).

Table 3.3: STERN-VOLMER Constants K_{SV} for **86**/Quencher Combinations.

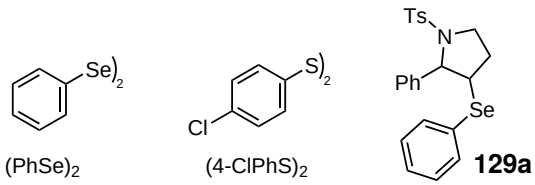

	$(PhSe)_2$	$(4\text{-}ClPhS)_2$	**129a**
K_{SV}	200±26.5 M^{-1}	110±23.1 M^{-1}	56.6±17.1 M^{-1}

The outcome suggests that when the three compounds are present in the reaction mixture with **86**, $(PhSe)_2$ will get oxidised first by the excited state photocatalyst. This results in a delay in the product-forming process, as **129a** will only be able to get oxidised and initiate the final release of the desired

product when a sufficiently low concentration of $(PhSe)_2$ is reached. This observation confirms previous reports on the inhibitory effect of $(PhSe)_2$ in the photoredox/Se-π-acid dual-catalytic lactonisation.[151] Theoretically, $(4\text{-ClPhS})_2$ might also show inhibition of product formation, as it exhibits a higher ability to quench the photocatalyst than **129a**. But experimental investigations showed a significant increase in product yield and reaction rate when 10 mol% of $(4\text{-ClPhS})_2$ was added, marking its influence to be worth investigating further.

Electrochemical investigations performed by H. Pesch revealed that $(4\text{-ClPhS})_2$ possesses a higher redox potential (E = 1.64 V vs. SCE in MeCN) than intermediate **129a** (E = 1.51 V vs. SCE in MeCN), which stands in reversed correlation to the quenching results and hints at a more complex role of $(4\text{-ClPhS})_2$ under photocatalytic conditions. Initial-rate experiments by Dr. S. Graf were conducted to investigate the influence of $(4\text{-ClPhS})_2$ on the product-forming process. The results support the initial argument that the dehydrodeselenylation is the rate-limiting step and $(4\text{-ClPhS})_2$ enhances its rate.[127,165]

By evaluating further electrochemical and synthetic experiments, it was proposed that the disulfide $(4\text{-ClPhS})_2$ serves as an electron-hole shuttle during the reaction, acting itself as an oxidant upon oxidation by the photoexcited catalyst **86**.[127] A long lifetime of in-situ formed $(4\text{-ClPhS})_2^{\cdot+}$ of 30 s is proposed to be the reason and enables the faster formation of oxidised intermediate **129a**$^{\cdot+}$. Additionally, supportive electrochemical investigations indicated a chemical follow-up reaction between **129a**$^{\cdot+}$ and $(4\text{-ClPhS})_2^{\cdot+}$. The so-formed interchalcogen species is proposed to accelerate the rate-limiting elimination step during the reaction, resulting in a faster product formation and, with this, an increased yield.

In conclusion, both electrochemical and synthetic investigations propose that the sulfur species $(4\text{-ClPhS})_2$ acts in a dual reaction-enhancing role during the Se-π-acid/photoredox intramolecular allylic amination, serving as an electron-hole shuttle and enabling the acceleration of the product-releasing step by interchalcogen formation, thus resulting in substantially improved product yields.[127]

3.1.4 Enantioselective Variant

Parts of the following investigation led to results published in 2024 in *ACS Catalysis*.[167]

To further extend the scope, Dr. T. Lei developed a series of chiral selenium compounds with a spiro-backbone that can act as Se-π-acid catalysts and induce chirality in the photoaerobic allylic esterification of alkenes.[167] Their application in the intramolecular allylic amination by Dr. S. Graf proved successful after optimisation studies, extending the racemic scope to the first enantioselective variant involving amines. In the course of the study, several substrates were screened for optimal conditions, which were synthesised as a part of this dissertation.[165] The substrates were prepared comparably to the methods used for the equivalent racemic investigation. Wittig-salt **130** was prepared from 5-aminopentan-1-ol **114** for six-membered rings according to

the procedure described above (cf. Scheme 3.1).

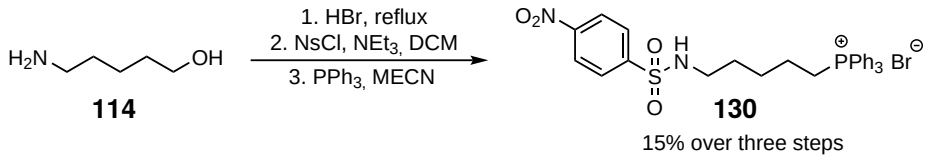

(3.4)

In addition, substrates with varying sulfonamides and vinylic substituents were synthesised from WITTIG-salt **131**.

Table 3.4: Synthesis of Varying Sulfonamides **134** from **131**.

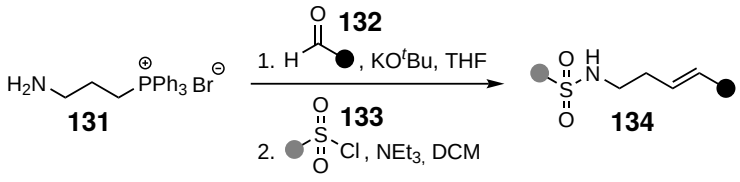

= *p*-nitrobenzene

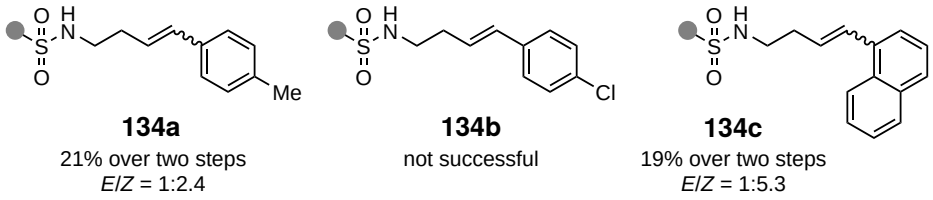

= *2,4,6*-trimethylbenzene

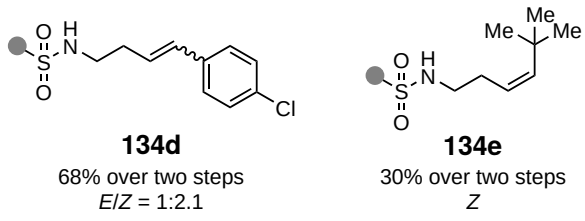

With these results, a first asymmetric variant of the photoredox/Se-π-acid dual catalytic approach towards allylic amines was developed. Asymmetrically substituted lactones and cyclic amines were readily synthesised with optimised reaction conditions, affording the desired products in good yields and enantioselectivity.[127,165]

In further studies, the expansion of this method towards an intermolecular variant was undertaken, accessing compounds with great pharmaceutical value, which is reported in the next chapters.

3.2 Racemic Intermolecular Allylic Amination with Sulfonamides

Parts of the following investigatory results were published in 2024 in *ACS Catalysis*.[168]

3.2.1 Preliminary Investigation

Following the intramolecular photoredox/Se-π-acid dual catalytic allylic amination of sulfonamides, the question arose whether the method could also be applied to an intermolecular approach, as Se-π-acid catalysed oxidative intermolecular allylic aminations with exogenous nucleophiles were not reported in the literature as yet. A preliminary reaction involved the exposure of *N*-methyl-*p*-toluene sulfonamide **137** and equimolar amounts of simple alkene (*E*)-dec-5-ene **138** with diphenyl diselenide $(PhSe)_2$ and photocatalyst (PC) **86** to blue light irradiation in *o*-xylene (Equation 3.5). The reaction conditions were chosen similar to the optimised conditions of the intramolecular allylic amination of sulfonamides discussed in Section 3.1. In this initial reaction, 20% conversion of **137** and 7% yield of the desired product were determined by quantitative NMR analysis with internal standard 1,3,5-trimethoxybenzene (TMB) after 22 h. Following purification *via* column chromatography afforded 6 mg of product **139**, corresponding to a 2% yield.

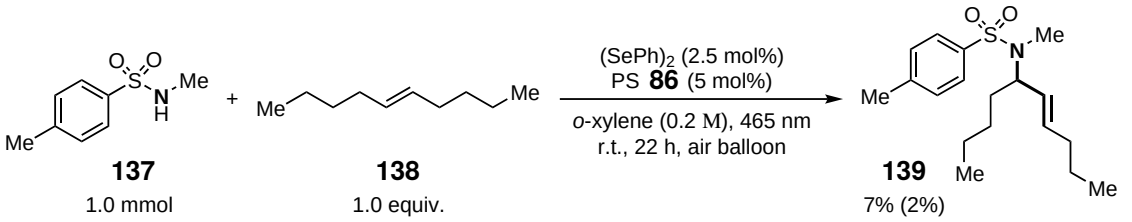

(3.5)

The constitution and configuration of **139** could be determined *via* ^{1}H NMR and 2D NMR analysis, including COSY, HSQC, and HMBC experiments (Table 3.5). Aromatic signals **a** in the region of 7.38–7.11 ppm were assigned to the two phenylic protons closest to the electron-withdrawing sulfonamide substituent, which deshields the adjacent protons and therefore results in a downfield shift. Three single proton signals were identified at 5.53–5.28, 5.08 and 4.34 ppm, which were proposed to belong to the two olefinic protons and the proton of the carbon bearing the *N*-bond. COSY analysis shows a signal coupling of peak **d** at 5.08 ppm to both the other protons **c** at 5.53–5.28 and **e** at 4.34 ppm. This resulted in the assignment of signal **d** to the olefinic proton closer to the C–N bond adjacent to both other signals.

Table 3.5: Assignment of ^{1}H NMR Signals of **139** and COSY-Couplings.

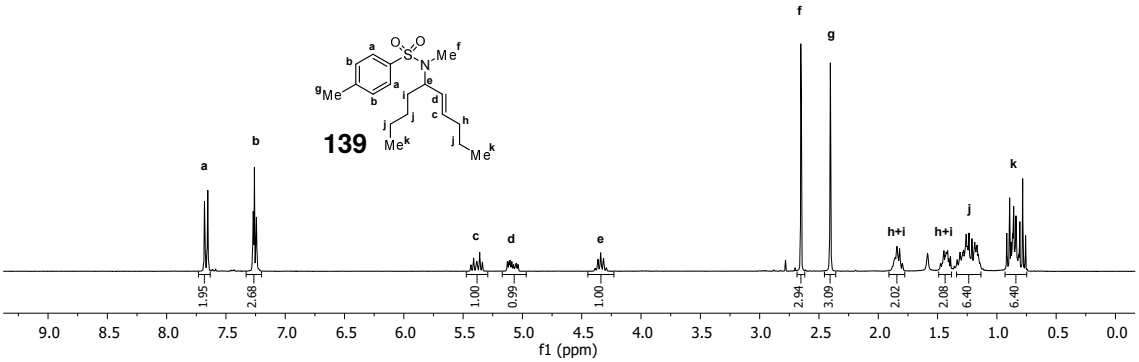

proton	coupling partner
a (7.76–7.55)	**b** (7.38–7.11 ppm)
b (7.38–7.11 ppm)	**a** (7.76–7.55), **g** (2.41 ppm)[a]
c (5.53–5.28 ppm)	**d** (5.08 ppm), **h** (1.95-–1.72 ppm)
d (5.08 ppm)	**c** (5.53–5.28 ppm), **e** (4.34 ppm)
e (4.34 ppm)	**d** (5.08 ppm), **i** (1.51–1.37 ppm)
f (2.65 ppm)	-
g (2.41 ppm)	**b** (7.26 ppm)[a]
h (1.95-–1.72 ppm)	**c** (5.53–5.28 ppm), **j** (1.36–1.07 ppm)
i (1.51–1.37 ppm)	**e** (4.34 ppm), **j** (1.36–1.07 ppm)
j (1.36–1.07 ppm)	**h** (1.95-–1.72 ppm), **i** (1.51–1.37 ppm), **k** (0.97–0.67 ppm)
k (0.97–0.67 ppm)	**j** (1.36–1.07 ppm)

[a]Small coupling signal.

HSQC analysis matched carbon signals at 134.2 and 58.7 ppm with signals **c** and **e**, respectively (Figure 3.3, left). This revealed proton **c** at 5.39 ppm to be attached to a sp^2 hybridised carbon, which holds for the second olefinic proton. Signal **e** at 4.34 ppm could be assigned to the proton of the amine-binding carbon. Furthermore, the coupling constant of the double bond signal at 5.08 ppm (dddt, J = 15.4, 7.0, 4.2, 1.4 Hz) indicates an (*E*)-configuration of **139**. HMBC-analysis enabled the allocation of the two methyl peaks **f** and **g**. Protons **g** at 2.41 ppm show interaction with aromatic carbons in the 125–144 ppm region, whereas protons **f** at 2.65 ppm do not interact with the aromatic region (Figure 3.3, right). As a result, signal **g** was assigned to the toluene-methyl and signal **f** at 2.65 ppm to the isolated *N*-substituent. Aliphatic signals **h**–**k** could be subsequently assigned to the alkyl chain according to their COSY-couplings (Table 3.5).

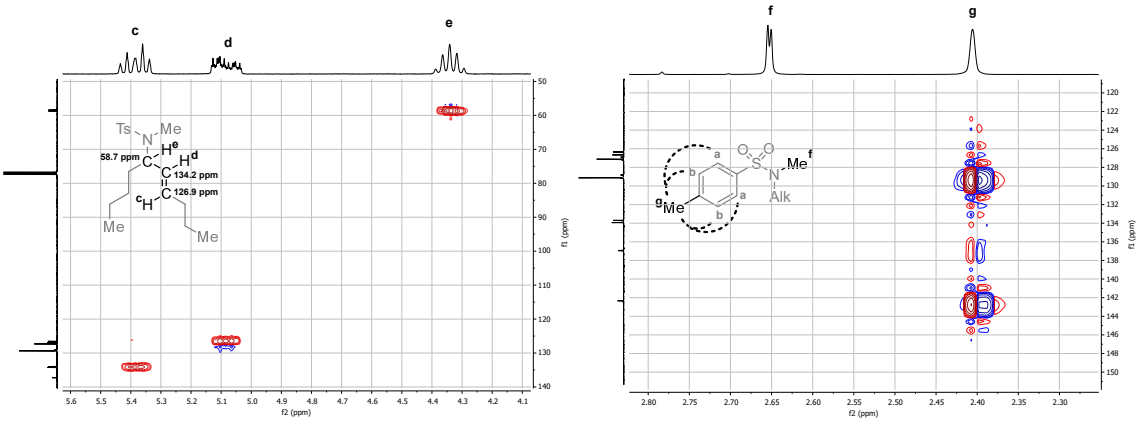

Figure 3.3: Excerpt of HSQC NMR- (left) and HMBC NMR- (right) experiment of **139**

Interestingly, ^{13}C NMR and HSQC analysis revealed that all carbons show a doubled peak-set. Several product conditions can result in such a doubling, one being a potential *E*/*Z* isomeric mixture. In the present case, ^{1}H NMR does not indicate an *E*/*Z*-mixture, as only coupling constants for the *E*-isomer are observed, and no second set of signals is identified for a potential *Z*-isomer. ^{13}C NMR analysis indicates an almost 1:1 ratio of the isomers, which is unlikely to be observed for an *E*/*Z*-mixture, as the *E*-conformer usually represents the thermodynamically more stable form. Another possibility for a signal doubling by diastereoselectivity is given when two stereocentres are available. This is not the case for product **139**, which possesses a stereocentre in position **e** but no second stereocentre, and is therefore unable to form diastereomers. A further explanation for the presented ^{13}C NMR-spectrum would be a hindrance in molecular rotation in product **139** and, with this, the presence of two rotamers. This has been observed in amide compounds on multiple occasions, where the OC–N bond exhibits a high double bond character, fixating its conformation into place and affording two rotamers visible in NMR analysis (Scheme 3.3, top).[19,169,170] Additional steric influence between large amine-substituents (grey circles) and the carbonyl O-atom might further restrict the rotational ability (Scheme 3.3, bottom). Rotamers are also occasionally observed in sulfonamides[171,172] but are not as thoroughly researched. Due to structural parallels to amides, a similar tendency towards the buildup of rotamers is thinkable in sulfonamides and would explain the doubling of signals for **139**. Another possibility would be a rotational hindrance in the C$^{\mathbf{O}}$-N rotation, which has previously been observed for sulfonamides.[172]

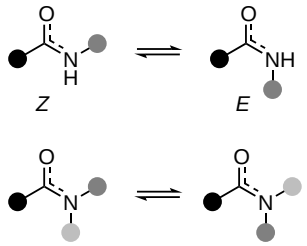

Scheme 3.3: Possible rotational conformers in amides.

High-temperature NMR experiments were performed in $CDCl_3$ and DMSO with temperatures of up to 120 °C to further investigate the presence of rotamers in the product mixture. Interestingly, the reduction in signal splitting which is usually detected with rotamers under these conditions was not observed, which could either be interpreted as the presence of two very highly trapped rotamers, or a different cause leading to the carbon signal doubling.

3.2.2 Reaction Optimisation and Mechanistic Investigation

With a promising first attempt towards the formation of **139**, the goal was then to ascertain the most advantageous reaction conditions for the photoredox/Se-π-acid dual catalytic transformation of **137** with **138** (Equation 3.6).

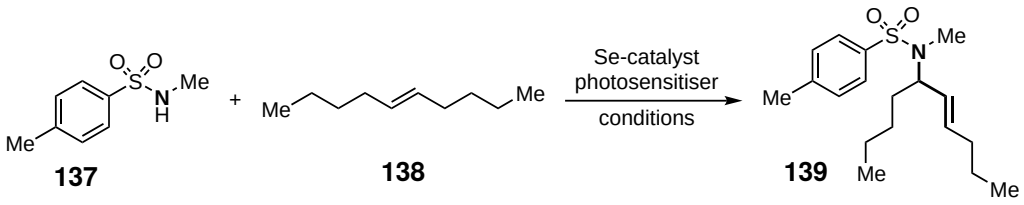

137 **138** **139** (3.6)

A temperature-controlled metal block and 40 mL reaction vials were used as the standardised setup to improve reproducibility. Variation in stoichiometry showed that the best result could be achieved with 5 equiv. of **137** in a 0.50 mmol scale of **138** in *o*-xylene (for detailed results, see Section 5.6, Table 5.3). Subsequent screening of solvents demonstrated a non-linear yield dependency on the solvent's relative polarity[173] (Table 3.6). Unlike in previous studies, where polar solvents such as MeCN[150,151,155,157] (relative polarity: 0.460) and 1,2-dichloroethane[156] (DCE, relative polarity: 0.327) were chosen to achieve high yields, in this case, solvents with a lower relative polarity ranging from 0.164 (1,4-dioxane) to 0.228 (EtOAc) achieved the most promising results. Solvents with low polarity, such as toluene and *o*-xylene, afforded low yields. This can be explained by the low solubility of photocatalyst **86** in nonpolar solvents, effecting a low concentration of the excited state photocatalyst available for the desired transformation. Interestingly, in contrast to these observations, *o*-xylene gave the best results in the very similar intramolecular variant discussed in Section 3.1.[127] Furthermore, solvents with polarity ranging from 0.259 ($CHCl_3$) to 0.355 (acetone) gave moderate yields, albeit with high conversion of **137** compared to previous results, except for DCE. This suggests the presence of side reactions, such as the SCHENCK-ene reaction.[155,174] Solvents with polarity of 0.444 (DMSO) and above led to low and up to no detectable product formation with highly varying conversion.

Table 3.6: Variation of Solvent in the Racemic Intermolecular Allylic Amination with Sulfonamides.[a]

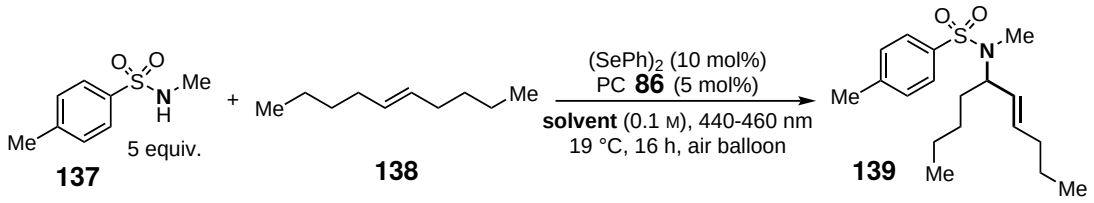

Entry	Solvent	Relative polarity[173]	Conversion of **137**[b,c] [%]	Yield[c] [%]
1	*o*-Xylene	(0.074[d])	22	3
2	Toluene	0.099	19	7
3	1,4-Dioxane	0.164	24	18
4[e]	PhCl	0.188	17	19
5[e]	THF	0.207	25	17
6[e]	EtOAc	0.228	29	21
7	$CHCl_3$	0.259	61	13
8	DCM	0.309	69	14
9	DCE	0.327	38	15
10	Acetone	0.355	67	15
11	DMSO	0.444	3	0
12	MeCN	0.460	14	6
13	EtOH	0.654	0	0
14	MeOH	0.762	5	0
15	HFIP	0.969	9	7

[a] 0.50 mmol of **138**. [b] Conversion of 0.50 mmol of **137**. [c] NMR yields and conversions were determined with TCE as the internal standard. [d] *p*-Xylene. [e] Average of two reactions.

In summary, both the intra- and intermolecular variants of the photoredox/selenium-π-acid dual catalytic allylic amination with sulfonamides require less polar solvents than previously reported variants.[150,151,155,157] Further variation in concentration, carried out with the most promising solvents PhCl, THF and EtOAc, and for comparison toluene, proved 0.1 M to be the leading condition for each solvent regarding yield and conversion (Table 5.5). PhCl, albeit exhibiting slightly lower yields than EtOAc, was chosen as the solvent for further optimisation studies due to a more auspicious conversion-to-yield ratio.

Proceeding from here, different selenium catalysts and photocatalysts, varying in their redox potentials, were investigated for a possibly improved interaction between one another and with the reaction intermediates, accompanied by a higher product yield. Various combinations, depicted in Table 3.7, were applied to the intermolecular allylic amination reaction for 8 h.

Table 3.7: Photophysical Properties and Results of Catalyst Variation in the Intermolecular Allylic Amination.

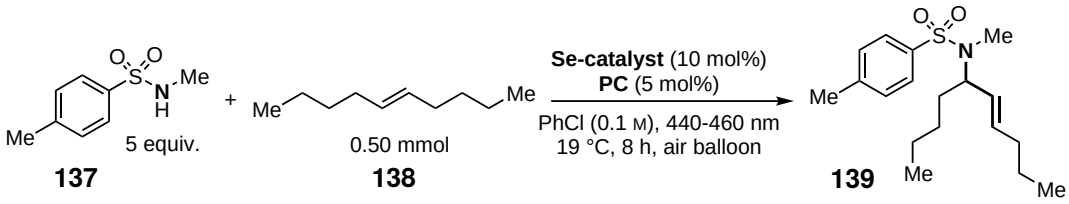

Se-catalysts

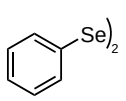

$(PhSe)_2$

E_{ap} = +1.35 V[a]

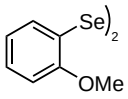

140

E_{ap} = +1.22 V[b]

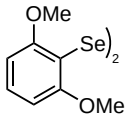

141

E_{ap} = +1.04 V[c]

with **86**	21%	9%	13%
with **143**	0%	0%	4%

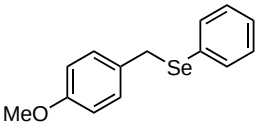

142

E = n.d.

with **86**	21%[f]
with **143**	0%

Hybrid-catalyst

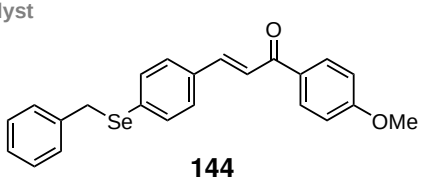

144

E = n.d.

0%[f]

Photocatalysts (PC)

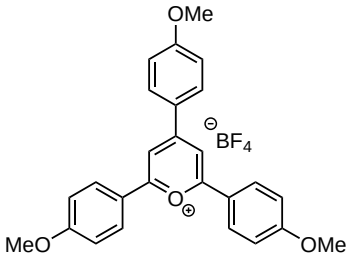

86

$E^*_{calcld.}$ = +1.74 V[d]

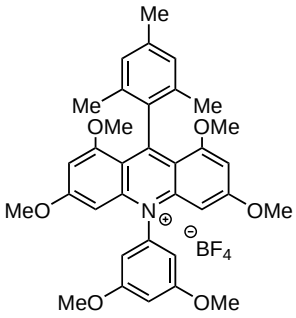

143

$E^*_{calcld.}$ = +1.65 V[e]

All potentials are given in V vs. SCE (saturated calomel electrode) in MeCN. $E_{calcld.}$ = calculated redox potential, E_{ap} = redox potential measured at the first anodic peak, E^* = redox potential of the excited state catalyst. [a] Kunai et al.[154] [b] Converted to V vs. SCE by adding 0.42 V to the reported value relative to $Fc^{+/0}$.[128,160,175] [c] Converted to V vs. SCE by subtracting 0.039 V from the reported value relative to Ag/AgCl.[153,160,176] [d] Converted to V vs. SCE by subtracting 0.141 V from the reported value relative to NHE.[150,152,153,160] [e] Joshi-Pangu et al.[177] [f] 20 mol% of Se-/hybrid-catalyst used.

Acridinium salts have previously been reported to enable C-N bond formation between sulfonamides and alkenes under photocatalytic conditions, albeit underlying a different mechanism than the title reaction enabled by the high potential of the salt (E^* = 2.18).[158,160,178] Here, the photoexcited acridinium salt directly activates a double bond towards a radical cationic species, which

in a later step recombines with the sulfonamide and affords the desired coupled product. **143** was chosen as a photocatalyst in the title reaction due to its lower redox potential with the goal to prevent interaction with the double bond and instead enable SET with the selenium catalyst present. But when applied under reaction conditions, acridinium salt **143** did not qualify as a productive photocatalyst in combination with the selenides, as low to no product formation was observed. This possibly results from a lower redox potential *E* than photocatalyst **86**. **86** on the other hand afforded the desired product with all of the investigated selenium catalysts. Lowering the redox potential of the diselenide with the goal to facilitate the electron transfer from the excited state photocatalyst did not result in higher yields, and no trend was detected. When applying 20 mol% of monoselenide **142**, a different approach was enforced, exploiting a homolytically breakable Se – benzyl bond as an alternative to the Se-Se bond.[179,180] Both catalysts gave the best results with 21% yield, which was achieved with 5 mol% of **86** in combination with either 10 mol% of diselenide $(PhSe)_2$ or 20 mol% of monoselenide **142**. A hybrid catalyst, theoretically both acting as a photocatalyst and a Se-π-acid, was also applied in the title reaction. The bifunctional catalyst was synthesised by Dr. K. Müller in the Breder group. Unfortunately, irradiation with blue light did not yield any product, even when prolonging the reaction time to 24 h.
To further elucidate the mechanistic properties of the reaction, the two most promising Se-catalysts $(PhSe)_2$ and **142** were subjected to a kinetic study.

Kinetic Observation

The kinetic investigation was performed on the transformation of **137** and **138** with photocatalyst **86** in PhCl (Figure 3.4). Reaction with 10 mol% of $(PhSe)_2$ shows that product formation was first detected only at 3 h, and the initiation phase proceeded until 5 h, after which a rapid rise in product formation was observed. An initiation phase was also seen in the intramolecular variant[127] and is associated with a higher quenching ability of the diselenide-catalyst compared to the in situ formed intermediate, which releases the desired product upon oxidation.

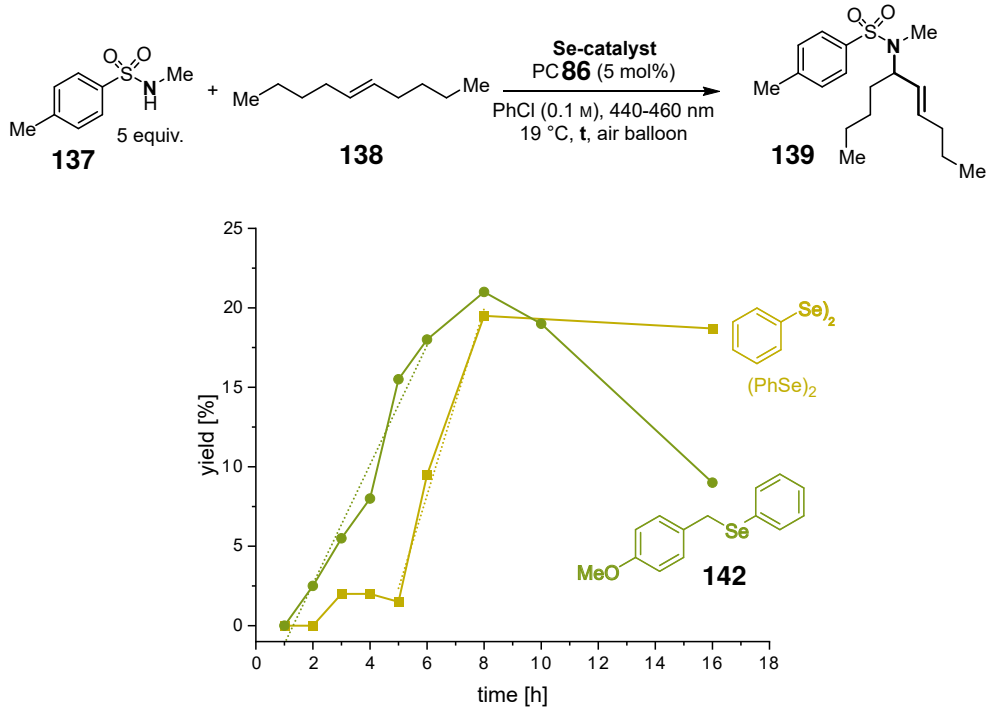

Figure 3.4: Yields of **139** in the reaction with $(PhSe)_2$ (10 mol%) or monoselenide **142** (20 mol%). Dotted lines show the rate of the reaction; after an initiation phase in case of $(PhSe)_2$.

With this in mind, it was considered that the application of a monoselenide-catalyst with a breakable Se-C bond could compete less with the intermediate and might reduce the initiation phase of the reaction. In fact, when applying 20 mol% of monoselenide **142** instead of $(PhSe)_2$, product formation was already observed at 2 h with a constant rise over the term of an additional 6 h. After 8 h of reaction time, product formation comes to a halt, and the yields even decrease with increased time. This indicates that product decomposition is present under reaction conditions and exceeds product formation at 8 h with **142** and somewhere between 8–16 h with $(PhSe)_2$. Comparing the kinetic product formation of the title reaction to the previously discussed intramolecular variant, it stands out that the intermolecular version is slower, reaching a yield of 21% only at 8 h, whereas yield in the intramolecular pathway exceeds 20% already before 2 h, even before 1 h when disulfide $(4\text{-ClPhS})_2$ was added. Previous studies in the BREDER- and other groups showed that final dehydrodeselenylation and, with this, the release of product presents the rate-limiting step in the mechanism of similar transformations.[104,127,128] Competing side reactions, such as the SCHENCK-ene reaction, might affect the product-forming process if elimination is too slow, as indicated in this intermolecular pathway.[155,174]

To verify the theory of a product decay under reaction conditions, a stability test of **139** was performed. No **138** was observed after reaction performance, which is why none was applied during the stability investigation. Mimicking the reaction conditions after approx. 8 h of reaction time, an excess amount of **137** was applied, as well as 50.0 µmol of $(PhSe)_2$ and 25.0 µmol of

photocatalyst **86** to 53 µmol of **139** in 5 mL PhCl. Three reactions were run under irradiation, stopping at 16, 40, and 112 h, respectively, to measure the residual amount of **139** *via* quantitative ^{1}H NMR analysis and with internal standard trichloroethylene (TCE) (Figure 3.5).

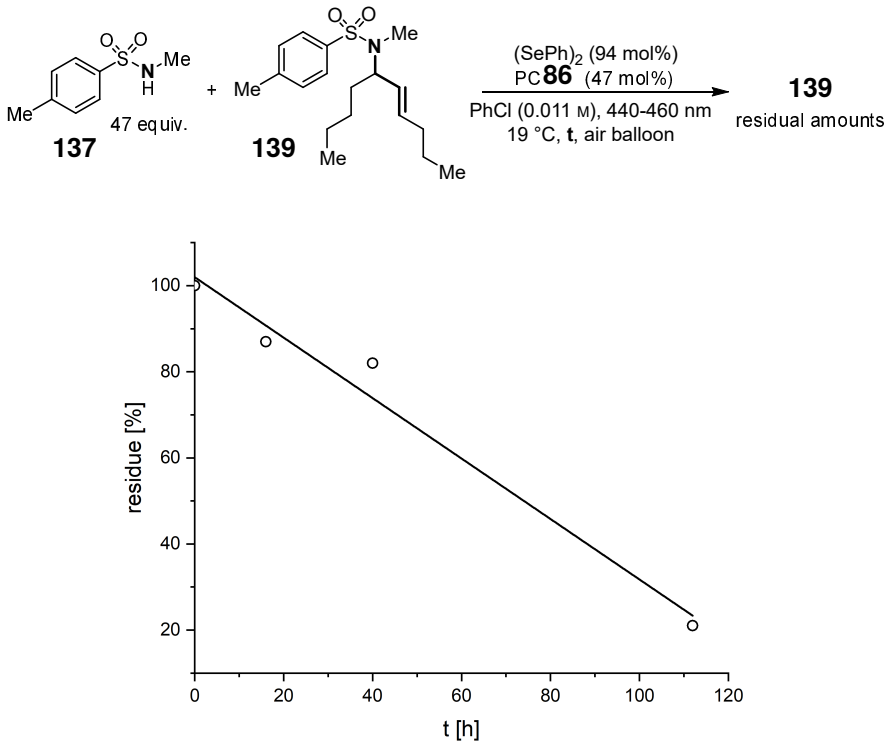

Figure 3.5: Residual amount of **139** after varying time under reaction conditions compared to applied amount, and interpolation.

The results show that **139** is unstable under reaction conditions, as indicated during the earlier kinetic investigation. Based on these observations, two strategies can be used to increase the yield. One strategy focuses on the increased lifetime and stability of the formed product. This could be reached by altering the applied reaction conditions, additives and starting materials. Another strategy involves the enhancement of the reaction rate. A successful elevation would already be observed after 8 h of reaction time, which is why this timespan was mainly used in the further validation of varying reaction parameters during the following optimisation procedure.

Further Optimisation Studies

In order to increase the reaction rate, it was aimed to address a possible insufficient single electron transfer between the excited state photocatalyst **86** ($E^*_{calcld.}$ = +1.74 V vs. SCE in MeCN)[150,152,153] and the $(PhSe)_2$ (E_{ap} = +1.35 V vs. SCE in MeCN)[128,154] and/or the selenofunctionalised intermediate under reaction conditions. An increased single-electron uptake, for example, could

increase the rate of product release from the selenofunctionalised intermediate. Previous studies on similar systems revealed that the redox potential of the selenofunctionalised intermediate is slightly higher than that of the corresponding diselenide, which is also proposed for our present conditions.[128] The presence of competitive side reactivity that interferes with the transfer is unlikely in PhCl, as the conversion matches the product yield (cf. Table 3.6, entry 4). Previous studies showed that the formation of unstable or short-lived radical intermediates might lead to the occurrence of a back-electron transfer (BET) from the radical species to the photocatalyst or another present species able to accept electrons. In this context, using so-called electron mediators can facilitate the kinetically slow redox processes by serving as electron shuttles and possessing 'stable and persistent radical ionic states'.[95,181] For a successful transfer between the PC and the diselenide, the electron mediator was proposed to require a marginally higher oxidation potential than the diselenide. As polyarenes proved successful in serving as electron mediators between **86** and a styrene-derivative ($E^*_{p/2}$ = +1.33 V vs. SCE in MeCN)[153,160,181] with almost the same redox potential as $(PhSe)_2$, biphenyl **145**, naphthalene **146**, and phenanthrene **147** were applied into the reaction with **86** and 10 mol% of $(PhSe)_2$ or $(o-anisylSe)_2$ **140** (Table 3.8).

Table 3.8: Variation of Redoxmediators in the Racemic Intermolecular Allylic Amination with Sulfonamides.[a]

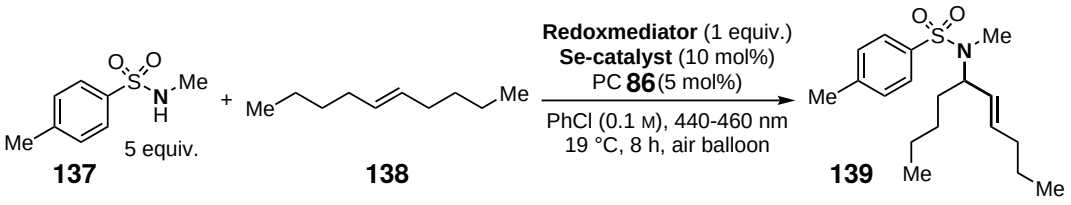

Redoxmediator	None	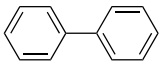 **145** $E_{1/2}$ = +1.95 V[b]	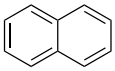 **146** $E_{1/2}$ = +1.54 V[c]	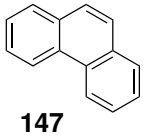 **147** $E_{1/2}$ = +1.50 V[c]	
Se-catalyst					
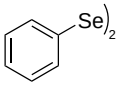 $(PhSe)_2$ E_{ap} = +1.35 V[d]	21% 19%	24% 26%	17% 19%	7% 10%	Yield Conversion
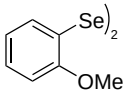 **140** E_{ap} = +1.22 V[e]	9% 9%	2% 1%	19% 23%	12% 24%	Yield Conversion

[a] 0.50 mmol of **138**. Conversion of 0.50 mmol of **137**. NMR yields were determined with TCE as the internal standard. Photosensitiser **86** ($E^*_{\text{calcld.}}$ = +1.74 V vs. SCE in MeCN).[150,152,153] E_{ap} = redox potential measured at the first anodic peak. $E_{1/2}$ = half-wave potential. [b] Guirado et al.[182] [c] Pysh et al.[183] [d] Kunai et al.[154] [e] Converted to V vs. SCE by adding 0.42 V to the reported value relative to $Fc^{+/0}$.[128,160,175]

The redox potentials of electron mediators **146** and **147** lie between those of **86** and diselenides and are proposed to aid with their electron transfer. And in fact, when diselenide **140** was used in the reaction, both mediators showed a definite increase in product formation. Unfortunately, the system could not exceed the previously afforded highest yield. In contrast, with $(PhSe)_2$, the application of the two mediators resulted in a decrease in yield, possibly due to a very narrow gap between the redox potentials of the photoactive species involved. Interestingly, when applying **145** as the redox mediator, which actually exhibits a redox potential even higher than the photocatalyst, a slight increase of 3%-points in yield was achieved with $(PhSe)_2$. Overall, the application of redox mediators did not increase the achievable yield to such an extent that it would justify the application of stoichiometric amounts of additive, significantly lowering the atom economy and raising the waste generated.

The previous kinetic investigation showed that the reaction seemed to slow down after 8 h. A theory is that either or both Se- and photocatalysts decompose during the reaction under the current conditions. In fact, the bright orange colour of the initial reaction mixture is decoloured at the end of the reaction. Therefore, a second addition of either or both photocatalyst **86** and monoselenide **142** after 6 h was investigated (for detailed results, see Subsection 5.6.1, Table 5.9). Only the addition of another 5 % of **86** led to a slight increase in yield after 12 h, but also a significantly higher conversion, indicating that i) more product was formed, but at the same time a similar amount decomposed, or ii) a higher amount of side reactions took place. The addition of an extra 20 mol% of monoselenide catalyst did not increase the yield or conversion. The addition of both catalysts increased conversion but lowered the yield, which indicates a faster product decomposition and/or a promotion of side reactions. In summary, a sufficiently higher yield in the reaction, justifying a second catalyst addition, could not be reached.

Previous reports on the intra- and intermolecular photo-aerobic/selenium-π-acid multi-catalytic allylic functionalisation of alkenes have shown that the application of a suitable base improved the reaction outcome.[155,156] This might result from deprotonation of the nucleophile - f.e. in the case of phosphate[156] - or the capture of occurring side products that might interfere with the product formation, as seen in the similar transformation.[122] The application of base-additives in the current intermolecular allylic amination was proposed to enhance the reaction rate, but only CaF_2 gave a slightly increased yield of 21 % after 6 h of irradiation, albeit with an increase in conversion, compared to the reaction without base, which afforded 18 % of the desired product (for detailed results, see Subsection 5.6.1, Table 5.10). All other bases, including carbonates and phosphates, resulted in very low or no product formation with low or no conversion, proposing an interference of the base with the desired product formation or even a quenching of the photocatalyst, which would explain the absent substrate conversion.
Following further optimisation investigations, the catalyst loading was evaluated. Several $(PhSe)_2$/**86** ratios were examined at different timescales, ranging from 10:5 to 50:25 (Figure 3.6. For detailed results, see Subsection 5.6.1, Table 5.12 ff.). The best result was achieved with 20 mol% of $(PhSe)_2$ and 10 mol% of photocatalyst **86**, yielding 28% after an 8 h reaction time.

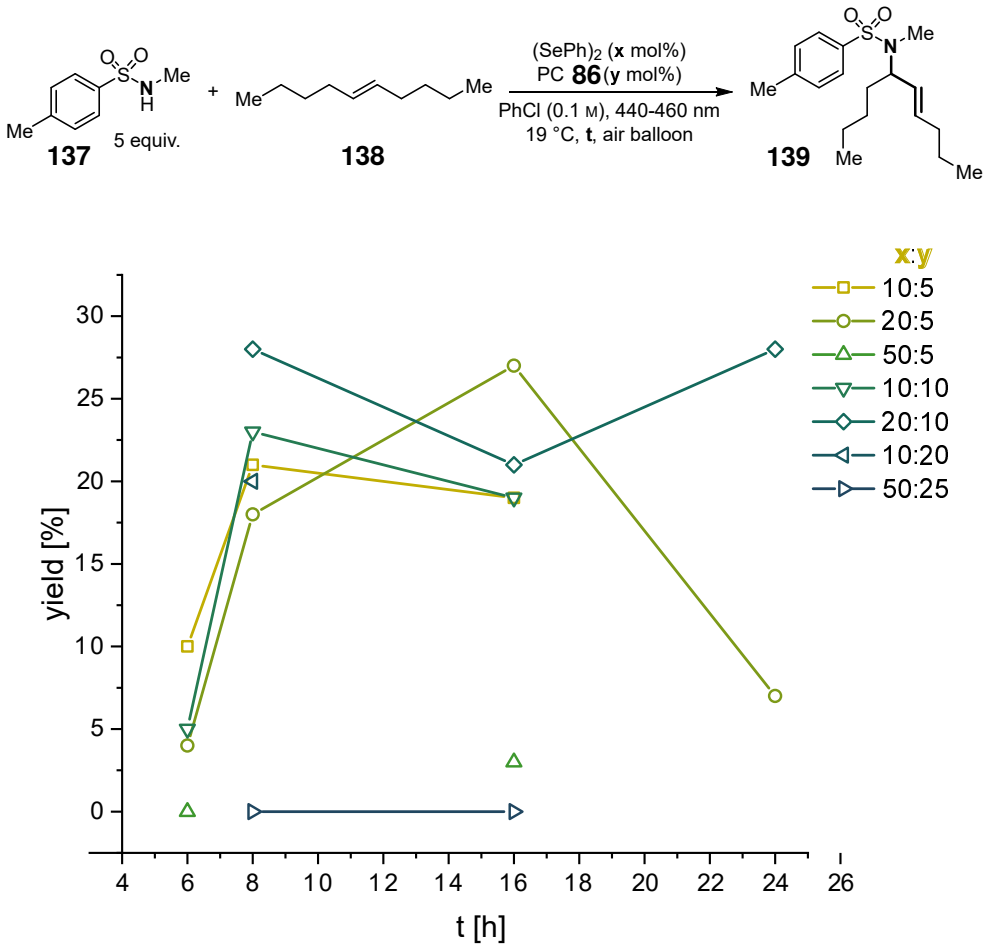

Figure 3.6: Screening of catalyst loading ($(PhSe)_2$/**86**) with varying reaction times in the intermolecular allylic amination with sulfonamides.

With the hitherto optimised reaction conditions, two further additives were tested to enhance product formation (for detailed results, see Subsection 5.6.1, Table 5.11). The addition of disulfide $(4\text{-ClPhS})_2$, which previously showed a rate-enhancing effect,[127] did not improve the present reaction. An increased substrate conversion suggests an indeed accelerated product formation, but accompanied by a higher product decay, overall leading to a lower yield of 20 % compared to 28 % without the addition of disulfide. Another possibility of the observed lower yield is the initiation of side reactions upon the addition of $(4\text{-ClPhS})_2$. By adding *o*-nitrobenzaldehyde to the reaction, the extension of the photocatalyst's lifespan was striven for. The aldehyde has previously been shown to suppress the generation of singlet oxygen, which might lead to the degradation of **86** and also to side reactions with the alkene starting material, such as the SCHENCK-ene reaction.[184] This and adding both additives simultaneously did not achieve the desired reaction enhancement, also with prolonged reaction times. Hints for degradation of the photocatalyst were observed in some reactions by the presence of an aldehyde-derived carbon signal in the ^{13}C-NMR spectra, which could present a degradation fraction of the pyrylium

catalyst. Also the discoulouring of the reaction mixture after some reaction time supports the observed degradation. Further alterations in reaction conditions, such as raising the temperature and a pure oxygen atmosphere, did not increase the yield (for detailed results, see Subsection 5.6.1, Table 5.14). Lastly, control experiments proved that $(PhSe)_2$, photocatalyst **86**, air, and blue light irradiation (448 nm) are crucial for the reaction. Leaving out irradiation but heating to 55 °C did not lead to any product formation or conversion of the substrate, which proves that the transformation is photocatalytic in nature (for detailed results, see Subsection 5.6.1, Table 5.15).

In summary, the first Se-π-acid catalysed intermolecular allylic amination involving an exogenous nucleophile was successfully performed with the conversion of simple decene **138** and *N*,4-dimethyl benzenesulfonamide **137** with the aid of photocatalyst **86**, acting as the oxidising species. Oxygen as the terminal oxidant renders the reaction ecologically friendly, as water is generated as the only by-product. Much effort was put into the optimisation of the intermolecular allylic amination of decene with sulfonamides. Kinetic studies showed that the reaction is productive until approximately 8 h, after which decomposition of the product under reaction conditions outperforms new formation. Efforts to enhance the reaction rate, for example, by increasing the electron transfer between the involved catalysts and onto substrates, were unsuccessful. Also, the enhancement of the rate-limiting step by the addition of $(4\text{-ClPhS})_2$, which proved productive in previous studies, did not result in the desired outcome. Further enhancement of the reaction rate or lifetime of reaction compounds was attempted by including various additives, which did not show a significant increase in product yield.
Under optimised reaction conditions, the transformation afforded the desired allylic amine **139** in 28% (24% isolated) yield in a 0.50 mmol scale and irradiation at 19 °C for 8 h with 20 mol% of $(PhSe)_2$ and 10 mol% of photocatalyst **86**.[168] Lastly, other alkene substrates were tested with these optimised reaction conditions in hand. β,γ-Unsaturated esters **148**, which previously proved to be suitable substrates in allylic functionalisation reactions, did not result in any product formation (for details see Chapter 5, Subsection 5.6.4). A different system might be successful in further enhancing the yield in the intermolecular allylic amination reaction.

3.3 Racemic Intermolecular Allylic Amination with Azoles

Parts of the following investigatory results were published in 2024 in *ACS Catalysis*.[168]

N-Heterocycles are common structural motifs in biologically active compounds. Within this class, *N*-allylic azoles show high potential as highly valued building blocks and starting materials for established pharmaceuticals, drug leads, and agrochemicals.[168,185–190] Against this background, it is to no surprise that method-based investigations into new synthetic protocols for the direct *N*-allylation of azoles, such as allylic substitutions[191,192] and hydroaminations,[193–196] have been made in recent decades. Among them, the direct oxidative coupling of olefins (C-H) with azoles (N-

H) provides a straightforward, highly atom-economic road towards new azole compounds but has so far been scarcely investigated.[56,99,197–199] Looking at this field in its current state, most protocols exhibit high specificity towards styrenes, terminal and/or symmetrically substituted olefins in order to reach high regioselectivity. With that background, it was discussed whether the developed method for the intermolecular photoredox/Se-π-acid allylic amination by the BREDER lab could be applied to the regioselective formation of allylic azoles. Although significant advancements have been made in azole allylations, effective protocols for 1,2-disubstituted alkenes that demonstrate strong electronic selectivity, as well as for 1,1,2-trisubstituted alkenes exhibiting MARKOVNIKOV regioselectivity, had yet to be developed.[168]

3.3.1 Preliminary Investigation

In regards to the previous results, Dr. T. LEI conducted preliminary investigations into the intermolecular allylic amination of alkene ethyl (*E*)-hex-3-enoate (**150a**) with 4-chloro-1H-pyrazole (**151a**) under photoaerobic/Se-π-acid dual catalytic conditions (Figure 3.7). **151a** was chosen as the model nucleophile in order to avoid possible electrophilic selenation of the heteroarene, which has been reported for 1H-pyrazole.[200–202] Standard conditions using 10 mol% of $(PhSe)_2$ and 5 mol% of photocatalyst **86**, irradiating in dichloroethane (DCE) for 21 h, afforded the desired allylic amine **152a** in 68% NMR yield. The result was reproduced in the course of this thesis, and further investigation revealed one major side product, namely, vinylic enamine isomer **153a** with 15% NMR yield. Proceeding from here, the mechanism is proposed to follow a route analogous to the reported photo-aerobic/selenium-π-acid dual catalytic lactonisation[151] *via* photoinduced activation of the double bond, forming a seleniranium ion, which opens up under nucleophilic attack (see Section 1.2, Scheme 1.21). A second oxidation facilitated by the excited photocatalyst enables the release of the desired allylic amine by dehydrodeselenylation under reformation of the double bond. None of the further possible isomers that result from a different binding site and/or the elimination of a different proton in the final step depicted at the bottom of Figure 3.7 were observed during analysis. The utilisation of β,γ-unsaturated ester **150a** enabled a preferential elimination site due to acidity bias and led to the formation of a conjugated double bond. This renders the reaction selective towards its allylic product **152a** with a ratio of 5:1 compared to the vinylic isomer **153a**.

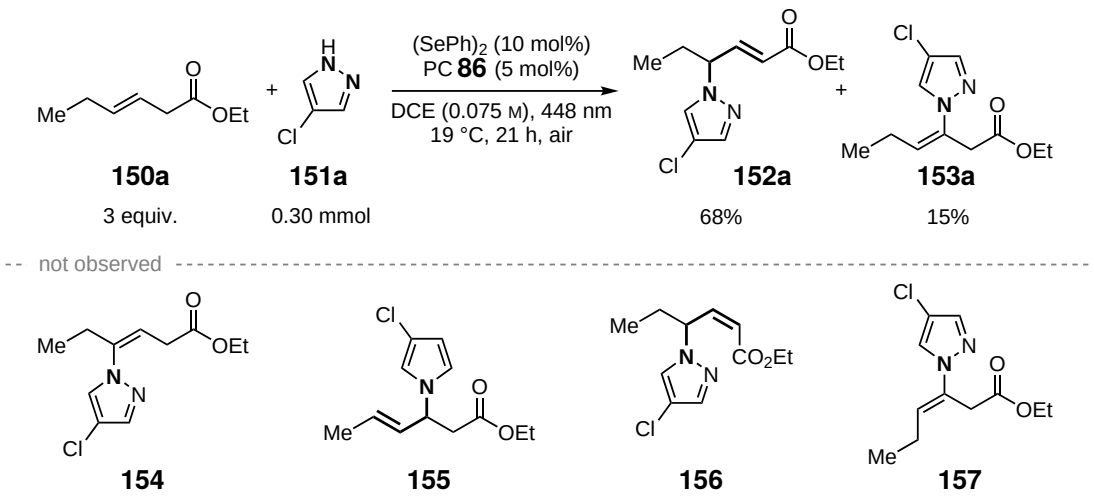

Figure 3.7: Regioselective outcome in the photo-aerobic/selenium-π-acid dual catalytic intermolecular allylic amination of **150a** with **151a**. NMR yields were determined with 1,4-dimethoxybenzene (DMB) as the internal standard.

Regarding the chemo- and regioselectivity, two more side products formed during the reaction were identified within the proceeding investigations and optimisation studies (Figure 3.8). Resulting from side reactions of the alkene starting material **150a**, both lactone 5-ethylfuran-2(5H)-one **158** and allylic hydroxide ethyl (*E*)-4-hydroxyhex-2-enoate **159** were identified by comparison to reported spectra and structural elucidation of the isolated material, respectively.

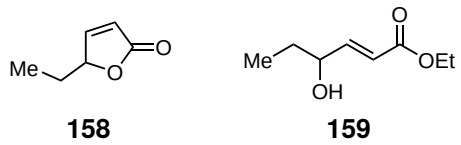

Figure 3.8: Detected side products in the intermolecular allylic amination with azoles.

The formation of lactone **158** is proposed to result from in situ hydrolysis of substrate **150a** towards its carboxylic acid, followed by a photo-aerobic/selenium-π-acid dual catalytic intramolecular cyclisation, which has been reported previously by the Breder group (Figure 3.9).[151]

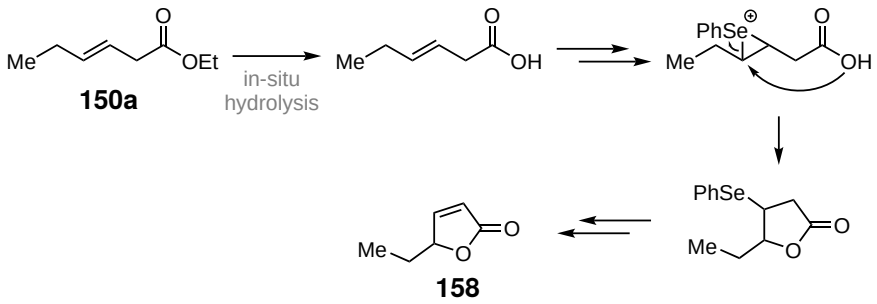

Figure 3.9: Mechanistic proposal for the formation of lactone-side product **158**.

Signals in the ^{1}H NMR analysis of the crude product mixture match the reported signals of the proposed lactone side product **158**.[151] A ^{1}H NMR comparison of the crude product mixture with isolated allylic product **152a** and hydroxy side product **159** is given in Figure 3.10.

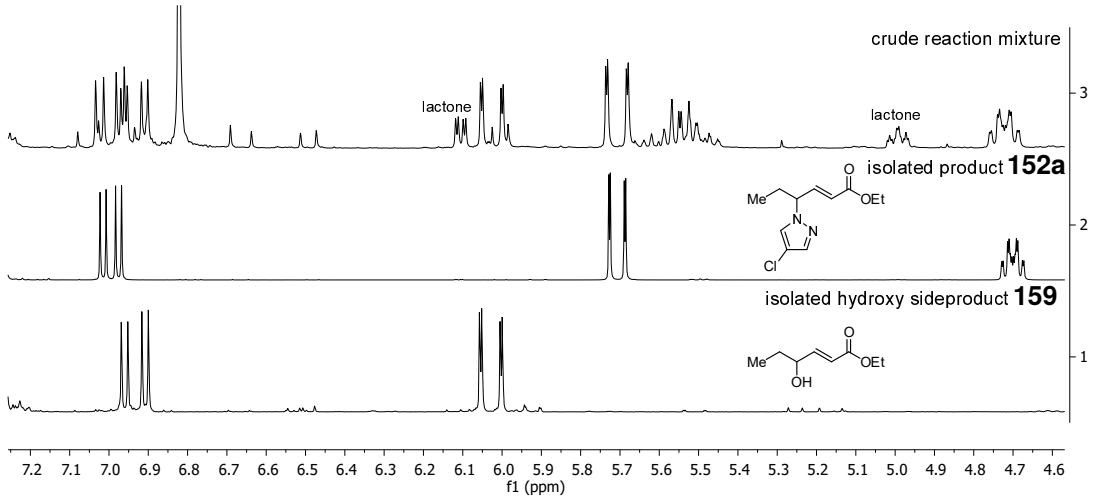

Figure 3.10: Excerpt of the crude ^{1}H NMR after the reaction of **150a** and **151a** (3), of the isolated allylic product **152a** (2) and the hydroxy side product **159** (1). The full spectra can be found in Chapter 6.

Two possible pathways towards the formation of the allylic hydroxide side product **159** are disclosed: i) Nucleophilic attack of H_2O at the in situ formed seleniraniumion intermediate, followed by equivalent oxidation-elimination steps catalysed by the present photocatalyst (Figure 3.11, path a). H_2O is formed in situ during the reformation of photocatalyst **86** in ground state with $^3O_2$, affording superoxide-anion $O_2^{\cdot-}$, which in further steps generates H_2O with H-atoms upon others abstracted from the amination reaction. Another possible introduction of H_2O into the reaction mixture could result from the used solvent or even the air, which would make the usage of molecular sieves during the reaction an interesting additive to investigate as it intercepts H_2O prior to interaction and has previously been proven to positively influence the reaction outcome in a similar transformation.[156] ii) A second possible pathway towards **159** might be the SCHENCK-ene reaction with singlet oxygen ($^1O_2$) (Figure 3.11, path b). Triplet-state excited photocatalyst ^{3}TAPT* is quenched by triplet oxygen $^3O_2$ from the air, affording $^1O_2$, which then can interact in a subsequent ene-reaction with isolated double bonds.[174,203] Upon further interaction with the reaction medium, the so-formed peroxide may afford the reduced hydroxy side product **159** However, the transition to ^{3}TAPT* from singlet-state excited photocatalyst ^{1}TAPT* is very low, with a quantum yield of the respective intersystem crossing (φ_{ISC}) of only 3%.[160,204]

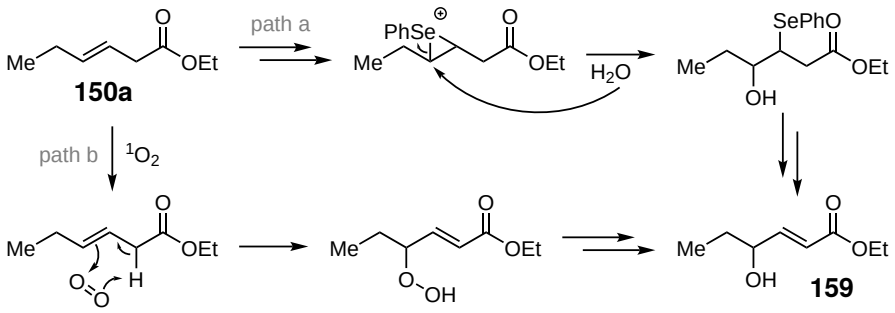

Figure 3.11: Mechanistic rationalisation of the formation of allylic hydroxide-side product **159**.

Regarding the findings of these side products, an excess of olefin is needed in the reaction to avoid a loss in yield. Moreover, during the investigation of the stoichiometry, a slight decrease in product formation was observed when applying **150a** as the limiting compound, but not as significant as expected (Table 3.9, entry 3). Interestingly, the allylic vs. vinylic product ratio was positively affected compared to the reaction with 3.0 equiv. of the alkene **150a** (Table 3.9, entry 1). The result indicates that side reactions of **150a** do not influence the reaction outcome significantly when used as the limiting compound. This may result from a reduced alkene concentration and, with this, a lower interaction with low-concentrated oxygen compounds, which are themselves outperformed by the *N*-nucleophile. This theory is also supported by the observation that both product yield and product ratio were lowered with equimolar amounts of the coupling partners (Table 3.9, entry 2).

Table 3.9: Stoichiometric Variation of Starting Materials in the Racemic Intermolecular Allylic Amination with Azoles.

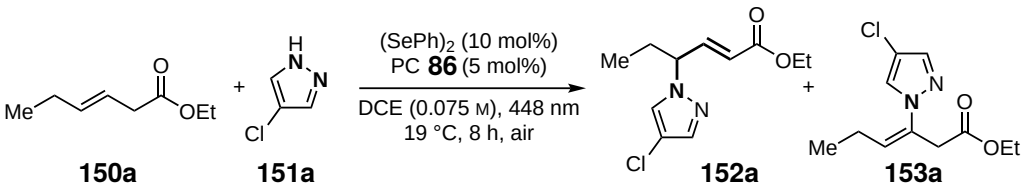

Entry	**150a**	**151a**	Yield [%]			**152a/153a**
			152a	**153a**	Total	
1	3.0 equiv.	0.30 mmol	65	11	76	6:1
2	0.30 mmol	1.0 equiv.	51	10	60	5:1
3	0.30 mmol	3.0 equiv.	62	9	71	7:1

NMR yields were determined with DMB as the internal standard. The average value of two reactions is given. All reactions showed 100% conversion of 1.0 equiv. of **151a**.

For further optimisation studies, **150a** was used as the excess compound to investigate the improvement of yield and product-to-side product ratio. With that goal in mind, it was argued

that a different electrochemical potential of the Se-catalyst might lead to an improved interaction with the excited state photocatalyst **86***, which has a reported potential of +1.74 V vs. SEC in MeCN.[150,152,153,160] As investigated by M. Wilken et al., the formed selenofunctionalised intermediates, which upon oxidation by excited state photocatalyst **86*** release the desired product in a rate-limiting step, possess a higher redox potential than the respective Se-catalysts.[128] Due to the broad similarity to our system, it was argued that this trend is also likely to hold true for the in situ formed selenoaminated intermediates in this reaction. In this manner, a lower redox potential of the Se-catalyst used in the desired allylic amination reaction might lead to a lower redox potential of the selenoaminated intermediate, which could then be oxidised more easily by the excited state photocatalyst **86***, leading to a facilitated release of the desired product and, with this, an increase in product yield. With this background in mind, selenium-catalysts with varying redox potentials *E* were applied to reaction conditions (Table 3.10).

Table 3.10: Variation of Se-Catalysts and the Influence of $(4\text{-ClPhS})_2$ in the Racemic Intermolecular Allylic Amination with Azoles.

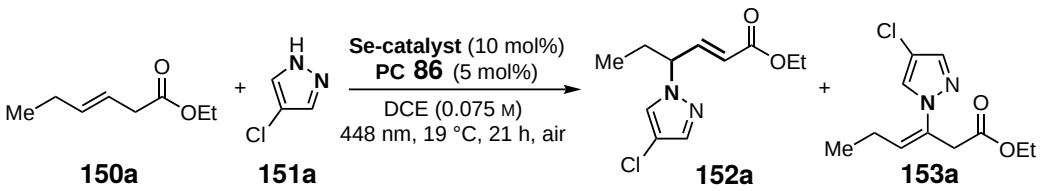

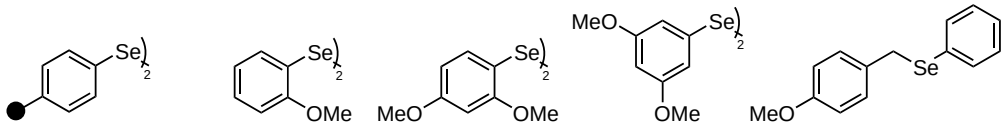

	E_{ap} = +1.35–+1.22 V[a,b]	E_{ap} = +1.22 V[b]	E_{ap} = +1.02 V[b]	E_{ap} = +1.33 V[b]	*E = n.d.*
● = H: $(PhSe)_2$	68%, 5:1				
= Me: **160**	65%, 5:1	64%, 3:1	62%, 6:1	62%, 5:1	51%, 9:1[c]
= OMe: **161**	67%, 5:1				
- with 5 mol% $(4\text{-ClPhS})_2$					
● = H: $(PhSe)_2$	69%, 13:1				
= Me: **160**	70%, 7:1	66%, 7:1	62%, 11:1	65%, 8:1	--
= OMe: **161**	67%, 10:1				

0.30 mmol (1.0 equiv.) of **151a**, 3.0 equiv. of **150a**. NMR yield of **152a** and ratio of the two isomers (**152a**:**153a**) were determined with DMB as the internal standard. Grayed entries were carried out by Dr. T. Lei. All potentials are given in V vs. SCE (saturated calomel electrode) in MeCN. E_{ap} = Potential measured at the first anodic peak. [a]Kunai et al.[154] [b]Converted to V vs. SCE by adding 0.42 V to the reported value relative to $Fc^{+/0}$.[128,160] [c]20 mol% of Se-catalyst used.

1,2-bis(2,4-dimethoxyphenyl)diselane (**162**), possessing the lowest reported redox potential, and

monoselenide **142** led to an increased selectivity towards the allylic product, even though accompanied by a reduced yield. Also, the other Se-catalysts with varying redox potentials did not result in the desired rise in yield either. Interestingly, when 5 mol% of disulfide additive $(4\text{-ClPhS})_2$ was added, all reactions showed both an increase in selectivity and yield towards the desired allylic amine **152a**, with the best result achieved by $(PhSe)_2$ as the selenium compound. The enhancing influence of $(4\text{-ClPhS})_2$ on the reaction outcome has been previously investigated and reported during the intramolecular allylic amination (see Section 3.1) and seems to have a positive influence on the present system.[127]

3.3.2 Kinetic Investigation and Reaction Optimisation

With these promising results in hand, further investigations towards a mechanistic understanding and an enhancement of the product yield and selectivity were conducted.

Kinetic Observation

A kinetic investigation revealed that complete conversion of the limiting reactant **151a** was achieved after 4 h, indicating a fast transformation of the starting materials. Afterwards, a slowing down of reaction rate is observed and a gain in total product yield of 18 percentage points over a further 17 h, possibly released from 20 mol% selenoaminated intermediate. This is supported by previous findings, which show that dehydrodeselenylation and release of the product are the rate-limiting step. After 18 h, only an increase in side product is observed, reducing the allylic-to-vinylic ratio. Approximately 17% of pyrazole was not successfully incorporated into either product and could not be accounted for, indicating side reactions or some form of decay.

Table 3.11: Kinetic Investigation of the Racemic Intermolecular Allylic Amination with Azoles.[a]

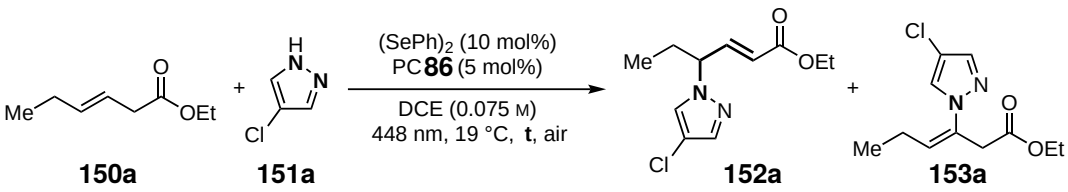

Entry	t [h]	Conversion[b] [%]	Yield[b] [%]			152a/153a
			152a	**153a**	Total	
1	2	38	25	4	29	6:1
2	4	100	57	8	65	7:1
3	6	100	63	11	74	6:1
4	8	100	65	11	76	6:1
5	18	100	68	11	79	6:1
6	21	100	68	15	83	5:1

[a] 0.30 mmol (1.0 equiv.) of **151a**, 3.0 equiv. of **150a**. Average value of two reactions given. [b] NMR yields and conversions were determined with DMB as the internal standard.

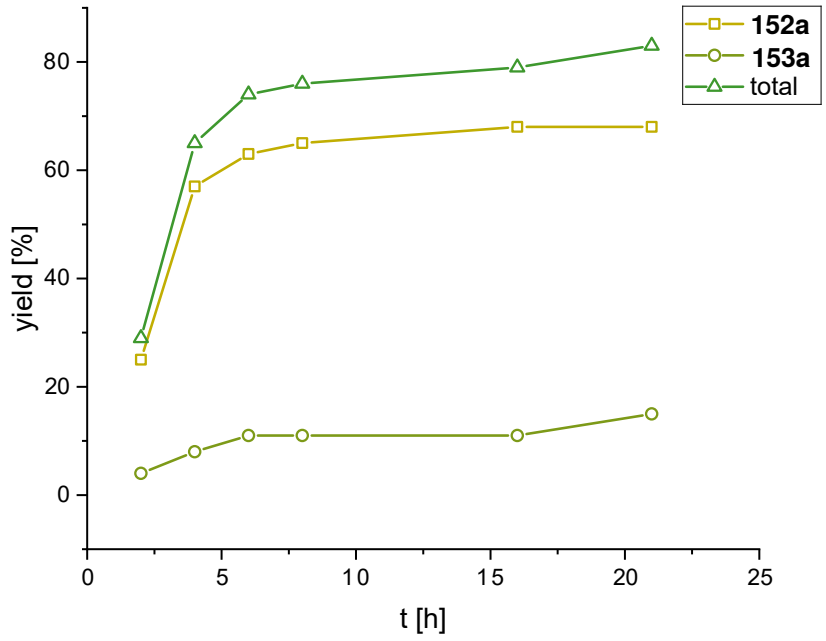

The reaction seems to stop after approximately 8 h and further investigations to elucidate the reason will be made. As a result, proceeding optimisation studies were mainly performed for 8 h, as at this point, an enhanced reaction rate, stability of nucleophile, and selectivity would be detectable

in the outcome.

Optimisation

With a better understanding of the underlying transformation, further variations in reaction conditions were performed. Changing the solvent from 1,2-dichloroethane to other, both polar and apolar media, resulted in a drop in yield and/or a reduced selectivity towards the desired allylic product **152a** (for detailed results, see Subsection 5.7.1, Table 5.19). Further variation in catalyst loading and concentration did not affect the reaction outcome significantly (for detailed results, see Subsection 5.7.1, Table 5.20), with the best conditions being 10 mol% of $(PhSe)_2$ and 5 mol% of photocatalyst **86** in DCE (0.075 M). Raising the temperature from 19 to 55°C resulted in a drop in product yield (for detailed results, see Subsection 5.7.1, Table 5.21), indicating the acceleration of side reactions or decay of products. Additionally, further photocatalysts besides **86** were tested (Table 3.12) but significantly decreased the yield. Pyrylium salt **166** with bis(trifluoromethanesulfonyl)azanide (NTf_2) as the counter ion was tested with different solvents, as it shows solubility in less polar solvents compared to **86**. However, the reaction outcome also produced a significantly lower yield.

Table 3.12: Variation of Se-Catalysts and the Influence of $(4\text{-ClPhS})_2$ in the Racemic Intermolecular Allylic Amination with Azoles.

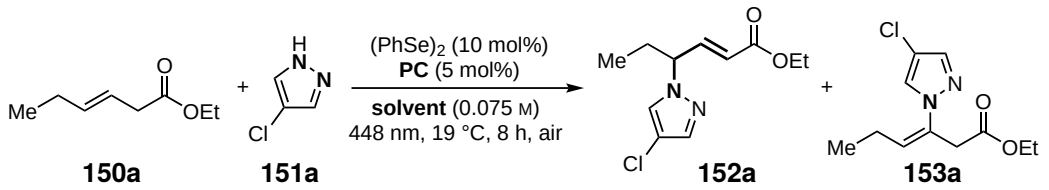

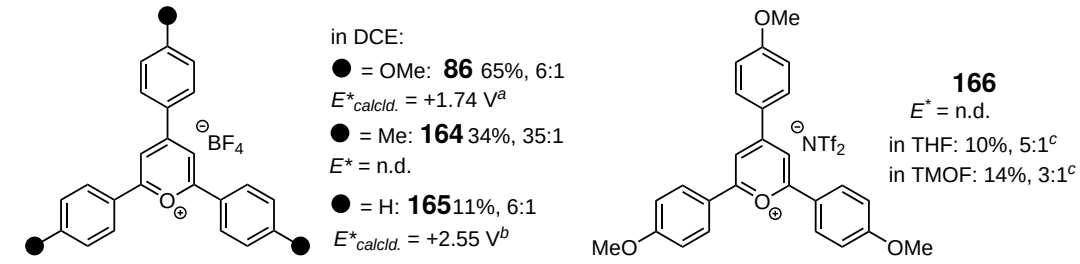

0.30 mmol (1.0 equiv.) of **151a**, 3.0 equiv. of **150a**. NMR yields of **152a** and the ratio of the two isomers (**152a**:**153a**) are given. These were determined with DMB as the internal standard. All potentials are given in V vs. SCE (saturated calomel electrode) and were recorded in MeCN. $E^*_{calcld.}$ = calculated potential of the excited state catalyst. [a]Converted to V vs. SCE by subtracting 0.141 V from the reported value relative to NHE.[150,152,153,160] [c]Romero et al.[160] [c]21 h reaction time. TMOF = trimethyl orthoformate.

Further investigations involved the inspection of the influence of several additives on the reaction outcome (Table 3.13, further details: Subsection 5.7.1, Table 5.23 and Table 5.24). The addition

of molecular sieves (MS) was tested to improve the product yield by in situ abstraction of the generated H_2O. The idea was to prevent the previously discussed side reaction towards the allylic hydroxy byproduct; instead, this resulted in a lower yield. So, the reaction with water does not compete under the present reaction conditions. Varying the base, which previously showed a better reaction outcome in similar transformations and was proposed to raise nucleophilicity by deprotonation of the amine,[155,156] did not lead to an improved reaction outcome.

Table 3.13: Kinetic Investigation of the Racemic Intermolecular Allylic Amination with Azoles.[a]

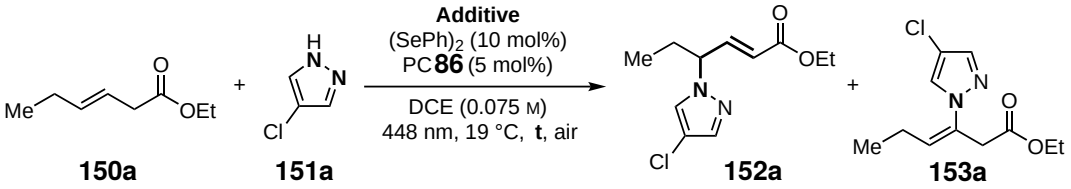

---	MS 3 Å	TEMPO	$(4\text{-ClPhS})_2$	Me_6Si_2	NaF	Li_2CO_3
6 h, 63%, 6:1 8 h, 65%, 6:1 21 h, 68%, 5:1	8 h, 53%, 13:1[b]	21 h, 0%, --[c]	8 h, 69%, 13:1[d]	21 h, 19%, 2:1[e,f] 21 h, 10%, 1:0[e,g]	6 h, 48%, 4:1[e]	6 h, 45%, 4:1[e]

KF_6P	CaF	Na_2HPO_4	TfOH	TFA	$Sc(OTf)_3$	
6 h, 46%, 5:1[e]	6 h, 64%, 6:1[e] 6 h, 64%, 5:1[h]	6 h, 24%, 4:1[e]	8 h, 0%, --[e]	8 h, 32%, 6:1[e]	8 h, 67%, 6:1[i] 8 h, 60%, 60:1[j]	21 h, 69%, 7:1[i] 21 h, 60%, 1:0[j] 21 h, 66%, 1:0[i,k]

$Zn(OTf)_2$	$AlCl_3$	$Yb(OTf)_3$
8 h, 63%, 6:1[i]	8 h, 30%, 5:1[j]	8 h, 68%, 6:1[i]

-- with 5 mol% $(4\text{-ClPhS})_2$ ----------

---	2-Nitrobenzaldehyde	$Sc(OTf)_3$	$Yb(OTf)_3$	NaBArF	$CaSO_4$
8 h, 69%, 13:1	8 h, 63%, 7:1[l] 21 h, 68%, 7:1[l]; 21 h, 63%, 6:1[j]	8 h, 58%, 1:0[j,m]	21 h,71%, 6:1[i]	21 h, 64%, 8:1[n]	21 h, 66%, 8:1[o]

AcOH	HFIP	MeOH
21 h, 68%, 11:1[e]	21 h, 68%, 10:1[l]	21 h, 62%, 13:1[e]

[a] 0.30 mmol of **151a**, 3.0 equiv. of **150a**. NMR yields of **152a** and ratios of the two isomers (**152a**:**153a**) were determined with DMB as the internal standard. Grayed entries were performed by Dr. T. Lei. [b] 9.14 mg of additive. [c] 20 mol% of additive. [d] 5 mol% of additive. [e] 1.0 equiv. of additive. [f] 1.0 mmol of **151a**, 3.0 equiv. of **150a**. [g] 1.0 mmol of **150a**, 3.0 equiv. of **151a**. [h] 4.0 equiv. of additive. [i] 2.5 mol% of additive. [j] 10 mol% of additive. [k] 9.00 mg of MS (4 Å) added. [l] 25 mol% of additive. [m] 10 mol% of $(4\text{-ClPhS})_2$ used. [n] 4 mol% of additive. [o] 1.22 equiv. of additive. MS = molecular sieves. TEMPO = 2,2,6,6-Tetramethylpiperidinyloxyl. NaBArF = Sodium tetrakis[3,5-bis(trifluoromethyl)phenyl]borate.

Silane, which in a previous study by the Breder group showed a benefit probably due to hindrance of degradation of the Se-catalyst, resulted in a significant decrease in yield during this transformation.[167,205] Remarkably, the usage of 10 mol% of Lewis-acid $Sc(OTf)_3$ led to a significantly improved allyl-to-vinyl ratio. This may result from an increased decay or reactivity of enamine

153a by the LEWIS-acid explaining the lack of improved yield of the desired allylic amine albeit unchanged full conversion compared to the reaction without additive.[206–208] Another explanation could be the coordination of the LEWIS-acid to the carbonyl O-atom, enhancing the acidity of the α-protons and with this favouring the formation of allylic product **152a** over vinylic **153a**.
After extensive research into the influence of altered reaction conditions, reactants, and the incorporation of additives, further efforts were directed towards broadening the scope of the reaction. Increasing the scale from 0.3 mmol to 1.0 mmol was intended to obtain more representative results in the following substrate scope (Table 3.14). Raising the amount of reaction mixture in the previously used 40 mL vials with varying concentrations (Table 3.14, entries 2-4) led to decreased yields compared to the 0.3 mmol scale (Table 3.14, entry 1). The reason for this might be the decreased light input into the larger reaction volume, as the surface area of the mixture exposed to irradiation remained unchanged.

Table 3.14: Scale-up of the Intermolecular Allylic Amination with Azoles.

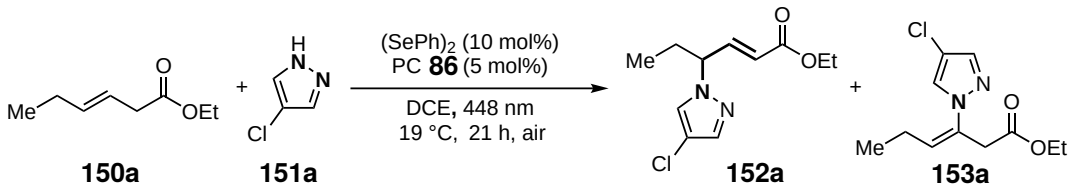

150a **151a** **152a** **153a**

Entry	**150a**	**151a**	Concentration [M]	Yield[a] [%]			**152a/153a**
				152a	**153a**	Total	
1[b]	3.0 equiv.	0.30 mmol	0.075	68	15	83	5:1
2[b]	3.0 equiv.	1.0 mmol	0.075	16	0	16	1:0
3[b]	3.0 equiv.	1.0 mmol	0.2	31	3	34	10:1
4[b]	3.0 equiv.	0.50 mmol	0.1	60	9	69	7:1
5[c]	3.0 equiv.	0.50 mmol	0.075	67	15	82	4:1
6[c]	3.0 equiv.	1.0 mmol	0.075	62	10	72	6:1
7[c]	3.0 equiv.	1.0 mmol	0.2	68 (68)	15 (13)	83 (81)	5:1
8[c,d]	3.0 equiv.	1.0 mmol	0.2	72	6	78	13:1
9[c]	1.0 mmol	3.0 equiv.	0.2	68 (68)	5 (3)	73 (71)	14:1
10[c,d]	1.0 mmol	3.0 equiv.	0.2	63	2.5	66	25:1

[a]NMR yields were determined with DMB as the internal standard. Isolated yields are given in parentheses. [b]40 mL reaction vial used. [c]100 mL round bottom flask used. [d](4-ClPhS)$_2$ (5 mol%) added.

To address this issue, a 100 mL round bottom flask was chosen as the reaction vessel in the following scale-up tests, increasing the light input surface. And indeed, when the same reaction conditions were applied to a 1.0 mmol scale, with 3.0 equiv. of the alkene compound **150a** and

a reaction concentration of 0.075 M, the results affording 62% of **152a** were very similar to the 0.3 mmol-scale reaction in the 40 mL vial (Table 3.14, entry 6). Reducing the amount of solvent and, with this, increasing the concentration to 0.2 M resulted in a further increase in yield to 68% of **152a** and an allyl/vinyl ratio of 5:1, comparable to the yield of the previously conducted smaller-scale reaction (Table 3.14, entry 7). When adding 5 mol% of additive $(4\text{-ClPhS})_2$ to the reaction, the yield of **152a** was further increased to 72% with an excellent allyl-to-vinyl ratio of 13:1 (Table 3.14, entry 8). This supports the previous observation that disulfide $(4\text{-ClPhS})_2$ positively influences the intermolecular allylic amination reaction towards higher yields of the desired allylic amine and increased selectivity. By reversing the stoichiometry and applying 1.0 mmol of **150a** as the limiting compound, the allylic compound was obtained with a 68% yield, and an even better ratio of 14:1 (Table 3.14, entry 9). Adding 5 mol% of $(4\text{-ClPhS})_2$ to these reaction conditions resulted again in a further increase of product ratio to 25:1 but a decreased yield of the desired allylic amine **152a** to 63% (Table 3.14, entry 10).

3.3.3 Synthesis of β,γ-unsaturated esters

With the optimised reaction conditions in hand, the synthesis of suitable alkene coupling partners was performed to expand the scope of the reaction. To observe the influence of substituents and functional groups on the outcome of the reaction, a variety of β,γ-unsaturated esters with different electron-withdrawing groups were synthesised. Esterification of (*E*)-hex-3-enoic acid (**167**) and (*E*)-hex-3-enedioic acid (**168**) with benzyl alcohol, assisted by acidic catalysis with *p*-TsOH·H_2O, afforded the desired esters benzyl (*E*)-hex-3-enoate (**150b**) and dibenzyl (*E*)-hex-3-enedioate (**150c**) (Table 3.15).[150]

Table 3.15: Synthesis of **150b** and **150c**.

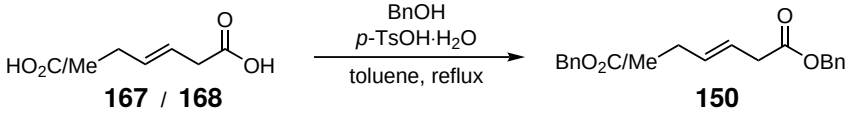

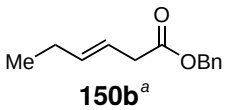	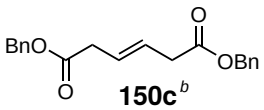
150b[a]	**150c**[b]
quant.	29%

[a](*E*)-hex-3-enoic acid **167** (24.9 mmol, 1.00 equiv.), *p*-TsOH·H_2O (4 mol%), BnOH (1.61 equiv.), 16 h. [b](*E*)-hex-3-enedioic acid **168** (10.0 mmol, 1.00 equiv.), *p*-TsOH·H_2O (22 mol%), BnOH (2.00 equiv.), 24.5 h.

An alternative route towards diester **150c** was performed by Dr. T. Lei (Equation 3.7).[168] In situ formation of an active ester with 1-ethyl-3-(3-dimethylaminopropyl)carbodiimid (EDAC), catalysed

by 4-(*N*,*N*-dimethylamino)pyridine (DMAP), afforded the desired product in 83% yield.

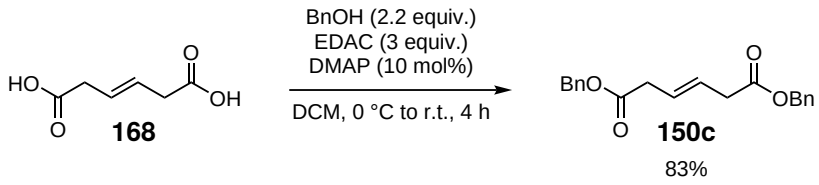

(3.7)

In the following, substrates with varying electron-withdrawing groups (EWG) were synthesised. The introduction of a cyanide functional group was achieved by the transformation of (*E*)-hex-2-en-1-ol **169** (Equation 3.8). The hydroxy group (-OH) of **169** is transferred into a good leaving group by dropwise addition to a solution of NaI and trimethylsilyl chloride (TMSCl) in MeCN. The reaction is proposed to be facilitated by the in situ formed complex $[MeCN\text{-}SiMe_3]^+I^-$, affording the respective allylic iodide.[209–211] The intermediate then undergoes nucleophilic substitution with KCN, affording the desired product **150d**.

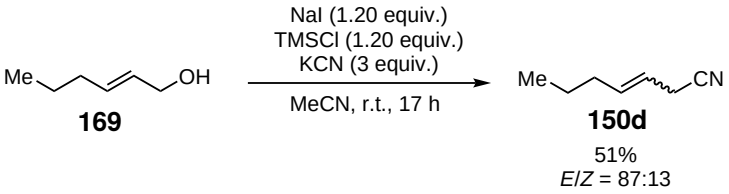

(3.8)

Additionally, two substrates with a sulfonylbenzene group as the electron-withdrawing group in β-position to the alkene were synthesised. The respective β-bromoalkene **170** is converted to its sulfonylbenzene **150e** (R = Me) and **150f** (R = Ph) by nucleophilic substitution with sodium benzenesulfinate (Table 3.16). When crotyl bromide **170a** was applied in the reaction, which consists of 85% *trans*- and 15% *cis*-alkene, a similar *E*/*Z* ratio of 91:9 in the product **150e** was afforded. The use of isomerically pure cinnamyl bromide **170b** resulted in the formation of **150f** exclusively in the *E* configuration.

Table 3.16: Synthesis of Sulfonylbenzenes But-2-en-1-ylsulfonyl benzene **150e** and Cinnamylsulfonyl benzene **150f**.

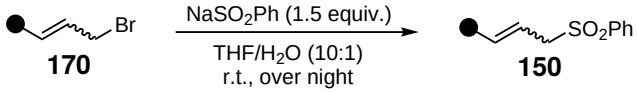

Me–⁄⁄–SO_2Ph	Ph–⁄⁄–SO_2Ph
150e	**150f**
quant.	68%
E/*Z* = 91:9	*E*

170a (R = Me): 85% *trans*, **170b** (R = Ph): only *trans*.

In a similar transformation, crotyl bromide **170a** (85% *trans*) afforded phosphonate **150g** by addition to diethyl phosphonate, which was previously treated with *n*BuLi (Equation 3.9).

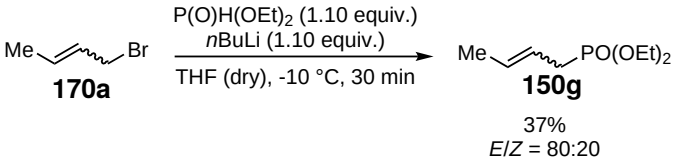

(3.9)

The NMR analysis of **150g** suggests two isomers present in the product mixture, proposed to be in an *E*/*Z* ratio of 80:20, resulting from the starting material with a similar ratio. Through ^{1}H NMR analysis, the corresponding signals could not be assigned to either *E*/*Z*-isomer due to overlap. So the proposed attribution was confirmed by 2D NMR analysis, with the minor isomer being the *Z*-isomer. Nuclear Overhauser Effect Spectroscopy (NOESY) NMR showed a coupling between H^a and H^b in the major signal, which is only expected for the *E*-isomer (Figure 3.12).

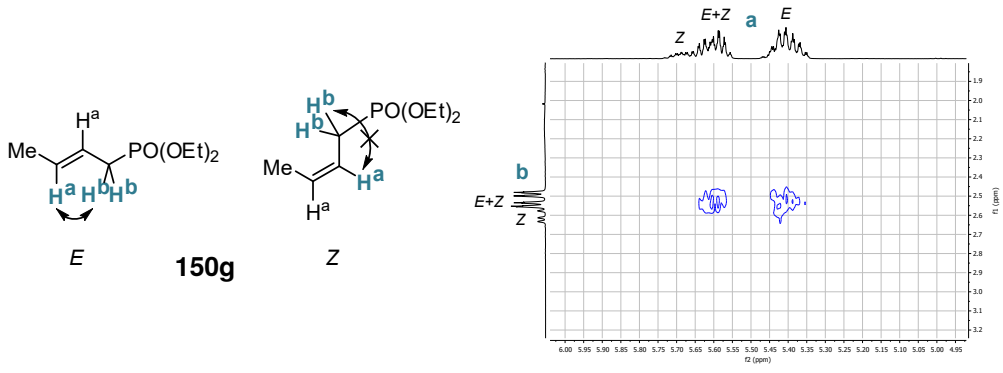

Figure 3.12: NOESY-Coupling expected for product **150g** and NOESY NMR experiment of **150g**.

Synthesis of **150h** was achieved by the formation of the active ester from (*E*)-hex-3-enoic acid

172a with *N*,*N*'-dicyclohexylcarbodiimide (DCC), and catalytic amounts of DMAP. Addition of oxazolidin-2-one **171** afforded the addition-elimination product **150h**.

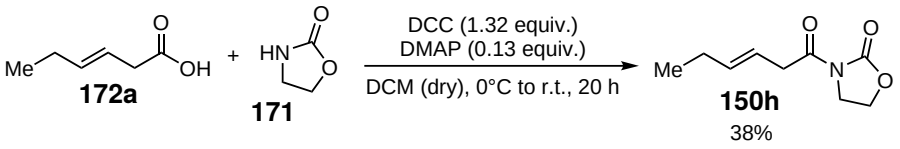

(3.10)

Further esters were synthesised by Dr. T. Lei or were bought from commercial vendors.[168] With a variety of starting materials in hand, their applicability in the previously optimised intermolecular photoaerobic/selenium-π-acid dual catalytic allylic amination with azoles was explored.

3.3.4 Intermolecular Allylic Amination

With the set of optimised conditions and various starting materials in hand, the substrate generality was examined. During the investigation of the substrate scope, it was found that for some substrates, the addition of $(4\text{-ClPhS})_2$ and/or the alteration of the solvent to a mixture of DCE and 1,1,1,3,3,3,-hexafluoropropanol (HFIP) led to a higher yield and/or selectivity. Also, some products performed better with reversed stoichiometry due to solubility issues. First, the alkene coupling partner was diversified by varying the ester moiety, incorporating several groups such as strained rings and various π-bonds, as well as acid-sensitive groups such as epoxides (**152b** to **152h**, Table 3.17). Remarkably, a present alkyne moiety remained intact after the reaction (**152f**). Diene compounds (**152g** and **152h**) displayed chemoselective transformation of *E*-alkenes in competition with *Z*-alkenes, forming α,β-unsaturated esters.[168] Such types of chemoselectivity are thought to arise from i) the −I effect exerted by the nearby oxygen (**152g** and **152h**) and ii) the elevated s-character of the carbon atoms in the alkyne. This characteristic likely makes the corresponding seleniranium ion less stable than the alkene's competing seleniranium ion.[168] This specific form of chemoselectivity (i.e., distinguishing between alkene and alkyne) has been noted in previous studies involving similar selenium-π-acid-catalyzed reactions, highlighting the remarkable effectiveness of this methodology in complex settings.[118] Conversely, the *Z*-isomer of alkene **150a** was transformed successfully and afforded **152a** with a slightly lower yield than with the *E*-configured starting material and an excellent regioselectivity. All reactions showed a preferential formation of the corresponding allylic product **152** compared to the vinylic isomer **153** with a minimum ratio of 5:1. Among others, **152b** was able to be isolated without any traces of **153b** noticeable in the performed analytical investigations. Instead, 8.20 mg (3%) of **153b** were able to be separated and identified.

Table 3.17: Variation of the Ester Moiety.

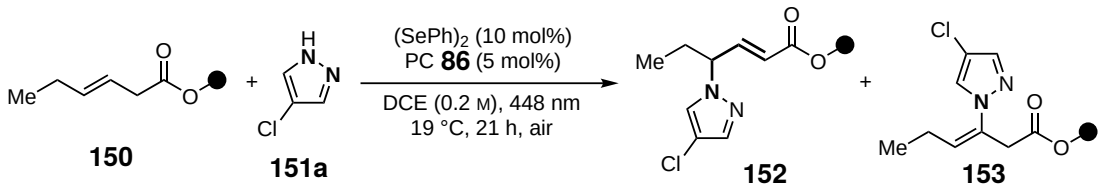

● =	Et	Ph	Bn	
	152a	**152b**	**152c**	**152d**
	68% (68%, r.r. = 14:1)[a] 51% (47%, r.r. = 26:1)[a,b]	62% (58%, r.r. = 8:1)[a]	61%, r.r. = 20:1 (55%, r.r. = 14:1)[a]	75%, r.r. = 33:1 (72%, r.r. = 7:1)[b]
	152e	**152f**	**152g**	**152h**
	74%, r.r. = 6:1 (73%, r.r. = 5:1)[b]	55% (60%, r.r. = 20:1)[b,c]	70% (66%, r.r. = 7:1)[b]	40% (43%, r.r. = 13:1)[b]

Yields of **152** and regioisomeric ratios (r.r. = **152**/**153**) are given. The respective NMR values were determined with DMB as the internal standard and are given in parentheses. Grayed substrates were synthesised by Dr. T. Lei.[168] [a] Alkene **150** (1.0 mmol, 1.0 equiv.), nucleophile **151a** (3.0 equiv.). [b] Ethyl (*Z*)-hex-3-enoate used as the alkene starting material. [c] Alkene **150** (3.0 equiv.), nucleophile **151a** (1.0 mmol, 1.0 equiv.). [d] (4-ClPhS)$_2$ (5 mol%) added.

Prolonging the alkyl moiety of the ester, as well as the incorporation of a variety of polar groups, readily led to the desired products with a yield ranging between 53 and 99%.[168] These results demonstrate the tolerance of the system towards standard functional groups such as halide, cyanide, arene, ether, and ester moieties. This is especially noteworthy, as previous reports on the oxidative allylic amination of azoles mostly covered alkenes without any functional groups.[56,99,197–199] The title reaction hereby enables a broader product scope and enhances the general value of the oxidative allylic amination of alkenes.

Excellent yields of 81–99% were obtained for symmetrically substituted diesters with both aliphatic and aromatic moieties without any vinylic isomer detected, indicating the preferential formation of the Hofmann product over the corresponding Zaytsev product (Table 3.18).[168] The symmetry of the diester reduces the total number of potential isomers and enhances the yields of the desired allylic products.

Table 3.18: Variation of Diester Moiety.

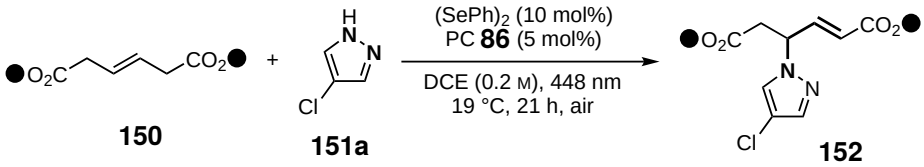

● =	Et	Bn
	152i	**152j**
	>99% (99%)[a] 76% (85%)[b]	81% (85%)[b] 89% (92%)[a]

The NMR yields were determined with DMB as the internal standard and are given in parentheses. Grayed substrates were synthesised by Dr. T. Lei. [a] Alkene **150** (3.0 mmol, 3.0 equiv.), nucleophile **151a** (1.0 equiv.). [b] Alkene **150** (1.0 mmol, 1.0 equiv.), nucleophile **151a** (3.0 equiv.).

Besides ester compounds, other electron-withdrawing groups such as malonyl, sulfate, cyanide, and phosphonate were able to induce acidity bias on the allylic positions, providing *N*-allylation products preferentially with good outcomes (Table 3.19). Other substitution patterns of olefins, such as trisubstituted and terminal alkenes, were readily transformed into the products, significantly expanding the scope of the applicable substrates, including substrates with different substitution patterns. A pleasant finding was when 1,1,2-trisubstituted alkene provided allylic azole **152n** in Markovnikov selectivity. For monosubstituted alkenes with electron withdrawing groups in the allylic position (i.e. **152l**, **152o**, **152s** **152v**, **152w**, and **152y**), the C–N bond forming process occurs at the terminal C-atom, which is less affected by the −I effect of the EWG. This definition is in accordance with the IUPAC definition of the Markovnikov selectivity, which states that its selectivity refers to the formation of the C–N bond at the carbon atom that electronically stabilises the positive charge best in the preceding seleniranium ion intermediate.[212] This has also been used in related contexts.[213] For the reactions depicted in Table 3.19, neither a distinct signal for the respective vinylic isomers **153** could be detected in the crude NMR analysis nor could any be isolated, once more demonstrating the high selectivity of the reaction.

Table 3.19: Variation of Substitution Pattern.

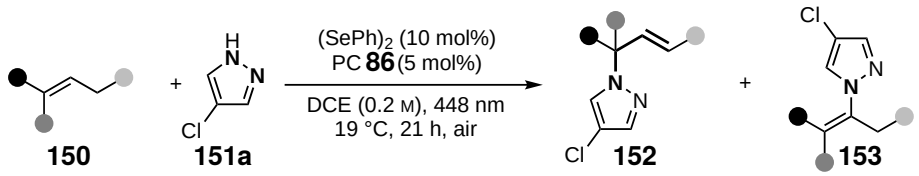

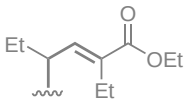	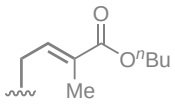	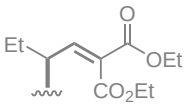	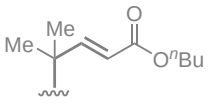	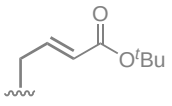
152k	**152l**	**152m**	**152n**	**152o**
67%	61%	not isolated	68%	66%
(66%)[a]	(63%)[a]	(n.d.)[b]	(65%)[a]	(62%)[a]
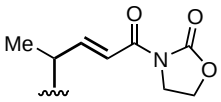	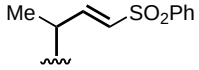	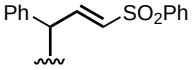	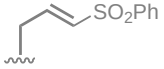	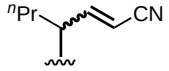
152p	**152q**	**152r**	**152s**	**152t**
not isolated	42%	not isolated	78%	26%
(27%)[c]	(39%)[c]	(n.d.)[c]	(78%)[a]	(27%)[a,d]
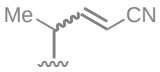	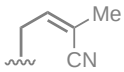	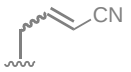	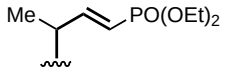	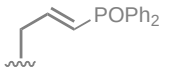
152u	**152v**	**152w**	**152x**	**152y**
75%	51%	78%	n.r.	64%
(80%)[a,e]	(53%)[a]	(78%)[a,f]		(62%)[a]

Yields of **152** and regioisomeric ratios (r.r. = **152**/**153**) are given. The respective NMR values were determined with DMB as the internal standard and are given in parentheses. Grayed substrates were synthesised by Dr. T. Lei. [a]Alkene **150** (3.0 equiv.), nucleophile **151a** (1.0 mmol, 1.0 equiv.). [b]Alkene **150** (1.0 mmol, 1.0 equiv.), nucleophile **151a** (6.5 equiv.). The di-aminated Michael addition-product **174** was formed (see Equation 3.11). [c]Alkene **150** (1.0 mmol, 1.0 equiv.), nucleophile **151a** (3.0 equiv.). [d]*E*/*Z* = 5:1 (3:1). 27.0 mg (10%) of the selenoaminated intermediate could be isolated and elucidated (see Subsection 5.7.4). [e]*E*/*Z* = 6:1 (4:1). [f]*E*/*Z* = 1:1 (1:1). n.d. = not determined, n.r. = no reaction.

Interestingly, when employing 1,1-substituted diester **150i** as the alkene compound, the in situ formed α,β-unsaturated diester (**152m**) can serve as an active enough Michael-acceptor to capture another *N*-nucleophile in a consecutive reaction, affording di-aminated product **174**, when 6.5 equiv. of pyrazole **151a** were used (Equation 3.11).[168]

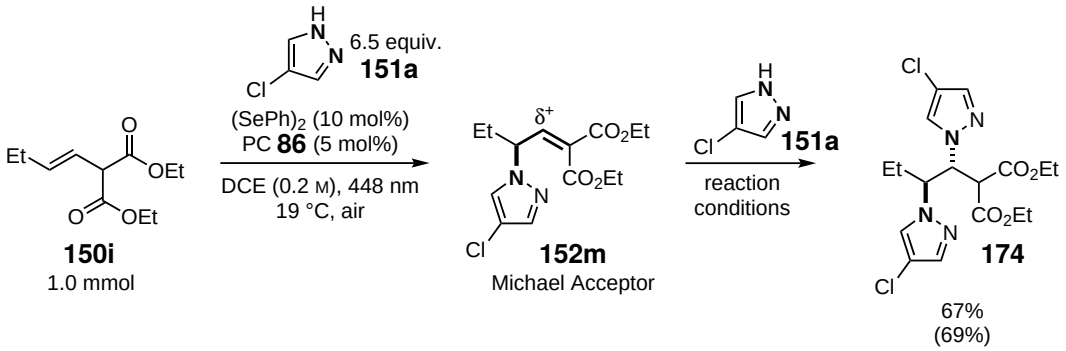

(3.11)

α,β-Unsaturated sulfonylbenzene **152r** was not successfully isolated. Instead, styrene isomer **173a** was formed and isolated in 16% yield. This probably resulted from preferential elimination of the more acidic benzylic proton in the product releasing step in comparison to the proton adjacent to the sulfonyl group in intermediate **175** (Equation 3.12). The ability of styrenes to absorb light or undergo SET with excited state photocatalysts[214,215] indicates side reactions of the starting material **150f** and/or follow-up reactions of the formed **152r** taking place, that may account for the low yield despite complete conversion of the starting material.

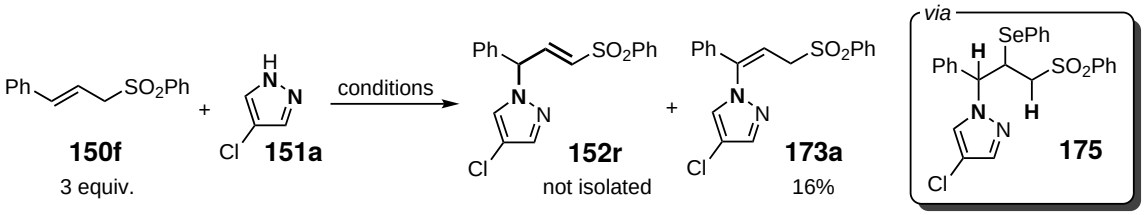

(3.12)

The isomer was identified by NMR analysis. ^{1}H NMR of the isolated material shows a doublet (2H) and triplet (1H) in the aliphatic region that couple with each other in a vicinal coupling (Figure 3.13) indicating a tertiary carbon atom present. A substitution in the β-position to the sulfonyl group was excluded, as a central tertiary carbon would separate the other two protons and would afford two singlet signals in the spectra. This led to the proposed structure of the styrylic product **173a**, which was presumably formed from **150f** by nucleophilic attack of **151a** in γ-position to the sulfonyl group. The following construction of a vinylic double bond might be driven by the formation of a conjugated π-system with the adjacent benzyl ring *via* elimination of the acidic benzylic proton, favoured over a conjugated system with the sulfonyl group.

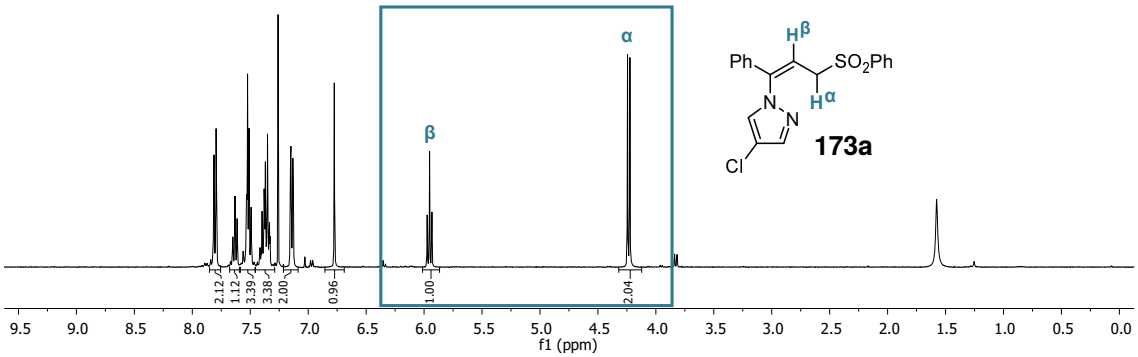

Figure 3.13: ^{1}H NMR spectrum of **173a**.

The configuration of **173a** was identified *via* 2D NMR analysis (Figure 3.14). Spatial coupling of the aliphatic protons of the *Z*-isomer **173a** with the aromatic protons would produce two coupling signals, whereas the *E*-isomer **173b** would only show a coupling of H^a with both aromatic rings (Figure 3.14, I.). The NOESY NMR experiment shows both H^a and H^b coupling to aromatic protons, indicating the *E*-configuration being present (Figure 3.14, II. left). The analysis also confirms that the aliphatic protons couple to different ring systems. COSY NMR experiment could identify two aromatic ring systems, as their respective protons only couple with each other. The downfield shifted sulfonylbenzene shows signals in the region of 7.4 to 7.78 ppm (Figure 3.14, II. right: green box) and another aromatic system (styrylic benzene) ranges from 7.0 to 7.4 ppm (Figure 3.14, II. right: yellow box). As expected, H^b shows coupling to protons of the styrylic benzene (yellow), whereas H^b couples with sulfonylbenzene (green).

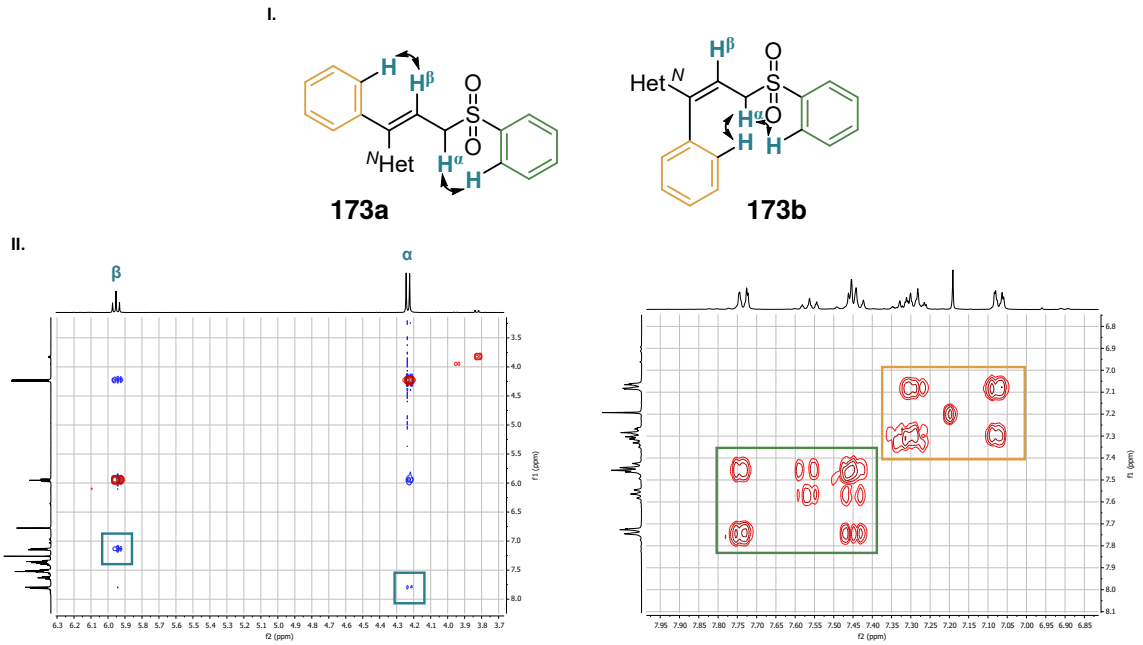

Figure 3.14: I. NOESY-Coupling expected for *E*-configured product **173a** and *Z*-configured product **173b**. II. Left: Excerpt of NOESY NMR experiment of **173**. Right: Excerpt of COSY NMR experiment of **173**.

To further express the utility and versatility of the title approach, the scope was expanded to simple alkenes (Table 3.20). Both 4-chloropyrazole **151a** and benzotriazole **151b** were applied to *trans*-7-tetradecene and cyclododecene (**152z** to **152ac**). A mixture of allylic and vinylic isomers was isolated in the case of the linear alkene. The desired allylic compounds were afforded in excellent purity for the cyclic alkene. Further, non-functionalised 1,1,2-trisubstituted alkenes were applied, affording **152ad** and **152ae** in MARKOVNIKOV-selectivity, complementing existing reports. Previous methods on photoredox catalytic amination of nonpolar alkenes through radical ionic π-bond activation typically exhibit *anti*-Markovnikov selectivity.[98,99,168] This indicates the intrinsic selective behaviour of the developed method towards the allylic compound over the vinylic one even without the interference of electron-withdrawing groups (compare with **152n**, Table 3.19).

Table 3.20: Simple Alkenes and MARKOVNIKOV-Selectivity.

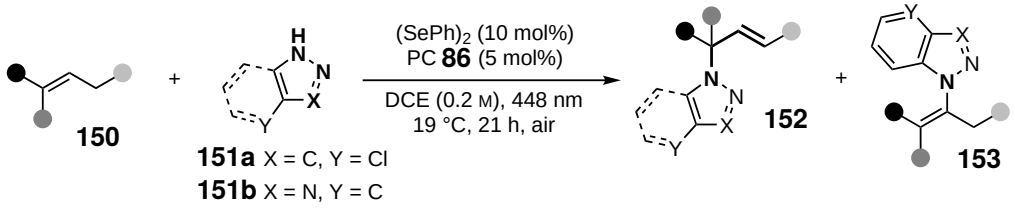

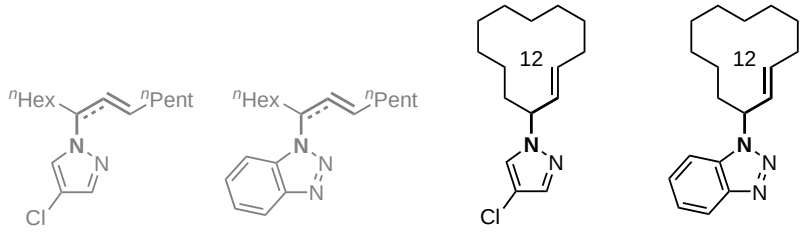

152z
50%, r.r = 4:1
(49%, r.r = 4:1)[a,c]

152aa
51%, r.r = 1:1
(60%, r.r = 1:1)[a,c]

152ab
31%
(33%)[a]

152ac
41%
(45%)[a]

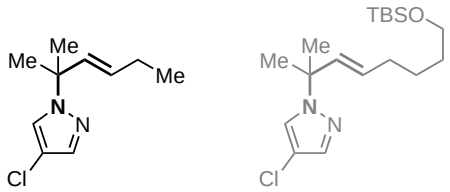

152ad
41%
(46%)[b,c]

152ae
34%
(46%)[a,c]

Yields of **152** and regioisomeric ratios (r.r. = **152**/**153**) are given. The respective NMR values were determined with DMB as the internal standard and are given in parentheses. [a]Alkene **150** (1.0 mmol, 1.0 equiv.), nucleophile **151a** (3.0 equiv.). [b]Alkene **150** (3.0 equiv.), nucleophile **151a** (1.0 mmol, 1.0 equiv.). n.r. = no reaction. [c](4-ClPhS)$_2$ (5 mol%) added.

Proceeding from these auspicious results, the scope of N-nucleophiles was regarded by coupling a variety of different azoles with asymmetrically substituted monoester **150a** (Table 3.21) and symmetrically substituted diester **150j** (Table 3.22). Functional groups such as halides, esters, arenes, and aldehydes once again proved the overall compatibility of the developed method.[168]

Table 3.21: Nucleophile **151** Variation with Monoester **150a**.

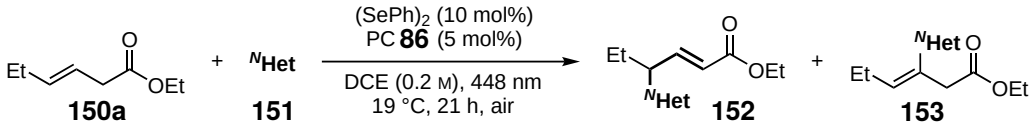

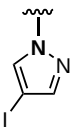	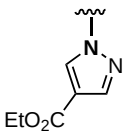	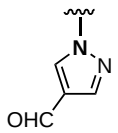	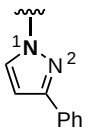	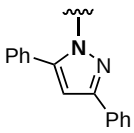
152af	**152ag**	**152ah**	**152ai**	**152aj**
64%	60%	24%	51%	38%
(64%, r.r. = 21:1)[a]	(62%, r.r. = 5:1)[a]	(37%, r.r. = 5:1)[a]	(53%)[a,b]	(65%, r.r. = n.d.)[a]
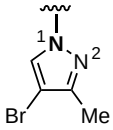	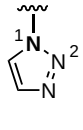	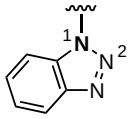	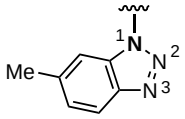	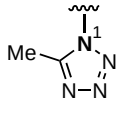
152ak	**152al**	**152am**	**152an**	**152ao**
57%	not isolated	*N*[1]: 61% (62%, r.r. = 4:1)	62%	36%
(58%)[a,b]	(55%)[a]	*N*[2]: 3% (n.d.)[a]	(61%, r.r. = 3:1)[a,c]	(40%, r.r. = 10:1)[a]
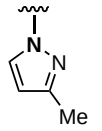	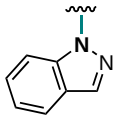	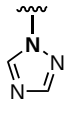	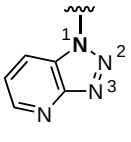	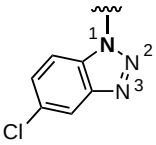
152ap	**152aq**	**152ar**	**152as**	**152at**
not isolated	not isolated	not isolated	not isolated	not isolated
(4%)[a,b]	(27%)[a]	(12%)[a]	(17%)[a]	(16%)[a]

Yields of **152** and regioisomeric ratios (r.r. = **152**/**153**) are given. The respective NMR values were determined with DMB as the internal standard and are given in parentheses. [a]Alkene **150** (1.0 mmol, 1.0 equiv.), nucleophile **151a** (3.0 equiv.). [b]N^1/N^2 = 5:1. [c]N^1/N^3 = 1:1. n.d. = not determined. [c]Second addition of both catalysts after 21 h. Overall reaction time of 41 h.

Several products arising from heteroarenes showed the formation of isomers with different *N*-connectivities, which were isolated collectively in products **152ai**, **152ak**, and **152an**. Missing NOESY-coupling of the phenyl ring to the aliphatic protons in **152ai** indicates the N^1-isomer, as depicted in Table 3.21, to be the major isomer. Contrarily, the aromatic proton of the major isomer

of **152ak** does show a NOESY coupling to aliphatic protons, which also indicates the N^1-isomer as depicted in Table 3.21 to be the major isomer. The analytical details are depicted in Chapter 6. On the other hand, the N^1 and N^2-isomers of compound **152am** could be isolated separately, with 61% of the N^1- and 3% of the N^2-isomer (for characterisation see Subsection 5.7.4). A small NOESY-coupling of the isolated methyl group with methylene (CH_2) of the aliphatic ethyl group suggests an N^1-connectivity in tetrazole product **152ao** (Figure 3.15). Additionally, 5% (4% NMR yield) of the corresponding vinylic isomer **153ao** was isolated and characterised.

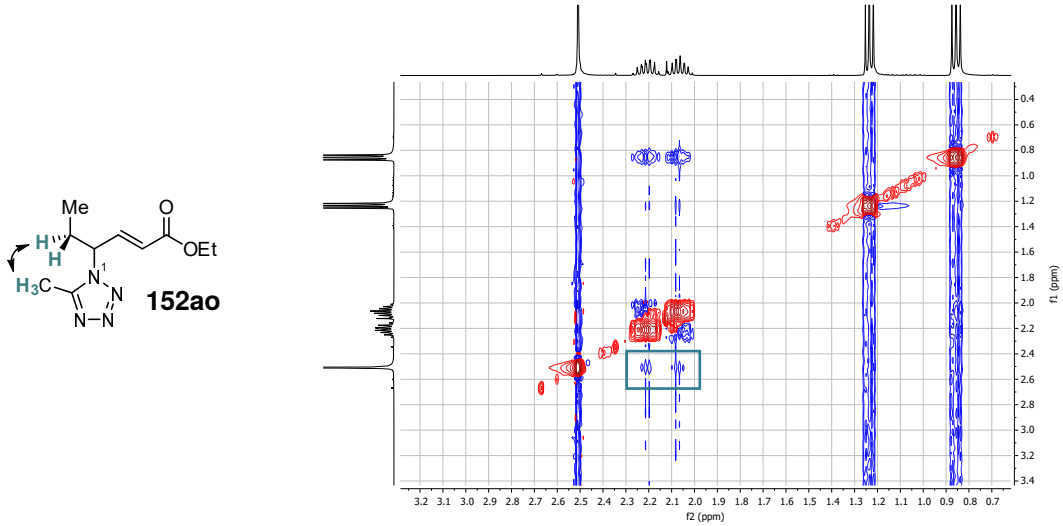

Figure 3.15: NOESY-Coupling of aromatic methyl group and excerpt of NOESY NMR experiment of **152ao**.

Notably, after 21 h of reaction time, the reaction mixture of **152ap** was clear, in contrast to the mostly observed orange coloured suspension, and TLC showed still a lot of starting material present. This was also noticed to be the case with other unsuccessful substrates (see Table 3.24). As a consequence, catalysts were readded and the reaction was let run for a further 20 h, after which an NMR yield of only 4% was determined and isolation was not attempted. These observations and results indicate that the amine may quench the photocatalyst and promote its decay, prohibiting product formation. In another reaction, amine 1H-[1,2,3]triazolo[4,5-b]pyridine in the reaction mixture for **152as** exhibited low solubility in the used solvent DCE, which is proposed to have led to a low yield. As a result, in equal cases, a solvent mixture of DCE/HFIP = 3:2 was used to enhance the solubility of the nucleophile (Table 3.22).

Excitingly, the reaction with 4-H pyrazole worked smoothly, contrary to the expected electrophilic addition of $(PhSe)_2$ to the heteroarene (Table 3.22, **152au**).[200–202] This inspired the further expansion of the nucleophilic pattern towards imidazoles, triazoles, and tetrazoles, which were found to give good results with perfect selectivity towards one *N*-isomer. NOESY analysis of tetrazoles **152ba**–**152bc** does not show any coupling of the substituent on the heteroarene to the alkyl chain, proposing a N^2-connectivity as depicted in Table 3.22 (for analytical details see Chapter 6).

Table 3.22: Nucleophile **151** Variation with Diester **150j**.

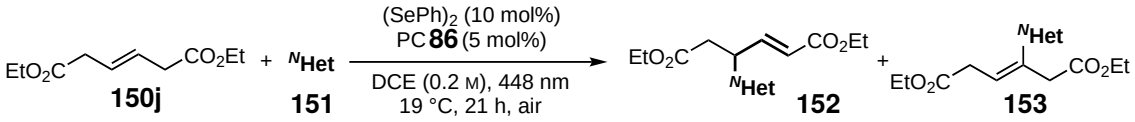

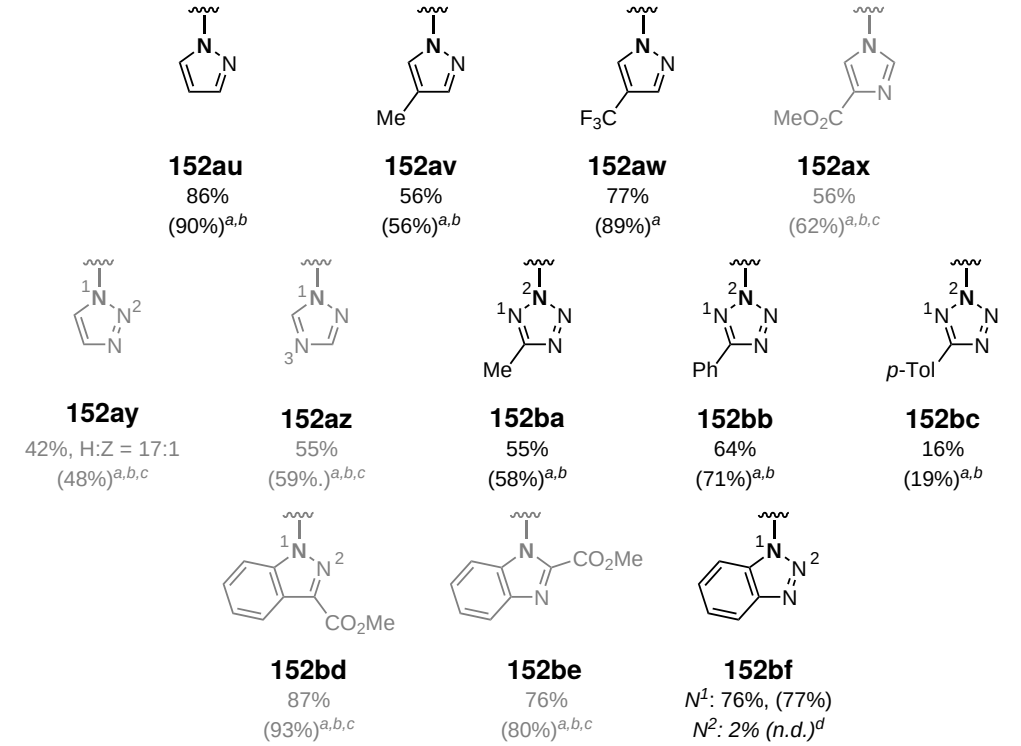

Yields of **152** and H:Z = HOFMANN:ZAYTSEV (**152**/**153**) elimination ratios are given. The respective NMR values were determined with DMB as the internal standard and are given in parentheses. Grayed substrates were synthesised and analysed by Dr. T. LEI.[168] [a] Alkene **150j** (3.0 equiv.), nucleophile **151** (1.0 mmol, 1.0 equiv.). [b] $(4\text{-ClPhS})_2$ (5 mol%) added. [c] DCE/HFIP = 3:2 used as the solvent. [d] Alkene **150j** (1.0 mmol, 1.0 equiv.), nucleophile **151** (3.0 equiv.).

In the next step, the method was tested in the course of late-stage derivatisation of known biologically active compounds that either performed as the designated nucleophile or alkene compound (Table 3.23). An ester derivative of Testosterone gave good yields with both 4-choropyrzole (**152bj**) and benzotriazole (**152bk**) in high regioselectivity. Derivatisation of commercially available pharmaceutical compounds Stanozolol, Irbesartan, and Valsartan, all decorated with an azole moiety, were also readily accepted in the transformation (**152bg** to **152bi**). Notably, the nucleophilic hydroxy moiety in compound **152bg** and the carboxylic acid in compound **152bi** remained intact and did not interfere with the reaction.

Table 3.23: Late-Stage Functionalisation of Biologically Active Compounds.

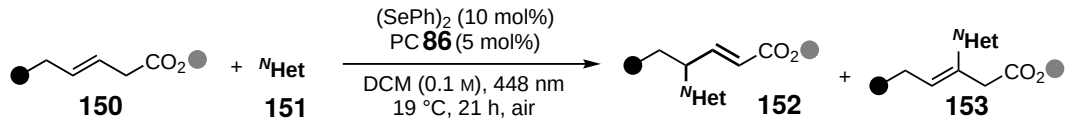

from Stanozolol

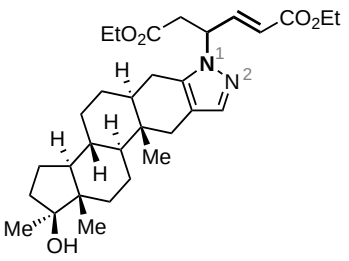

152bg
48%, d.r. = 1:1
(51%, 4:1)[a,b,c,d]

from Irbesartan

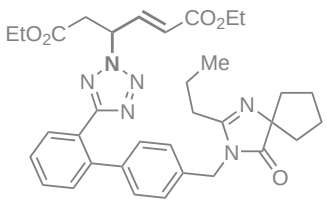

152bh
35%
(53%)[a,b,c]

from Valsartan

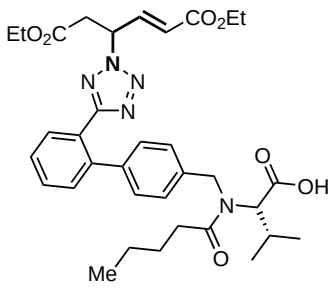

152bi
not isolated
(37%)[a,b]

from Testosterone

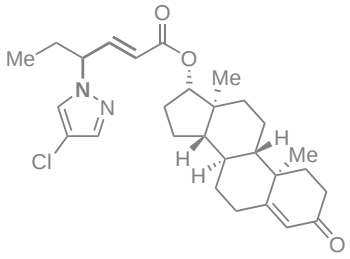

152bj
74%, r.r. = 11:1, d.r. = 1:1
(76%)[b,e]

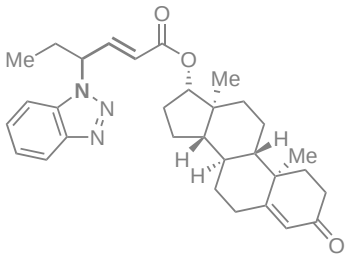

152bk
58%, d.r. = 1:1
(62%)[b,e]

Yields of **152** and regioisomeric ratios (r.r. = **152**/**153**) are given. The respective NMR values were determined with DMB as the internal standard and are given in parentheses. Grayed substrates were synthesised by Dr. T. Lei. [a] Alkene **150** (3.0 equiv.), nucleophile **151** (1.0 mmol, 1.0 equiv.). [b] $(4\text{-ClPhS})_2$ (5 mol%) added. [c] DCE/HFIP = 3:2 used as solvent. [d] N^1/N^2 = 5:1. [e] Alkene **150** (1.0 mmol, 1.0 equiv.), nucleophile **151** (3.0 equiv.).

During the substrate investigation, several N-nucleophiles did not lead to the desired product formation under the optimised reaction conditions (Table 3.24). For example, in the attempted coupling of alkene **150a** with N-heteroarenes bearing only one nitrogen atom, such as pyrrole (**152bl**) and **152bm**, no product was identified in the crude reaction mixture *via* ^{1}H NMR analysis. Some electron-rich variants of imidazole and pyrazole (**152bn** to **152bp**) did not produce any product in contrast to electron-poor variants (see above), indicating that an electron-poor heterocycle is necessary for the transformation. Primary amines proved to be unsuccessful, as well, when incorporated next to a second nitrogen atom, such as in **152br**. Succinimide and sulfonamides were unsuccessful

as well. These results indicate the necessity of a heteroaromat acting as the nucleophile, which shows better results when possessing a lower electron density compared to analogues with elecron donating groups. When comparing the pK_a values in DMSO of successful with unsuccessful substrates, which may hint at the heteroarenes' reactivity and nucleophilicity, no trend could be detected.[216] Even though it seems that a lower pK_a value is beneficial for the reaction outcome, pyrazole falls out of that spectrum as it possesses a relatively high pK_a value.

Table 3.24: Unsuccessful Nucleophiles.

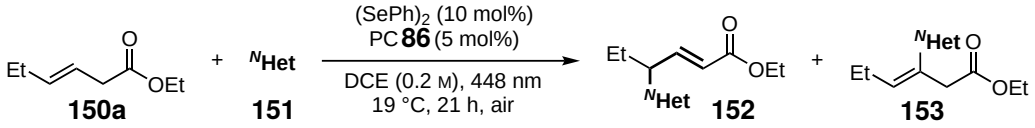

		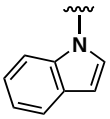	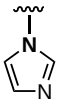	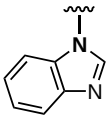	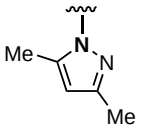
	152bl	**152bm**	**152bn**	**152bo**	**152bp**
pK_a (DMSO)[b]	23.0	21.0	18.6	16.4	-
	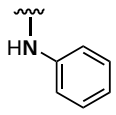	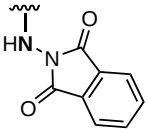	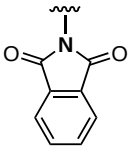	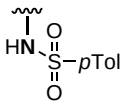	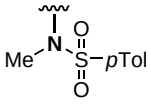	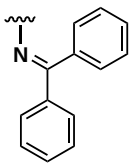
	152bq	**152br**	**152bs**	**152bt**	**152bu**	**152bv**
	30.6	-	-	16.1[c]	-	25.0
-- comparison to succesful nucleophiles						
		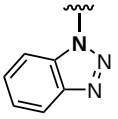	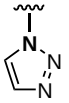	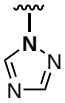		
	152a	**152am**	**152al**	**152ar**		
pK_a (DMSO)[b]	19.8	11.9	13.9	14.8		
NMR yield	68%	62%	55%	12%		

Alkene **150a** (1.0 mmol, 1.0 equiv.), nucleophile **151** (3.0 equiv.). [b] pK_a values of the nucleophiles in DMSO.[216,217] [b] pK_a value of $PhSO_2NH_2$.

Some of the amines **151** that would result in the depicted products in Table 3.24 exhibit low redox potentials, such as indole (E = +1.16 V vs. SCE in MeCN),[175] imidazole (E = +1.15 V vs. SCE in MeCN),[175] and aniline (E = +0.95 V vs. SCE in MeCN)[175] compared to pyrazole (E = +2.21 V

vs. SCE in MeCN).[175] In consequence, these amines are more easily oxidised and could quench the photoredoxcatalyst **86** (E = +1.74 V vs. SCE in MeCN)[150,152,153] and, with this, inhibit the formation of the respective products.
Due to the challenge of olefin activation in the presence of *N*-heteroarenes, followed by alterable site selectivity in the coupling step, only a few contributions have been made previously. Early reports employ stoichiometric amounts of strong oxidants (NBS, TBHP, DDQ) transforming alkenes with N-nucleophiles, mainly focusing on non-heteroarenes.[197–199] In 2022, the group of Gevorgyan reported an elegant photoinduced Pd-catalysed coupling for the buildup of N-allylic amines initiated by allylic C-H atom abstraction under the assistance of substoichiometric aryl halide, including two cases for heteroaryl rings and showing high regioselectivities (see also Equation 1.3 in Subsection 1.1.1). More recently, Lei, Cai, and coworkers reported a related N-allylation of azoles via a radical-cationic intermediate to mainly provide terminal alkene products.[99] Regiocontrol in the 1,2 position was achieved for mono- and trisubstituted alkene substrates due to their sterically and electronically easily differentiable environment. Yet, a protocol with 1,2-regiocontrol in 1,2-disubstituted alkenes remained elusive and with this, a synthetically useful process for the regioselective C-H, N-H coupling to afford N-allylic heteroarenes, with a broad alkene and azole scope and high functional group tolerance, is still required.
During the course of this thesis, the first highly regioselective and widely applicable Se-π-acid catalysed intermolecular allylic amination protocol with exogenous nucleophiles was developed. The transformation is made possible by a dual catalytic interaction with photocatalyst **86** acting as the oxidant. Various allylic azoles were synthesised from olefins *via* π-bond activation and in high selectivity towards the allylic product compared to its vinylic isomer, exploiting acidity bias and the formation of a conjugated system as the driving force. It is noteworthy that also simple olefinic carbohydrates without any heteroatoms were readily transformed into the respective functionalised products. Alkenes of various connectivity, such as terminal, 1,2-disubstituted and trisubstituted olefins, were both applied and synthesised successfully in the title transformation. Incorporation of the dual catalytic system enables the formation of Markovnikov products *via* photoredoxcatalysis, which complements previous methods.[98,99] All in all, the method proves to be of high synthetic value with a wide variety of starting materials able to be transformed to their corresponding allylic azoles, especially with the applicability in the late-stage functionalisation of biologically active compounds.

3.4 Enantioselective Intermolecular Allylic Amination with Azoles

Parts of the following investigatory results were published in 2024 in *ACS Catalysis*.[168]

Having established a robust protocol for the N-allylation of heteroarenes, initial efforts were made towards an enantioselective variant. Chiral Se-π-acid catalysts have previously shown the ability

to induce chirality in alkene functionalisation reactions.[218,219] First investigations towards the enantioselective photo-aerobic Se-π-acid catalysed intramolecular allylic lactonisation were made with enantiomeric ratios (e.r.) of up to 83.5:16.5 by applying MARKUOKA's catalyst.[118,220] In 2023, new asymmetric catalysts exhibiting a rigid spiro-backbone were designed by the BREDER group and successfully applied to the photo-aerobic Se-π-acid catalysed intramolecular allylic lactonisation and amination.[167] Their application to an intermolecular system was first investigated during the course of this thesis.

3.4.1 Preliminary Investigation

The reaction of monoester **150a** (3.0 equiv.) and chloropyrazole **151a** (0.30 mmol, 1.0 equiv.) was conducted with varying chiral Se-catalysts **136** (10–20 mol%) and photocatalyst **86** (5 mol%) in DCM (0.075 M) under irradiation with blue light (λ_{max} = 448 nm) (Table 3.25). All reactions afforded allylic amine **150a** with chiral information, marking this the first intermolecular example for the enantioselective photoaerobic/Se-π-acid dual catalytic functionalisation.
Out of the various catalysts, the highest enantiomeric excess (*ee*) was achieved with 20 mol% of MARUOKA's monoselenide (**136d**) (43%), with the second-highest yield (40%). The highest yield was achieved with 10 mol% DENMARK's diselenide catalyst (**136e**) (44%) but with an *ee* of only 25%. BREDER's spiro catalysts **136b**–**136a** afforded overall lower *ee*'s with an average of 35% (median: 33%) and lower yields (average: 20, median: 22). The rise in catalyst loading of photocatalyst **86** from 5 to 10 mol% did not influence the outcome. Only small amounts of isomer **153a** (1–6%) were formed in the investigated reactions.

Table 3.25: Variation of Chiral Se-Catalysts **136** in the Asymmetric Allylic Amination of **150a** with **151a**.

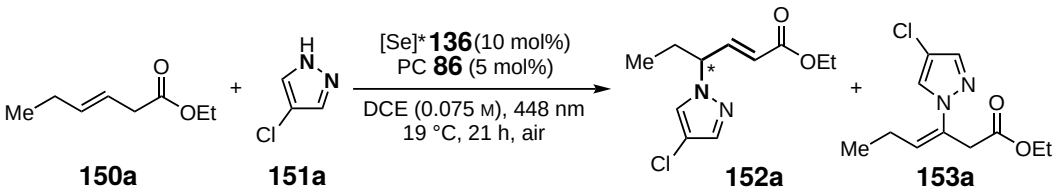

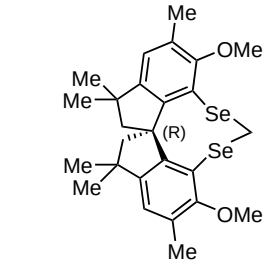

136b

24%, *ee* = 33%[a]

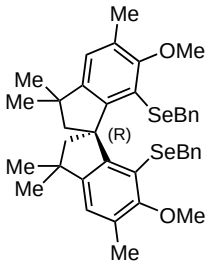

136a

20%, *ee* = 31%
22%, *ee* = 32%[a]

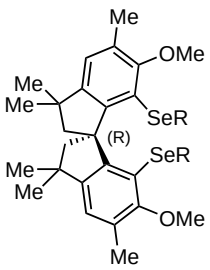

136c

R = 2,5-diOMeBn
13%, *ee* = 40%

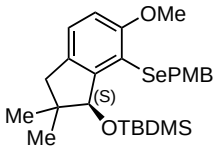

136d

40%, *ee* = 43%[b]

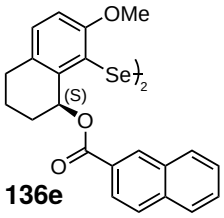

136e

44%, *ee* = 25%

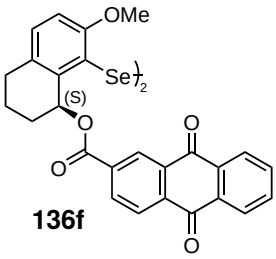

136f

3%, *ee* = n.d.[c]

0.30 mmol (1.0 equiv.) of **151a**, 3.0 equiv. of **150a**. Se-catalyst purity $\geq$ 99%. NMR yields are given and were determined with DMB as the internal standard. [a] 10 mol% TAPT used. [b] 20 mol% **136d** used. [c] 5 mol% **136f** and no **86** used. n.d. = not determined.

A kinetic investigation of the transformation with **136a** and varying stoichiometry showed that the reaction proceeded more slowly than its racemic equivalent (Figure 3.16, Table 5.29). Complete conversion was reached after 27.5 h when 3.0 equiv. of either starting material is applied, albeit reaching a yield of only 20–21%. A yield plateau was reached after 21 h, or even after 6 h for the reaction with 5.0 equiv. of pyrazole **151a**. The high conversion with a low yield outcome indicates slow product formation accompanied by yield-diminishing side reactions, such as the SCHENCK-ene oxidation (Section 3.3).[155,168,174] A product decay is proposed to be unlikely due to the long plateau phases. As a result, further investigations into advancing the reaction rate were performed.

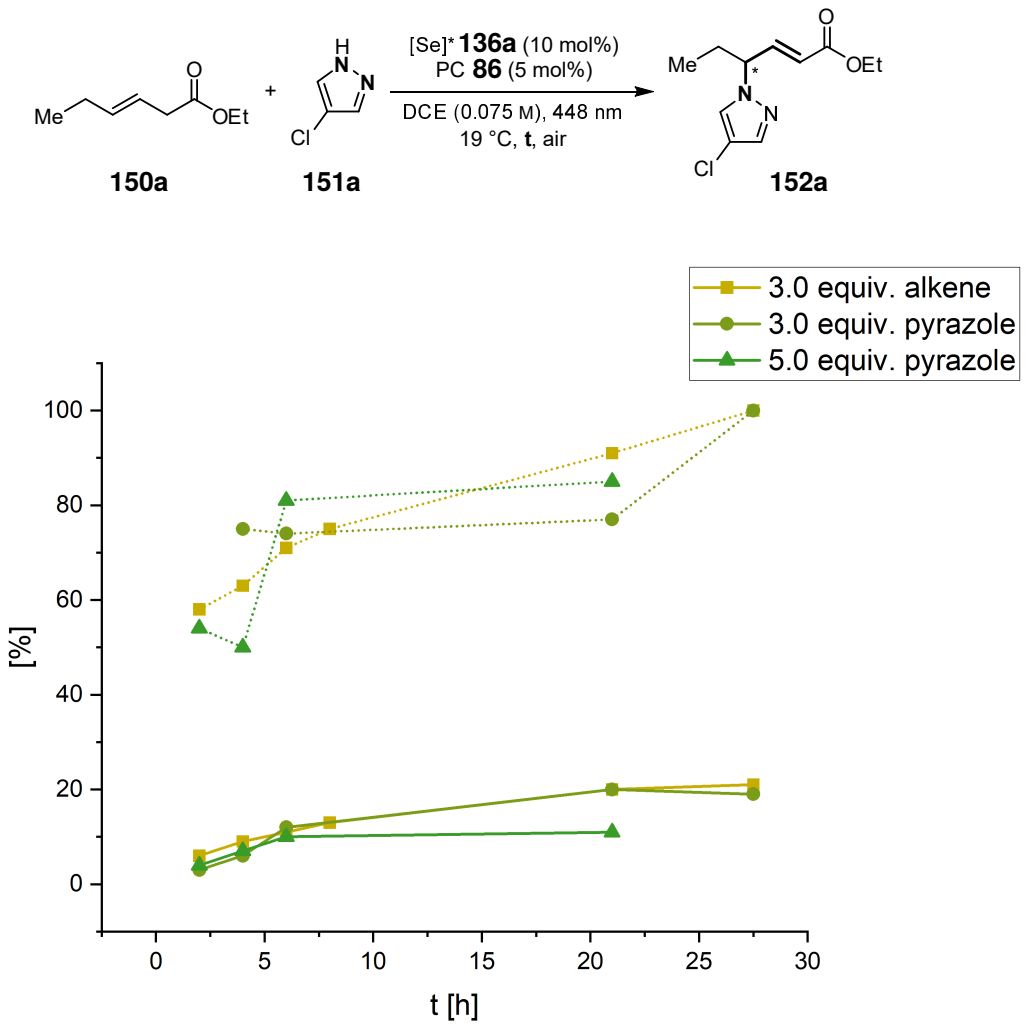

Figure 3.16: Kinetic investigation of the enantioselective amination of **150a** with **151a** using chiral Se-catalyst **136a**. 0.30 mmol of limiting compound used. Conversions and NMR yields were determined with DMB as the internal standard. Dotted lines show conversion of 1.0 equiv. of **151a**, bold lines show yield of **152a**.

3.4.2 Reaction Optimisation

In the following, many efforts towards enhancing the reaction yield and stereoselectivity were undertaken. For this, variations in reaction conditions and additives were tested with **136a** as the chiral catalyst (Table 3.26). $Sc(OTf)_3$ and $Zn(OTf)_2$ were applied, to potentially aid in the elimination step by coordination to the carbonyl O-tom and/or the Se. Whilst using 10 mol% of photocatalyst **86**, the addition of 2.5 mol% of either Lewis acid did not influence the outcome (Table 3.26, entry 3 and 5). 10 mol% $Sc(OTf)_3$ slightly raised the yield by 4%-points and the *ee* by 5 percentage points (Table 3.26, entry 4). The addition of $(4\text{-ClPhS})_2$, which in previous cases had enhanced the reaction outcome by raising the yield (see Section 3.1),[127,167] regioselectivity (see Section 3.3)[168] and/or stereoselectivity.,[167] proved to be detrimental in this case. The addition

of or 5 mol% of $(4\text{-ClPhS})_2$ even lowered the *ee* and did not influence the yield (Table 3.26, entry 6). Further alteration in reaction conditions, such as increasing the concentration, lowering the reaction temperature, or reversing the stoichiometry of the two substrates, all led to a decrease in yield and a similar or lower *ee* (Table 3.26, entries 7–9).

Table 3.26: Optimisation of the Enantioselective Intermolecular Allyic Amination of Ethyl (*E*)-hex-3-enoate **150a**.[a]

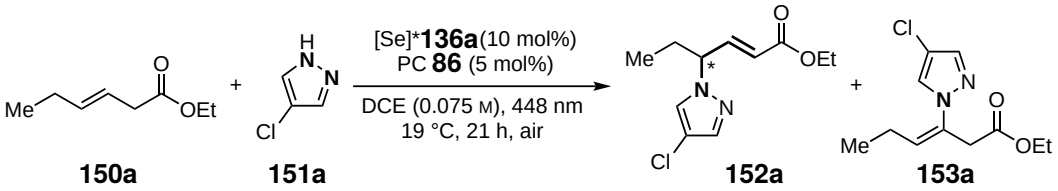

150a **151a** **152a** **153a**

Entry	Comment	Conv.[b] [%] of **150a**	Yield[b] [%] **152a**	**153a**	*ee* [%]
1	-	91	20	2	31
2[c]	-	87	22	1	32
3[c]	2.5 mol% $Sc(OTf)_3$	100	23	0	31
4[c]	10 mol% $Sc(OTf)_3$	100	26	0	37
5[c]	2.5 mol% $Zn(OTf)_2$	100	22	0	30
6	5 mol% $(4\text{-ClPhS})_2$	100	22	2	26
7	0.2 M	100	18	0	30
8	Reaction at -3 °C.	100	15	1	22
9	0.30 mmol **150a**, 3.00 equiv. **151a**	70	18	3	n.d.
10	Benzyl (*E*)-hex-3-enoate instead of **150a**	100	47	3	25
11	Acetone as Solvent	45	4	0	n.d.
12	MeCN as Solvent	67	15	2	n.d.
13	Toluene as Solvent	58	6	0	n.d.
14	*o*-Xylene as Solvent	86	6	0	n.d.

[a] 0.30 mmol (1.0 equiv.) of **151a**, 3.0 equiv. of **150a**. Se-catalyst purity $\geq$ 99%.
[b] Conversions and NMR yields were determined with DMB as the internal standard.
[c] 10 mol% of **86** used. n.d. = not determined.

The application of benzyl (*E*)-hex-3-enoate (**150b**) as the alkene compound afforded the desired product in an increased yield of 47% but a lower *ee* of 25%. Applying solvents with higher and lower polarity than DCE did not show any trends, all affording lower yields without complete

conversions after 21 h, seeming to slow down the reaction. The formation of vinylic side product **153a** was very low overall, with a range from 0 to 3%, probably resulting from a generally lower product formation. The value of the side product should be surveyed carefully, as a small signal-to-noise ratio in ^{1}H NMR analysis leads to a high uncertainty in detecting these low amounts. LEWIS-acid application suppresses the formation of the vinylic regioisomer, which was previously hinted at in the equivalent racemic protocol (Section 3.3, Table 3.13). Other trends towards the formation of vinylic side product **153a** could not be detected.

During the investigation of the racemic intermolecular allylic amination, it was found that the usage of symmetrically substituted diester **150j** afforded significantly higher yields and very good regioselectivity towards the desired allylic amine product in comparison to monoester **150a** (Section 3.3). With this in mind, the enantioselective variant by the usage of varying chiral Se-catalysts was also performed with diester **150j** in the reaction with **151a**, using photocatalyst **86** in DCE (4 mL), irradiating with blue light (λ_{max} = 448 nm) for 21 h (Table 3.27 and Table 5.30).

Table 3.27: Variation of Chiral Se-Catalysts **136** in the Asymmetric Allylic Amination of **150j** with **151a**.

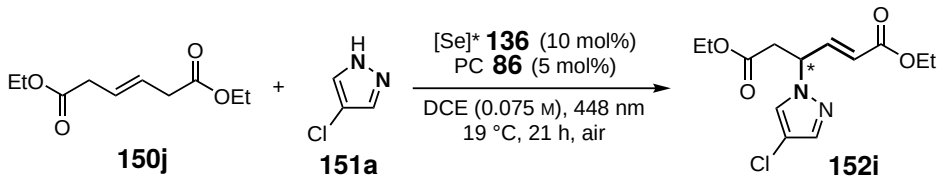

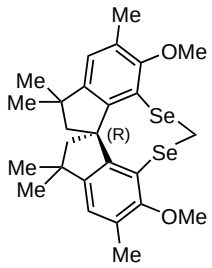

136b

42%, *ee* = 72%
35%, *ee* = 75%[a]
30%, *ee* = 84%[a,b]

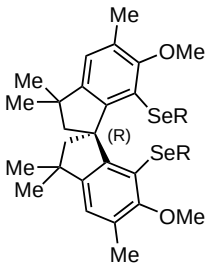

136a R = Bn
44%, *ee* = 67%
136c R = 2,5-diOMeBn
29%, *ee* =78%

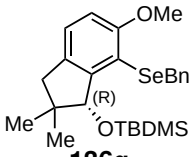

136g

64%, *ee* = -26%[a,b,c]

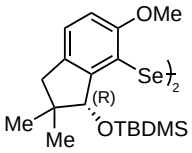

136h

64%, *ee* = -52%[a,b]

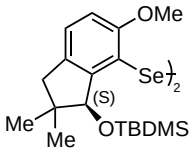

136i

75%, *ee* = 35%[d]

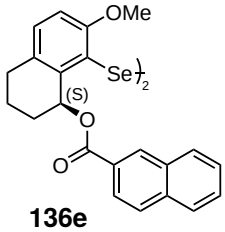

136e

70%, *ee* = 32%

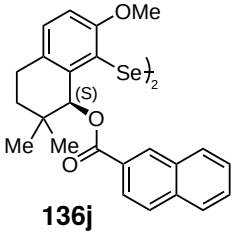

136j

66%, *ee* = 21%[a]

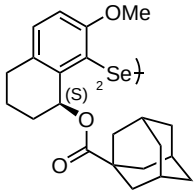

136k

71%, *ee* = -10%[a]

0.30 mmol (1.0 equiv.) of **151a**, 3.0 equiv. of **150j**. Se-catalyst purity $\geq$ 99%, unless otherwise noted. NMR yields were determined with DMB as the internal standard. [a]Newly synthesised Se-catalyst **136b** used. [b]20 mol% **136** used. [c]**136h** purity = 80–90% *ee*. [d]**136i** purity = 98% *ee*.

To our delight, employment of 10 mol% of BREDER's spiro-catalysts **136b**–**136c** afforded *ee*'s of 67–78%. A freshly synthesised batch of **136b** led to a slight decrease in yield and an increase in *ee* compared to an older batch, proposing a slow catalyst degradation over time, increasing the reaction rate accompanied by a lower enantioselective induction. When the loading of bridged catalyst **136b** was raised from 10 to 20 mol%, the *ee* could further increase from 75 to 84%. Albeit overall good *ee*'s, the yield could not exceed 44% using spiro-catalysts. Contrary to these results, catalytic structures based on MARUOKA's[118] (**136g**–**136i**) and DENMARK's[124] (**136e**–**136k**) catalysts afforded higher yields ranging from 64–75%, but could not compete with the previously achieved enantioselectivity. Interestingly, when DENMARK-type catalysts (**136e**–**136k**) were applied, the selectivity towards the other product-enantiomer increased with increasing bulkiness of

the ester-moiety.

Kinetic investigations with catalysts **136b** and **136c** were performed to examine the product formation and the development of the *ee* over time (Figure 3.17 and Table 5.35). When visualising the results, it was immediately seen that the *ee* decreases over time, which has also been observed in the enantioselective lactonisation.[167] This might result from partial oxidation of the selenium,[221,222] which affords an oxygenated species that still possesses some catalytic activity, albeit with low or opposite enantioselectivity.[167] The product formation has a high rate during the first 8 h of reaction time, after which it decreases. After 8 h, the conversion also did not improve significantly when the reaction time was prolonged to 21 h. Product formation and conversion of the starting material show a similar development over time, however, with a 30% difference. In conclusion, consumption of the starting material, for example, by side reactions or decay, occurs preferentially over allylic amine formation.

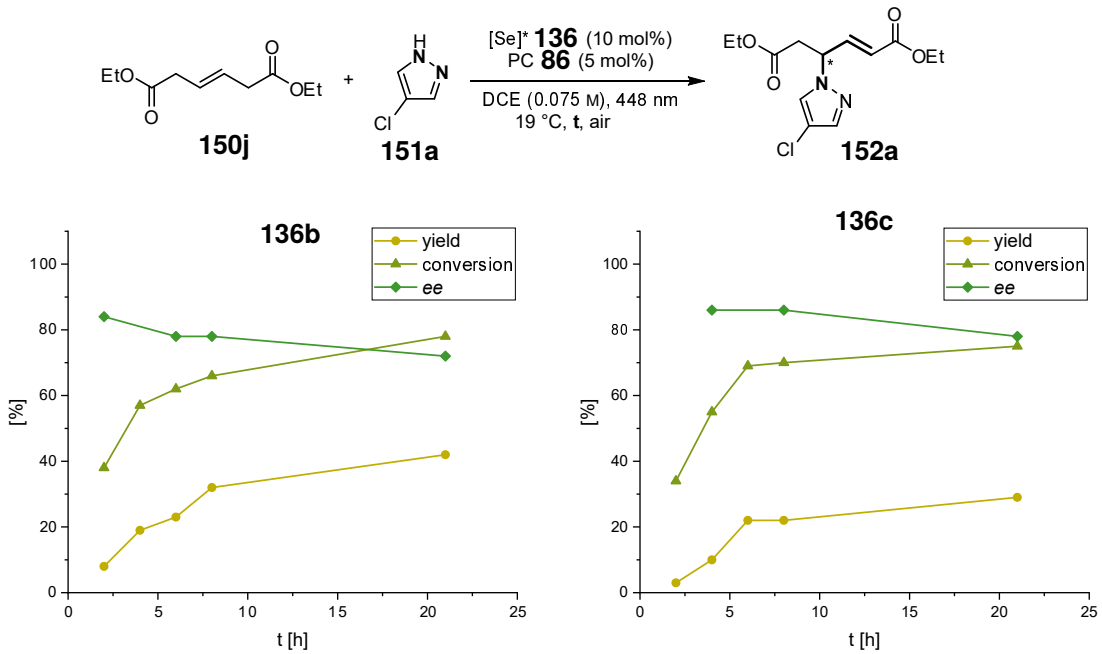

Figure 3.17: Kinetic investigation of the enantioselective amination of **150j** (3.0 equiv.) with **151a** (0.30 mmol, 1.0 equiv.) using chiral Se-catalyst **136b** and **136c**. 0.30 mmol of limiting compound used. Conversions and NMR yields were determined with DMB as the internal standard.

Proceeding from here, further investigations were conducted for 8 h, which was set as the favoured compromise between a high *ee* and conversion. The improvement in yield was investigated with spiro-catalyst **136b**. For this, various solvents ranging from polar-protic (HFIP) to apolar-aprotic (toluene) were applied to the reaction (for detailed results, see Section 5.8, Table 5.31). This investigation showed consensus with the racemic variant of the reaction and confirmed DCE to be the best-performing solvent (32% yield and 78% *ee*, which could be increased to 84% with a newly synthesised catalyst **136b**). MeCN also afforded product **152a** with a high *ee* of 84%,

albeit a lowered yield of 14%. To further improve the yield, several additives were applied to the reaction conditions (for detailed results, see Section 5.8, Table 5.32). Disulfide $(4\text{-ClPhS})_2$, which previously showed a positive influence in similar reactions, was added to the reaction conditions with DCE and MeCN. Other disulfides were also tested, but no increase in yield and a similar *ee* for all outcomes was observed. Further additives, such as LEWIS acids and Me_6Si_2, did not positively influence the reaction outcome or even entirely prevent product formation. Further variations, such as changing the concentration or reaction temperature, reversing the stoichiometry of the starting materials, or reducing the O_2 concentration, either led to a decrease in *ee*, product yield, or even both. A variation in catalyst loading with 5-20 mol% of **136b** and 2.5-10 mol% of **86** in various combinations did not result in the desired improvement in yield (for detailed results, see Section 5.8, Table 5.34). Neither the yield nor the enantioselective outcome was significantly affected by the catalyst loading. Finally, the upscale to a 1.0 mmol protocol was conducted with slightly adapted reaction conditions. The best outcome for the larger scale was found with a 0.2 M reaction mixture instead of 0.075 M and a prolonged the reaction time from 8 to 21 h (for detailed results, see Section 5.8, Table 5.33 and Subsection 5.8.3).
At this point of reaction optimisation, it was concluded that for the already invested effort, the best result for the asymmetric variant of the intermolecular allylic amination of alkenes with azoles was achieved. Further effort could preferably be invested in exploring the racemic substrate scope and investigating the influence of chiral counter ions on enantioselectivity.

3.4.3 Asymmetric Intermolecular Allylic Amination

With the optimised reaction conditions in hand, 1H-benzo[d][1,2,3]triazole **151b** was utilised as an additional nucleophile substrate in order to investigate further applicability (Table 3.28). Compared to the reaction with chloropyrazole as the nucleophile, a very similar result was achieved for the 0.3 mmol reaction, affording 31% yield and an *ee* of 80%. Scaling up the reaction to 1.0 mmol yielded 17% after 8 h and a comparable yield (29%) and *ee* (84%) after 21 h. The same goes for the scaled-up reaction with chloropyrazole **151a**, giving 31% yield and an *ee* of 82%.

Table 3.28: Asymmetric Intermolecular Allylic Amination[a]

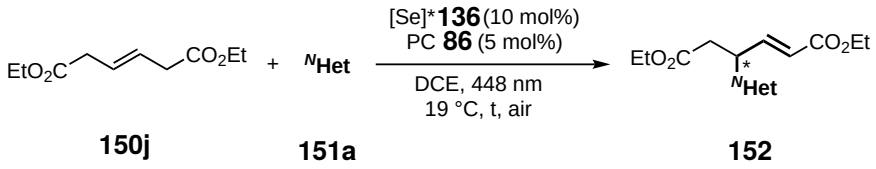

150j **151a** **152**

152i	**152bf**
0.3 mmol: 30% (32%), *ee* = 84[b]	0.3 mmol: 27% (31%), *ee* = 80[b]
1.0 mmol: 29% (31%), *ee* = 82[c]	1.0 mmol: 24% (29%), *ee* = 84[c]

[a] All reactions were performed with 3.0 euqiv. of **151**. NMR yields were determined with DMB as the internal standard and are given in parentheses. [b] 8 h, 0.075 M. [c] 21 h, 0.2 M.

3.4.4 Chiral Counter Ions

Further investigating a possible chiral induction during the Se-π-acid/photoredox dual catalytic allylic amination process, another approach was proposed to proceed *via* a chiral counterion, introduced to the reaction media by the photocatalyst Figure 3.18.

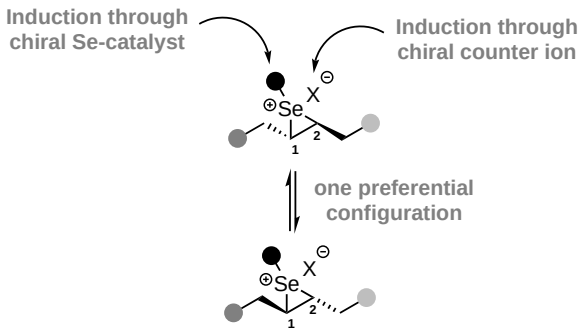

Figure 3.18: Influence of chiral induction onto the preferred configuration of the seleniranium ion intermediate.

Previous reports have already attributed anionic chiral counterions to have a stereoselective-inducing effect in certain transformations. In 2014, Jacobsen and coworkers reported a Se-π-acid catalysed enantioselective protocol, where a chiral anion, coordinated to the positively charged seleniranium ion, was able to successfully influence the stereoselective nucleophilic attack, affording the desired products with *ee*'s of up to 92% (Equation 3.13).[223] Differently accelerated

ring-opening of the seleniranium ion leads to the highly enantioselective outcome through dynamic kinetic resolution.[223,224]

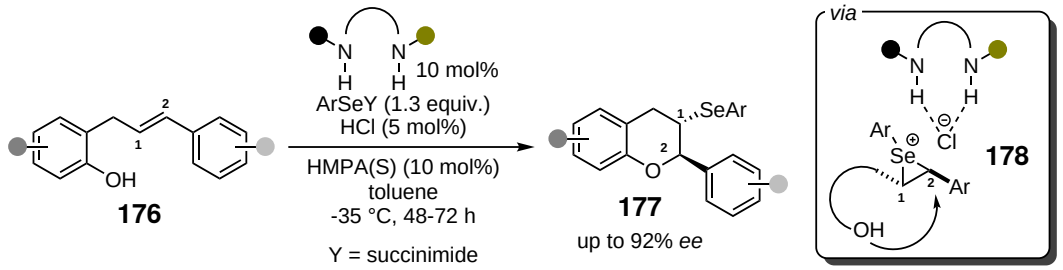

(3.13)

Ion-pairing catalysis has also been reported in light-induced transformations.[225] In this field, Nicewicz reported using an oxopyrylium photoredox catalyst with a chiral counter ion in an asymmetric radical cation Diels-Alder reaction.[226] With the application of chiral BINOL-derived phosphoric acids, the group could obtain the desired products in enantiomeric ratios of up to 75:25, laying the foundation of this system for further applications.

Catalyst Synthesis

With this background, an asymmetric counterion directed catalytic (ACDC) approach of the Se-π-acid/photoredox dual catalytic allylic amination was attempted for the first time. For this purpose, catalyst starting material (*Z*)-1,3,5-tris(4-methoxyphenyl)pent-2-ene-1,5-dione (**179**) was prepared by Dr. T. Lei, following a procedure by Morse et al. (Equation 3.14).[226] **86** was subjected to superstoichiometric amounts of basic Al_2O_3 and NaAc and stirred at 75°C for 23 h in a solvent mixture of EtOH and H_2O. Workup and precipitation afforded **179** in 88% yield.

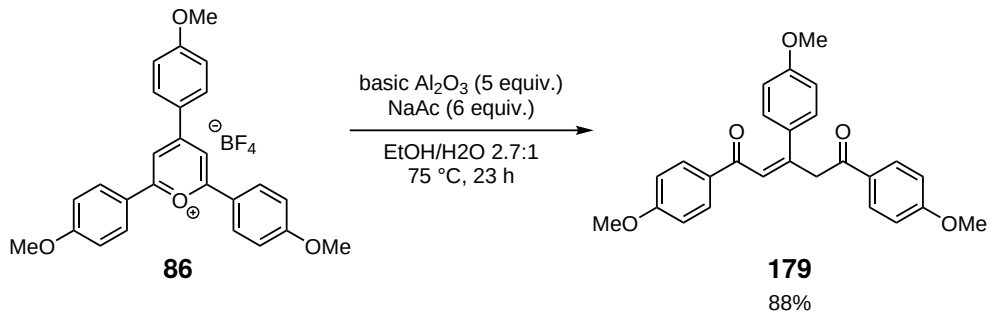

(3.14)

Subsequently, converting **179** with an acidic compound such as a chiral phosphoric acid, afforded pyrylium salts **180a**–**180d** consisting of a 2,4,6-tris(4-methoxyphenyl)pyrylium-cation (TAP^+) with varying chiral counteranions.

Table 3.29: Synthesis of photocatalysts **180a**–**180d** with varying chiral counteranions.[a]

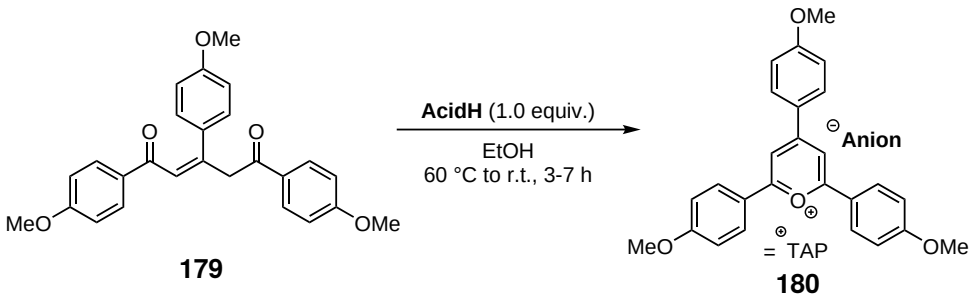

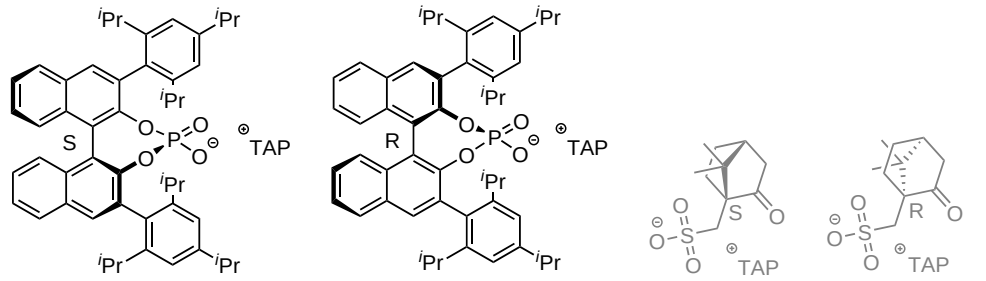

[a] Isolated yields given. Grayed catalysts were synthesised by Dr. T. Lei.

Application of ACDC Catalysts

Synthesised catalysts **180a**–**180d** were then tested under the previously optimised conditions of the racemic Se-π-acid/photoredox dual catalytic intermolecular allylic amination with azoles (Table 3.30). Chiral photocatalyst **180a** was applied in the reaction in combination with non-chiral Se-catalyst $(PhSe)_2$. Additionally, photocatalysts **180a**–**180d** were applied in the reaction in combination with ciral Se-catalyst **136c**. Comparing the results with the racemic reaction (yield = 68%), it shows that the achieved yield was substantially lower with one (average yield = 22%) or two (average yield = 10%) chiral compounds. This might be due to a more sterically demanding surrounding either by the chiral counterion, the chiral Se-catalyst, or both. This might lead to a hindered intermolecular nucleophilic attack or a less efficient elimination step. As seen previously, the application of chiral Se-catalysts with racemic photocatalyst **86** in the previous study achieved significantly lower yields (20%, with an *ee* of 31%) compared to the application of racemic Se-catalyst $(PhSe)_2$ (68%) (Subsection 3.4.1). The application of photocatalyst with chiral counterion **180a** afforded a similar yield of 23%, albeit a lower *ee* of 4%. This result shows that chiral counterions can induce chirality during intermolecular allylic amination, albeit in a very low amount.

Table 3.30: Photosensitiser with Chiral Counter Anions Used in the Asymmetric Intermolecular Allylic Amination of **150a** with **151a**.[a]

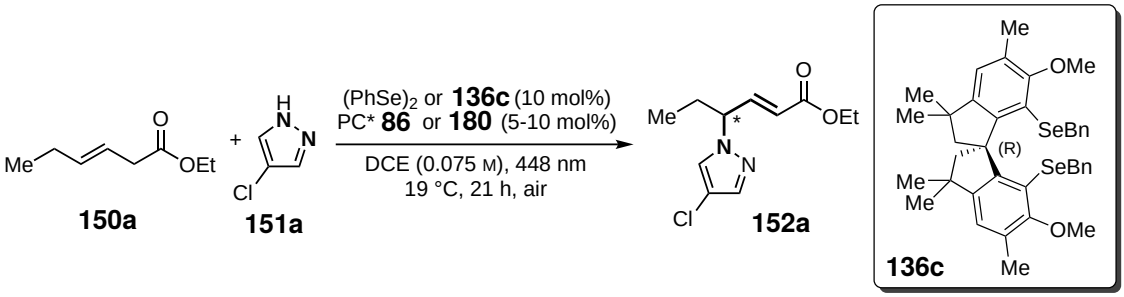

with $(PhSe)_2$

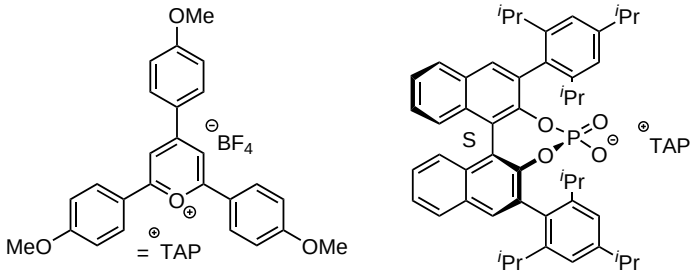

86
68%, *ee* = -[b]

180a
23%, *ee* = 4%[b]

with **136c**

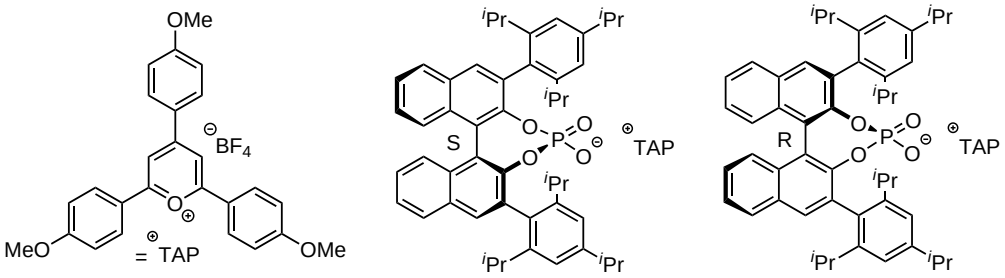

86
20%, *ee* = 31%[b]

180a
7%, *ee* = 11%[b]

180b
7%, *ee* = 14%[b]

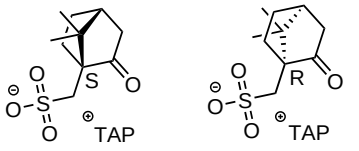

180c
13%, *ee* = 29%[c]

180d
14%, *ee* = 33%[c]

NMR yields were determined with DMB as the internal standard. [a]**150a** (0.30 mmol, 1.0 equiv.), **151a** (3.0 equiv.). [b]5 mol% of photocatalyst used. [c]10 mol% of photocatalyst used.

A reason for this outcome could be an insufficient control of the seleniranium ion scrambling and/or

a low selectivity towards one enantiomer by inefficient coordination of the counterion.[223,224] Consequently, the question arose whether accumulating two chiral compounds would result in a positive collaboration and an enhanced enantiomeric outcome. For this, several photocatalysts with chiral counterions **180** were applied in combination with chiral Se-catalyst **136c**. Photosensitisers **180a** and **180b**, bearing a chiral phosphoric acid as the counterion, both resulted in a low yield of 7% and an average *ee* of 13%. When photocatalysts **180c** and **180d** with a camphor sulfonic acid (CSA) as the chiral counterion were used, the yield doubled to an average of 14%, and the *ee* rose to 33% in the highest outcome. These results, though, did not exceed the reaction of **136c** with racemic photocatalyst **86**, which indicates that the application of chiral counter anions suppresses the chirality-inducing step rather than improves enantioselectivity during the reaction. Another indication supporting this theory is that the smaller CSA anions have a minor effect compared to the larger phosphoric acid.

After the course of these investigations, B. List published an elegant protocol for the enantioselective [2+2]-cyclo addition reaction, with stereoselective induction enabled by photocatalyst TAP^+ with chiral counter ions, affording *ee*'s of up to 96%.[227] The most successful chiral counter ion is characteristic due to its space-consuming and rigid structure, indicating a space-demanding anion needed for a successful transformation. Additionally, the aciditiy of the counter anion seems to have an effect on the transformation and should be investigated.

4 Summary And Outook

The aim of this thesis was the development of regioselective protocols for the inter- and intramolecular oxidative allylic amination of simple alkenes with exogenous N-nucleophiles, not derived from the oxidant. The transformation was proposed to be accomplished by a dual catalytic system consisting of a photoredox catalyst and a selenium-π-acid, which previously proved to be highly applicable in the allylic functionalisation with O-nucleophiles by the group of BREDER.[150,151,155–157] The first project involved the intramolecular allylic amination of sulfonamides **111** and the successful expansion of the scope from five-membered heterocycles **113** and **112** to six-membered heterocycles **122** (Equation 4.1).[127]

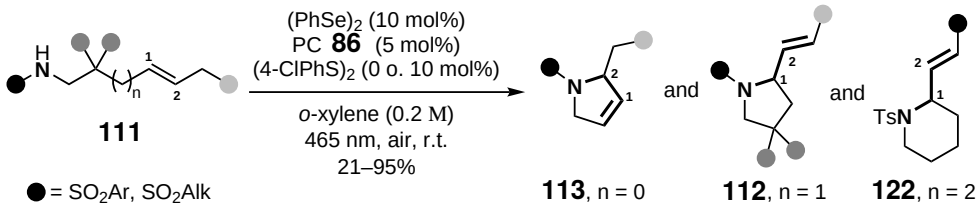

(4.1)

The role of the disulfide was elucidated by mechanistic investigations involving upon others quenching experiments and electrochemical investigations. It was found that the disulfide exhibits a dual function during the reaction, for once serving as an electron hole shuttle, promoting the formation of the $(PhSe)_2$ radical cation, which itself engages in the interaction with the double bond. Secondly, $(4\text{-}ClPhS)_2$ is proposed to form an interchalcogen species with the selenoaminated intermediate, which enables a faster elimination step. Both functions are suggested to enhance the reaction rate and increase the product yield. In a further study, the method could be expanded to an enantioselective variant using newly developed chiral selenium spiro catalysts.[124]

The second project involved the intermolecular allylic amination of simple alkenes with sulfonamides (Equation 4.2).[168] A lot of effort was put into the optimisation of the reaction, which led to the development of a stable protocol for the transformation of **138** with **137**. First reported method with the usage of exogenous nucleophiles with Se-π-acid catalysis.

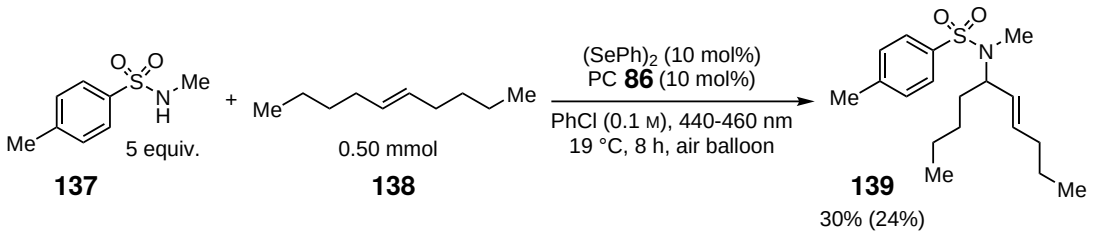

(4.2)

Lastly, a highly regioselective intermolecular process for the allylic amination of alkenes with azoles was developed (Equation 4.3).[168] The broad substrate scope proved high functional group tolerance. The application of alkenes with different connectivity such as 1,2- 1,1,2- and terminal olefins all lead to a highly selective outcome of the favoured allylic amines **152** versus the vinylic regioisomer **153**. Compared to classical thermal Pd-catalysed protocols, the developed method was able to transform internal alkenes in high regioselectivity. Unsummetrically substituted olefins lead to the formation of the respective MARKOVNIKOV products, which complements previous allylic amination protocols *via* photocatalysis, which afforded the *anti*-MARKOVNIKOV products. The applicability of the developed protocol was demonstrated by successful late-stage functionalisation of drug analogs and natural products derivatisation.

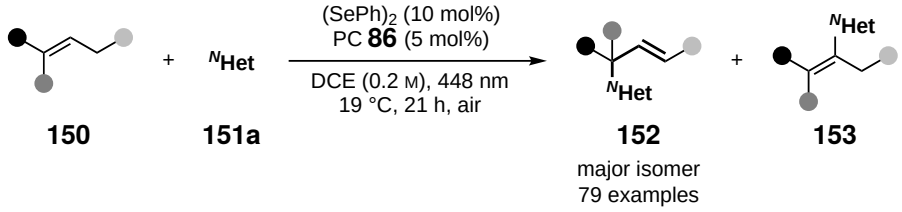

(4.3)

Efforts towards the further development of an enantioselective variant were conducted. Simple amines were successfully transformed with spiro selenium catalysts developed by the BREDER group, with a high enantiomeric excess of up to 84% and an isolated yield of up to 30%. Further investigations and optimisation may lead to a successful increase in yield. Additionally, the influence of chiral counter anions of the photocatalysts was investigated and led to first promising results, albeit low yields and enantiomeric excess, but room for improvement. The employment of counter anions with a higher steric demand could lead to an improved outcome, as B. LIST and coworkers showed in their enantioselective [2+2] cycloadditions.[227]

5 Experimental Section

5.1 General Remarks

5.1.1 Preparative Methods

5.1.2 Solvents and Reagents

Unless otherwise noted, starting materials and solvents were obtained from commercial suppliers and used without further purification. Starting material **131** was synthesised and provided by Dr. S. Graf.[127,165] Hybrid catalyst **144** was synthesised and provided by Dr. K. Müller. Chiral Se-catalysts **136a**–**136c** were synthesised and provided by Dr. T. Lei,[167] **136d**, **136e**, **136i**–**136k** were synthesised and provided by Dr. S. Park[228] and **136g**, **136h** were synthesised and provide by L. d'Heureuse.[118,121] **136f** was synthesised and provided by C. Nagel. Starting Material **179** and ACDC-catalysts **180c**, **180d** were synthesised and provided by Dr. T. Lei.
Solvents for thin layer chromatography and liquid chromatography were technical grade and distilled prior to use. Solvents used in reactions were pro analysi (p.A.) grade. The used H_2O is deionised and provided by the university of Regensburg. DCM and EtOH were dried by storing over molecular sieves under N_2-atmosphere for several days. Anhydrous toluene and THF were either obtained from distillation over sodium under N_2-atmosphere or from a *MBraun* MB-SPS-5 solvent purification system and then stored over molecular sieves under N_2-atmosphere. Other dry solvents were obtained commercially and used without further purification. Percentages (%) always refer to weight-% unless otherwise noted.

5.1.3 Chromaographic Methods

Thin layer chromatography (TLC): TLC was carried out on silica gel coated aluminium plates from *Macherey-Nagel* (Alugram Sil G/UV254). Visualisation was enabled by exposure to UV light (λ = 254 nm) [UV] and by treatment with *p*-anisaldehyde stain [*p*-anisaldehyde] (composition: 270 mL EtOH, 7.4 mL *p*-anisaldehyde, 10 mL H_2SO_4 conc., 3 mL AcOH) or permanganate stain [$KMnO_4$] (composition: 3 g $KMnO_4$, 20 g K_2CO_3, 5 mL aqueous NaOH (5%), 300 mL H_2O) and subsequent heating with a heat gun. Reported are the R_f values (substance level/solvent front level).

Column Chromatography: Column Chromatography was performed manually using forced flow or *via* an automated flash column from *Advion* (puriFlash 5.050) on Silica 60 (0.035–0.075 mm,

70–230 mesh ASTM) from *Acros* or from *Büchi* (Pure C185 Flash). Solvent mixtures are understood as volume/volume.

5.1.4 Instrumental Analysis

Nuclear Magnetic Resonance (NMR) Spectroscopy: NMR spectra were recorded at 300 MHz (^{1}H) and 75 MHz (^{13}C) on a *Bruker* Avance 300 spectrometer or at 400 MHz (^{1}H), 101 MHz (^{13}C), 376 MHz (^{19}F), 162 MHz (^{31}P) and 76 MHz (^{77}Se) on a *Bruker* Avance III HD 400 or at 151 MHz (^{13}C) on a *Bruker* Avance III 600 HD, if not otherwise specified. Chemical shifts δ are given in parts per million (ppm) and refer to the residual proton signal of the used solvent (Table 5.1). Coupling constants (*J*) are given in Hertz (Hz). Spectral splitting patterns (multiplicity) are designated as: s (singlet), bs (broad singlet), d (doublet), t (triplet), q (quartet), quint. (quintet), hept. (heptet), m (multiplet). COSY, NOESY, HSQC and HMBC experiments were carried out to identify the structure of some molecules.

Table 5.1: Deuterated Solvents and their Respective Solvent Residual Signals in ^{1}H- and ^{13}C NMR Spectra.[229]

Solvent	^{1}H-shift (multiplicity)	^{13}C-shift
$CDCl_3$	7.26 (s)	77.2
MeCN-d_3	1.94 (quint.)	1.32, 118.3
DMSO-d_6	2.50 (quint.)	39.5

Quantitative NMR (qNMR): For the intermolecular allylic amination reactions with sulfonamides qNMR analysis was carried out by homogeniously diluting the crude reaction mixture in $CHCl_3$. A defined aliquot of an appropriate internal standard was added, the mixture was stirred and a sample was added to a NMR tube containing $CDCl_3$. For intramolecular allylic aminations and allylic aminations with azoles and azines qNMR analysis was carried out by firstly adding a defined aliquot of an appropriate internal standard and then diluting the mixture with $CDCl_3$. By analysis of the ^{1}H NMR the yield of the reaction could be determined by comparison of the integral of the internal standard to the characteristic signals of the reaction compounds. As internal standard the following were utilised:[230]

Trichloroethylene (TCE)	^{1}**H NMR** ($CDCl_3$): δ 6.45 (s, 1H)
1,1,2,2-Tetrachloroethane	^{1}**H NMR** ($CDCl_3$): δ 5.90 (s, 2H)
1,3,5-Trimethoxybenzene (TMB)	^{1}**H NMR** ($CDCl_3$): δ 6.08 (s, 3H), 3.75 (s, 9H)
1,4-Dimethoxybenzene (DMB)	^{1}**H NMR** ($CDCl_3$): δ 6.83 (s, 4H), 3.76 (s, 6H)

Infrared Spectroscopy (IR): IR spectra were recorded on a *Agilent* Cary 630 FT-IR spectrometer with attenuated total reflexion (ATR) sampling module.

High Resolution Mass Spectrometry (HRMS): Electronspray ionisation (ESI) and atmospheric pressure chemical ionisation (APCI) HRMS spectra were measured on an *Agilent* Q-TOF 6540 UHD mass spectrometer. Electron ionisation (EI) HRMS spectra were measured on a *Jeol* AccuTOF GCX.

Melting Points (m.p.): M.p. were measured on a melting point meter M5000 from *A.KRÜSS Optronic*.

High Performance Liquid Chromatography (HPLC): HPLC analyses were performed on an *Agilent* 1260 Infinity. The signals were detected *via* a diode array detector (DAD). The enantiomers were separated on a Chiralpak IA or Chiralcel OD column from *Daicel*. As solvent, a mixture of isopropanol and n-hexane was used.

Optical Rotations: Optical rotations were measured on a P-2000 polarimeter from *Jasco*.

5.2 Experimental Procedures

5.3 Synthesis of Arylselenides and Photosensitiser

2,4,6-tris(4-methoxyphenyl)pyrylium tetrafluoroborate (TAPT) (86)[152]

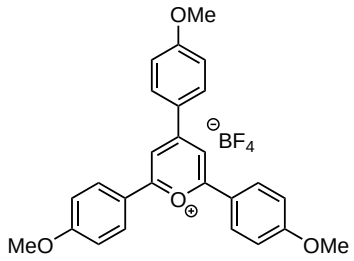

86

To a solution of 1-(4-methoxyphenyl)ethan-1-one (30.0 g, 200 mmol, 2.00 equiv.) in 10 mL dry toluene under N_2-atmosphere, 4-methoxybenzaldehyde (13.6 g, 100 mmol, 1.00 equiv.) and $BF_3 \cdot Et_2O$ (29.6 mL, 34.0 g, 240 mmol, 2.40 equiv.) were added. The resulting dark red mixture was heated to 100 °C and stirred for 2 h, upon which the solution turns darker over time. After cooling to r.t., the formed Et_2O was removed under reduced pressure. The residue was then dissolved in acetone (500 mL) and separated into three parts and 1-2 L of Et_2O was added each. The resulting precipitate was filtered and carefully washed with Et_2O and ice cold acetone, before it was dried on vacuum affording **86** (10.1 g, 20.7 mmol, 21%) as an orange solid.

M.p. = 342 °C. **IR** [cm^{-1}]: 3120, 3082, 2978, 2940, 2844, 2113, 1629, 1588, 1484, 1461, 1305, 1878, 1015, 925. ^{1}**H NMR** (300 MHz, MeCN-d_3): δ 8.35–8.08 (m, 8H), 7.29–6.95 (m, 6H), 3.99–3.93 (m, 9H).^{13}**C NMR** (101 MHz, MeCN-d_3): δ 169.5, 166.8, 166.2, 163.6, 132.8, 131.5, 125.6, 122.2, 116.5, 116.4, 112.1, 56.9, 56.8. **HRMS** (ESI) calcd. for $[C_{26}H_{23}O_4]^+$ ($[M - BF_4^-]^+$), m/z = 399.1591; found 399.159.

1,2-bis(2-methoxyphenyl)diselane (140)

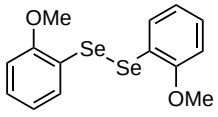

140

To a solution of 1-bromo-2-methoxybenzene (2.52 mL, 3.79 g, 20.3 mmol, 1.00 equiv.) in dry THF under a N_2-atmosphere, ^{t}BuLi (1.7 M in pentane, 25.0 mL, 42.5 mmol, 1.1 equiv.) was added dropwise at -78 °C. After stirring for 15 min, the solution was allowed to warm to 0°C. Se-powder (1.76 g, 22.3 mmol, 1.10 equiv.) was added and the resulting mixture was stirred for 15 min at 0°C and 1 h at r.t.. the reaction was then quenched with 1 M aqueous HCl (20 mL). H_2O (100 mL) was added and the mixture was extracted with Et_2O (3 × 100 mL). The combined organic phases were washed with brine (100 mL), dried over Na_2SO_4, filtered and the solvent was removed under reduced pressure. The residual orange oil was redissolved in EtOH (50 mL), two pellets of NaOH were added and the resulting solution was vigorously stirred open to air for 2 h. The solvent was removed under reduced pressure and the residue was purified *via* column chromatography (*n*-pentane/EA, 90:10) affording **140** (2.14 g, 5.75 mmol, 57%) as a yellow solid.

TLC: R_f = 0.37 (PE/EtOAc, 90:10) [UV, *p*-anisaldehyde]. **M.p.** = 83 °C. **IR** [cm^{-1}]: 3056, 3004,

2963, 2837, 1572, 1465, 1431, 1234, 1182, 1122, 1051, 1017. **^{1}H NMR** (300 MHz, $CDCl_3$): δ 7.55 (dd, *J* = 7.7, 1.6 Hz, 2H), 7.21 (ddd, *J* = 8.1, 7.4, 1.6 Hz, 2H), 6.87 (td, *J* = 7.5, 1.2 Hz, 2H), 6.82 (dd, *J* = 8.2, 1.2 Hz, 2H), 3.91 (s, 6H). **^{13}C NMR** (101 MHz, $CDCl_3$): δ 156.9, 130.7, 128.2, 122.0, 118.8, 110.2, 56.0. **^{77}Se NMR** (76 MHz, $CDCl_3$): δ 332.1. **HRMS** (EI) calcd. for $[C_{14}H_{15}O_2Se_2]^{\cdot+}$ ($[M]^{\cdot+}$), m/z = 373.9319; found 373.9316.

(4-methoxybenzyl)(phenyl)selane (142)

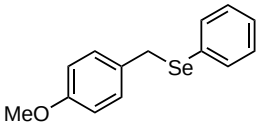

142

To a solution of $(PhSe)_2$ (936 mg, 3.00 mmol, 1.00 equiv.) in dry THF (15 mL) and dry EtOH (15 mL) under a N_2-atmosphere, $NaBH_4$ (340 mg, 9.00 mmol, 3.00 equiv.) was added at 0 °C. After warming to r.t., 1-(chloromethyl)-4-methoxybenzene (1.16 mL, 937 mg, 6.00 mmol, 2.00 equiv.) was added and the resulting mixture was stirred for 2 h, before quenched by addition of H_2O (20 mL). The resulting two phases were separated and the aqueous phase was extracted with EtOAc (3 × 30 mL). The combined organic phases were washed with brine, dried over Na_2SO_4 and filtered. The solvent was removed under reduced pressure and the residue was purified *via* column chromatography (pentane/EtOAc, 100:0 to 95:5) affording **142** (1.53 g 5.52 mmol, 92%) as a colourless solid.

To a solution of $(PhSe)_2$ (4.68 g, 15.0 mmol, 1.00 equiv.) in dry THF (75 mL) and dry EtOH (75 mL) under a N_2-atmosphere, $NaBH_4$ (1.70 g, 45.0 mmol, 3.00 equiv.) was added at 0 °C. After warming to r.t., 1-(chloromethyl)-4-methoxybenzene (4.07 mL, 4.70 g, 30 mmol, 2.00 equiv.) was added and the resulting mixture was stirred for 2 h, before quenched by addition of H_2O (20 mL). The resulting two phases were separated and the aqueous phase was extracted with EtOAc (3 × 100 mL). The combined organic phases were washed with brine (100 mL), dried over Na_2SO_4 and filtered. The solvent was removed under reduced pressure and the residue was purified *via* column chromatography (PE/EtOAc, 100:0 to 20:1) affording **142** (7.30 g 26.3 mmol, 88%) as a yellowish solid.

TLC: R_f = 0.37 (PE/EtOAc, 99:1) [UV]. **M.p.** = 73 °C. **IR** [cm^{-1}]: 3124, 3045, 3008, 2967, 2837, 2058, 1607, 1580, 1510, 1435, 1238, 1033. **^{1}H NMR** (400 MHz, $CDCl_3$): δ 7.55–7.39 (m, 2H), 7.32–7.21 (m, 3H), 7.19–7.07 (m, 2H), 6.83–6.54 (m, 2H), 4.09 (s, 2H), 3.79 (s, 3H). **^{13}C NMR** (101 MHz, $CDCl_3$): δ 158.7, 133.6, 130.8, 130.7, 130.1, 129.1, 127.3, 114.0, 55.4, 31.9. **^{77}Se NMR** (76 MHz, $CDCl_3$): δ 372.5. **HRMS** (EI) calcd. for $[C_{14}H_{14}OSe]^{\cdot+}$ ($[M]^{\cdot+}$), m/z = 278.0212; found 278.0204.

5.4 Racemic Intramolecular Allylic Amination with Sulfonamides

5.4.1 Optimisation of Reaction Conditions

5.4.2 Fluorescence Quenching Experiments (Stern-Volmer)

Fluorescence quenching measurements were performed on a Jobinyvon Fluorolog by Horiba in quartz cuvettes (1 × 1 cm). For fluorescence quenching measurements, a 0.2 mM stock solution of **86**, a 2.0 mM stock solution of $(PhSe)_2$, a 2.0 mM, and a 6.0 mM stock solution of $(4\,ClPhS)_2$ and a 6.0 mM stock solution of the intermediate **129a** in MeCN were prepared. From these stock solutions, samples were prepared with a final **86** concentration of 10 µM and quencher concentrations in the range of 0–5.7 mM (0–570 equiv.). Every sample was measured three to five times and an average value of the fluorescence intensity was used for analysis. The obtained intensities $\frac{I_0}{I} - 1$ were plotted against the quencher concentration c_q, where $_0$ equals the fluorescence intensity of the unquenched photocatalyst derived from the sample containing no quencher and I equals the intensity of the quenched sample. The Stern-Volmer constants K_{SV} of the quenchers were obtained from the slopes of these plots following the Stern-Volmer equation.

$$\frac{I_0}{I} - 1 = K_{SV} \cdot c_q \tag{5.1}$$

Fluorescence quenching was conducted at an absorption g_{Abs} = 443 nm and an emission g_{Em} = 540 nm. The resulting Stern-Volmer constants are summarised in Table 5.2.

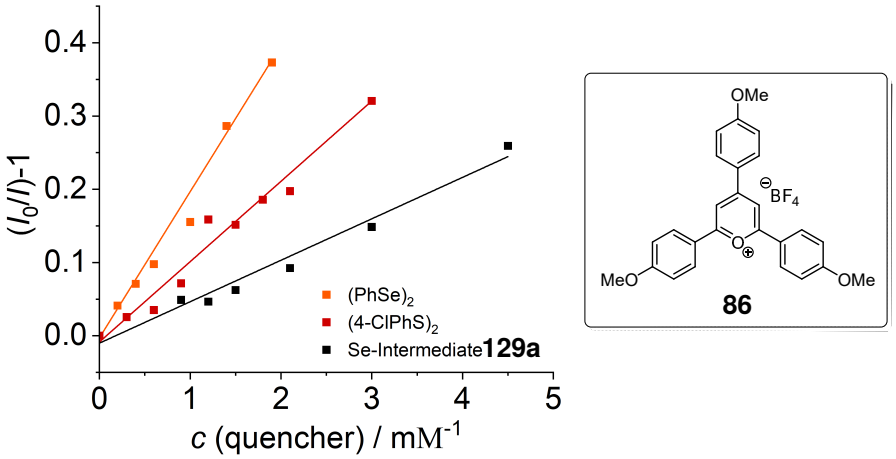

Figure 5.1: Stern-Volmer quenching experiments.

Table 5.2: STERN-VOLMER Constants for **86**/Quencher Combinations.

	$(PhSe)_2$	$(4\text{-}ClPhS)_2$	**129a**
Constant	200±26.5 M^{-1}	110±23.1 M^{-1}	56.6±17.1 M^{-1}

5.4.3 Substrate Synthesis

N-(5-Bromopentyl)-4-methylbenzenesulfonamide (116)[162,231]

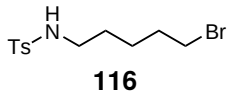

116

Step 1: 5-Aminopentan-1-ol (10.5 mL, 10.0 g, 96.9 mmol, 1.00 equiv.) was added to 85 mL HBr (aqueous solution, 47%) and stirred under reflux for 3 h. After cooling to r.t., the solvent was removed on vacuum into a cooling trap by slowly elevating the temperature to 70 °C. Removal of the solvent gave 21.8 g of crude 5-bromopentan-1-amine hydrobromide, which was used without further purification.

Step 2: NEt_3 (8.32 mL, 6.07 g, 60.0 mmol, 2.73 equiv.) was added slowly to a solution of 4.94 g of the crude 5-bromopentan-1-amine hydrobromide (equals 22.0 mmol and 1.00 equiv. at full conversion) in 80 mL DCM. The reaction mixture was cooled to 0 °C and TsCl (3.89 g, 20.0 mmol, 0.91 equiv.) was added. After stirring at r.t. for 3 h, another 8.32 mL NEt_3 (6.07 g, 60.0 mmol, 2.73 equiv.) were added and the solution was stirred at r.t. for further 16 h. After confirmation of the consumption of TsCl via TLC, H_2O (70 mL) was added, and the two formed phases were separated. The aqueous phase was extracted with DCM (2 × 50 mL). The combined organic phases were washed with 2 M aqueous HCl (50 mL), brine (50 mL), sat. aqueous $NaHCO_3$ solution (50 mL) and brine (50 mL), dried over Na_2SO_4 and filtered, before the solvent was removed under reduced pressure. Purification via column chromatography (PE/EtOAc, 80:20) afforded **116** (4.07 g, 12.7 mmol, 58% over two steps) as a colourless solid.

TLC: R_f = 0.23 (PE/EtOAc, 80:20) [UV, $KMnO_4$]. **M.p.** = 71 °C. **IR** [cm^{-1}]: 3273, 2948, 2859, 1595, 1420, 1319, 1293, 1256, 1156, 1088, 1062, 1021, 902, 816. ^{1}**H NMR** (400 MHz, $CDCl_3$): δ 7.75 (d, *J* = 8.3 Hz, 2H), 7.40–7.25 (m, 2H), 4.75 (t, *J* = 6.2 Hz, 1H), 3.33 (t, *J* = 6.7 Hz, 2H), 2.93 (q, *J* = 6.6 Hz, 2H), 2.43 (s, 3H), 1.86–1.70 (m, 2H), 1.56–1.31 (m, 4H). ^{13}**C NMR** (101 MHz, $CDCl_3$): δ 143.6, 137.0, 129.9, 127.2, 43.0, 33.5, 32.2, 28.9, 25.2, 21.7. **HRMS** (ESI) calcd. for $[C_{12}H_{19}BrNO_2S]^+$ ($[M+H]^+$), m/z = 320.0314; found 320.0310.

(5-((4-Methylphenyl)sulfonamido)pentyl)triphenylphosphonium bromide (117)[232]

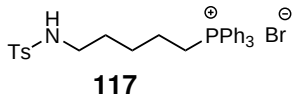

117

To a solution of *N*-(5-bromopentyl)-4- methyl-benzenesulfonamide **116** (1.28 g, 4.00 mmol, 1.00 equiv.) in 10 mL MeCN, PPh_3 (1.26 g, 4.80 mmol, 1.20 equiv.) was added and the resulting mixture was stirred under reflux for 16 h. After cooling to r.t., the solvent was removed under reduced pressure. The residue was then again

dissolved in iPrOH (100 mL). Et_2O (175 mL) was added and a colourless precipitate formed, which was filtered, washed with Et_2O and dried on vacuum, affording **117** (1.15 g, 1.98 mmol, 49%) as a colourless solid.

To a solution of *N*-(5-bromopentyl)-4- methyl-benzenesulfonamide **116** (9.00 g, 28.1 mmol, 1.00 equiv.) in 35 mL MeCN, PPh_3 (8.85 g, 33.7 mmol, 1.20 equiv.) was added and the resulting mixture was stirred under reflux for 18 h. During cooling to r.t., colourless precipitate formed. The flask was put into the freezer for 13 days. After warming to r.t., the precipitated was fitlered and washed with icecold EtOAc (300 mL). Drying under vacuum for one day afforded **117** (11.2 g, 19.2 mmol, 68%) as a colourless solid.

M.p. = 202 °C. **IR** [cm^{-1}]: 3019, 2930, 2833, 1588, 1431, 1327, 1162, 1107, 991. ^{1}**H NMR** (400 MHz, DMSO – d_6): δ 7.96–7.85 (m, 3H), 7.85–7.70 (m, 12H), 7.68–7.59 (m, 2H), 7.49 (t, *J* = 5.9 Hz, 1H), 7.37 (d, *J* = 8.0 Hz, 2H), 3.61–3.47 (m, 2H), 2.64 (q, *J* = 6.3 Hz, 2H), 2.36 (s, 3H), 1.55–1.30 (m, 6H). ^{13}**C NMR** (101 MHz, DMSO – d_6): δ 142.5, 137.5, 134.9, 134.8, 133.6, 133.5, 130.3, 130.1, 129.6, 126.5, 118.9, 118.1, 42.0, 28.0, 26.9, 26.8, 21.3, 21.3, 20.9, 20.4, 19.9. ^{31}**P NMR** (162 MHz, DMSO – d_6): δ 25.2. **HRMS** (ESI) calcd. for $[C_{30}H_{33}NO_2PS]^+$ ([M-Br^-]$^+$), m/z = 502.1964; found 502.1960.

5-((4-Methylphenyl)sulfonamido)pentyl 4-methylbenzenesulfonate (118)

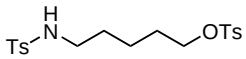

118

To a solution of 5-aminopentan-1-ol (2.06 g, 20.0 mmol, 1.00 equiv.) in DCM (80 ml), NEt_3 (8.32 mL, 6.07 g, 60.0 mmol, 3.00 equiv.) was added and the mixture was then cooled to 0 °C. TsCl (7.63 g, 40.0 mmol, 2.00 equiv.) was slowly added. The solution was then stirred at r.t. for 19 h, turning yellow at first and brown over time. An additional portion of NEt_3 (8.32 mL, 6.07 g, 60.0 mmol, 3.00 equiv.) was added, resulting in white fog forming in the flask. 4 h later, further NEt_3 (8.32 mL, 6.07 g, 60.0 mmol, 3.00 equiv.) was added, and 30 min later, NEt_3 (8.32 mL, 6.07 g, 60.0 mmol, 3.00 equiv.) was added yet again. After another 23 h of stirring, the formed colourless solid was filtered off and washed with DCM (50 ml). The brown filtrate was then washed successively with 1 M aqueous HCl (3 × 40 ml), H_2O (3 × 40 ml), sat. aqueous $NaHCO_3$ solution (40 ml) and brine (40 ml). The organic phase was dried over Na_2SO_4 and filtered, before the solvent was removed under reduced pressure. Purification via column chromatography (PE/EtOAc, 90:10 to 70:30) afforded **118** (5.41 g, 13.2 mmol, 66%) as a colourless oil.

TLC: R_f = 0.18 (PE/EtOAc, 80:20) [UV]. **IR** [cm^{-1}]: 3291, 2926, 2866, 1599, 1454, 1424, 1353, 1159, 1096. ^{1}**H NMR** (400 MHz, $CDCl_3$): δ 7.84–7.58 (m, 4H), 7.39–7.27 (m, 4H), 4.33 (s, 1H), 3.97 (t, *J* = 6.3 Hz, 2H), 2.89 (q, *J* = 6.1 Hz, 2H), 2.49–2.36 (m, 6H), 1.70–1.52 (m, 2H), 1.50–1.37 (m, 2H), 1.36–1.24 (m, 2H). ^{13}**C NMR** (101 MHz, $CDCl_3$): δ 145.0, 143.6, 137.0, 133.2, 130.0, 129.9, 128.0, 127.2, 70.2, 43.0, 29.1, 28.4, 22.6, 21.8, 21.7. **HRMS** (ESI) calcd. for $[C_{19}H_{26}NO_5S_2]^+$ ([M+H]$^+$), m/z = 412.1247; found 412.1254.

(5-((4-Methylphenyl)sulfonamido)pentyl)triphenylphosphonium 4-methylbenzenesulfonate (119)

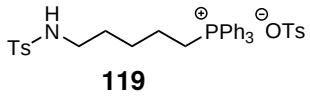

119

To a solution of 5-((4-methylphenyl)sulfonamido)pentyl 4-methylbenzenesulfonate (**118**) (5.36 g, 13.0 mmol, 1.00 equiv.) in MeCN (21 ml), PPh_3 (4.10 g, 15.6 mmol, 1.20 equiv.) was added and the mixture was heated to 100 °C, resulting in a brown solution. After 24 h, the temperature was increased to 120 °C and the solution was stirred for another 96 h, before cooled to r.t.. The solvent was removed under reduced pressure and the brown residue was dissolved in DCM and residual PPh_3 was precipitated by addition of Et_2O (150 mL). The solvent of the filtrate was removed under reduced pressure and the residue was dissolved again in 30–50 mL MeCN and was extracted with hexane (2 × 70 mL and 4 × 100 mL) until almost no PPh_3 could be detected in the polar phase via TLC. The solvent of the MeCN-phase was removed. Purification via column chromatography (EA to EA/MeOH, 70:30) afforded (**119**) (5.16 g, 7.66 mmol, 59%) as an off-white solid.

IR [cm^{-1}]: 3425, 3146, 3064, 2926, 2870, 2233, 1599, 1439,1323, 1185, 1156, 1118, 1036, 913, 816, 723, 678. ^{1}**H NMR** (400 MHz, $CDCl_3$): δ 8.03–7.68 (m, 19H), 7.31 (d, *J* = 7.8 Hz, 2H), 7.18 (d, *J* = 7.7 Hz, 2H), 3.77–3.50 (m, 2H), 3.13–2.80 (m, 2H), 2.49 (s, 3H), 2.43 (s, 3H), 1.79 (s, 6H). ^{13}**C NMR** (101 MHz, $CDCl_3$): δ 144.0, 142.4, 138.9, 137.7, 135.0, 134.9, 133.7, 133.6, 130.6, 130.5, 129.5, 128.5, 127.3, 126.3, 119.0, 118.2, 43.1, 27.6, 27.4, 22.0, 21.9, 21.6, 21.5, 21.4. ^{31}**P NMR** (162 MHz, $CDCl_3$): δ 25.2. **HRMS** (ESI) calcd. for $[C_{30}H_{33}NO_2PS]^+$ ($[M-OTs^-]^+$), m/z = 502.1964; found 502.1967.

N-(8,8-Dimethylnon-5-en-1-yl)-4-methylbenzenesulfonamide (120c)

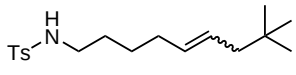

120c

To a suspension of (5-((4-methylphenyl)sulfonamido)pentyl)triphenyl phosphonium 4-methylbenzenesulfonate (**119**) (6.74 g, 10.0 mmol, 2.00 equiv.) in dry THF (17 mL) under a N_2-atmosphere, KOtBu (2.24 g, 20.0 mmol, 4.00 equiv.) was added at 0 °C. Upon addition, the suspension turned viscous making stirring impossible, wherefore additional dry THF (30 mL) was added. After 30 min. of stirring at r.t., the mixture was again cooled to 0 °C and a solution of 3,3-dimethylbutanal (628 µL, 501 mg, 5.00 mmol, 1.00 equiv.) in dry THF (1.5 mL) was added dropwise. The reaction was stirred at r.t., until the consumption of the aldehyde was confirmed via TLC after 23 h. The mixture was quenched with 1 M aqueous HCl (50 mL) and extracted with Et_2O (3 × 70 mL). The combined organic phases were washed with H_2O (2 × 70 mL) and brine, dried over Na_2SO_4, filtered and the solvent was removed under reduced pressure. Purification via column chromatography (PE/EtOAc, 90:10) afforded **120c** (770 mg, 2.38 mmol, 48%) as a slightly yellow oil and an *E*/*Z*-ratio of 1:10.

TLC: R_f = 0.44 (PE/EtOAc, 80:20) [UV, *p*-Anisaldehyde]. **IR** [cm^{-1}]: 3280, 3012, 2948, 2866, 1599, 1461, 1424, 1323, 1156, 1092, 813. ^{1}**H NMR** (400 MHz, $CDCl_3$): δ 7.83–7.60 (m, 2H+2H,

E+*Z*), 7.38–7.27 (m, 2H+2H, *E*+*Z*), 5.52–5.24 (m, 2H+2H, *E*+*Z*), 4.44 (t, *J* = 6.1 Hz, 1H+1H, *E*+*Z*), 3.05–2.81 (m, 2H+2H, *E*+*Z*), 2.43 (s, 3H+3H, *E*+*Z*), 1.96 (qd, *J* = 7.3, 1.3 Hz, 2H+2H, *E*+*Z*), 1.90–1.77 (m, 2H+2H, *E*+*Z*), 1.53–1.39 (m, 2H+2H, *E*+*Z*), 1.39–1.19 (m, 2H+2H, *E*+*Z*), 0.86 (s, 9H, *Z*), 0.84 (s, 9H, *E*). ^{13}**C NMR** (101 MHz, $CDCl_3$): δ 143.5, 137.2, 130.4, 129.8, 127.5, 127.3, 43.3, 41.2, 31.3, 29.4, 29.3, 26.7, 26.7, 21.7. **HRMS** (ESI) calcd. for $[C_{18}H_{30}NO_2S]^+$ ($[M+H]^+$), m/z = 324.1992; found 324.1992.

4-Methyl-*N*-(7-phenylhept-5-en-1-yl)benzenesulfonamide (a) and (*E*)-4-Methyl-*N*-(7-phenylhept-6-en-1-yl)benzenesulfonamide (b) (120d)

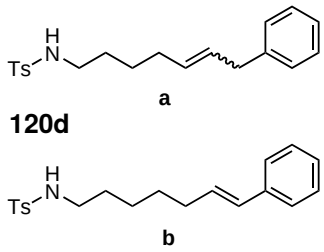

a

120d

b

To a suspension of (5-((4-methylphenyl)sulfonamido)pentyl)triphenyl phosphonium bromide **117** (2.33 g, 4.00 mmol, 2.00 equiv.) in dry THF (8 mL) under a N_2-atmosphere, KO^{t}Bu (898 mg, 8.00 mmol, 4.00 equiv.) was added at 0 °C. After 30 min. of stirring at r.t., the mixture was again cooled to 0 °C and a solution of 2-phenylacetaldehyde (233 µL, 240 mg, 2.00 mmol, 1.00 equiv.) in dry THF (2 mL) was added. The reaction was stirred at r.t., until the consumption of the aldehyde was confirmed via TLC after 19 h. The mixture was quenched with 1 M aqueous HCl (50 mL) and extracted with Et_2O (3 × 50 mL). The combined organic phases were washed with H_2O (2 × 50 mL) and brine (50 mL), dried over Na_2SO_4, filtered and the solvent was removed under reduced pressure. Purification via column chromatography (PE/EtOAc, 95:5 to 80:20) afforded **120d** (621 mg, 1.81 mmol, 90%) as a colourless oil and a mixture of regioisomers ($\Delta^{6,7}/\Delta^{7,8}$ = 3.3:1).

TLC: R_f = 0.52 (PE/EtOAc, 70:30) [UV, *p*-Anisaldehyde]. **IR** [cm^{-1}]: 2945, 2859, 1595, 1454, 1334, 1163, 1092, 928, 723. ^{1}**H NMR** (400 MHz, $CDCl_3$, mixture): δ 7.84–7.65 (m, 2H+2H, a+b), 7.37–7.24 (m, 5H+5H, a+b), 7.25–7.08 (m, 2H+2H, a+b), 6.35 (dt, *J* = 15.8, 1.5 Hz, 1H, b), 6.24–6.01 (m, 1H, b), 5.62–5.47 (m, 1H, a), 5.48–5.34 (m, 1H, a), 4.80–4.53 (m, 1H+1H, a+b), 3.41–3.25 (m, 2H, a), 3.01–2.82 (m, 2H+2H, a+b), 2.42 (s, 3H+3H, a+b), 2.21–2.02 (m, 2H+1H, a+b), 2.02–1.87 (m, 1H, b), 1.56–1.29 (m, 4H+6H, a+b). ^{13}**C NMR** (101 MHz, $CDCl_3$): δ 143.5, 141.1, 137.8, 137.1, 137.1, 131.1, 130.6, 130.2, 130.1, 129.8, 129.6, 128.8, 128.8, 128.6, 128.5, 128.5, 128.4, 127.2, 127.0, 126.0, 126.0, 43.3, 43.2, 39.1, 33.5, 32.9, 31.9, 29.6, 29.5, 29.2, 29.1, 28.9, 26.7, 26.6, 26.4, 26.2, 21.6. **HRMS** (ESI) calcd. for $[C_{20}H_{26}NO_2S]^+$ ($[M+H]^+$), m/z = 344.1679; found 344.1679.

4-Methyl-*N*-(6-phenylhex-5-en-1-yl)benzenesulfonamide (120e)

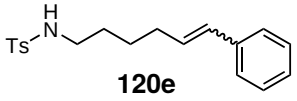

120e

To a solution of (5-((4-methylphenyl)sulfonamido)pentyl)triphenyl-phosphonium bromide **117** (4.66 g, 8.00 mmol, 2.00 equiv.) in dry THF (16 mL) under a N_2-atmosphere, KO^{t}Bu (1.80 g, 16.0 mmol, 4.00 equiv.) was added at 0 °C. After 30 min. of stirring at r.t., the

mixture was again cooled to at 0 °C and a solution of benzaldehyde (425 mg, 4.00 mmol, 1.00 equiv.) in dry THF (2 mL) was added. The reaction was stirred at r.t., until the consumption of the aldehyde was confirmed via TLC after 19 h. The mixture was quenched with 1 M aqueous HCl (50 mL) and extracted with Et_2O (3 × 50 mL). The combined organic phases were washed with H_2O (2 × 50 mL) and brine (50 mL), dried over Na_2SO_4, filtered and the solvent was removed under reduced pressure. Purification via column chromatography (PE/EA = 80:20) afforded **120e** (890 mg, 2.70 mmol, 68%) as a colourless oil and a *E*/*Z*-ratio of 1:1.4.

TLC: R_f = 0.24 (PE/EtOAc, 80:20) [UV]. **IR** [cm^{-1}]: 3276, 3027, 2930, 2863, 1599, 1495, 1446, 1320, 1156, 1092. ^{1}**H NMR** (300 MHz, $CDCl_3$): δ 7.84–7.59 (m, 2H+2H, *E*+*Z*), 7.46–6.98 (m, 7H+7H, *E*+*Z*), 6.51–6.21 (m, 1H+1H, *E*+*Z*), 6.12 (dt, *J* = 15.9, 6.8 Hz, 1H, *E*), 5.55 (dt, *J* = 11.6, 7.2 Hz, 1H, *Z*), 4.71–4.44 (m, 1H+1H, *E*+*Z*), 3.03–2.72 (m, 2H+2H, *E*+*Z*), 2.47–2.37 (m, 3H+3H, *E*+*Z*), 2.27 (qd, *J* = 7.2, 1.8 Hz, 1H+1H, *E*+*Z*), 2.15 (qd, *J* = 7.0, 1.5 Hz, 1H+1H, *E*+*Z*), 1.63–1.32 (m, 4H+4H, *E*+*Z*). ^{13}**C NMR** (101 MHz, $CDCl_3$): δ 143.5, 137.7, 137.6, 137.1, 137.1, 132.1, 130.5, 130.1, 129.9, 129.9, 129.8, 129.5, 128.8, 128.6, 128.6, 128.6, 128.3, 128.2, 127.2, 127.1, 126.7, 126.1, 125.6, 77.4, 62.8, 58.6, 43.2, 43.2, 43.1, 32.5, 31.7, 29.4, 29.3, 29.2, 28.0, 26.9, 26.3, 23.1, 21.7. **HRMS** (ESI) calcd. for $[C_{19}H_{24}NO_2S]^+$ ($[M+H]^+$), m/z = 330.1522; found 330.1525.

5.4.4 Synthesis of Intermediates

2-Phenyl-3-(phenylselanyl)-1-tosylpyrrolidine (129a)[151]

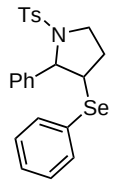

129a

To a solution of (*E*)-4-methyl-*N*-(4-phenylbut-3-en-1-yl)benzenesulfonamide (151 mg, 500 µmol, 1.00 equiv.) in dry DCM (2.5 mL), NEt_3 (69.3 µL, 50.6 mg, 500 µmol, 1.00 equiv.) and PhSeBr (130 mg, 550 µ mol, 1.10 equiv.). After confirmation of the consumption of the starting material *via* TLC, the reaction mixture was washed with 1 M aqueous HCl (2 × 5 mL), sat. aqueous $NaHCO_3$ (2 × 5 mL) and brine (5 mL). The combined aqueous layers were then extracted with DCM (5 mL), before the combined organic layers were dried over Na_2SO_4, filtered and the solvent removed under reduced pressure. Purification *via* column chromatography (DCM) afforded **129a** (135 mg, 296 µmol, 59%) as a lightly yellow oil.

TLC: R_f = 0.51 (DCM) [UV, *p*-anisaldehyde]. **IR** [cm^{-1}]: 3060, 3030, 2974, 2881, 2359, 1599, 1476, 1439, 1346, 1159, 1096, 1006, 816, 742, 697, 667. ^{1}**H NMR** (300 MHz, $CDCl_3$): δ 7.79–7.58 (m, 2H), 7.40–7.14 (m, 12H + $CHCl_3$), 4.69 (d, *J* = 2.6 Hz, 1H), 3.78 (ddd, *J* = 9.4, 7.5, 3.1 Hz, 1H), 3.67–3.51 (m, 2H), 2.47 (s, 3H), 2.32 (dddd, *J* = 13.6, 9.7, 7.5, 5.9 Hz, 1H), 1.79 (ddt, *J* = 13.3, 6.5, 3.2 Hz, 1H). ^{13}**C NMR** (101 MHz, $CDCl_3$): δ 143.5, 142.0, 135.0, 134.5, 129.6, 129.3, 128.5, 128.3, 128.2, 127.8, 127.5, 126.1, 69.3, 49.7, 48.3, 30.1, 21.6. ^{77}**Se NMR** (76 MHz, $CDCl_3$): δ 377.8. **HRMS** (ESI) calcd. for $[C_{23}H_{24}NO_2SSe]^+$ ($[M+H]^+$), m/z = 458.0688; found 458.0695.

3-((4-Methoxyphenyl)selanyl)-2-phenyl-1-tosylpyrrolidine (129b)[233]

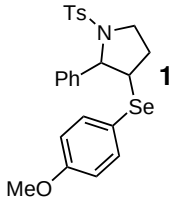

129b

To a solution of (*E*)-4-methyl-*N*-(4-phenylbut-3-en-1-yl)benzenesulfonamide (603 mg, 2.00 mmol, 1.00 equiv.) and 1,2-bis(4-methoxyphenyl)diselane (447 mg, 1.20 mmol, 0.60 equiv.) in DCM (40 mL), DEAD (188 µL, 209 mg, 1.20 mmol, 0.60 equiv.) and TfOH (8.85 µL, 15.0 mg, 100 µ mol, 5 mol%). The reaction mixture was stirred for 19 h, before the solvent was concentrated under reduced pressure. Purification *via* column chromatography (Pentane/EtOAc, 85:15) afforded **129b** (424 mg, 872 µmol, 44%) as a lightly yellow oil.

TLC: R_f = 0.28 (PE/EtOAc, 80:20) [UV, *p*-anisaldehyde]. **IR** [cm^{-1}]: 3034, 3027, 2930, 1737, 1588, 1491, 1450, 1346, 1286, 1245, 1156, 1096, 1025, 813, 753, 701, 667. ^{1}**H NMR** (300 MHz, $CDCl_3$): δ 7.77–7.62 (m, 2H), 7.38–7.13 (m, 9H + $CHCl_3$), 6.87–6.72 (m, 2H), 4.65 (d, *J* = 2.9 Hz, 1H), 3.82 (s, 3H), 3.79–3.69 (m, 1H), 3.60 (td, *J* = 9.3, 6.6 Hz, 1H), 3.45 (dt, *J* = 6.2, 3.3 Hz, 1H), 2.46 (s, 3H), 2.34–2.13 (m, 1H), 1.74 (ddt, *J* = 13.6, 6.9, 3.5 Hz, 1H). ^{13}**C NMR** (101 MHz, $CDCl_3$): δ 160.2, 143.6, 142.1, 137.6, 134.8, 129.7, 128.6, 128.0, 127.5, 126.2, 118.3, 115.1, 69.3, 55.5, 50.2, 48.4, 30.2, 21.8. ^{77}**Se NMR** (76 MHz, $CDCl_3$): δ 360.1. **HRMS** (ESI) calcd. for $[C_{23}H_{26}NO_3SSe]^+$ ([M+H]$^+$), m/z = 488.0793; found 488.0805.

3-((4-Chlorophenyl)thio)-2-phenyl-1-tosylpyrrolidine (129c)[151][233]

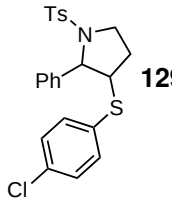

129c

To a solution of 1,2-bis(4-chlorophenyl)disulfane (144 mg, 500 µmol, 0.50 equiv.) in dry CCl_4 (1 mL) under a N_2-atmosphere, Br_2 (25.7 µL, 79.9 mg, 500 µmol, 0.50 equiv.) in CCl_4 (0.25 mL) was added at °C.. Residual amounts of Br_2 were dissolved in additional CCl_4 (0.25 mL) and added to the brown, clear solution. The mixture was stirred at °C for 30 min, before it was allowed to warm to r.t. and continued to stir for 2 h. During this time, in a second flask, (*E*)-4-methyl-*N*-(4-phenylbut-3-en-1-yl)benzenesulfonamide (301 mg, 1.00 mmol, 1.00 equiv.) was dissolved in 6 mL dry DCM under a N_2-atmosphere, before NEt_3 (139 µL, 101 mg, 1.00 mmol, 1.00 equiv.) was added. After the 2 h, this was added to the bromine-mixture and stirring was continued for another 5 h. Then, the reaction mixture was washed with 1 M aqueous HCl (2 × 15 mL), sat. aqueous $NaHCO_3$ (1 × 15 mL) and brine. The combined aqueous layers were extracted with DCM (20 mL) and the organic phase was dried over Na_2SO_4, filtered and the solvent was removed under reduced pressure. NMR analysis of the crude reaction mixture showed, that the desired product **129c** was not formed during this reaction.

To a solution of (*E*)-4-methyl-*N*-(4-phenylbut-3-en-1-yl)benzenesulfonamide (151 mg, 500 µmol, 1.00 equiv.) and 1,2-bis(4-chlorophenyl)disulfane (86.2 mg, 300 µmol, 0.60 equiv.) in DCM (10 mL), DEAD (47.1 µL, 52.2 mg, 300 µmol, 0.60 equiv.) and TfOH (2.21 µL, 3.75 mg, 25.0 µ mol, 5 mol%) were added. The reaction mixture was stirred for 18 h, before the solvent was concentrated under reduced pressure. Purification *via* column chromatog-

raphy (Pentane/EtOAc, 90:10 to 85:15) afforded **129c** (112 mg, 252 µmol, 50%) as a colourless oil.

To a solution of (*E*)-4-methyl-*N*-(4-phenylbut-3-en-1-yl)benzenesulfonamide (1.51 g, 5.00 mmol, 1.00 equiv.) and 1,2-bis(4-chlorophenyl)disulfane (862 mg, 3.00 mmol, 0.60 equiv.) in DCM (100 mL), DEAD (471 µL, 522 mg, 3.00 mmol, 0.60 equiv.) and TfOH (22.1 µL, 37.5 mg, 250 µ mol, 5 mol%) were added. The reaction mixture was stirred for 40 h, before the solvent was concentrated under reduced pressure. Two-time purification *via* column chromatography (Pentane/EtOAc, 85:15) afforded **129c** (899 mg, 2.02 mmol, 41%) as a colourless oil.

TLC: R_f = 0.40 (PE/EtOAc, 80:20) [UV, *p*-anisaldehyde]. **IR** [cm^{-1}]: 3064, 3030, 2922, 1737, 1599, 1476, 1450, 1390, 1346, 1156, 1092, 1010, 880, 812, 749, 701, 671. ^{1}**H NMR** (400 MHz, $CDCl_3$): δ 7.76–7.58 (m, 2H), 7.30 (ddd, *J* = 8.5, 6.9, 1.5 Hz, 4H), 7.27–7.18 (m, 5H), 7.14–6.99 (m, 2H), 4.61 (d, *J* = 2.3 Hz, 1H), 3.78 (ddd, *J* = 9.5, 7.7, 3.0 Hz, 1H), 3.62 (td, *J* = 9.6, 6.6 Hz, 1H), 3.55 (dt, *J* = 5.7, 2.7 Hz, 1H), 2.47 (s, 3H), 2.30 (dddd, *J* = 13.5, 9.7, 7.7, 5.9 Hz, 1H), 1.76 (ddt, *J* = 13.1, 6.3, 3.0 Hz, 1H). ^{13}**C NMR** (101 MHz, $CDCl_3$): δ 143.6, 141.5, 134.7, 134.0, 133.7, 132.1, 129.6, 129.3, 128.6, 127.9, 127.7, 126.1, 68.7, 55.7, 47.9, 29.4, 21.7. **HRMS** (ESI) calcd. for $[C_{23}H_{23}ClNO_2S_2]^+$ ($[M+H]^+$), m/z = 444.0853; found 444.0860.

5.5 Enantioselective Intramolecular Allylic Amination with Sulfonamides

5.5.1 Substrate Synthesis

General Procedure 1

To a 0.6 M solution of the respective WITTIG-salt (2.00 equiv.) in dry THF under a N_2-atmosphere, KO*t*Bu (4.00 equiv.) was added at 0 °C. The resulting suspension was stirred at r.t. for 30 min, before it was again cooled to 0 °C. At this temperature, a 2 M solution of the aldehyde (1.00 equiv.) in dry THF was added. The reaction mixture was then allowed to warm to r.t. and stirred for the given time, before H_2O (20 mL) was added. 1 M aqueous HCl was added, until a pH of 1 was reached. Then, Et_2O was added and the phases were separated. Na_2CO_3 was added to the aqueous phase until a pH of 9 was reached and the phase was extracted with Et_2O (3 × 100 mL). Removal of the solvent of the combined organic phases afforded the crude intermediate, which was again diluted in DCM to afford a 0.25 M solution. 4-Nitrobenzenesulfonyl chloride (NsCl) or 2,4,6-trimethylbenzenesulfonyl chloride (2-mesitylenesulfonyl chloride, $MesSO_2Cl$) (1.20 equiv.) was added and the mixture was cooled to 0 °C, when NEt_3 (2.00 equiv.) was added. After allowing the reaction to warm to r.t. and stir for the given time, the solvent was removed under reduced pressure and the residue was purified *via* column chromatography, affording the target compound.

(5-((4-Nitrophenyl)sulfonamido)pentyl)triphenylphosphonium bromide (130)[162],[231]

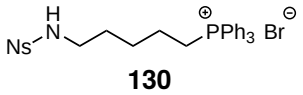

130

Step 1: 80 mL HBr (aqueous solution, 47%) was added to 5-aminopentan-1-ol (10.2 g, 98.7 mmol, 1.00 equiv.) in portion the resulting solution was stirred under reflux for 4 h. After cooling to r.t., the solvent was removed on vacuum into a cooling trap by slowly elevating the temperature to 70 °C. Removal of the solvent gave 34.32 g of crude 5-bromopentan-1-amine hydrobromide, which was used without further purification.

Step 2: NEt_3 (27.7 mL, 20.2 g, 200 mmol, 5.00 equiv.) was added in portions to a solution of 9.88 g of the crude 5-bromopentan-1-amine hydrobromide (equals 40.0 mmol and 1.00 equiv. at full conversion) in 150 mL DCM. Then, the reaction mixture was cooled with a water bath while NsCl (8.86 g, 40.0 mmol, 1.00 equiv.) was added in portions. As no precipitate was formed, another 27.7 mL of NEt_3 (20.2 g, 200 mmol, 5.00 equiv.) were added and a colourless precipitate formed. After stirring at r.t. for 3 h, TLC still showed NsCl present in the reactio mixture and further 27.7 mL NEt_3 (20.2 g, 200 mmol, 5.00 equiv.) were added and the suspension was continued to stir at r.t. for 30 min. After confirmation of the consumption of NsCl via TLC, H_2O (100 mL) was added, and the two formed phases were separated. The aqueous phase was extracted with DCM (2 × 70 mL). The combined organic phases were washed with 1 M aqueous HCl (2 × 100 mL) and 2 M aqueous HCl (2 × 60 mL) and brine (100 mL). The organic phase was dried over

Na_2SO_4 and filtered, before the solvent was removed under reduced pressure. Purification via column chromatography (PE/EtOAc, 50:50) afforded *N*-(5-bromopentyl)-4-nitrobenzenesulfonamide (7.30 g, unpure) as an orange oil, which was used without further purification.
Step 3: To a solution of 7.30 g of crude *N*-(5-bromopentyl)-4-nitrobenzenesulfonamide (20.8 mmol and 1.00 equiv. if used as pure compound) in 30 mL MeCN, PPh_3 (6.54 g, 24.9 mmol, 1.20 equiv) was added and the resulting mixture was stirred under reflux for 20 h. After cooling to r.t., the solvent was removed under reduced pressure. Purification *via* column chromatography afforded **130** (3.75 g, 6.11 mmol, 15.3% over three steps) as a beige solid.
IR [cm^{-1}]: 3392, 2866, 3056, 2937, 2192, 1539, 1439, 1368, 1334, 1163, 1111, 917, 723, 690. ^{1}**H NMR** (300 MHz, Methanol – d_4): δ 8.03–7.96 (m, 1H), 7.92–7.84 (m, 3H), 7.83–7.68 (m, 15H), 3.44–3.33 (m, 2H), 2.97 (t, *J* = 6.3 Hz, 2H), 1.79–1.45 (m, 6H). ^{13}**C NMR** (101 MHz, Methanol – d_4):δ 136.3, 136.3, 135.0, 134.8, 134.8, 134.7, 133.5, 131.6, 131.5, 131.4, 125.8, 120.3, 119.5, 43.5, 29.8, 28.3, 28.2, 23.0, 22.9, 22.9, 22.5. ^{31}**P NMR** (162 MHz, Methanol – d_4): δ 23.7. **HRMS** (ESI) calcd. for $[C_{29}H_{30}N_2O_4PS]^+$ ($[M\text{-}Br^-]^+$), m/z = 533.1658; found 533.1665.

4-Nitro-*N*-(4-(*p*-tolyl)but-3-en-1-yl)benzenesulfonamide (134a)[155][231]

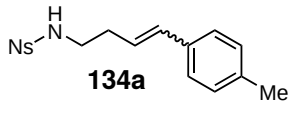

134a

According to general procedure **1**: (3-Aminopropyl)triphenylphosphonium bromide (4.00 g, 10.0 mmol, 2.00 equiv., prepared by Dr. S. Graf[165]), KO*t*Bu (2.24 g, 20.0 mmol, 4.00 equiv.), 4-methylbenzaldehyde (590 µL, 601 mg, 5.00 mmol, 1.00 equiv.), 19 h. Workup afforded crude 4-(*p*-tolyl)but-3-en-1-amine. Then, NsCl (1.33 g, 6.00 mmol, 1.20 equiv.), NEt_3 (1.39 mL, 1.01 g, 10.0 mmol, 2.00 equiv.), over night. Purification (PE/EtOAc, 80:20), afforded **134a** (367 mg, 1.06 mmol, 21% over two steps) as an orange oil with a *E*/*Z*-ratio of 1:2.4.
TLC: R_f = 0.19 (PE/EtOAc, 80:20) [UV, *p*-anisaldehyde]. **IR** [cm^{-1}]: 3343, 3094, 3019, 2922, 2732, 1595, 1536, 1439, 1409, 1342, 1163, 1066, 969, 947, 854, 783, 731. ^{1}**H NMR** (300 MHz, $CDCl_3$): δ 8.20–8.02 (m, 1+1H, *E*+*Z*), 7.85–7.55 (m, 3+1H, *E*+*Z*), 7.18–6.97 (m, 4+4H, *E*+*Z*), 6.49 (dd, *J* = 11.7, 1.9 Hz, 1H, *Z*), 6.32 (d, *J* = 16.0 Hz, 1H, *E*), 5.92 (dt, *J* = 15.9, 7.1 Hz, 1H, *E*), 5.46 (dt, *J* = 11.6, 7.2 Hz, 1H, *Z*), 5.37 (t, *J* =5.9 Hz, NH, *E*+*Z*), 3.35–3.17 (m, 2+2H, *E*+*Z*), 2.53 (qd, *J* = 7.0, 1.9 Hz, 2H, *Z*), 2.42 (qd, *J* = 6.8, 1.4 Hz, 2H, *E*), 2.36–2.30 (m, 3+3H, *E*+*Z*). ^{13}**C NMR** (101 MHz, $CDCl_3$): δ 148.0, 137.5, 136.9, 134.0, 134.0, 133.9, 133.5, 133.5, 133.4, 132.9, 132.4, 131.0, 129.3, 129.1, 129.0, 128.7, 128.6, 126.4, 126.1, 125.5, 125.5, 124.2, 43.9, 43.6, 33.3, 28.8, 21.3, 21.3. **HRMS** (ESI) calcd. for $[C_{17}H_{19}N_2O_4S]^+$ ($[M+H]^+$), m/z = 347.1060; found 347.1064.

N-(4-(4-Chlorophenyl)but-3-en-1-yl)-4-nitrobenzenesulfonamide (134b)[155][231]

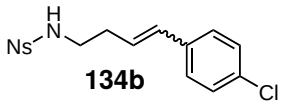

134b

According to general procedure **1**: (3-Aminopropyl)triphenylphosphonium bromide (4.80 g, 12.0 mmol, 2.00 equiv., prepared by Dr. S. GRAF[165]), KO*t*Bu (2.69 g, 24.0 mmol, 4.00 equiv.), 4-chlorobenzaldehyde (843 mg, 6.00 mmol, 1.00 equiv.), over night. Workup afforded crude 4-(4-chlorophenyl)but-3-en-1-amine. Then, NsCl (1.60 g, 7.20 mmol, 1.20 equiv.) NEt_3 (1.66 mL, 1.21 g, 12.0 mmol, 2.00 equiv.), over night. Purification (PE/EtOAc, 80:20). This procedure did not afford the desired product **134b**.

N-(4-(Naphthalen-1-yl)but-3-en-1-yl)-4-nitrobenzenesulfonamide (134c)[155][231]

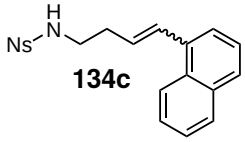

134c

According to general procedure **1**: (3-Aminopropyl)triphenylphosphonium bromide (4.80 g, 12.0 mmol, 2.00 equiv., prepared by Dr. S. GRAF[165]), KO*t*Bu (2.69 g, 24.0 mmol, 4.00 equiv.), 1-naphthaldehyde (815 µL, 937 mg, 6.00 mmol, 1.00 equiv.), over night. Workup afforded crude 4-(naphthalen-1-yl)but-3-en-1-amine. Then, NsCl (1.60 g, 7.20 mmol, 1.20 equiv.), NEt_3 (1.66 mL, 1.21 g, 12.0 mmol, 2.00 equiv.), 20 h. Purification (PE/EtOAc, 80:20), afforded **134c** (444 mg, 1.16 mmol, 19% over two steps) as yellow solid with a *E*/*Z*-ratio of 1:5.3.

TLC: R_f = 0.17 (PE/EtOAc, 80:20) [UV, *p*-anisaldehyde]. **IR** [cm^{-1}]: 3347, 3094, 3012, 3056, 2945, 2885, 2501, 2386, 2259, 1592, 1536, 1439, 1264, 1163, 1074, 969, 910, 779, 727. **^{1}H NMR** (400 MHz, $CDCl_3$): δ 8.12 (dd, *J* = 7.8, 1.4 Hz, 1H, *E*), 8.02–7.96 (m, 1H, *E*), 7.95–7.89 (m, 1H, *Z*), 7.89–7.80 (m, 2+2H, *E*+*Z*), 7.79–7.68 (m, 1+1H, *E*+*Z*), 7.65–7.34 (m, 6+6H, *E*+*Z*), 7.19 (dd, *J* = 7.0, 1.1 Hz, 1H, *Z*), 7.11 (d, *J* = 15.5 Hz, 1H, *E*), 7.00 (dd, *J* = 11.4, 1.8 Hz, 1H, *Z*), 5.99 (dt, *J* = 15.5, 7.1 Hz, 1H, *E*), 5.82 (dt, *J* = 11.4, 7.2 Hz, 1H, *Z*), 5.46 (t, *J* = 5.9 Hz, 1H, *E*), 5.35 (t, *J* = 6.1 Hz, 1H, *Z*), 3.44–3.33 (m, 2H, *E*), 3.24 (q, *J* = 6.6 Hz, 2H, *Z*), 2.57 (qd, *J* = 6.8, 1.5 Hz, 2H, *E*), 2.34 (qd, *J* = 6.9, 1.7 Hz, 2H, *Z*). **^{13}C NMR** (101 MHz, $CDCl_3$): δ 147.8, 134.6, 134.1, 134.0, 133.7, 133.6, 133.3, 133.3, 132.8, 132.6, 131.7, 131.1, 130.9, 130.7, 130.6, 129.0, 128.8, 128.6, 128.5, 128.0, 127.7, 126.3, 126.3, 126.2, 126.1, 125.3, 125.2, 124.8, 123.8, 123.7, 43.9, 43.7, 33.8, 28.9. **HRMS** (ESI) calcd. for $[C_{20}H_{19}N_2O_4S]^+$ ($[M+H]^+$), m/z = 383.1060; found 383.1058.

N-(4-(4-Chlorophenyl)but-3-en-1-yl)-2,4,6-trimethylbenzenesulfonamide (134d)[155][231]

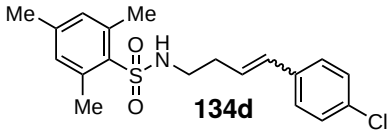

134d

To a solution of (3-aminopropyl)triphenylphosphonium bromide (5.07 g, 12.7 mmol, 1.33 equiv., prepared by Dr. S. GRAF[165]) in dry THF (21 mL) under a *N2*-atmosphere, KO*t*Bu (2.84 g, 25.3 mmol, 2.66 equiv.) was added at 0 °C.

The resulting suspension was stirred at r.t. for 30 min, before it was again cooled to 0 °C. At this temperature, a solution of 4-chlorobenzaldehyde (1.34 g, 9.50 mmol, 1.00 equiv.) in dry THF (5 mL) was added. The reaction mixture was then allowed to warm to r.t. and stirred for 5.5 h, before H_2O (20 mL) was added. The phases were separated and the aqueous phase was extracted with Et_2O (3 × 100 mL). Removal of the solvent of the combined organic phases afforded crude 4-(4-chlorophenyl)but-3-en-1-amine, which was again diluted in DCM (36 mL). $MesSO_2Cl$ (2.49 g, 11.4 mmol, 1.20 equiv.) was added and the mixture was cooled to 0 °C, when NEt_3 (2.63 mL, 1.92 g, 19.0 mmol, 2.00 equiv.) was added. After allowing the reaction to warm to r.t. and stir over night, the solvent was removed under reduced pressure and the residue was purified *via* column chromatography (PE/EtOAc, 80:20), affording **134d** (2.34 g, 6.43 mmol, 68% over two steps) as slightly yellow oil with an *E*/*Z*-ratio of 1:2.1.

TLC: R_f = 0.34 and 0.37 (PE/EtOAc, 80:20) [UV, *p*-anisaldehyde]. **IR** [cm^{-1}]: 3302, 2974, 2941, 2255, 1603, 1491, 1320, 1152, 1088, 906, 842, 727. ^{1}**H NMR** (400 MHz, $CDCl_3$): δ 7.30–7.20 (m, 2+2H, *E*+*Z*), 7.22–7.14 (m, 2H, *E*), 7.12–7.03 (m, 2H, *Z*), 6.93 (s, 2H, *E*), 6.90 (s, 2H, *Z*), 6.44 (dt, *J* = 11.6, 1.9 Hz, 1H, *Z*), 6.27 (dt, *J* = 15.8, 1.4 Hz, 1H, *E*), 5.94 (dt, *J* = 15.8, 7.1 Hz, 1H, *E*), 5.50 (dt, *J* = 11.6, 7.2 Hz, 1H, *Z*), 4.71 (dt, *J* = 20.6, 6.3 Hz, 1+1H, *E*+*Z*), 3.04 (dq, *J* = 15.6, 6.6 Hz, 2+2H, *E*+*Z*), 2.61 (s, 6H, *E*), 2.58 (s, 6H, *Z*), 2.41 (qd, *J* = 7.0, 1.9 Hz, 2H, *Z*), 2.34 (qd, *J* = 6.7, 1.4 Hz, 2H, *E*), 2.31–2.24 (m, J = 1.8 Hz, 3+3H, *E*+*Z*). ^{13}**C NMR** (101 MHz, $CDCl_3$): δ 142.3, 142.3, 139.1, 139.1, 135.4, 135.2, 133.8, 133.8, 133.1, 132.8, 132.1, 132.0, 131.9, 130.9, 130.0, 128.7, 128.6, 128.5, 127.4, 126.7, 42.4, 42.0, 33.1, 28.7, 23.1, 23.0, 21.0. **HRMS** (ESI) calcd. for $[C_{19}H_{23}ClNO_2S]^+$ ($[M+H]^+$), m/z = 364.1133; found 364.1135.

(*Z*)-*N*-(5,5-Dimethylhex-3-en-1-yl)-2,4,6-trimethylbenzenesulfonamide (134e)[155][231]

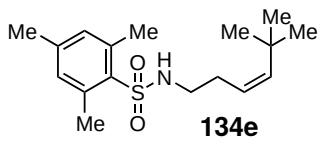

134e

According to general procedure **1**: (3-Aminopropyl)triphenylphosphonium bromide (5.07 g, 12.7 mmol, 1.33 equiv., prepared by Dr. S. Graf[165]), KO*t*Bu (2.84 g, 25.3 mmol, 2.66 equiv.), pivalaldehyde (1.87 mL, 1.48 g, 9.50 mmol, 1.00 equiv.), over night. Workup afforded crude 5,5-dimethylhex-3-en-1-amine. Then, $MesSO_2Cl$ (2.49 g, 11.4 mmol, 1.20 equiv.), NEt_3 (2.63 mL, 1.92 g, 19.0 mmol, 2.00 equiv.), over night. Purification (PE/EtOAc, 90:10), afforded **134e** (890 mg, 2.88 mmol, 30% over two steps) as a slightly yellow solid.

TLC: R_f = 0.57 (PE/EtOAc, 80:20) [UV, *p*-anisaldehyde]. **M.p.** = 68 °C. **IR** [cm^{-1}]: 3306, 2956, 2870, 1603, 1461, 1409, 164, 1323, 1189, 1156, 1074, 1036, 783, 731. ^{1}**H NMR** (300 MHz, $CDCl_3$): δ 6.99–6.89 (m, 2H), 5.43 (dt, *J* = 12.0, 1.8 Hz, 1H), 4.93 (dt, *J* = 12.0, 7.4 Hz, 1H), 4.48 (bs, 1H), 2.91 (t, *J* = 6.9 Hz, 2H), 2.63 (s, 6H), 2.35 (qd, *J* = 7.0, 1.8 Hz, 2H), 2.30 (s, 3H), 1.05 (s, 9H). ^{13}**C NMR** (75 MHz, $CDCl_3$): δ 143.6, 142.3, 139.2, 133.6, 132.1, 123.6, 42.8, 33.5, 31.2, 28.4, 23.1, 21.1. **HRMS** (ESI) calcd. for $[C_{17}H_{28}NO_2S]^+$ ($[M+H]^+$), m/z = 310.1835; found 310.1825.

5.6 Racemic Intermolecular Allylic Amination with Sulfonamides

5.6.1 Optimisation of Reaction Conditions

General Procedure 2

Into a 40 mL vial were added (*E*)-dec-5-ene (**138**, 70.1 mg, 0.50 mmol, 1.0 equiv.), *N*-methyl-*p*-toluenesulfonamide **137** and solvent and the resulting mixture was stirred under reaction temperature for 5–10 min. Then, $(PhSe)_2$, photocatalyst (PC) 2,4,6-tris(4-methoxyphenyl)pyrylium tetrafluoroborate (**86**) and further additives, if stated, were added, the vial was sealed with a screw cap including a septum and equipped with a balloon filled with air. The reaction was performed in a temperature-controlled metal block by irradiation with blue light (λ_{max} = 440–460 nm) with a stirring speed of 550 rpm. When the reaction was stopped, the reaction mixture was transferred into a round bottom flask using DCM and the solvent was removed under reduced pressure. To the dried reaction mixture, 15–18 mg of the internal standard 1,3,5-trimethoxybenzene (TMB) or 25–50 µL of trichloroethylene (TCE) or 1,1,2,2-tetrachloroethane was added. $CHCl_3$ was added until a homogenous solution was formed and approx. 0.25 mL were withdrawn and added into a NMR tube containing 0.25 mL $CDCl_3$ for quantitative ^{1}H NMR analysis.

Table 5.3: Optimisation of Stoichiometry in the Racemic Intermolecular Allylic Amination with Sulfonamides.[a]

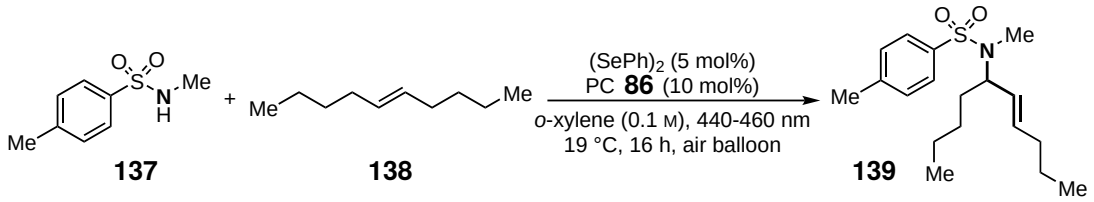

Entry	n (**138**) [mmol]	**137** [equiv.]	Conversion of **137**[b,c] [%]	Yield[c] [%]
1[d]	1.0	1.0	20	7
2	0.50	2.0	n.d.	4
3	0.50	5.0	n.d.	6
4[e]	0.50	5.0	n.d.	2
5	0.50	10	n.d.	2

[a] 0.50 mmol of **138**. Reactions were performed in a 40 mL reaction vial. [b] Conversion of 0.50 mmol of **137**. [c] NMR yields and conversions were determined with 1,1,2,2-tetrachloroethane as the internal standard. [d] Reaction in a 250 mL round bottom flask, 22 h, $(PhSe)_2$ (2.5 mol%), **86** (5 mol%), crisallisation dish covered with LED strips (λ_{max} = 465 nm). The NMR yield was determined with TMB as the internal standard. [e] Air balloon instead of open vial. n.d. = not determined.

Table 5.4: Variation of Solvent in the Racemic Intermolecular Allylic Amination with Sulfonamides.[a]

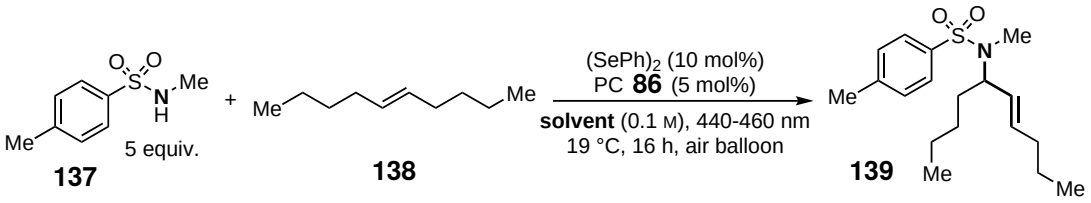

Entry	Solvent	Conversion of **137**[c] [%]	Yield[c] [%]
1	Toluene	19	7
2	*o*-Xylene	22	3
3	1,4-Dioxane	24	18
4[e]	PhCl	17	19
5[e]	THF	25	17
6[e]	EtOAc	29	21
7	$CHCl_3$	61	13
8	DCM	69	14
9	DCE	38	15
10	Acetone	67	15
11	DMSO	3	0
12	MeCN	14	6
13	EtOH	0	0
14	MeOH	5	0
15	HFIP	9	7
16[e,f]	PhCl	19	21
17[f,g]	DCE	n.d.	9
18[f]	DCE/HFIP (3:2)	n.d.	13

[a] 0.50 mmol of **138**. [b] Conversion of 0.50 mmol of **137**. [c] NMR yields and conversions were determined with TCE as the internal standard. [d] *p*-Xylene. [e] Average of two reactions. [f] 8 h. [g] 10 mol% of $(4\text{-ClPhS})_2$ added.

Table 5.5: Optimisation of Concentration in Different Solvents in the Racemic Intermolecular Allylic Amination with Sulfonamides.[a]

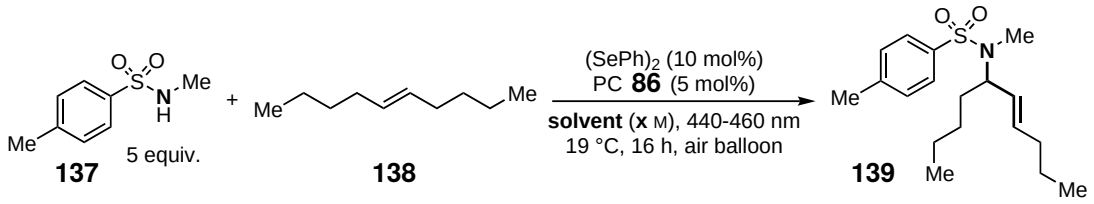

Entry	Solvent	c [**x** mol/L]	Conversion of **137**[b,c] [%]	Yield[c] [%]
1	EtOAc	0.05	6	7
2[d]	EtOAc	0.10	29	21
3	EtOAc	0.20	21	13
4	EtOAc	0.50	21	10
5[e]	EtOAc	0.10	34	8
6	PhCl	0.025	11	10
7[d]	PhCl	0.05	22	19
8[d]	PhCl	0.10	17	19
9	PhCl	0.20	15	13
10	PhCl	0.50	9	3
11[d,e]	PhCl	0.10	34	37
12[d,f]	PhCl	0.10	11	12
13	Toluene	0.05	n.d.	5
14[d]	Toluene	0.10	19	7
15	Toluene	0.20	0	0
16	Toluene	0.50	0	0
17[e]	Toluene	0.10	0	0
18	THF	0.05	15	14
19[d]	THF	0.10	25	17
20	THF	0.20	15	12
21	THF	0.50	32	10

[a] 0.50 mmol of **138**. [b] Conversion of 0.50 mmol of **137**. [c] NMR yields and conversions were determined with TCE as the internal standard. [d] Average of two reactions. [e] **137** (0.10 mmol, 1.0 equiv.), **138** (5.0 equiv.), $(PhSe)_2$ (50 mol%), **86** (25 mol%). [f] **137** (0.50 mmol, 1.0 equiv.), **138** (5.0 equiv.).

Table 5.6: Variation of Catalysts in the Racemic Intermolecular Allylic Amination with Sulfonamides.[a]

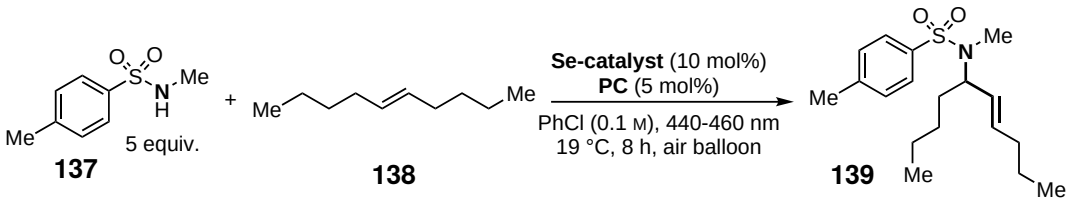

Entry	t [h]	Se-catalyst	PC	Conversion of **137**[b,c]	Yield[c] [%]
1	8	$(PhSe)_2$	**86**	19	21
2	8	$(PhSe)_2$	**143**	24	0
3	8	**140**	**86**	9	9
4	8	**140**	**143**	17	0
5	8	**141**	**86**	24	13
6	8	**141**	**143**	13	4
7[d]	6	**142**	**86**	20	18
8[d]	8	**142**	**86**	25	21
9[d]	6	**144**		0	0
10[d]	24	**144**		0	0

[a]0.50 mmol of **138**. [b]Conversion of 0.50 mmol of **137**. [c]NMR yields and conversions were determined with TCE as the internal standard. PC = photocatalyst. [d]20 mol% of Se-catalyst/Hybrid-catalyst. Average of two reactions.

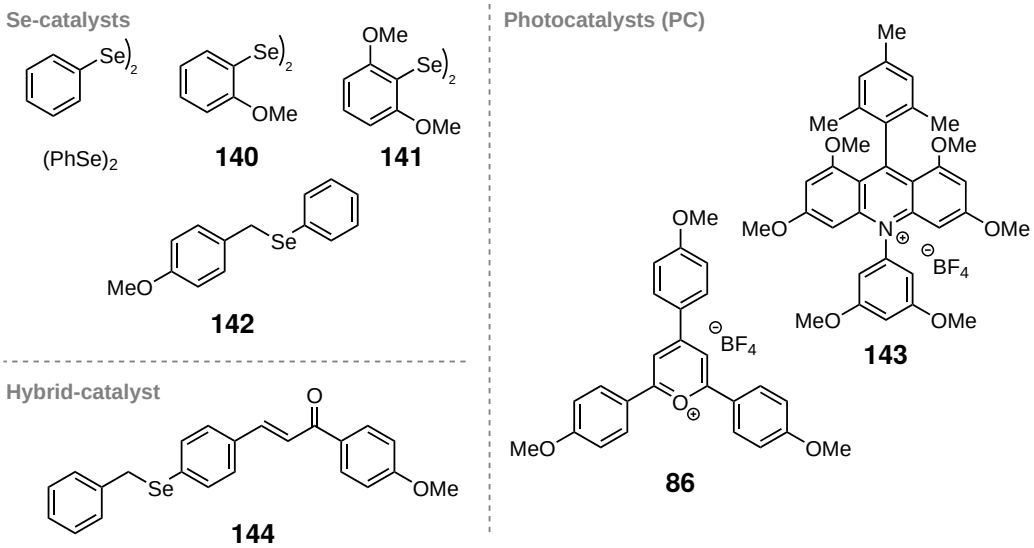

Table 5.7: Variation of Redoxmediators in the Racemic Intermolecular Allylic Amination with Sulfonamides.[a]

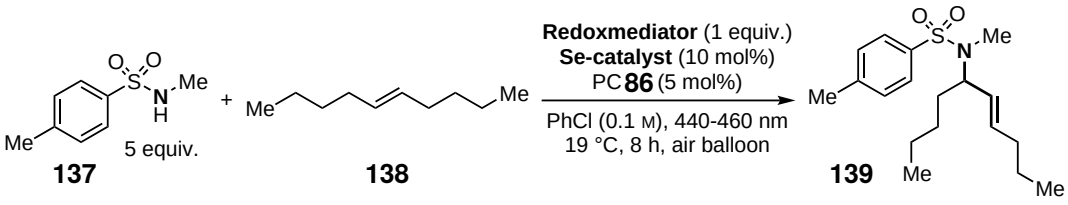

Entry	Se-catalyst	Redoxmediator	Conversion of **137**[b,c]	Yield[c] [%]
1	$(PhSe)_2$	-	19	21
2	**140**	-	9	9
3	$(PhSe)_2$	**145**	26	24
4	$(PhSe)_2$	**146**	19	17
5	$(PhSe)_2$	**147**	10	7
6	**140**	**145**	1	2
6	**140**	**146**	23	19
6	**140**	**147**	24	12

[a]0.50 mmol of **138**. [b]Conversion of 0.50 mmol of **137**. [c]NMR yields and conversions were determined with TCE as the internal standard.

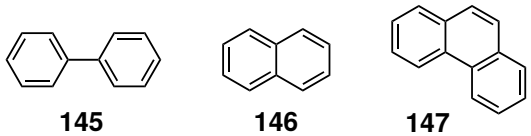

Table 5.8: Change of Light Source in the Racemic Intermolecular Allylic Amination with Sulfonamides.[a]

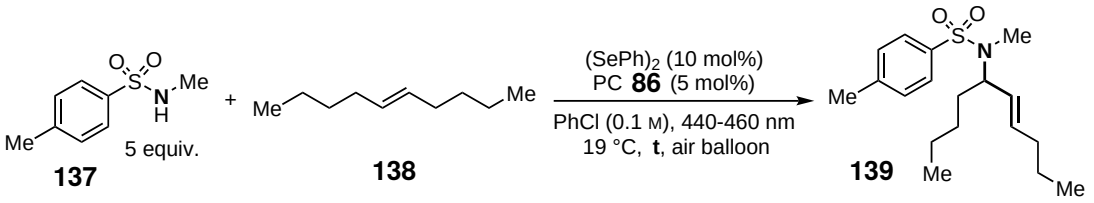

Entry	t [h]	Light Source	Average Intensity [lux]	Average Power [mW]	Conversion of **137**[b,c]	Yield[c] [%]
1	8	61-20	21 703	393	18	22
2[d]	8	124-20-1	44 098	463	20	20
3[e]	16	61-20	21 703	393	17	19
4[e]	16	124-20-1	44 098	463	17	19

[a]0.50 mmol of **138**. λ_{max} between 440 and 460 nm. [b]Conversion of 0.50 mmol of **137**. [c]NMR yields and conversions were determined with TCE as the internal standard. [d]Average of two reactions. [e]Average of three reactions.

Table 5.9: Second Addition of Catalysts in the Racemic Intermolecular Allylic Amination with Sulfonamides.[a]

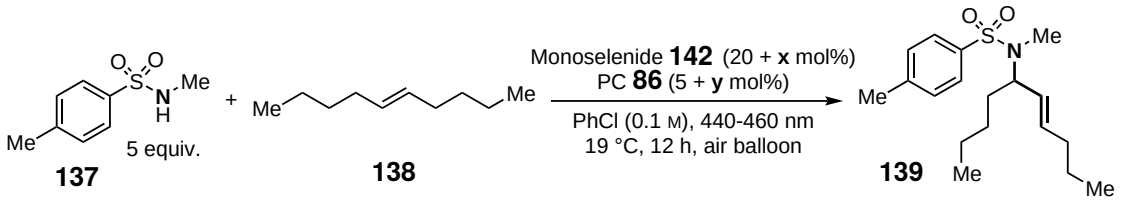

Entry	t [h]	**x** [mol%]	**y** [mol%]	Conversion of **137**[b,c]	Yield[c] [%]
1	8	-	-	25	21
2	10	-	-	17	19
3	16	-	-	14	9
4	12	20	-	16	6
5	12	-	5	39	24
6	12	20	5	33	14

[a]0.50 mmol of **138**, second addition of catalyst(s) after 6 h reaction time. Average value of two reactions given. [b]Conversion of 0.50 mmol of **137**. [c]NMR yields and conversions were determined with TCE as the internal standard.

Table 5.10: Variation of Base in the Racemic Intermolecular Allylic Amination with Sulfonamides.[a]

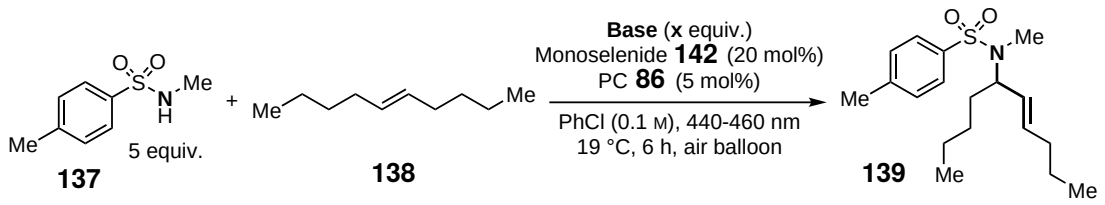

Entry	Base	**x** [equiv.]	Conversion of **137**[b,c]	Yield[c] [%]
1	-	-	20	18
2	Li_2CO_3	4	2	0
3	Na_2CO_3	4	3	0
4	K_2CO_3	4	0	0
5	Cs_2CO_3	4	0	0
6	$NaHCO_3$	4	6	0
7	Na_2HPO_4	4	4	0
8	$KHCO_3$	4	14	5
9	NaH_2PO_4	4	2	0
10	K_2HPO_4	4	0	0
11	CaF_2	4	34	21
12	CsF	1.5	10	5

[a]0.50 mmol of **138**. Average value of two reactions given. [b]Conversion of 0.50 mmol of **137**. [c]NMR yields and conversions were determined with TCE as the internal standard.

Table 5.11: Addition of 4,4'-Dichloro diphenyl disulfide $(4\text{-ClPhS})_2$ and/or *o*-Nitrobenzaldehyde **183** in the Racemic Intermolecular Allylic Amination with Sulfonamides.[a]

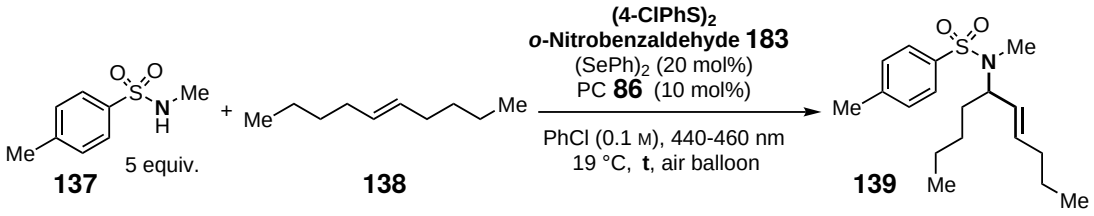

Entry	t [h]	$(4\text{-ClPhS})_2$ [mol%]	**183** [mol%]	Conversion of **137**[b,c]	Yield[c] [%]
1	4	20	-	19	6
2	8	-	-	30	28
3		20	25	21	20
4		-	25	n.d.	6
5		20	-	38	21
6	16	-	-	23	21
7		20	25	22	23
8[d]		20	25	40	25
9		20	-	52	19
10	24	-	-	26	28
11		-	25	n.d.	22

[a]0.50 mmol of **138**. Average value of two reactions given. [b]Conversion of 0.50 mmol of **137**. [c]NMR yields and conversions were determined with TCE as the internal standard. [d]Second addition of $(PhSe)_2$ (20 mol%) and **86** (10 mol%) after 8 h.

Table 5.12: Screening of Catalyst Loading with Varying Reaction Time in the Racemic Intermolecular Allylic Amination with Sulfonamides.[a]

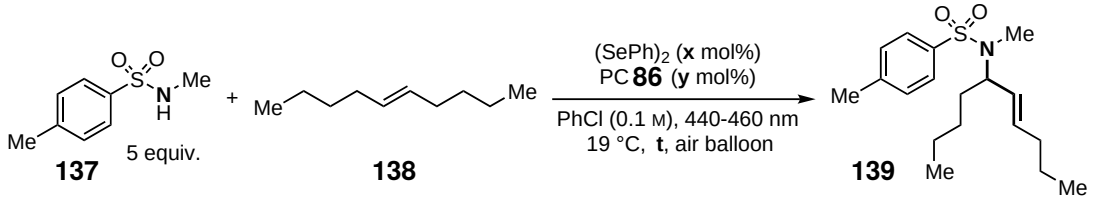

Entry	t [h]	**x** [mol%]	**y** [mol%]	Conversion of **137**[b,c]	Yield[c] [%]
1	6	10	5	9	10
2		10	10	1	5
3		20	5	2	4
4		50	5	0	0
5	8	10	5	19	21
6		10	10	20	23
7		10	20	18	20
8		20	5	19	18
9		20	10	30	28
10		50	25	4	0
11	16	10	5	17	19
12		10	10	19	19
13		20	5	25	27
14		20	10	23	21
15		50	5	0	3
16		50	25	0	0
17	24	20	5	6	7
18		20	10	26	28

[a] 0.50 mmol of **138**. Average value of two reactions given. [b] Conversion of 0.50 mmol of **137**. [c] NMR yields and conversions were determined with TCE as the internal standard.

Table 5.13: Screening of Temperature in the Racemic Intermolecular Allylic Amination with Sulfonamides.[a]

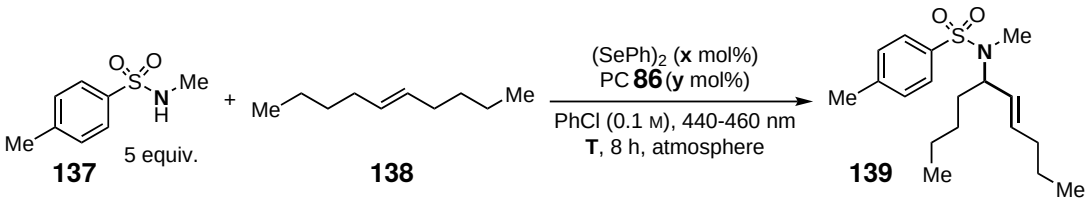

Entry	$(PhSe)_2$/**86** **x**:**y** [mol%]	T [°C]	Conversion of **137**[b,c]	Yield[c] [%]
1	10:10	19	20	23
2		30	0	0
3	20:10	19	30	28
4		30	25	26
5		50	15	17

[a]0.50 mmol of **138**. Average value of two reactions given. [b]Conversion of 0.50 mmol of **137**. [c]NMR yields and conversions were determined with TCE as the internal standard.

Table 5.14: Reaction under Oxygen Atmosphere in the Racemic Intermolecular Allylic Amination with Sulfonamides.[a]

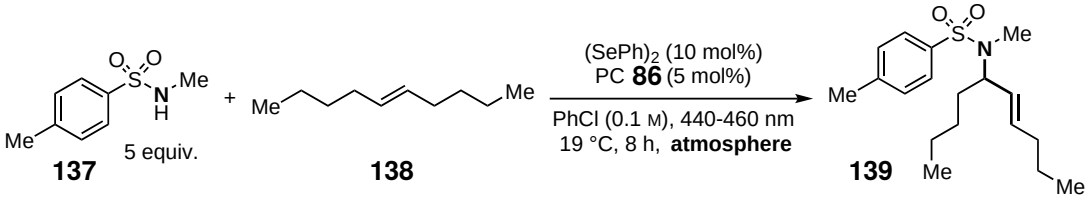

Entry	Atmosphere	Conversion of **137**[b,c]	Yield[c] [%]
1	air balloon	19	21
2	O_2	0	0

[a]0.50 mmol of **138**. Average value of two reactions given. [b]Conversion of 0.50 mmol of **137**. [c]NMR yields and conversions were determined with TCE as the internal standard.

Table 5.15: Control Experiments in the Racemic Intermolecular Allylic Amination with Sulfonamides.[a]

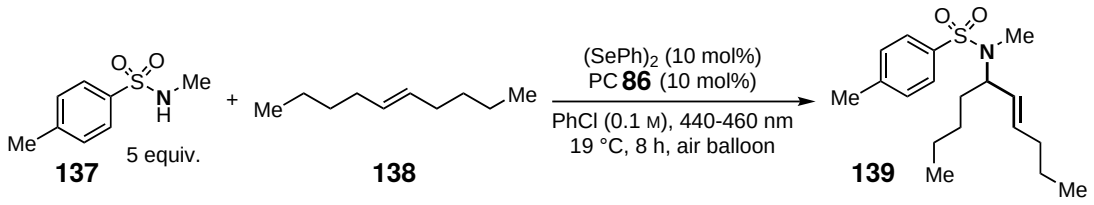

Entry	Deviation from Standard Conditions	Conversion of **137**[b,c]	Yield[c] [%]
1	-	20	23
2	No $(PhSe)_2$ $(PhSe)_2$	0	0
3	No PC **86**	0	0
4	N_2-atmosphere	0	0
5	No irradiation	0	0
6	No irradiation, 55 °C	0	0

[a]0.50 mmol of **138**. Average value of two reactions given. [b]Conversion of 0.50 mmol of **137**. [c]NMR yields and conversions were determined with TCE as the internal standard.

5.6.2 Kinetic Investigations

Kinetic Measurement of the Racemic Intermolecular Allylic Amination with Sulfonamides.

According to general procedure **2** with 5 equiv. of **137**, 5 mol% of PC **86** and the given amount of Se-catalyst in 5 mL PhCl. The reactions were run for the given time in Table 5.16.

Table 5.16: Kinetic Investigation of the Racemic Intermolecular Allylic Amination with Sulfonamides and Two Different Se-catalystst.[a]

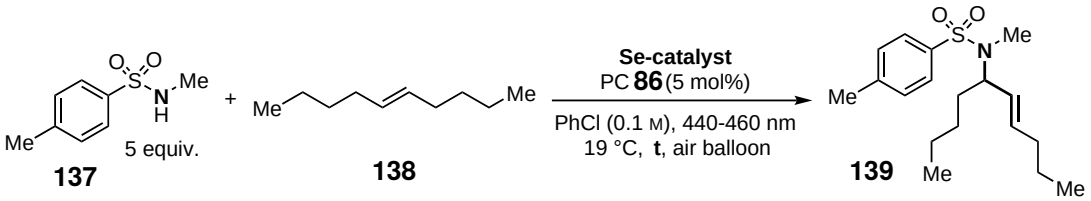

		$(PhSe)_2$ (10 mol%)		Monoselenide **142** (20 mol%)	
Entry	t [h]	Conversion of **137**[b,c] [%]	Yield[c] [%]	Conversion of **137**[b,c] [%]	Yield[c] [%]
1	1	0	0	0	0
2	2	0	0	3	3
3	3	4	2	5	6
4	4	1	2	8	8
5	5	1	2	15	16
6	6	9	10	20	18
7	8	19	21	25	21
8	10	-	-	17	19
9	16	17	19	14	9

[a]0.50 mmol of **138**. Average value of two reactions given. [b]Conversion of 0.50 mmol of **137**. [c]NMR yields and conversions were determined with TCE as the internal standard..

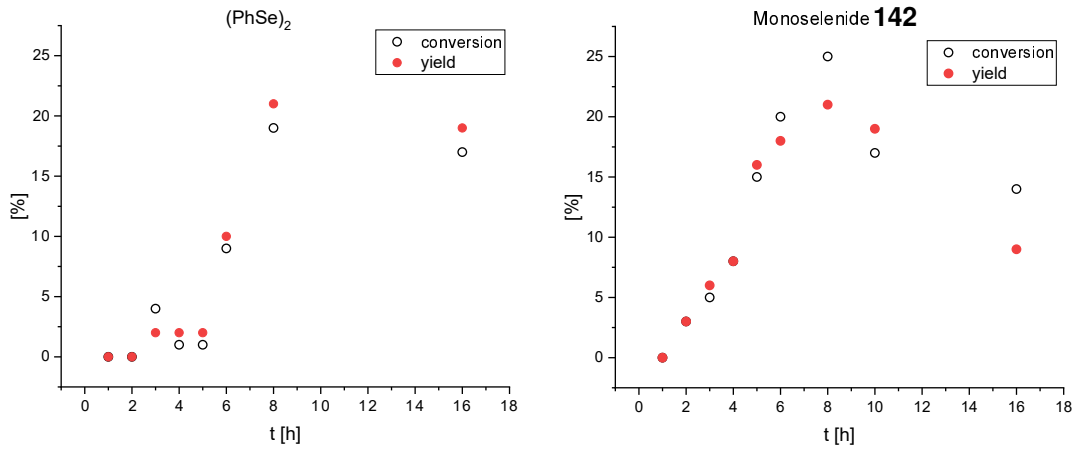

Variation of Catalyst Loading

The reactions were conducted according to the general procedure **2** of the optimisation.

Table 5.17: Kinetic Investigation of the Racemic Intermolecular Allylic Amination with Sulfonamides with Varying Catalyst Loading.[a]

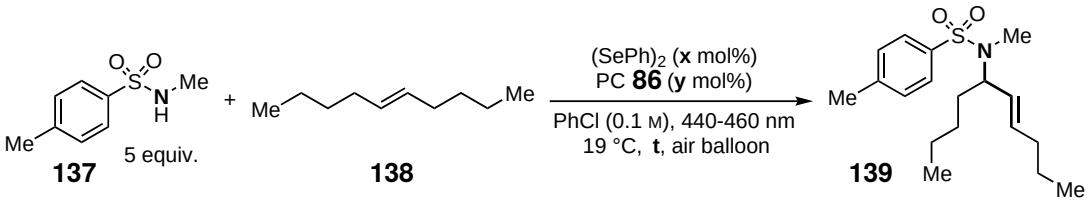

137 **138** **139**

Entry	$(PhSe)_2$/**86** **x**:**y** [mol%]	t [h]	Conversion of **137**[b], *c* [%]	Yield[c] [%]
1	10:5	6	9	10
2		8	19	21
3		16	17	19
4	10:10	6	1	5
5		8	20	23
6		16	19	19
8	10:20	8	18	20
9	20:5	6	2	4
10		8	19	18
11		16	25	27
12		24	6	7
13	20:10	8	30	28 (24)
14		16	23	21
15		24	26	28
16	50:5	6	0	0
17		16	0	3
18	50:25	8	4	0
19		16	0	0

[a]0.50 mmol of **138**. Average value of two reactions given. [b]Conversion of 0.50 mmol of **137**. [c]NMR yields and conversions were determined with TCE as the internal standard.

Measurement of Product Decay

The reactions were conducted according to the general procedure **2** of the optimisation with the conditions depicted in Table 5.18. The reaction conditions were chosen to mimick the conditions after approx. 8 h of the formation of product **139**.

Table 5.18: Kinetic Investigation of Decay of **139** under Reaction Conditions.

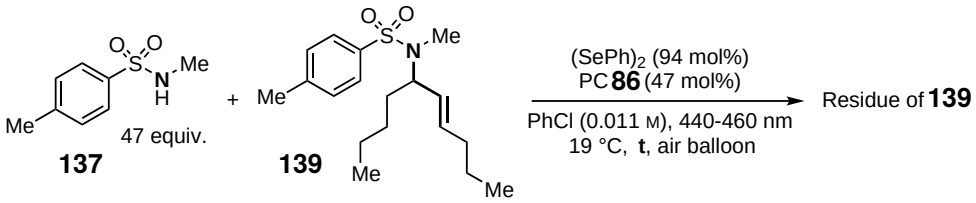

Entry	n (**139**) [µmol]	t [h]	Conversion of **137**[a] [%]	Residue of **139**[a] [µmol]	[%]
1	52.7	16	0	46.0	87
2	52.6	40	0	43.2	82
3	52.8	112	16	11.0	21

[a] Conversions/Residues were determined *via* ^{1}H NMR analysis and TCE as the internal standard.

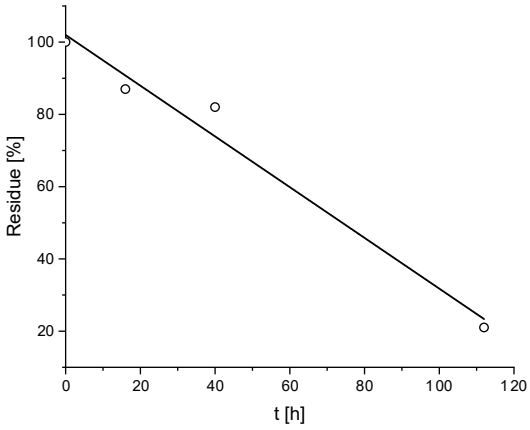

5.6.3 Substrate Synthesis

Methyl (*E*)-hex-3-enoate (148)

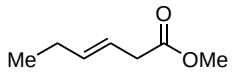

148

To a solution of methyl (*E*)-hex-3-enoate (**148**) (573 mg, 5.01 mmol, 1.00 equiv.) in MeOH (10 mL), H_2SO_4 (conc.) (1 mL) was added and stirred at r.t. for 21 h, until consumption of the starting material was confirmed *via* TLC. $NaHCO_3$ (30 mL) was added and the solution was extracted with DCM (3 × 20 mL). The combined organic phases were washed with H_2O and brine, dried over Na_2SO_4, filtered and the solvent was carefully removed under reduced pressure, affording **148** (443 mg, 3.46 mmol, 69%) as a slightly yellow liquid.

TLC: R_f = 0.5 (PE/EtOAc, 2:1) [$KMnO_4$]. **IR** [cm^{-1}]: 2963, 2851, 1737, 1435, 1357, 1320, 1256, 1163, 1122, 1018, 969. ^{1}**H NMR** (300 MHz, $CDCl_3$): δ 5.71–5.37 (m, 2H), 3.66 (s, 3H), 3.10–2.91 (m, 2H), 2.20–1.87 (m, 2H), 0.96 (t, J = 7.5 Hz, 3H). ^{13}**C NMR** (75 MHz, $CDCl_3$): δ 172.7, 136.5, 120.6, 51.8, 38.0, 25.6, 13.5. **HRMS** (EI) calcd. for $[C_7H_{12}O_2]^{\cdot+}$ ($[M]^{\cdot+}$), m/z = 128.08318; found 128.08332.

5.6.4 Synthesis of Allylic Sulfonamides

(*E*)-*N*-(Dec-6-en-5-yl)-*N*,4-dimethylbenzenesulfonamide (139)

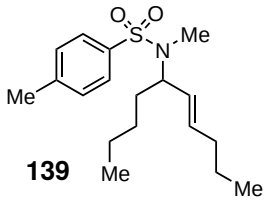

139

(*E*)-Dec-5-ene (**138**, 70.2 mg, 500 µmol, 1.00 equiv.), *N*,4-dimethylbenzenesulfonamide (**137**, 464 mg, 2.50 mmol, 5.00 equiv.), TAPT (**86**, 24.4 mg, 50.1 µmol, 10 mol%), $(PhSe)_2$, 31.2 mg, 100 µmol, 20 mol%) and PhCl (5 mL) were added into a 40 mL vial. The vial was then equipped with a balloon filled with air and the resulting mixture was stirred under water cooling at 19 °C and irradiated for 8 h. Afterwards, the reaction mixture was transferred into a round bottom flask using DCM and the solvent was removed under reduced pressure. After purification (PE/EtOAc, 95:5 to 90:10), the product was isolated as a lightly yellow oil (39.0 mg, 121 µmol, 24%). Crude ^{1}H NMR analysis: 30% yield.

TLC: R_f = 0.39 (PE/EtOAc, 9:1) [UV, *p*-anisaldehyde]. **IR** [cm^{-1}]: 2960, 2870, 1718, 1599, 1494, 1461, 1334, 1156, 1088, 969, 921, 813. **^{1}H NMR** (300 MHz, $CDCl_3$): δ 7.76–7.55 (m, 2H), 7.38–7.11 (m, 2H + $CHCl_3$), 5.53–5.28 (m, 1H), 5.08 (dddt, *J* = 15.4, 7.0, 4.2, 1.4 Hz, 1H), 4.34 (quint., *J* = 7.0 Hz, 1H), 2.65 (d, *J* = 1.2 Hz, 3H), 2.41 (s, 3H), 1.95–1.72 (m, 2H), 1.51–1.37 (m, 2H), 1.36–1.07 (m, 6H), 0.97–0.67 (m, 6H). **^{13}C NMR** (101 MHz, $CDCl_3$): δ 142.8, 142.7, 137.3, 137.3, 134.2, 134.0, 129.4, 127.4, 127.3, 126.9, 126.6, 58.7, 58.4, 34.4, 34.3, 32.0, 31.8, 31.2, 28.5, 28.5, 28.4, 22.4, 22.1, 22.1, 21.5, 21.5, 19.4, 14.0, 13.9, 13.8, 13.6. **HRMS** (ESI) calcd. for $[C_{18}H_{30}NO_2S]^+$ ($[M+H]^+$), m/z = 324.1994; found 324.1992.

Methyl (*E*)-4-((*N*,4-Dimethylphenyl)sulfonamido)hex-2-enoate (149)

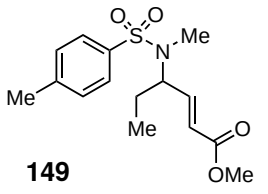

149

Methyl (E)-hex-3-enoate (**148**, 64.3 mg, 501 µmol, 1.00 equiv.), *N*,4-dimethylbenzenesulfonamide (**137**, 463 mg, 2.50 mmol, 4.99 equiv.), TAPT (**86**, 24.4 mg, 50.1 µmol, 10 mol%), $(PhSe)_2$ (31.2 mg, 100 µmol, 20 mol%) and PhCl (5 mL) were added into a 40 mL vial. The vial was then equipped with a balloon filled with air and the resulting mixture was stirred under water cooling at 19 °C and irradiated for 8 h. Afterwards, the reaction mixture was transferred into a round bottom flask using DCM and the solvent was removed under reduced pressure. Purification *via* column chormatography did not give the desired product.

5.7 Racemic Intermolecular Allylic Amination with Azoles

5.7.1 Optimisation of Reaction Conditions

General Procedure 3

Into a 40 mL vial were added ethyl (*E*)-hex-3-enoate (**150a**), 4-chloropyrazole (**151a**), $(SePh)_2$, photocatalyst (**86**) and further additives, if stated. Solvent was added and the vial was sealed with a screw cap including a septum and equipped with two cannulas, leaving the mixture open to air. The reaction was performed in a temperature-controlled metal block by irradiation with blue light (λ_{max} = 448 nm) with a stirring speed of 400–550 rpm. When the reaction was stopped, the mixture was transferred into a round bottom flask using DCM and the solvent was removed under reduced pressure. To the dried reaction mixture, 10-25 mg of the internal standard 1,4-dimethoxybenzene (DMB) were added and the mixture was dissolved in $CDCl_3$ (1-2 mL), homogenised in an ultrasonic bath and then withdrawn for quantitative ^{1}H NMR analysis.

Table 5.19: Optimisation of Stoichiometry and Solvent in the Racemic Intermolecular Allylic Amination with Azoles.[a]

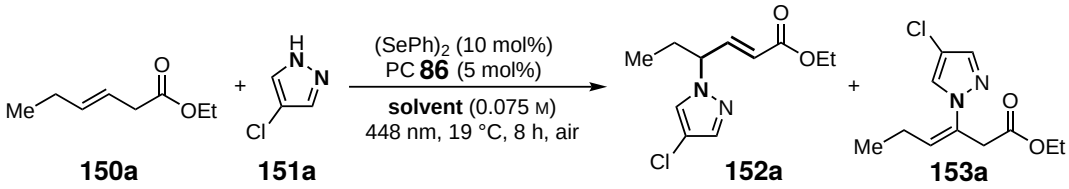

150a **151a** **152a** **153a**

Entry	**150a**	**151a**	Solvent	Conversion[a,b] [%]	Yield[b] [%]		
					152a	**153a**	Total
1[c]	0.30 mmol	3.0 equiv.	DCE	100	62	9	71
2[c]	0.30 mmol	1.0 equiv.	DCE	100	51	10	60
3[c]	3.0 equiv.	0.30 mmol	DCE	100	65	11	76
4	3.0 equiv.	0.30 mmol	MeCN	55	20	4	24
5	3.0 equiv.	0.30 mmol	$CHCl_3$	70	63	13	76
6	3.0 equiv.	0.30 mmol	Acetone	49	18	3	21
7	3.0 equiv.	0.30 mmol	Toluene	46	4	1	5

[a]Conversion of 1.0 equiv. of **151a**. [b]Conversions and NMR yields were determined with DMB as the internal standard. [c]Average value of two reactions.

Table 5.20: Optimisation Catalyst Loading and Concentration in the Racemic Intermolecular Allylic Amination with Azoles.[a]

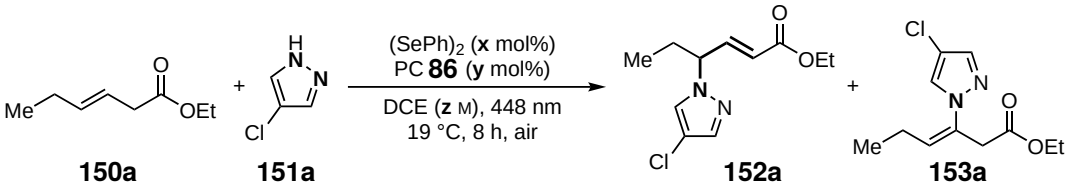

150a **151a** **152a** **153a**

Entry	**x** [mol%]	**y** [mol%]	**z** [mol/L]	Conversion[b] [%]	Yield[b] [%]		
					152a	**153a**	Total
1	10	5	0.075	100	65	11	76
2	10	10	0.075	100	65	10	75
3	20	5	0.075	100	62	11	73
4	20	10	0.075	100	65	10	75
5	10	5	0.15	100	65	12	76
6	10	5	0.0375	100	59	10	69

[a]0.30 mmol (1.0 equiv.) of **151a**, 3.0 equiv. of **150a**. Average value of two reactions given. [b]Conversions and NMR yields were determined with DMB as the internal standard.

Table 5.21: Optimisation of Temperature in the Racemic Intermolecular Allylic Amination with Azoles.[a]

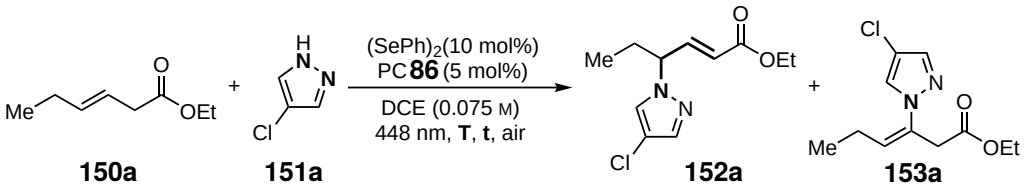

150a **151a** **152a** **153a**

Entry	t [h]	T [°C]	Additive	Conversion[b] [%]	Yield[b] [%]		
					152a	**153a**	Total
1	6	19	-	100	63	11	74
2	6	55	-	100	59	8	67
3	6	55	9.12 mg MS (4 Å)	100	54	13	66
4[c]	21	55	9.02 mg MS (4 Å)	100	54	5	58

[a]0.30 mmol (1.0 equiv.) of **151a**, 3.0 equiv. of **150a**. Average value of two reactions given. [b]Conversions and NMR yields were determined with DMB as the internal standard. [c]Second addition of $(PhSe)_2$ (10 mol%) and **86** (5 mol%) after 8 h.

Table 5.22: Variation of Catalysts in the Racemic Intermolecular Allylic Amination with Azoles.[a]

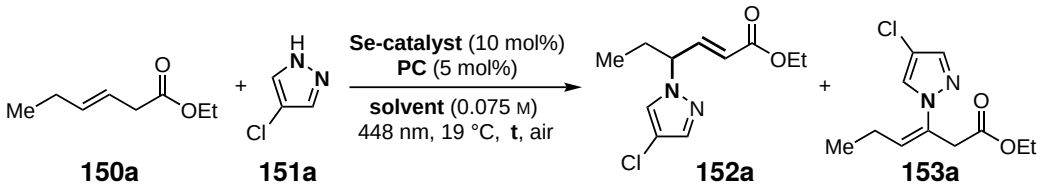

150a **151a** **152a** **153a**

Entry	Se-catalyst	PC	t [h]	Solvent	Conversion[b] [%]	Yield[b] [%]		
						152a	**153a**	Total
1[f]	$(PhSe)_2$	**86**	21	DCE	100	68	15	83
2[c]	$(PhSe)_2$	**86**	21	DCE	100	68	12	80
3[c,d]	$(PhSe)_2$	**86**	21	DCE	100	69	5	74
4[c]	**160**	**86**	21	DCE	100	65	14	79
5[c,d]	**160**	**86**	21	DCE	100	70	10	80
6[c]	**140**	**86**	21	DCE	100	64	21	85
7[c,d]	**140**	**86**	21	DCE	100	66	10	76
8[c]	**161**	**86**	21	DCE	100	67	12	79
9[c,d]	**161**	**86**	21	DCE	100	67	7	74
10[c]	**162**	**86**	21	DCE	100	62	10	72
11[c,d]	**162**	**86**	21	DCE	100	62	6	68
12[c]	**163**	**86**	21	DCE	100	62	12	74
13[c,d]	**163**	**86**	21	DCE	100	65	8	72
14[e]	**142**	**86**	21	DCE	100	51	6	57
15	$(PhSe)_2$	**164**	8	DCE	100	34	1	35
16	$(PhSe)_2$	**165**	8	DCE	100	11	2	13
17	$(PhSe)_2$	**166**	21	THF	48	10	2	12
18	$(PhSe)_2$	**166**	21	TMOF	46	14	5	19

[a]0.30 mmol (1.0 equiv.) of **151a**, 3.0 equiv. of **150a**. [b]Conversions and NMR yields were determined with DMB as the internal standard. [c]Reaction conducted by Dr. T. Lei. [d](4-ClPhS) (5 mol%) added. [e]20 mol% of Se-catalyst used. [f]Average value of two reactions given. TMOF = trimethyl orthoformate.

Se-catalysts

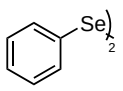

$(PhSe)_2$

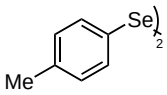

160

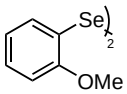

140

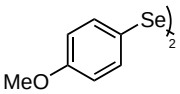

161

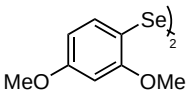

162

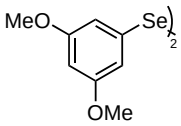

163

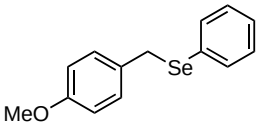

142

PC

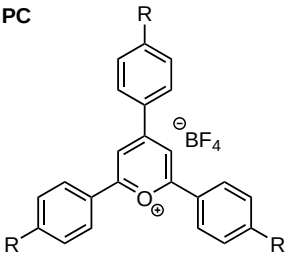

86 R = OMe
164 R = Me
165 R = H

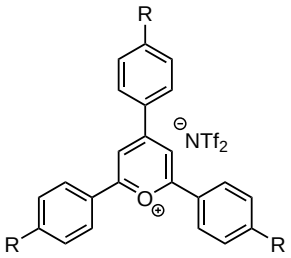

166 R = OMe

Table 5.23: Variation of Additives in the Racemic Intermolecular Allylic Amination with Azoles.[a]

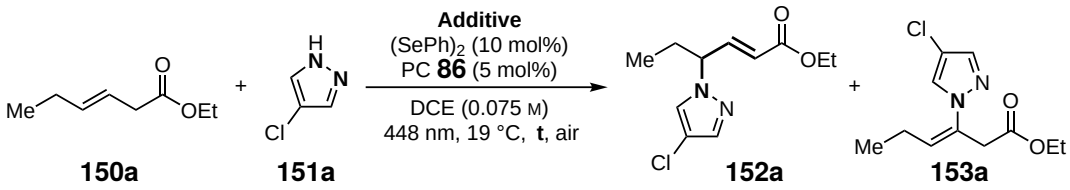

Entry	t [h]	Additive	Amount	Conv.[b] [%]	Yield[b] [%]		
					152a	**153a**	Total
1	8	MS (3 Å)	9.14 mg	100	53	4	57
2[c]	21	MS (4 Å)	9.03 mg	100	57	8	65
3[e]	21	TEMPO	20 mol%	13	0	0	0
4[d,e]	21	$(4\text{-ClPhS})_2$	5 mol%	100	69	5	74
5[e,f]	21	Me_6Si_2	1.0 equiv.	n.d.	19	8	27
6[e,g]	21	Me_6Si_2	1.0 equiv.	85	10	0	10
1	6	NaF	1.0 equiv.	100	48	11	59
2	6	Li_2CO_3	1.0 equiv.	100	45	12	57
3	6	KF_6P	1.0 equiv.	100	46	10	56
4	6	CaF_2	1.0 equiv.	100	64	11	75
5	6	CaF_2	4.0 equiv.	100	64	12	76
6[e]	6	Na_2HPO_4	1.0 equiv.	50	24	6	30
7	8	TfOH	1.0 equiv.	100	0	0	0
8	8	TfOH, $AlCl_3$	1.0 equiv., 10 mol%	100	0	0	0
9	8	TFA	1.0 equiv.	84	32	5	37
10	8	$Sc(OTf)_3$	2.5 mol%	100	67	11	78
11	21	$Sc(OTf)_3$	2.5 mol%	100	69	10	79
12	8	$Sc(OTf)_3$	10 mol%	n.d.	60	1	61
13[e]	21	$Sc(OTf)_3$	10 mol%	100	60	0	60
14	8	$Sc(OTf)_3$, $(4\text{-ClPhS})_2$	both 10 mol%	n.d.	58	0	58
15[e]	21	$Sc(OTf)_3$, MS (4 Å)	10 mol%, 9.00 mg	100	66	0	66
16	8	$Zn(OTf)_2$	2.5 mol%	100	63	10	73
17	8	$AlCl_3$	10 mol%	100	30	6	36
18[d,e]	21	$Yb(OTf)_3$	2.5 mol%	100	68	12	80

[a]0.30 mmol (1.0 equiv.) of **151a**, 3.0 equiv. of **150a**. Average value of two reactions given. [b]Conversions and NMR yields were determined with DMB as the internal standard. [c]Second addition of $(PhSe)_2$ (10 mol%) and **86** (5 mol%) catalysts after 8 h. [d]Reaction performed by Dr. T. Lei. [e]Single determination. [f]1.0 mmol (1.0 equiv.) of **151a**, 3.0 equiv. of **150a**. [g]1.0 mmol (1.0 equiv.) of **150a**, 3.0 equiv. of **151a**. MS = molecular sieves. TEMPO = 2,2,6,6-Tetramethylpiperidinyloxyl.

Table 5.24: Variation of Additives in the Racemic Intermolecular Allylic Amination with Azoles.[a]

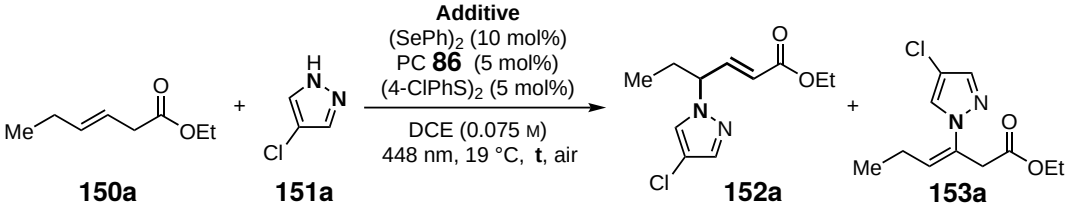

Entry	t [h]	Additive	Amount	Conv.[b] [%]	Yield[b] [%]		
					152a	**153a**	Total
1[c]	21	MS (4 Å)	9.14 mg	100	53	4	57
2[d,e]	8	$Sc(OTf)_3$	10 mol%	88–100	58	0	58
3[c]	8	2-Nitrobenzaldehyde	25 mol%	100	63	9	72
4[c]	21	2-Nitrobenzaldehyde	25 mol%	100	68	10	78
5[c]	21	2-Nitrobenzaldehyde	10 mol%	100	63	14	77
6[c]	21	$CaSO_4$	1.2 equiv.	100	66	8	75
7[c]	21	NaBArF	4 mol%	100	64	8	72
8[c]	21	$Yb(OTf)_3$	2.5 mol%	100	71	12	83
9[c]	21	AcOH	1.0 equiv.	n.d.	68	6	74
10[c]	21	HFIP	25 mol%	n.d.	68	7	74
11[c]	21	MeOH	1.0 equiv.	n.d.	62	5	67

[a] 0.30 mmol (1.0 equiv.) of **151a**, 3.0 equiv. of **150a**. [b] Conversions and NMR yields were determined with DMB as the internal standard. [c] Reaction performed by Dr. T. Lei. [d] 10 mol% of $(4\text{-ClPhS})_2$ added. [e] Average value of two reactions given. NaBArF = Sodium tetrakis[3,5-bis(trifluoromethyl)phenyl]borate. n.d. = not determined.

Table 5.25: Control Experiments in the Racemic Intermolecular Allylic Amination with Azoles.[a]

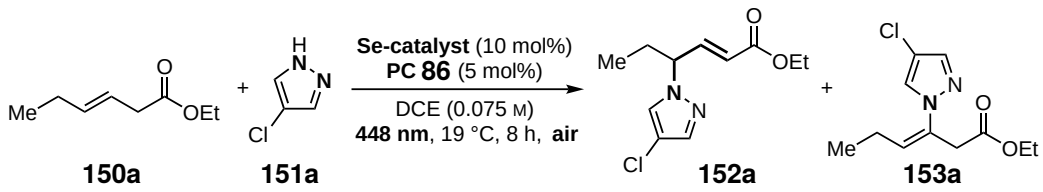

150a **151a** **152a** **153a**

Entry	Deviation from Standard Conditions	Conversion[b] [%]	Yield[b] [%]		
			152a	**153a**	Total
1	-	100	65	11	76
2	No $(PhSe)_2$	24	0	0	0
3[c]	No PC **86**	0	0	2	2
4	N_2-atmosphere	20	0	0	0
5	No irradiation	88	0	0	0

[a] 0.30 mmol (1.0 equiv.) of **151a**, 3.0 equiv. of **150a**. Average value of two reactions given. [b] Conversions and NMR yields were determined with DMB as the internal standard. [c] 6 h.

Table 5.26: Scale-up of the Intermolecular Allylic Amination with Azoles.

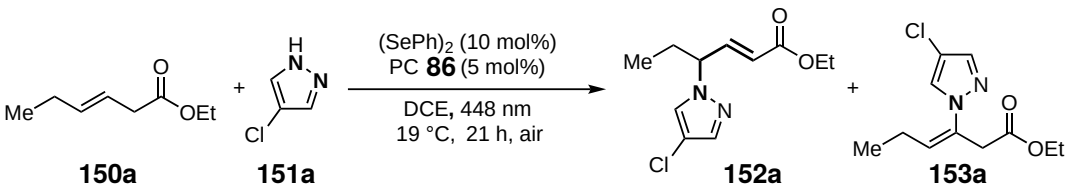

Entry	**150a**	**151a**	Concentration [M]	Yield[a] [%]			**152a/153a**
				152a	**153a**	Total	
1[b]	3.0 equiv.	0.30 mmol	0.075	68	15	83	5:1
2[b]	3.0 equiv.	1.0 mmol	0.075	16	0	16	1:0
3[b]	3.0 equiv.	1.0 mmol	0.2	31	3	34	10:1
4[b]	3.0 equiv.	0.50 mmol	0.1	60	9	69	7:1
5[c]	3.0 equiv.	0.50 mmol	0.075	67	15	82	4:1
6[c]	3.0 equiv.	1.0 mmol	0.075	62	10	72	6:1
7[c]	3.0 equiv.	1.0 mmol	0.2	68 (68)	15 (13)	83 (81)	5:1
8[c,d]	3.0 equiv.	1.0 mmol	0.2	72	6	78	13:1
9[c]	1.0 mmol	3.0 equiv.	0.2	68 (68)	5 (3)	73 (71)	14:1
10[c,d]	1.0 mmol	3.0 equiv.	0.2	63	2.5	66	25:1

[a]NMR yields were determined with DMB as the internal standard. Isolated yields are given in parentheses. [b]40 mL reaction vial used. [c]100 mL round bottom flask used. [d](4-ClPhS)$_2$ (5 mol%) added.

5.7.2 Kinetic Investigations

Kinetic Measurement of the Racemic Intermolecular Allylic Amination with Azoles.

Table 5.27: Kinetic Investigation of the Racemic Intermolecular Allylic Amination with Azoles.[a]

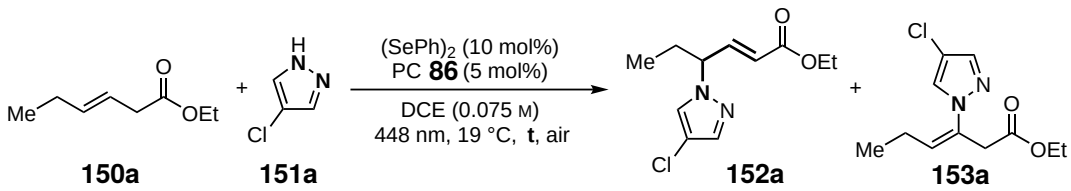

150a **151a** **152a** **153a**

Entry	t [h]	Conversion[b] of **151a** [%]	Yield[b] [%]		
			152a	**153a**	Total
1	2	38	25	4	29
2	4	100	57	8	65
3	6	100	63	11	74
4	8	100	65	11	76
5	18	100	68	11	79
6	21	100	68	15	83

[a] 0.30 mmol (1.0 equiv.) of **151a**, 3.00 equiv. of **150a**. Average value of two reactions given. [b] NMR yields and conversions were determined with DMB as the internal standard.

5.7.3 Substrate Synthesis

Benzyl (*E*)-hex-3-enoate (150b)[150]

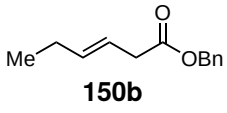

150b

Into a solution of (*E*)-hex-3-enoic acid (3.0 mL, 2.85 g, 24.9 mmol, 1.00 equiv.) in toluene (20 mL) in a DEAN-STARK apparatus, benzyl alcohol (4.16 mL, 4.33 g, 40.0 mmol, 1.61 equiv.) and *p*-TsOH·H_2O (190 mg, 999 µmol, 4 mol%) were added. The resulting mixture was stirred at 150 °C for 16 h, before it was allowed to cool to r.t.. EtOAc (50 mL) was added and the solution was washed with sat. aqueous $NaHCO_3$ solution (3 × 50 mL) and brine (50 mL). The combined aqueous phases were back extracted with EtOAc (50 mL) and the united organic phases were dried over Na_2SO_4, filtered and the solvent was removed under reduced pressure. Purification *via* column chromatography (PE/EtOAc, 10:1) afforded **150b** (5.64 g, 27.6 mmol, >99%) as a colourless oil.

TLC: R_f = 0.61 (PE/EtOAc, 90:10) [UV, *p*-anisaldehyde]. **IR** [cm^{-1}]: 3064, 3034, 2963, 1737, 1488, 1454, 1379, 1316, 1234, 1152, 969, 738, 697. ^{1}**H NMR** (300 MHz, $CDCl_3$): δ 7.46–7.31 (m, 5H), 5.73–5.43 (m, 2H), 5.13 (s, 2H), 3.19–2.90 (m, 2H), 2.20–1.93 (m, 2H), 0.99 (t, *J* = 7.4 Hz,

3H). ^{13}**C NMR** (75 MHz, $CDCl_3$): δ 172.2, 136.6, 136.1, 128.7, 128.3, 128.3, 120.5, 66.4, 38.2, 25.6, 13.6. **HRMS** (EI) calcd. for $[C_{13}H_{16}O_2]^{\cdot+}$ ($[M]^{\cdot+}$), m/z = 204.11448; found 204.11491.

Dibenzyl (*E*)-hex-3-enedioate (150c)

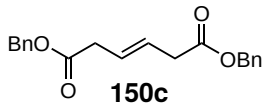

150c

Into a solution of (*E*)-hex-3-enedioic acid (1.44 g, 10.0 mmol, 1.00 equiv.) in toluene (20 mL) in a DEAN-STARK apparatus, *p*-TsOH·H_2O (381 mg, 2.21 mmol, 22 mol%) is added. The resulting solution is heated to reflux (150 °C), when benzyl alcohol (2.1 mL, 2.16 g, 20.0 mmol, 2.00 equiv.) in 20 mL toluene is added drop wise with a dropping funnel over a time span of 4 h. The resulting solution is stirred at 150 °C for another 20.5 h. After cooling to r.t., the reaction mixture was diluted with 100 mL EtOAc and washed with sat. aqueous $NaHCO_3$ solution (3 × 100 mL). The combined aqueous phases were back extracted with EtOAc (100 mL). The united organic phases were washed with brine (100 mL), dried over Na_2SO_4, filtered and the solvent was removed under reduced pressure. Purification *via* column chromatography (PE/EtOAc, 95:5 to 90:10) afforded **150c** (931 g, 2.87 mmol, 29%) as a colourless solid.

TLC: R_f = 0.29 (PE/EtOAc, 10:1) [UV]. **M.p.** = 38 °C. **IR** [cm^{-1}]: 3064, 3034, 2956, 2896, 173, 1241, 1148, 969, 738, 701. ^{1}**H NMR** (300 MHz, $CDCl_3$): δ 7.41–7.30 (m, 10H), 5.73 (ddd, *J* = 5.5, 3.8, 1.6 Hz, 2H), 5.13 (s, 4H), 3.19–3.04 (m, 4H). ^{13}**C NMR** (101 MHz, $CDCl_3$): δ 171.5, 135.9, 128.7, 128.4, 128.4, 126.1, 66.7, 38.0. **HRMS** (ESI) calcd. for $[C_{20}H_{21}O_4]^+$ ($[M+H]^+$), m/z = 325.1434; found 325.1436.

Hept-3-enenitrile (150d)[150]

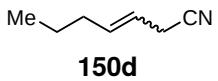

150d

To a solution of NaI (3.61 g, 24.1 mmol, 1.20 equiv.) in MeCN (30 mL), TMSCl (3.05 mL, 2.61 mg, 24.0 mmol, 1.20 equiv.) was added dropwise. Then, (*E*)-hex-2-en-1-ol (**169**) (2.36 mL, 2.00 g, 20.0 mmol, 1.00 equiv.) was added to the suspension. After letting the reaction mixture stir at r.t. for 30 min, KCN (3.92 g, 60.2 mmol, 3.00 equiv.) was added stirring was continued for 17 h. Then, H_2O (20 mL) was added and the aqueous phase was extracted with Et_2O (3 × 30 mL). The combined organic phases were washed with sat. aqueous $Na_2S_2O_3$ solution (30 mL) and 1 M aqueous $Na_2S_2O_3$ solution (30 mL), dried over Na_2SO_4, filtered and the solvent was removed under reduced pressure. Purification *via* column chromatography (PE/EtOAc, 90:10) afforded **150d** (1.11 g, 10.2 mmol, 51%) as a yellow liquid with a *E*/*Z*-ratio of 87:13.

TLC: R_f = 0.43 (PE/EtOAc, 90:10) [UV, $KMnO_4$]. **IR** [cm^{-1}]: 2960, 2930, 2874, 2363, 2251, 1707, 1461, 1416, 969. ^{1}**H NMR** (400 MHz, $CDCl_3$): δ 5.81 (dtt, *J* = 15.4, 6.8, 1.7 Hz, 1H, *E*), 5.68 (dtt, *J* = 10.8, 7.5, 1.7 Hz, 1H, *Z*), 5.47–5.18 (m, 1H, *E*+*Z*), 3.13–2.95 (m, 2H, *E*+*Z*), 2.19–1.95 (m, 2H, *E*+*Z*), 1.49–1.30 (m, 2H, *E*+*Z*), 0.99–0.85 (m, 3H, *E*+*Z*). ^{13}**C NMR** (101 MHz, $CDCl_3$): δ 136.3 (*E*), 136.1(*Z*), 118.0 (*Z*), 117.3 (*E*), 117.1 (*Z*), 34.3 (*E*), 29.4 (*Z*), 22.3 (*Z*), 22.1 (*E*), 20.6 (*E*), 15.7 (*Z*), 13.8 (*Z*), 13.7 (*E*). **HRMS** (EI) calcd. for $[C_7H_{11}N]^{\cdot+}$ ($[M]^{\cdot+}$), m/z = 109.08860;

found 109.08790 and 109.08842 (major GC signal).

(But-2-en-1-ylsulfonyl)benzene (150e)[150]

150e

To a solution of crotyl bromide (85% *trans*, 1.03 mL, 1.35 g, 10.0 mmol, 1.00 equiv.) in THF/H_2O (10:1, 42 mL), sodium benzenesulfinate (2.46 g, 15.0 mmol, 1.50 equiv.) was added and the mixture was stirred at r.t. for 16 h. Then, the solution was diluted with each 50 mL H_2O and EtOAc. The phases were separated and the organic layer was washed with H_2O (50 mL). The combined aqueous layers were back extracted with EtOAc (50 mL) and the united organic phases were then dried over Na_2SO_4, filtered and the solution was removed under reduced pressure. Purification *via* column chromatography (PE/EtOAc, 80:20) afforded **150e** (2.48 g, 12.7 mmol, >99%) as a colourless oil with a *E*/*Z*-ratio of 91:9.

TLC: R_f = 0.26 (PE/EtOAc, 80:20) [UV]. **IR** [cm^{-1}]: 3034, 2970. 2919, 1670, 1584, 1480, 144, 1297, 1141, 1085, 965, 760, 731, 690. ^{1}**H NMR** (300 MHz, $CDCl_3$): δ 7.92–7.77 (m, 2+2H, *E*+*Z*), 7.69–7.43 (m, 3+3H, *E*+*Z*), 5.89–5.70 (m, 2H, *Z*), 5.62–5.46 (m, 1H, *E*), 5.39 (dddt, *J* = 15.4, 7.2, 5.8, 1.5 Hz, 1H, *E*), 3.88–3.58 (m, 2H, *E*+*Z*), 1.72–1.11 (m, 3H, *E*+*Z*). ^{13}**C NMR** (75 MHz, $CDCl_3$): δ 138.5 (*Z*), 138.5 *E*, 136.6 (*E*), 134.1 (*Z*), 133.7 (*Z*), 133.7 (*E*), 129.1 (*Z*), 129.0 (*E*), 128.5 (*Z*), 128.5 (*E*), 117.0 (*E*), 116.3 (*Z*), 60.1 (*E*), 54.9 (*Z*), 18.2 (*E*), 12.8 (*Z*). **HRMS** (ESI) calcd. for $[C_{10}H_{13}O_2S]^+$ ([M+H]$^+$), m/z = 197.0631; found 197.0630.

(Cinnamylsulfonyl)benzene (150f)[150]

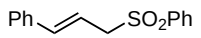

150f

To a solution of cinnamyl bromide (1.48 mL, 1.97 g, 10.0 mmol, 1.00 equiv.) in THF/H_2O (10:1, 37 mL), sodium benzenesulfinate (2.46 g, 15.0 mmol, 1.50 equiv.) was added and the mixture was stirred at r.t. for 14.5 h. Then, the solution was diluted with each 50 mL H_2O and EtOAc. The phases were separated and the organic layer was washed with H_2O (50 mL). The combined aqueous layers were back extracted with EtOAc (50 mL) and the united organic phases were then dried over Na_2SO_4, filtered and the solution was removed under reduced pressure. Purification *via* column chromatography (PE/EtOAc, 80:20 to 70:30) afforded **150f** (1.76 g, 6.81 mmol, 68%) as a colourless solid.

TLC: R_f = 0.36 (PE/EtOAc, 80:20) [UV, *p*-anisaldehyde]. **M.p.** = 113 °C. **IR** [cm^{-1}]: 3056, 2974, 2903, 2371, 1901, 1584, 1495, 1446, 1402, 1320, 1238, 1080, 980, 734, 690. ^{1}**H NMR** (300 MHz, $CDCl_3$): δ 7.94–7.82 (m, 2H), 7.71–7.60 (m, 1H), 7.59–7.48 (m, 2H), 7.38–7.21 (m, 5H+$CHCl_3$), 6.37 (dt, *J* = 15.9, 1.2 Hz, 1H), 6.10 (dt, *J* = 15.8, 7.5 Hz, 1H), 3.96 (dd, *J* = 7.6, 1.1 Hz, 2H). ^{13}**C NMR** (75 MHz, $CDCl_3$): δ 139.3, 138.5, 135.8, 133.9, 129.2, 128.8, 128.6, 126.7, 115.2, 60.6. **HRMS** (ESI) calcd. for $[C_{15}H_{15}O_2S]^+$ ([M+H]$^+$), m/z = 259.0787; found 259.0787.

Diethyl but-2-en-1-ylphosphonate (150g)[150]

150g

To a solution of diethyl phosphonate (1.42 mL, 1.52 g, 11.0 mmol, 1.10 equiv.) in dry THF (34 mL) under a N_2-atmosphere, *n*BuLi (4.4 mL, 705 mg, 2.50 M in hexane, 11.0 mmol, 1.10 equiv.) was added dropwise at -10 °C and stirred for 10 min. Then, a solution of crotyl bromide (85% *trans*, 1.03 mL, 1.35 g, 10.0 mmol, 1.00 equiv.) in dry THF (3 mL) was added dropwise and the reaction mixture was stirred at -10 °C for 30 min. Then, sat. aqueous NH_4Cl solution (30 mL) was added and the phases were separated. The aqueous phase was extracted with DCM (3 × 30 mL), before the combined organic layers were washed with brine (50 mL) and dried over Na_2SO_4, filtered and the solvent was removed under reduced pressure. Purification *via* column chromatography (PE/Et_2O, 2:1 to 1:2) afforded **150g** (707 mg, 3.68 mmol, 37%) as a colourless oil with a *E*/*Z*-ratio of 80:20.

TLC: R_f = 0.16 (PE/EtOAc, 80:20) [UV]. **IR** [cm^{-1}]: 3452, 2982, 2915, 1651, 1446, 1394, 1245, 1021, 962. ^{1}**H NMR** (400 MHz, $CDCl_3$): δ 5.74–5.53 (m, 1H, *E*+*Z*), 5.49–5.29 (m, 1H, *E*+*Z*), 4.20–3.95 (m, 4H, *E*+*Z*), 2.72–2.41 (m, 2H, *E*+*Z*), 1.75–1.57 (m, 3H, *E*+*Z*), 1.30 (td, *J* = 7.1, 1.4 Hz, 6H, *E*+*Z*). ^{13}**C NMR** (101 MHz, $CDCl_3$): δ 130.8 (d, J_{CP} = 14.8 Hz, *E*), 128.8 (d, J_{CP} = 14.4 Hz, *Z*), 119.7 (d, J_{CP} = 11.3 Hz, *E*), 118.9 (d, J_{CP} = 11.1 Hz, *Z*), 62.0 (d, J_{CP} = 6.7 Hz, *Z*, 61.9 (d, J_{CP} = 6.6 Hz, *E*), 30.5 (d, J_{CP} = 140.0 Hz, *E*), 25.6 (d, J_{CP} = 140.4 Hz, *Z*), 18.2 (d, J_{CP} = 2.6 Hz, *E*, 16.6 (d, J_{CP} = 6.0 Hz, *E*), 13.7 (*Z*) , 13.0 (d, J_{CP} = 2.7 Hz, *Z*). ^{31}**P NMR** (162 MHz, $CDCl_3$): δ 28.8. **HRMS** (EI) calcd. for $[C_8H_{17}O_3P]^{\cdot+}$ ($[M]^{\cdot+}$), m/z = 192.09098; found 192.09118 (major) and 192.09117 (minor).

(*E*)-3-(Hex-3-enoyl)oxazolidin-2-one (150h)[129]

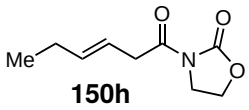

150h

To a solution of oxazolidin-2-one (1.74 g, 20.0 mmol, 1.00 equiv.) in dry DCM (25 mg) under a N_2-atmosphere, DMAP (320 mg, 2.62 mmol, 0.13 equiv.) and (*E*)-hex-3-enoic acid (3.08 mL, 2.97 g, 26.0 mmol, 1.30 equiv.) were added. DCC (5.45 g, 26.4 mmol, 1.32 equiv.) was added at 0 °C and the mixture was stirred at r.t. for 20 h. Then, the formed precipitate was filtered and washed with DCM. The filtrate was washed with sat. aqueous $NaHCO_3$ solution (2 × 50 mL), dried over Na_2SO_4, filtered and the solvent was removed under reduced pressure. Purification *via* column chromatography (PE/EtOAc, 70:30) afforded **150h** (1.40 g, 7.61 mmol, 38%) as a lightly yellow liquid.

TLC: R_f = 0.27 (PE/EtOAc, 70:30) [UV, $KMnO_4$]. **IR** [cm^{-1}]: 2967, 2922, 1771, 1696, 1480, 1387, 1331, 1219, 1185, 1103, 1036, 962, 760, 701. ^{1}**H NMR** (300 MHz, $CDCl_3$): δ 5.75–5.44 (m, 2H), 4.49–4.28 (m, 2H), 4.01 (dd, *J* =+8.7, 7.5 Hz, 2H), 3.73–3.41 (m, 2H), 2.20–1.85 (m, 2H), 0.98 (t, *J* = 7.4 Hz, 3H). ^{13}**C NMR** (101 MHz, $CDCl_3$): 172.1, 153.6, 137.1, 120.0, 62.2, 42.6, 38.8, 25.7, 13.5. **HRMS** (ESI) calcd. for $[C_9H_{14}NO_3]^{\cdot+}$ ($[M]^{\cdot+}$), m/z = 184.0968; found 184.0968.

5.7.4 Synthesis of Allylic Azoles and Azines

General Procedure 4

Into a 100 mL round bottom flask were added alkene (**150**), amine (**151**), $(SePh)_2$ (10 mol%), photocatalyst **86** (5 mol%) and 5 mL of the stated solvent (DCE or DCE/HFIP = 3:2). If indicated, $(4\text{-ClPhS})_2$ (14.4 mg, 50.0 µmol, 5 mol%) was added. The flask was sealed with a septum including two cannulas, leaving it open to air. The reaction mixture was then vigorously stirred at 19 °C under irradiation with blue light for the given time. After reaction, the solvent was removed under reduced pressure. The NMR yield of the allylic product and the ratio of the allylic (**152**) and vinylic (**153**) isomer was determined with internal standard 1,4-dimethoxybenzene (DMB). If no obvious signal for the vinylic isomer in the crude ^{1}H NMR was detected, no total yield is given and the ratio is given at >10:1. Further purification *via* column chromatography afforded the target compound.

Ethyl (*E*)-4-(4-chloro-1H-pyrazol-1-yl)hex-2-enoate (152a)

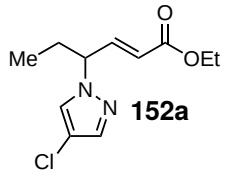

152a

According to general procedure **4**: Ethyl (*E*)-hex-3-enoate (**150a**) (142 mg, 1.00 mmol, 1.00 equiv.), 4-chloro-1H-pyrazole (**151a**) (308 mg, 3.00 mmol, 3.00 equiv.), TAPT (24.3 mg, 50.0 µmol, 5 mol%), $(PhSe)_2$ (31.6 mg, 101 µmol, 10 mol%) and DCE, 21 h. Purification (PE/EtOAc, 9:1) afforded **152a** (166 mg, 684 µmol, 68%) as a colourless oil (crude ^{1}H NMR yield: 68%) and vinylic isomer **153a** (8.20 mg, 33.8 µmol, 3%) as a lightly yellow oil (Crude ^{1}H NMR yield: 5%).

TLC: R_f = 0.51 (PE/EtOAc, 4:1) [UV, $KMnO_4$]. **IR** [cm^{-1}]: 3131, 2878, 2974, 2937, 1778, 1715, 1659, 1435, 1368, 1312, 1271, 1182, 1036, 969, 824, 790, 742. **^{1}H NMR** (300 MHz, $CDCl_3$): δ 7.48–7.40 (m, 1H), 7.40–7.34 (m, 1H), 7.08–6.84 (m, 1H), 5.67 (dq, *J* = 15.8, 1.5 Hz, 1H), 4.68 (dtq, *J* = 9.1, 6.1, 1.5 Hz, 1H), 4.23–4.05 (m, 2H), 2.19–1.77 (m, 2H), 1.34–1.15 (m, 3H), 0.96–0.66 (m, 3H). **^{13}C NMR** (75 MHz, $CDCl_3$): δ 165.8, 145.2, 138.1, 126.3, 123.0, 110.3, 65.3, 60.8, 27.3, 14.3, 10.6. **HRMS** (EI) calcd. for $[C_{11}H_{15}ClN_2O_2]^{\cdot+}$ ($[M]^{\cdot+}$), m/z = 242.08166; found 242.08108.

Vinylic Isomer: **Ethyl (*Z*)-3-(3-chloro-1H-pyrrol-1-yl)hex-3-enoate (153a)**

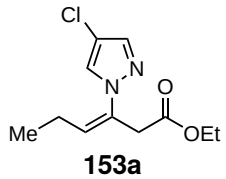

153a

TLC: R_f = 0.54 (PE/EtOAc, 80:20) [UV]. **IR** [cm^{-1}]: 3138, 2974, 2363, 1737, 1681, 1431, 1372, 1341, 1252, 1178, 1029, 969, 842, 790. **^{1}H NMR** (400 MHz, $CDCl_3$): δ 7.56–7.47 (m, 2H), 5.51 (t, *J* = 7.3 Hz, 1H), 4.08 (q, *J* = 7.2 Hz, 2H), 3.57–3.47 (m, 2H), 2.11 (quint., *J* = 7.5 Hz, 2H), 1.19 (t, *J* = 7.1 Hz, 3H), 1.02 (t, *J* = 7.5 Hz, 3H). **^{13}C NMR** (101 MHz, $CDCl_3$): δ 170.2, 138.5, 131.7, 129.6, 128.9, 110.3, 61.1, 41.0, 21.0, 14.2, 14.0. **HRMS** (EI) calcd. for $[C_{11}H_{15}ClN_2O_2]^{\cdot+}$ ($[M]^{\cdot+}$), m/z = 242.08166; found 242.08199.

According to general procedure **4**: Ethyl (*E*)-hex-3-enoate (**150a**) (427 mg, 3.00 mmol, 3.00 equiv.), 4-chloro-1H-pyrazole (**151a**) (103 mg, 1.00 mmol, 1.00 equiv.), TAPT (24.5 mg, 50.4 µmol, 5 mol%), $(PhSe)_2$ (31.5 mg, 101 µmol, 10 mol%) and DCE, 21 h. Purification (PE/EtOAc, 9:1) afforded **152a** (166 mg, 684 µmol, 68%) as a colourless oil (crude ^{1}H NMR yield: 68%) and 13% of vinylic isomer **153a** (crude ^{1}H NMR yield: 15%).

According to general procedure **4**: Ethyl (*Z*)-hex-3-enoate (**150a**) (142 mg, 1.00 mmol, 1.00 equiv.), 4-chloro-1H-pyrazole (**151a**) (308 mg, 3.00 mmol, 3.00 equiv.), TAPT (24.3 mg, 50.0 µmol, 5 mol%), $(PhSe)_2$ (31.2 mg, 100 µmol, 10 mol%) and DCE, 21 h. Purification (PE/EtOAc, 9:1) afforded **152a** (123 mg, 507 µmol, 51%) as a lightly yellow oil (crude ^{1}H NMR yield: 47%) and no vinylic isomer **153a** (crude ^{1}H NMR yield: 2%).

Phenyl (*E*)-4-(4-chloro-1H-pyrazol-1-yl)hex-2-enoate (152b)

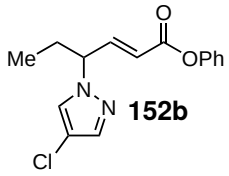

152b

According to general procedure **4**: Phenyl (*E*)-hex-3-enoate (**150k**) (190 mg, 1.00 mmol, 1.00 equiv.), 4-chloro-1H-pyrazole (**151a**) (308 mg, 3.00 mmol, 3.00 equiv.), TAPT (24.4 mg, 50.1 µmol, 5 mol%), $(PhSe)_2$ (31.3 mg, 100 µmol, 10 mol%) and DCE, 21 h. Purification (PE/EtOAc, 95:5) afforded **152b** (179 mg, 616 µmol, 62%) as a lightly yellow oil. Crude NMR yield: 58%.

TLC: R_f = 0.56 (PE/EtOAc, 80:20) [UV]. **IR** [cm^{-1}]: 3131, 2937, 2974, 1737, 1656, 1595, 1490, 1312, 1193, 1163, 973, 824, 690. ^{1}**H NMR** (300 MHz, $CDCl_3$): δ 7.51 (d, *J* = 0.7 Hz, 1H), 7.45 (d, *J* = 0.7 Hz, 1H), 7.42–7.33 (m, 2H), 7.26–7.17 (m, 2H), 7.13–7.04 (m, 2H), 5.90 (dd, *J* = 15.7, 1.5 Hz, 1H), 4.79 (dtd, *J* = 9.1, 5.9, 1.6 Hz, 1H), 2.23–1.92 (m, 2H), 0.95 (t, *J* = 7.4 Hz, 3H). ^{13}**C NMR** (101 MHz, $CDCl_3$): δ 164.2, 150.6, 147.4, 138.4, 129.6, 126.5, 126.1, 122.2, 121.6, 110.6, 65.4, 27.4, 10.7. **HRMS** (ESI) calcd. for $[C_{15}H_{16}ClN_2O_2]^+$ ([M+H]$^+$), m/z = 291.0895; found 291.0895.

Vinylic Isomer: **Phenyl (*Z*)-3-(4-chloro-1H-pyrazol-1-yl)hex-3-enoate (153b)**

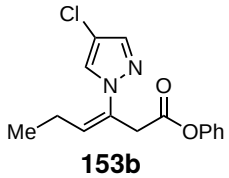

153b

153b (21.2 mg, 72.2 µmol, 7%) as a lightly yellow oil. Crude ^{1}H NMR yield: 7%.

TLC: R_f = 0.60 (PE/EtOAc, 80:20) [UV]. **IR** [cm^{-1}]: 3138, 2967, 2933, 1759, 1595, 1491, 1431, 1342, 1238, 1193, 1133, 969, 693. ^{1}**H NMR** (400 MHz, $CDCl_3$): δ 7.57 (d, *J* = 2.2 Hz, 2H), 7.38–7.31 (m, 2H), 7.23–7.18 (m, 1H), 7.05–6.84 (m, 2H), 5.61 (t, *J* = 7.3 Hz, 1H), 3.78 (d, *J* = 1.0 Hz, 2H), 2.16 (quint., *J* = 7.4 Hz, 2H), 1.06 (t, *J* = 7.5 Hz, 3H). ^{13}**C NMR** (101 MHz, $CDCl_3$): δ 168.8, 150.6, 138.7, 131.2, 129.8, 129.5, 129.0, 126.1, 121.5, 110.6, 41.1, 21.1, 14.0. **HRMS** (ESI) calcd. for $[C_{15}H_{16}ClN_2O_2]^+$ ([M+H]$^+$), m/z = 291.0892; found 291.0895.

Benzyl (*E*)-4-(4-chloro-1H-pyrazol-1-yl)hex-2-enoate (152c)

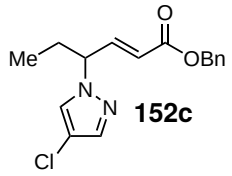

152c

According to general procedure **4**: Benzyl (*E*)-hex-3-enoate (**150b**) (204 mg, 1.00 mmol, 1.00 equiv.), 4-chloro-1H-pyrazole (**151a**) (308 mg, 3.00 mmol, 3.00 equiv.), TAPT (22.5 mg, 46.2 µmol, 5 mol%), $(PhSe)_2$ (31.2 mg, 100 µmol, 10 mol%) and DCE, 21 h. Purification (PE/EtOAc, 90:10) afforded **152c** (185 mg, 608 µmol, 61%) as a lightly yellow oil. Crude NMR yield: 55%.

TLC: R_f = 0.23 (PE/EtOAc, 80:20) [UV]. **IR** [cm^{-1}]: 3131, 3064, 3034, 2971, 2878, 1718, 1659, 1457, 1383, 1271, 1163, 969, 842, 697. **^{1}H NMR** (300 MHz, $CDCl_3$): δ 7.47 (s, 1H), 7.39 (s, 1H), 7.38–7.31 (m, 5H), 7.06 (dd, *J* = 15.7, 6.0 Hz, 1H), 5.75 (dd, *J* = 15.7, 1.5 Hz, 1H), 5.17 (s, 2H), 4.70 (dddd, *J* = 8.6, 7.1, 4.2, 1.3 Hz, 1H), 2.22–1.77 (m, 3H), 0.88 (td, *J* = 7.4, 1.2 Hz, 3H). **^{13}C NMR** (101 MHz, $CDCl_3$): δ 165.6, 145.9, 138.1, 135.7, 128.7, 128.5, 128.5, 126.4, 122.5, 110.3, 66.7, 65.3, 27.3, 10.6. **HRMS** (EI) calcd. for $[C_{16}H_{17}ClN_2O_2]^{\cdot+}$ ($[M]^{\cdot+}$), m/z = 304.09731; found 304.09681.

Diethyl (*E*)-4-(4-chloro-1H-pyrazol-1-yl)hex-2-enedioate (152i)

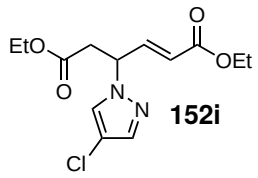

152i

According to general procedure **4**: Diethyl (*E*)-hex-3-enedioate (**150j**) (601 mg, 3.00 mmol, 3.00 equiv.), 4-chloro-1H-pyrazole (**151a**) (103 mg, 1.00 mmol, 1.00 equiv.), TAPT (24.3 mg, 50.0 µmol, 5 mol%), $(PhSe)_2$ (31.2 mg, 100 µmol, 10 mol%) and DCE, 21 h. Purification (PE/EtOAc, 15:1) afforded **152i** (308 mg, 1.02 mmol, >99%) as a colourless oil. Crude NMR yield: 99%. Reaction conducted by Dr. T. Lei.[168]

According to general procedure **4**: Diethyl (*E*)-hex-3-enedioate (**150j**) (201 mg, 1.00 mmol, 1.00 equiv.), 4-chloro-1H-pyrazole (**151a**) (310 mg, 3.02 mmol, 3.01 equiv.), TAPT (24.3 mg, 50.0 µmol, 5 mol%), $(PhSe)_2$ (31.4 mg, 101 µmol, 10 mol%) and DCE, 21 h. Purification (PE/EtOAc, 15:1) afforded **152i** (228 mg, 758 µmol, 76%) as a slightly yellow oil. Crude NMR yield: 85%.

TLC: R_f = 0.23 (PE/EtOAc, 5:1) [UV]. **IR** [cm^{-1}]: 3131, 2982, 2937, 1718, 1662, 1372, 1312, 1271, 1178, 1025, 969, 857. **^{1}H NMR** (300 MHz, $CDCl_3$): δ 7.54–7.39 (m, 2H), 7.01 (dd, *J* = 15.7, 6.0 Hz, 1H), 5.71 (dd, *J* = 15.7, 1.5 Hz, 1H), 5.33 (dtd, *J* = 8.8, 5.8, 1.6 Hz, 1H), 4.28–4.04 (m, 4H), 3.22 (dd, *J* = 16.6, 8.7 Hz, 1H), 2.91 (dd, *J* = 16.6, 5.6 Hz, 1H), 1.27 (t, *J* = 7.1 Hz, 2H), 1.21 (t, *J* = 7.1 Hz, 2H). **^{13}C NMR** (101 MHz, $CDCl_3$): δ 169.5, 165.4, 143.6, 138.6, 127.4, 123.6, 110.4, 61.3, 60.9, 59.3, 38.3, 14.2, 14.1. **HRMS** (APCI) calcd. for $[C_{13}H_{18}ClN_2O_4]^+$ ($[M+H]^+$), m/z = 301.0950; found 301.0953.

Dibenzyl (*E*)-4-(4-chloro-1H-pyrazol-1-yl)hex-2-enedioate (152j)

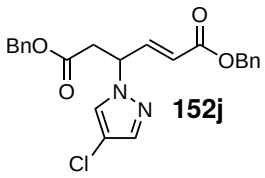

152j

According to general procedure **4**: Dibenzyl (*E*)-hex-3-enedioate (**150c**) (324 mg, 1.00 mmol, 1.00 equiv.), 4-chloro-1H-pyrazole (**151a**) (308 mg, 3.00 mmol, 3.00 equiv.), TAPT (24.4 mg, 50.1 µmol, 5 mol%), $(PhSe)_2$ (31.2 mg, 100 µmol, 10 mol%) and DCE, 21 h. Purification (PE/EtOAc, 90:10) afforded **152j** (345 mg, 812 mmol, 81%) as a colourless solid. Crude NMR yield: 85%.

According to general procedure **4**: Dibenzyl (*E*)-hex-3-enedioate (**150c**) (973 mg, 3.00 mmol, 3.00 equiv.), 4-chloro-1H-pyrazole (**151a**) (103 mg, 1.00 mmol, 1.00 equiv.), TAPT (24.3 mg, 50.0 µmol, 5 mol%), $(PhSe)_2$ (31.2 mg, 100 µmol, 10 mol%) and DCE, 21 h. Purification (PE/EtOAc, 30:1 to 15:1) afforded **152j** (376 mg, 885 µmol, 89%) as a slightly yellow oil. Crude NMR yield: 92%. Reaction conducted by Dr. T. Lei.[168]

TLC: R_f = 0.38 (PE/EtOAc, 80:20) [UV]. **M.p.** = 67.9 °C. **IR** [cm^{-1}]: 3131, 3034, 2952, 1722, 1659, 1454, 1383, 1308, 1267, 1156, 969, 842, 697. ^{1}**H NMR** (400 MHz, $CDCl_3$): δ 7.45 (s, 1H), 7.39 (s, 1H), 7.38–7.30 (m, 8H), 7.28–7.23 (m, 2H), 7.04 (dd, *J* = 15.7, 5.9 Hz, 1H), 5.75 (dd, *J* = 15.7, 1.5 Hz, 1H), 5.33 (dtd, *J* = 8.9, 5.6, 1.6 Hz, 1H), 5.16 (s, 2H), 5.10 (d, *J* = 2.7 Hz, 2H), 3.29 (dd, *J* = 16.6, 8.9 Hz, 1H), 2.95 (dd, *J* = 16.6, 5.4 Hz, 1H). ^{13}**C NMR** (101 MHz, $CDCl_3$): δ 169.4, 165.3, 144.2, 138.7, 135.6, 135.3, 128.7, 128.6, 128.6, 128.6, 128.4, 127.6, 123.5, 110.6, 67.2, 66.9, 59.4, 38.3. **HRMS** (ESI) calcd. for $[C_{23}H_{22}ClN_2O_4]^+$ ($[M+H]^+$), m/z = 425.1263; found 425.1269.

Dibenzyl (*E*)-4-(4-chloro-1H-pyrazol-1-yl)hex-2-enedioate (152j)

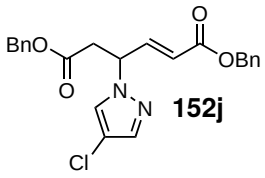

152j

According to general procedure **4**: Dibenzyl (*E*)-hex-3-enedioate (**150c**) (324 mg, 1.00 mmol, 1.00 equiv.), 4-chloro-1H-pyrazole (**151a**) (308 mg, 3.00 mmol, 3.00 equiv.), TAPT (24.4 mg, 50.1 µmol, 5 mol%), $(PhSe)_2$ (31.2 mg, 100 µmol, 10 mol%) and DCE, 21 h. Purification (PE/EtOAc, 90:10) afforded **152j** (345 mg, 812 mmol, 81%) as a colourless solid. Crude NMR yield: 85%.

According to general procedure **4**: Dibenzyl (*E*)-hex-3-enedioate (**150c**) (973 mg, 3.00 mmol, 3.00 equiv.), 4-chloro-1H-pyrazole (**151a**) (103 mg, 1.00 mmol, 1.00 equiv.), TAPT (24.3 mg, 50.0 µmol, 5 mol%), $(PhSe)_2$ (31.2 mg, 100 µmol, 10 mol%) and DCE, 21 h. Purification (PE/EtOAc, 30:1 to 15:1) afforded **152j** (376 mg, 885 µmol, 89%) as a slightly yellow oil. Crude NMR yield: 92%. Reaction conducted by Dr. T. Lei.[168]

TLC: R_f = 0.38 (PE/EtOAc, 80:20) [UV]. **M.p.** = 67.9 °C. **IR** [cm^{-1}]: 3131, 3034, 2952, 1722,

1659, 1454, 1383, 1308, 1267, 1156, 969, 842, 697. **^{1}H NMR** (400 MHz, $CDCl_3$): δ 7.45 (s, 1H), 7.39 (s, 1H), 7.38–7.30 (m, 8H), 7.28–7.23 (m, 2H), 7.04 (dd, *J* = 15.7, 5.9 Hz, 1H), 5.75 (dd, *J* = 15.7, 1.5 Hz, 1H), 5.33 (dtd, *J* = 8.9, 5.6, 1.6 Hz, 1H), 5.16 (s, 2H), 5.10 (d, *J* = 2.7 Hz, 2H), 3.29 (dd, *J* = 16.6, 8.9 Hz, 1H), 2.95 (dd, *J* = 16.6, 5.4 Hz, 1H). **^{13}C NMR** (101 MHz, $CDCl_3$): δ 169.4, 165.3, 144.2, 138.7, 135.6, 135.3, 128.7, 128.6, 128.6, 128.6, 128.4, 127.6, 123.5, 110.6, 67.2, 66.9, 59.4, 38.3. **HRMS** (ESI) calcd. for $[C_{23}H_{22}ClN_2O_4]^+$ ($[M+H]^+$), m/z = 425.1263; found 425.1269.

Dibenzyl (*E*)-4-(4-chloro-1H-pyrazol-1-yl)hex-2-enedioate (152p)

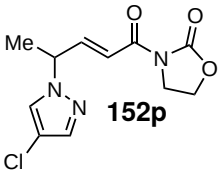

152p

According to general procedure **4**: (*E*)-3-(Hex-3-enoyl)oxazolidin-2-one (**150h**) (184 mg, 1.00 mmol, 1.00 equiv.), 4-chloro-1H-pyrazole (**151a**) (308 mg, 3.00 mmol, 3.00 equiv.), TAPT (24.21 mg, 49.8 µmol, 5 mol%), $(PhSe)_2$ (31.3 mg, 100 µmol, 10 mol%) and DCE, 21 h. Purification (PE/EtOAc, 50:50 to pure EA) did not afford the desired product **152p**. Crude NMR yield: 27%.

(*E*)-4-chloro-1-(4-(phenylsulfonyl)but-3-en-2-yl)-1H-pyrazole (152q)

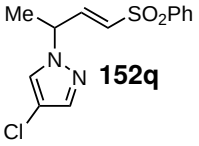

152q

According to general procedure **4**: (But-2-en-1-ylsulfonyl)benzene (**150e**) (196 mg, 1.00 mmol, 1.00 equiv.), 4-chloro-1H-pyrazole (**151a**) (308 mg, 3.00 mmol, 3.00 equiv.), TAPT (24.6 mg, 50.5 µmol, 5 mol%), $(PhSe)_2$ (31.1 mg, 99.6 µmol, 10 mol%) and DCE, 21 h. Two-time purification (PE/EtOAc, 80:20) afforded **152q** (123 mg, 416 µmol, 42%) as a lightly yellow oil. Crude NMR yield: 39%.

TLC: R_f = 0.12 (PE/EtOAc, 80:20) [UV]. **IR** [cm^{-1}]: 3135, 3064, 2989, 2926, 2255, 1633, 1446, 1387, 1312, 1148, 1085, 969, 834, 723, 686. **^{1}H NMR** (400 MHz, $CDCl_3$): δ 7.88–7.80 (m, 2H), 7.63 (tt, *J* = 6.8, 1.3 Hz, 1H), 7.57–7.53 (m, 2H), 7.42 (dd, *J* = 14.1, 0.7 Hz, 2H), 7.05 (dd, *J* = 15.1, 4.9 Hz, 1H), 6.15 (dd, *J* = 15.1, 1.7 Hz, 1H), 5.07 (qdd, *J* = 7.1, 4.9, 1.7 Hz, 1H), 1.67 (d, *J* = 7.1 Hz, 3H). **^{13}C NMR** (101 MHz, $CDCl_3$): δ 144.5, 139.7, 138.4, 133.9, 131.8, 129.6, 127.9, 125.9, 110.8, 58.1, 19.4. **HRMS** (ESI) calcd. for $[C_{13}H_{14}ClN_2O_2S]^+$ ($[M+H]^+$), m/z = 297.0459; found 297.0458.

(*Z*)-4-chloro-1-(1-phenyl-3-(phenylsulfonyl)prop-1-en-1-yl)-1H-pyrazole (173a)

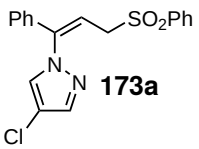

173a

According to general procedure **4**: (Cinnamylsulfonyl)benzene (**150f**) (259 mg, 1.00 mmol, 1.00 equiv.), 4-chloro-1H-pyrazole (**151a**) (308 mg, 3.00 mmol, 3.00 equiv.), TAPT (24.5 mg, 50.3 µmol, 5 mol%), $(PhSe)_2$ (31.7 mg, 102 µmol, 10 mol%) and DCE, 21 h. Two-time purification (PE/EtOAc, 80:20) afforded **173a** (58.1 mg, 162 µmol, 16%) as a colourless oil. Crude NMR yield could not be determined.

TLC: R_f = 0.28 (PE/EtOAc, 80:20) [UV]. **IR** [cm^{-1}]: 3135, 3064, 2922, 2255, 1655, 1446, 1308, 1141, 1085, 973, 910, 727, 686. ^{1}**H NMR** (400 MHz, $CDCl_3$): δ 7.88–7.77 (m, 2H), 7.72–7.59 (m, 1H), 7.59–7.45 (m, 3H), 7.46–7.32 (m, 3H), 7.20–7.08 (m, 2H), 6.77 (d, *J* = 0.7 Hz, 1H), 5.95 (t, *J* = 8.2 Hz, 1H), 4.23 (d, *J* = 8.2 Hz, 2H). ^{13}**C NMR** (75 MHz, $CDCl_3$): δ 144.2, 139.4, 138.4, 135.7, 133.9, 130.2, 129.3, 129.1, 129.1, 129.0, 128.3, 127.1, 111.7, 111.1, 55.2. **HRMS** (ESI) calcd. for $[C_{18}H_{16}ClN_2O_2]^+$ ($[M+H]^+$), m/z = 359.0616; found 359.0622.

(*E*)-4-(4-Chloro-1H-pyrazol-1-yl)hept-2-enenitrile (152t)

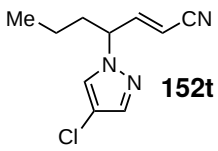

152t

According to general procedure **4**: (*E*)-Hept-3-enenitrile (**150d**) (110 mg, 1.01 mmol, 1.00 equiv.), 4-chloro-1H-pyrazole (**151a**) (308 mg, 2.98 mmol, 3.00 equiv.), TAPT (24.3 mg, 50.0 µmol, 5 mol%), $(PhSe)_2$ (31.3 mg, 100 µmol, 10 mol%) and DCE, 21 h. Purification (PE/EtOAc, 92:8 to 80:20) afforded **152t** (46.0 mg, 219 µmol, 22%) as a lightly yellow oil. Crude NMR yield: 17%. The *Z*-isomer **156a** was afforded as slightly yellow particles (7.00 mg, 33.4 µmol, 3%). Crude NMR yield: 6%. Se-intermediate **184a**: Crude NMR yield: 12%.

According to general procedure **4**: (*E*)-Hept-3-enenitrile (**150d**) (329 mg, 3.01 mmol, 3.00 equiv.), 4-chloro-1H-pyrazole (**151a**) (103 mg, 1.00 mmol, 1.00 equiv.), TAPT (24.4 mg, 50.1 µmol, 5 mol%), $(PhSe)_2$ (31.2 mg, 100 µmol, 10 mol%) and DCE, 21 h. Purification (PE/EtOAc, 90:10) afforded **152t** (55.0 mg, 262 µmol, 26%) as a lightly yellow oil with a *E*/*Z*-ratio of 5:1. Crude NMR yield: 27%, *E*/*Z*-ratio = 3:1. The Se-intermediate **184a** was afforded as a colourless oil (37.0 mg, 101 µmol, 10%). Crude NMR yield: 15%.

TLC: R_f = 0.51 (PE/EtOAc, 80:20) [UV]. **IR** [cm^{-1}]: 3131, 2963, 2933, 2873, 2363, 2337, 2229, 1737, 1640, 1431, 1387, 1320, 969, 842. ^{1}**H NMR** (300 MHz, $CDCl_3$): δ 7.50 (s, 1H), 7.39 (d, *J* = 0.7 Hz, 1H), 6.81 (dd, *J* = 16.4, 5.7 Hz, 1H), 5.20 (dd, *J* = 16.3, 1.6 Hz, 1H), 4.79 (dtd, *J* = 9.5, 5.8, 1.7 Hz, 1H), 2.21–1.99 (m, 1H), 1.86 (ddt, *J* = 14.0, 9.5, 6.1 Hz, 1H), 1.36–1.13 (m, 2H + silicon grease), 0.94 (t, *J* = 7.4 Hz, 3H). ^{13}**C NMR** (101 MHz, $CDCl_3$): δ 152.2, 138.7, 126.6, 116.3, 110.9, 101.8, 63.7, 35.6, 19.2, 13.6. **HRMS** (EI) calcd. for $[C_{10}H_{12}ClN_3]^{\cdot+}$ ($[M]^{\cdot+}$), m/z = 209.07143; found 209.07104.

Z-Isomer: **(*Z*)-4-(4-Chloro-1H-pyrazol-1-yl)hept-2-enenitrile (156a)**

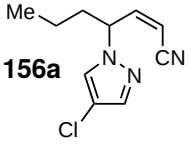

156a

TLC: R_f = 0.47 (PE/EtOAc, 80:20) [UV]. **IR** [cm^{-1}]: 3131, 2963, 2930, 2878, 2225, 1461, 1435, 1316, 969, 842, 790, 746. ^{1}**H NMR** (400 MHz, $CDCl_3$): δ 7.48 (s, 1H), 7.45 (d, *J* = 0.7 Hz, 1H), 6.75 (dd, *J* = 11.0, 9.3 Hz, 1H), 5.49 (dd, *J* = 11.0, 0.9 Hz, 1H), 5.06 (td, *J* = 8.9, 6.3 Hz, 1H), 2.21–2.03 (m, 1H), 1.95–1.76 (m, 1H), 1.36–1.11 (m, 2H + silicon grease), 0.96 (t, *J* = 7.3 Hz, 3H). ^{13}**C NMR** (101 MHz, $CDCl_3$): δ 151.5, 138.8, 127.2, 114.9, 110.3, 101.4, 62.6, 36.4, 18.9,

13.6. **HRMS** (APCI) calcd. for $[C_{10}H_{13}ClN_3]^+$ ([M+H]$^+$), m/z = 210.0793; found 210.0796.

Se-intermediate: **4-(4-Chloro-1H-pyrazol-1-yl)-3-(phenylselanyl)heptanenitrile (184a)**

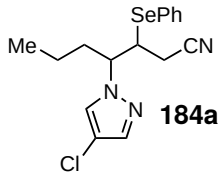

184a

TLC: R_f = 0.67 (PE/EtOAc, 80:20) [UV]. **IR** [cm^{-1}]: 3131, 3056, 2960, 2933, 2874, 2356, 2251, 1577, 1465, 1439, 1387, 1320, 969, 742, 683. ^{1}**H NMR** (400 MHz, $CDCl_3$): δ 7.70–7.52 (m, 2H), 7.47 (s, 1H), 7.45 (d, *J* = 0.7 Hz, 1H), 7.44–7.30 (m, 3H), 4.16 (ddd, *J* = 11.0, 9.5, 3.2 Hz, 1H), 3.65 (ddd, *J* = 9.5, 6.5, 4.2 Hz, 1H), 2.46 (dd, *J* = 17.4, 4.2 Hz, 1H), 2.34–2.17 (m, 2H), 2.16–1.99 (m, 1H), 1.23–1.00 (m, 2H), 0.90 (t, *J* = 7.3 Hz, 3H). ^{13}**C NMR** (101 MHz, $CDCl_3$): δ 139.1, 136.1, 136.1, 129.8, 129.8, 129.3, 128.7, 126.5, 117.5, 110.0, 65.4, 43.3, 35.4, 22.4, 19.5, 13.6. ^{77}**Se NMR** (76 MHz, $CDCl_3$): δ 381.4. **HRMS** (APCI) calcd. for $[[C_{16}H_{19}ClN_3[80\,Se]]^+$ ([M+H]$^+$), m/z = 368.0427; found 368.0431.

(*E*)-4-Chloro-1-(cyclododec-1-en-1-yl)-1H-pyrazole (152ab)

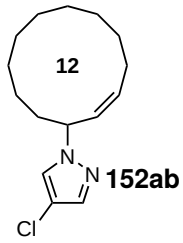

152ab

According to general procedure **4**: (*Z*)-Cyclododecene (**150l**) (166 mg, 1.00 mmol, 1.00 equiv.), 4-chloro-1H-pyrazole (**151a**) (308 mg, 3.00 mmol, 3.00 equiv.), TAPT (24.3 mg, 50.0 µmol, 5 mol%), $(PhSe)_2$ (31.2 mg, 100 µmol, 10 mol%) and DCE, 21 h. Purification (PE/EtOAc, 95:5 to 90:10) afforded **152ab** (84.0 mg, 315 µmol, 31%) as a slightly yellow solid. Crude NMR yield: 33%.

According to general procedure **4**: (*Z*)-Cyclododecene (**150l**) (160 mg, 964 µmol, 1.00 equiv.), 4-chloro-1H-pyrazole (**151a**) (308 mg, 3.01 mmol, 3.12 equiv.), TAPT (24.4 mg, 50.1 µmol, 5 mol%), $(PhSe)_2$ (31.3 mg, 100 µmol, 10 mol%), $(4\text{-}ClPhS)_2$ (14.4 mg, 50.1 µmol, 5 mol%) and DCE, 21 h. Purification (PE/EtOAc, 30:1) afforded **152ab** (128 mg, 478 µmol, 50%) as a colourless solid. Crude NMR yield: 53%. This reaction was conducted by Dr. T. Lei.[168]

TLC: R_f = 0.85 (PE/EtOAc, 80:20) [UV]. **M.p.** = 49.8 °C. **IR** [cm^{-1}]: 2926, 2855, 1461, 1387, 1308, 1167, 969, 835. ^{1}**H NMR** (400 MHz, $CDCl_3$): δ 7.41 (d, *J* = 2.0 Hz, 2H), 5.77 (ddd, *J* = 14.9, 10.4, 4.4 Hz, 1H), 5.58 (ddd, *J* = 15.2, 9.3, 1.6 Hz, 1H), 4.56 (ddd, *J* = 11.2, 9.3, 3.9 Hz, 1H), 2.35–2.20 (m, 1H), 2.19–2.08 (m, 1H), 2.08–1.92 (m, 1H), 1.87–1.73 (m, 1H), 1.70–1.54 (m, 2H), 1.55 – 1.10 (m, 12H + H_2O). ^{13}**C NMR** (101 MHz, $CDCl_3$): δ 137.2, 136.7, 128.6, 125.5, 109.5, 66.1, 33.2, 32.0, 26.0, 26.0, 25.2, 24.7, 24.7, 24.4, 23.3. **HRMS** (APCI) calcd. for $[C_{15}H_{24}ClN_2]^+$ ([M+H]$^+$), m/z = 267.1623; found 267.1626.

(*Z*)-1-(Cyclododec-2-en-1-yl)-1H-benzo[d][1,2,3]triazole (152ac)

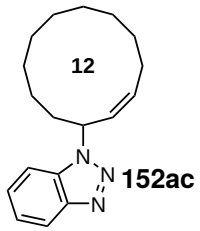

According to general procedure **4**: (*Z*)-Cyclododecene (**150l**) (166 mg, 1.00 mmol, 1.00 equiv.), 1H-benzo[d][1,2,3]triazole (**151b**) (357 mg, 3.00 mmol, 3.00 equiv.), TAPT (24.3 mg, 50.0 µmol, 5 mol%), $(PhSe)_2$ (31.2 mg, 100 µmol, 10 mol%) and DCE, 21 h. Purification (PE/EtOAc, 90:10, twice) afforded **152ac** (117 mg, 413 µmol, 41%) as a slightly yellow solid. Crude NMR yield: 45%.

According to general procedure **4**: (*Z*)-Cyclododecene (**150l**) (160 mg, 964 µmol, 1.00 equiv.), 1H-benzo[d][1,2,3]triazole (**151a**) (357 mg, 3.00 mmol, 3.11 equiv.), TAPT (24.4 mg, 50.1 µmol, 5 mol%), $(PhSe)_2$ (31.3 mg, 100 µmol, 10 mol%), $(4\text{-ClPhS})_2$ (14.4 mg, 50.1 µmol, 5 mol%) and DCE, 21 h. Purification (PE/EtOAc, 30:1) afforded **152ab** (153 mg, 540 µmol, 56%) as a colourless solid. Crude NMR yield: 52%. This reaction was conducted by Dr. T. Lei.[168]

TLC: R_f = 0.60 (PE/EtOAc, 80:20) [UV]. **M.p.** = 86.7 °C. **IR** [cm^{-1}]: 2926, 2855, 1614, 1454, 1267, 1238, 1159, 1074, 977, 746. ^{1}**H NMR** (400 MHz, $CDCl_3$): δ 8.05 (d, *J* = 8.4 Hz, 1H), 7.56 (d, *J* = 8.3 Hz, 1H), 7.50–7.40 (m, 1H), 7.39–7.29 (m, 1H), 5.88 (dd, *J* = 6.5, 2.8 Hz, 2H), 5.18 (ddt, *J* = 8.7, 6.1, 4.0 Hz, 1H), 2.40–2.28 (m, 1H), 2.28–2.14 (m, 2H), 2.08–1.88 (m, 1H), 1.82–1.58 (m, 2H), 1.57–1.20 (m, 12H + H_2O). ^{13}**C NMR** (101 MHz, $CDCl_3$): δ 146.3, 136.8, 132.4, 128.1, 126.9, 123.8, 120.2, 110.1, 63.3, 32.7, 31.9, 26.0, 25.9, 25.2, 24.8, 24.8, 24.4, 23.6. **HRMS** (ESI) calcd. for $[C_{18}H_{26}N_3]^+$ ($[M+H]^+$), m/z = 284.2121; found 284.2128.

(*E*)-4-Chloro-1-(2-methylhex-3-en-2-yl)-1H-pyrazole (152ad)

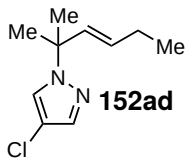

According to general procedure **4**: 2-Methylhex-2-ene (**150m**) (295 mg, 3.00 mmol, 3.00 equiv.), 4-chloro-1H-pyrazole (**151a**) (103 mg, 1.00 mmol, 1.00 equiv.), TAPT (24.4 mg, 50.1 µmol, 5 mol%), $(PhSe)_2$ (31.2 mg, 100 µmol, 10 mol%), $(4\text{-ClPhS})_2$ (14.4 mg, 50.0 µmol, 5 mol%) and DCE, 21 h. Purification (PE/EtOAc, 100:0 to 97:3, Puriflash Advion) afforded **152ad** (82.0 mg, 413 µmol, 41%) as a lightly yellow oil. Crude NMR yield: 46%.

TLC: R_f = 0.51 (PE/EtOAc, 95:5) [UV, $KMnO_4$]. **IR** [cm^{-1}]: 3146, 3027, 2967, 2937, 2878, 1461, 1387, 1327, 1271, 1167, 969, 835, 790. ^{1}**H NMR** (300 MHz, $CDCl_3$): δ 7.59–7.34 (m, 2H), 5.76–5.49 (m, 2H), 2.17–2.00 (m, 2H), 1.62 (s, 6H), 1.00 (t, *J* = 7.5 Hz, 3H). ^{13}**C NMR** (101 MHz, $CDCl_3$): δ 137.0, 133.4, 132.0, 125.0, 109.1, 62.1, 27.8, 25.3, 13.4. **HRMS** (EI) calcd. for $[C_{10}H_{15}ClN_2]^{\cdot+}$ ($[M]^{\cdot+}$), m/z = 198.09183; found 198.09179.

Ethyl (*E*)-4-(4-iodo-1H-pyrazol-1-yl)hex-2-enoate (152af)

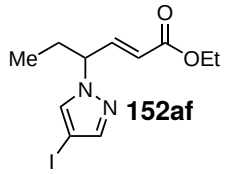

According to general procedure **4**: Ethyl (*E*)-hex-3-enoate (**150a**) (143 mg, 1.01 mmol, 1.00 equiv.), 4-iodo-1H-pyrazole (**151c**) (582 mg, 3.00 mmol, 2.98 equiv.), TAPT (24.4 mg, 50.1 µmol, 5 mol%), $(PhSe)_2$ (31.3 mg, 100 µmol, 10 mol%) and DCE, 21 h. Purification (PE/EtOAc, 95:5) afforded **152af** (214 mg, 640 µmol, 64%) as a colourless oil. Crude ^{1}H NMR yield: 64%; vinylic isomer **153af**: 3%.

TLC: R_f = 0.55 (PE/EtOAc, 80:20) [UV]. **IR** [cm^{-1}]: 3124, 2974, 2937, 1715, 1659, 1428, 1368, 1308, 1271, 1182, 1036, 977, 939, 850. **^{1}H NMR** (400 MHz, $CDCl_3$): δ 7.55 (d, *J* = 0.6 Hz, 1H), 7.45 (d, *J* = 0.6 Hz, 1H), 7.00 (dd, *J* = 15.7, 6.2 Hz, 1H), 5.71 (dd, *J* = 15.7, 1.5 Hz, 1H), 4.76 (dtd, *J* = 8.9, 6.1, 1.5 Hz, 1H), 4.17 (q, *J* = 7.1 Hz, 2H), 2.18–1.86 (m, 2H), 1.26 (t, *J* = 7.1 Hz, 3H), 0.88 (t, *J* = 7.3 Hz, 3H). **^{13}C NMR** (101 MHz, $CDCl_3$): δ 165.8, 145.2, 144.7, 132.8, 123.1, 65.1, 60.9, 56.5, 27.4, 14.3, 10.6. **HRMS** (EI) calcd. for $[C_{11}H_{15}IN_2O_2]^{\cdot+}$ ($[M]^{\cdot+}$), m/z = 334.01727; found 334.01688.

Ethyl (*E*)-1-(6-ethoxy-6-oxohex-4-en-3-yl)-1H-pyrazole-4-carboxylate (152ag)

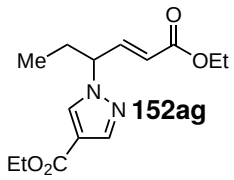

According to general procedure **4**: Ethyl (*E*)-hex-3-enoate (**150a**) (143 mg, 1.01 mmol, 1.00 equiv.), ethyl 3H-pyrazole-4-carboxylate (**151d**) (422 mg, 3.01 mmol, 2.99 equiv.), TAPT (24.4 mg, 50.2 µmol, 5 mol%), $(PhSe)_2$ (31.2 mg, 100 µmol, 10 mol%) and DCE, 21 h. Purification (PE/EtOAc/DCM, 90:10:5) afforded **152ag** (169 mg, 603 µmol, 60%) as a colourless oil. Crude ^{1}H NMR yield: 62%.

TLC: R_f = 0.31 (PE/EtOAc, 80:20) [UV, $KMnO_4$]. **IR** [cm^{-1}]: 3124, 2978, 2937, 1715, 1662, 1554, 1230, 1174, 1126, 1025,977, 768. **^{1}H NMR** (300 MHz, $CDCl_3$): 7.95 (d, *J* = 0.6 Hz, 1H), 7.91 (d, *J* = 0.7 Hz, 1H), 7.02 (dd, *J* = 15.7, 6.1 Hz, 1H), 5.72 (dd, *J* = 15.7, 1.5 Hz, 1H), 4.77 (dtd, *J* = 8.9, 6.1, 1.5 Hz, 1H), 4.29 (q, *J* = 7.1 Hz, 2H), 4.18 (q, *J* = 7.1 Hz, 2H), 2.23–1.87 (m, 2H), 1.34 (t, *J* = 7.1 Hz, 3H), 1.26 (t, *J* = 7.1 Hz, 3H), 0.89 (t, *J* = 7.4 Hz, 3H). **^{13}C NMR** (75 MHz, $CDCl_3$): δ 165.7, 163.0, 144.8, 141.4, 131.9, 123.3, 115.4, 65.2, 60.9, 60.4, 27.4, 14.5, 14.3, 10.6. **HRMS** (ESI) calcd. for $[C_{14}H_{21}N_2O_4]^+$ ($[M]^+$), m/z = 281.1496; found 281.1504.

Vinylic Isomer: **Ethyl (*Z*)-1-(1-ethoxy-1-oxohex-3-en-3-yl)-1H-pyrazole-4-carboxylate (153ag)**

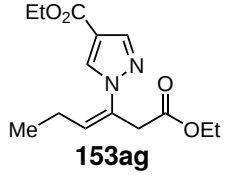

153ag (38.0 mg, 136 µmol, 14%, 86% purity) as a lightly yellow oil including 14% (5.32 mg) of **152ag**. Crude ^{1}H NMR yield: 13%.

TLC: R_f = 0.32 (PE/EtOAc, 80:20) [UV, $KMnO_4$]. **^{1}H NMR** (300 MHz, $CDCl_3$): δ 8.03–7.93 (m, 2H), 5.63–5.53 (m, 1H), 4.30 (q, *J* = 7.1 Hz, 2H), 4.07 (q, *J* = 7.1 Hz, 2H), 3.55 (d, *J* = 0.9 Hz, 2H), 2.20–2.00 (m, 2H), 1.34 (t, *J* = 7.1 Hz, 3H), 1.18 (t, *J* = 7.1 Hz, 3H), 1.02 (t, *J* = 7.5 Hz, 2H). **^{13}C NMR**

(75 MHz, $CDCl_3$): δ 170.1, 163.1, 141.5, 134.5, 131.4, 130.7, 115.2, 61.2, 60.4, 40.9, 21.0, 14.5, 14.2, 14.0. **HRMS** (ESI) calcd. for $[C_{10}H_{17}N_4O_2]^+$ ($[M]^+$), m/z = 281.1496; found 281.1502.

Ethyl (*E*)-4-(4-formyl-1H-pyrazol-1-yl)hex-2-enoate (152ah)

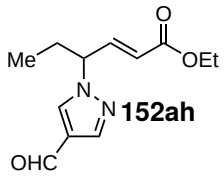

152ah

According to general procedure **4**: Ethyl (*E*)-hex-3-enoate (**150a**) (142 mg, 1.00 mmol, 1.00 equiv.), 1H-pyrazole-4-carbaldehyde (**151e**) (288 mg, 3.00 mmol, 3.00 equiv.), TAPT (24.3 mg, 50.0 µmol, 5 mol%), $(PhSe)_2$ (31.2 mg, 100 µmol, 10 mol%) and DCE, 21 h. Purification (PE/EtOAc, 80:20) afforded **152ah** (57.0 mg, 241 µmol, 24%) as a slightly yellow oil. Crude ^{1}H NMR yield: 37%.

TLC: R_f = 0.44 (PE/EtOAc, 60:40) [UV, $KMnO_4$]. **IR** [cm^{-1}]: 3124, 2974, 1733, 1681, 1543, 1450, 1372, 1178, 1029, 962, 757. ^{1}**H NMR** (400 MHz, $CDCl_3$): δ 9.87 (s, 1H), 8.02 (s, 1H), 7.96 (s, 1H), 7.03 (dd, *J* = 15.7, 6.3 Hz, 1H), 5.77 (dd, *J* = 15.7, 1.4 Hz, 1H), 4.81 (dtd, *J* = 7.8, 6.2, 1.4 Hz, 1H), 4.19 (q, *J* = 7.1 Hz, 2H), 2.23–1.94 (m, 2H), 1.27 (t, *J* = 7.2 Hz, 3H), 0.90 (t, *J* = 7.4 Hz, 3H). ^{13}**C NMR** (101 MHz, $CDCl_3$): δ 184.2, 165.6, 144.3, 141.2, 131.9, 124.5, 123.7, 65.4, 61.0, 27.5, 14.3, 10.6. **HRMS** (EI) calcd. for $[C_{12}H_{16}N_2O_3]^{\cdot+}$ ($[M]^{\cdot+}$), m/z = 236.11554; found 236.10460.

Vinylic Isomer: **Ethyl (*Z*)-3-(4-formyl-1H-pyrazol-1-yl)hex-3-enoate (153ah)**

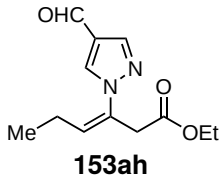

153ah

153ah (14.0 mg, 59.3 µmol, 6%) as a lightly yellow oil. Crude ^{1}H NMR yield: 8%.

TLC: R_f = 0.52 (PE/EtOAc, 60:40) [UV]. **IR** [cm^{-1}]: 3120, 2974, 2937, 2878, 1718, 1685, 1543, 1454, 1318, 1312, 1275, 1182, 1036, 977, 760. ^{1}**H NMR** (400 MHz, $CDCl_3$): δ 9.89 (s, 1H), 8.04 (s, 2H), 5.63 (t, *J* = 7.4 Hz, 1H), 4.07 (q, *J* = 7.1 Hz, 2H), 3.56 (s, 2H), 2.09 (quint., *J* = 7.5 Hz, 2H), 1.17 (t, *J* = 7.1 Hz, 3H), 1.03 (t, *J* = 7.5 Hz, 3H). ^{13}**C NMR** (101 MHz, $CDCl_3$): δ 184.2, 170.0, 140.9, 134.9, 131.4, 131.3, 124.2, 61.2, 40.8, 21.0, 14.2, 13.9.

Hydroxy byproduct: **Ethyl (*E*)-4-hydroxyhex-2-enoate (159)**

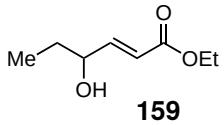

159

During purification, 13 mg (82.2 µmol, 8%) of hydroxy-byproduct ethyl (*E*)-4-hydroxyhex-2-enoate (**159**) were able to be isolated.

TLC: R_f = 0.63 (PE/EtOAc, 60:40) [UV]. **IR** [cm^{-1}]: 3448, 3105, 2919, 2863, 1595, 1446, 1305, 1148, 1088, 1029, 939, 816, 753. ^{1}**H NMR** (300 MHz, $CDCl_3$): δ 6.93 (ddd, *J* = 15.8, 5.1, 0.5 Hz, 1H), 6.03 (ddd, *J* = 15.9, 1.7, 0.6 Hz, 1H), 4.30–3.98 (m, 3H), 1.99 (d, *J* = 18.7 Hz, 1H), 1.72–1.51 (m, 2H), 1.29 (td, *J* = 7.2, 0.6 Hz, 3H), 0.96 (t, *J* = 7.5 Hz, 3H). ^{13}**C NMR** (101 MHz, $CDCl_3$): δ 166.7, 150.0, 120.5, 72.5, 60.6, 29.7, 14.4, 9.6. **HRMS** (APCI) calcd. for $[C_{10}H_{17}O_5]^+$ ($[M+H]^+$),

m/z = 217.1070; found 217.1071.

Ethyl (*E*)-4-(3-phenyl-1H-pyrazol-1-yl)hex-2-enoate (*N*1-isomer) and ethyl (*E*)-4-(5-phenyl-1H-pyrazol-1-yl)hex-2-enoate (*N*2-isomer) (152ai)

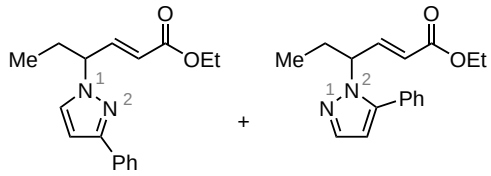

*N*1-isomer **152ai** *N*2-isomer

According to general procedure **4**: Ethyl (*E*)-hex-3-enoate (**150a**) (143 mg, 1.01 mmol, 1.00 equiv.), 3-phenyl-1H-pyrazole (**151f**) (432 mg, 3.00 mmol, 2.98 equiv.), TAPT (24.5 mg, 50.3 µmol, 5 mol%), $(PhSe)_2$ (31.2 mg, 99.9 µmol, 10 mol%) and DCE, 21 h. Purification (Hexane/EtOAc, 93:7 to 85:15, Puriflash Büchi) afforded **152ai** (145 mg, 510 µmol, 51%) as a colourless oil with a *N*1/*N*2 ratio of 5:1. Crude ^{1}H NMR yield: allylic isomer **152ai**: 53%; a signal of vinylic isomer **153ai** was not identified.

TLC: R_f = 0.51 (PE/EtOAc, 80:20) [UV]. **IR** [cm^{-1}]: 2974, 2937, 1715, 1659, 1498, 1457, 1368, 1308, 1271, 1233, 1177, 1036, 977, 749, 693. ^{1}**H NMR** (400 MHz, $CDCl_3$): δ 7.85–7.76 (m, 2H, *N*1), 7.64 (d, *J* = 1.8 Hz, 1H, *N*2), 7.49–7.27 (m, 4H + 5H, *N*1 + *N*2), 7.18–7.06 (m, 1H + 1H, *N*1 + *N*2), 6.60 (d, *J* = 2.4 Hz, 1H, *N*1), 6.29 (d, *J* = 1.8 Hz, 1H, *N*2), 5.76 (dd, *J* = 15.7, 1.5 Hz, 1H, *N*1), 5.67 (dd, *J* = 15.7, 1.6 Hz, 1H, *N*2), 4.83 (dtd, *J* = 9.0, 6.1, 1.5 Hz, 1H, *N*1), 4.79–4.70 (m, 1H, *N*2), 4.18 (q, *J* = 7.1 Hz, 2H + 2H, *N*1 + *N*2), 2.30–1.86 (m, 2H + 2H, *N*1 + *N*2), 1.33–1.23 (m, 3H + 3H, *N*1 + *N*2), 0.94 (t, *J* = 7.4 Hz, 3H, *N*1), 0.73 (t, *J* = 7.3 Hz, 3H, *N*2). ^{13}**C NMR** (101 MHz, $CDCl_3$): δ 166.2, 166.1, 151.6, 147.0, 146.1, 144.8, 139.7, 133.6, 130.7, 129.4, 129.3, 128.9, 128.9, 128.7, 127.8, 125.8, 122.7, 122.3, 106.0, 103.2, 64.8, 60.9, 60.8, 60.7, 27.9, 27.7, 14.3, 10.8, 10.7. **HRMS** (EI) calcd. for $[C_{17}H_{20}N_2O_2]^{\cdot+}$ ($[M]^{\cdot+}$), m/z = 284.15193; found 284.15138 (minor) and 284.15186 (major).

Ethyl (*E*)-4-(3,5-diphenyl-1H-pyrazol-1-yl)hex-2-enoate (152aj)

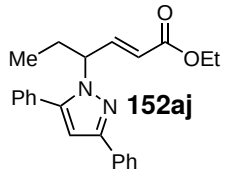

152aj

According to general procedure **4**: Ethyl (*E*)-hex-3-enoate (**150a**) (51.9 mg, 365 µmol, 1.00 equiv.), 3,5-diphenyl-1H-pyrazole (**151g**) (240 mg, 1.09 mmol, 2.99 equiv.), TAPT (8.87 mg, 18.3 µmol, 5 mol%), $(PhSe)_2$ (11.5 mg, 36.9 µmol, 10 mol%) and DCE, 21 h. Purification (PE/EtOAc, 95:5) afforded **152aj** (50.3 mg, 140 µmol, 38%) as a colourless oil. Crude ^{1}H NMR yield: allylic isomer **152aj**: 65%; a signal of vinylic isomer **153aj** was not identified. **TLC**: R_f = 0.51 (PE/EtOAc, 80:20) [UV, $KMnO_4$]. **IR** [cm^{-1}]: 3060, 2971, 2930, 1718, 1659, 1305, 1271, 1178, 1033, 980, 910, 760, 693. ^{1}**H NMR** (400 MHz, $CDCl_3$): δ 7.93–7.83 (m, 2H), 7.51–7.35 (m, 7H), 7.35–7.29 (m, 1H), 7.22 (ddd, *J* = 15.7, 5.9, 0.7 Hz, 1H), 6.60 (s, 1H), 5.77 (ddd, *J* = 15.7, 1.5, 0.7 Hz, 1H), 4.76 (dtd, *J* = 9.7, 5.6, 1.5 Hz, 1H), 4.20 (q, *J* = 7.1 Hz, 2H), 2.40–2.24 (m, 1H), 2.02–1.86 (m, 1H), 1.29 (t, *J* = 7.1 Hz, 3H), 0.79 (t, *J* = 7.3 Hz, 3H). ^{13}**C NMR** (101 MHz, $CDCl_3$): δ 166.3, 151.4, 147.3, 146.1, 133.8, 130.7, 129.2,

128.9, 128.9, 128.7, 127.8, 125.9, 122.3, 103.3, 61.2, 60.7, 28.0, 14.3, 10.8. **HRMS** (EI) calcd. for $[C_{23}H_{24}N_2O_2]^{\cdot+}$ ($[M]^{\cdot+}$), m/z = 360.18323; found 360.18236.

Ethyl (*E*)-4-(4-bromo-3-methyl-1H-pyrazol-1-yl)hex-2-enoate (*N*1-isomer) and ethyl (*E*)-4-(4-bromo-5-methyl-1H-pyrazol-1-yl)hex-2-enoate (*N*2-isomer) (152ak)

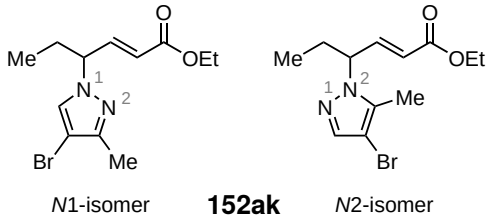

*N*1-isomer **152ak** *N*2-isomer

According to general procedure **4**: Ethyl (*E*)-hex-3-enoate (**150a**) (142 mg, 1.00 mmol, 1.00 equiv.), 4-bromo-3-methyl-1H-pyrazole (**151h**) (484 mg, 3.01 mmol, 3.01 equiv.), TAPT (24.3 mg, 50.0 µmol, 5 mol%), $(PhSe)_2$ (31.4 mg, 101 µmol, 10 mol%) and DCE, 21 h. Purification (PE/EtOAc, 95:5 to 90:10 Puriflash Advion) afforded **152ak** (172 mg, 571 µmol, 57%) as a slightly yellow oil. Crude ^{1}H NMR yield: allylic isomer **152ak**: 58%; a signal of vinylic isomer **153ak** was not identified.

TLC: R_f = 0.50 (PE/EtOAc, 80:20) [UV, $KMnO_4$]. **IR** [cm^{-1}]: 3127, 2974, 2933, 2878, 1718, 1659, 1368, 1312, 1275, 1238, 1178, 1059, 980, 861, 828. **^{1}H NMR** (400 MHz, $CDCl_3$): δ 7.48 (s, 1H, *N*2), 7.35 (s, 1H, *N*1), 7.08–6.90 (m, 1H + 1H, *N*1 + *N*2), 5.71 (dd, *J* = 15.7, 1.5 Hz, 1H, *N*1), 5.58 (dd, *J* = 15.8, 1.6 Hz, 1H, *N*2), 4.73–4.54 (m, 1H + 1H, *N*1 + *N*2), 4.25–4.11 (m, 2H + 2H, *N*1 + *N*2), 2.26–2.19 (m, 3H + 3H, *N*1 + *N*2), 2.13–1.86 (m, 2H + 2H, *N*1 + *N*2), 1.31–1.20 (m, 3H + 3H, *N*1 + *N*2), 0.95–0.81 (m, 3H + 3H, *N*1 + *N*2). **^{13}C NMR** (101 MHz, $CDCl_3$): δ 165.9, 147.7, 145.7, 145.5, 139.4, 137.2, 128.8, 122.9, 122.4, 94.1, 93.7, 62.1, 60.8, 27.3, 26.9, 14.3, 12.1, 10.9, 10.7, 9.8. **HRMS** (EI) calcd. for $[C_{12}H_{17}BrN_2O_2]^{\cdot+}$ ($[M]^{\cdot+}$), m/z = 300.04679; found 300.04620 (major) and 300.04620 (minor).

Ethyl (*E*)-4-(1H-1,2,3-triazol-1-yl)hex-2-enoate (152al)

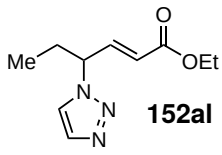

152al

According to general procedure **4**: Ethyl (*E*)-hex-3-enoate (**150a**) (142 mg, 1.00 mmol, 1.00 equiv.), 1H-1,2,3-triazole (**151i**) (174 µL, 207 mg, 3.00 mmol, 3.01 equiv.), TAPT (24.4 mg, 50.2 µmol, 5 mol%), $(PhSe)_2$ (31.2 mg, 100 µmol, 10 mol%) and DCE, 21 h. Purification (Hexane/EtOAc, 97:3 to 45:55, puriflash Büchi) did not afford the desired product **152al**. Crude NMR yield: 55%.

Ethyl (*E*)-4-(1H-benzo[d][1,2,3]triazol-1-yl)hex-2-enoate (152am)

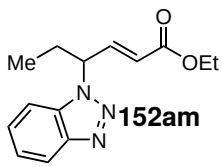

152am

According to general procedure **4**: Ethyl (*E*)-hex-3-enoate (**150a**) (142 mg, 1.00 mmol, 1.00 equiv.), 1H-benzo[d][1,2,3]triazole (**151b**) (358 mg, 3.01 mmol, 3.00 equiv.), TAPT (24.3 mg, 50.0 µmol, 5 mol%), $(PhSe)_2$ (31.2 mg, 100 µmol, 10 mol%) and DCE, 21 h. Purification (PE/EtOAc, 90:10) afforded **152am** (157 mg, 605 µmol, 61%) as a lightly yellow oil

(crude ^{1}H NMR yield: 62%), **153am** (44.0 mg, 170 µmol, 17%) as a lightly yellow oil (crude ^{1}H NMR yield: 15%) and **185a** (7.00 mg, 27.0 µmol, 3%) as colourless particles (crude ^{1}H NMR yield: not detectable).

TLC: R_f = 0.31 (PE/EtOAc, 4:1) [UV, $KMnO_4$]. **IR** [cm^{-1}]: 3064, 2974, 2937, 2878, 1718, 1659, 1454, 1271, 1238, 1185, 1036, 977, 746. **^{1}H NMR** (400 MHz, $CDCl_3$): δ 8.09 (dt, *J* = 8.3, 1.0 Hz, 1H), 7.52–7.46 (m, 2H), 7.44–7.32 (m, 1H), 7.20 (dd, *J* = 15.7, 6.0 Hz, 1H), 5.76 (dd, *J* = 15.8, 1.6 Hz, 1H), 5.40 (dtd, *J* = 9.3, 6.0, 1.6 Hz, 1H), 4.16 (q, *J* = 7.1 Hz, 2H), 2.49–2.34 (m, 1H), 2.35–2.20 (m, 1H), 1.24 (t, *J* = 7.1 Hz, 3H), 0.91 (t, *J* = 7.4 Hz, 3H). **^{13}C NMR** (101 MHz, $CDCl_3$): δ 165.6, 146.3, 143.9, 132.6, 127.6, 124.3, 123.6, 120.4, 109.7, 62.2, 61.0, 26.9, 14.2, 10.8. **HRMS** (APCI) calcd. for $[C_{14}H_{18}N_3O_2]^+$ ([M]$^+$), m/z = 260.1394; found 260.1399.

Vinylic Isomer: **Ethyl (*Z*)-3-(1H-benzo[d][1,2,3]triazol-1-yl)hex-3-enoate (153am)**

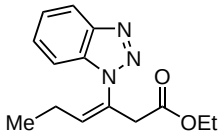

153am

TLC: R_f = 0.44 (PE/EtOAc, 4:1) [UV, $KMnO_4$]. **IR** [cm^{-1}]: 3064, 2974, 1737, 1614, 1454, 1275, 1178, 1059, 1029, 749. **^{1}H NMR** (400 MHz, $CDCl_3$): δ 8.07 (dt, *J* = 8.3, 1.0 Hz, 1H), 7.57–7.43 (m, 2H), 7.42–7.33 (m, 1H), 5.96 (tt, *J* = 7.4, 0.9 Hz, 1H), 3.93 (q, *J* = 7.2 Hz, 2H), 3.71 (d, *J* = 0.9 Hz, 2H), 1.89–1.77 (m, 2H), 0.97 (td, *J* = 7.3, 5.5 Hz, 6H). **^{13}C NMR** (101 MHz, $CDCl_3$): δ 169.6, 145.2, 134.7, 133.6, 127.8, 127.7, 124.0, 119.9, 110.7, 61.1, 41.9, 21.3, 13.8, 13.4. **HRMS** (ESI) calcd. for $[C_{11}H_{15}ClN_2O_2]^+$ ([M]$^+$), m/z = 260.1394; found 260.1398.

N2-Isomer: **Ethyl (*E*)-4-(2H-benzo[d][1,2,3]triazol-2-yl)hex-2-enoate (185a)**

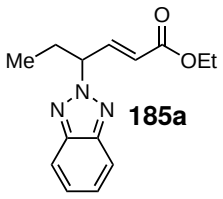

185a

TLC: R_f = 0.67, (PE/EtOAc, 80:20) [UV]. **IR** [cm^{-1}]: 3064, 2974, 2930, 1722, 1662, 1450, 1367, 1316, 1271, 1178, 1036, 977, 850, 746. **^{1}H NMR** (300 MHz, $CDCl_3$): δ 7.94–7.81 (m, 2H), 7.46–7.33 (m, 2H), 7.23 (dd, *J* = 15.7, 6.9 Hz, 1H), 5.84 (dd, *J* = 15.8, 1.3 Hz, 1H), 5.44 (dddd, *J* = 9.0, 7.1, 5.9, 1.4 Hz, 1H), 4.18 (q, *J* = 7.1 Hz, 2H), 2.43 (ddq, *J* = 14.6, 9.0, 7.4 Hz, 1H), 2.29–2.13 (m, 1H), 1.26 (t, *J* = 7.1 Hz, 3H), 0.91 (t, *J* = 7.4 Hz, 3H). **^{13}C NMR** (101 MHz, $CDCl_3$): 165.7, 144.4, 144.0, 126.7, 123.9, 118.3, 69.4, 60.9, 28.1, 14.3, 10.6. **HRMS** (EI) calcd. for $[C_{14}H_{17}N_3O_2]^{\cdot+}$ ([M]$^{\cdot+}$), m/z = 259.13153; found 259.13130.

According to general procedure **4**: Ethyl (*E*)-hex-3-enoate (**150a**) (425 mg, 2.99 mmol, 2.97 equiv.), 1H-benzo[d][1,2,3]triazole (**151b**) (120 mg, 1.01 mmol, 1.00 equiv.), TAPT (24.2 mg, 50.0 µmol, 5 mol%), $(PhSe)_2$ (31.2 mg, 100 µmol, 10 mol%) and DCE, 39 h. After 22 h, second addition of TAPT (24.3 mg, 50.0 µmol, 5 mol%) and $(PhSe)_2$ (31.2 mg, 100 µmol, 10 mol%). Crude ^{1}H NMR yield: **152am**: 37%, **153am**: 17%.

Ethyl (*E*)-4-(5-methyl-1H-benzo[d][1,2,3]triazol-1-yl)hex-2-enoate (*N*1-isomer) and ethyl (*E*)-4-(6-methyl-1H-benzo[d][1,2,3]triazol-1-yl)hex-2-enoate (*N*3-isomer) (152an)

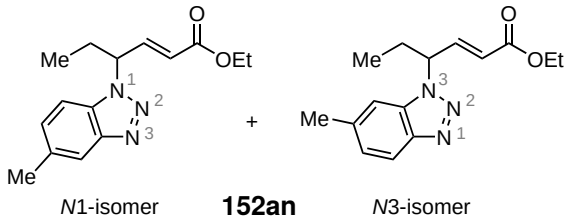

*N*1-isomer **152an** *N*3-isomer

According to general procedure **4**: Ethyl (*E*)-hex-3-enoate (**150a**) (142 mg, 1.00 mmol, 1.00 equiv.), 5-methyl-1H-benzo[d][1,2,3]triazole (**151j**) (401 mg, 3.01 mmol, 3.01 equiv.), TAPT (24.3 mg, 49.9 µmol, 5 mol%), $(PhSe)_2$ (31.3 mg, 100 µmol, 10 mol%) and DCE, 21 h. Purification (PE/EtOAc, 95:5 to 90:10) afforded **152an** (169 mg, 618 µmol, 62%) as a slightly yellow oil and a mixture of isomers (*N*1/*N*2 = 1:1). Crude ^{1}H NMR yield: 61%.

TLC: R_f = 0.28 (PE/EtOAc, 80:20) [UV, $KMnO_4$]. **IR** [cm^{-1}]: 2974, 2933, 1718, 1662, 1461, 1368, 1312, 1275, 1238, 1185, 1040, 980, 805. **^{1}H NMR** (400 MHz, $CDCl_3$): δ 7.97 (d, *J* = 8.5 Hz, 0.43H), 7.90–7.81 (m, 0.57H), 7.43–7.30 (m, 1H), 7.27–7.16 (m, 2H), 5.77 (dd, *J* = 15.8, 1.6 Hz, 1H), 5.39 (ddtd, *J* = 10.8, 9.3, 6.0, 1.6 Hz, 1H), 4.18 (qd, *J* = 7.1, 2.2 Hz, 2H), 2.54 (dd, *J* = 3.8, 0.9 Hz, 3H), 2.42 (ddtd, *J* = 14.6, 9.3, 7.3, 5.2 Hz, 1H), 2.27 (ddd, *J* = 13.9, 7.4, 6.3 Hz, 1H), 1.27 (td, *J* = 7.1, 2.1 Hz, 3H), 0.93 (td, *J* = 7.4, 2.7 Hz, 3H). **^{13}C NMR** (75 MHz, $CDCl_3$): δ 165.7, 147.0, 144.0, 134.3, 129.8, 126.5, 123.5, 119.4, 109.3, 62.2, 60.9, 26.9, 21.6, 14.3, 10.9. **HRMS** (EI) calcd. for $[C_{15}H_{19}N_3O_2]^{\cdot+}$ ($[M]^{\cdot+}$), m/z = 273.14718; found 273.14678 and 273.14719.

Vinylic Isomer: **Ethyl (*Z*)-3-(5-methyl-1H-benzo[d][1,2,3]triazol-1-yl)hex-3-enoate (*N*1-isomer) and ethyl (*Z*)-3-(6-methyl-1H-benzo[d][1,2,3]triazol-1-yl)hex-3-enoate (*N*3-isomer) (153an)**

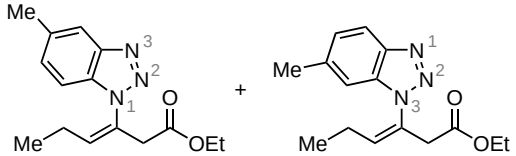

*N*1-isomer **153an** *N*3-isomer

153an (41.0 mg, 150 µmol, 15%) as a lightly yellow oil and a mixture of isomers (41:59). Crude ^{1}H NMR yield: 18%.

TLC: R_f = 0.38 (PE/EtOAc, 80:20) [UV]. **IR** [cm^{-1}]: 2971, 2933, 1733, 1495, 1457, 1402, 1372, 1327, 1238, 1178, 1066, 1029, 805. **^{1}H NMR** (400 MHz, $CDCl_3$): 7.92 (*N*1, d, *J* = 8.5 Hz, 1H), 7.82 (*N*3, s, 1H), 7.39 – 7.30 (*N*3, m, 2H), 7.21 (*N*1, s, 1H), 7.19 (*N*1, dd, *J* = 8.5, 1.4 Hz, 1H), 6.03 – 5.85 (*N*1+*N*3, m, 1+1H), 3.98 – 3.88 (*N*1+*N*3, m, 2+2H), 3.69 (*N*1+*N*3, s, 2+2H), 2.52 (*N*1, s, 1H), 2.51 (*N*3, s, 2H), 1.88 – 1.76 (*N*1+*N*3, m, 2H), 1.03 – 0.91 (*N*1+*N*3,m, 6H). **^{13}C NMR** (101 MHz, $CDCl_3$): δ 169.8, 145.8, 143.9, 138.6, 134.6, 134.5, 134.2, 132.3, 130.1, 127.9, 127.9, 126.4, 119.4, 118.9, 110.4, 110.0, 61.2, 41.9, 22.2, 21.6, 21.4, 21.4, 14.0, 13.9, 13.5. **HRMS** (ESI) calcd. for $[C_{15}H_{20}N_3O_2]^+$ ($[M]^+$), m/z = 274.1550; found 274.1552.

Ethyl (*E*)-4-(5-methyl-1H-tetrazol-1-yl)hex-2-enoate (152ao)

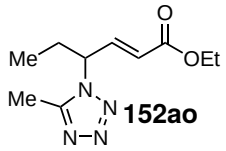

152ao

According to general procedure **4**: Ethyl (*E*)-hex-3-enoate (**150a**) (143 mg, 1.01 mmol, 1.00 equiv.), 5-methyl-1H-tetrazole (**151k**) (253 mg, 3.01 mmol, 3.01 equiv.), TAPT (24.4 mg, 50.2 µmol, 5 mol%), $(PhSe)_2$ (31.3 mg, 100 µmol, 10 mol%) and DCE, 21 h. Purification (PE/EtOAc, 95:5 to 90:10) afforded **152ao** (81.0 mg, 361 µmol, 36%) as a colourless oil. Crude ^{1}H NMR yield: 40%.

TLC: R_f = 0.18 (PE/EtOAc, 80:20) [UV, $KMnO_4$]. **IR** [cm^{-1}]: 2978, 2941, 2881, 122, 1662, 1461, 1506, 1368, 1312, 1271, 1185, 1029, 977, 828, 731. **^{1}H NMR** (300 MHz, $CDCl_3$): δ 7.06 (dd, *J* = 15.7, 7.0 Hz, 1H), 5.84 (dd, *J* = 15.8, 1.3 Hz, 1H), 5.34 (dddd, *J* = 8.6, 7.2, 6.1, 1.3 Hz, 1H), 4.19 (q, *J* = 7.1 Hz, 2H), 2.54 (s, 3H), 2.36–1.95 (m, 2H), 1.27 (t, *J* = 7.1 Hz, 3H), 0.89 (t, *J* = 7.4 Hz, 3H). **^{13}C NMR** (75 MHz, $CDCl_3$): δ 165.4, 163.3, 142.6, 124.4, 66.2, 61.0, 27.5, 14.3, 11.1, 10.4. **HRMS** (ESI) calcd. for $[C_{10}H_{17}N_4O_2]^+$ ($[M]^+$), m/z = 225.1346; found 225.1352.

Vinylic Isomer: **Ethyl (*Z*)-3-(5-methyl-1H-tetrazol-1-yl)hex-3-enoate (153ao)**

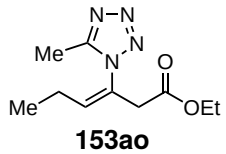

153ao

153ao (12.0 mg, 53.5 µmol, 5%) as a colourless oil. Crude ^{1}H NMR yield: 4%.

TLC: R_f = 0.50 (PE/EtOAc, 80:20) [UV, $KMnO_4$]. **IR** [cm^{-1}]: 2974, 2937, 1737, 1510, 1461, 1394, 1342, 1252, 1182, 1029, 872, 723. **^{1}H NMR** (400 MHz, $CDCl_3$): δ 5.77–5.61 (m, 1H), 4.10 (q, *J* = 7.2 Hz, 2H), 3.66 (d, *J* = 1.0 Hz, 2H), 2.56 (s, 3H), 2.50–2.35 (m, 2H), 1.18 (t, *J* = 7.2 Hz, 3H), 1.08 (t, *J* = 7.5 Hz, 3H). **^{13}C NMR** (101 MHz, $CDCl_3$): δ 169.5, 162.2, 132.1, 128.2, 61.3, 40.6, 21.6, 14.1, 13.7, 11.0. **HRMS** (ESI) calcd. for $[C_{10}H_{17}N_4O_2]^+$ ($[M]^+$), m/z = 225.1346; found 225.1352.

Ethyl (*E*)-4-(3-methyl-1H-pyrazol-1-yl)hex-2-enoate (152ap)

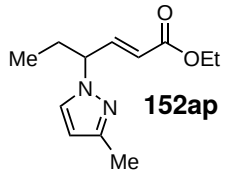

152ap

According to general procedure **4**: Ethyl (*E*)-hex-3-enoate (**150a**) (144 mg, 1.01 mmol, 1.00 equiv.), 3-methyl-1H-pyrazole (**151l**) (242 µL, 247 mg, 3.01 mmol, 2.97 equiv.), TAPT (24.5 mg, 50.3 µmol, 5 mol%), $(PhSe)_2$ (31.2 mg, 100 µmol, 10 mol%) and DCE. After 21 h, TLC analysis indicates still a lot of starting material present. TAPT (24.4 mg, 50.2 µmol, 5 mol%) and $(PhSe)_2$ (31.1 mg, 99.7 µmol, 10 mol%) were added again and the reaction was stirred for further 20 h. Purification was not attempted due to a low crude NMR yield of 4%.

Ethyl (*E*)-4-(1H-indazol-1-yl)hex-2-enoate (152aq)

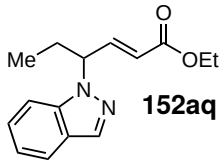

152aq

According to general procedure **4**: Ethyl (*E*)-hex-3-enoate (**150a**) (142 mg, 1.00 mmol, 1.00 equiv.), 2H-indazole (**151m**) (355 mg, 3.00 mmol, 3.01 equiv.), TAPT (24.3 mg, 50.0 µmol, 5 mol%), $(PhSe)_2$ (31.4 mg, 101 µmol, 10 mol%) and DCE, 21 h. Purification was not attempted due to a low crude NMR yield of 27%.

Ethyl (*E*)-4-(1H-1,2,4-triazol-1-yl)hex-2-enoate (152ar)

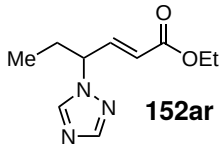

152ar

According to general procedure **4**: Ethyl (*E*)-hex-3-enoate (**150a**) (143 mg, 1.01 mmol, 1.00 equiv.), 1H-1,2,4-triazole (**151n**) (207 mg, 3.00 mmol, 3.00 equiv.), TAPT (24.4 mg, 50.2 µmol, 5 mol%), $(PhSe)_2$ (31.2 mg, 100 µmol, 10 mol%) and DCE, 21 h. Purification was not attempted due to a low crude NMR yield of 12%.

Ethyl (*E*)-4-(1H-1,2,4-triazol-1-yl)hex-2-enoate (152as)

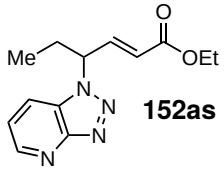

152as

According to general procedure **4**: Ethyl (*E*)-hex-3-enoate (**150a**) (144 mg, 1.01 mmol, 1.00 equiv.), 1H-[1,2,3]triazolo[4,5-b]pyridine (**151o**) (360 mg, 3.00 mmol, 3.00 equiv.), TAPT (24.3 mg, 50.0 µmol, 5 mol%), $(PhSe)_2$ (31.3 mg, 100 µmol, 10 mol%) and DCE, 21 h. Purification was not attempted due to a low crude NMR yield of 17%.

Ethyl (*E*)-4-(5-chloro-1H-benzo[d][1,2,3]triazol-1-yl)hex-2-enoate (152at)

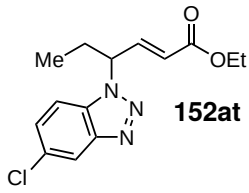

152at

According to general procedure **4**: Ethyl (*E*)-hex-3-enoate (**150a**) (143 mg, 1.01 mmol, 1.00 equiv.), 5-chloro-1H-benzo[d][1,2,3]triazole (**151p**) (462 mg, 3.01 mmol, 3.00 equiv.), TAPT (24.4 mg, 50.2 µmol, 5 mol%), $(PhSe)_2$ (31.5 mg, 101 µmol, 10 mol%) and DCE, 21 h. Purification was not attempted due to a low crude NMR yield of 16%.

Diethyl (*E*)-4-(1H-pyrazol-1-yl)hex-2-enedioate (152au)

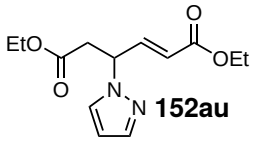

According to general procedure **4**: Diethyl (*E*)-hex-3-enedioate (**150j**) (604 mg, 3.02 mmol, 3.01 equiv.), 1H-pyrazole (**151q**) (68.2 mg, 1.00 mmol, 1.00 equiv.), TAPT (24.3 mg, 50.0 µmol, 5 mol%), $(PhSe)_2$ (31.4 mg, 101 µmol, 10 mol%), $(4\text{-}ClPhS)_2$ (14.5 mg, 50.3 µmol, 5 mol%) and DCE, 21 h. Purification (PE/EtOAc, 97:3 to 80:20, Puriflash Advion) afforded **152au** (228 mg, 857 µmol, 86%) as a slightly yellow oil. Crude NMR yield: 90%.

TLC: R_f = 0.26 (PE/EtOAc, 80:20) [UV, $KMnO_4$]. **IR** [cm^{-1}]: 3124, 2982, 2937, 1722, 1662, 1398, 1271, 1185, 1096, 1044, 980, 752. ^{1}**H NMR** (400 MHz, $CDCl_3$): δ 7.56 (d, *J* = 1.8 Hz, 1H), 7.45 (dd, *J* = 2.3, 0.7 Hz, 1H), 7.06 (dd, *J* = 15.7, 5.8 Hz, 1H), 6.34–6.20 (m, 1H), 5.69 (dd, *J* = 15.7, 1.6 Hz, 1H), 5.41 (dtd, *J* = 8.5, 5.9, 1.6 Hz, 1H), 4.28–4.01 (m, 5H), 3.24 (dd, *J* = 16.5, 8.4 Hz, 1H), 2.95 (dd, *J* = 16.5, 6.0 Hz, 1H), 1.25 (t, *J* = 7.1 Hz, 3H), 1.19 (t, *J* = 7.1 Hz, 3H). ^{13}**C NMR** (101 MHz, $CDCl_3$): δ 169.8, 165.7, 144.5, 140.2, 129.4, 123.4, 105.9, 61.2, 60.9, 58.8, 38.8, 14.3, 14.2. **HRMS** (ESI) calcd. for $[C_{13}H_{19}N_2O_4]^+$ ($[M+H]^+$), m/z = 267.1339; found 267.1340.

Diethyl (*E*)-4-(4-methyl-1H-pyrazol-1-yl)hex-2-enedioate (152av)

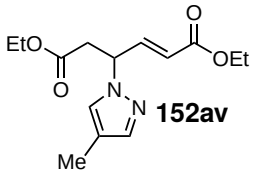

According to general procedure **4**: Diethyl (*E*)-hex-3-enedioate (**150j**) (601 mg, 3.01 mmol, 3.01 equiv.), 4-methyl-1H-pyrazole (**151r**) (77.3 µL, 82.1 mg, 1.00 mmol, 1.00 equiv.), TAPT (24.5 mg, 50.3 µmol, 5 mol%), $(PhSe)_2$ (31.3 mg, 100 µmol, 10 mol%), $(4\text{-}ClPhS)_2$ (14.5 mg, 50.3 µmol, 5 mol%) and DCE, 21 h. Purification (PE/EtOAc, 98:2 to 75:25, Puriflash Advion) afforded **152av** (157 mg, 560 µmol, 56%) as a slightly yellow oil. Crude NMR yield: 56%.

TLC: R_f = 0.31 (PE/EtOAc, 80:20) [UV, $KMnO_4$]. **IR** [cm^{-1}]: 3090, 2982, 2937, 1722, 1662, 1372, 1312, 1271, 1159, 1029, 984, 861. ^{1}**H NMR** (400 MHz, $CDCl_3$): δ 7.36 (s, 1H), 7.24–7.16 (m, 1H), 7.03 (dd, *J* = 15.7, 5.8 Hz, 1H), 5.69 (dd, *J* = 15.7, 1.6 Hz, 1H), 5.33 (dtd, *J* = 8.4, 5.9, 1.6 Hz, 1H), 4.24–4.04 (m, 5H), 3.22 (dd, *J* = 16.4, 8.4 Hz, 1H), 2.92 (dd, *J* = 16.4, 6.0 Hz, 1H), 2.06 (t, *J* = 0.6 Hz, 3H), 1.26 (t, *J* = 7.1 Hz, 3H), 1.20 (t, *J* = 7.1 Hz, 3H). ^{13}**C NMR** (101 MHz, $CDCl_3$): δ 169.9, 165.8, 144.7, 140.5, 128.2, 123.3, 116.5, 61.2, 60.9, 58.7, 38.6, 14.3, 14.2, 9.0. **HRMS** (EI) calcd. for $[C_{14}H_{20}N_2O_4]^{\cdot+}$ ($[M]^{\cdot+}$), m/z = 280.14176; found 280.14138.

Diethyl (*E*)-4-(4-(trifluoromethyl)-1H-pyrazol-1-yl)hex-2-enedioate (152aw)

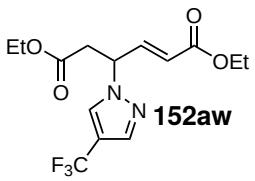

According to general procedure **4**: Diethyl (*E*)-hex-3-enedioate (**150j**) (604 mg, 3.02 mmol, 2.99 equiv.), 4-(trifluoromethyl)-1H-pyrazole (**151s**) (137 mg, 1.01 mmol, 1.00 equiv.), TAPT (24.4 mg, 50.2 µmol, 5 mol%), $(PhSe)_2$ (31.2 mg, 100 µmol, 10 mol%) and DCE, 21 h. Purification (PE/EtOAc, 90:10) afforded **152aw** (258 mg, 772 µmol, 77%) as a slightly yellow oil. Crude NMR yield: 89%.

TLC: R_f = 0.32 (PE/EtOAc, 80:20) [UV, $KMnO_4$]. **IR** [cm^{-1}]: 3124, 2986, 1722, 1662, 1580, 1409, 1372, 1238, 1189, 1118, 1029, 969, 869, 686. ^{1}**H NMR** (400 MHz, $CDCl_3$): δ 7.83–7.60 (m, 2H), 7.03 (dd, *J* = 15.7, 6.1 Hz, 1H), 5.77 (dd, *J* = 15.7, 1.5 Hz, 1H), 5.39 (dtd, *J* = 8.8, 5.7, 1.5 Hz, 1H), 4.27–3.89 (m, 4H), 3.25 (dd, *J* = 16.7, 8.8 Hz, 1H), 2.94 (dd, *J* = 16.7, 5.4 Hz, 1H), 1.27 (t, *J* = 7.1 Hz, 3H), 1.19 (t, *J* = 7.1 Hz, 3H). ^{13}**C NMR** (101 MHz, $CDCl_3$): δ 169.4, 165.4, 143.1, 137.8 (q, J_{C-F} = 2.7 Hz), 129.1 (q, J_{C-F} = 3.6 Hz), 124.2, 113.0 (q, J_{C-F} = 38.4 Hz), 77.2, 61.5, 61.1, 59.5, 38.6, 14.3, 14.1. ^{19}**F NMR** (376 MHz, $CDCl_3$): δ -57.0. **HRMS** (ESI) calcd. for $[C_{14}H_{18}F_3N_2O]^+$ ([M+H]$^+$), m/z = 335.1213; found 335.1216.

Diethyl (*E*)-4-(5-methyl-2H-tetrazol-2-yl)hex-2-enedioate (152ba)

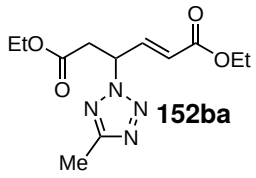

152ba

According to general procedure **4**: Diethyl (*E*)-hex-3-enedioate (**150j**) (601 mg, 3.00 mmol, 3.00 equiv.), 5-methyl-1H-tetrazole (**151t**) (84.0 mg, 1.00 mmol, 1.00 equiv.), TAPT (24.4 mg, 50.1 µmol, 5 mol%), $(PhSe)_2$ (31.4 mg, 101 µmol, 10 mol%), $(4\text{-ClPhS})_2$ (14.4 mg, 50.0 µmol, 5 mol%) and DCE, 21 h. Purification (PE/EtOAc, 88:12 to 62:38, Puriflash Advion) afforded **152ba** (154 mg, 547 µmol, 55%) as a slightly yellow oil. Crude NMR yield: 58%.

TLC: R_f = 0.29 (PE/EtOAc, 80:20) [UV, $KMnO_4$]. **IR** [cm^{-1}]: 2982, 2941, 1722, 1662, 1506, 1372, 1312, 1271, 1185, 1025, 977. ^{1}**H NMR** (400 MHz, $CDCl_3$): δ 7.01 (dd, J = 15.7, 6.7 Hz, 1H), 5.99–5.88 (m, 1H), 5.81 (dd, *J* = 15.7, 1.4 Hz, 1H), 4.33–3.97 (m, 4H), 3.34 (dd, *J* = 16.8, 8.3 Hz, 1H), 3.07 (dd, *J* = 16.8, 6.2 Hz, 1H), 2.53 (s, 3H), 1.26 (t, *J* = 7.1 Hz, 3H), 1.20 (t, *J* = 7.1 Hz, 3H). ^{13}**C NMR** (101 MHz, $CDCl_3$): δ 168.6, 165.1, 163.4, 141.2, 125.1, 61.6, 61.1, 60.4, 38.2, 14.2, 14.1, 11.1. **HRMS** (ESI) calcd. for $[C_{12}H_{19}N_4O_4]^+$ ([M+H]$^+$), m/z = 283.1401; found 283.1402.

Hydroxy byproduct: **Diethyl (*E*)-4-hydroxyhex-2-enedioate (186)**

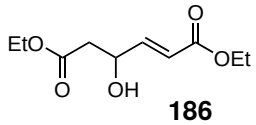

186

During purification, 25 mg of hydroxy-byproduct diethyl (*E*)-4-hydroxyhex-2-enedioate (**186**) were able to be isolated.

TLC: R_f = 0.26 (PE/EtOAc, 80:20) [UV, $KMnO_4$]. **IR** [cm^{-1}]: 3481, 2982, 2937, 1718, 1662, 1305, 1267, 1174, 1111, 1036. ^{1}**H NMR** (400 MHz, $CDCl_3$): δ 6.90 (dd, *J* = 15.6, 4.3 Hz, 1H), 6.13 (dd, *J* = 15.7, 1.8 Hz, 1H), 4.71 (dtd, *J* = 8.3, 3.9, 1.8 Hz, 1H), 4.19 (qd, *J* = 7.1, 4.9 Hz, 4H), 2.87 (bs, 1H), 2.65 (dd, *J* = 16.7, 3.7 Hz, 1H), 2.52 (dd, *J* 16.6, 8.7 Hz, 1H), 1.28 (td, *J* = 7.1, 4.2 Hz, 6H). ^{13}**C NMR** (101 MHz, $CDCl_3$): δ 172.0, 166.4, 147.3, 121.4, 67.3, 61.3, 60.7, 40.5, 14.4, 14.3. **HRMS** (APCI) calcd. for $[C_{10}H_{17}O_5]^+$ ([M+H]$^+$), m/z = 217.1070; found 217.1071.

Diethyl (*E*)-4-(5-phenyl-2H-tetrazol-2-yl)hex-2-enedioate (152bb)

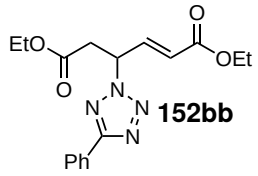

152bb

According to general procedure **4**: Diethyl (*E*)-hex-3-enedioate (**150j**) (600 mg, 3.00 mmol, 3.00 equiv.), 5-phenyl-1H-tetrazole (**151u**) (146 mg, 1.00 mmol, 1.00 equiv.), TAPT (24.3 mg, 50.0 µmol, 5 mol%), $(PhSe)_2$ (31.4 mg, 100 µmol, 10 mol%), $(4\text{-}ClPhS)_2$ (14.5 mg, 50.4 µmol, 5 mol%) and DCE, 21 h. Purification (PE/EtOAc, 96:4 to 62:38, Puriflash Advion) afforded **152bb** (220 mg, 639 µmol, 64%) as a lightly yellow oil. Crude NMR yield: 71%.

TLC: R_f = 0.35 (PE/EtOAc, 80:20) [UV]. **IR** [cm^{-1}]: 2982, 1722, 1662, 1450, 1372, 1316, 1271, 1185, 1025, 977, 734, 693. ^{1}**H NMR** (400 MHz, $CDCl_3$): δ δ 8.23–8.04 (m, 2H), 7.55–7.40 (m, 3H), 7.09 (dd, *J* = 15.7, 6.7 Hz, 1H), 6.05 (dtd, *J* = 8.1, 6.5, 1.4 Hz, 1H), 5.89 (dd, *J* = 15.7, 1.4 Hz, 1H), 4.26–4.06 (m, 4H), 3.44 (dd, *J* = 16.8, 8.3 Hz, 1H), 3.16 (dd, *J* = 16.8, 6.3 Hz, 1H), 1.27 (t, *J* = 7.1 Hz, 3H), 1.21 (t, *J* = 7.2 Hz, 3H). ^{13}**C NMR** (101 MHz, $CDCl_3$): δ 168.6, 165.5, 165.1, 141.1, 130.7, 129.0, 127.2, 127.1, 125.2, 61.7, 61.2, 60.8, 38.3, 14.3, 14.2. **HRMS** (ESI) calcd. for $[C_{17}H_{21}N_4O_4]^+$ ([M+H]$^+$), m/z = 345.1557; found 345.1562.

Diethyl (*E*)-4-(5-(p-tolyl)-1H-tetrazol-1-yl)hex-2-enedioate (152bc)

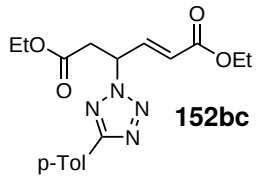

152bc

According to general procedure **4**: Diethyl (*E*)-hex-3-enedioate (**150j**) (601 mg, 3.00 mmol, 3.00 equiv.), 5-(p-tolyl)-1H-tetrazole (**151v**) (160 mg, 1.00 mmol, 1.00 equiv.), TAPT (24.5 mg, 50.4 µmol, 5 mol%), $(PhSe)_2$ (31.3 mg, 100 µmol, 10 mol%) and DCE, 21 h. Purification (PE/EtOAc, 90:10) afforded **152bc** (41.0 mg, 114 µmol, 11%) as a slightly yellow oil. Crude NMR yield: 20%.

According to general procedure **4**: Diethyl (*E*)-hex-3-enedioate (**150j**) (603 mg, 3.01 mmol, 3.00 equiv.), 5-(p-tolyl)-1H-tetrazole (**151v**) (161 mg, 1.01 mmol, 1.00 equiv.), TAPT (24.4 mg, 50.1 µmol, 5 mol%), $(PhSe)_2$ (31.3 mg, 100 µmol, 10 mol%), $(4\text{-}ClPhS)_2$ (14.4 mg, 50.1 µmol, 5 mol%) and DCE, 21 h. Purification (PE/EtOAc, 98:2 to 62:38, Puriflash Advion) afforded **152bc** (58.8 mg, 164 µmol, 16%) as a slightly yellow oil. Crude NMR yield: 19%.

TLC: R_f = 0.38 (PE/EtOAc, 80:20) [UV, $KMnO_4$]. **IR** [cm^{-1}]: 2982, 2937, 1722, 1465, 1372, 1316, 1271, 1185, 1021, 977, 831, 757. ^{1}**H NMR** (400 MHz, $CDCl_3$): δ 8.08–7.96 (m, 2H), 7.36–7.21 (m, 3H), 7.09 (dd, *J* = 15.7, 6.7 Hz, 1H), 6.04 (dtd, *J* = 8.1, 6.5, 1.4 Hz, 1H), 5.88 (dd, *J* = 15.7, 1.4 Hz, 1H), 4.25–4.05 (m, 4H), 3.43 (dd, *J* = 16.8, 8.3 Hz, 1H), 3.15 (dd, *J* = 16.8, 6.4 Hz, 1H), 2.41 (s, 3H), 1.27 (t, *J* = 7.1 Hz, 3H), 1.21 (t, *J* = 7.1 Hz, 3H). ^{13}**C NMR** (101 MHz, $CDCl_3$): δ 168.6, 165.6, 165.2, 141.2, 140.8, 129.7, 127.0, 125.2, 124.4, 61.6, 61.2, 60.7, 38.3, 21.6, 14.3, 14.2. **HRMS** (ESI) calcd. for $[C_{18}H_{23}N_4O_4]^+$ ([M+H]$^+$), m/z = 359.1714; found 359.1719.

Diethyl (E)-4-(1H-benzo[d][1,2,3]triazol-1-yl)hex-2-enedioate (152bf)

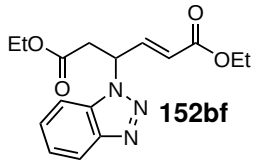

152bf

According to general procedure **4**: Diethyl (*E*)-hex-3-enedioate (**150j**) (202 mg, 1.01 mmol, 1.00 equiv.), 1H-benzo[d][1,2,3]triazole (**151b**) (358 mg, 3.01 mmol, 2.98 equiv.), TAPT (24.5 mg, 50.3 µmol, 5 mol%), $(PhSe)_2$ (31.2 mg, 100 µmol, 10 mol%) and DCE, 21 h. Purification (PE/EtOAc, 80:20) afforded **152bf** (242 mg, 763 µmol, 76%) as a slightly yellow oil. Crude ^{1}H NMR yield: 77%.

N2-isomer: **185b** (7.00 mg, 22.1 µmol, 2%) as a slightly yellow oil. Crude ^{1}H NMR yield: not detectable.

TLC: R_f = 0.13 (PE/EtOAc, 80:20) [UV, $KMnO_4$]. **IR** [cm^{-1}]: 3064, 2982, 2937, 1722, 1662, 1454, 1472, 1275, 1185, 1025, 749. ^{1}**H NMR** (300 MHz, $CDCl_3$): δ 8.08 (dt, *J* = 8.4, 1.0 Hz, 1H), 7.60–7.46 (m, 2H), 7.39 (ddd, *J* = 8.1, 6.3, 1.6 Hz, 1H), 7.14 (dd, *J* = 15.7, 6.0 Hz, 1H), 5.94 (dtd, *J* = 8.6, 6.0, 1.6 Hz, 1H), 5.72 (dd, *J* = 15.7, 1.5 Hz, 1H), 4.25–3.94 (m, 4H), 3.57 (dd, *J* = 16.8, 8.6 Hz, 1H), 3.24 (dd, *J* = 16.8, 6.0 Hz, 1H), 1.23 (t, *J* = 7.1 Hz, 3H), 1.14 (t, *J* = 7.1 Hz, 3H). ^{13}**C NMR** (101 MHz, $CDCl_3$): δ 169.3, 165.2, 146.0, 142.6, 132.8, 127.8, 124.3, 124.1, 120.2, 109.4, 61.4, 60.9, 55.9, 38.3, 14.1, 14.0. **HRMS** (APCI) calcd. for $[C_{16}H_{20}N_3O_4]^+$ ($[M+H]^+$), m/z = 318.1448; found 318.1450.

N2-Isomer: **Diethyl (*E*)-4-(2H-benzo[d][1,2,3]triazol-2-yl)hex-2-enedioate (185b)**

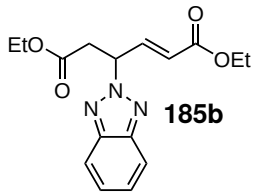

185b

TLC: R_f = 0.38, (PE/EtOAc, 80:20) [UV]. **IR** [cm^{-1}]: 3068, 2982, 2937, 1722, 1372, 1271, 1182, 1029, 977, 749. ^{1}**H NMR** (400 MHz, $CDCl_3$): δ 7.96–7.75 (m, 2H), 7.44–7.35 (m, 2H), 7.16 (dd, *J* = 15.7, 6.6 Hz, 1H), 6.07 (dtd, *J* = 8.1, 6.4, 1.4 Hz, 1H), 5.80 (dd, *J* = 15.7, 1.4 Hz, 1H), 4.24–4.03 (m, 4H), 3.54 (dd, *J* = 16.7, 8.4 Hz, 1H), 3.18 (dd, *J* = 16.7, 6.3 Hz, 1H), 1.25 (t, *J* = 7.1 Hz, 3H), 1.17 (t, *J* = 7.1 Hz, 3H). ^{13}**C NMR** (101 MHz, $CDCl_3$): δ 169.0, 165.3, 144.3, 142.5, 126.7, 124.3, 118.3, 63.3, 61.3, 60.9, 38.6, 14.1, 14.0. **HRMS** (ESI) calcd. for $[C_{16}H_{20}N_3O_4]^+$ ($[M+H]^+$), m/z = 318.1448; found 318.1449.

According to general procedure **4**: Diethyl (*E*)-hex-3-enedioate (**150j**) (602 mg, 3.01 mmol, 2.98 equiv.), 1H-benzo[d][1,2,3]triazole (**151a**) (120 mg, 1.01 mmol, 1.00 equiv.), TAPT (24.5 mg, 50.4 µmol, 5 mol%), $(PhSe)_2$ (31.4 mg, 101 µmol, 10 mol%) and DCE, 21 h. Purification (PE/EtOAc, 80:20) afforded **152bf** (174 mg, 548 µmol, 55%) as a slightly yellow oil. Crude ^{1}H NMR yield: 52%.

N2-isomer: **185b** (11.0 mg, 34.7 µmol, 3%) as a slightly yellow oil. Crude ^{1}H NMR yield: not detectable.

Diethyl (*E*)-4-((1S,3aS,3bR,5aS,10aS,10bS,12aS)-1-hydroxy-1,10a,12a-trimethyl-2,3,3a,3b,4,5,5a,6,10,10a,10b,11,12,12a-tetradecahydrocyclopenta[5,6]naphtho[1,2-f]indazol-7(1H)-yl)hex-2-enedioate (152bg, *N*1-isomer) and diethyl (*E*)-4-((1S,3aS,3bR,5aS,10aS,10bS,12aS)-1-hydroxy-1,10a,12a-trimethyl-2,3,3a,3b,4,5,5a,6,10,10a,10b,11,12,12a-tetradecahydrocyclopenta[5,6]naphtho[1,2-f]indazol-8(1H)-yl)hex-2-enedioate (152bg, *N*2-isomer)

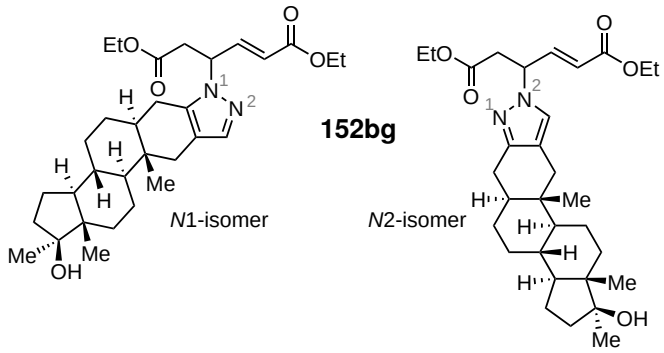

According to general procedure **4**: Diethyl (*E*)-hex-3-enedioate (**150j**) (600 mg, 3.00 mmol, 3.00 equiv.), Stanozolol (**151w**) (329 mg, 1.00 mmol, 1.00 equiv.), TAPT (24.3 mg, 50.0 µmol, 5 mol%), $(PhSe)_2$ (31.4 mg, 101 µmol, 10 mol%), $(4\text{-}ClPhS)_2$ (14.3 mg, 49.9 µmol, 5 mol%) and HFIP/DCE (2:3), 48 h. Two times purification (PE/EtOAc, 96:4 to 62:38, Puriflash Advion) afforded **152bg** in three fractions: Pure *N*2-isomer (187.6 mg, 356 µmol, 36%) as a slightly yellow oil. A *N*1/*N*2 mixture with ratio 1:1 (*N*2: 16.4 mg, 31.1 µmol, 3%; *N*1: 18.4 mg, 34.9 µmol, 4%) as a slightly yellow oil. And a *N*1/*N*2 mixture with ratio 6:1 (*N*2: 4.17 mg, 7.92 µmol, 1%; *N*1: 25.6 mg, 48.6 µmol, 5%) as a slightly yellow oil. Crude NMR yield: *N*2: 46%; *N*1: n.d..

***N*2-isomer**: **TLC**: R_f = 0.39 (DCM/MeCN, 10:1) [UV]. **IR** [cm^{-1}]: 3526, 2922, 2851, 2251, 1718, 1372, 1271, 1156, 1098, 1029, 910, 980, 727. ^{1}**H NMR** (400 MHz, $CDCl_3$): δ 7.08 (s, 1H), 7.02 (dd, *J* = 15.7, 6.0 Hz, 1H), 5.72 (ddd, *J* = 15.7, 4.4, 1.5 Hz, 1H), 5.34–5.16 (m, 1H), 4.22–3.95 (m, 4H), 3.15 (ddd, *J* = 16.3, 7.8, 3.6 Hz, 1H), 2.89 (ddd, *J* = 16.3, 6.6, 2.6 Hz, 1H), 2.68–2.49 (m, 2H), 2.32–2.17 (m, 1H), 2.05 (d, *J* = 15.2 Hz, 1H), 1.87–1.10 (m, 24H + H_2O), 0.95–0.76 (m, 5H), 0.72 (d, *J* = 7.4 Hz, 3H). ^{13}**C NMR** (101 MHz, $CDCl_3$): δ 169.9, 165.7, 148.6, 144.8, 126.7, 123.0, 115.5, 81.7, 61.0, 60.7, 58.5, 53.8, 50.6, 45.4, 42.5, 39.0, 38.8, 36.7, 36.3, 34.8, 31.7, 31.5, 29.3, 27.6, 25.8, 23.3, 20.8, 14.2, 14.1, 13.9, 11.5. **HRMS** (ESI) calcd. for $[C_{31}H_{47}N_2O_5]^+$ ($[M+H]^+$), m/z = 527.3479; found 527.3488.

***N*1-isomer (containing small amounts of *N*2-isomer)**: **TLC**: R_f = 0.26 (DCM/MeCN, 10:1) [UV]. **IR** [cm^{-1}]: 3511, 2922, 1722, 1659, 1446, 1372, 1308, 1271, 1182, 1029, 936, 731. ^{1}**H NMR** (400 MHz, $CDCl_3$): δ 7.28 (s, 1H), 7.12 (s, 0H), 7.09–6.88 (m, 1H), 5.75 (dd, *J* = 15.7, 4.3 Hz, 0H), 5.53 (ddt, *J* = 53.9, 15.6, 1.2 Hz, 1H), 5.35–5.10 (m, 1H), 4.25–3.96 (m, 4H), 3.35 (dt, *J* = 15.9, 9.3 Hz, 1H), 3.18 (dd, *J* = 16.4, 7.5 Hz, 0H), 2.92 (ddd, *J* = 16.6, 5.4, 2.8 Hz, 1H), 2.57 (ddd, *J* = 22.8, 15.7, 4.8 Hz, 2H), 2.43 (dd, *J* = 16.2, 5.0 Hz, 0H), 2.26 (dd, *J* = 16.3,

11.4 Hz, 1H), 2.15–1.97 (m, 2H), 1.90–1.10 (m, 24H + H_2O), 0.98–0.76 (m, 6H), 0.70 (s, 3H). ^{13}**C NMR** (101 MHz, $CDCl_3$): δ 170.2, 165.9, 145.0, 138.2, 137.7, 122.7, 115.4, 81.8, 77.5, 77.4, 77.2, 76.8, 61.1, 60.8, 55.1, 53.9, 50.7, 45.5, 42.3, 39.1, 38.2, 38.0, 36.7, 36.5, 35.1, 31.6, 29.8, 29.3, 25.9, 25.7, 23.4, 20.9, 14.3, 14.0, 11.5. **HRMS** (ESI) calcd. for $[C_{31}H_{47}N_2O_5]^+$ ($[M+H]^+$), m/z = 527.3479; found 527.3488 and 527.3489.

***N*-((2'-(2-((*E*)-1,6-diethoxy-1,6-dioxohex-4-en-3-yl)-2H-tetrazol-5-yl)-[1,1'-biphenyl]-4-yl)methyl)-*N*-pentanoyl-*D*-valine (152bi)

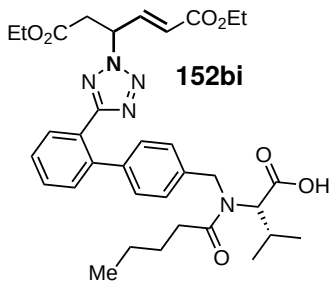

According to general procedure **4**: Ethyl (*E*)-hex-3-enoate (**150a**) (603 mg, 3.01 mmol, 3.00 equiv.), *N*-((2'-(1H-tetrazol-5-yl)-[1,1'-biphenyl]-4-yl)methyl)-*N*-pentanoyl-*L*-valine (Valsartan) (**151x**) (425 mg, 1.00 mmol, 1.00 equiv.), TAPT (24.3 mg, 50.0 µmol, 5 mol%), $(PhSe)_2$ (31.4 mg, 101 µmol, 10 mol%), 1,2-bis(4-chlorophenyl)disulfane (14.3 mg, 49.8 µmol, 5 mol%) and DCE, 21 h. Purification (PE/EtOAc, 95:5 to 0:100 EtOAc with Puriflash Advion) did not afford the desired product **152bi**. Crude NMR yield: 42%.

5.8 Enantioselective Intermolecular Allylic Amination with Azoles

5.8.1 Optimisation of the Amination of Ethyl (*E*)-hex-3-enoate 150a

General Procedure 5

Into a 40 mL vial were added ethyl (*E*)-hex-3-enoate (**150a**), 4-chloropyrazole (**151a**), chiral Se-catalyst **136**, photocatalyst (**86**) and further additives, if stated. DCE was added and the vial was sealed with a screw cap including a septum and equipped with two cannulas, leaving the mixture open to air. The reaction was performed in a temperature-controlled metal block by irradiation with blue light (λ_{max} = 448 nm) with a stirring speed of 400–550 rpm. When the reaction was stopped, the mixture was transferred into a round bottom flask using DCM and the solvent was removed under reduced pressure. To the dried reaction mixture, 10-25 mg of the internal standard 1,4-dimethoxybenzene (DMB) was added and the mixture was dissolved in $CDCl_3$ (1-2 mL), homogenised in an ultrasonic bath and then withdrawn for quantitative ^{1}H NMR analysis.

Table 5.28: Optimisation of the Enantioselective Intermolecular Allyic Amination of Ethyl (*E*)-hex-3-enoate **150a**.[a]

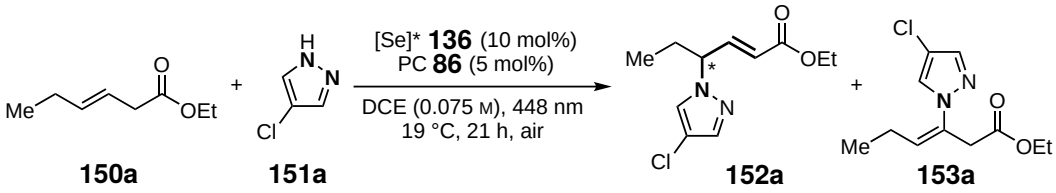

150a **151a** **152a** **153a**

Entry	Comment	[Se]* **136**	Conv.[b] [%]	Yield[b] [%]		*ee*
				152a	**153a**	
1	10 mol% **86**	**136b**	93	24 (21)	3	33
2	10 mol% **86**	**136a**	87	22 (25)	1	32
3	-	**136a**	91	20 (12)	2	31
4	-	**136c**	100	13	1	40
5	20 mol% **136**	**136d**	100	40	6	43
6	-	**136e**	100	44	4	25
7	5 mol% **136**, no **86**	**136f**	27	3	1	n.d.
8	10 mol% **86**, 2.5 mol% $Sc(OTf)_3$	**136a**	100	23	0	31
9	10 mol% **86**, 10 mol% $Sc(OTf)_3$	**136a**	100	26	0	37
10	10 mol% **86**, 2.5 mol% $Zn(OTf)_2$	**136a**	100	22	0	30
11	5 mol% $(4\text{-ClPhS})_2$	**136a**	100	22	2	26
12	0.2 M	**136a**	100	18	0	30
13	Reaction at -3 °C.	**136a**	100	15	1	22
14	0.3 mmol **150a**, 3.0 equiv. **151a**	**136a**	70	18	3	n.d.
15	Benzyl (*E*)-hex-3-enoate instead of **150a**	**136a**	100	47	3	25
16	Acetone as Solvent	**136a**	45	4	0	n.d.
17	MeCN as Solvent	**136a**	67	15	2	n.d.
18	Toluene as Solvent	**136a**	58	6	0	n.d.
19	*o*-Xylene as Solvent	**136a**	86	6	0	n.d.

[a]0.30 mmol (1.0 equiv.) of **151a**, 3.0 equiv. of **150a**. Isolated yields in parentheses. Se-catalyst purity $\geq$ 99%. [b]Conversions and NMR yields were determined with DMB as the internal standard. n.d. = not determined.

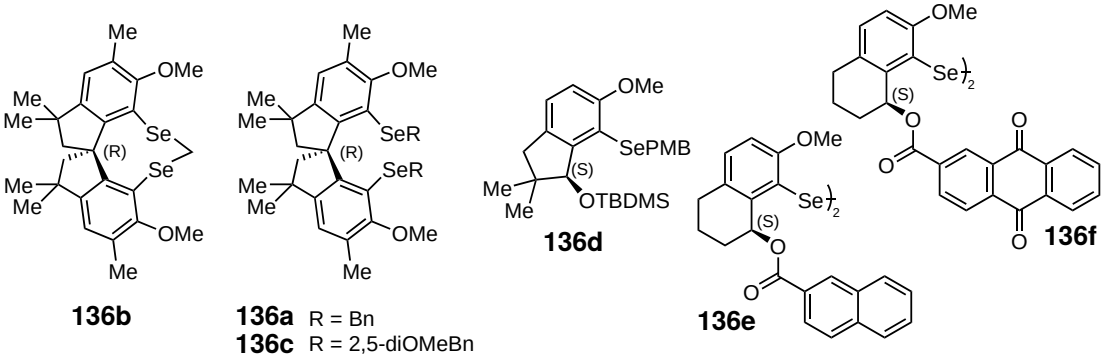

Kinetic Investigation

Table 5.29: Kinetic Investigation of the Asymmetric Amination of Ethyl (*E*)-hex-3-enoate **150a**.[a]

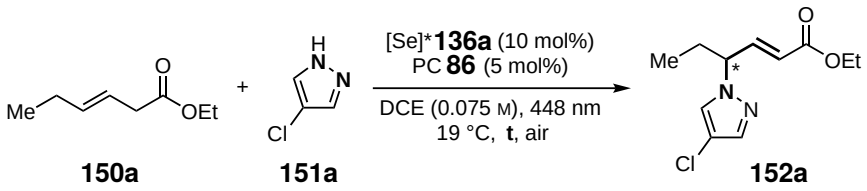

	Entry	t [h]	Conversion[b] [%]	Yield[b] [%]	*ee*
3 equiv. of **150a**	1	2	58	6	n.d.
	2	4	63	9	n.d.
	3	6	71	11	n.d.
	4	8	75	13	n.d.
	5	21	91	20	31
	6	27.5	100	21	n.d.
3 equiv. of **151a**	7	2	n.d.	3	n.d.
	8	4	75	6	n.d.
	9	6	74	12	n.d.
	10	21	77	20	25
	11	27.5	100	19	n.d.
5 equiv. of **151a**	12	2	54	4	n.d.
	13	4	50	7	n.d.
	14	6	81	10	n.d.
	15	21	85	11	n.d.

[a]0.30 mmol of limiting compound. [b]Conversions and NMR yields were determined with DMB as the internal standard. n.d. = not determined.

5.8.2 Optimisation of the Amination of Diethyl (*E*)-hex-3-enedioate (150j)

General Procedure 6

Into a 40 mL vial were added diethyl (*E*)-hex-3-enedioate (**150j**), 4-chloropyrazole (**151a**), chiral Se-catalyst **136**, photocatalyst (**86**) and further additives, if stated. DCE was added and the vial was sealed with a screw cap including a septum and equipped with two cannulas, leaving the mixture open to air. The reaction was performed in a temperature-controlled metal block by irradiation with blue light (λ_{max} = 448 nm) with a stirring speed of 400–550 rpm. When the reaction was stopped, the mixture was transferred into a round bottom flask using DCM and the solvent was removed under reduced pressure. To the dried reaction mixture, 10-25 mg of the internal standard 1,4-dimethoxybenzene (DMB) was added and the mixture was dissolved in $CDCl_3$ (1-2 mL), homogenised in an ultrasonic bath and then withdrawn for quantitative ^{1}H NMR analysis. Further purification *via* column chromatography afforded the target compound. The enantiomeric excess (*ee*) of product **152** was determined *via* chiral HPLC-analysis.

Table 5.30: Catalyst Screening in the Enantioselective Intermolecular Allyic Amination of Diethyl (*E*)-hex-3-enedioate (**150j**).[a]

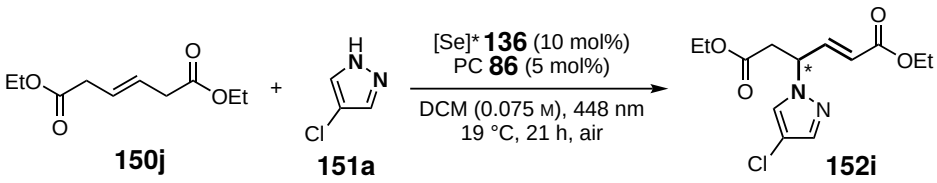

Entry	Comment	[Se]* **136**	Conversion[b] [%]	Yield[b] [%]	*ee*
1	-	**136b**	>78	42	72
2	-	**136b**[c]	61	35	75
3	20 mol% **136**	**136b**[c]	86	30	84
4	-	**136a**	89	44	67
5	-	**136c**	75	29	78
6	20 mol% **136**	**136g**[d]	100	64	-26
7	20 mol% **136**	**136h**	100	64	-52
8		**136i**[e]	100	75	35
9	-	**136e**	100	70	32
10		**136j**	100	66	21
11		**136k**	100	71	-10

[a] 0.30 mmol (1.0 equiv.) of **151a**, 3.0 equiv. of **150j**. Se-catalyst purity $\geq$ 99%, unless otherwise noted. [b] Conversions and NMR yields were determined with DMB as the internal standard. [c] Newly synthesised Se-catalyst **136b**. [d] 80-90% *ee*. [e] 98% *ee*.

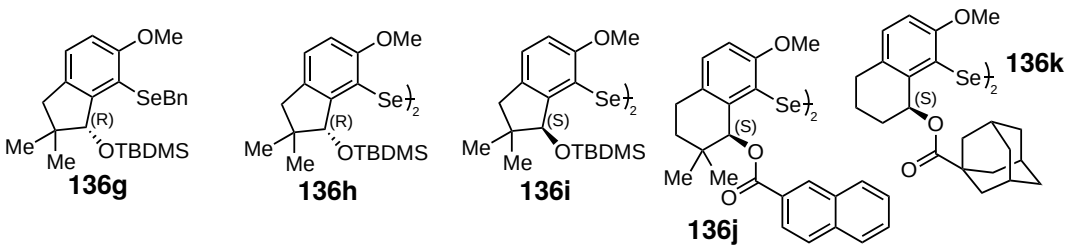

Table 5.31: Solvent Variation in the Enantioselective Intermolecular Allyic Amination of Diethyl (*E*)-hex-3-enedioate (**150j**).[a]

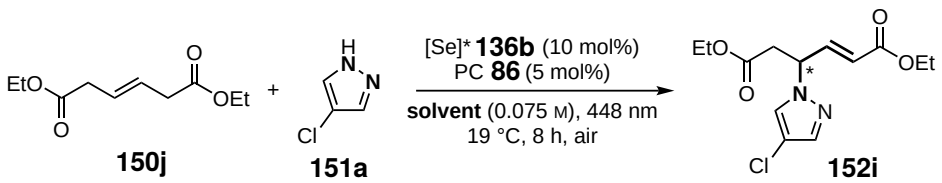

Entry	Solvent	Conversion[b] [%]	Yield[b] [%]	*ee*
1	MeCN	30	14	84
2	EtOAc	8	0	n.d.
3	Toluene	18	2	n.d.
4	THF[c]	38	0	n.d.
5	DCE	66	32	78
6[d]	DCE	66	32 (30)	84
7[d]	Acetone	54	7	84
8[d]	HFIP	24	< 6	n.d.
9[d]	$CHCl_3$	51	17	79

[a] 0.30 mmol of **151a**, 3.00 equiv. of **150j**. Isolated yields in parentheses. [b] Conversions and NMR yields were determined with DMB as the internal standard. [c] Distilled prior to use. [d] Newly synthesised Se-catalyst **136b**. n.d. = not determined.

Table 5.32: Additive Variation in the Enantioselective Intermolecular Allyic Amination of Diethyl (*E*)-hex-3-enedioate (**150j**).[a]

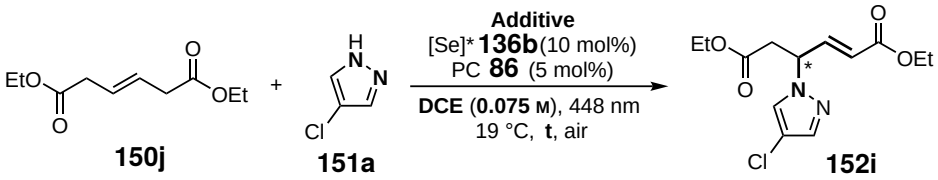

Entry	Additive	solvent	t [h]	Conv.[b] [%]	Yield[b] [%]	*ee*
1	5 mol% $(4\text{-ClPhS})_2$	MeCN	8	56	27	87
2	5 mol% $(4\text{-ClPhS})_2$	MeCN	21	77	35	74
3	10 mol% $(4\text{-ClPhS})_2$	MeCN	8	74	28	85
4	5 mol% $(4\text{-ClPhS})_2$	DCE	8	81	33	82
5[c]	5 mol% $(4\text{-ClPhS})_2$	DCE	21	83	35	83
6	10 mol% $(4\text{-ClPhS})_2$	DCE	8	73	29	82
7	20 mol% $(4\text{-ClPhS})_2$	DCE	8	86	24	80
8	5 mol% $(^t\text{BuS})_2$	DCE	8	71	33	83
9	5mol% $(4\text{-OMePhS})_2$	DCE	8	78	26	82
10	1.00 equiv. Me_6Si_2	DCE	8	35	0	n.d.
11	10 mol% $Sc(OTf)_3$	DCE	8	70	30	74
12	10 mol% $ZnCl_2$	DCE	8	51	23	83
13	10 mol% $ZnCl_2$[d]	DCE	8	49	20	78
14	1.00 equiv. SiO_2	DCE	8	59	30	86
15	1.00 equiv. AcOH, 5 mol% $4\text{-}(ClPhS)_2$	DCE	8	68	31	80

[a] 0.30 mmol of **151a**, 3.00 equiv. of **150j**. Isolated yields in parentheses. Newly synthesised Se-catalyst **136b** used. [b] Conversions and NMR yields were determined with DMB as the internal standard. [c] 20 mol% **136b**. [d] 1.9 M in MeTHF. n.d. = not determined.

Table 5.33: Further Optimisation of the Enantioselective Intermolecular Allyic Amination of Diethyl (*E*)-hex-3-enedioate (**150j**).[a]

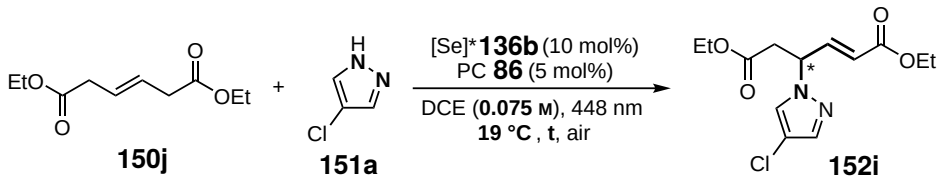

Entry	Comment	solvent	t [h]	Conv.[b] [%]	Yield[b] [%]	*ee*
1	0.15 M	DCE	8	57	26	83
2	0.0375 M	DCE	8	51	20	84
3	0 °C.	DCE	8	56	26	86
4	55 °C.	DCE	8	73	35	43
5[c]	reversed stoichiometry	DCE	8	34	19	76
6	Reduced O_2-concentration	DCE	8	61	30	78
6[e]	1H-benzo[d][1,2,3]triazole **151b** instead of **151a**	DCE	7	62	31 (27)	80
8[d,e]	1 mmol 1H-benzo[d][1,2,3]triazole **151b** instead of **151a**	DCE	8	33	17	n.d.
9[d,e]	1 mmol 1H-benzo[d][1,2,3]triazole **151b** instead of **151a**	DCE	21	38	29 (24)	84
10	1 mmol **151a**	DCE	21	61	31 (29)	82

[a] 0.30 mmol of **151a**, 3.0 equiv. of **150j**. Isolated yields in parentheses. Newly synthesised Se-catalyst **136b** used. [b] Conversions and NMR yields were determined with DMB as the internal standard. [c] 0.30 mmol of **150j**, 3.0 equiv. of **151a**. [d] 1.00 mmol of **151b**, 3.00 equiv. of **150j**. [e] 0.2 M. n.d. = not determined.

Table 5.34: Variation in Catalyst Loading and Second Addition in the Enantioselective Intermolecular Allyic Amination of Diethyl (*E*)-hex-3-enedioate (**150j**).[a]

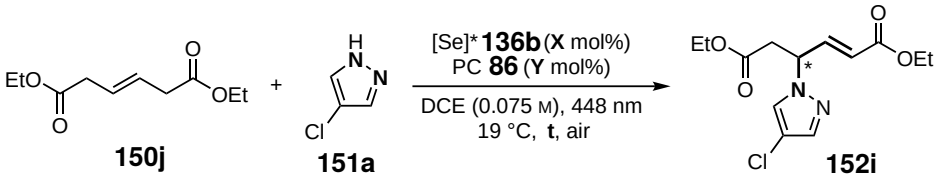

Entry	**X** [mol%]	**Y** [mol%]	t [h]	Conv.[b] [%]	Yield[b] [%]	*ee*
1	5	5	8	45	17	75
2	10	5	8	66	32 (30)	84
3	20	5	8	74	29	87
4	10	2.5	8	57	34	83
5	10	10	8	59	28	86
6	20	10	8	77	23	87
7[c]	10	5	21	85	38	83
8[d]	10	5	21	73	43	71
9[e]	10	5	21	82	35	83

[a] 0.30 mmol of **151a**, 3.00 equiv. of **150j**. Isolated yields in parentheses. Newly synthesised Se-catalyst **136b** used. [b] Conversions and NMR yields were determined with DMB as the internal standard. [c] Second addition of 10 mol% **136b** and 5 mol% **86** after 6 h. [d] Second addition of 5 mol% **86** after 6 h. [e] Second addition of 10 mol% **136b** after 6 h.

Kinetic Investigation

Table 5.35: Kinetic Investigation of the Asymmetric Amination of Diethyl (*E*)-hex-3-enedioate **150j** with Catalysts **136a** and **136c**.[a]

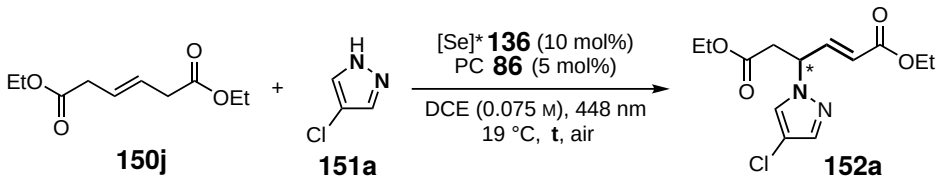

	136b					136c			
Entry	t [h]	Conv.[b] [%]	Yield[b] [%]	*ee*	Entry	t [h]	Conv.[b] [%]	Yield[b] [%]	*ee*
1	2	38	8	84	6	2	34	3	n.d.
2	4	57	19	n.d.	7	4	55	10	86
3	6	62	23	78	8	6	69	22	n.d.
4	8	66	32	78	9	8	70	22	86
5	21	>78	42	72	10	21	75	29	78

[a] 3.0 equiv. of **150j**, 0.30 mmol, (1.0 equiv.) of **151a**. [b] Conversions and NMR yields were determined with DMB as the internal standard. n.d. = not determined.

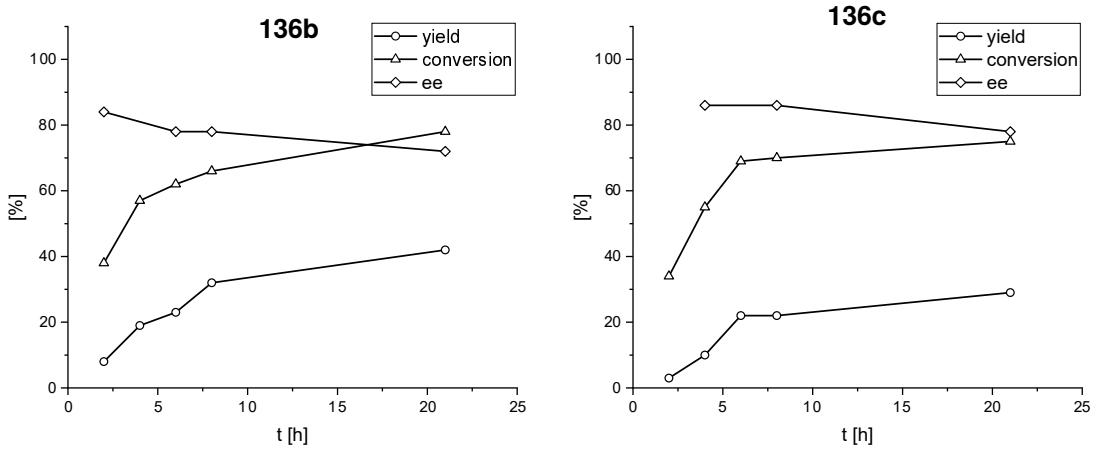

5.8.3 Enantioselective Synthesis of Allylic Azoles and Azines

General Procedure 7

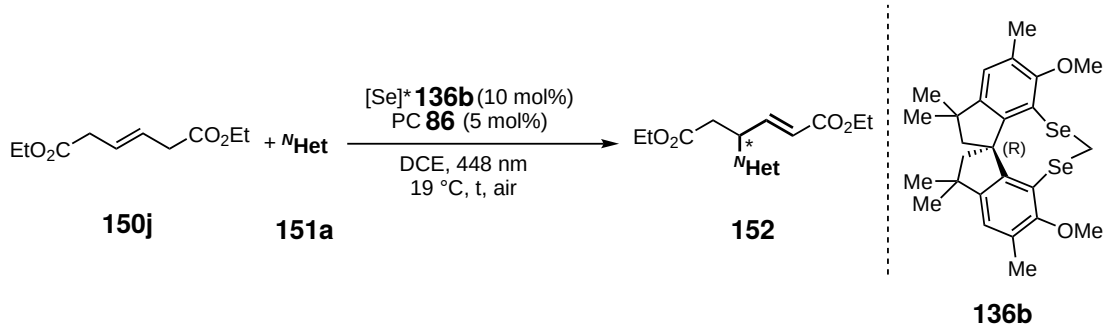

150j **151a** **152** **136b**

Into a 100 mL round bottom flask were added alkene (**150**), amine (**151**), **136b** (10 mol%), photocatalyst **86** (5 mol%) and DCE. The flask was sealed with a septum including two cannulas, leaving it open to air. The reaction mixture was then vigorously stirred at 19 °C under irradiation with blue light (λ_{max} = 448 nm) for the given time in a temperature-controlled metal block. After reaction, the solvent was removed under reduced pressure. The NMR yield of the allylic product **152** was determined with internal standard 1,4-dimethoxybenzene (DMB). Further purification *via* column chromatography afforded the target compound. The enantiomeric excess (*ee*) of product **152** was determined *via* chiral HPLC-analysis.

Diethyl (*E*)-4-(4-chloro-1H-pyrazol-1-yl)hex-2-enedioate (152i)

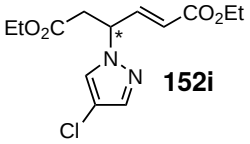

152i

According to general procedure **6**: 40 mL vial, diethyl (*E*)-hex-3-enedioate (**150j**) (182 mg, 909 µmol, 3.03 equiv.), 4-chloro-1H-pyrazole (**151a**) (30.8 mg, 300 µmol, 1.00 equiv.), **86** (7.36 mg, 15.1 µmol, 5 mol%), **136b** (16.1 mg, 30.1 µmol, 10 mol%) and DCE (4 mL), 8 h. Purification (PE/EtOAc, 9:1), afforded **152i** (22.0 mg, 90.7 µmol, 30%, 84% *ee*) as a colourless oil (crude ^{1}H NMR yield: 32%).

HPLC: t_R = 29.805 min (minor), 31.770 min (major) [IC-3, hexane/^{i}PrOH = 90:10, flow rate 0.5 ml/min, 25 °C].

According to general procedure **7**: 100 mL round bottom flask, diethyl (*E*)-hex-3-enedioate (**150j**) (601 mg, 3.00 mmol, 3.00 equiv.), 4-chloro-1H-pyrazole (**151a**) (103 mg, 1.00 mmol, 1.00 equiv.), **86** (24.3 mg, 50.0 µmol, 5 mol%), **136b** (53.5 mg, 100 µmol, 10 mol%) and DCE (5 mL), 21 h. Purification (PE/EtOAc, 9:1), afforded **152i** (85.9 mg, 286 µmol, 29%, 82% *ee*) as a lightly yellow oil (crude ^{1}H NMR yield: 31%).

HPLC: t_R = 30.522 min (minor), 32.470 min (major). [IC-3, hexane/^{i}PrOH = 90:10, flow rate 0.5 ml/min, 25 °C]. **Optical rotation**: $[\alpha]_D^{25}$ = -13.6 (*c* 0.95, $CHCl_3$).

Diethyl (E)-4-(1H-benzo[d][1,2,3]triazol-1-yl)hex-2-enedioate (152bf)

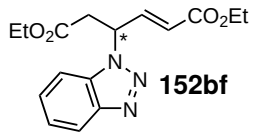

According to general procedure **6**: 40 mL vial, diethyl (*E*)-hex-3-enedioate (**150j**) (181 mg, 904 µmol, 3.00 equiv.), 1H-benzo[d][1,2,3]triazole (**151b**) (35.9 mg, 301 µmol, 1.00 equiv.), **86** (7.35 mg, 15.1 µmol, 5 mol%), **136b** (16.1 mg, 30.0 µmol, 10 mol%) and DCE (4 mL), 8 h. Purification (PE/EtOAc, 9:1 to 8:2), afforded **152bf** (26.0 mg, 81.9 µmol, 27%, 80% *ee*) as a slightly yellow oil (crude ^{1}H NMR yield: 31%).

HPLC: t_R = 15.885 min (minor), 18.719 min (major) [IB-3, hexane/^{i}PrOH = 90:10, flow rate 0.8 ml/min, 25 °C].

According to general procedure **7**: 100 mL round bottom flask, diethyl (*E*)-hex-3-enedioate (**150j**) (601 mg, 3.00 mmol, 3.00 equiv.), 1H-benzo[d][1,2,3]triazole (**151b**) (119 mg, 1.00 mmol, 1.00 equiv.), **86** (24.3 mg, 50.0 µmol, 5 mol%), **136b** (53.5 mg, 100 µmol, 10 mol%) and DCE (5 mL), 21 h. Purification (PE/EtOAc, 9:1 to 8:2), afforded **152i** (75.0 mg, 236 µmol, 24%, 84% *ee*) as a lightly yellow oil (crude ^{1}H NMR yield: 29%).

HPLC: t_R = 15.817 min (minor), 18.540 min (major). [IB-3, hexane/^{i}PrOH = 90:10, flow rate 0.8 ml/min, 25 °C]. **Optical rotation**: $[\alpha]_D^{25}$ = 2.74 (*c* 0.95, $CHCl_3$).

5.9 Asymmetric Counderanion Directed Catalysis (ACDC)

5.9.1 Synthesis of Photosensitiser with Chiral Counterions

(Z)-1,3,5-tris(4-methoxyphenyl)pent-2-ene-1,5-dione (179)[226]

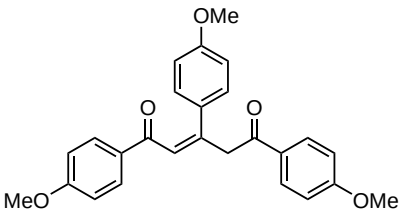

179

Conducted by Dr. T. Lei: To to a suspension of 2,4,6-tris(4-methoxyphenyl)pyrylium tetrafluoroborate (**86**, 1.46 g, 3.00 mmol, 1.00 equiv.) and basic Al_2O_3 (1.53 g, 15.0 mmol, 5.00 equiv.) in 20 mL EtOH, NaAc (1.48 g, 18.0 mmol, 6.00 equiv.) in 7.5 mL H_2O was added. The mixture was stirred at 75 °C for 23 h, before it was allowed to cool to r.t.. The remaining solid was filtered and washed with DCM. Then, the solvent of the filtrate was removed under reduced pressure and the residue was again dissolved in DCM and H_2O. The phases were separated and the aqueous phase was extracted with DCM. The combined organic phases were washed with H_2O, before the solvent was removed under reduced pressure. The residue was purified via column chromatography (pentane/EtOAc, 30:1) affording **179** (1.11 g, 2.65 mmol, 88%) as a yellow oil, which later solidified into a dark orange solid.

TLC: R_f = 0.29 (PE/EtOAc, 3:1) [UV]. **M.p.** = 39.5 °C. **IR** [cm^{-1}]: 3056, 3004, 2960, 2840, 2356, 1677, 1603, 1513, 1424, 1316, 1260, 1029, 1170, 831. ^{1}**H NMR** (400 MHz, $CDCl_3$): δ 8.08–8.02 (m, 2H), 8.01–7.94 (m, 2H), 7.54–7.46 (m, 2H), 7.39 (s, 1H), 6.98–6.86 (m, 6H), 4.83 (s, 2H), 3.87 (d, *J* = 3.5 Hz, 6H), 3.83 (s, 3H). ^{13}**C NMR** (101 MHz, $CDCl_3$): δ 195.2, 189.6, 163.6, 163.3, 160.7, 151.8, 134.4, 132.5, 130.7, 130.7, 130.3, 128.4, 122.0, 114.2, 113.9, 113.8, 55.6, 55.6, 55.5, 42.4. **HRMS** (ESI) calcd. for $[C_{26}H_{25}O_5]^+$ ([M+H]$^+$), m/z = 417.1697; found 417.1700.

2,4,6-tris(4-methoxyphenyl)pyrylium (2s,11bS)-2,6-bis(2,4,6-triisopropylphenyl)dinaphtho[2,1-d:1',2'-f][1,3,2]dioxaphosphepin-4-olate 4-oxide (180a)[226]

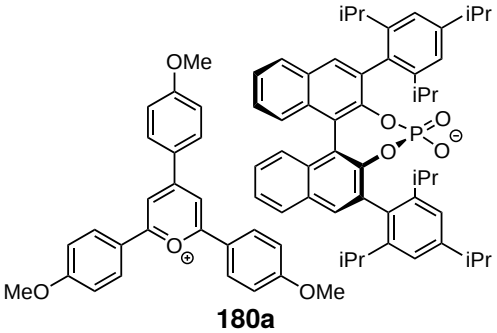

180a

Into a 50 mL round bottom flask were added **179** (62.5 mg, 150 µmol, 1.00 equiv.), (2s,4R,11bS)-4-hydroxy-2,6-bis(2,4,6-triisopropylphenyl)dinaphtho[2,1-d:1',2'-f][1,3,2]dioxaphosphepine 4-oxide ((S)-TRIP) (113 mg, 150 µmol, 1.0 equiv.) and 2 mL EtOH. The resulting mixture was heated to 60 °C, upon which the starting materials dissolved, and stirred for 4 h. Then, the solution was cooled to r.t. and continued to stir for 3 h, before the solvent was

removed under reduced pressure. The residual dark red solid was dissolved in acetone (1 mL) and the product was precipitated by addition of hexane (50 mL). The flask was stored in the fridge for 1 h, before the precipitated was filtered off and washed with hexane. The resulting solid was dried on vacuum affording **180a** (36.0 mg, 31.3 µmol, 21%, 95.3% purity) as a red solid including 4.7% of starting material **179** (sm).

IR [cm^{-1}]: 2960, 2870, 1588, 1513, 1241, 1178, 1092, 1021, 906, 835, 727. **^{1}H NMR** (400 MHz, $CDCl_3$): δ 8.46 (s, 2H), 8.23 (d, *J* = 8.7 Hz, 2H), 8.16 (d, *J* = 8.5 Hz, 4H), 7.88 (d, *J* = 8.1 Hz, 2H), 7.82 (s, 2H), 7.47–7.27 (m, 6H), 6.88 (d, *J* = 1.7 Hz, 2H), 6.84–6.79 (m, 2H), 6.69 (d, *J* = 8.5 Hz, 4H), 6.27 (d, *J* = 8.4 Hz, 2H), 3.60 (s, 6H), 3.34 (s, 3H), 3.13 (s, 2H), 2.81 (quint., *J* = 6.8 Hz, 2H), 2.59 (quint., *J* = 7.0 Hz, 2H), 1.19–0.83 (m, 36H). **^{13}C NMR** (151 MHz, $CDCl_3$): δ 195.2 (sm), 189.5 (sm), 166.7, 165.4, 164.3, 163.6 (sm), 163.3 (sm), 161.8, 160.7 (sm), 151.8 (sm), 148.1, 147.4, 147.0, 134.4 (sm), 133.8, 133.6, 133.1, 132.5 (sm), 132.2, 131.8, 130.7 (sm), 130.7 (sm), 130.6, 130.3 (sm), 130.3, 128.4 (sm), 128.1, 127.5, 125.5, 124.5, 123.6, 123.1, 122.0 (sm), 121.2, 121.0, 120.1, 115.4, 115.3, 114.2 (sm), 113.9 (sm), 113.8 (sm), 110.5, 55.6, 55.6 (sm), 55.5 (sm), 55.4, 42.4 (sm), 34.1, 30.9, 30.9, 30.8, 26.5, 25.0, 24.0, 23.8, 23.7, 23.6. **^{31}P NMR** (162 MHz, $CDCl_3$): δ 4.6. **HRMS** (ESI) calcd. for $[C_{26}H_{23}O_4]^+$ ([M − (S)-TRIP$^-$]$^+$), m/z = 399.1591; found 399.1594; calcd. for $[C_{50}H_{56}O_4P]^-$ ([M − TAP$^+$]$^-$), m/z = 751.3922; found 751.3923.

2,4,6-tris(4-methoxyphenyl)pyrylium (2r,11cS)-2,6-bis(2,4,6-triisopropylphenyl)dinaphtho[2,1-d:1',2'-f][1,3,2]dioxaphosphepin-4-olate 4-oxide (180b)[226]

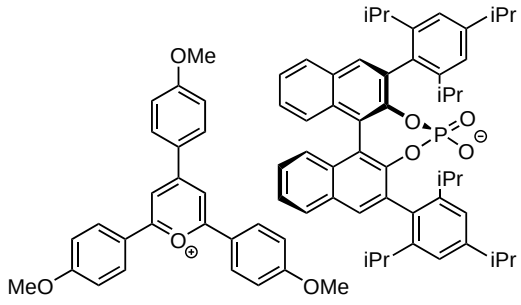

180b

Into a round bottom flask were added **179** (62.5 mg, 150 µmol, 1.00 equiv.), (2r,4R,11cS)-4-hydroxy-2,6-bis(2,4,6-triisopropylphenyl)dinaphtho[2,1-d:1',2'-f][1,3,2]dioxaphosphepine 4-oxide ((R)-TRIP) (113 mg, 150 µmol, 1.00 equiv.) and 2 mL EtOH. The resulting mixture was heated to 60 °C, upon which the starting materials dissolved, and stirred for 4 h. Then, the solution was cooled to r.t. and continued to stir for 2 h and 20 min, before the solvent was removed under reduced pressure. The residual dark red solid was dissolved in acetone (1 mL) and the product was precipitated by addition of hexane (50 mL). The flask was stored in the fridge for 1 h, before the precipitated was filtered off and washed with hexane. The resulting solid was dried on vacuum affording **180b** (32.0 mg, 27.8 µmol, 19%, 94.4% purity) as a red solid including 5.6% of starting material **179** (sm).

IR [cm^{-1}]: 3056, 2960, 2870, 1588, 1513, 1245, 1178, 1025, 910, 835, 731. **^{1}H NMR** (400 MHz, $CDCl_3$): δ 8.47 (s, 2H), 8.23 (d, *J* = 8.8 Hz, 2H), 8.16 (d, *J* = 8.6 Hz, 4H), 7.88 (d, *J* = 8.1 Hz, 2H), 7.82 (s, 2H), 7.48–7.25 (m, 6H), 6.88 (d, *J* = 1.7 Hz, 2H), 6.84 (s, 2H), 6.71 (d, *J* = 8.6 Hz,

4H), 6.30 (d, *J* = 8.5 Hz, 2H), 3.61 (s, 6H), 3.35 (s, 3H), 3.07 (s, 2H), 2.88–2.71 (m, 2H), 2.61 (d, *J* = 7.1 Hz, 2H), 1.17–0.81 (m, 36H). **^{13}C NMR** (151 MHz, $CDCl_3$): δ 195.2 (sm), 189.6 (sm), 166.8, 165.5, 164.4, 163.6 (sm), 163.3 (sm), 161.9, 160.7 (sm), 151.8 (sm), 148.1, 147.6, 147.1, 134.4 (sm), 133.5, 133.0, 132.5 (sm), 132.3, 132.0, 130.7 (sm), 130.7 (sm), 130.6, 130.4, 130.3 (sm), 128.4 (sm), 128.1, 127.5, 125.7, 124.7, 123.6, 122.9, 122.0 (sm), 121.3, 121.0, 120.1, 115.5, 115.4, 114.2 (sm), 113.9 (sm), 113.8 (sm), 113.5, 110.5, 55.7, 55.6 (sm), 55.6 (sm), 55.5, 55.5 (sm), 55.5, 42.4 (sm), 34.2, 30.9, 26.6, 25.1, 24.1, 23.8, 23.7, 23.4. **^{31}P NMR** (162 MHz, $CDCl_3$): δ 4.5. **HRMS** (ESI) calcd. for $[C_{26}H_{23}O_4]^+$ ([M − (R)-TRIP$^-$]$^+$), m/z = 399.1591; found 399.1594; calcd. for $[C_{50}H_{56}O_4P]^-$ ([M − TAP$^+$]$^-$), m/z = 751.3922; found 751.3921.

2,4,6-tris(4-methoxyphenyl)pyrylium ((1S,4R)-7,7-dimethyl-2-oxobicyclo[2.2.1]heptan- 1-yl)methanesulfonate (180c)[226]

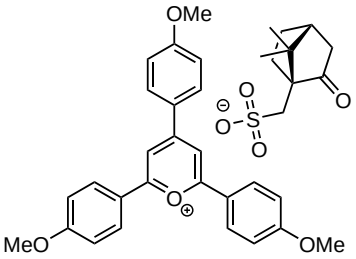

180c

Conducted by Dr. T. Lei: Into a round bottom flask were added **179** (83.3 mg, 200 µmol, 1.00 equiv.), ((1S,4R)-7,7-dimethyl-2-oxobicyclo[2.2.1]heptan-1-yl)methanesulfonic acid ((S)-CSA) (46.5 mg, 200 µmol, 1.00 equiv.) and 2 mL EtOH. The resulting mixture was heated to 60 °C and stirred for 3 h, before the solvent was removed under reduced pressure. The residue was dissolved in 2 mL MeOH and extracted with hexane (5 × 2 mL). As the MeOH-phase still contained some impurity (verified via TLC), it was added dropwise into 50 mL Et_2O. The formed precipitated was filtered, washed with Et_2O and dried on vacuum, affording **180c** (100 mg, 159 mmol, 79%) as a red solid.

M.p. = 235.7 °C. **IR** [cm^{-1}]: 3444, 3083, 2952, 2844, 1737, 1588, 1513, 1487, 1312, 1245, 1178, 1126, 1036, 835. **^{1}H NMR** (400 MHz, $CDCl_3$): δ 8.59–8.44 (m, 4H), 8.23 (d, *J* = 8.9 Hz, 4H), 6.99 (d, *J* = 9.0 Hz, 3H), 6.94 (d, *J* = 8.9 Hz, 2H), 3.87 (s, 6H), 3.81 (s, 3H), 3.62 (d, *J* = 14.7 Hz, 1H), 3.17–2.96 (m, 2H), 2.38 (dt, *J* = 18.1, 4.0 Hz, 1H), 2.17–2.02 (m, 2H), 1.80 (ddd, *J* = 14.3, 9.8, 4.6 Hz, 1H), 1.45–1.33 (m, 1H), 1.30 (s, 3H), 0.94 (s, 3H). **^{13}C NMR** (101 MHz, $CDCl_3$): δ 217.6, 167.0, 165.8, 164.7, 161.9, 133.6, 130.6, 124.1, 121.0, 115.7, 115.6, 110.5, 59.1, 55.8, 48.1, 47.5, 43.3, 42.9, 27.4, 25.0, 20.6, 20.2. **HRMS** (ESI) calcd. for $[C_{26}H_{23}O_4]^+$ ([M-CSA$^-$]$^+$), m/z = 399.1591 ; found 399.1595.

2,4,6-tris(4-methoxyphenyl)pyrylium ((1R,4S)-7,7-dimethyl-2-oxobicyclo[2.2.1]heptan- 1-yl)methanesulfonate (180d)[226]

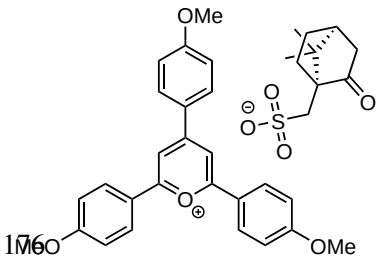

180d

Conducted by Dr. T. Lei: Into a round bottom flask were added **179** (83.3 mg, 200 µmol, 1.00 equiv.), ((1R,4S)-7,7-dimethyl-2-oxobicyclo[2.2.1]heptan-1-yl)methanesulfonic acid ((R)-CSA) (46.5 mg, 200 µmol, 1.00 equiv.) and 2 mL EtOH. The resulting

mixture was heated to 60 °C and stirred for 3 h, before the solvent was removed under reduced pressure. The residue was dissolved in 2 mL MeOH and extracted with hexane (5 × 2 mL). After separation, the MeOH-phase was added dropwise into 50 mL Et_2O. The formed precipitated was filtered, washed with Et_2O and dried on vacuum, affording **180d** (93.0 mg, 147 mmol, 74%) as a red solid.

M.p. = 228.5 °C. **IR** [cm^{-1}]: 3448, 3079, 2952, 2878, 2356, 1737, 1633, 1592, 1513, 1491, 1312, 1245,1182, 1030, 835. ^{1}**H NMR** (300 MHz, $CDCl_3$): δ 8.50 (d, *J* = 10.1 Hz, 4H), 8.23 (d, *J* = 8.9 Hz, 4H), 6.99 (d, *J* = 8.9 Hz, 3H), 6.94 (d, *J* = 8.9 Hz, 2H), 3.87 (s, 6H), 3.81 (s, 3H), 3.62 (d, *J* = 14.7 Hz, 1H), 3.16–2.96 (m, 2H), 2.39 (dt, *J* = 18.1, 4.0 Hz, 1H), 2.14–2.02 (m, 2H), 1.80 (ddd, *J* = 14.3, 9.8, 4.7 Hz, 1H), 1.39 (ddd, *J* = 13.3, 9.2, 3.7 Hz, 1H), 1.30 (s, 3H), 0.94 (s, 3H). ^{13}**C NMR** (101 MHz, $CDCl_3$): δ 217.6, 167.0, 165.9, 164.8, 162.1, 133.7, 130.7, 124.2, 121.1, 115.8, 115.6, 110.7, 59.1, 55.9, 48.1, 47.5, 43.3, 42.9, 27.4, 25.0, 20.7, 20.2. **HRMS** (ESI) calcd. for $[C_{26}H_{23}O_4]^+$ ([M-CSA$^-$]$^+$), m/z = 399.1591 ; found 399.1594.

5.9.2 Application onto Intermolecular Allylic Amination with Azoles

General Procedure 8

Into a 40 mL vial were added ethyl (*E*)-hex-3-enoate (**150a**) (3.0 equiv.), 4-chloro-1H-pyrazole (**151a**) (0.30 mmol, 1.0 equiv.), the respective selenium-catalyst (10 mol%), photosensitiser (5–10 mol%) and 4 mL DCE. The screw cap was equipped with two blue cannulas and the resulting mixture was vigorously stirred at 19 °C for 21 h. The solvent was removed and the NMR yield was determined with internal standard 1,4-dimethoxybenzene. The crude mixture was then purified via column chromatography (PE/EtOAc, 90:10) to receive a clean fraction for HPLC-analysis of the desired product **152a**.

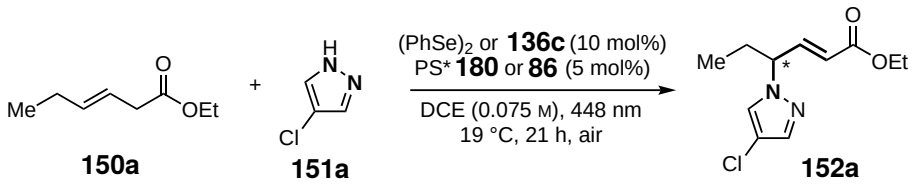

Table 5.36: Enantioselective Intermolecular Amination *via* Counteranion Directed Catalysis.

Entry	Photosensitiser [mol%]	Se-Catalyst	Conversion[a] [%]	Yield[a] [%]	*ee*[b] [%]
1	TAPT (**86**) [5]	$(PhSe)_2$	100	68	-
2	TAPT (**86**) [5]	**136c**	91	20	31
3	**180a** [5]	$(PhSe)_2$	n.d.	23	4
4	**180a** [5]	**136c**	40	7	11
5	**180b** [5]	**136c**	43	7	14
6	**180c** [10]	**136c**	10	13	29
7	**180d** [10]	**136c**	78	14	33

[a]NMR yields and conversions were determined with 1,4-dimethoxybenzene as the internal standard. [b]Enantiomeric excess (*ee*) was determined by chiral stationary phase HPLC analysis.

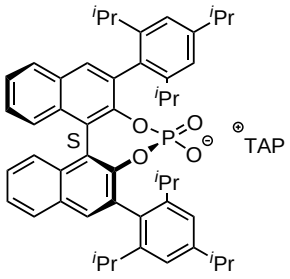

180a

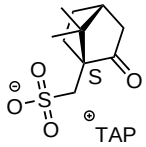

180c

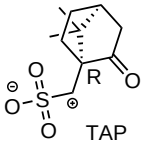

180d

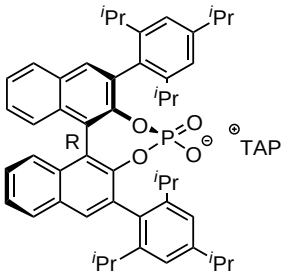

180b

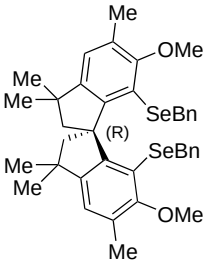

136c

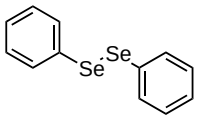

$(PhSe)_2$

6 Spectra

2,4,6-tris(4-methoxyphenyl)pyrylium tetrafluoroborate (TAPT) (86) (^{1}H NMR: 300 MHz, ^{13}C NMR: 101 MHz, MeCN-d_3; IR)

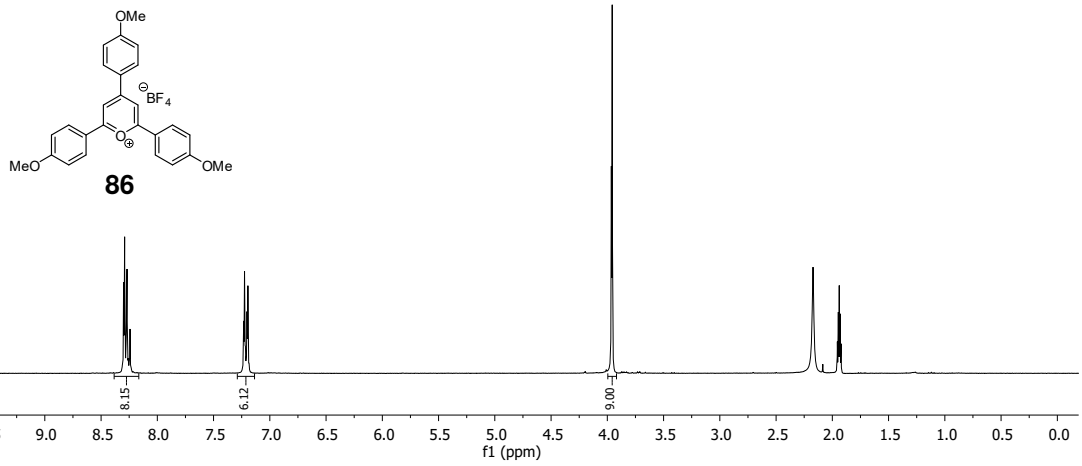

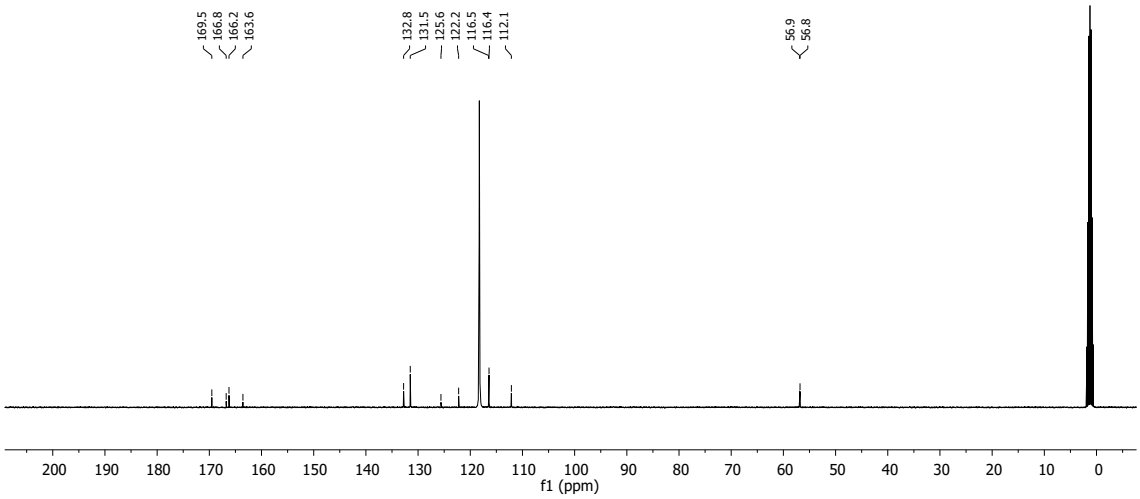

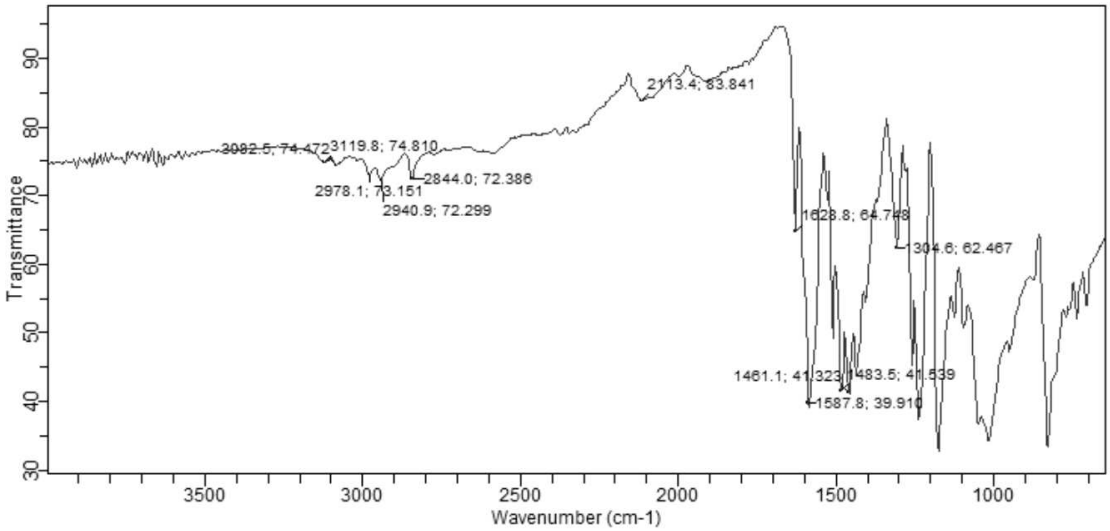
Transmittance
Wavenumber (cm-1)
3500
3000
2500
2000
1500
1000
90
80
70
60
50
40
30
3082.5; 74.472
3119.8; 74.810
2978.1; 73.151
2940.9; 72.299
2844.0; 72.386
2113.4; 83.841
1628.8; 64.748
1304.6; 62.467
1461.1; 41.323
1483.5; 41.539
1587.8; 39.910

1,2-bis(2-methoxyphenyl)diselane (140) (^{1}H NMR: 300 MHz, ^{13}C NMR: 101 MHz, ^{77}Se NMR: 76 MHz, $CDCl_3$; IR)

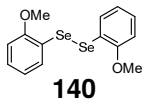

140

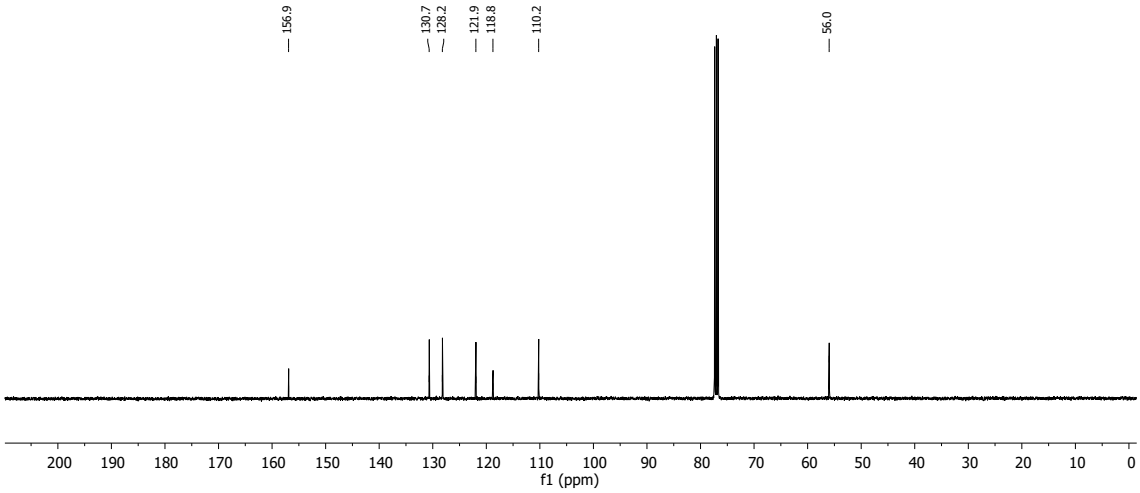

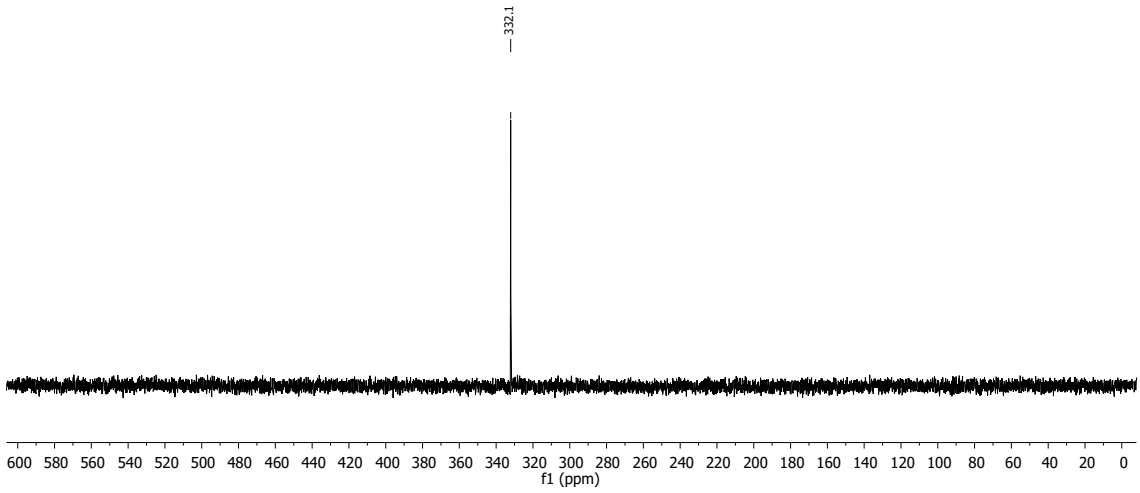

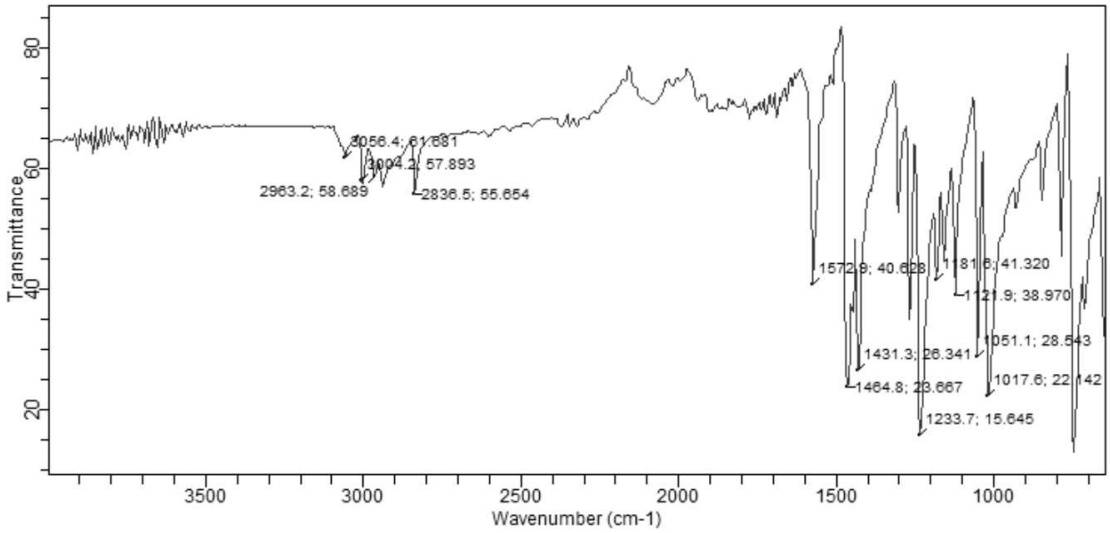
Transmittance
80
60
40
20
3500
3000
2500
2000
1500
1000
Wavenumber (cm-1)
3056.4; 61.681
3004.2; 57.893
2963.2; 58.689
2836.5; 55.654
1572.9; 40.628
1181.6; 41.320
1121.9; 38.970
1431.3; 26.341
1051.1; 28.543
1464.8; 23.667
1017.6; 22.142
1233.7; 15.645

(4-methoxybenzyl)(phenyl)selane (142) (^{1}H NMR: 400 MHz, ^{13}C NMR: 101 MHz, ^{77}Se NMR: 76 MHz, $CDCl_3$; IR)

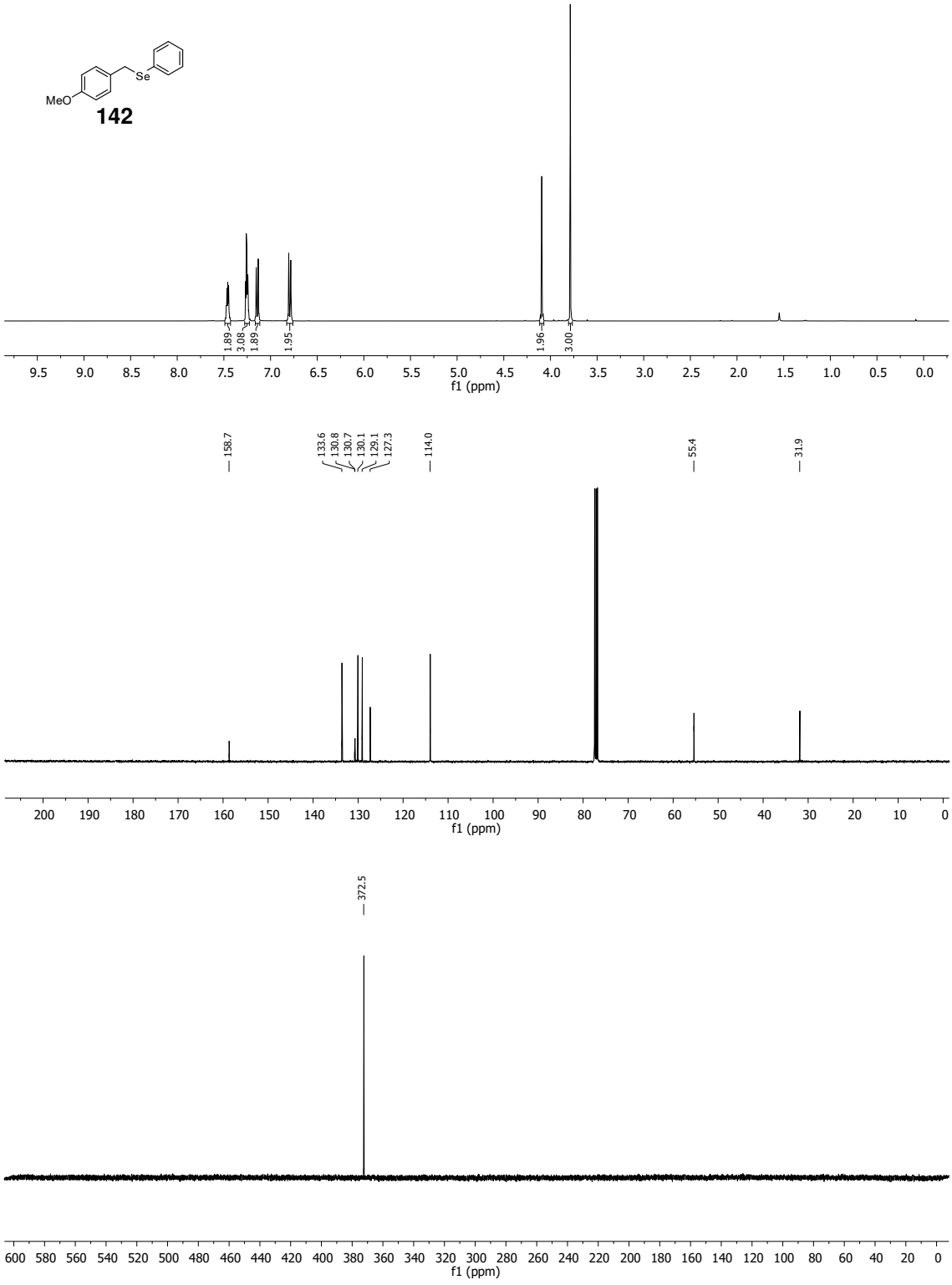

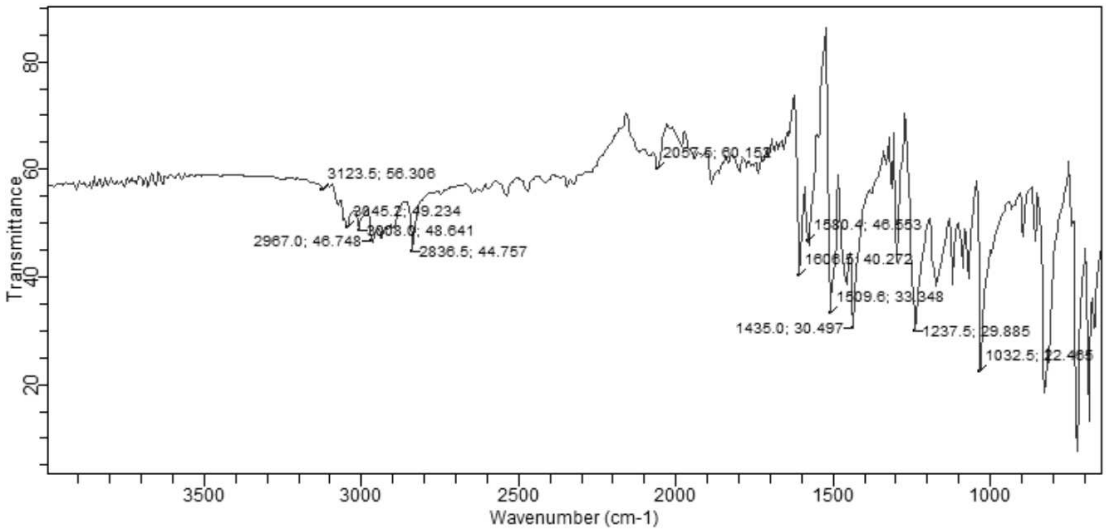
Transmittance
80
60
40
20
3500
3000
2500
2000
1500
1000
Wavenumber (cm-1)
3123.5; 56.306
2967.0; 46.748
2836.5; 44.757
1580.4; 46.553
1606.5; 40.272
1509.6; 33.348
1435.0; 30.497
1237.5; 29.885
1032.5; 22.466

***N*-(5-Bromopentyl)-4-methylbenzenesulfonamide (116) (^{1}H NMR: 400 MHz, ^{13}C NMR: 101 MHz, $CDCl_3$; IR)**

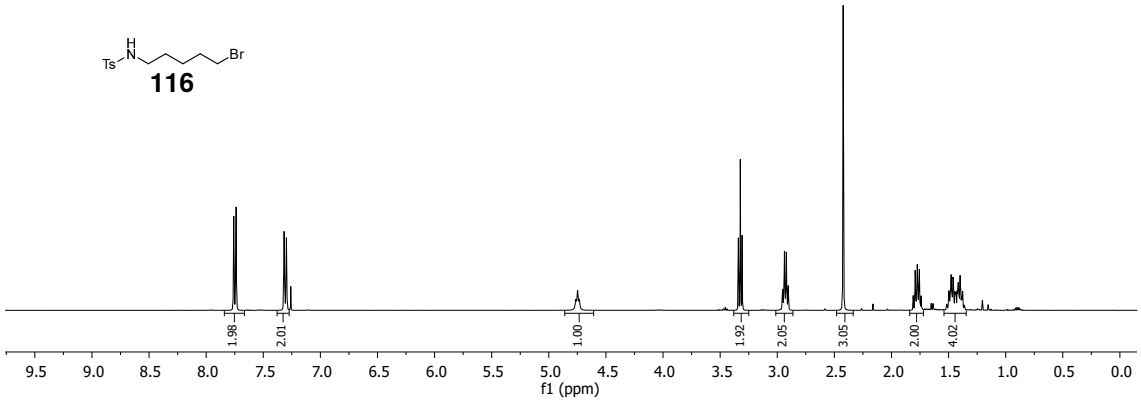

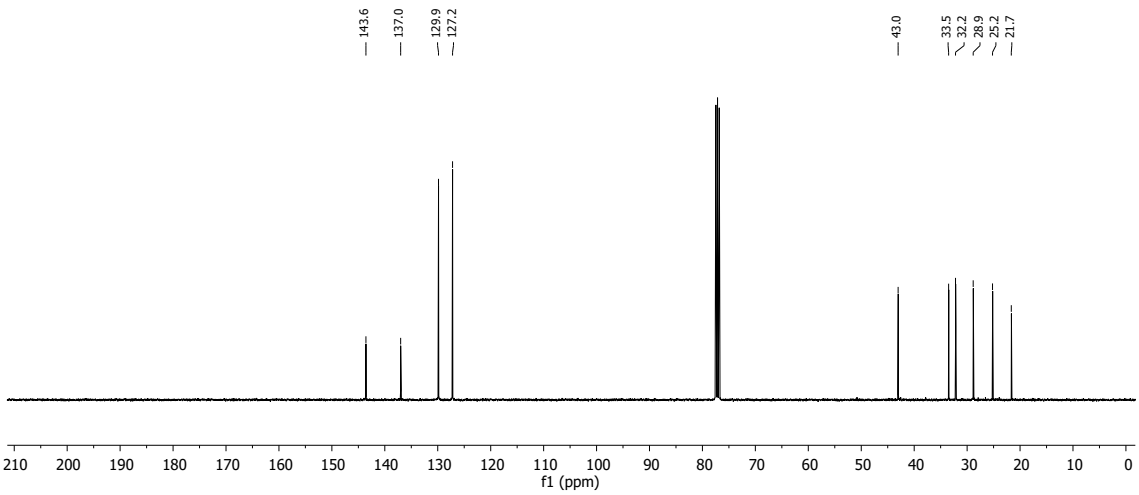

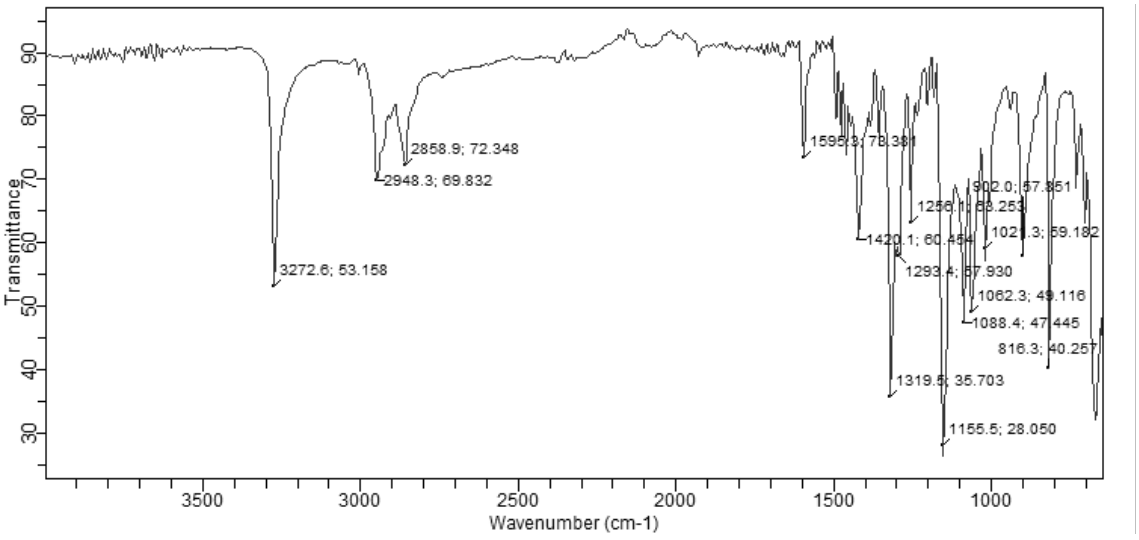

(5-((4-M ethylphenyl)sulfonamido)pentyl)triphenylphosphonium bromide (117) (^{1}H NMR: 400 MHz, ^{13}C NMR: 101 MHz, ^{31}P NMR: 162 MHz, DMSO – d_6; IR)

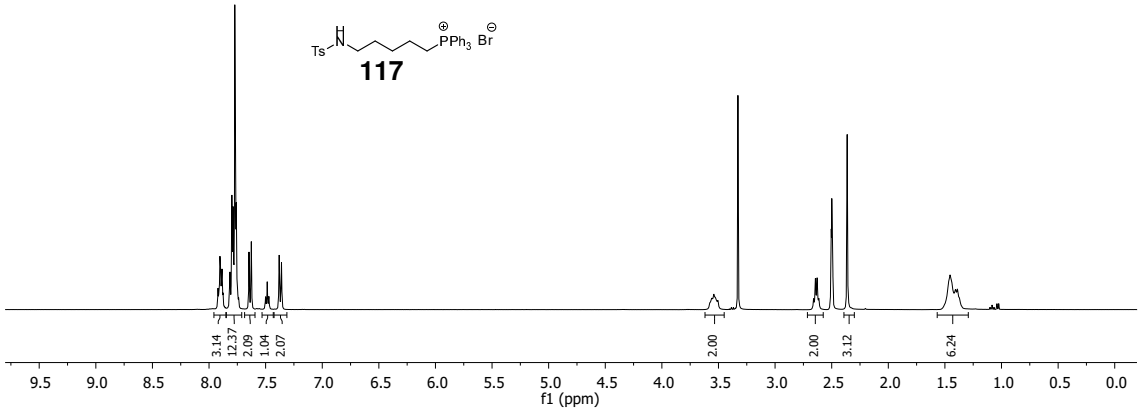

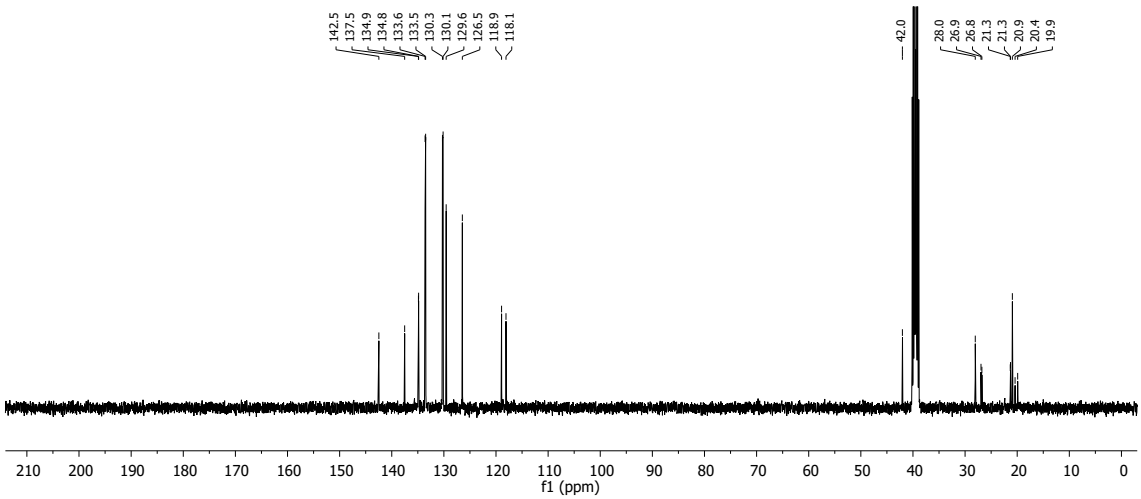

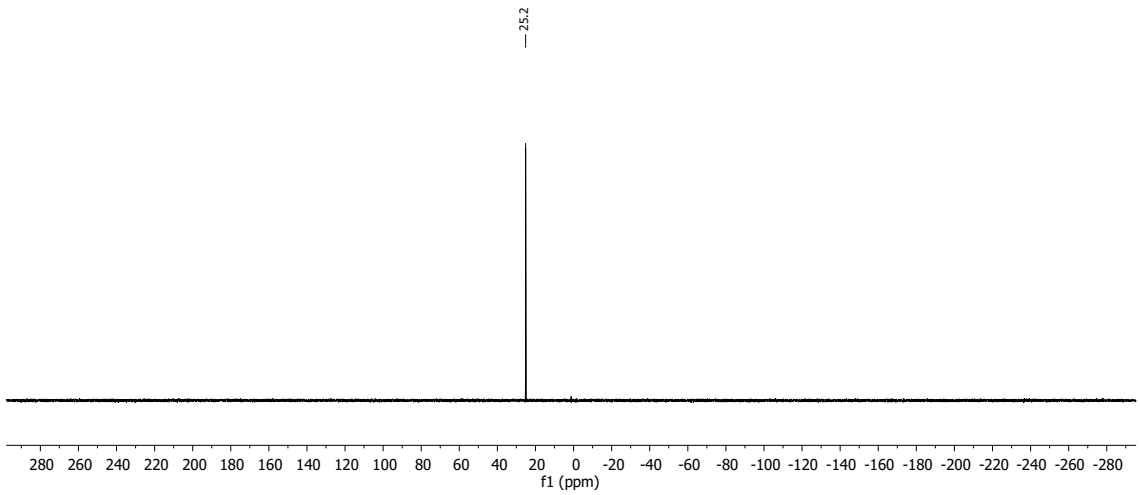

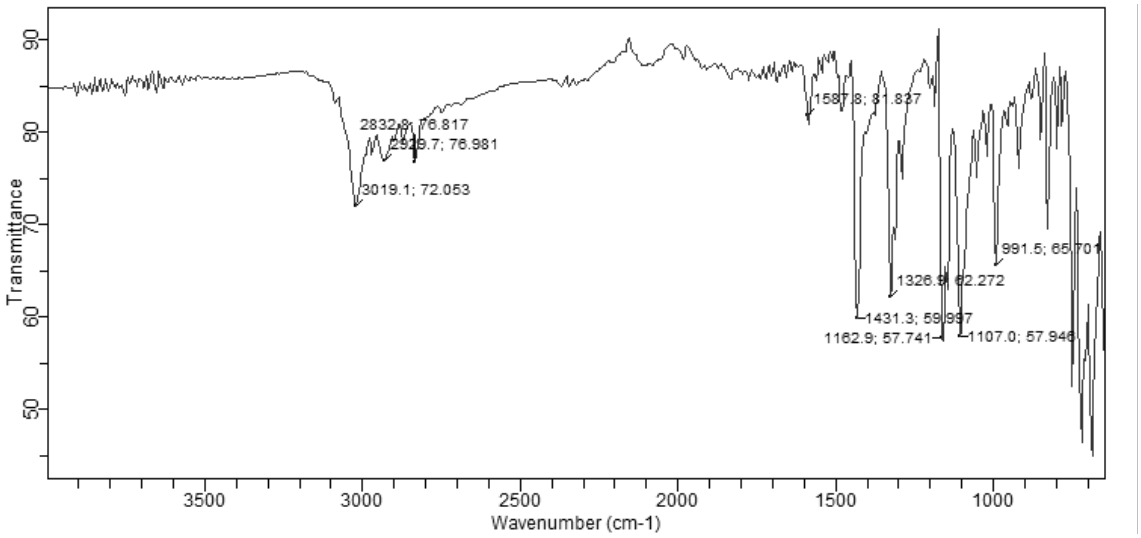
Transmittance
90
80
70
60
50
3500
3000
2500
2000
1500
1000
Wavenumber (cm-1)
2832.8; 76.817
2919.7; 76.981
3019.1; 72.053
1587.8; 81.837
1326.9; 62.272
991.5; 65.701
1431.3; 59.997
1162.9; 57.741
1107.0; 57.946

5-((4-methylphenyl)sulfonamido)pentyl 4-methylbenzenesulfonate (118) (^{1}H NMR: 400 MHz, ^{13}C NMR: 101 MHz, $CDCl_3$; IR)

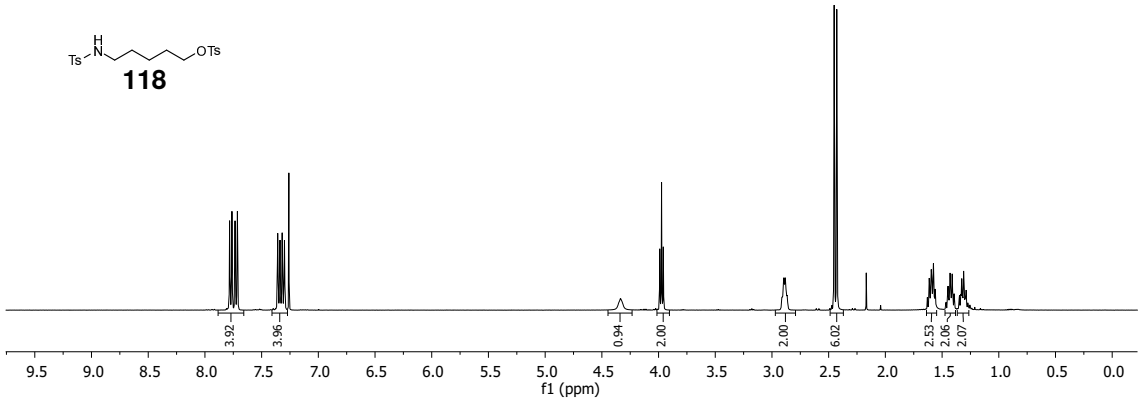

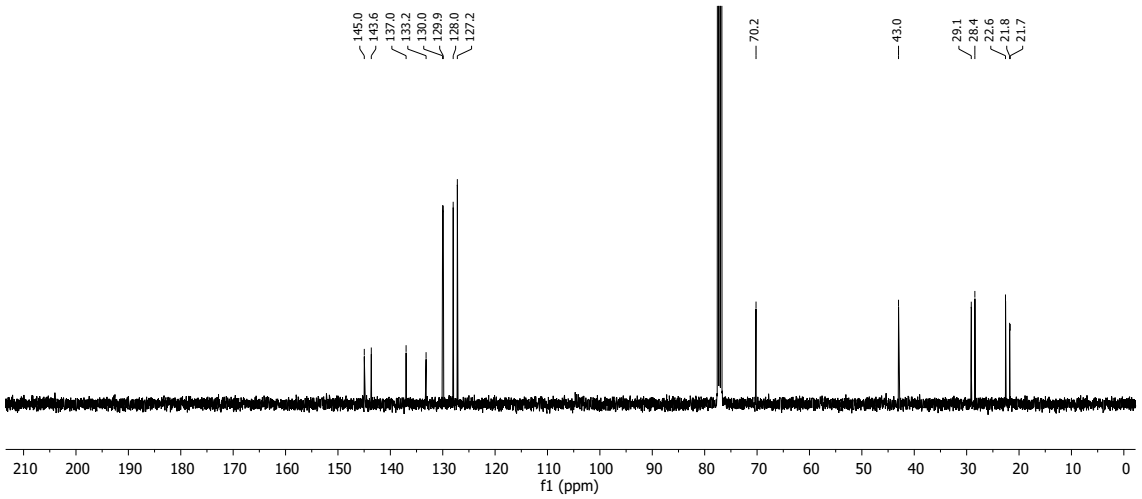

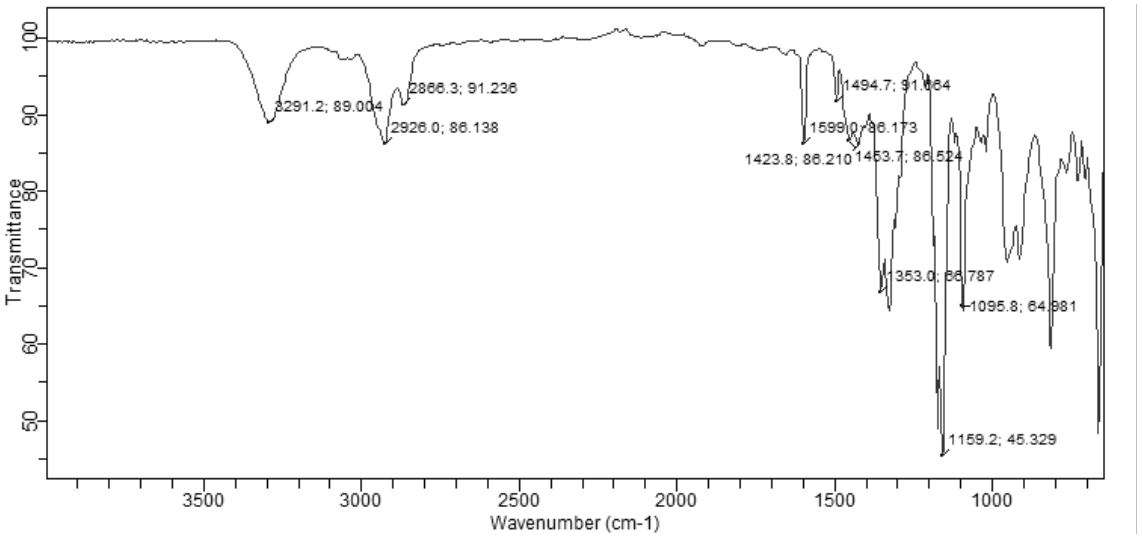

(5-((4-methylphenyl)sulfonamido)pentyl)triphenylphosphonium 4-methylbenzenesulfonate (119) (^{1}H NMR: 400 MHz, ^{13}C NMR: 101 MHz, ^{31}P NMR: 162 MHz $CDCl_3$; IR)

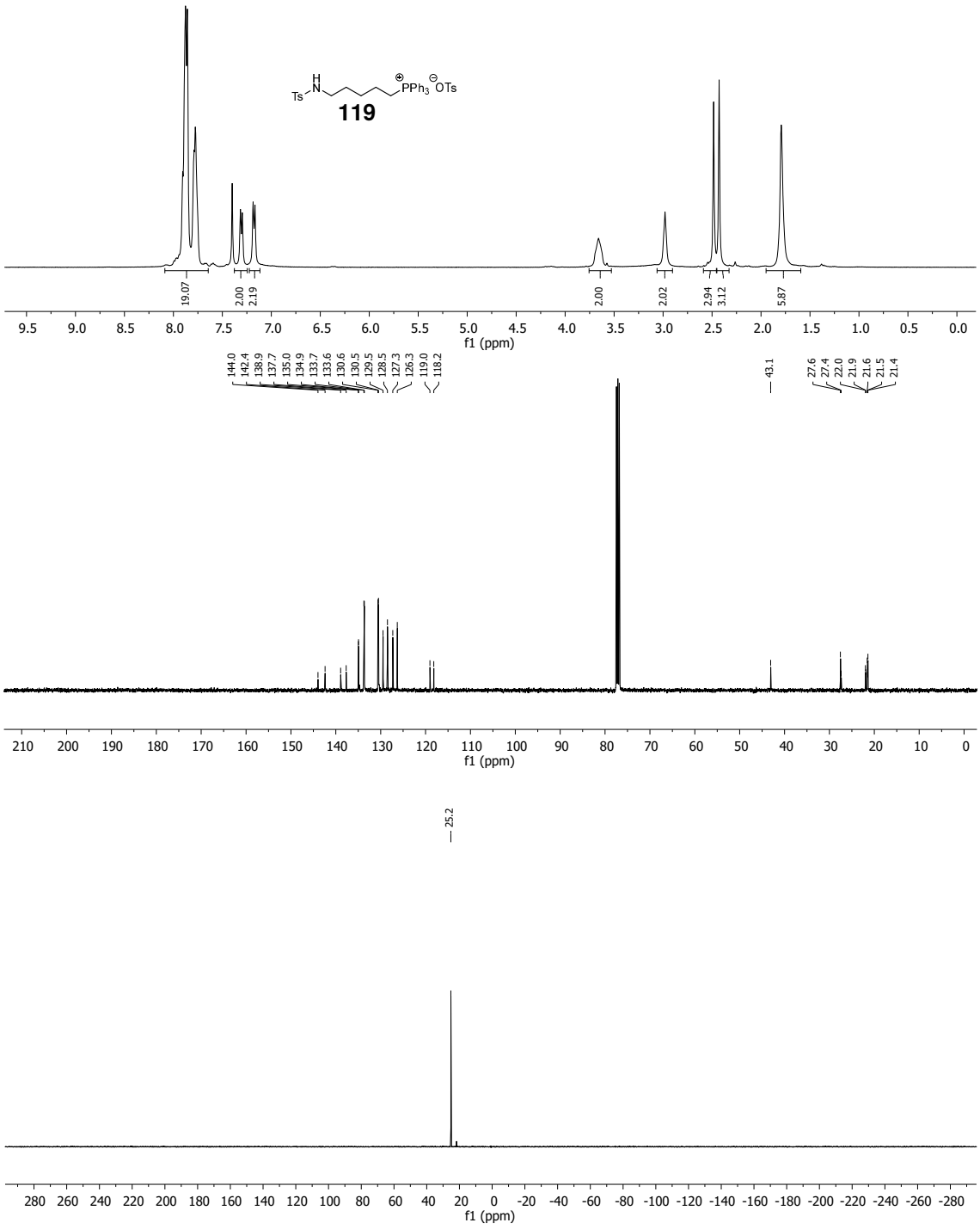

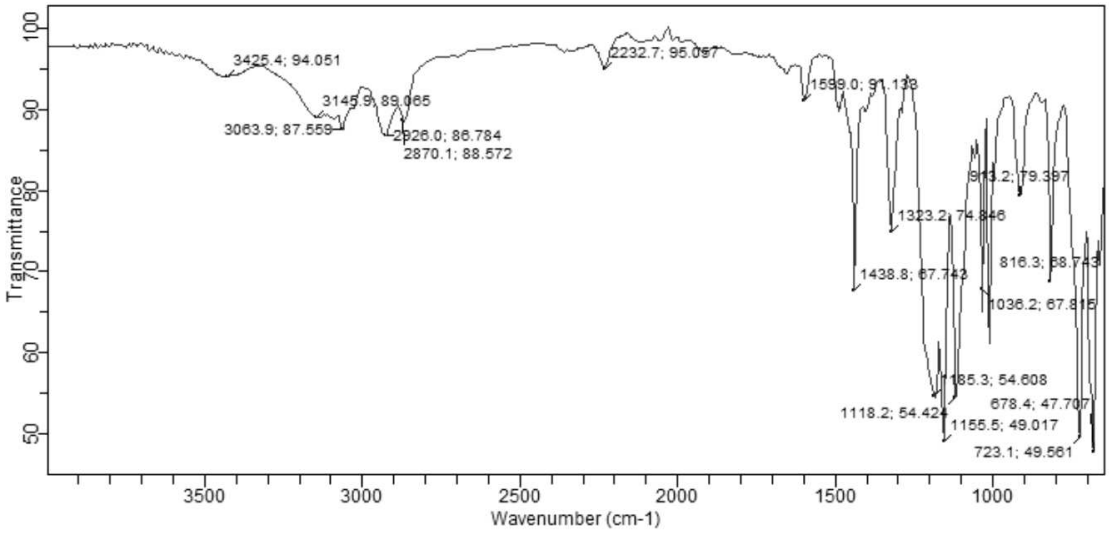
Transmittance
Wavenumber (cm-1)
3425.4; 94.051
3145.9; 89.065
3063.9; 87.559
2926.0; 86.784
2870.1; 88.572
2232.7; 95.057
1599.0; 91.138
1323.2; 74.846
1438.8; 67.742
1118.2; 54.424
1155.5; 49.017
723.1; 49.561
816.3; 58.743
1036.2; 67.815
678.4; 47.707

(*E*)-*N*-(8,8-Dimethylnon-5-en-1-yl)-4-methylbenzenesulfonamide (120c) (^{1}H NMR: 400 MHz, ^{13}C NMR: 101 MHz, $CDCl_3$; IR)

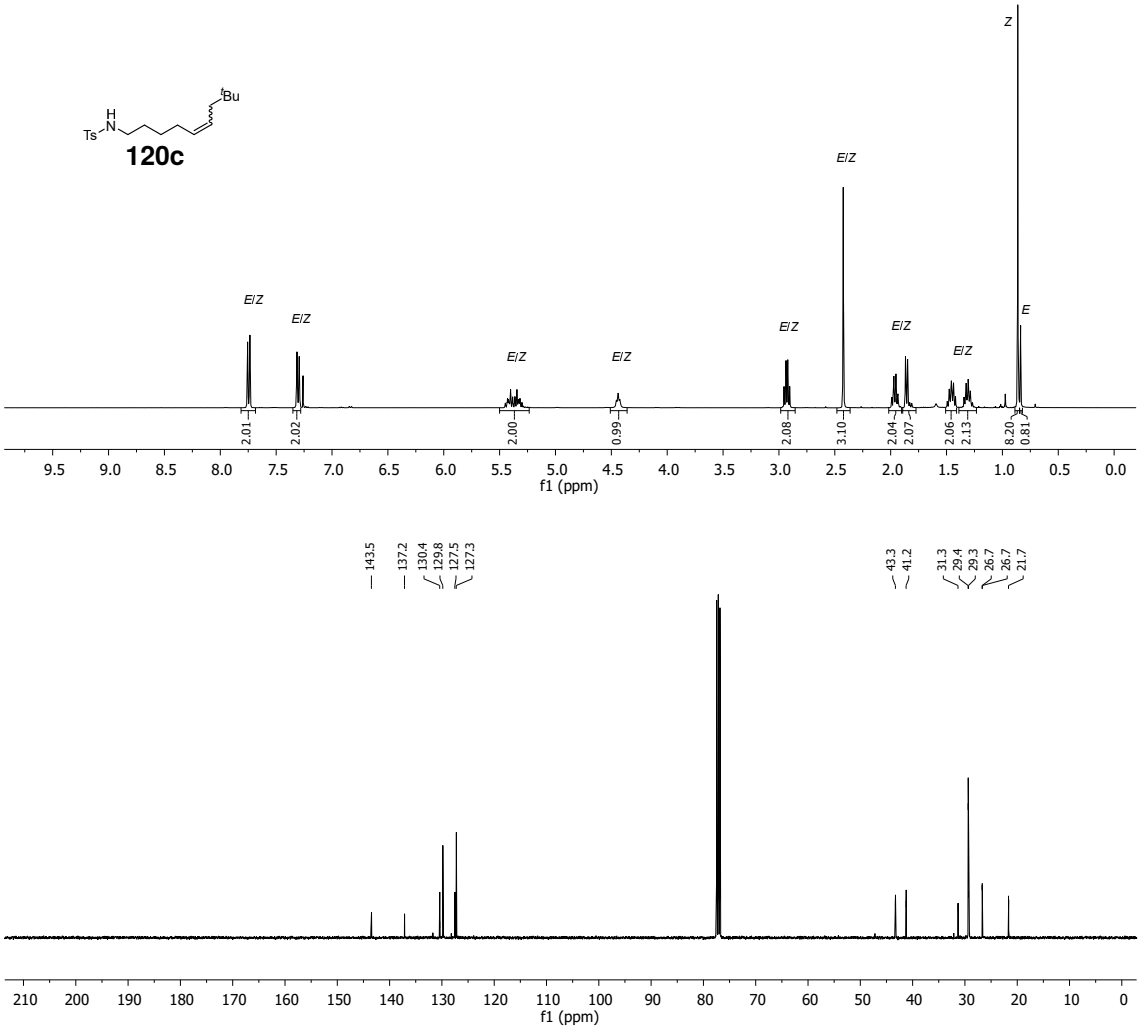

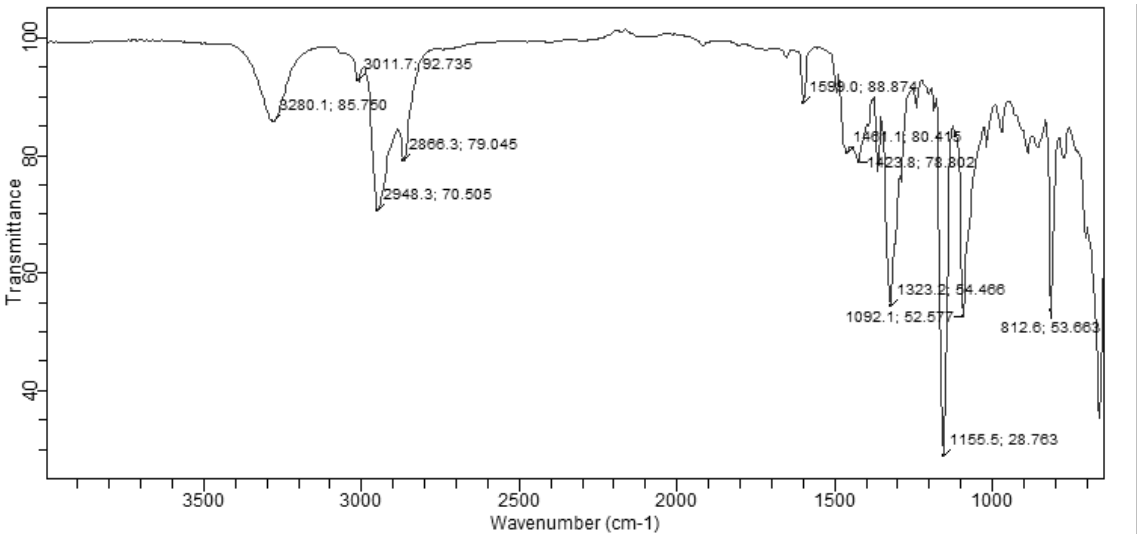
Transmittance
100
80
60
40
3500
3000
2500
2000
1500
1000
Wavenumber (cm-1)
3280.1; 85.750
3011.7; 92.735
2866.3; 79.045
2948.3; 70.505
1599.0; 88.874
1461.1; 80.415
1423.8; 78.302
1323.2; 54.466
1092.1; 52.577
812.6; 53.663
1155.5; 28.763

(*E*)-4-methyl-N-(7-phenylhept-5-en-1-yl)benzenesulfonamide and (*E*)-4-methyl-N-(7-phenylhept-6-en-1-yl)benzenesulfonamide (120d) (^{1}H NMR: 400 MHz, ^{13}C NMR: 101 MHz, NOESY, $CDCl_3$; IR)

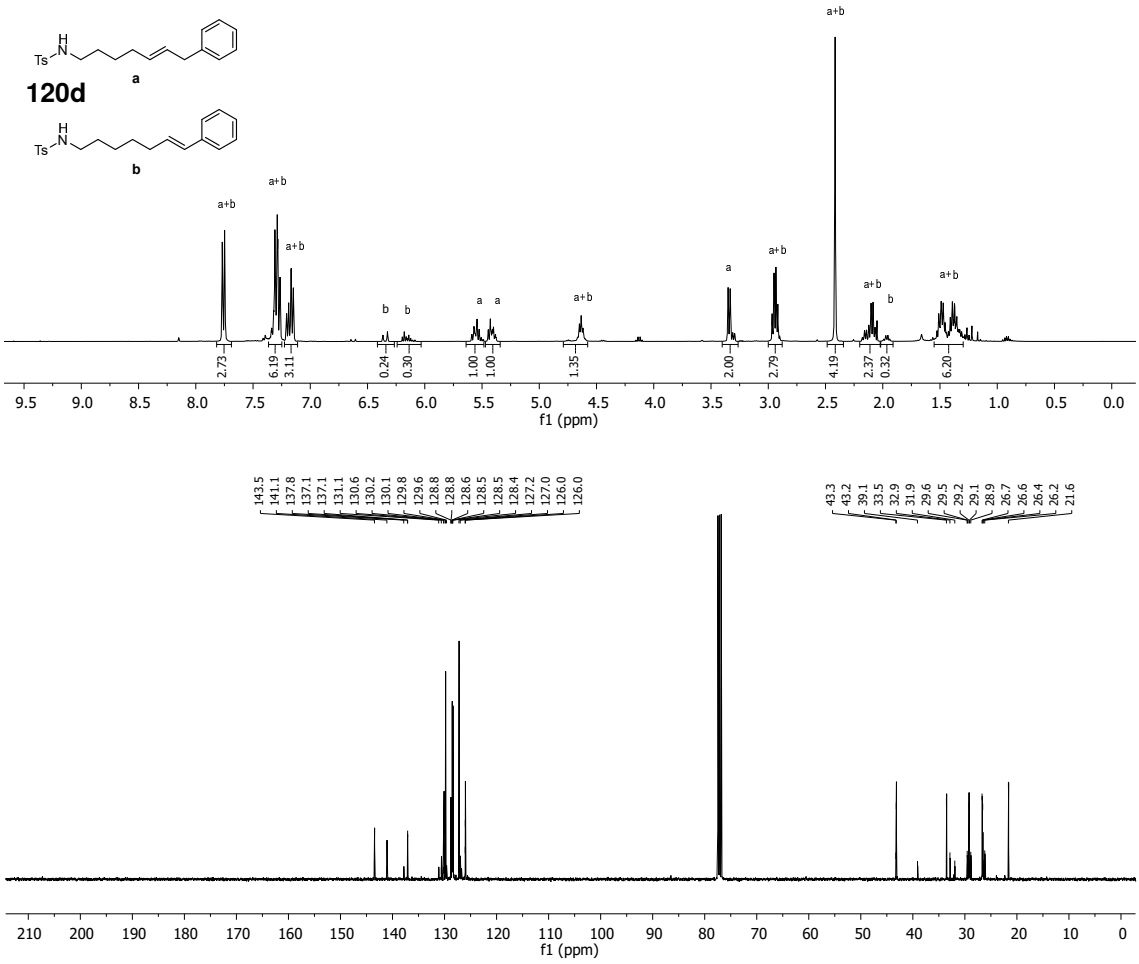

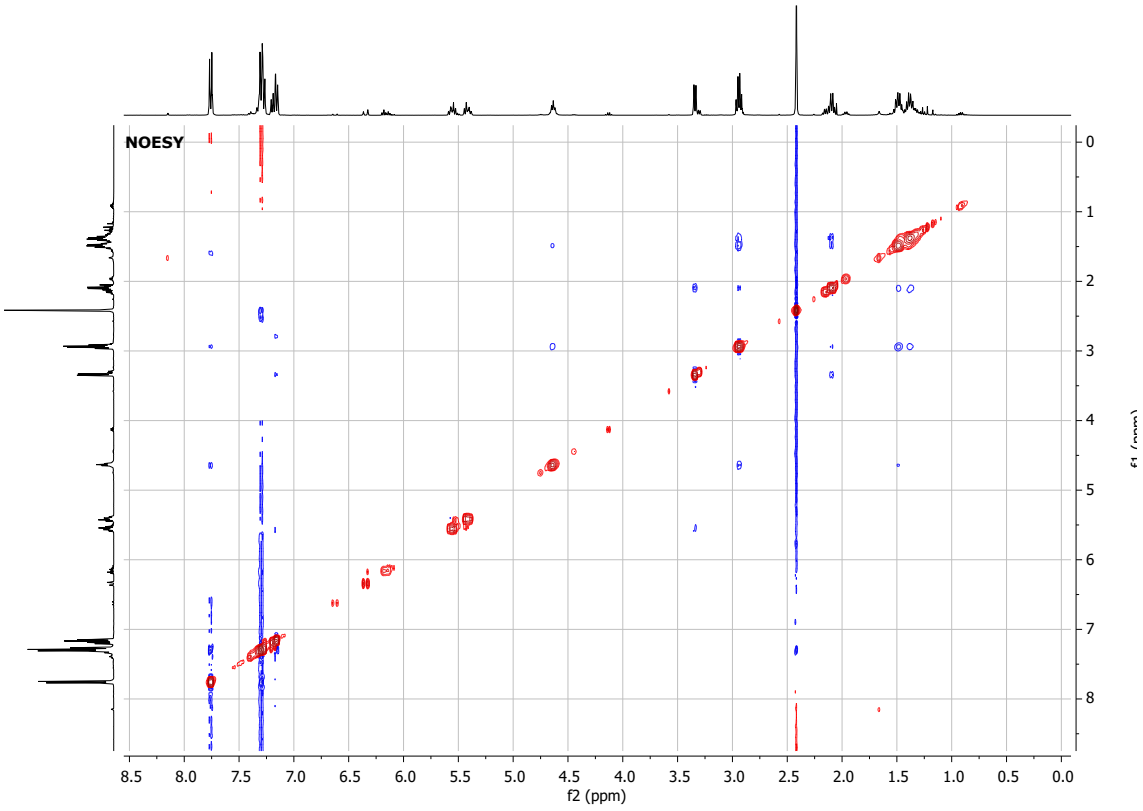
NOESY
8.5
8.0
7.5
7.0
6.5
6.0
5.5
5.0
4.5
4.0
3.5
3.0
2.5
2.0
1.5
1.0
0.5
0.0
f2 (ppm)
0
1
2
3
4
5
6
7
8

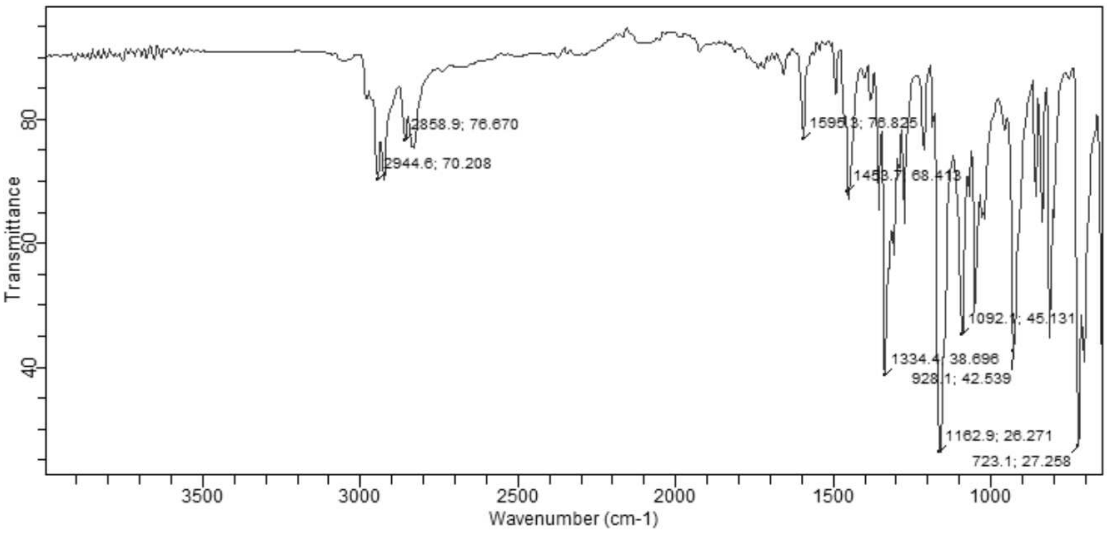
Transmittance
80
60
40
2858.9; 76.670
2944.6; 70.208
1595.3; 76.825
1092.1; 45.131
1334.4; 38.696
928.1; 42.539
1162.9; 26.271
723.1; 27.258
3500
3000
2500
2000
1500
1000
Wavenumber (cm-1)

4-methyl-*N*-(6-phenylhex-5-en-1-yl)benzenesulfonamide (120e) (^{1}H NMR: 300 MHz, ^{13}C NMR: 101 MHz, $CDCl_3$; IR)

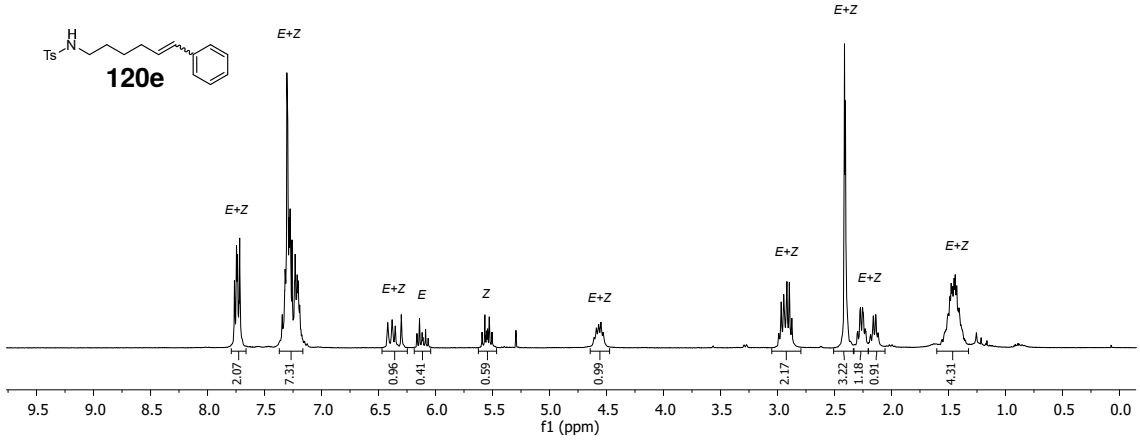

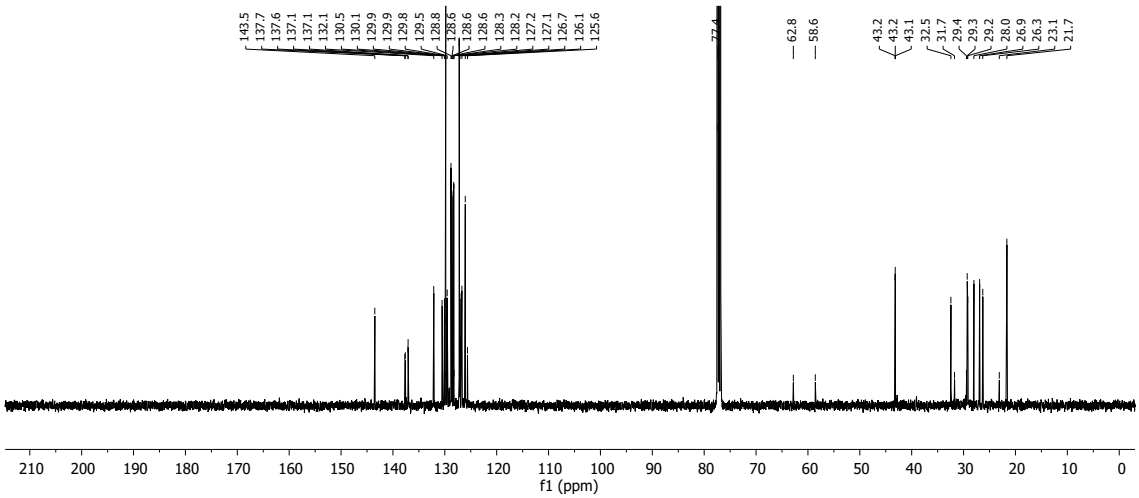

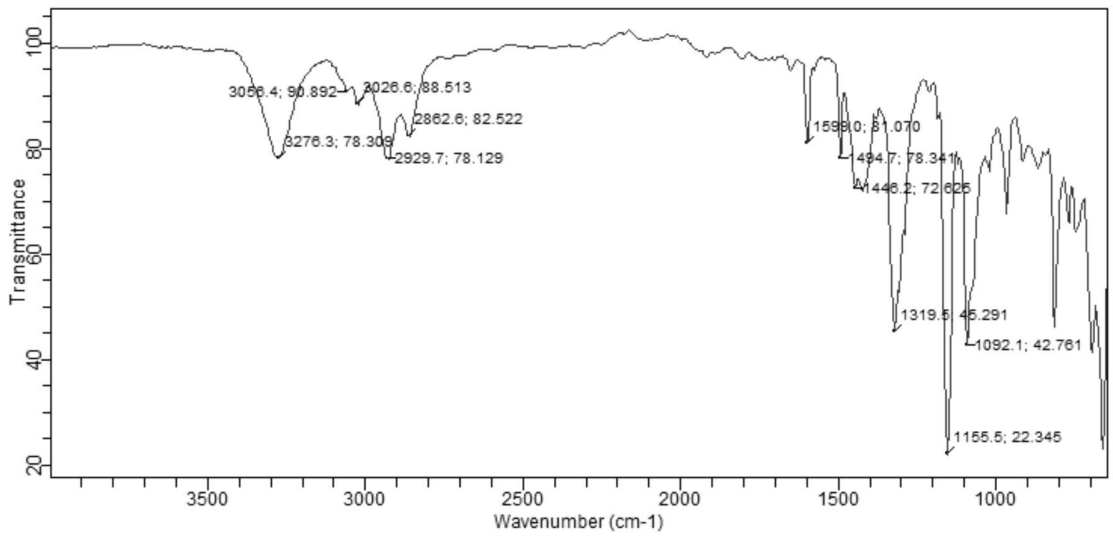

2-Phenyl-3-(phenylselanyl)-1-tosylpyrrolidine (129a) (^{1}H NMR: 300 MHz, ^{13}C NMR: 101 MHz, ^{77}Se NMR: 76 MHz, $CDCl_3$; IR)

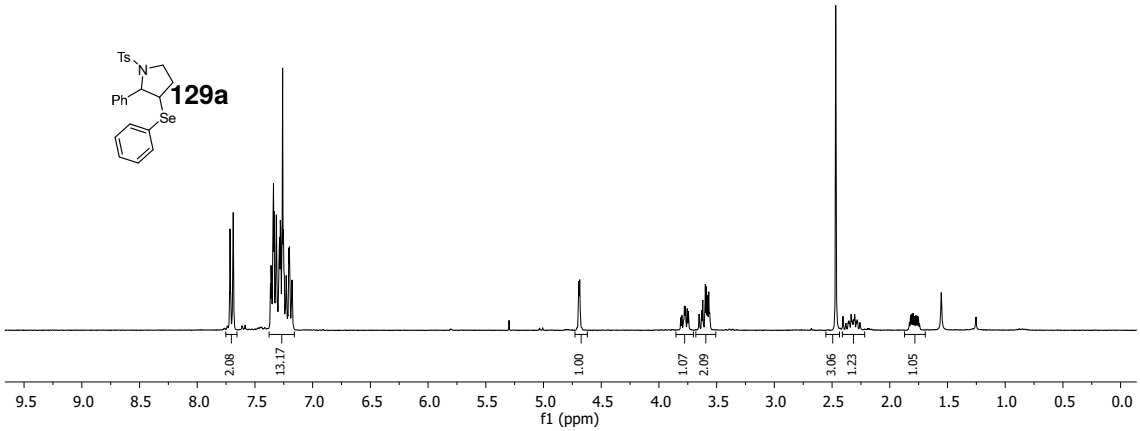

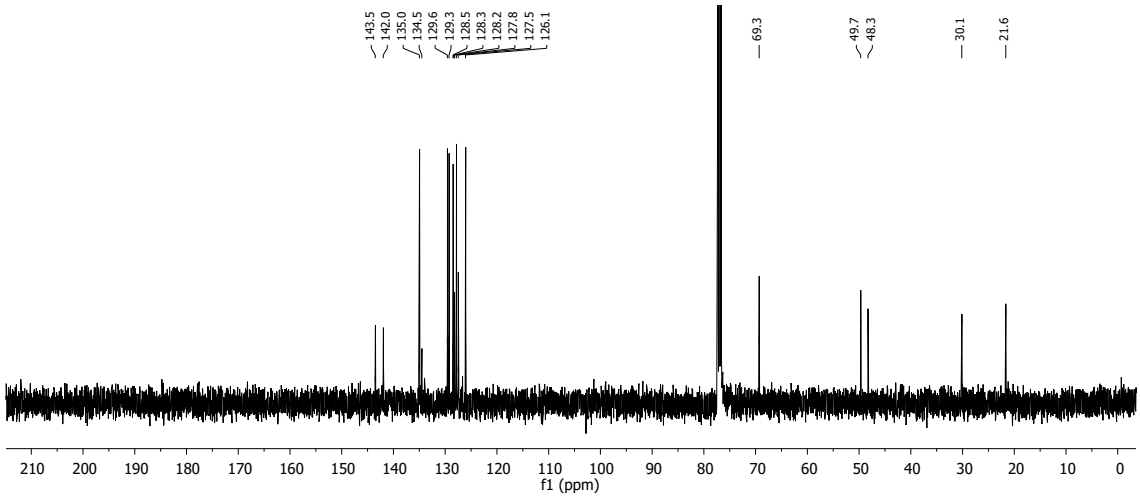

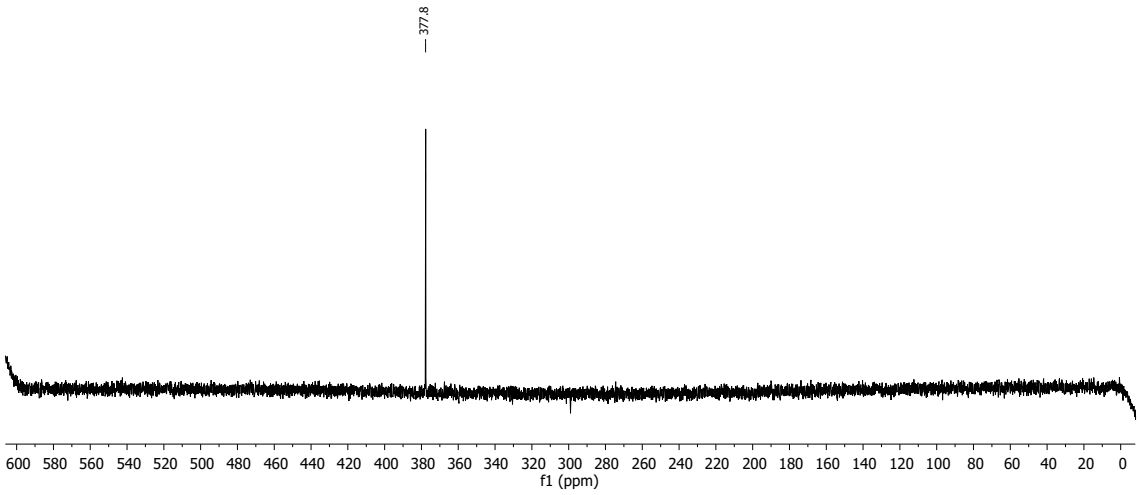

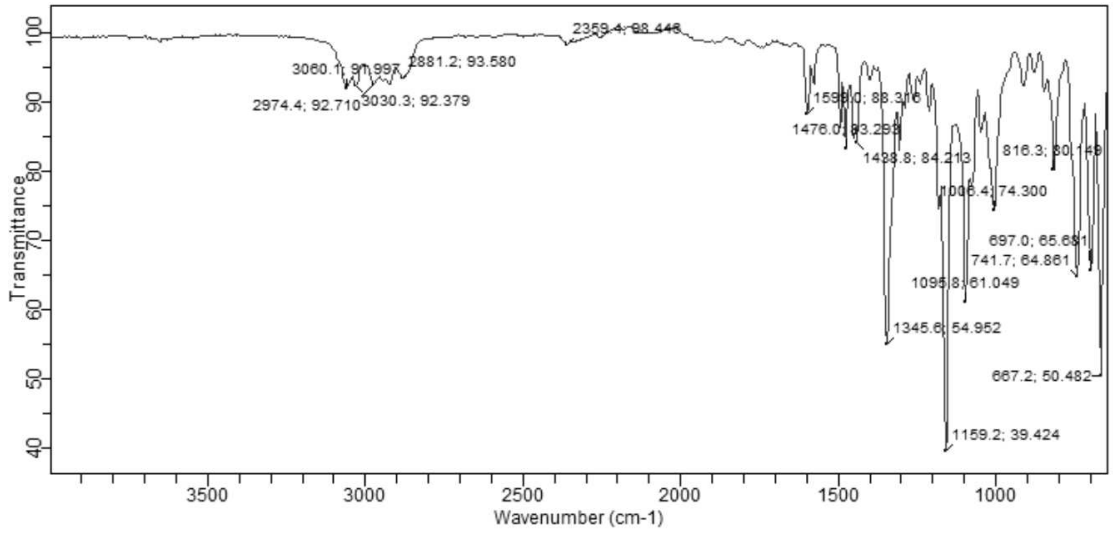
Transmittance
Wavenumber (cm-1)
3500
3000
2500
2000
1500
1000
100
90
80
70
60
50
40
2974.4; 92.710
3030.3; 92.379
2881.2; 93.580
2359.4; 98.448
1476.0; 93.293
1345.6; 54.952
1159.2; 39.424
667.2; 50.482
1095.8; 61.049
741.7; 64.861
697.0; 65.681
816.3; 80.148
1006.4; 74.300

3-((4-Methoxyphenyl)selanyl)-2-phenyl-1-tosylpyrrolidine (129b) (^{1}H NMR: 300 MHz, ^{13}C NMR: 101 MHz, ^{77}Se NMR: 76 MHz, $CDCl_3$; IR)

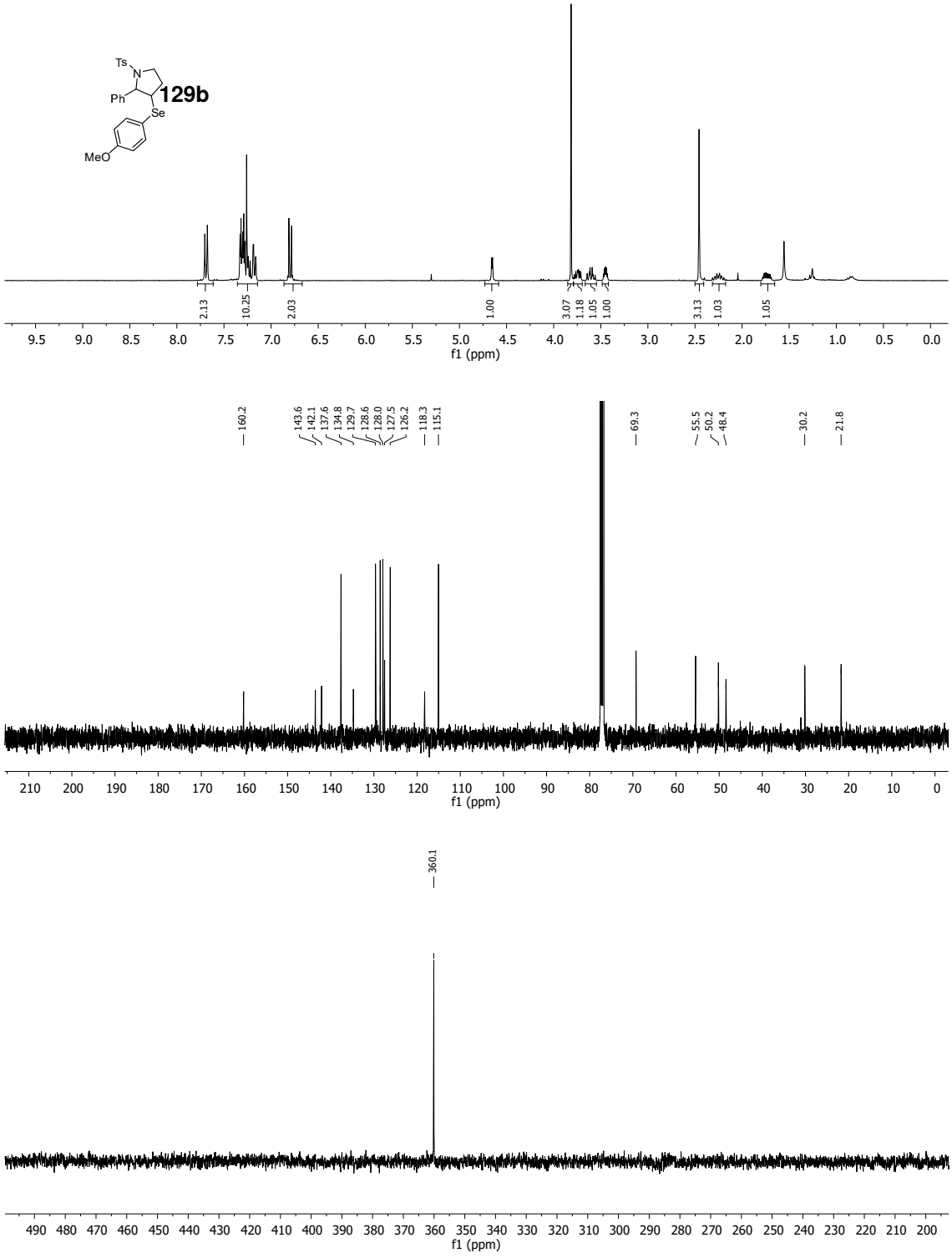

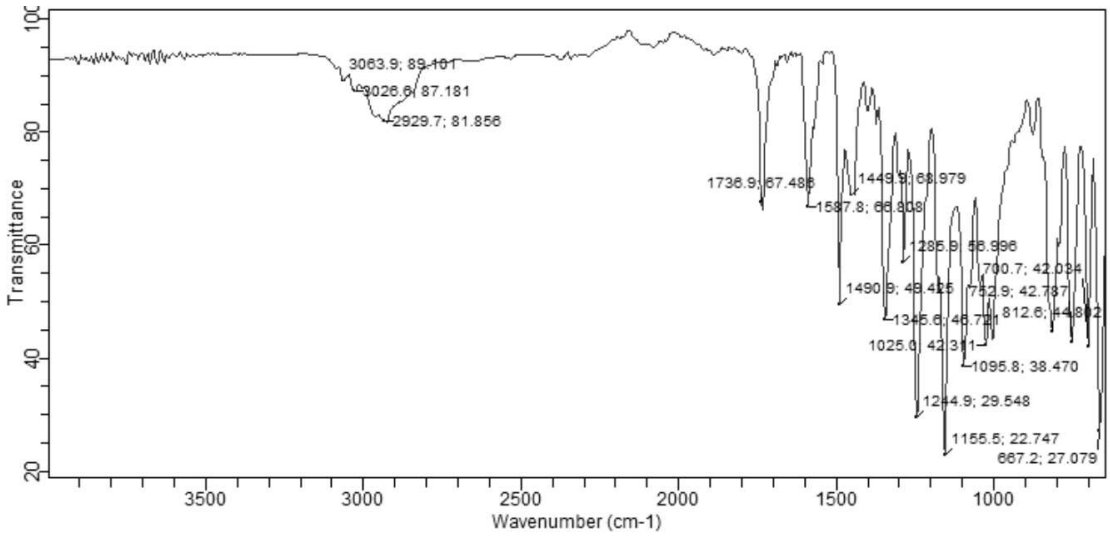
Transmittance
Wavenumber (cm-1)
3500
3000
2500
2000
1500
1000
3063.9; 89.161
3026.6; 87.181
2929.7; 81.856
1736.9; 67.486
1587.8; 66.808
1449.9; 68.979
1490.9; 48.415
1345.6; 46.721
1025.0; 42.311
1285.9; 56.996
700.7; 42.034
752.9; 42.787
812.6; 44.802
1095.8; 38.470
1244.9; 29.548
1155.5; 22.747
667.2; 27.079

3-((4-Chlorophenyl)thio)-2-phenyl-1-tosylpyrrolidine (129c) (^{1}H NMR: 400 MHz, ^{13}C NMR: 101 MHz, $CDCl_3$; IR)

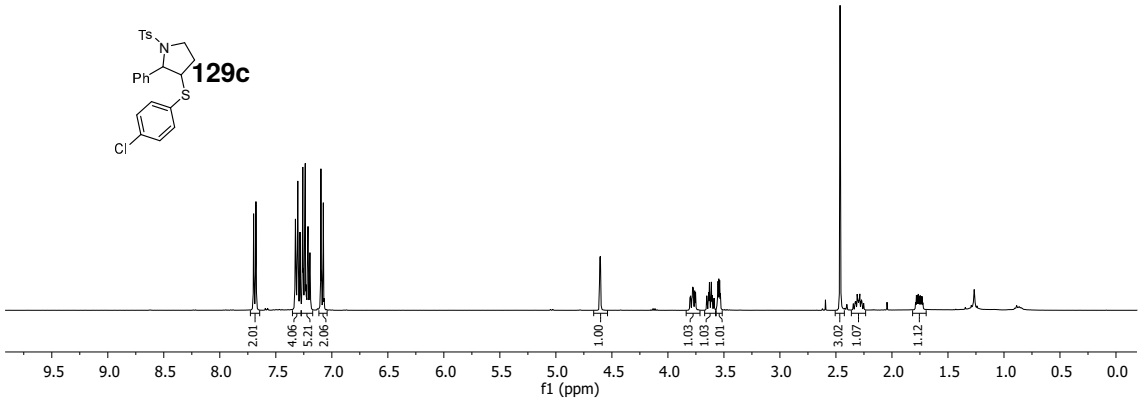

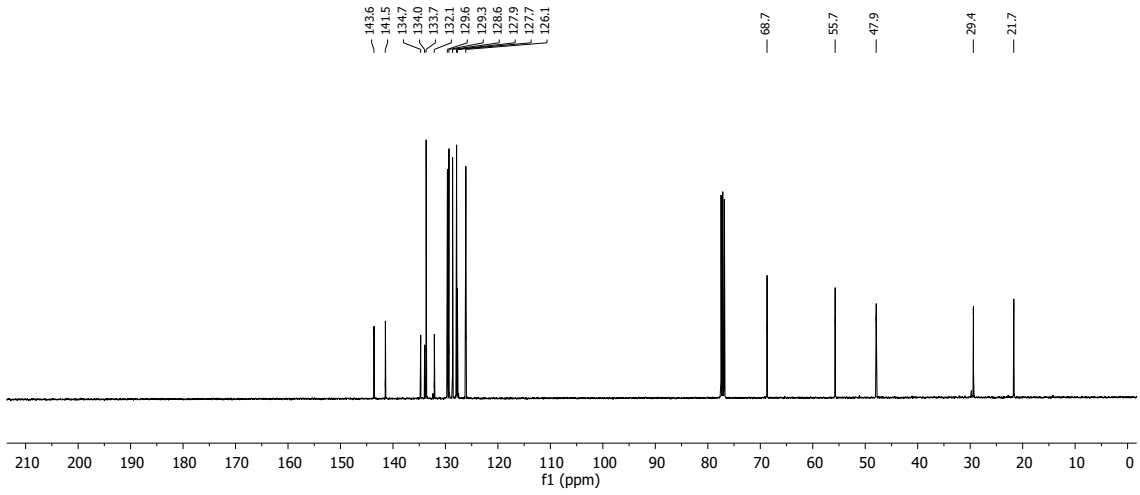

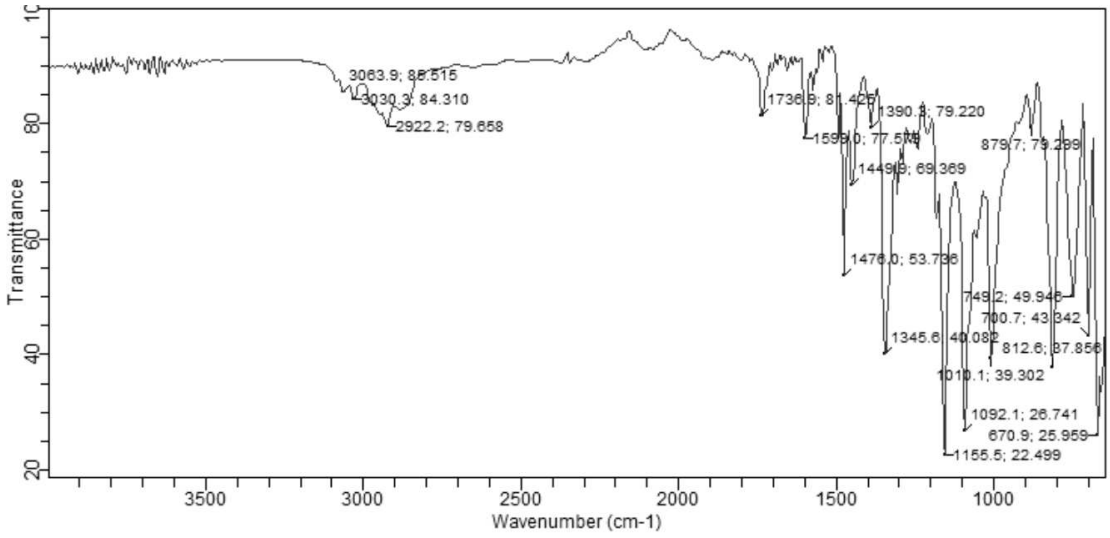

(5-((4-Nitrophenyl)sulfonamido)pentyl)triphenylphosphonium bromide (130) (^{1}H NMR: 300 MHz, ^{13}C NMR: 101 MHz, ^{31}P NMR: 162 MHz Methanol – d_4; IR)

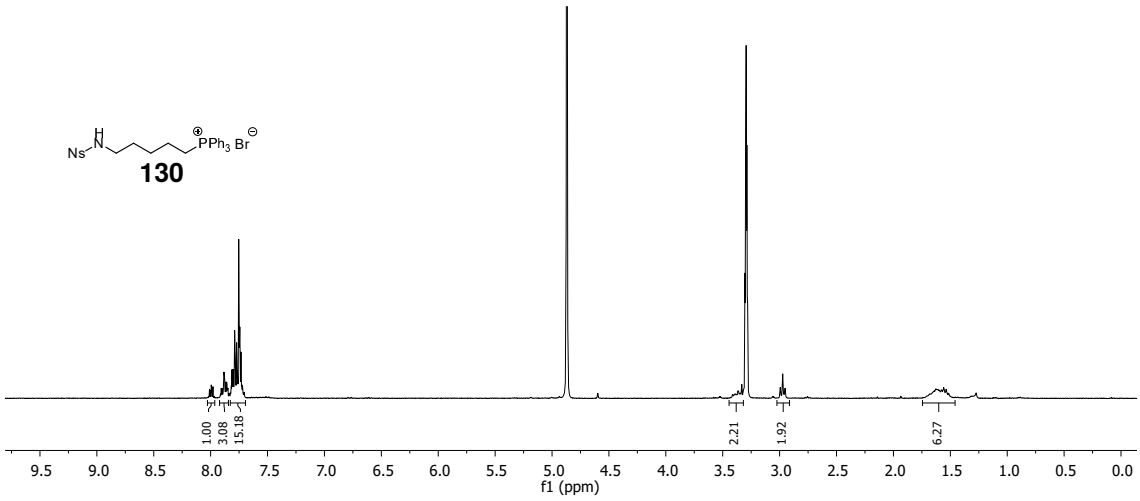

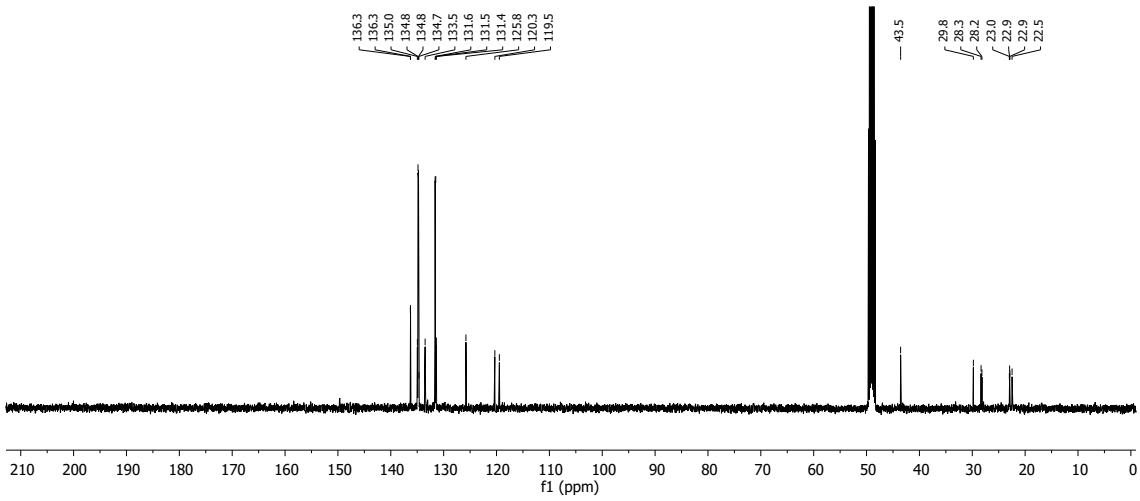

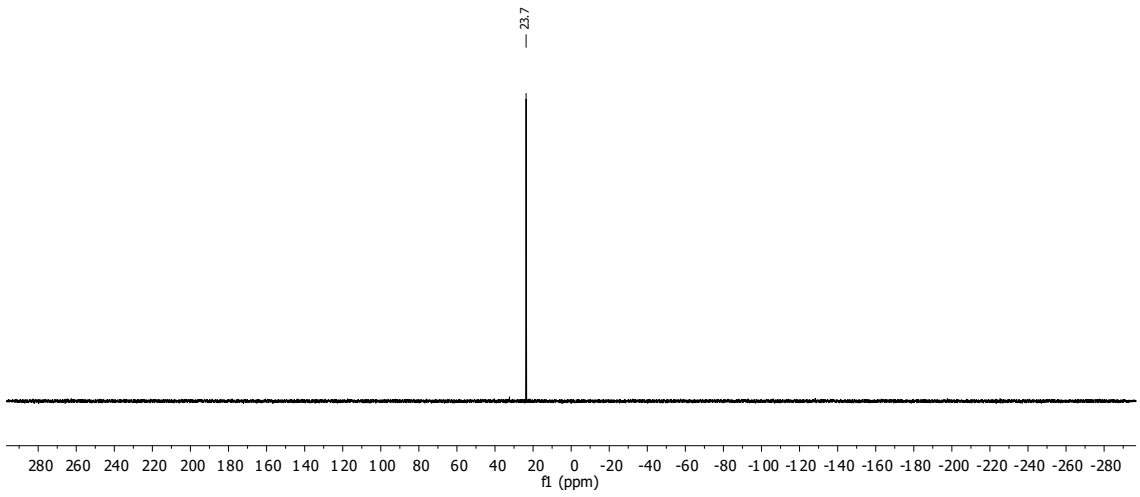

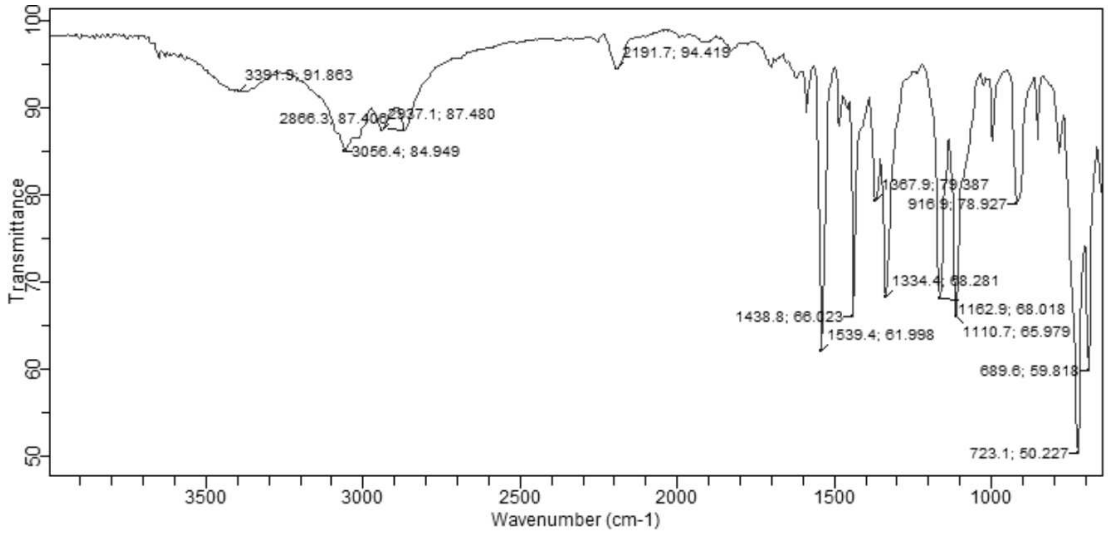
Transmittance
Wavenumber (cm-1)
3391.9; 91.863
2866.3; 87.406
2937.1; 87.480
3056.4; 84.949
2191.7; 94.419
1438.8; 66.023
1539.4; 61.998
1334.4; 68.281
1067.9; 79.387
916.9; 78.927
1162.9; 68.018
1110.7; 65.979
689.6; 59.818
723.1; 50.227

4-Nitro-*N*-(4-(*p*-tolyl)but-3-en-1-yl)benzenesulfonamide (134a) (^{1}H NMR: 300 MHz, ^{13}C NMR: 101 MHz, $CDCl_3$; IR)

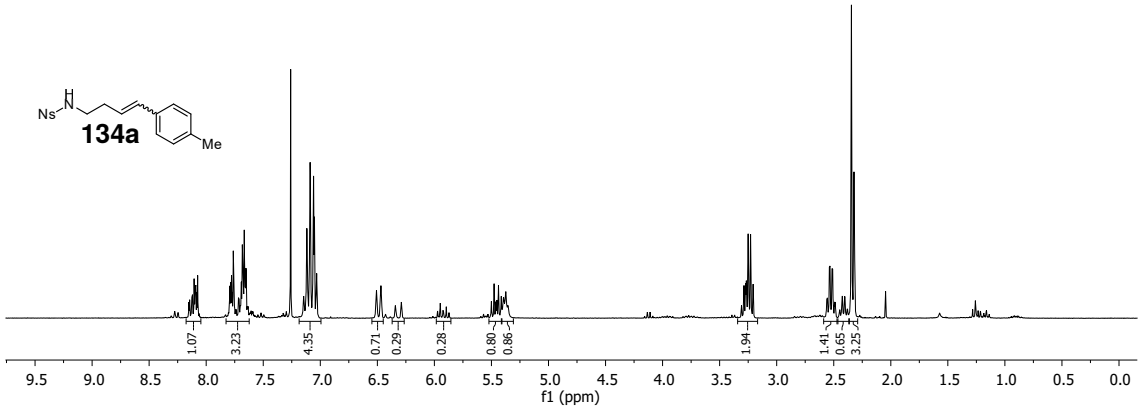

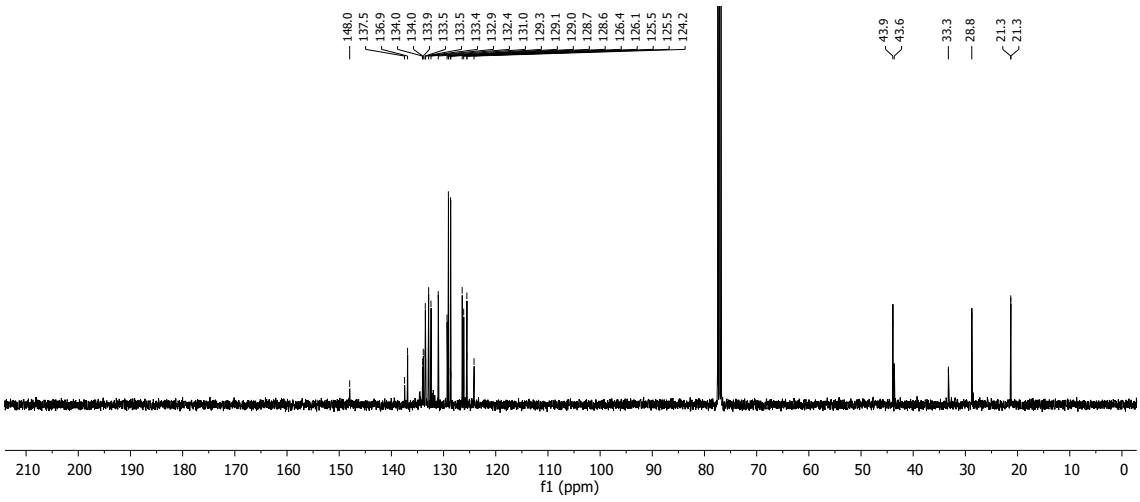

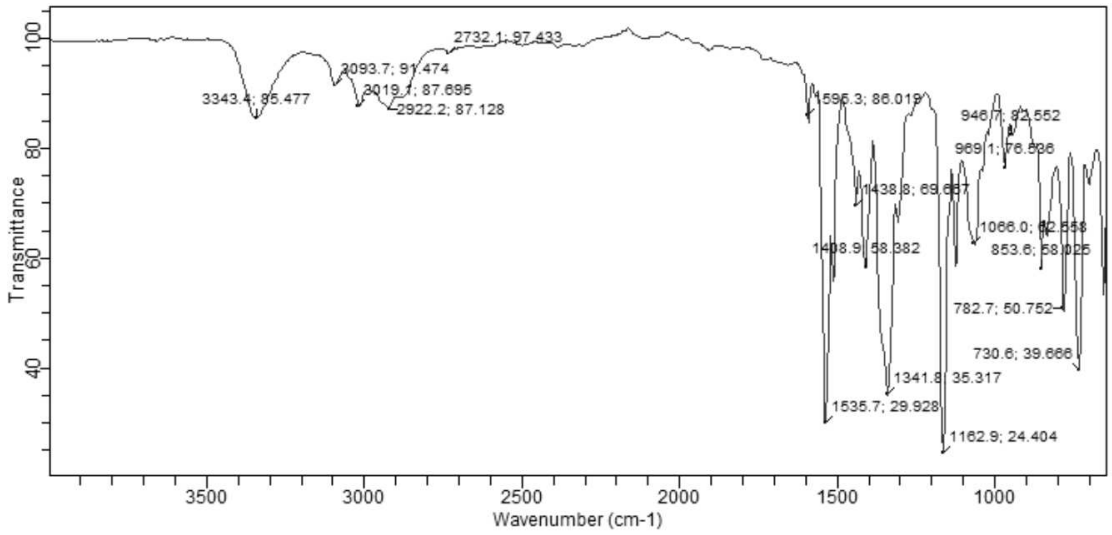

_N_-(4-(Naphthalen-1-yl)but-3-en-1-yl)-4-nitrobenzenesulfonamide (134c) (^{1}H NMR: 400 MHz, ^{13}C NMR: 101 MHz, $CDCl_3$; IR)

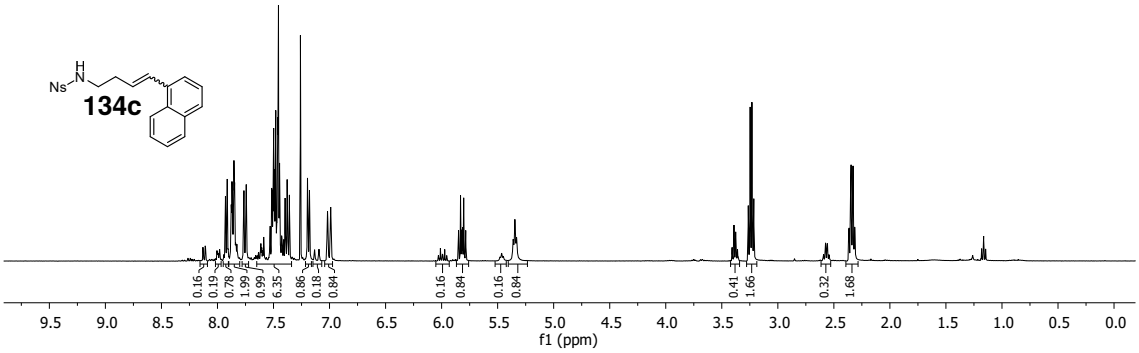

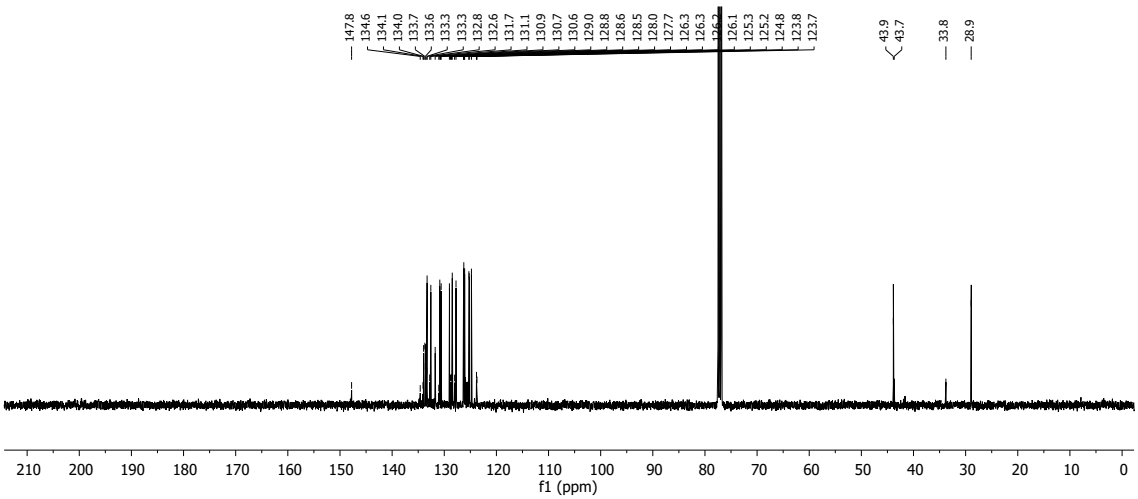

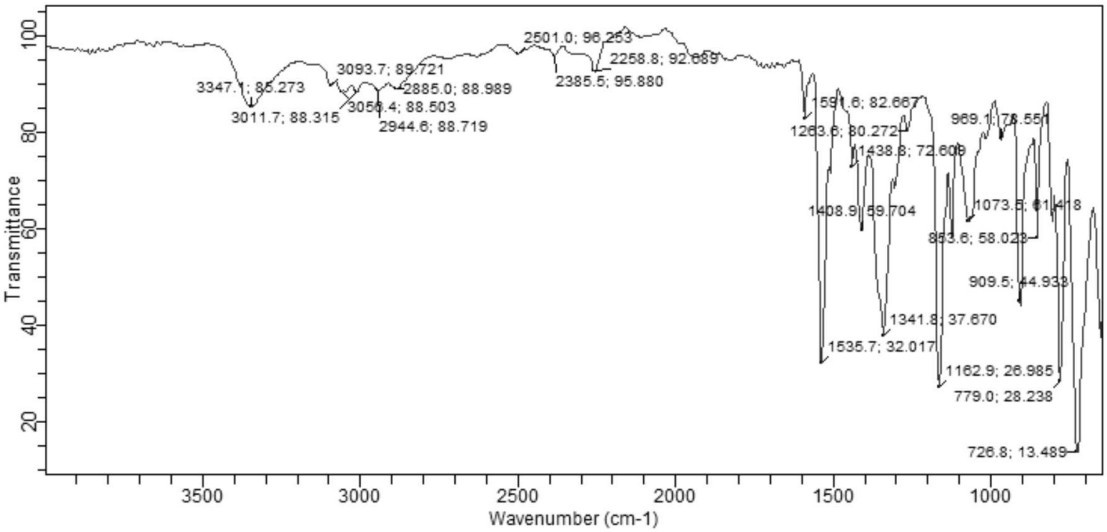

***N*-(4-(4-Chlorophenyl)but-3-en-1-yl)-2,4,6-trimethylbenzenesulfonamide (134d) (^{1}H NMR: 400 MHz, ^{13}C NMR: 101 MHz, $CDCl_3$; IR)**

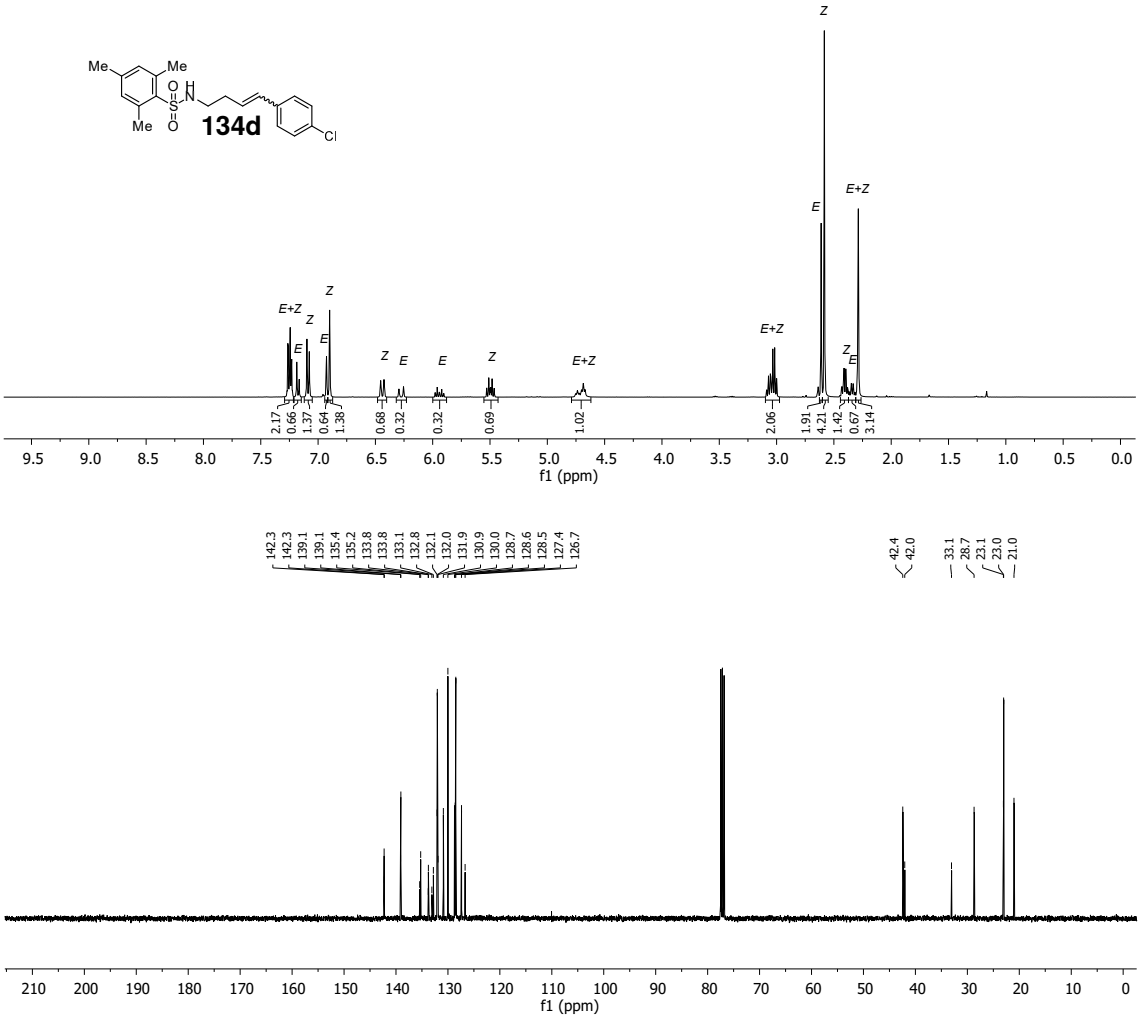

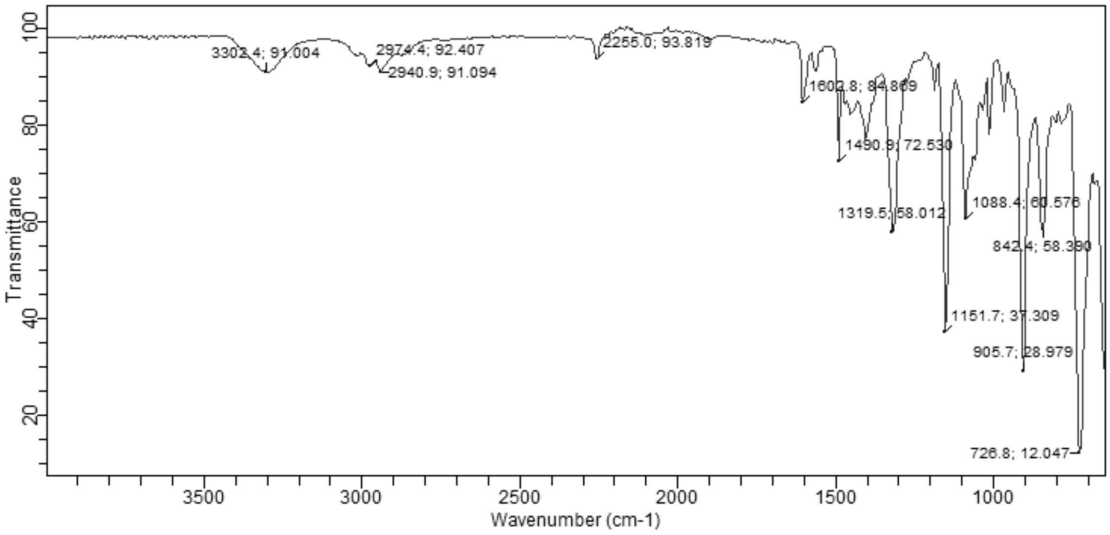
Transmittance
100
80
60
40
20
3302.4; 91.004
2974.4; 92.407
2940.9; 91.094
2255.0; 93.819
1602.8; 84.869
1490.9; 72.530
1319.5; 58.012
1088.4; 60.578
842.4; 58.390
1151.7; 37.309
905.7; 28.979
726.8; 12.047
3500
3000
2500
2000
1500
1000
Wavenumber (cm-1)

(*Z*)-*N*-(5,5-Dimethylhex-3-en-1-yl)-2,4,6-trimethylbenzenesulfonamide (134e) (^{1}H NMR: 300 MHz, ^{13}C NMR: 75 MHz, $CDCl_3$; IR)

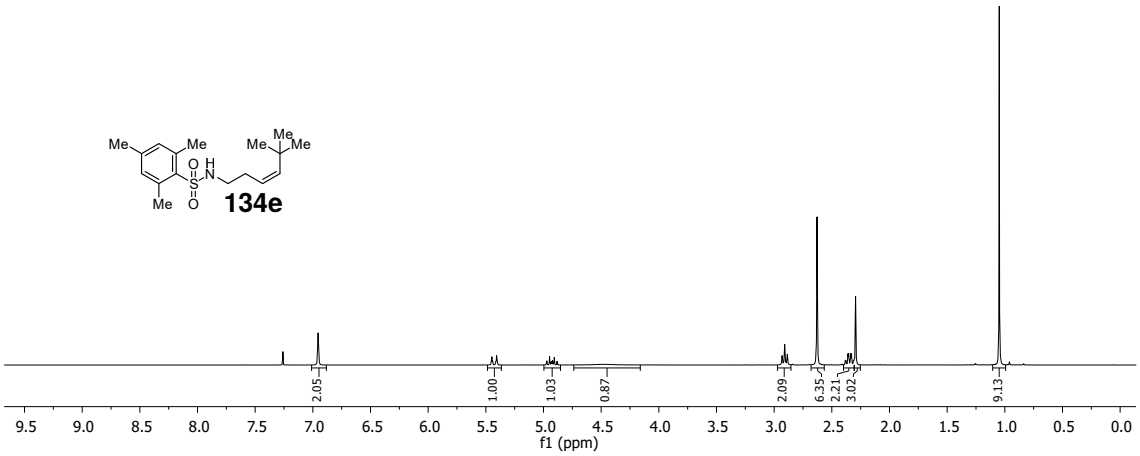

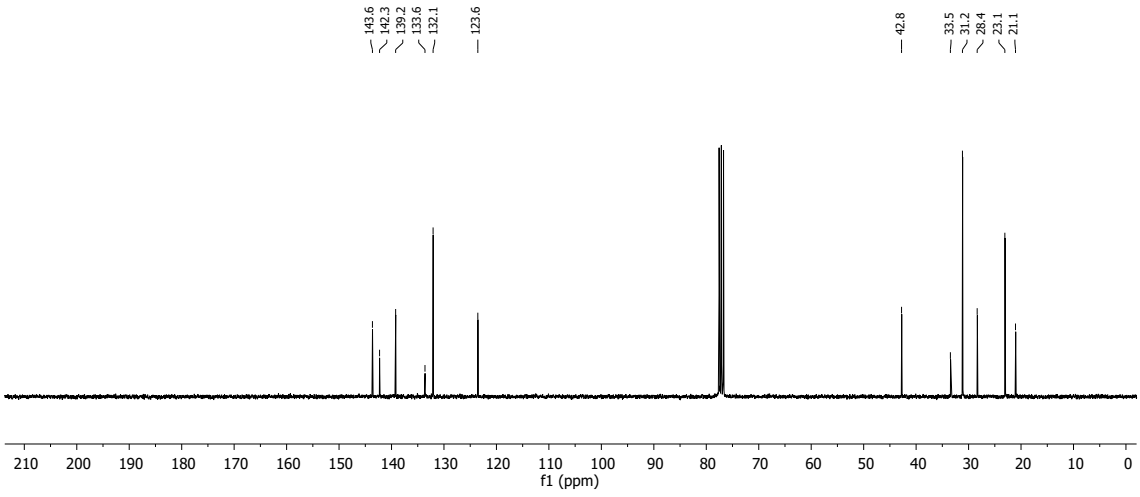

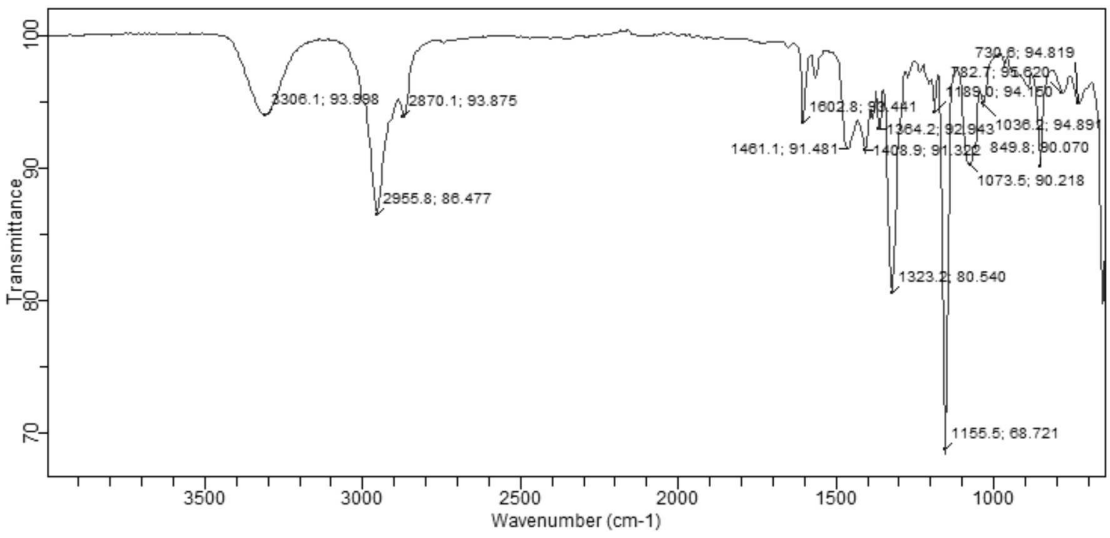

Methyl (*E*)-hex-3-enoate (148) (^{1}H NMR: 300 MHz, ^{13}C NMR: 75 MHz, $CDCl_3$; IR)

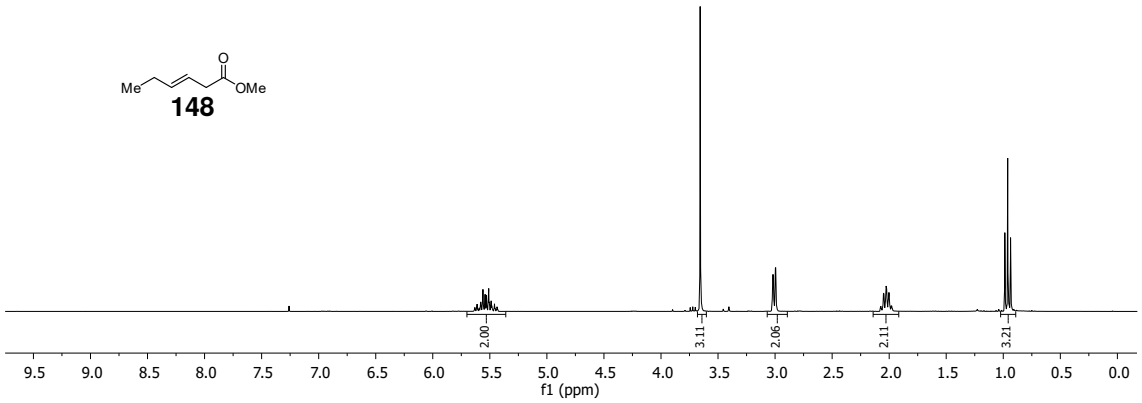

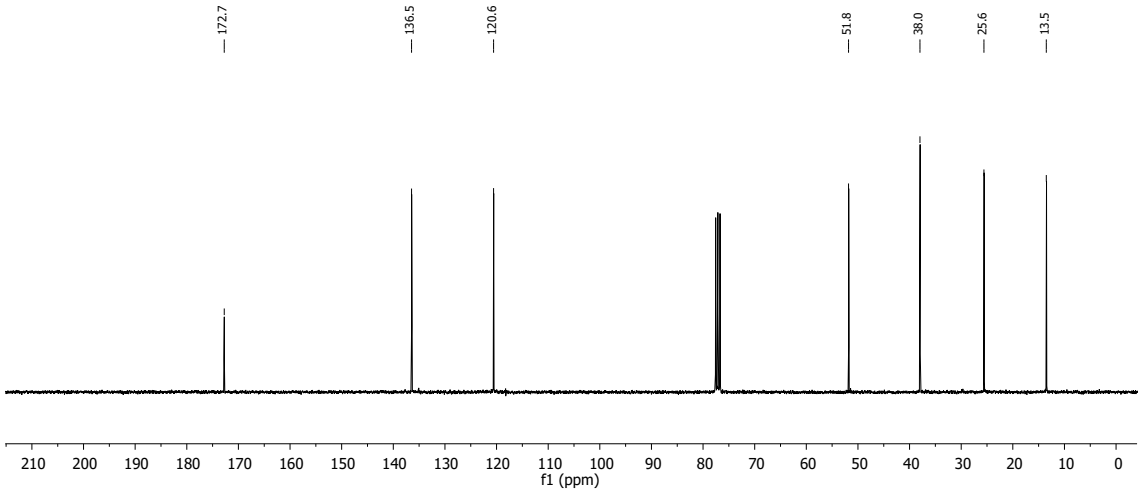

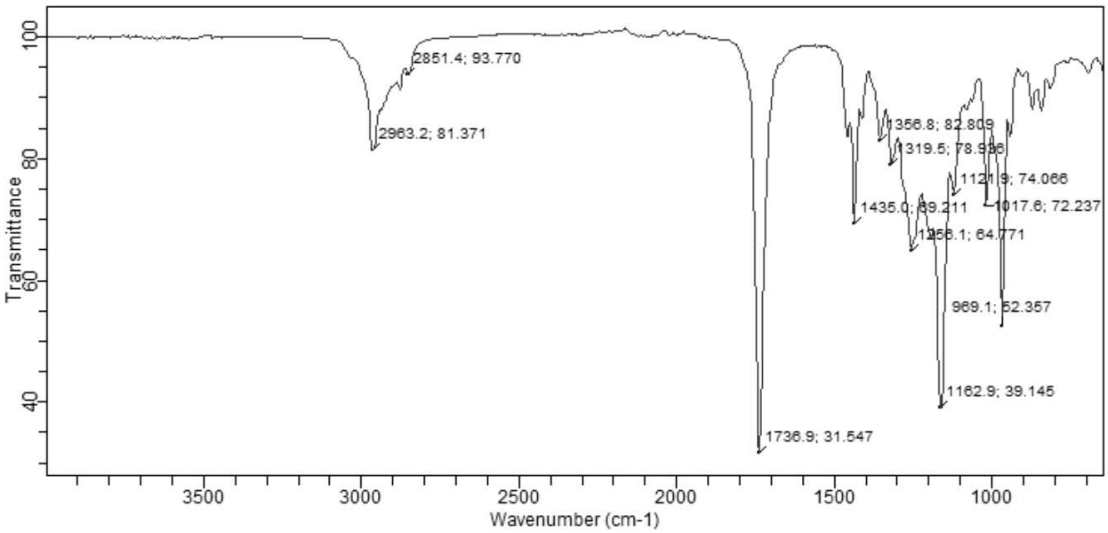

(*E*)-*N*-(Dec-6-en-5-yl)-*N*,4-dimethylbenzenesulfonamide (139) (^{1}H NMR: 300 MHz, ^{13}C NMR: 101 MHz, $CDCl_3$; IR; 2D NMR: COSY, HSQC, HMBC, $CDCl_3$)

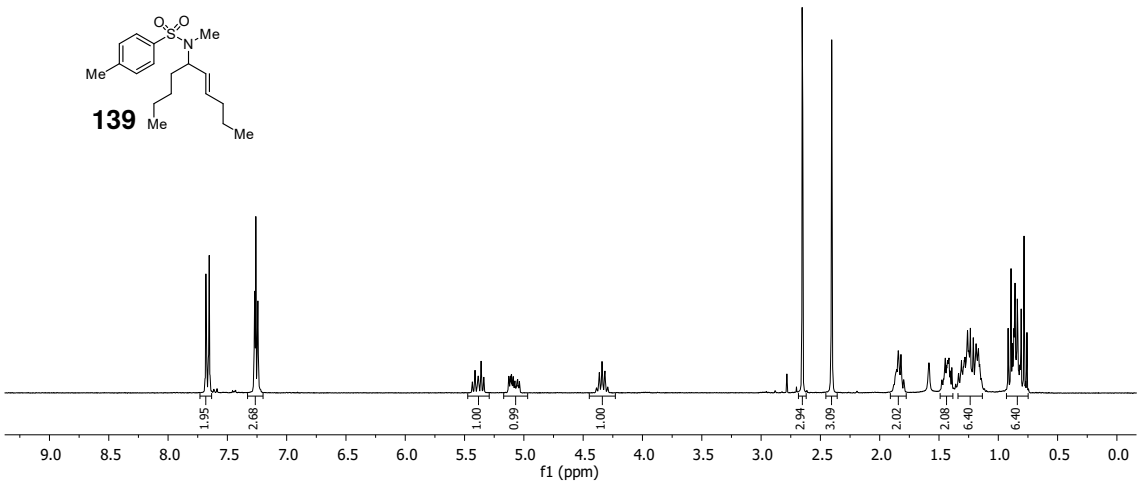

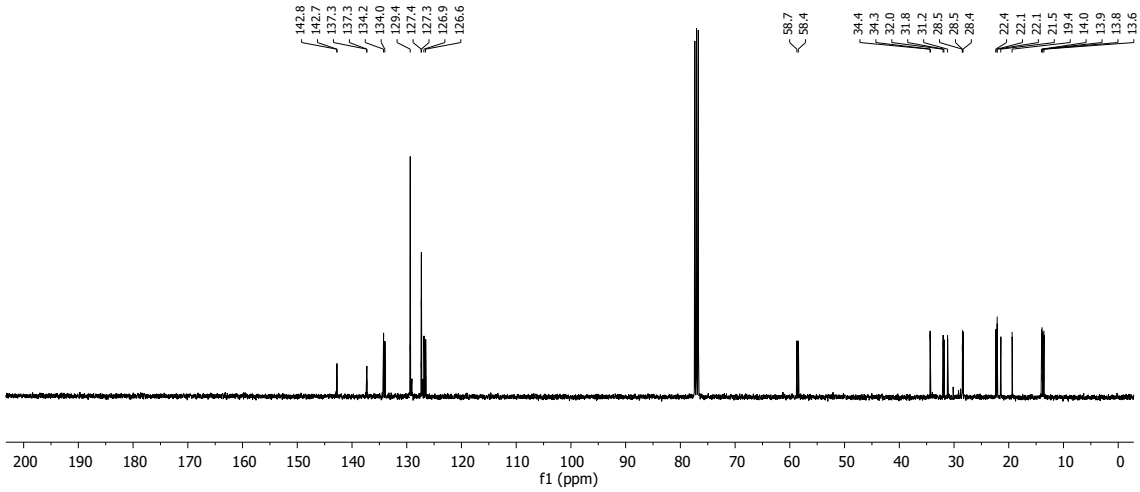

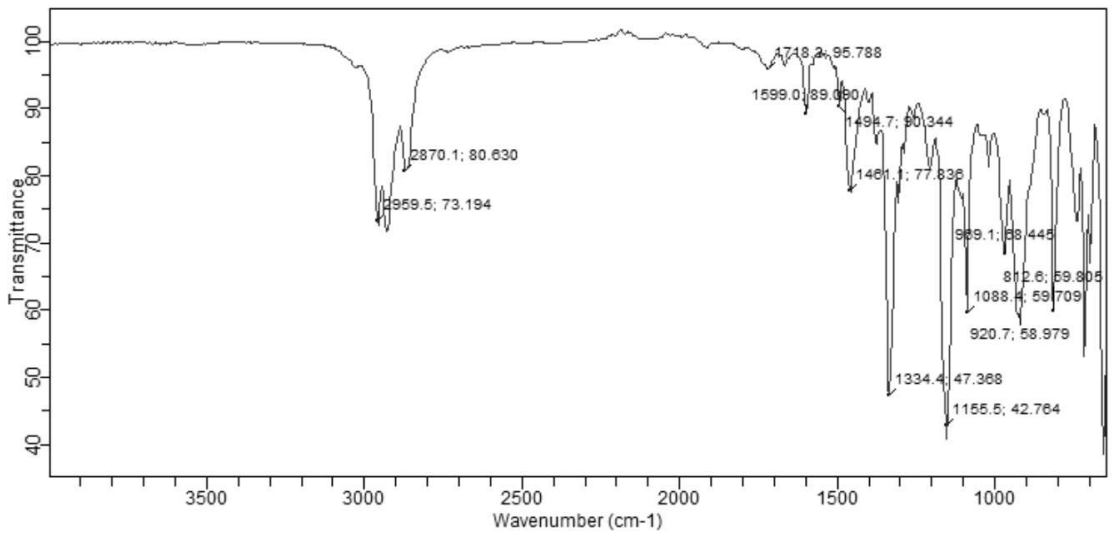

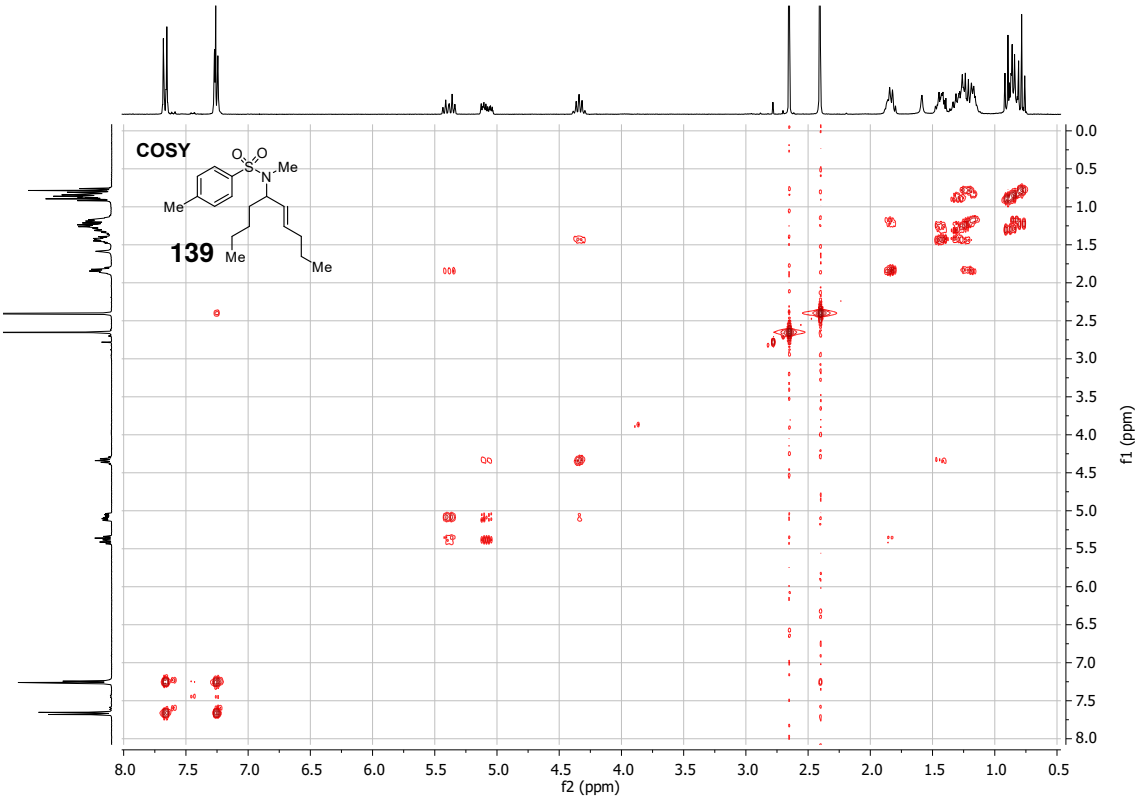
COSY
Me
Me
139
Me
Me
f2 (ppm)
f1 (ppm)

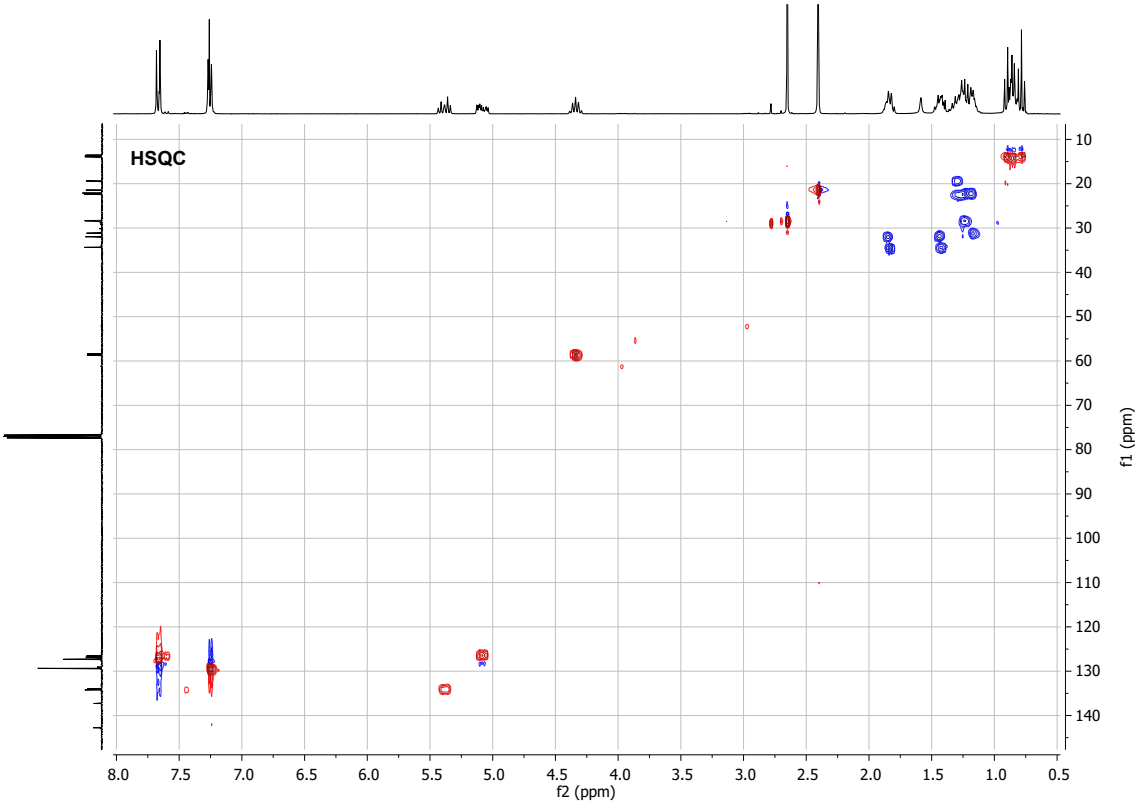
HSQC
f2 (ppm)
f1 (ppm)

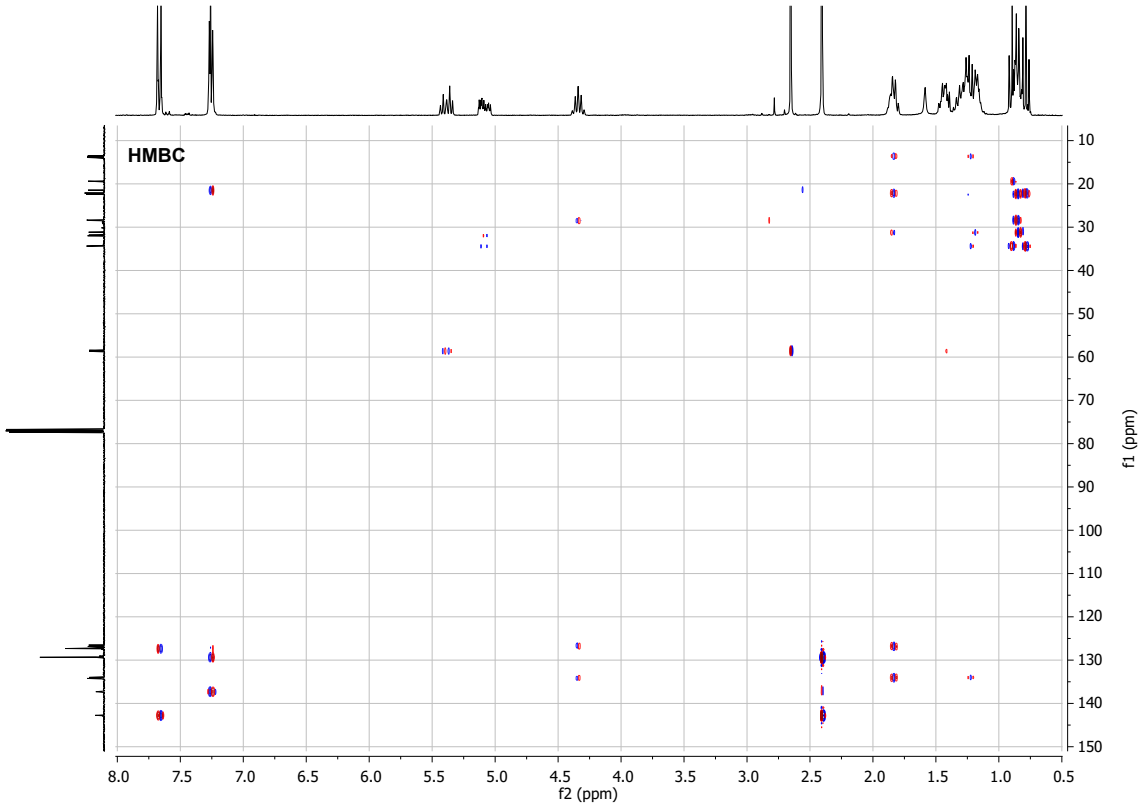
HMBC
f2 (ppm)
f1 (ppm)
8.0
7.5
7.0
6.5
6.0
5.5
5.0
4.5
4.0
3.5
3.0
2.5
2.0
1.5
1.0
0.5
10
20
30
40
50
60
70
80
90
100
110
120
130
140
150

Benzyl (*E*)-hex-3-enoate (150b) (^{1}H NMR: 300 MHz, ^{13}C NMR: 75 MHz, $CDCl_3$; IR)

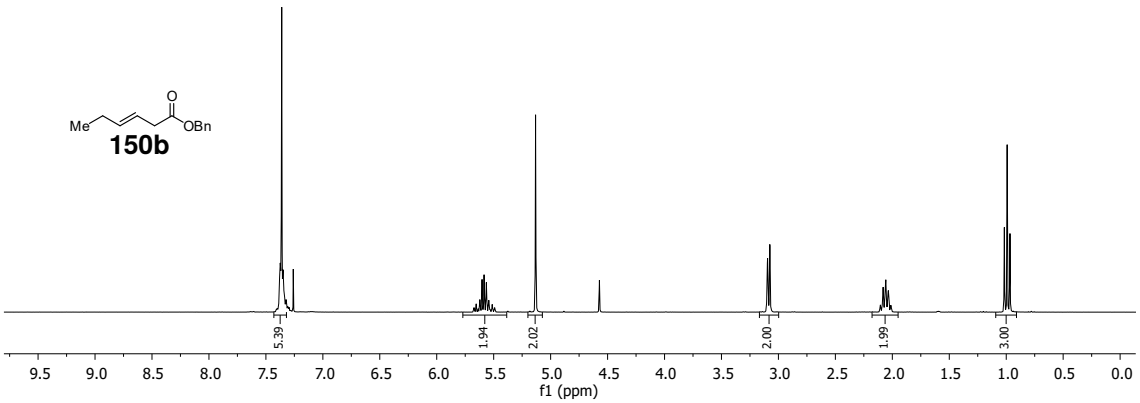

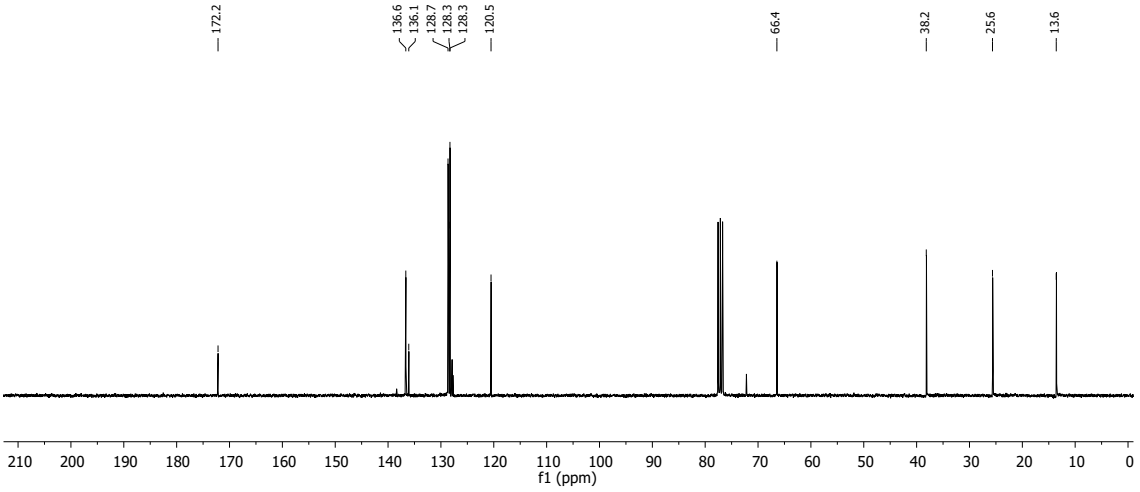

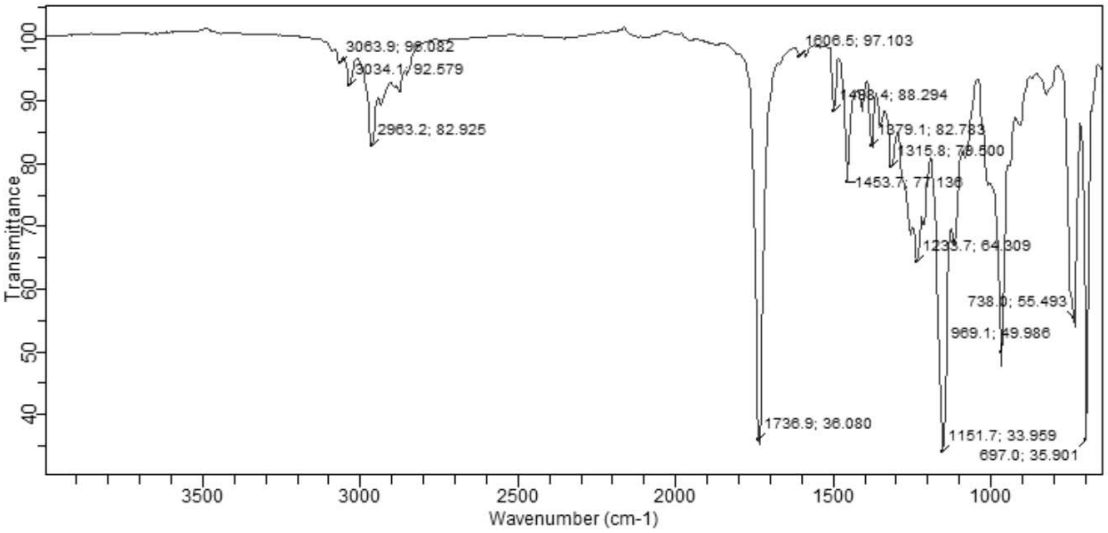

Dibenzyl (*E*)-hex-3-enedioate (150c) (^{1}H NMR: 300 MHz, ^{13}C NMR: 101 MHz, $CDCl_3$; IR)

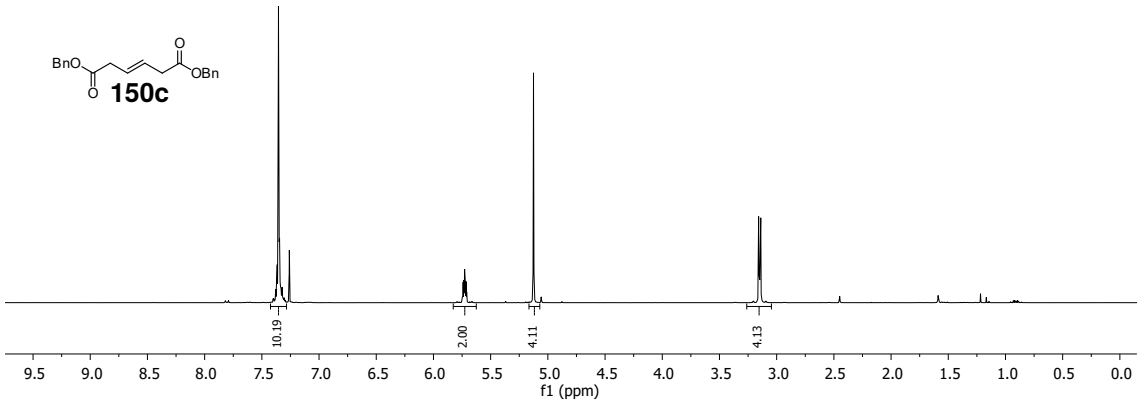

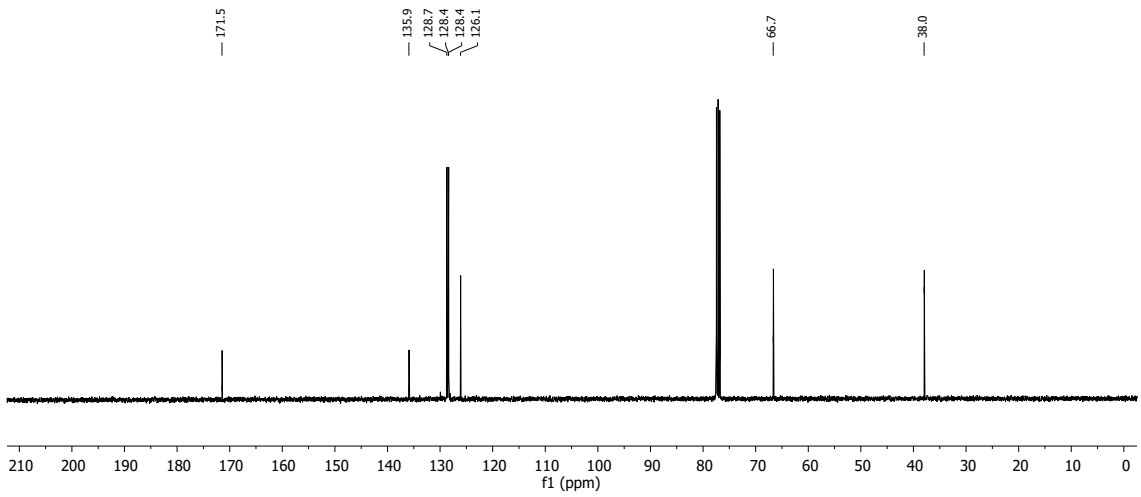

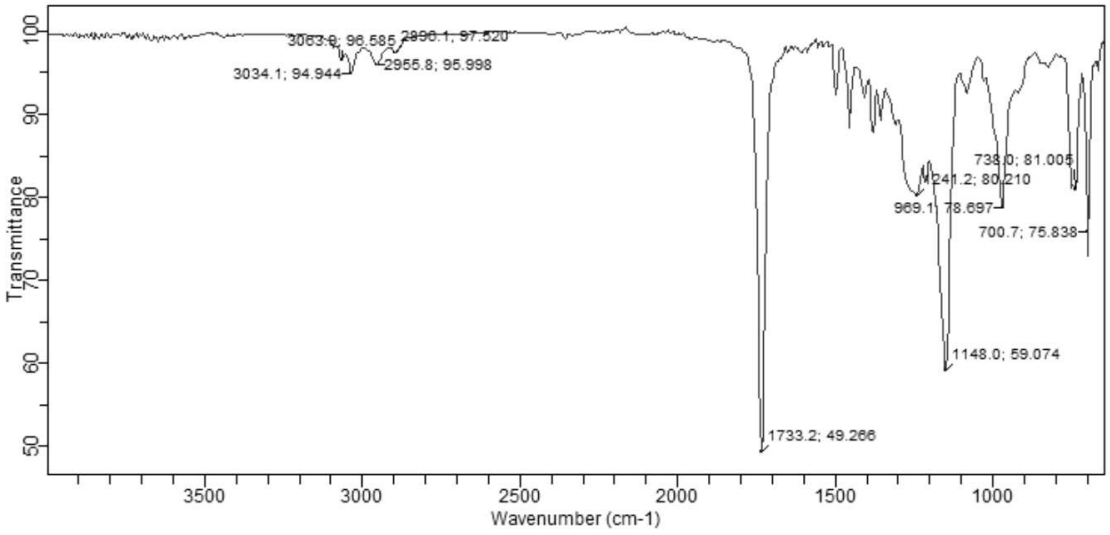

Hept-3-enenitrile (150d) (^{1}H NMR: 400 MHz, ^{13}C NMR: 101 MHz, $CDCl_3$; IR)

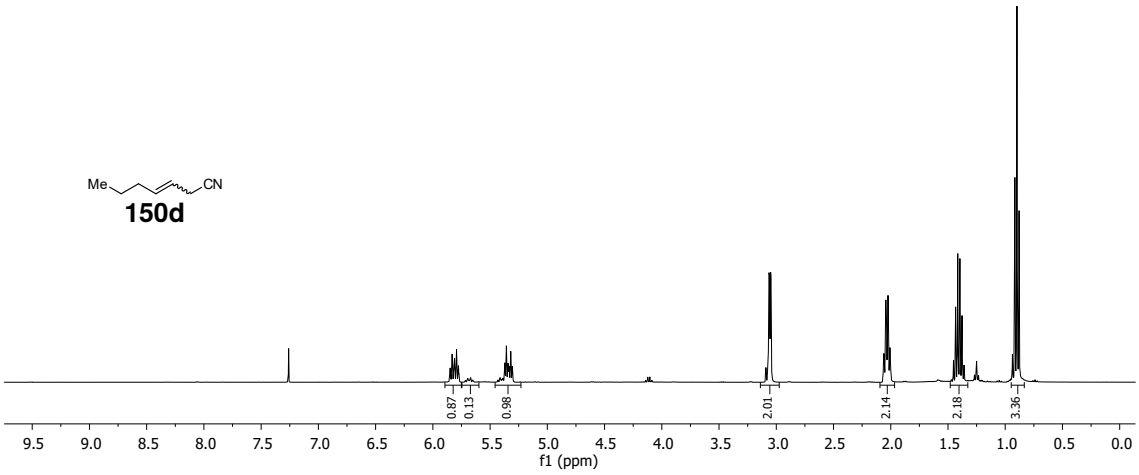

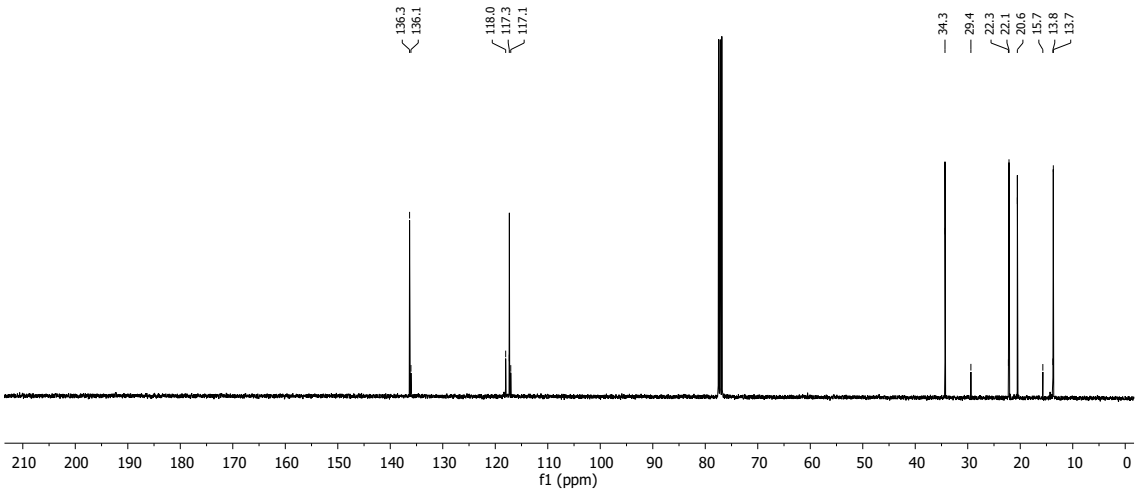

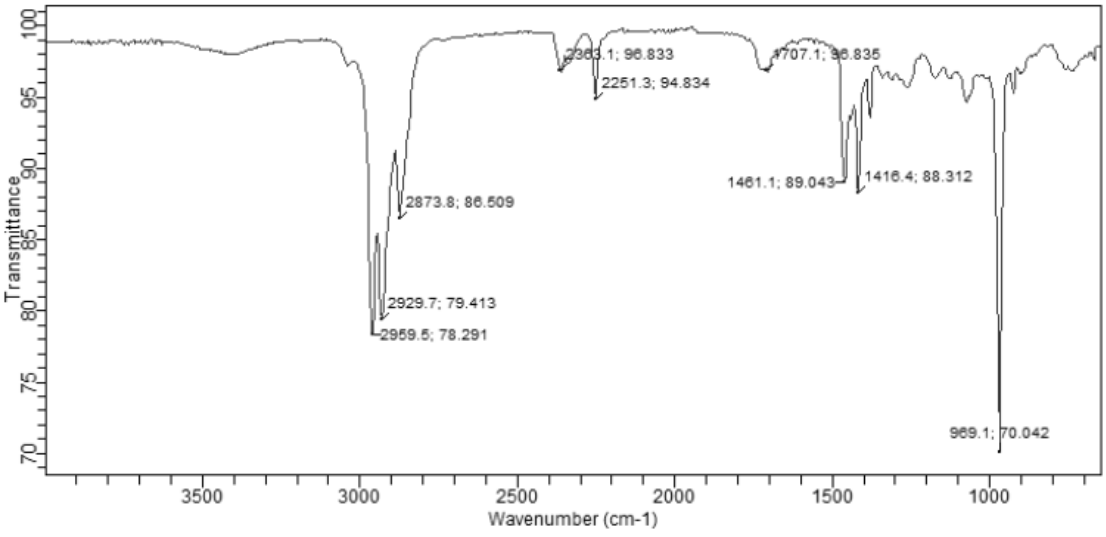

(But-2-en-1-ylsulfonyl)benzene (150e) (^{1}H NMR: 300 MHz, ^{13}C NMR: 75 MHz, $CDCl_3$; IR)

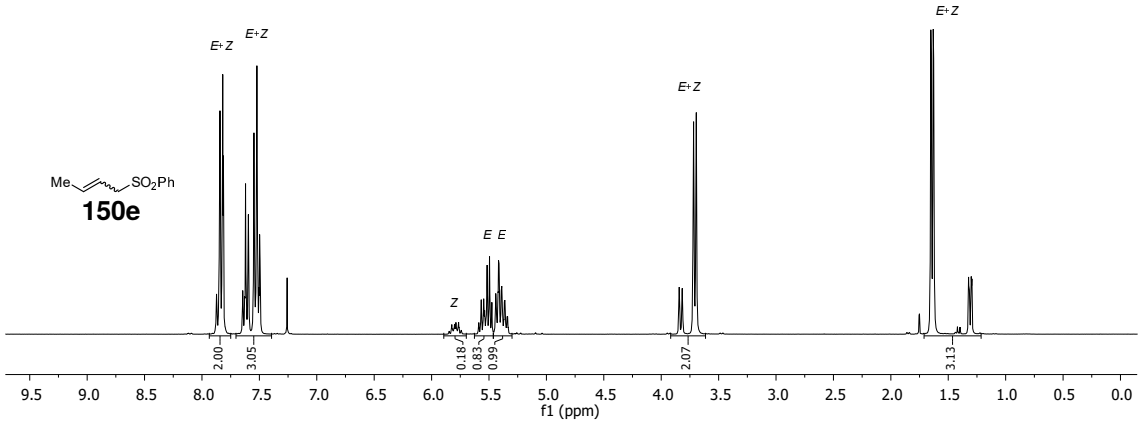

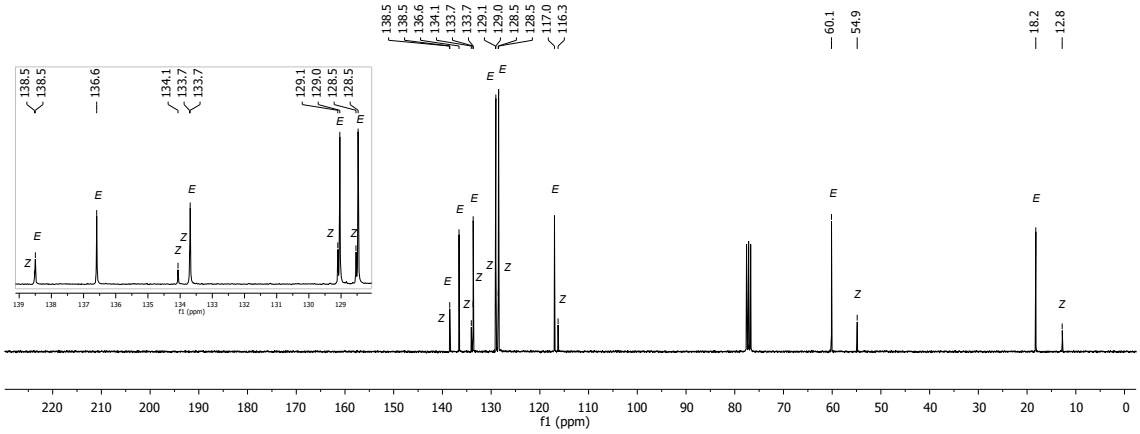

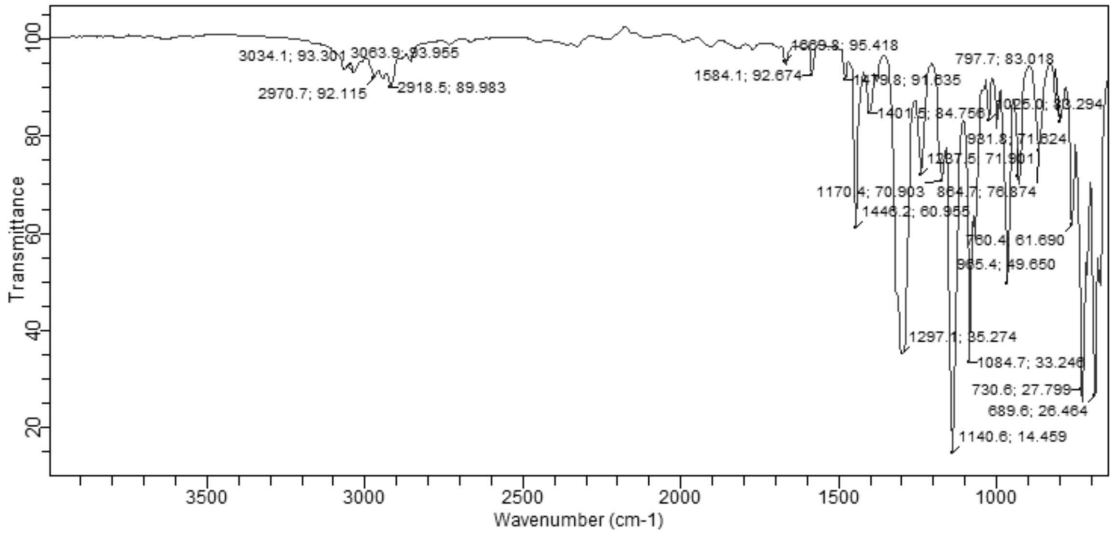

(Cinnamylsulfonyl)benzene (150f) (^{1}H NMR: 300 MHz, ^{13}C NMR: 75 MHz, $CDCl_3$; IR)

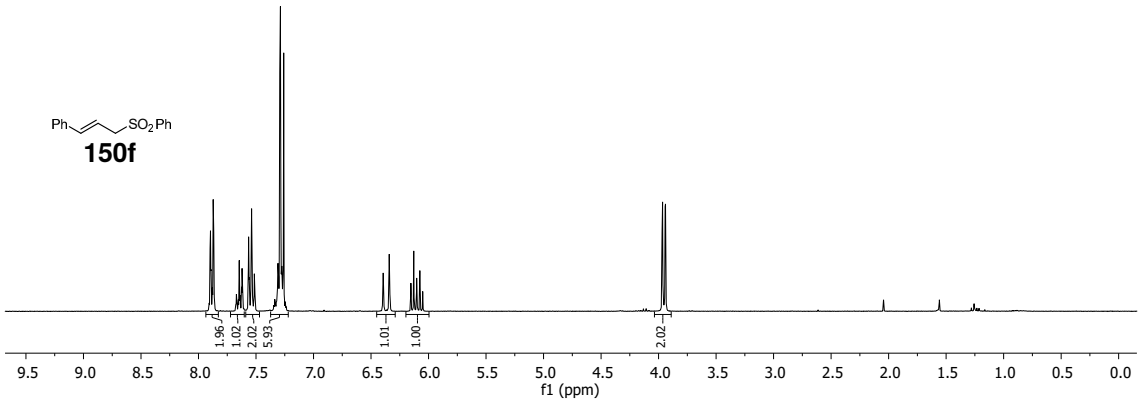

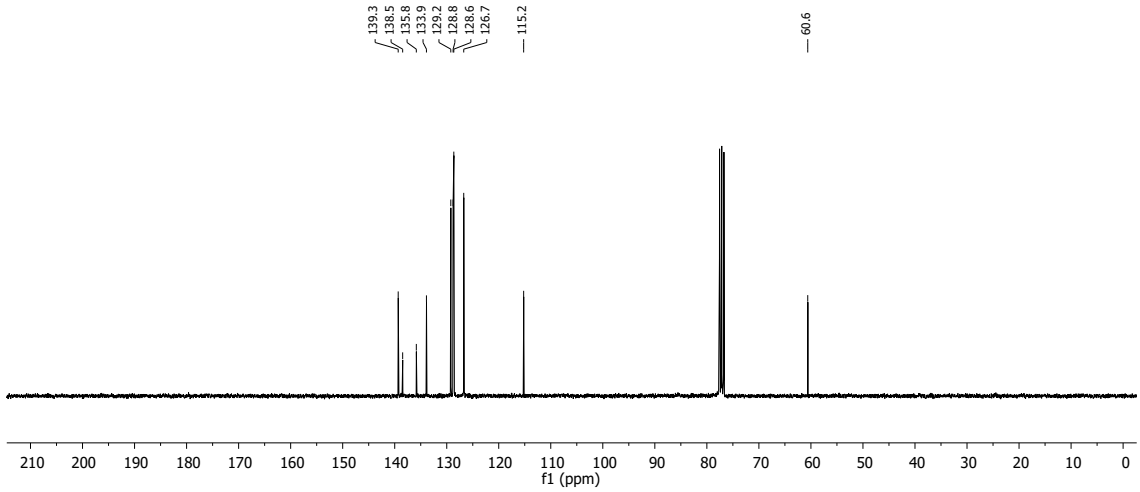

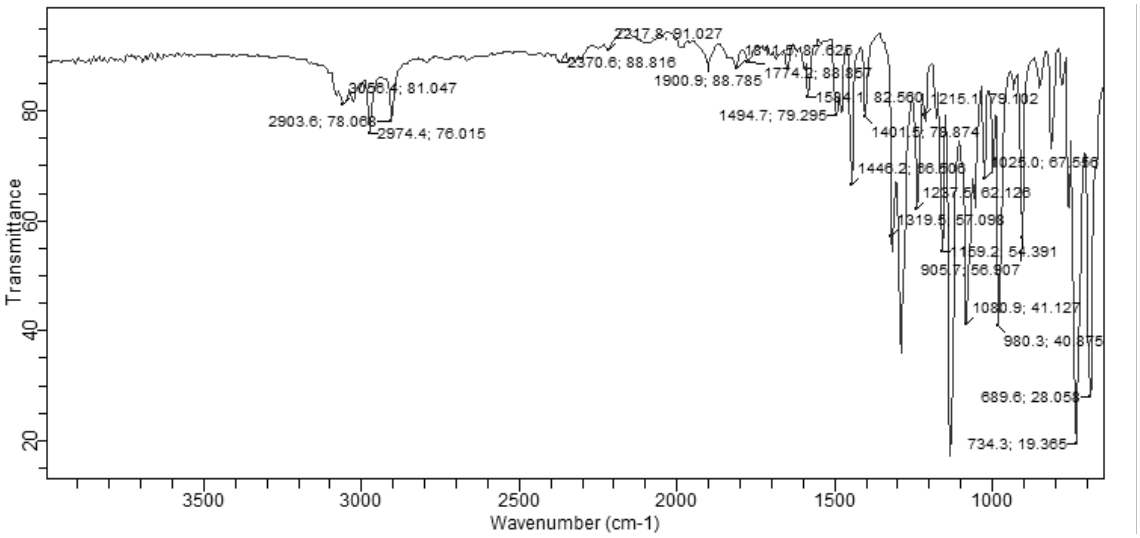

Diethyl but-2-en-1-ylphosphonate (150g) (^{1}H NMR: 400 MHz, ^{13}C NMR: 101 MHz, NOESY, $CDCl_3$; IR)

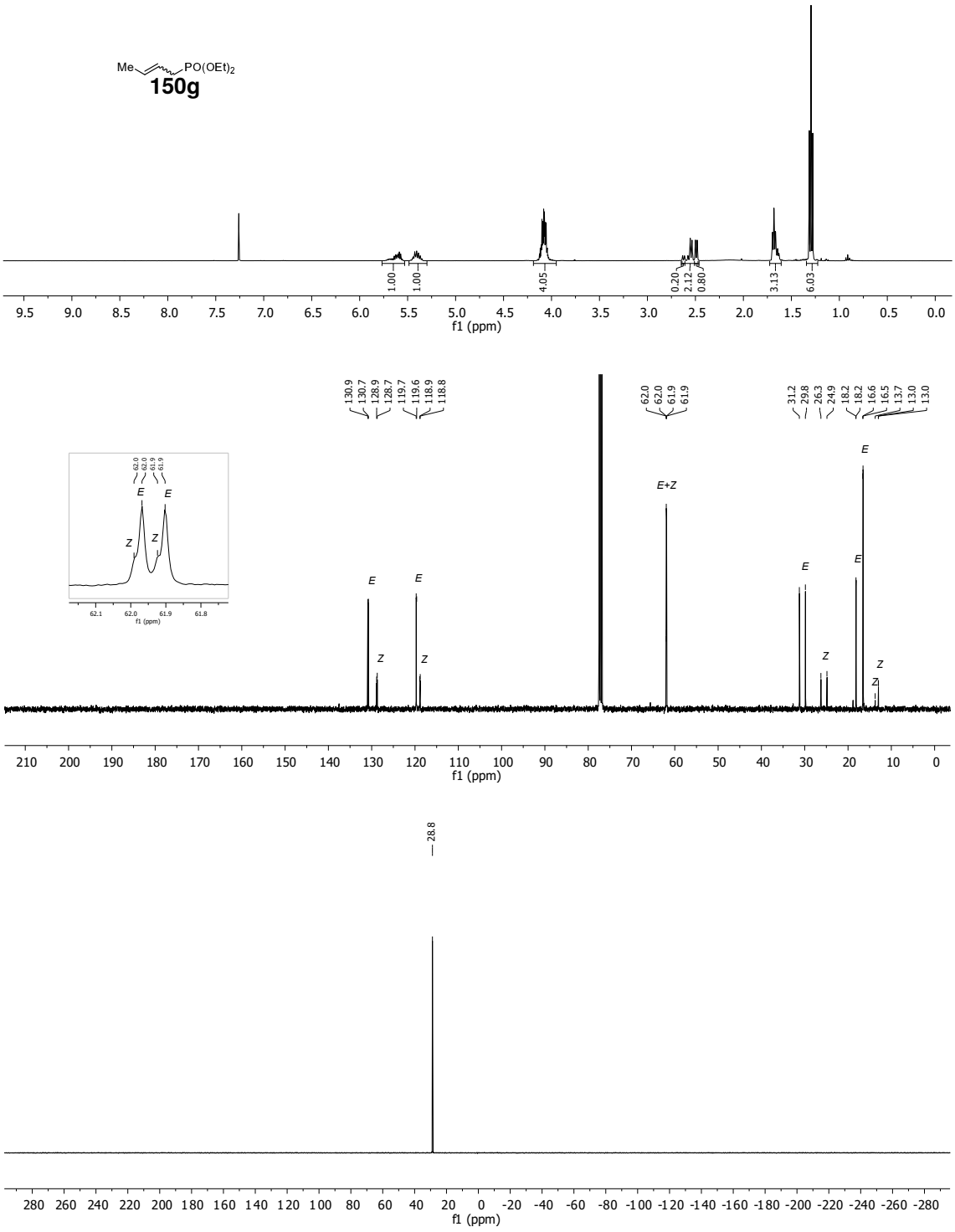

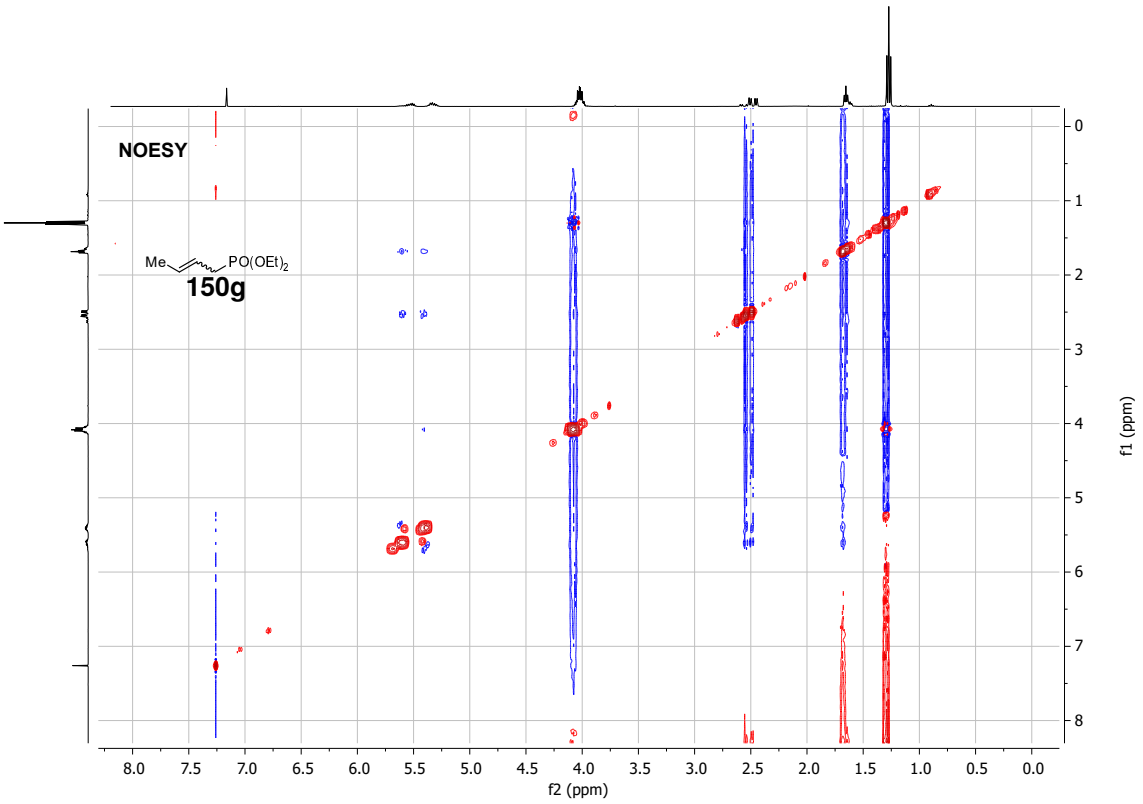
NOESY
Me
PO(OEt)2
150g
f2 (ppm)
f1 (ppm)

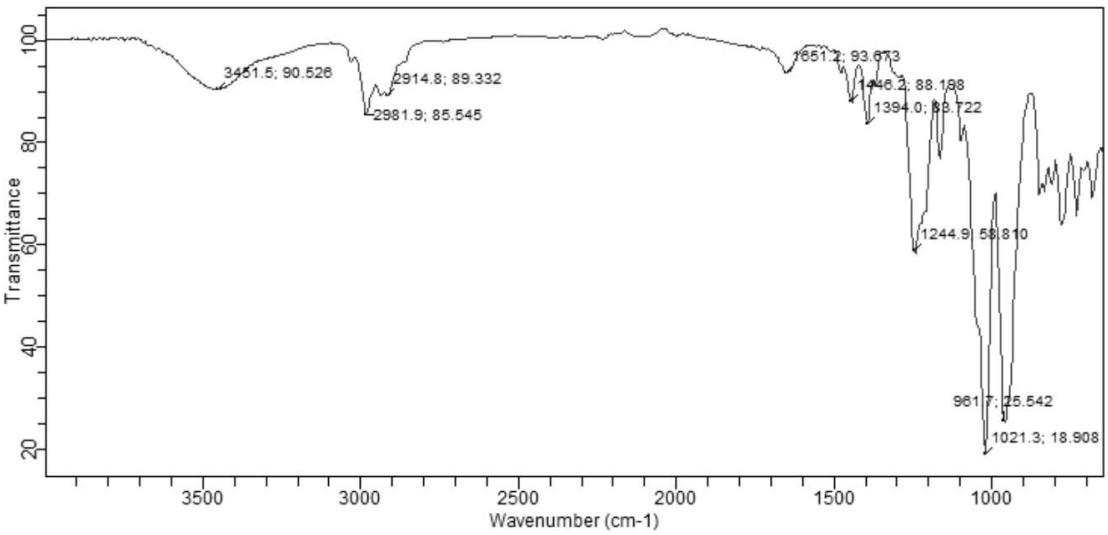
3451.5; 90.526
2914.8; 89.332
2981.9; 85.545
1651.2; 93.673
1446.2; 88.188
1394.0; 89.722
1244.9; 58.810
961.7; 25.542
1021.3; 18.908
Transmittance
Wavenumber (cm-1)

(*E*)-3-(Hex-3-enoyl)oxazolidin-2-one (150h)(^{1}H NMR: 300 MHz, ^{13}C NMR: 101 MHz, $CDCl_3$; IR)

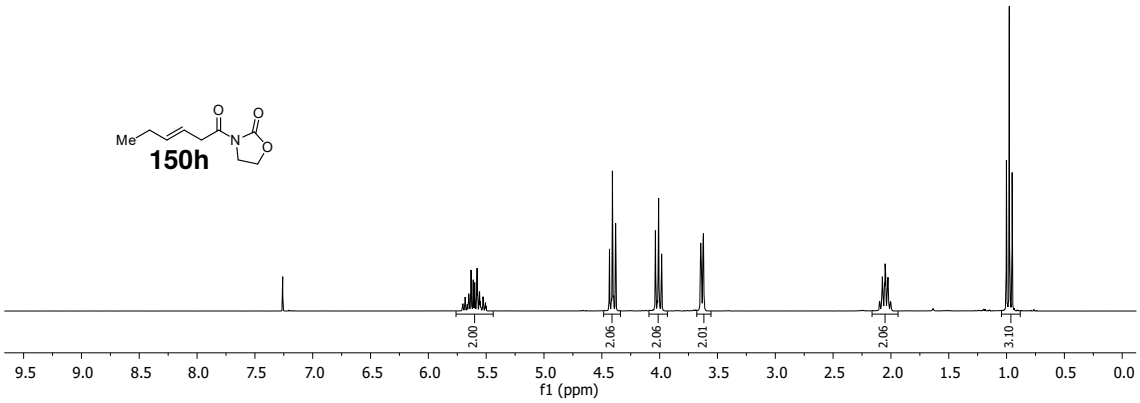

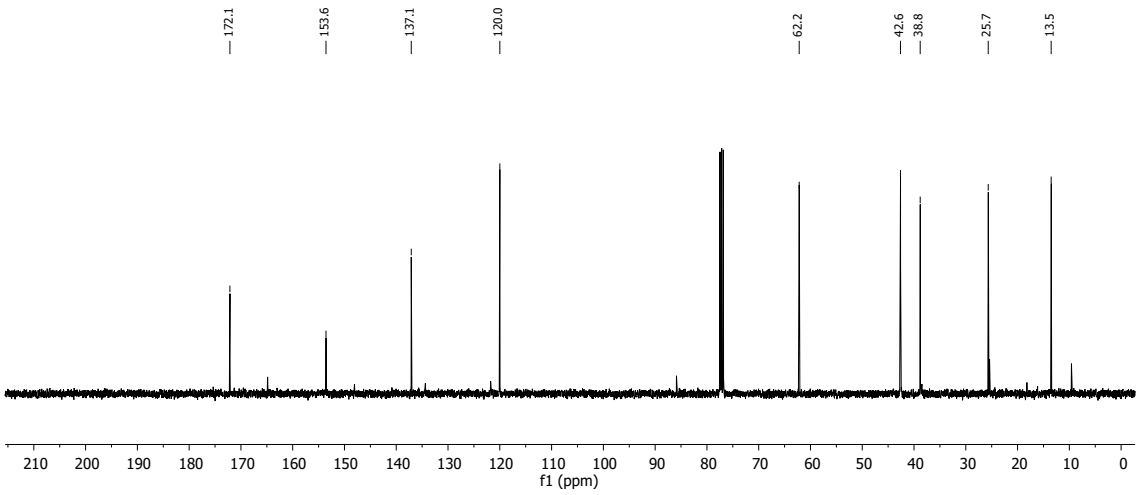

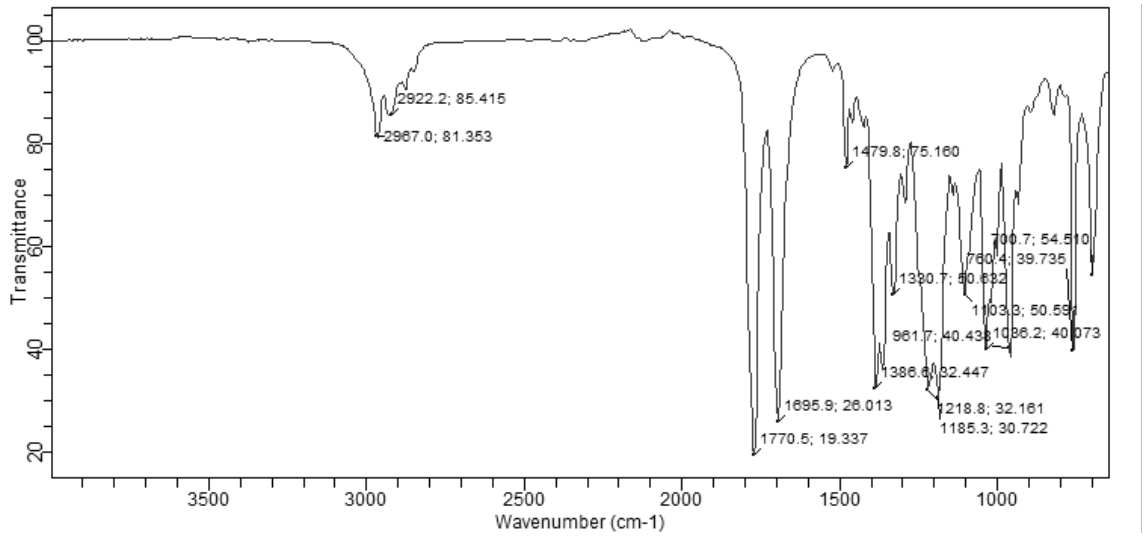

Ethyl (*E*)-4-(4-chloro-1H-pyrazol-1-yl)hex-2-enoate (152a) (^{1}H NMR: 300 MHz, ^{13}C NMR: 75 MHz, $CDCl_3$; IR)

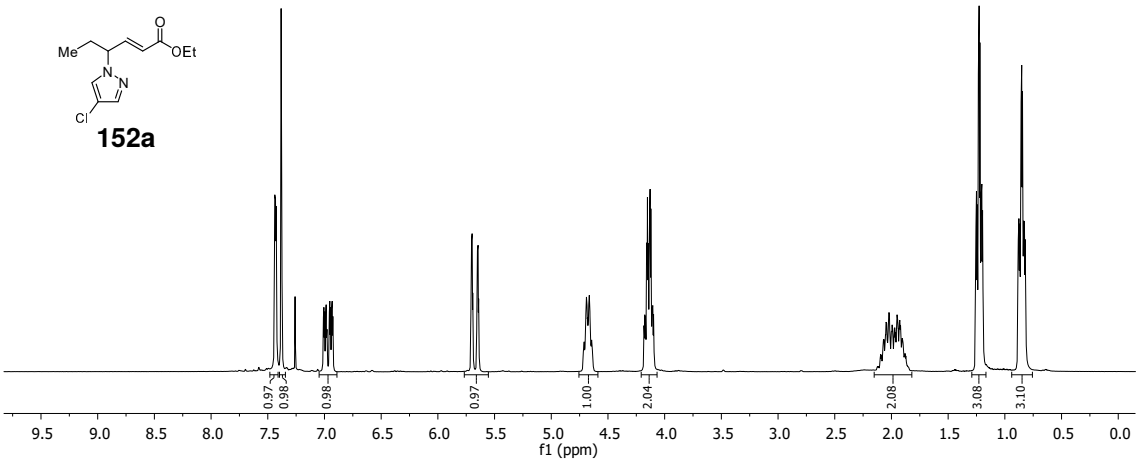

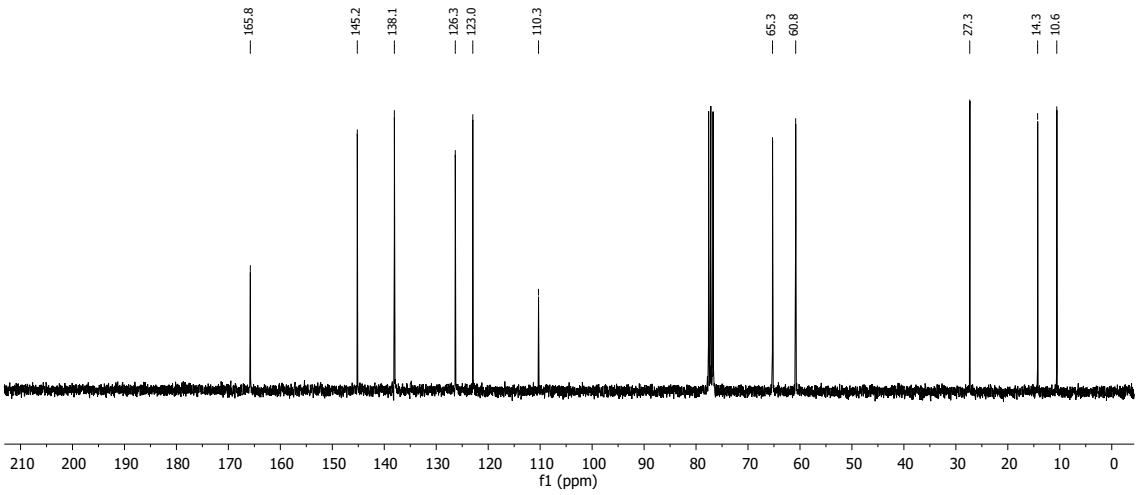

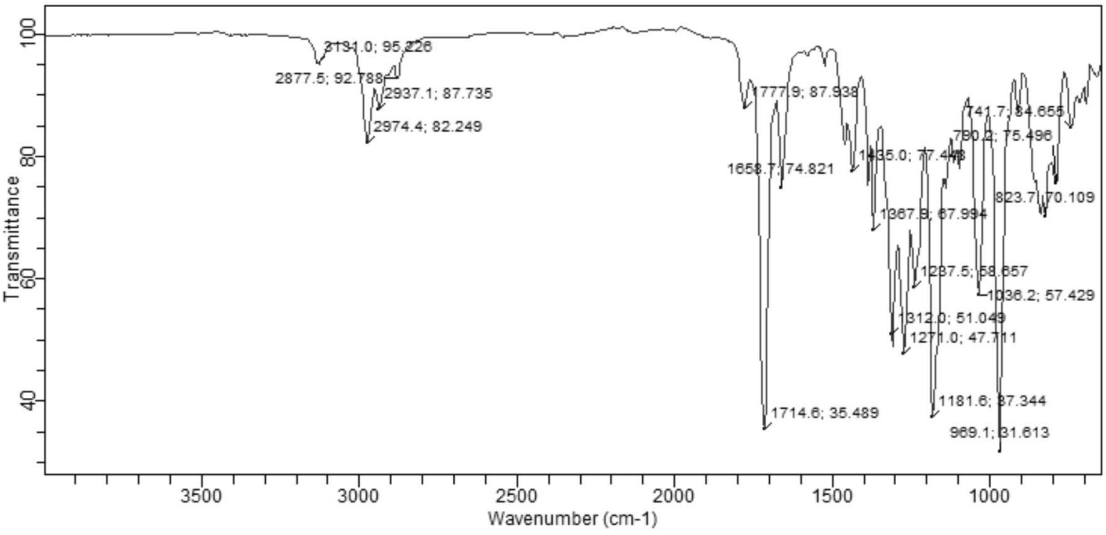

Ethyl (*Z*)-3-(3-chloro-1H-pyrrol-1-yl)hex-3-enoate (153a) (^{1}H NMR: 400 MHz, ^{13}C NMR: 101 MHz, $CDCl_3$; IR)

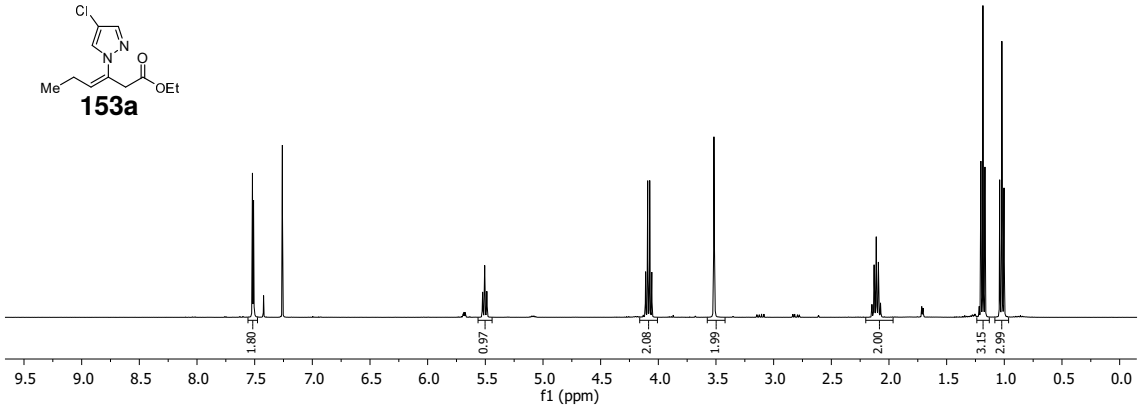

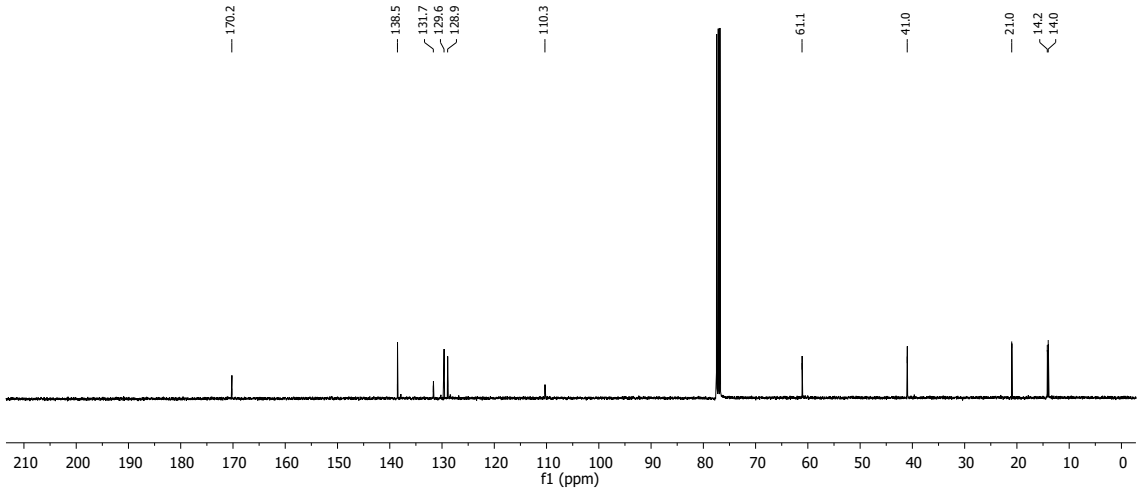

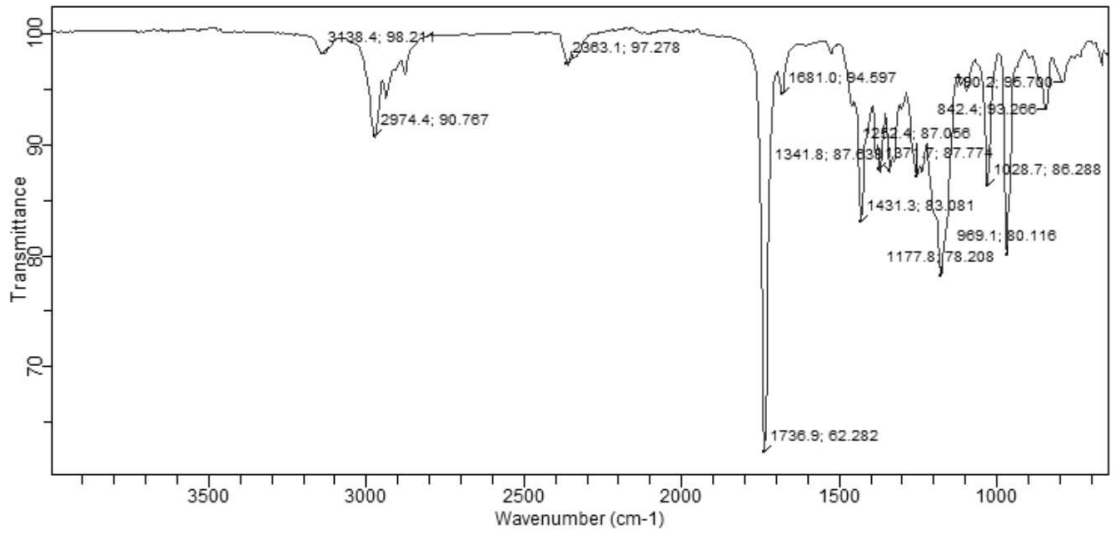

Phenyl (*E*)-4-(4-chloro-1H-pyrazol-1-yl)hex-2-enoate (152b) (^{1}H NMR: 300 MHz, ^{13}C NMR: 101 MHz, $CDCl_3$; IR)

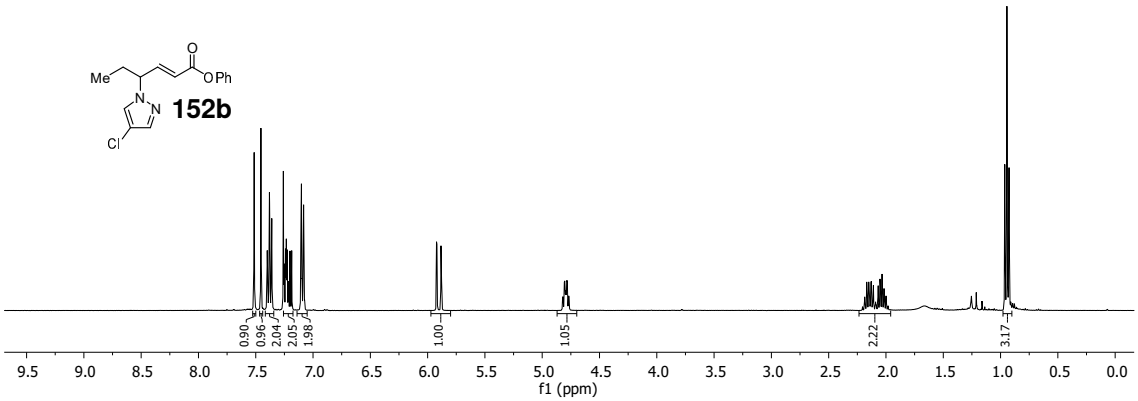

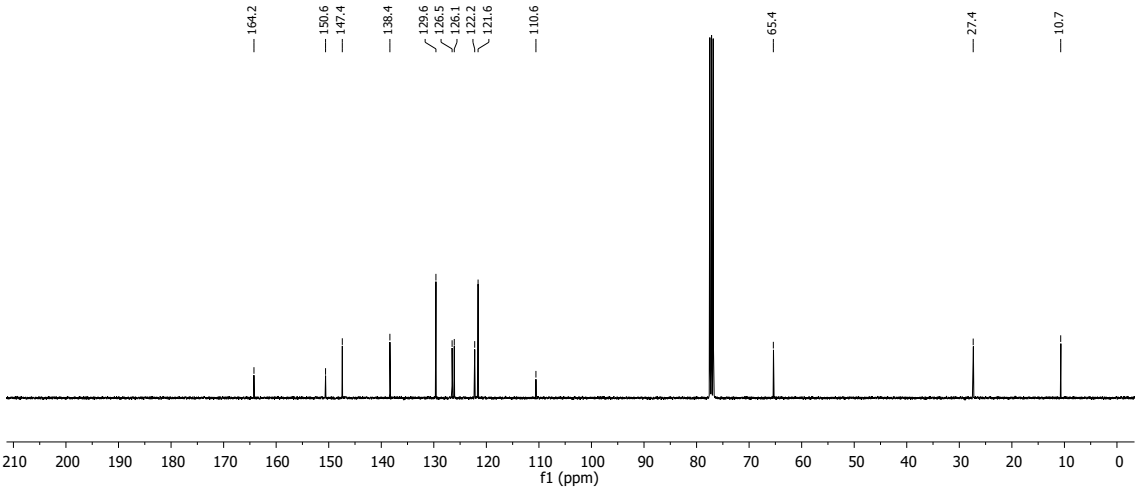

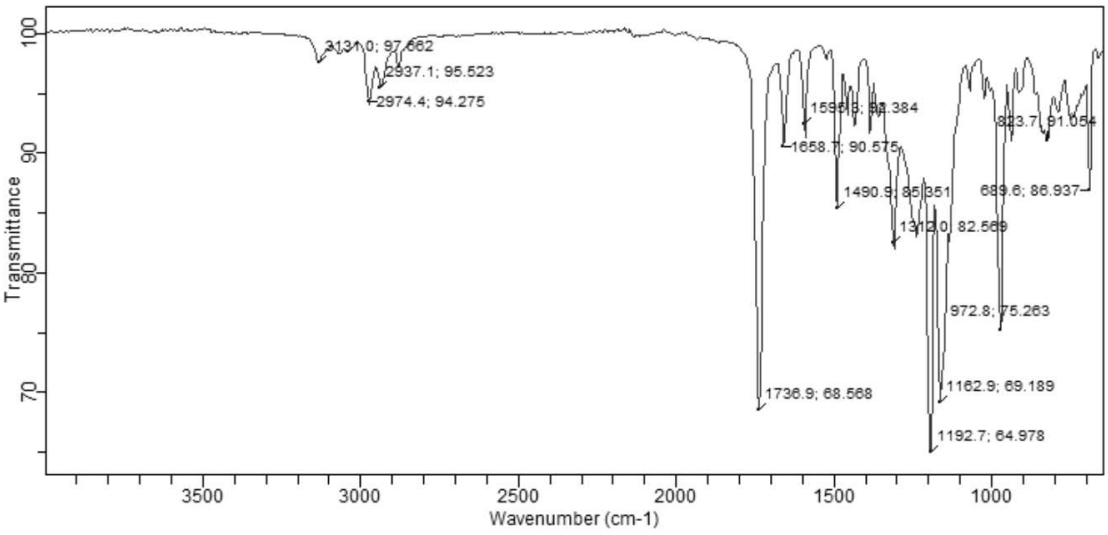

Phenyl (*Z*)-3-(4-chloro-1H-pyrazol-1-yl)hex-3-enoate (153b) (^{1}H NMR: 400 MHz, ^{13}C NMR: 101 MHz, $CDCl_3$; IR)

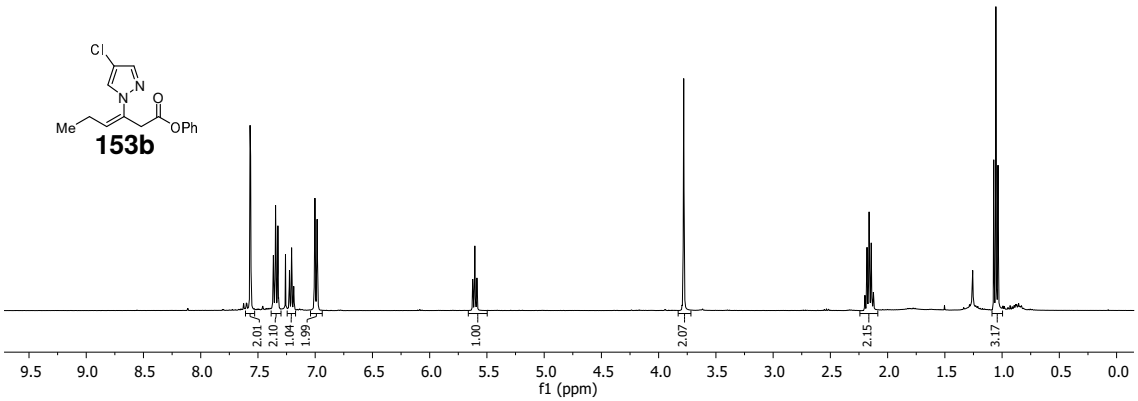

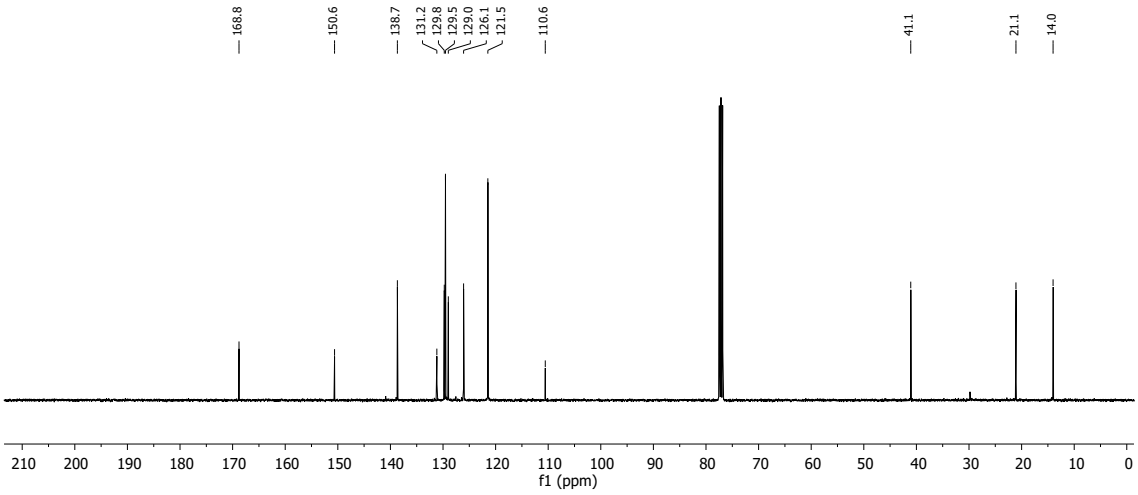

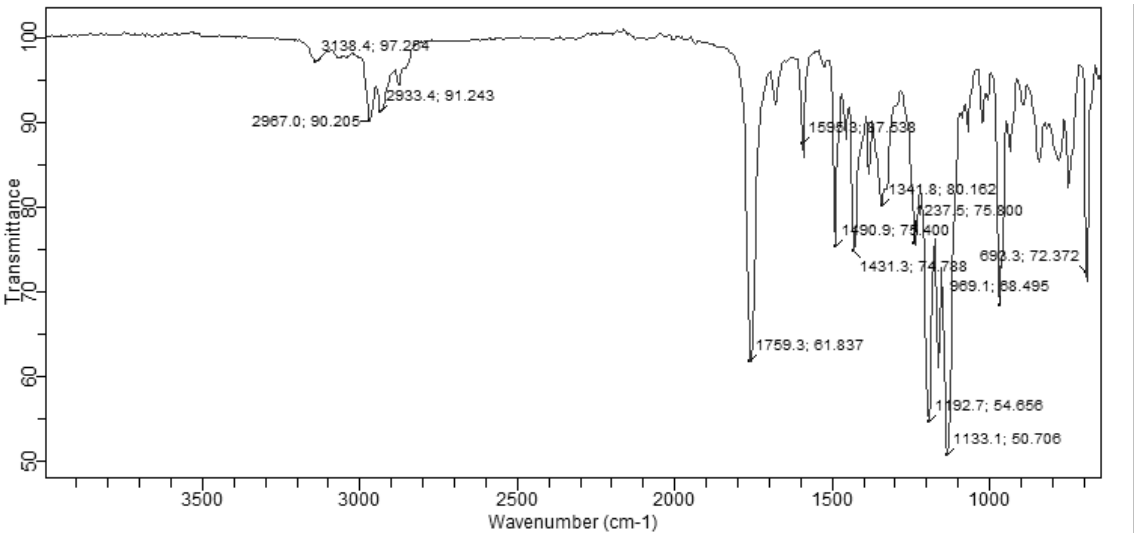

Benzyl (*E*)-4-(4-chloro-1H-pyrazol-1-yl)hex-2-enoate (152c) (^{1}H NMR: 300 MHz, ^{13}C NMR: 101 MHz, $CDCl_3$; IR)

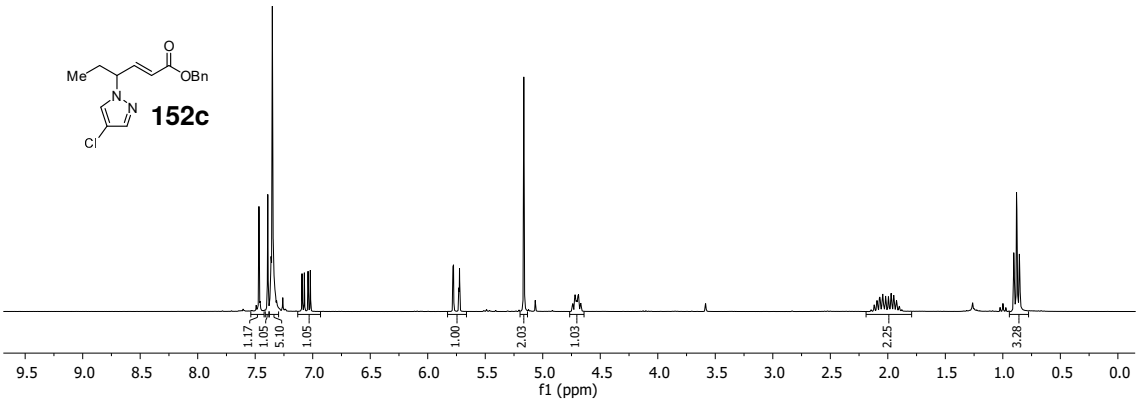

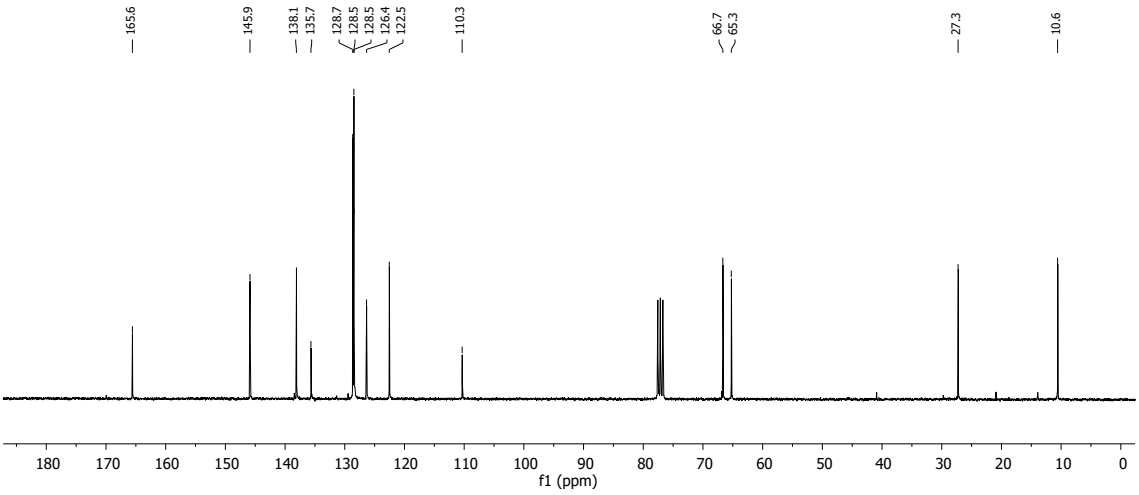

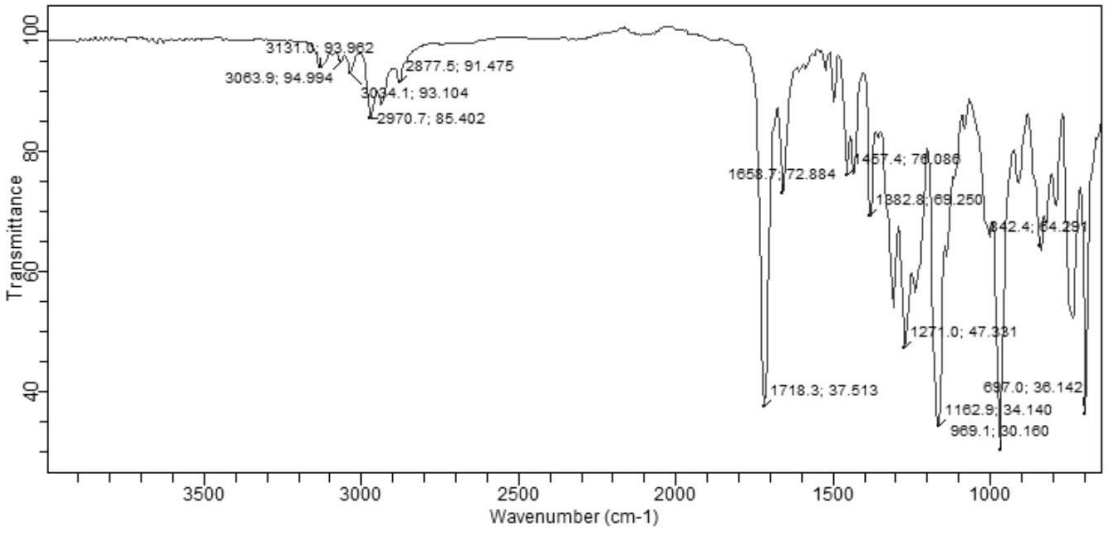

Diethyl (*E*)-4-(4-chloro-1H-pyrazol-1-yl)hex-2-enedioate (152i) (^{1}H NMR: 300 MHz, ^{13}C NMR: 101 MHz, $CDCl_3$; IR)

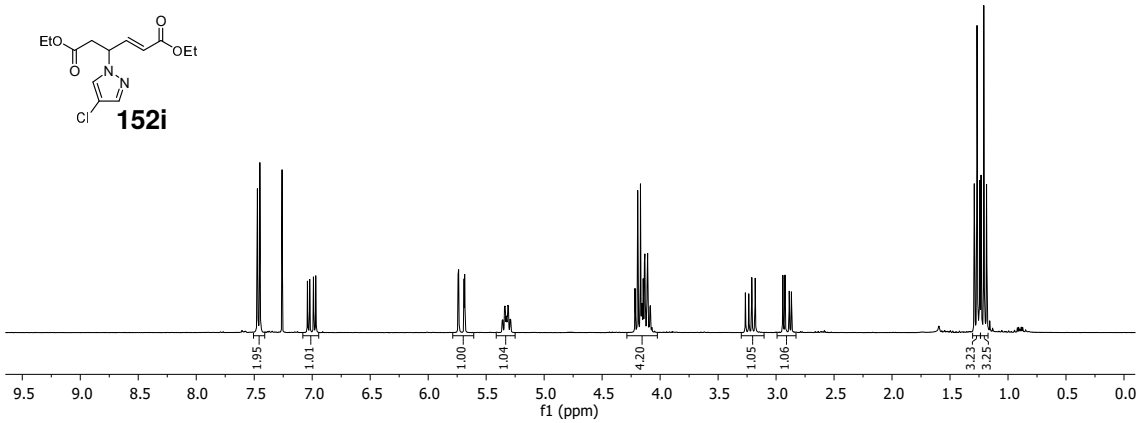

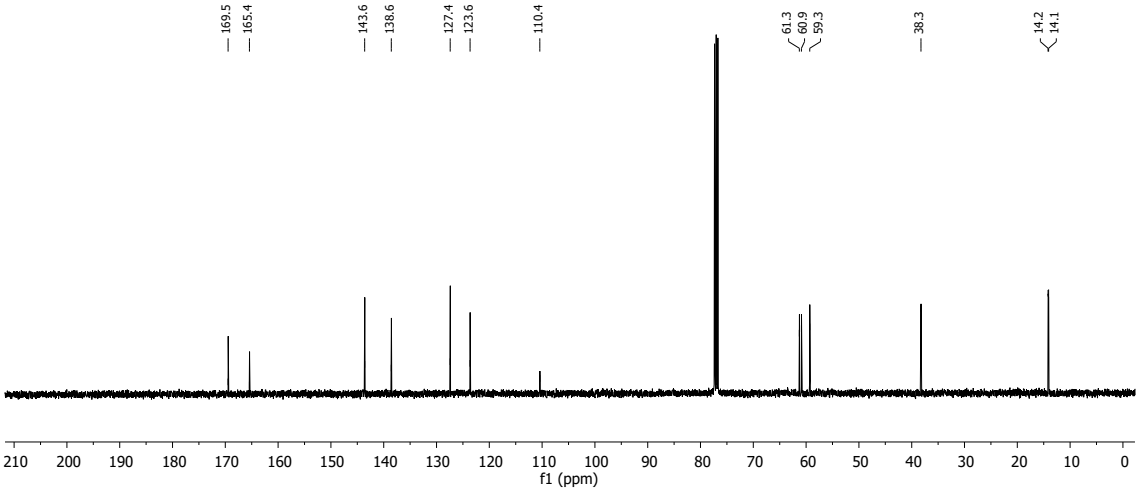

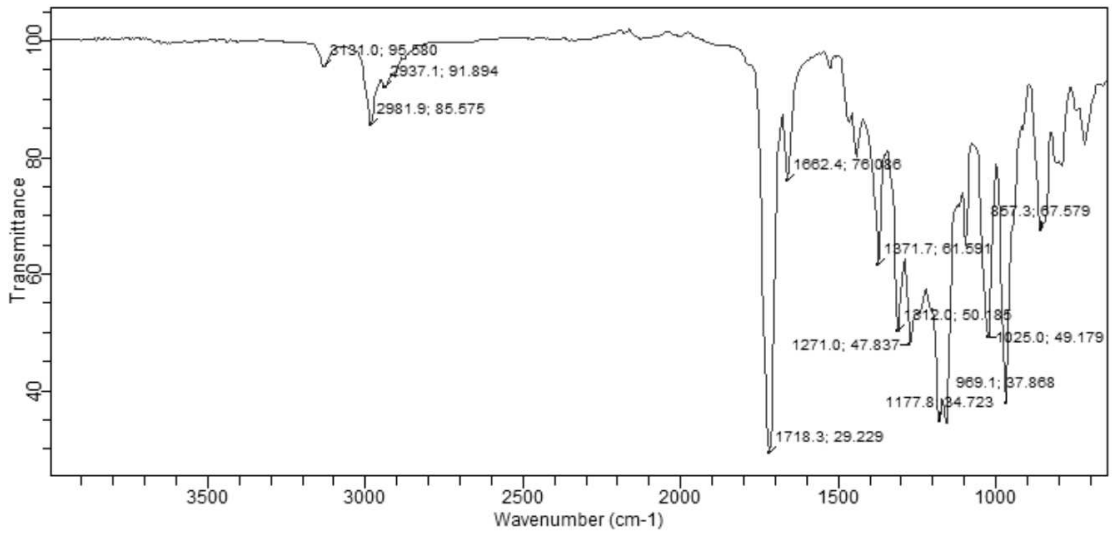

Dibenzyl (*E*)-4-(4-chloro-1H-pyrazol-1-yl)hex-2-enedioate (152j) (^{1}H NMR: 400 MHz, ^{13}C NMR: 101 MHz, $CDCl_3$; IR)

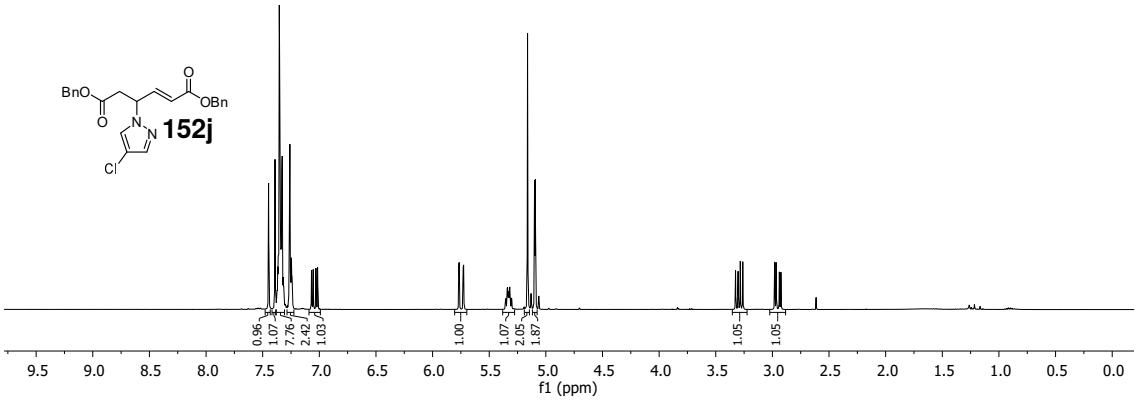

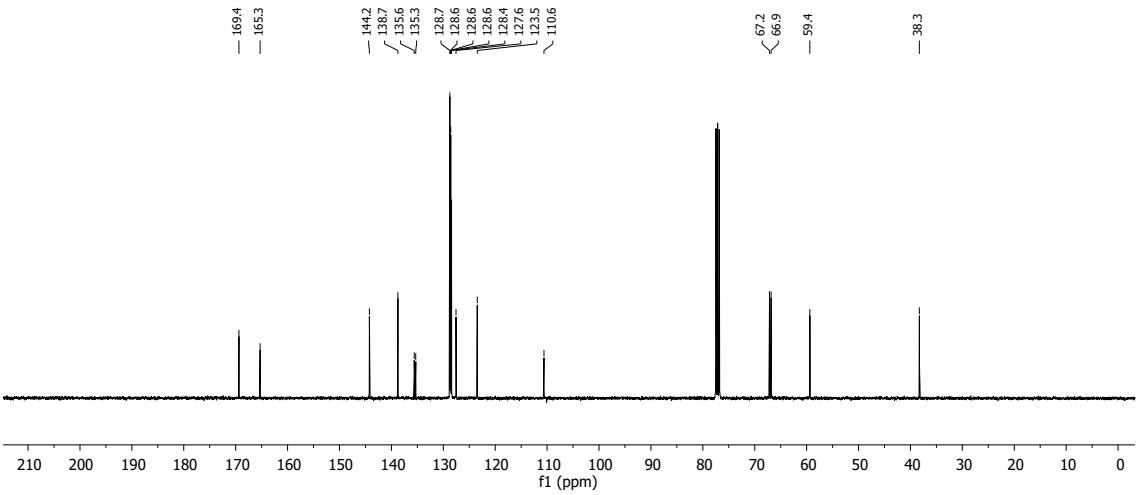

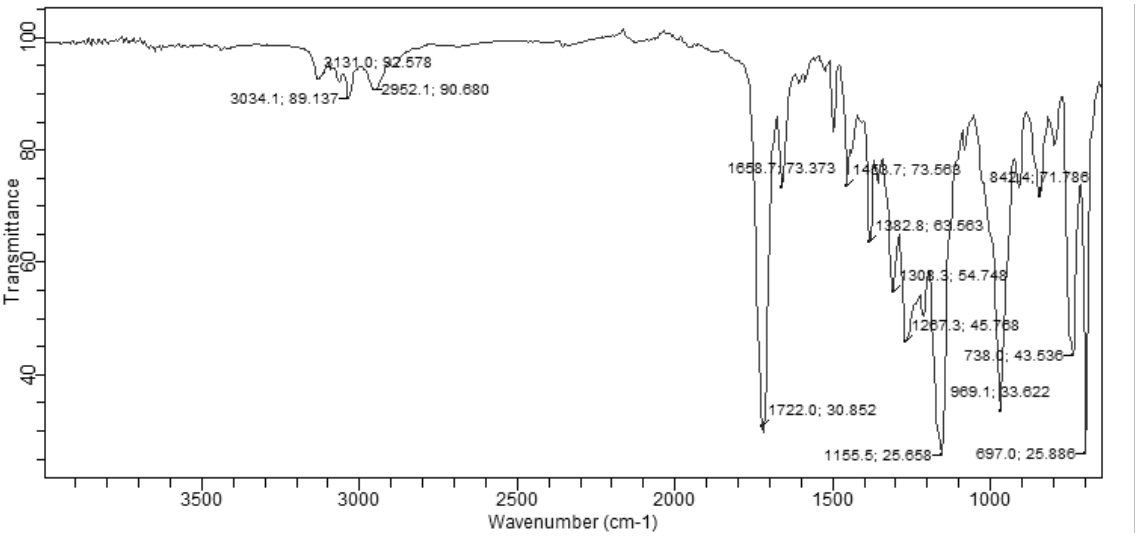

(*E*)-4-chloro-1-(4-(phenylsulfonyl)but-3-en-2-yl)-1H-pyrazole (152q) (^{1}H NMR: 400 MHz, ^{13}C NMR: 101 MHz, $CDCl_3$; IR)

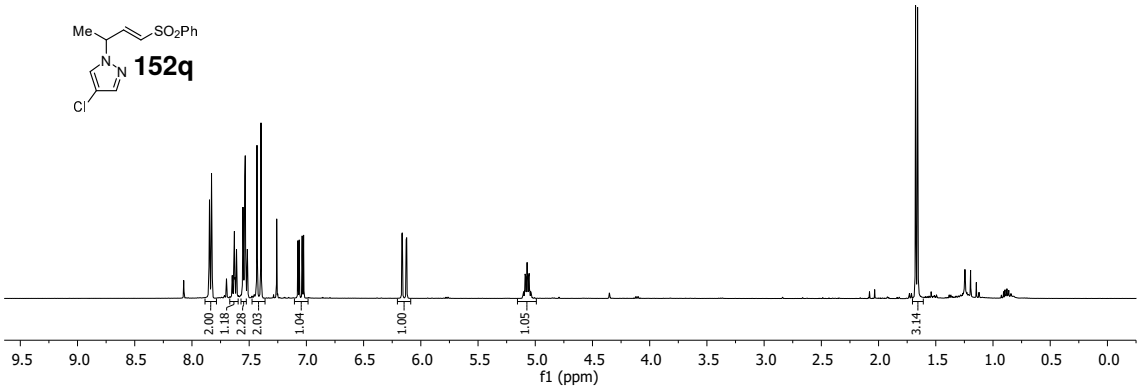

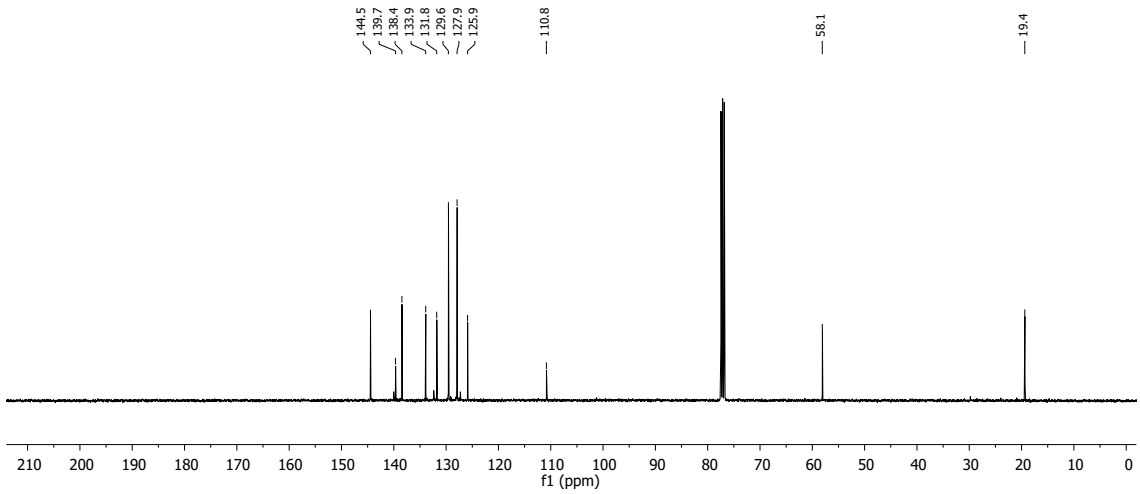

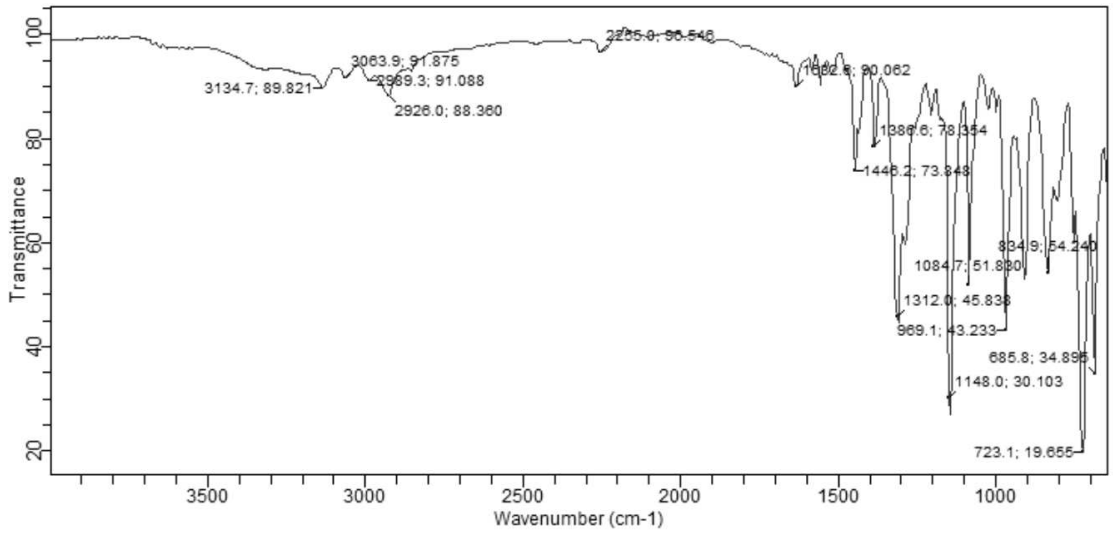

(*Z*)-4-chloro-1-(1-phenyl-3-(phenylsulfonyl)prop-1-en-1-yl)-1H-pyrazole (173a) (^{1}H NMR: 400 MHz, ^{13}C NMR: 75 MHz, $CDCl_3$; IR)

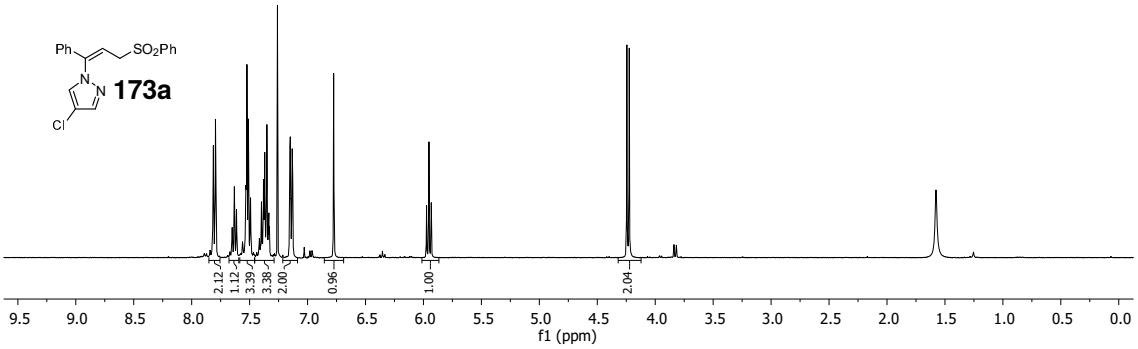

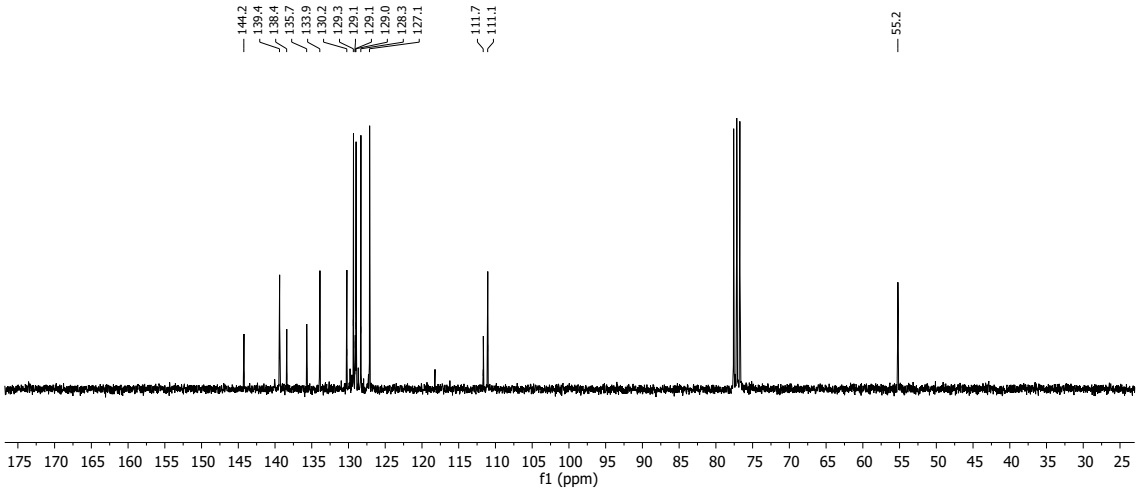

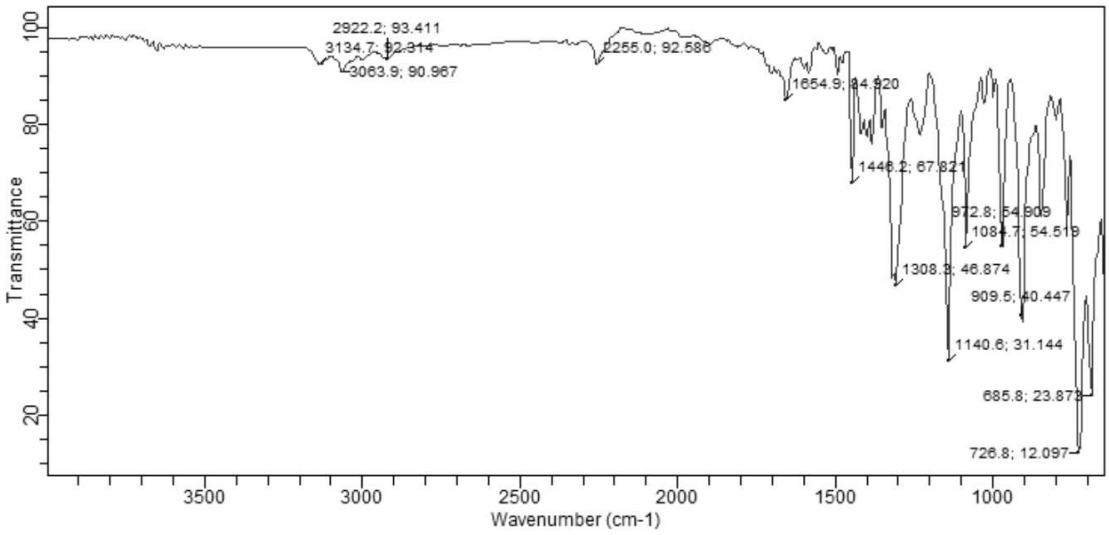

(*E*)-4-(4-chloro-1H-pyrazol-1-yl)hept-2-enenitrile (152t) (^{1}H NMR: 300 MHz, ^{13}C NMR: 101 MHz, $CDCl_3$; IR)

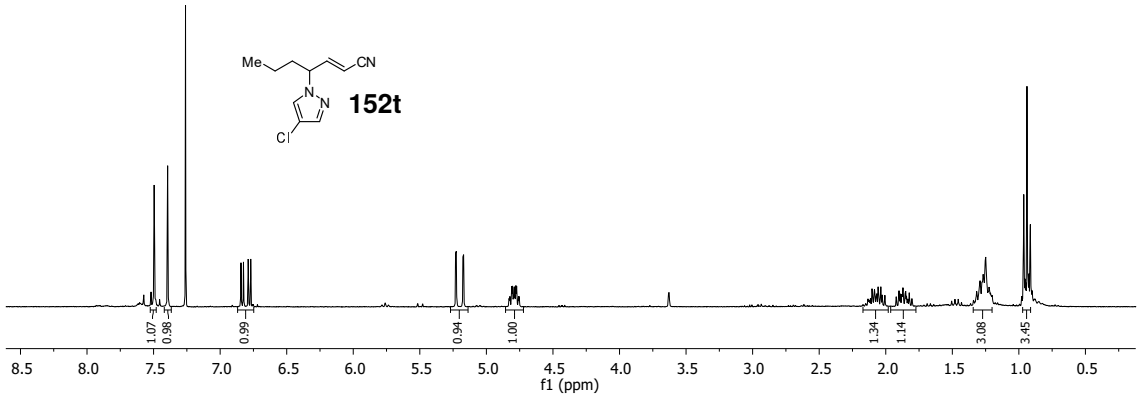

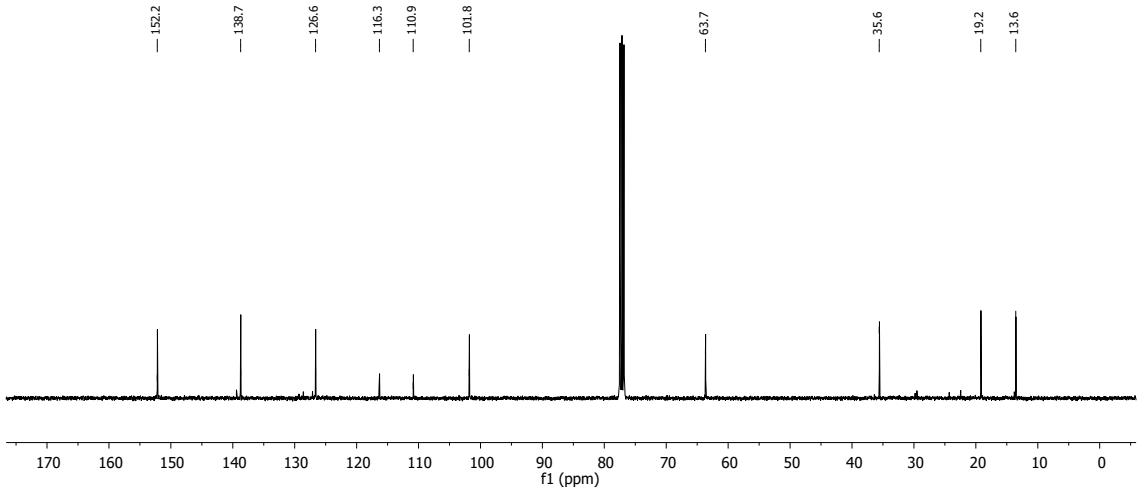

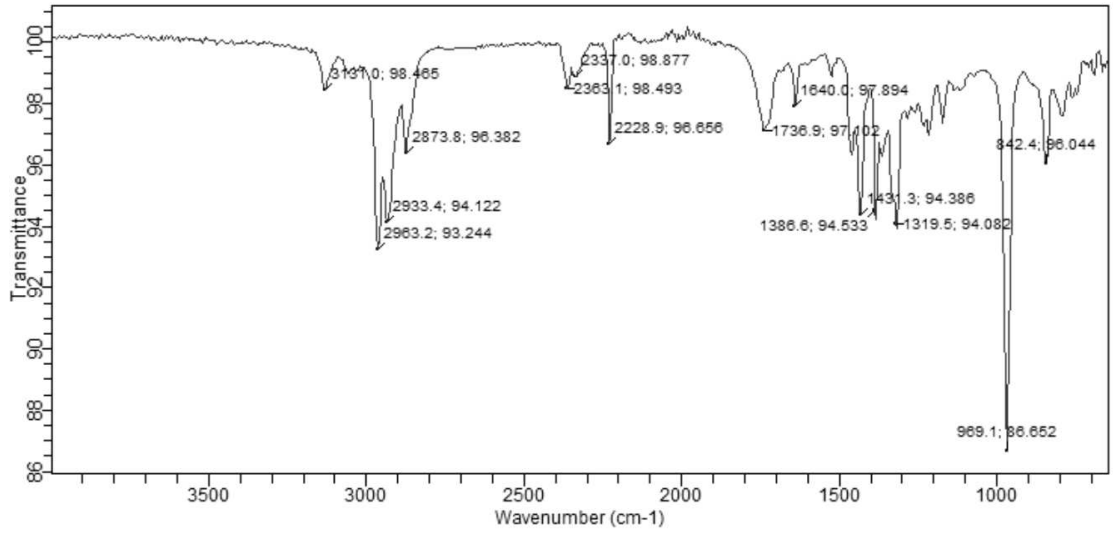

(*Z*)-4-(4-chloro-1H-pyrazol-1-yl)hept-2-enenitrile (156a) (^{1}H NMR: 400 MHz, ^{13}C NMR: 101 MHz, $CDCl_3$; IR)

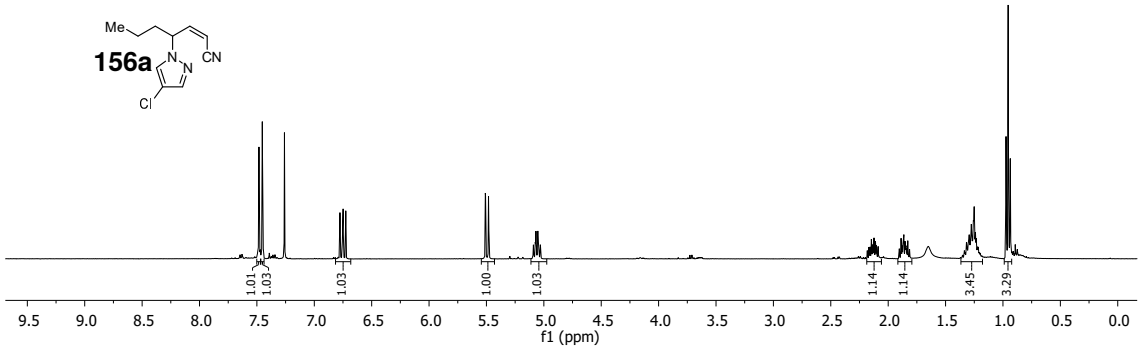

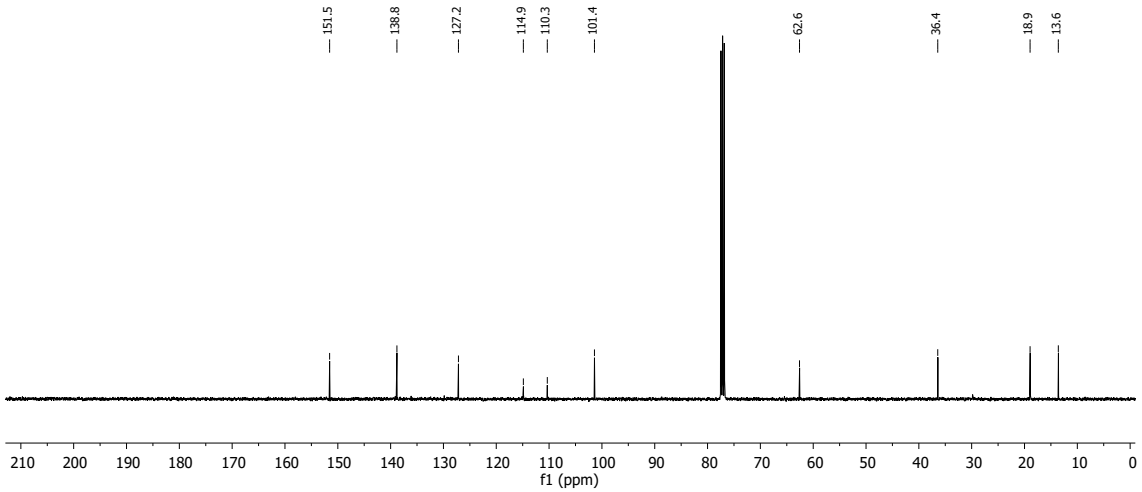

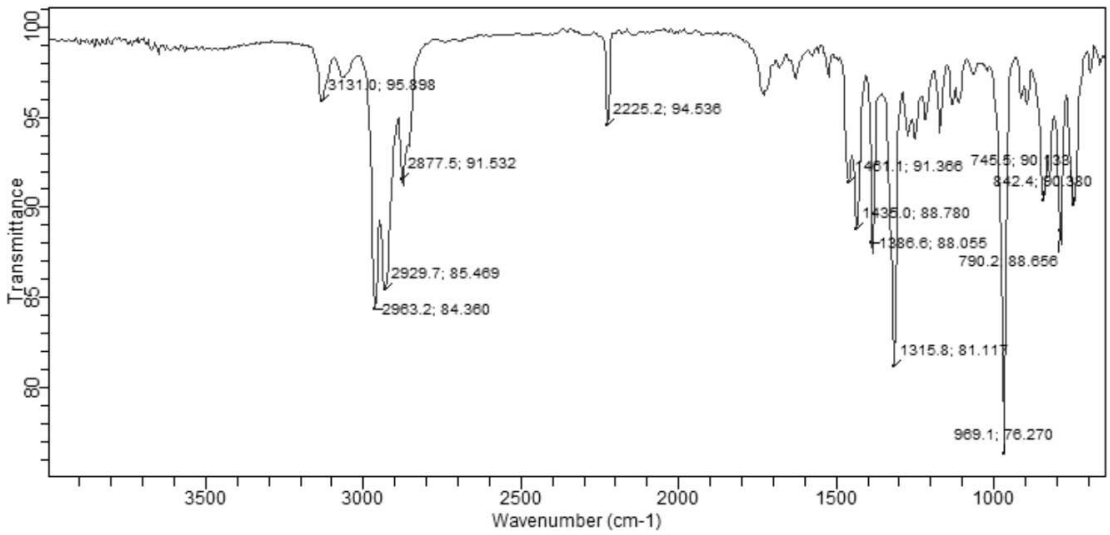

4-(4-chloro-1H-pyrazol-1-yl)-3-(phenylselanyl)heptanenitrile (184a) (^{1}H NMR: 400 MHz, ^{13}C NMR: 101 MHz, ^{77}Se NMR: 76 MHz, $CDCl_3$; IR)

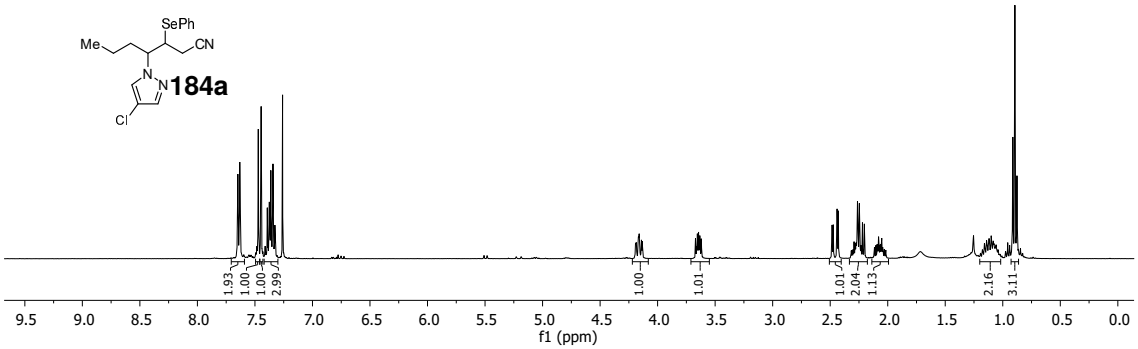

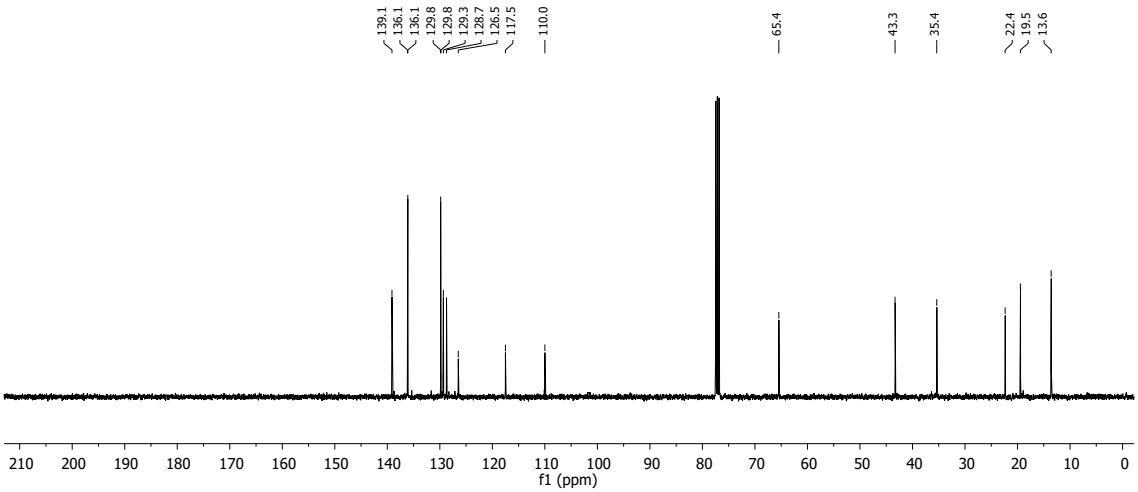

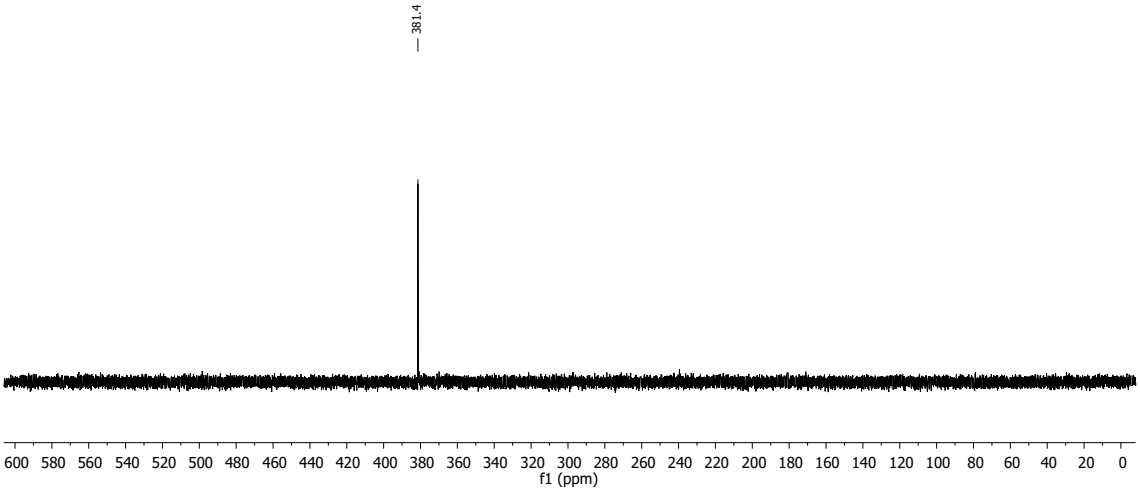

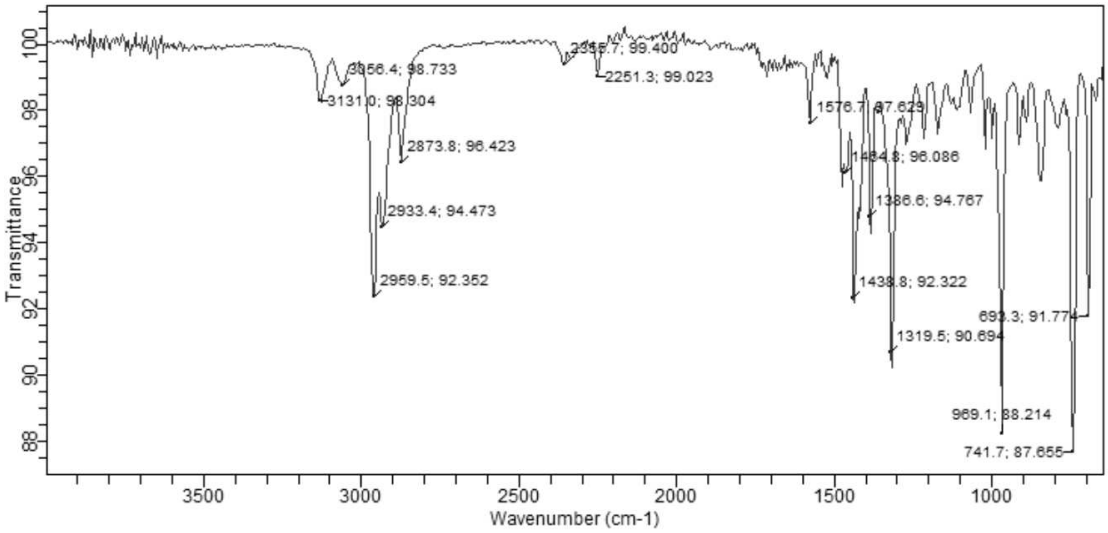
Transmittance
Wavenumber (cm-1)
3500
3000
2500
2000
1500
1000
100
98
96
94
92
90
88
3131.0; 98.304
2959.5; 92.352
2933.4; 94.473
2873.8; 96.423
2251.3; 99.023
1576.7; 97.623
1319.5; 90.694
969.1; 88.214
741.7; 87.655

(*E*)-4-Chloro-1-(cyclododec-1-en-1-yl)-1H-pyrazole (152ab) (^{1}H NMR: 400 MHz, ^{13}C NMR: 101 MHz, $CDCl_3$; IR)

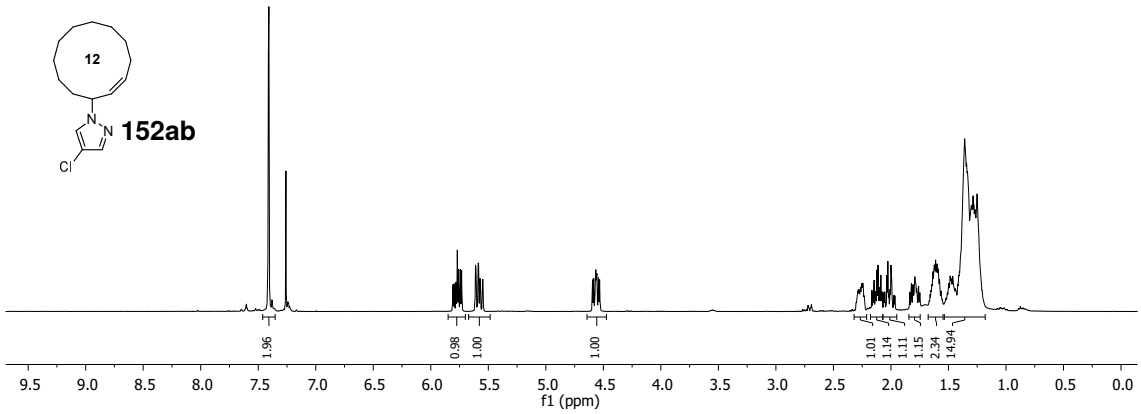

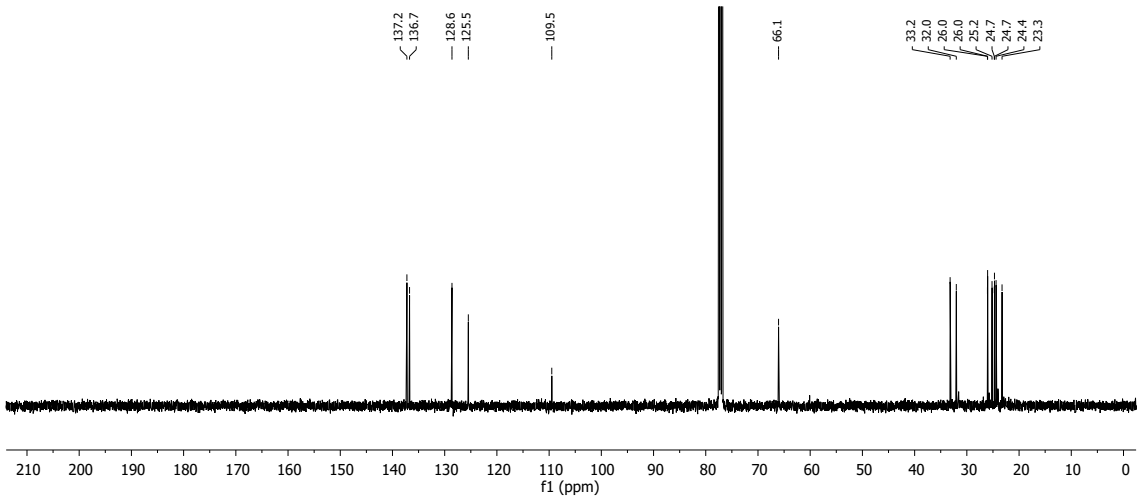

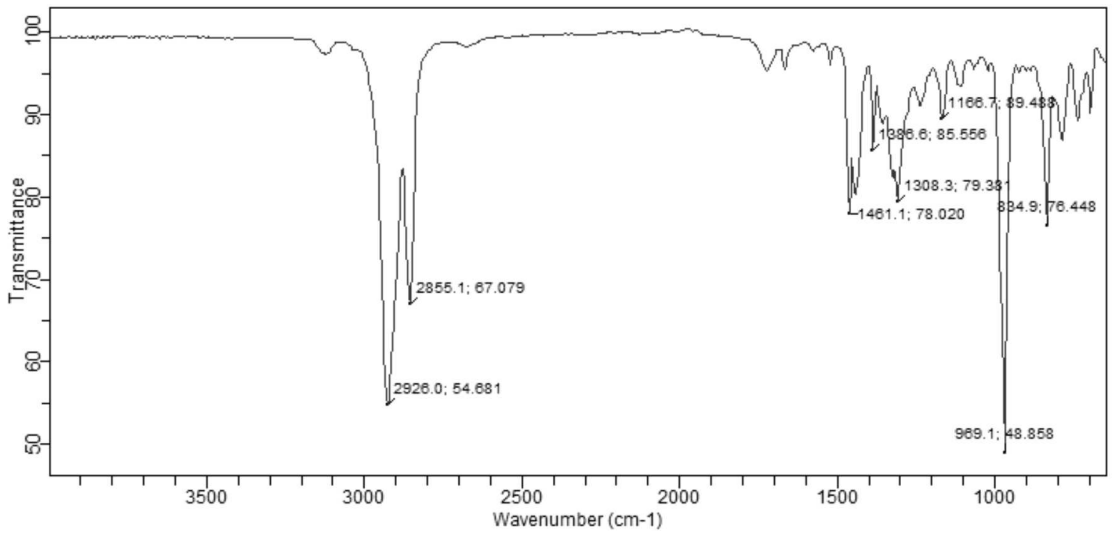

(*Z*)-1-(Cyclododec-2-en-1-yl)-1H-benzo[d][1,2,3]triazole (152ac) (^{1}H NMR: 400 MHz, ^{13}C NMR: 101 MHz, $CDCl_3$; IR)

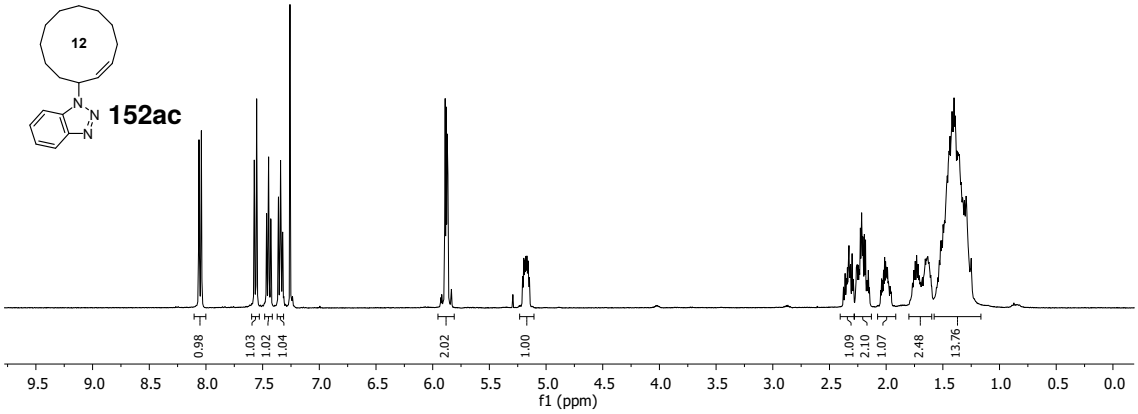

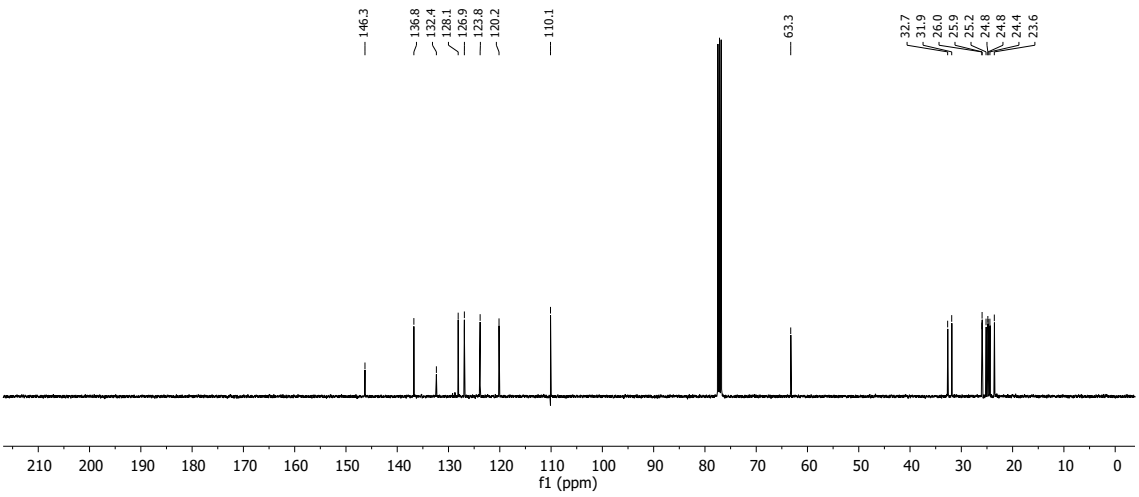

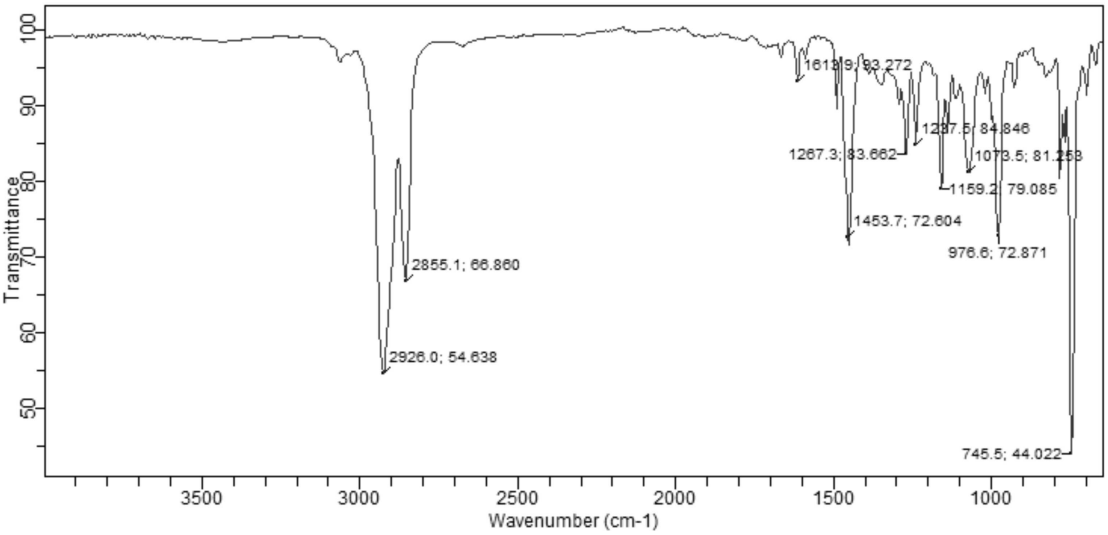

(*E*)-4-Chloro-1-(2-methylhex-3-en-2-yl)-1H-pyrazole (152ad) (^{1}H NMR: 300 MHz, ^{13}C NMR: 101 MHz, $CDCl_3$; IR)

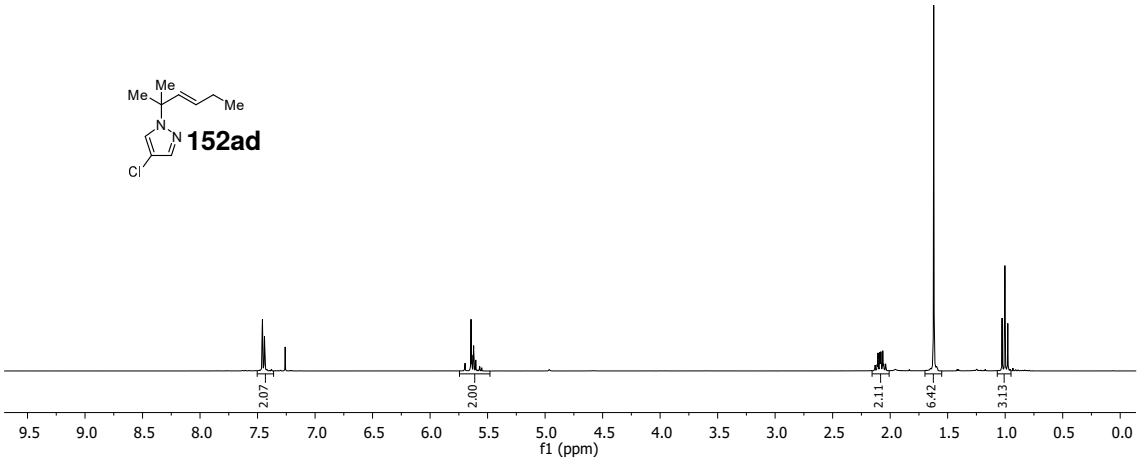

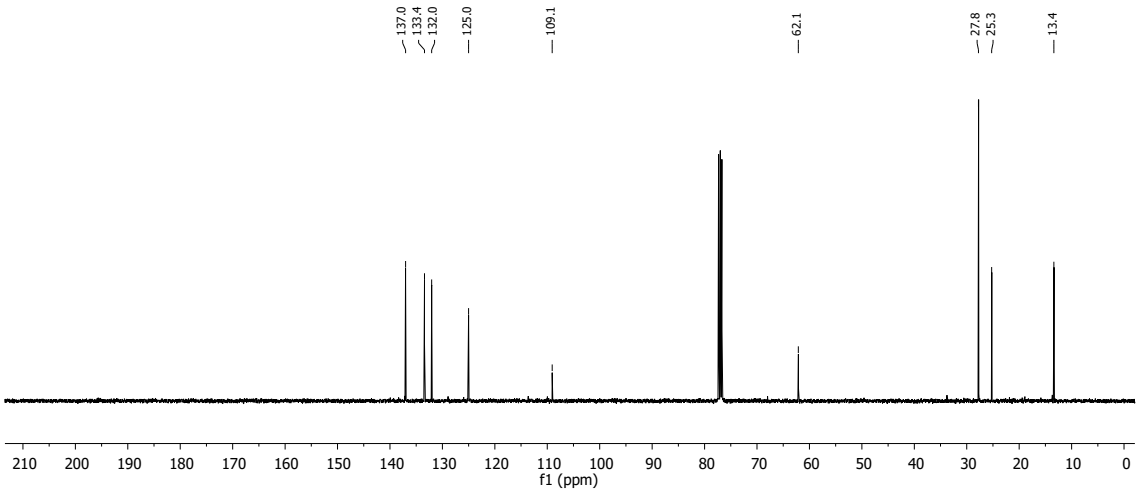

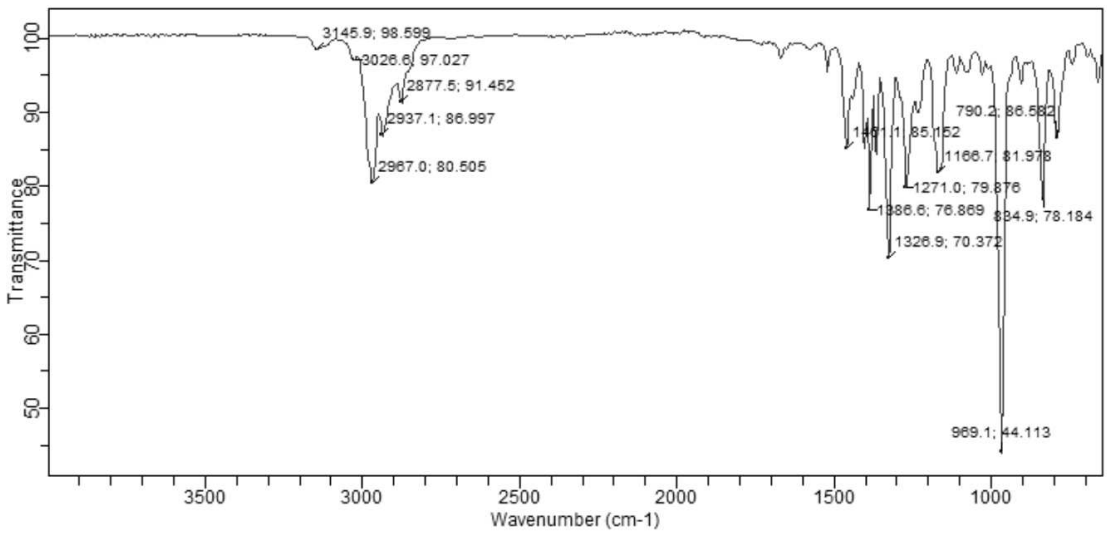

Ethyl (*E*)-4-(4-iodo-1H-pyrazol-1-yl)hex-2-enoate (152af) (^{1}H NMR: 400 MHz, ^{13}C NMR: 101 MHz, $CDCl_3$; IR)

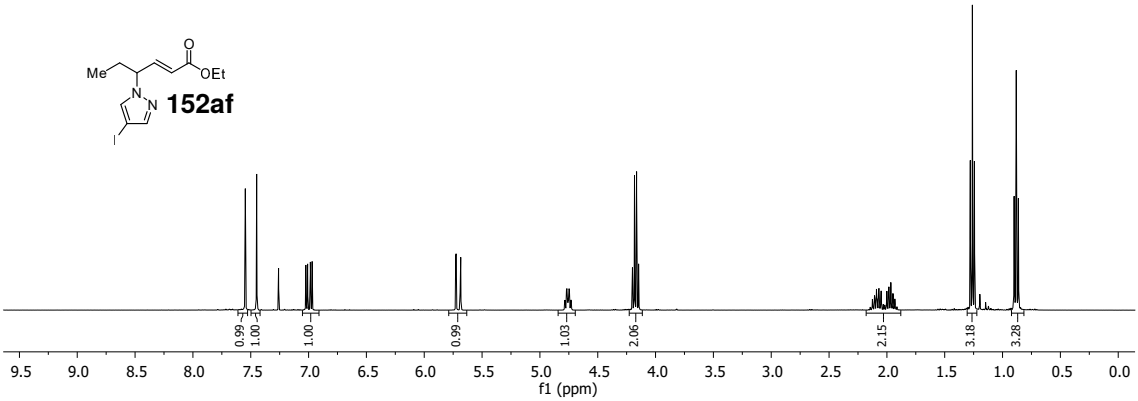

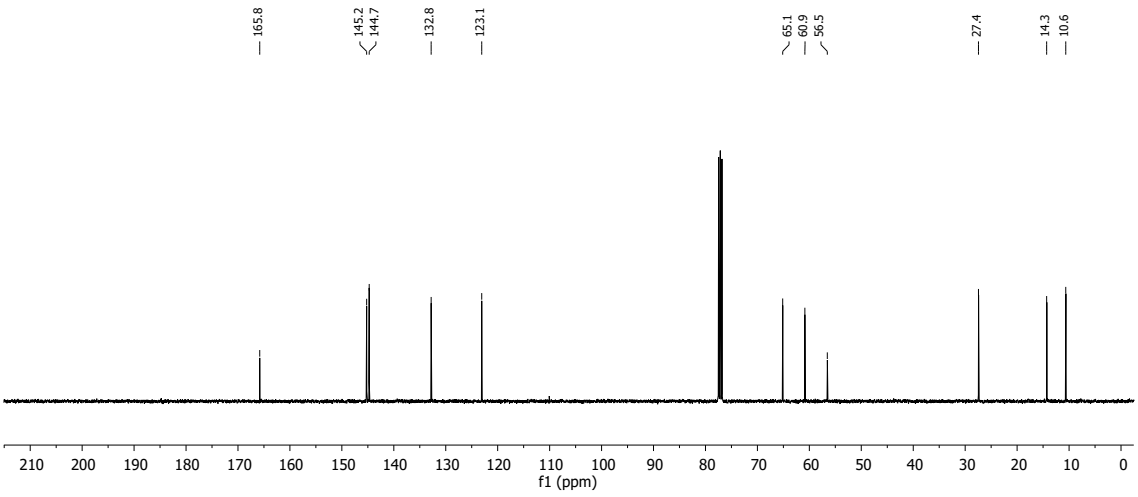

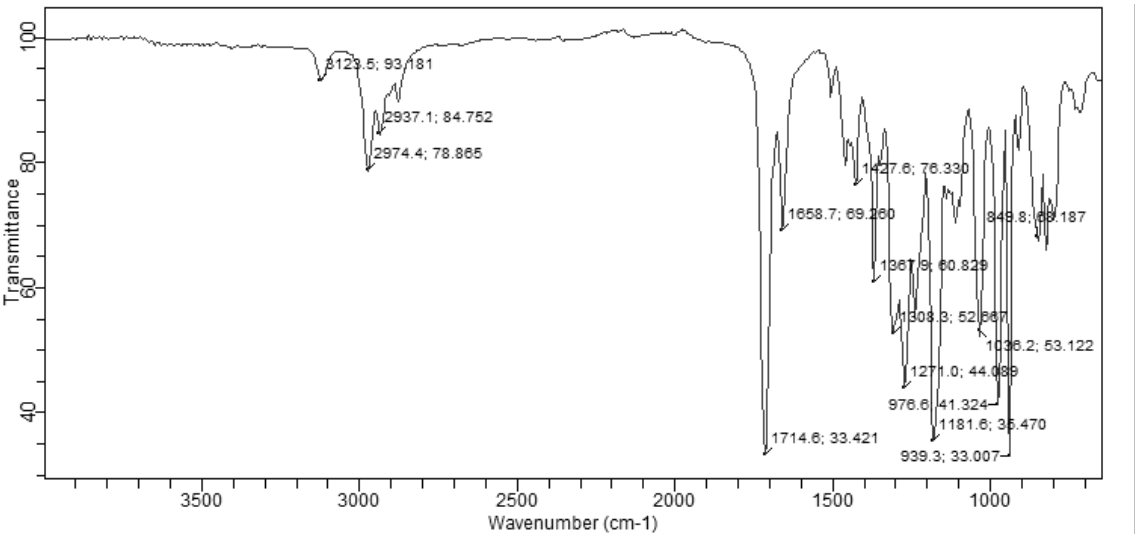

Ethyl (*E*)-1-(6-ethoxy-6-oxohex-4-en-3-yl)-1H-pyrazole-4-carboxylate (152ag) (^{1}H NMR: 300 MHz, ^{13}C NMR: 75 MHz, $CDCl_3$; IR)

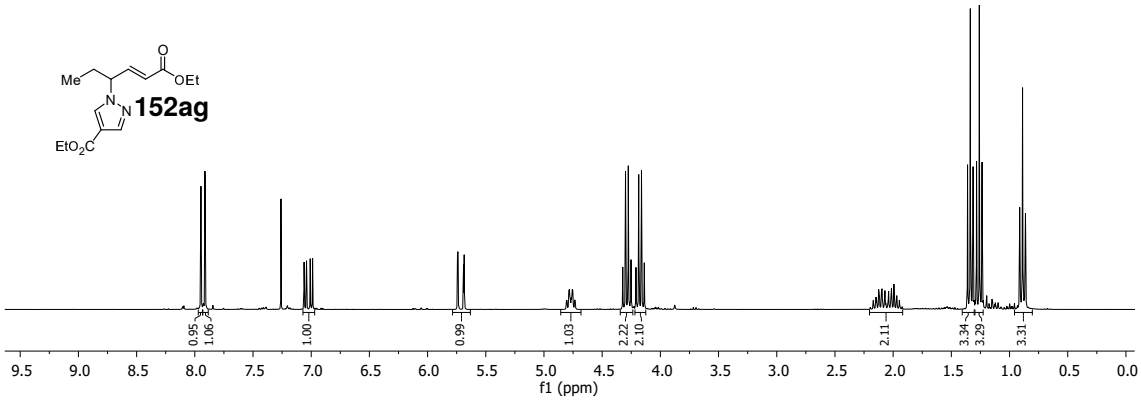

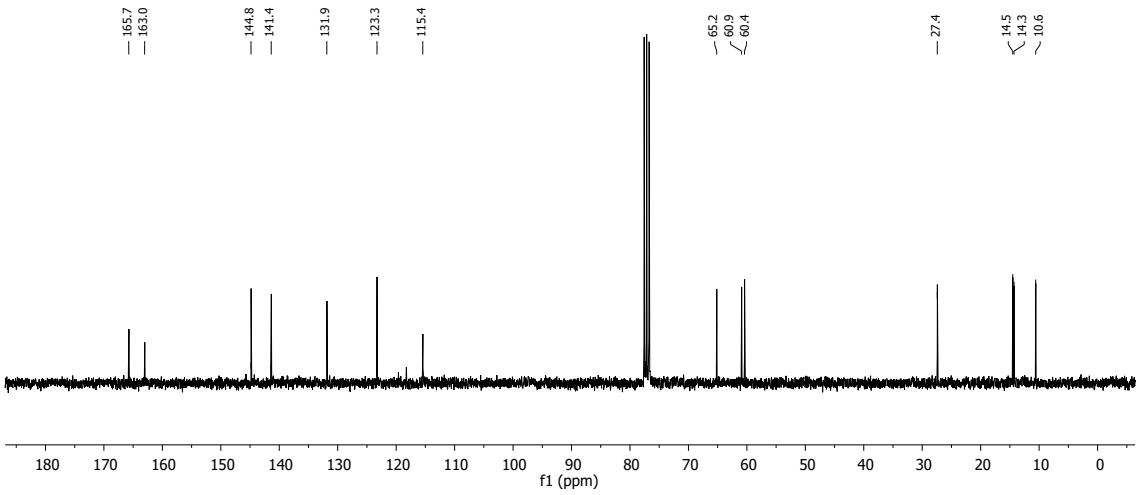

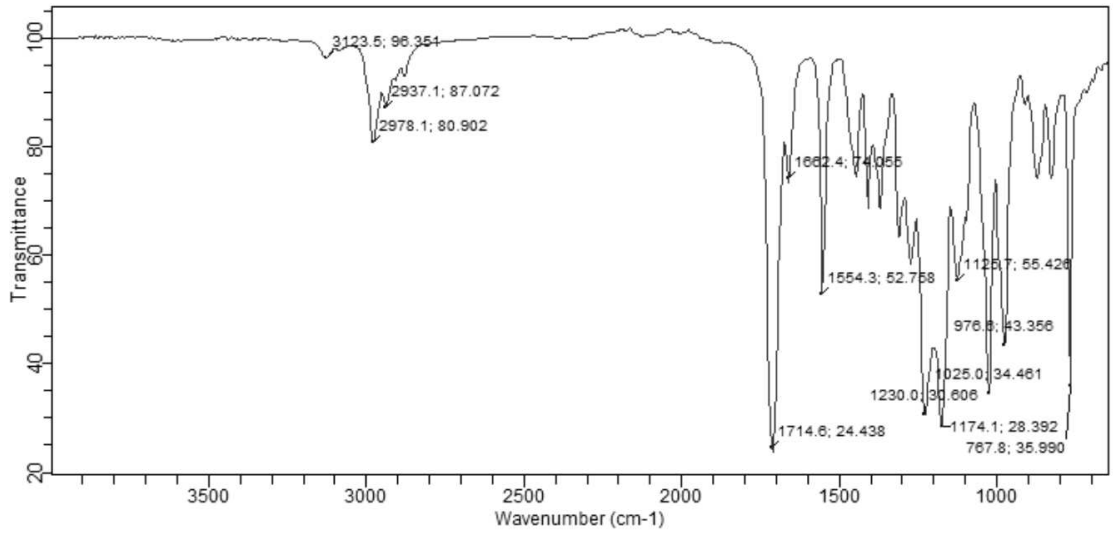

Ethyl (*Z*)-1-(1-ethoxy-1-oxohex-3-en-3-yl)-1H-pyrazole-4-carboxylate (153ag) (^{1}H NMR: 300 MHz, ^{13}C NMR: 75 MHz, $CDCl_3$)

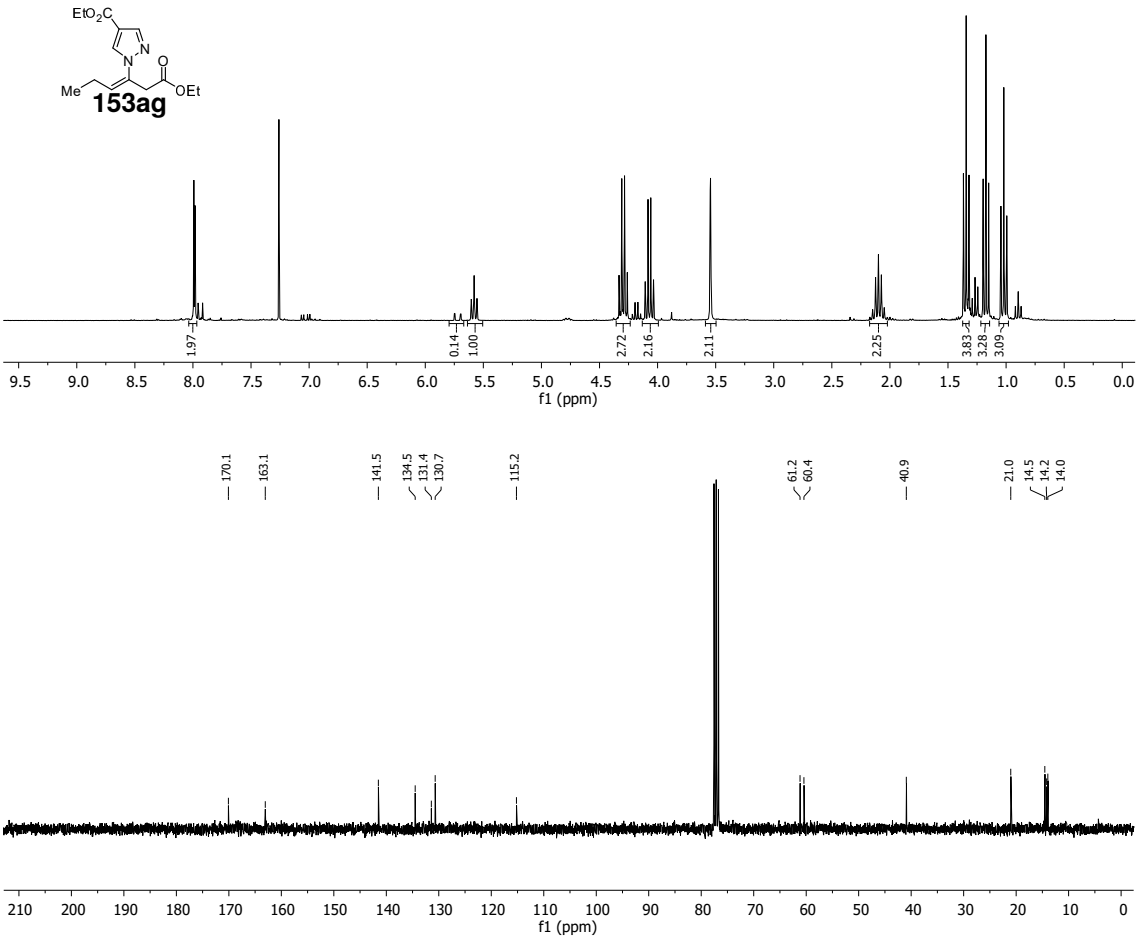

Ethyl (*E*)-4-(4-formyl-1H-pyrazol-1-yl)hex-2-enoate (152ah) (^{1}H NMR: 400 MHz, ^{13}C NMR: 101 MHz, $CDCl_3$; IR)

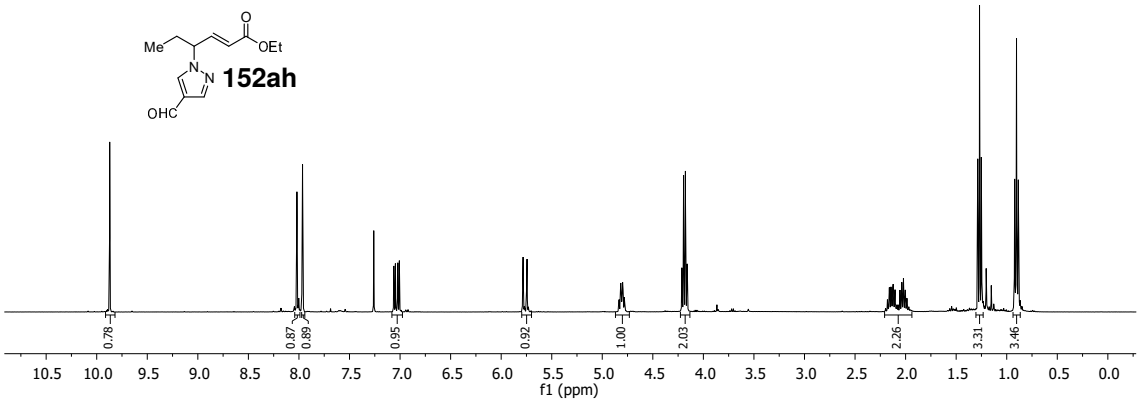

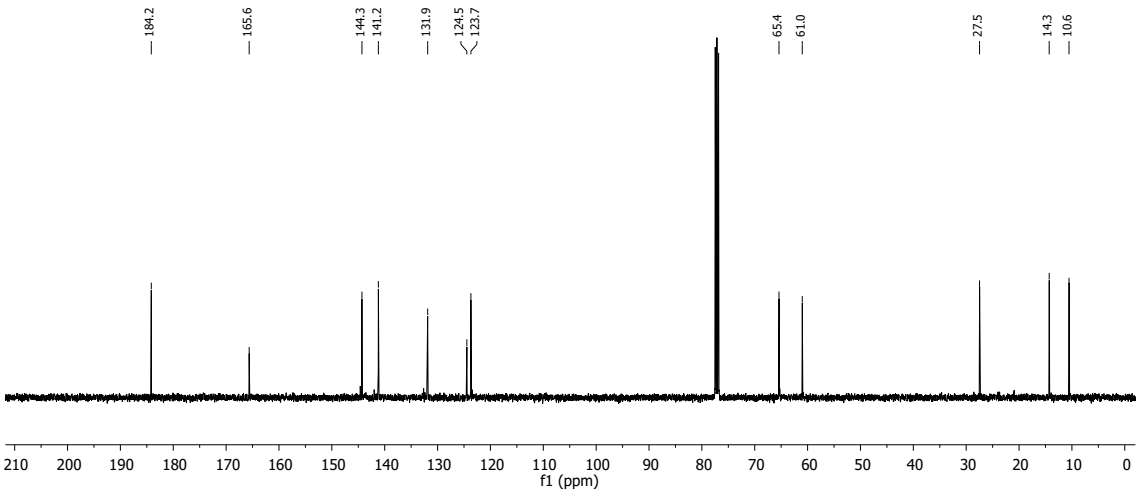

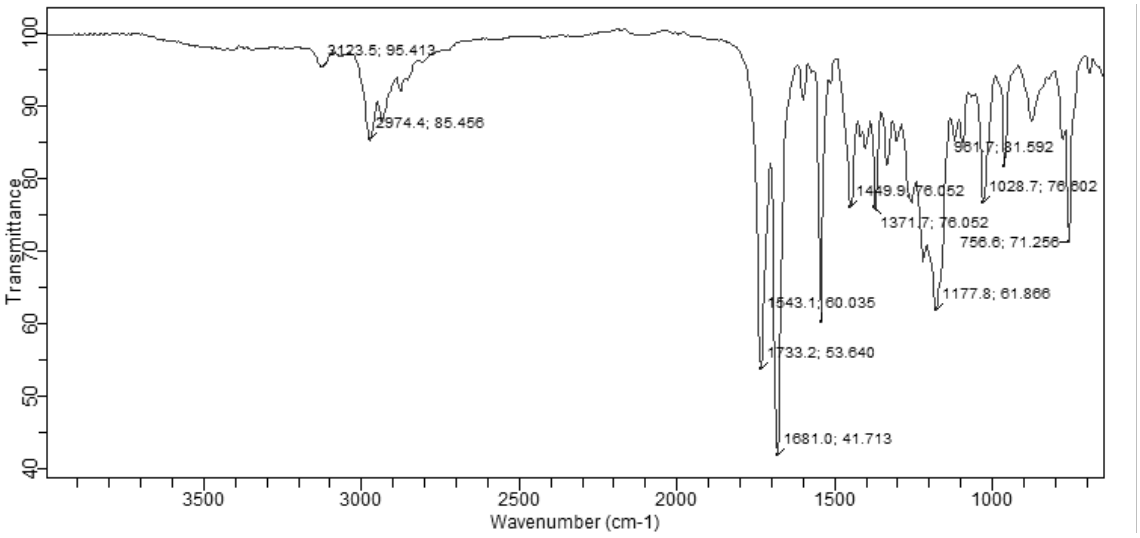

Ethyl (*Z*)-3-(4-formyl-1H-pyrazol-1-yl)hex-3-enoate (153ah) (^{1}H NMR: 400 MHz, ^{13}C NMR: 101 MHz, $CDCl_3$; IR)

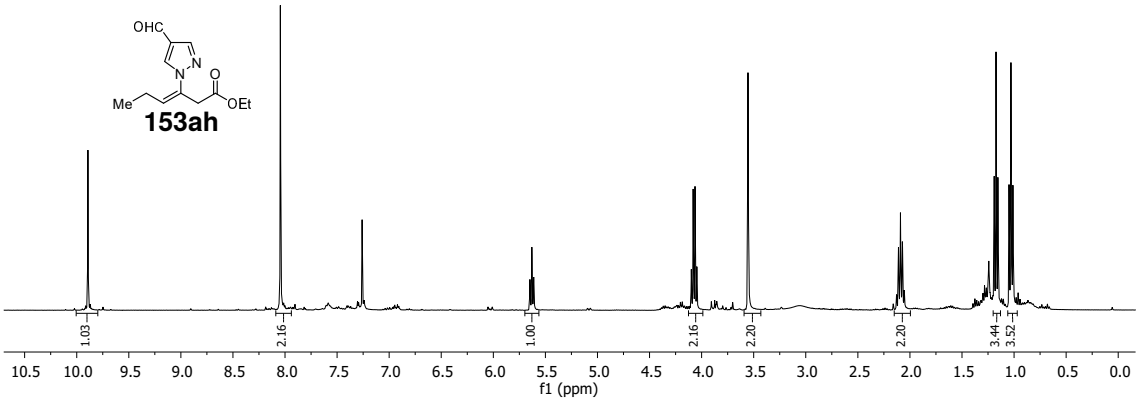

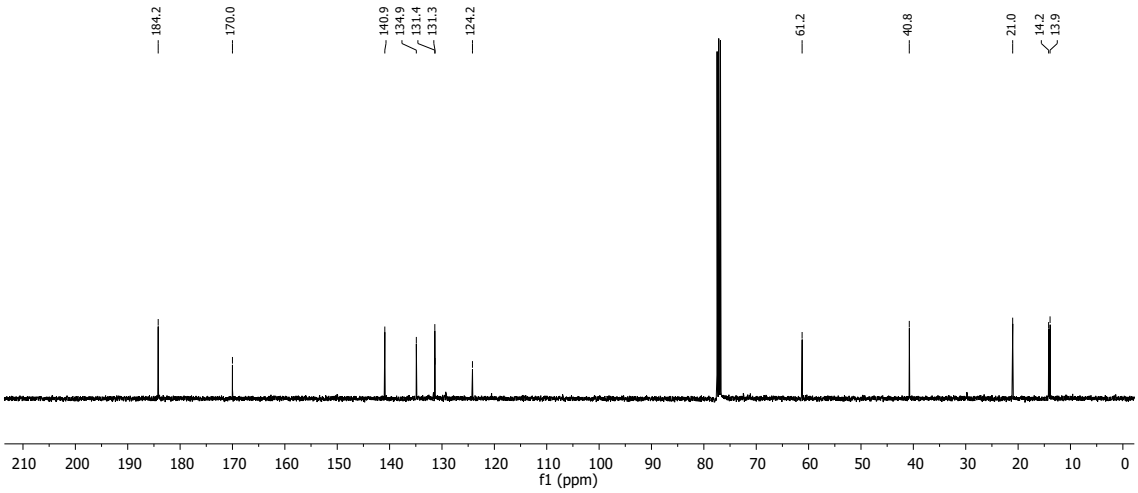

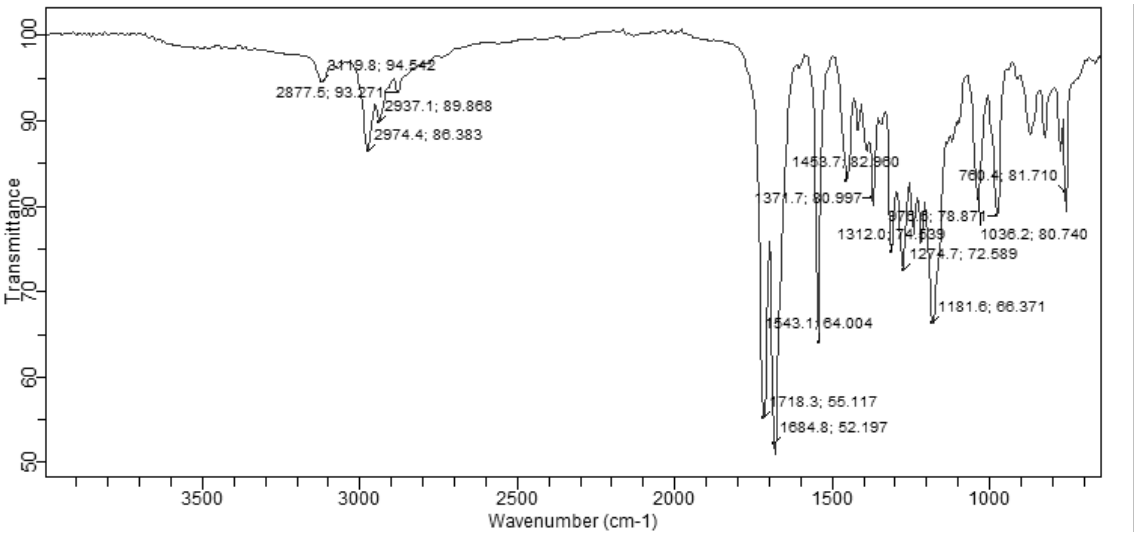

Ethyl (*E*)-4-(3-phenyl-1H-pyrazol-1-yl)hex-2-enoate (*N*1-isomer) and ethyl (*E*)-4-(5-phenyl-1H-pyrazol-1-yl)hex-2-enoate (*N*2-isomer) (152ai) (^{1}H NMR: 400 MHz, ^{13}C NMR: 101 MHz, NOESY, $CDCl_3$; IR)

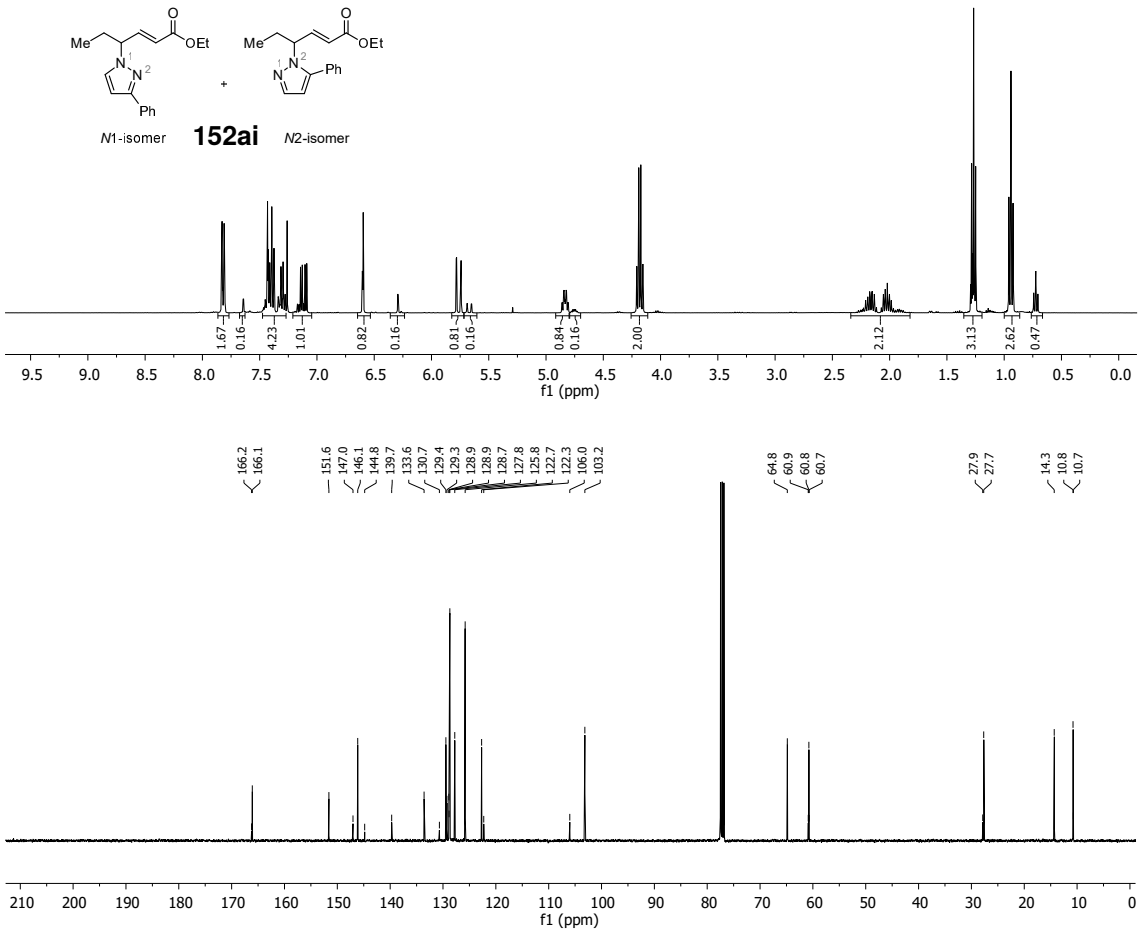

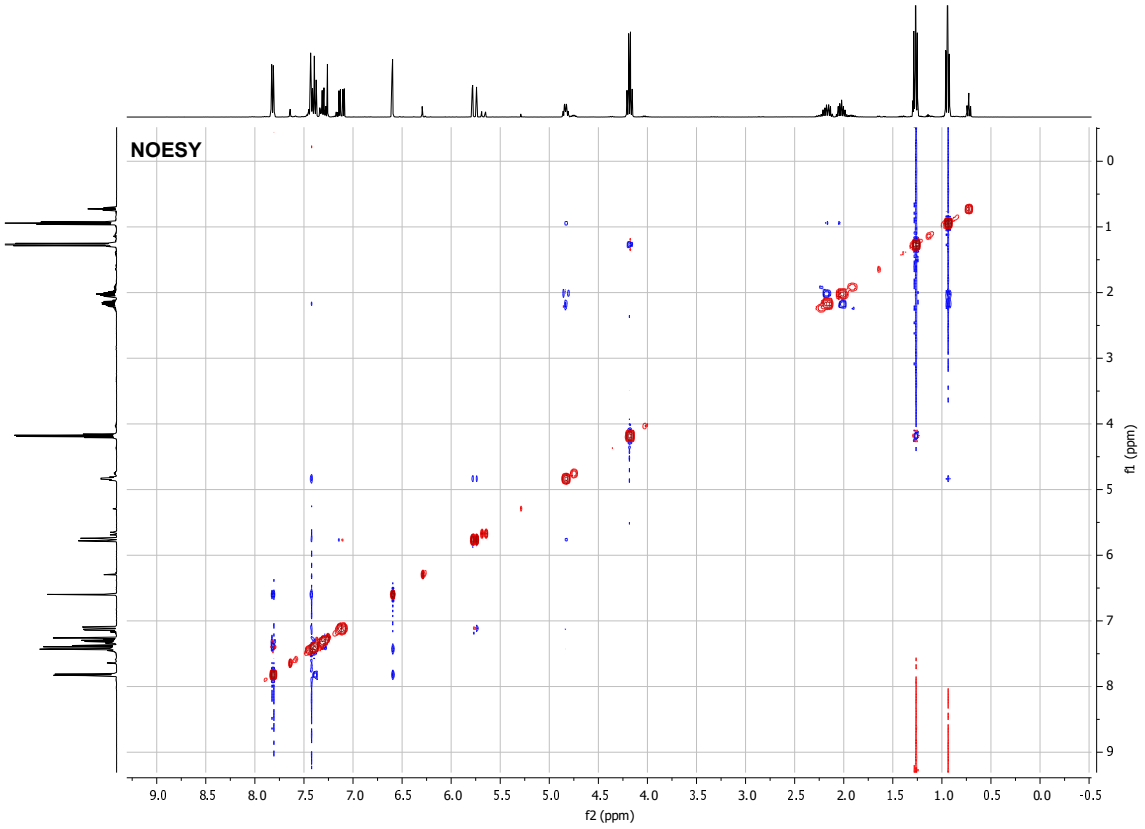
NOESY
f2 (ppm)
f1 (ppm)

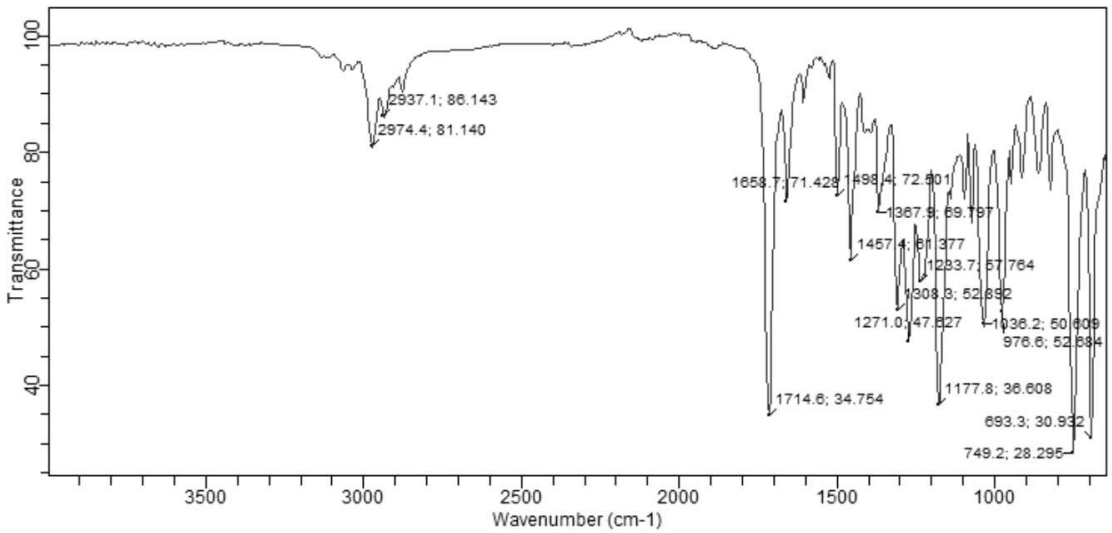
Transmittance
Wavenumber (cm-1)
2937.1; 86.143
2974.4; 81.140
1658.7; 71.428
1498.4; 72.501
1367.9; 69.797
1457.4; 61.377
1283.7; 57.764
1308.3; 52.892
1271.0; 47.527
1036.2; 50.609
976.6; 52.584
1714.6; 34.754
1177.8; 36.608
693.3; 30.932
749.2; 28.295

Ethyl (*E*)-4-(3,5-diphenyl-1H-pyrazol-1-yl)hex-2-enoate (152aj) (^{1}H NMR: 400 MHz, ^{13}C NMR: 101 MHz, $CDCl_3$; IR)

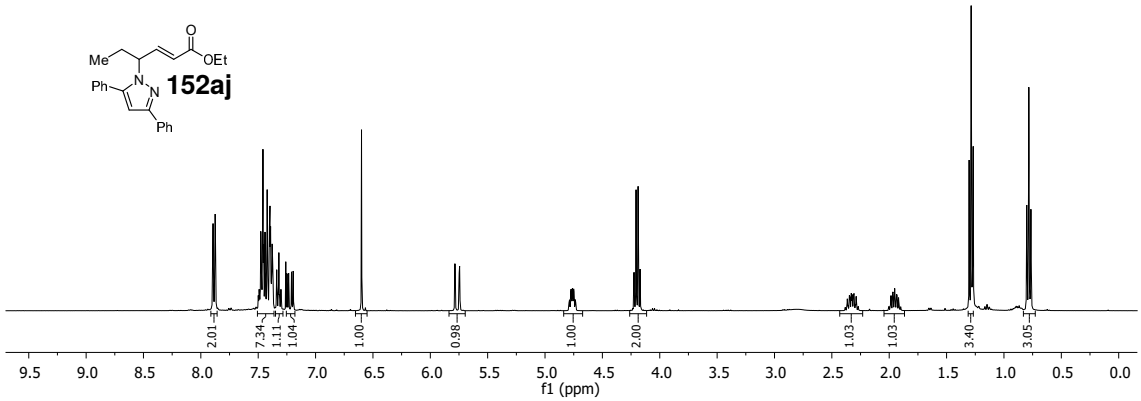

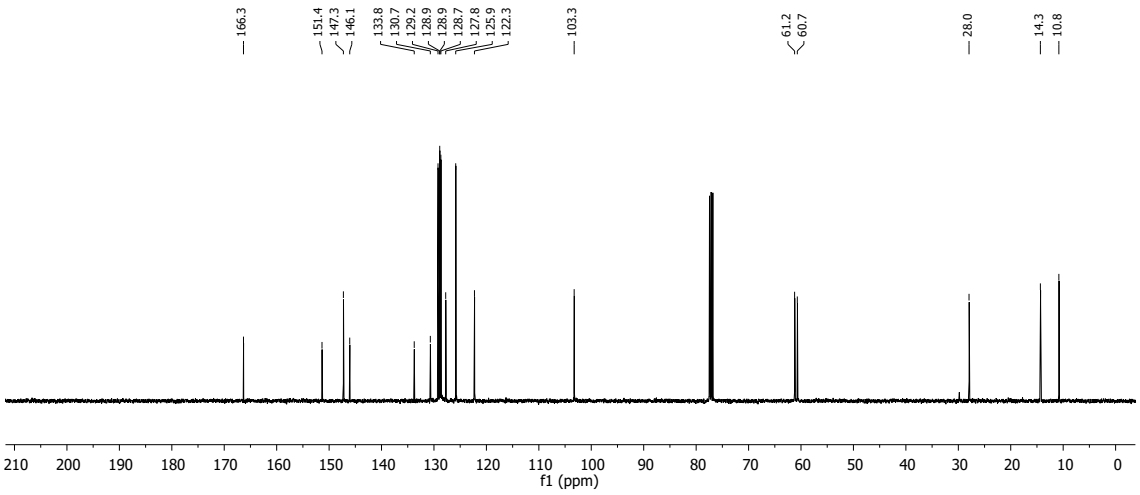

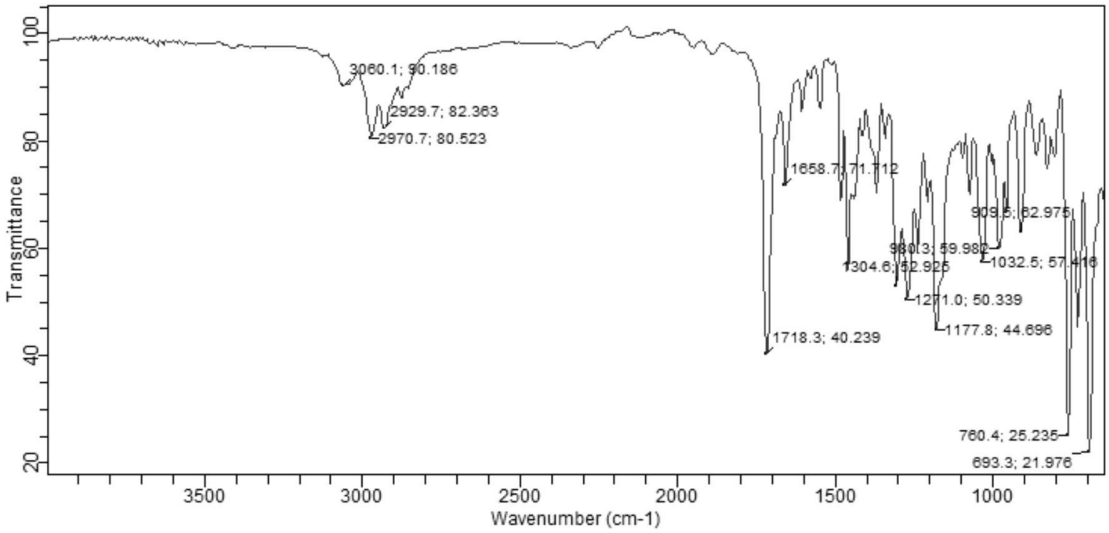

Ethyl (*E*)-4-(4-bromo-3-methyl-1H-pyrazol-1-yl)hex-2-enoate (N1-siomer) and ethyl (*E*)-4-(4-bromo-5-methyl-1H-pyrazol-1-yl)hex-2-enoate (N2-isomer) (152ak) (^{1}H NMR: 400 MHz, ^{13}C NMR: 101 MHz, NOESY, $CDCl_3$; IR)

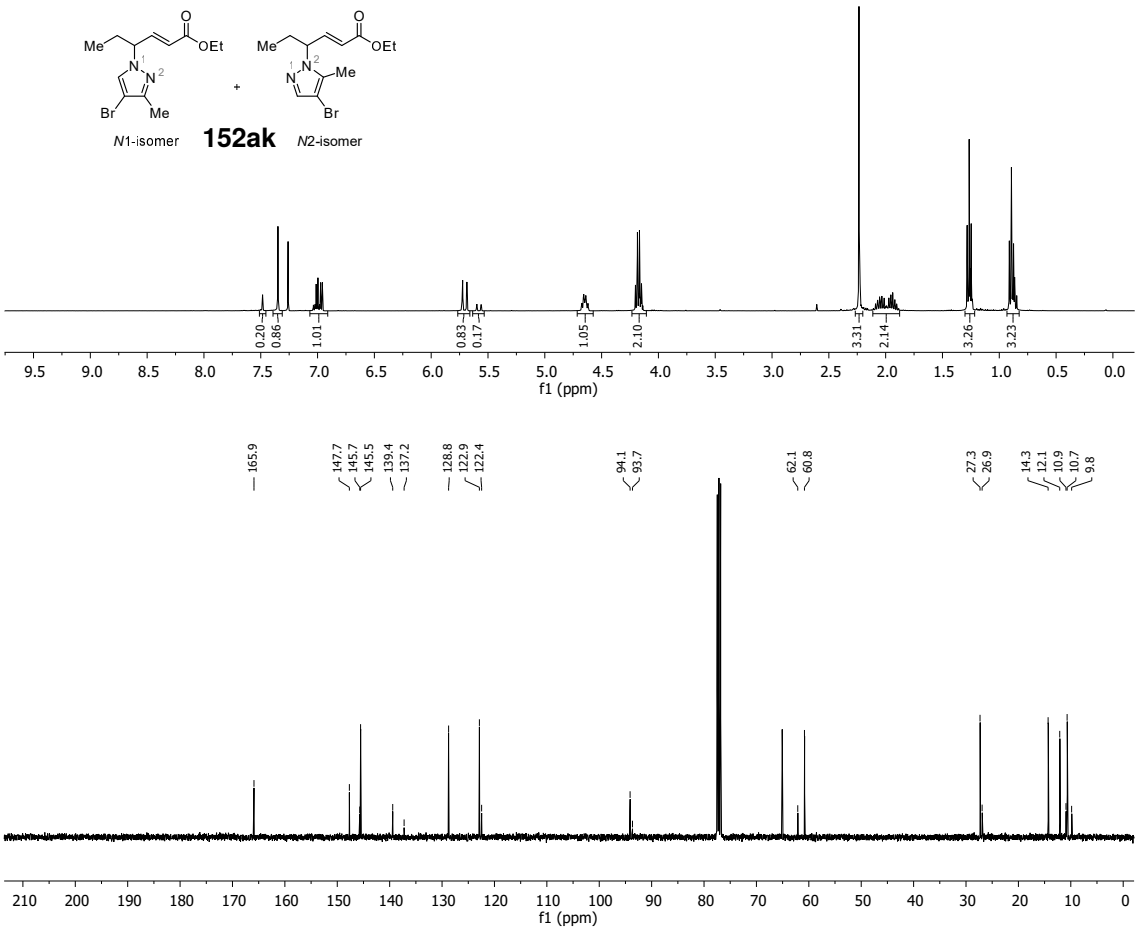

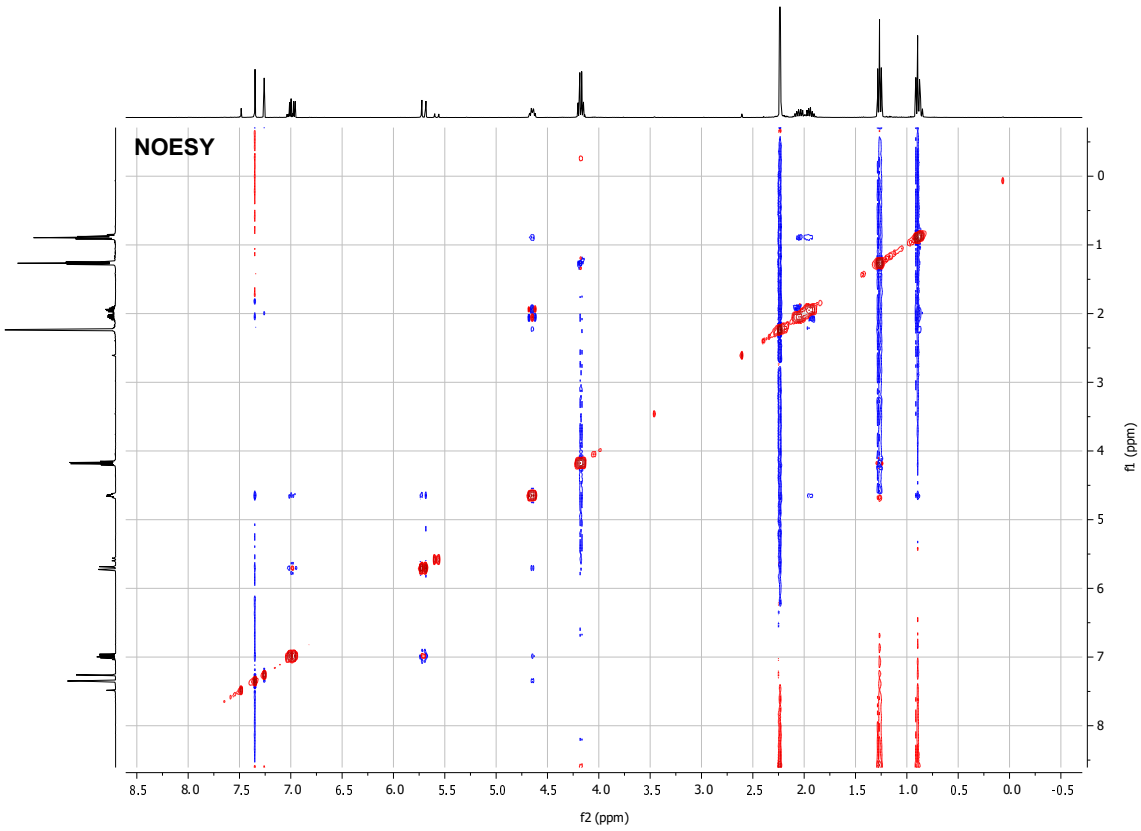
NOESY
f2 (ppm)
f1 (ppm)

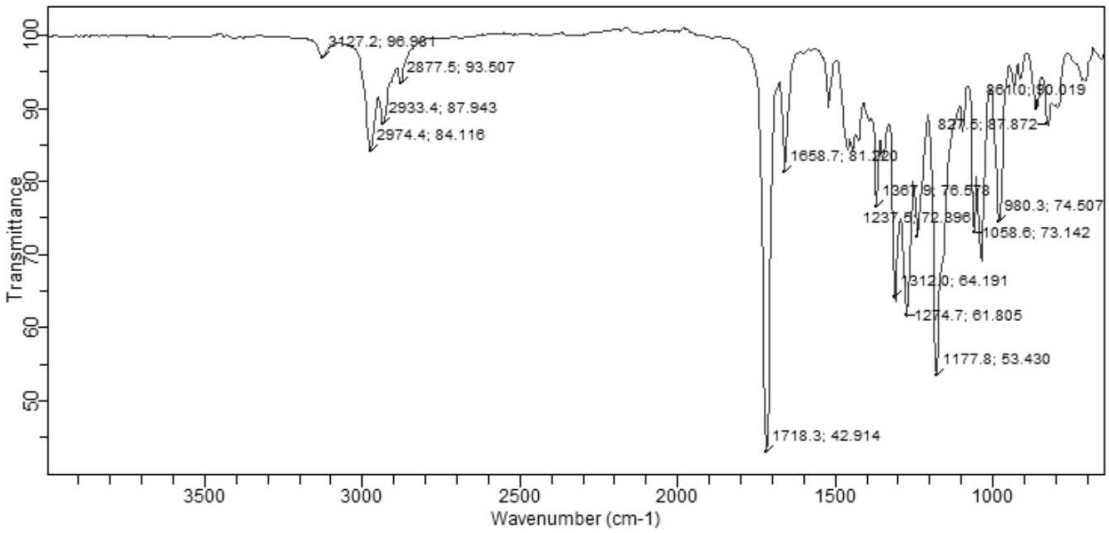
Transmittance
Wavenumber (cm-1)
3127.2; 96.981
2877.5; 93.507
2933.4; 87.943
2974.4; 84.116
1658.7; 81.220
1718.3; 42.914
1237.5; 72.396
1058.6; 73.142
1312.0; 64.191
1274.7; 61.805
1177.8; 53.430
827.5; 87.872
980.3; 74.507

Ethyl (*E*)-4-(1H-benzo[d][1,2,3]triazol-1-yl)hex-2-enoate (152am) (^{1}H NMR: 400 MHz, ^{13}C NMR: 101 MHz, $CDCl_3$; IR)

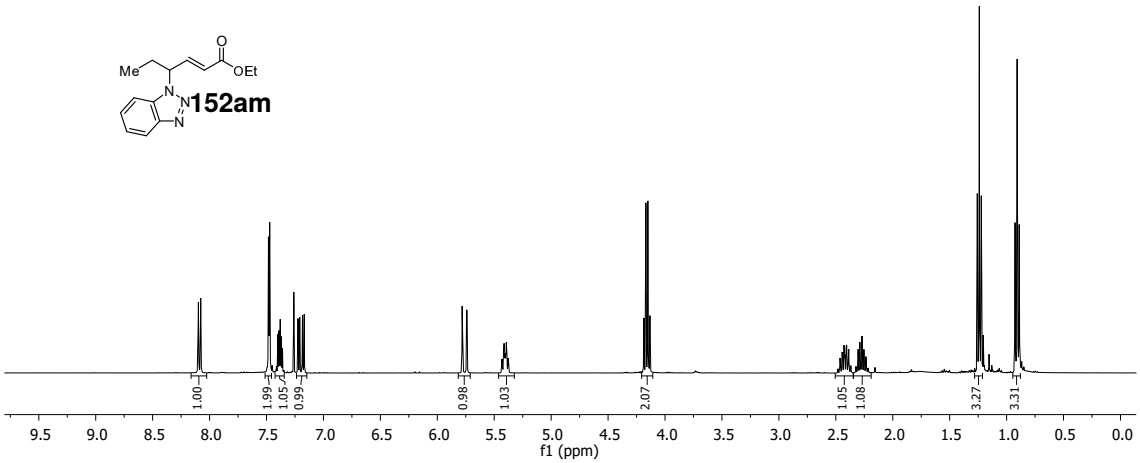

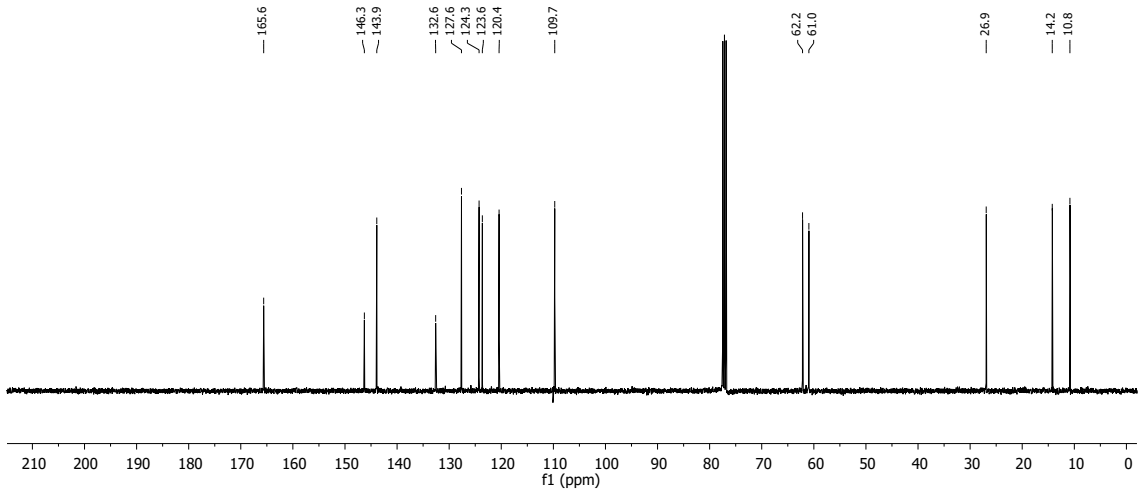

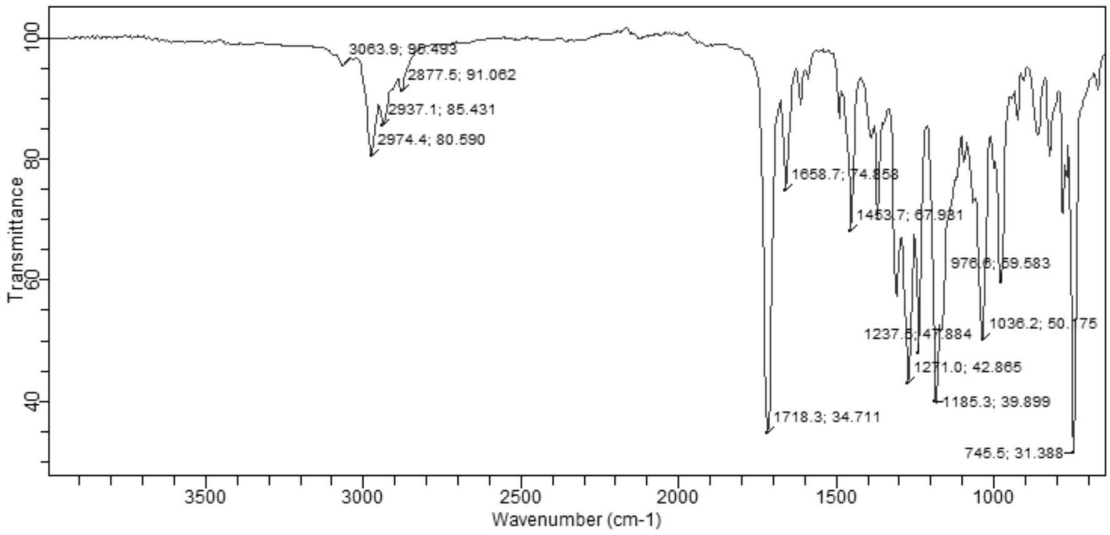

Ethyl (*Z*)-3-(1H-benzo[d][1,2,3]triazol-1-yl)hex-3-enoate (153am) (^{1}H NMR: 400 MHz, ^{13}C NMR: 101 MHz, $CDCl_3$; IR)

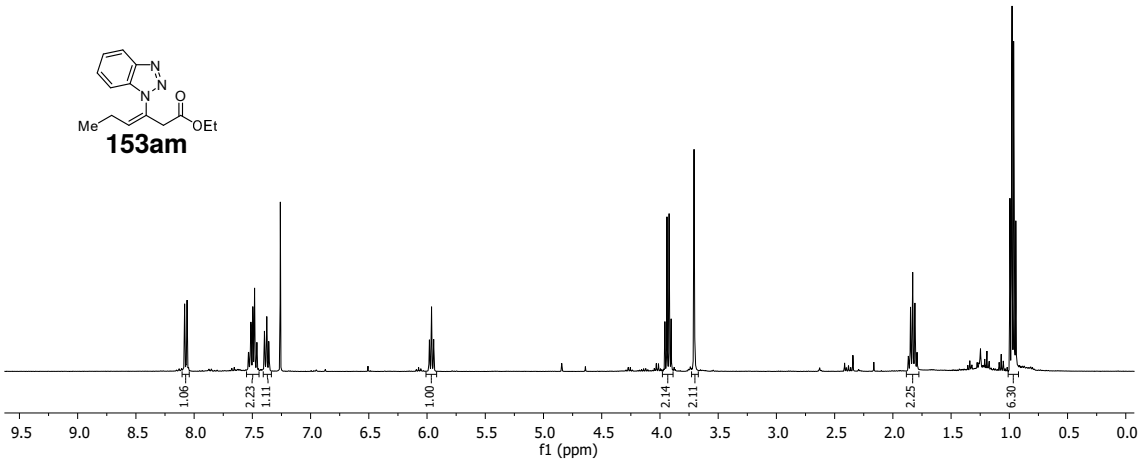

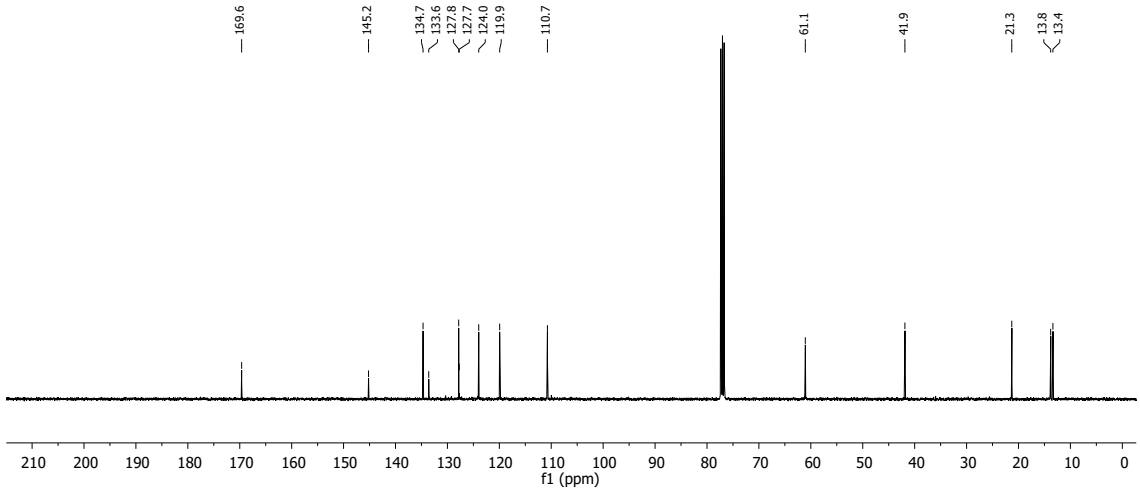

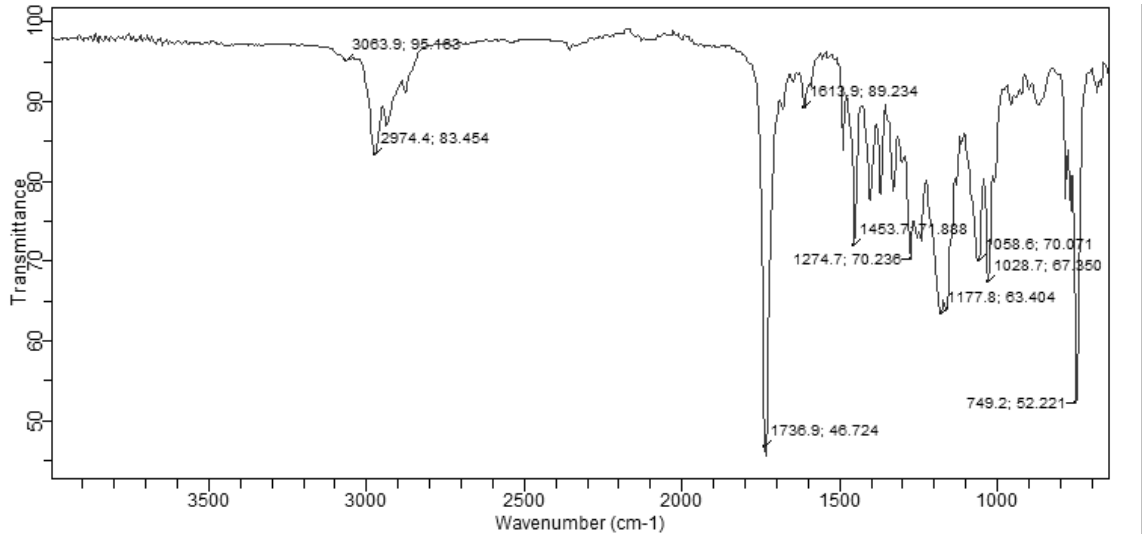

Ethyl (*E*)-4-(2H-benzo[d][1,2,3]triazol-2-yl)hex-2-enoate (185a) (^{1}H NMR: 300 MHz, ^{13}C NMR: 101 MHz, $CDCl_3$; IR)

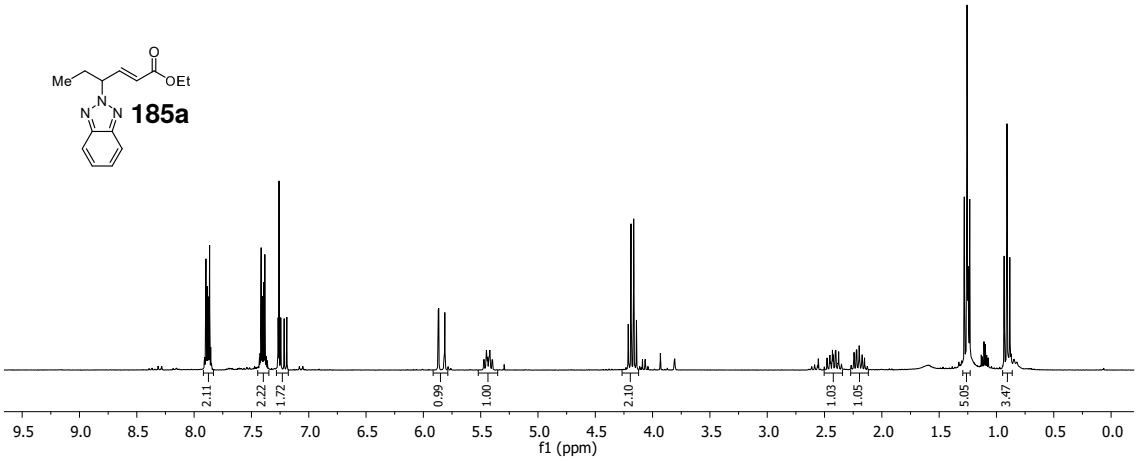

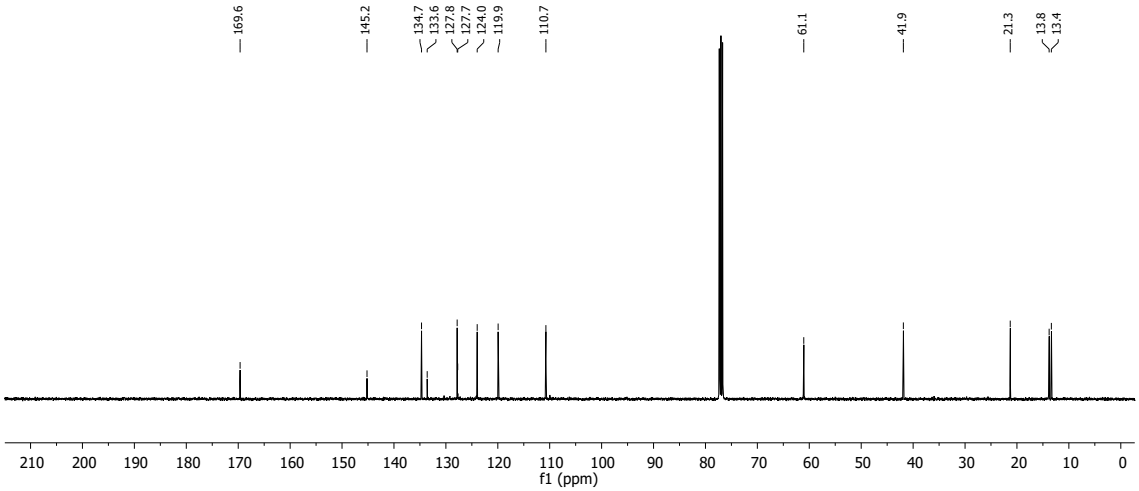

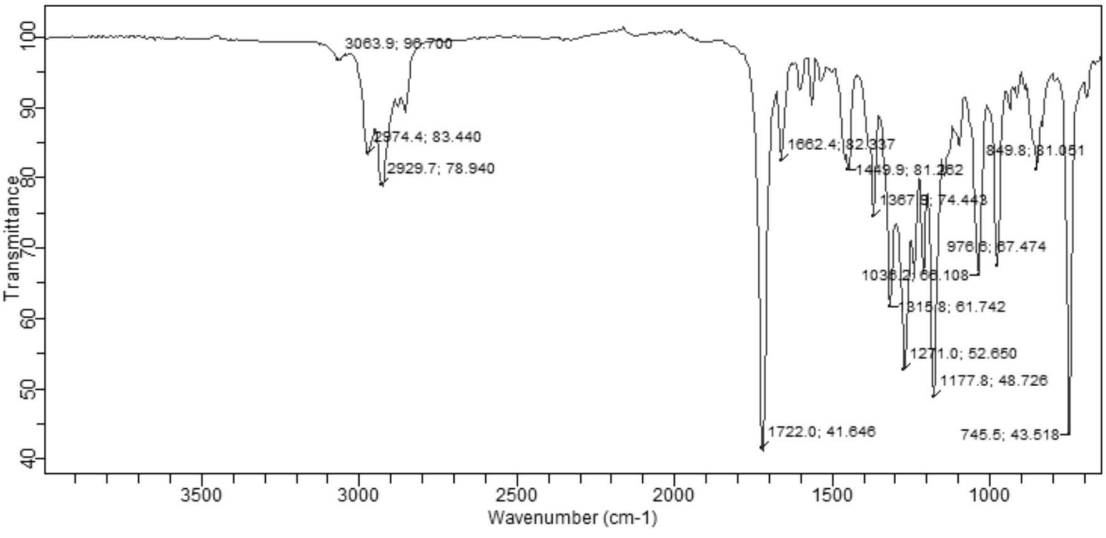

Ethyl (*E*)-4-(5-methyl-1H-benzo[d][1,2,3]triazol-1-yl)hex-2-enoate (C5-isomer) and ethyl (*E*)-4-(6-methyl-1H-benzo[d][1,2,3]triazol-1-yl)hex-2-enoate (C6-isomer) (152an) (^{1}H NMR: 400 MHz, ^{13}C NMR: 75 MHz, $CDCl_3$; IR)

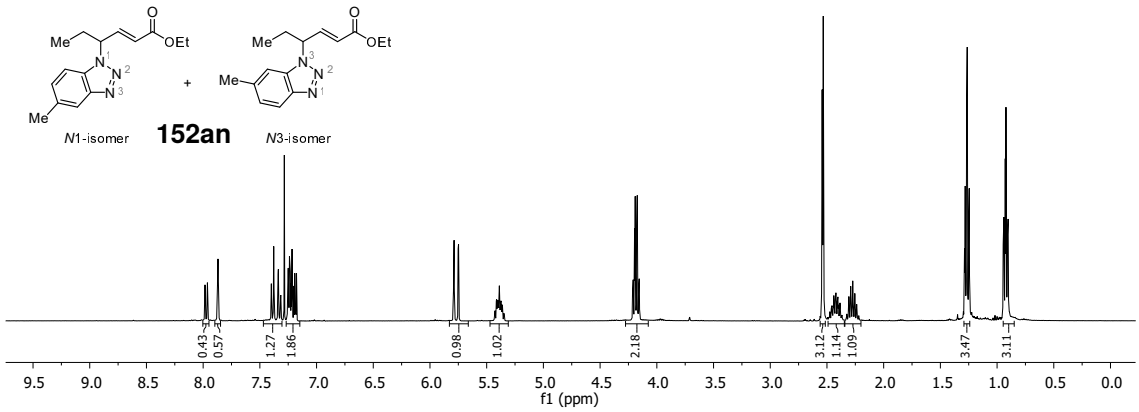

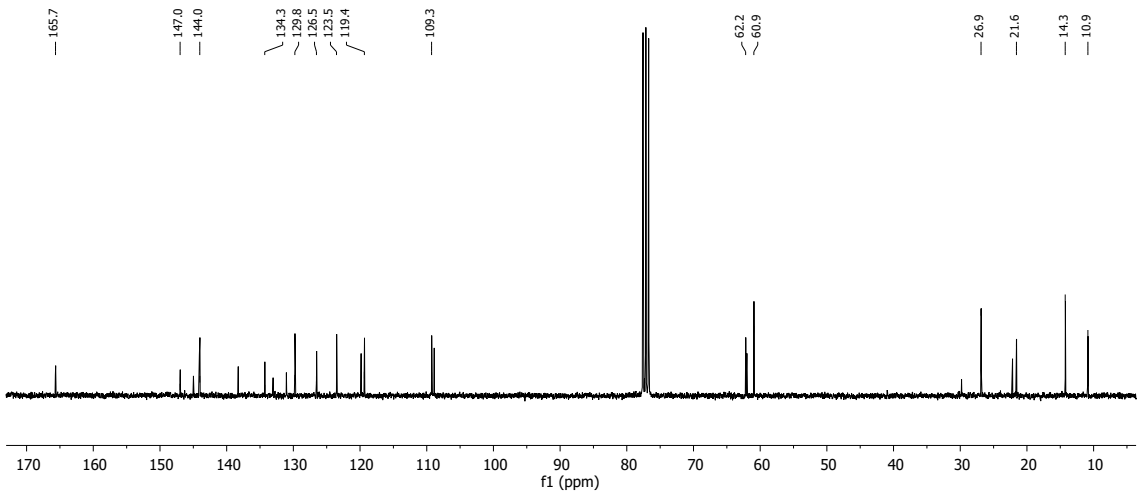

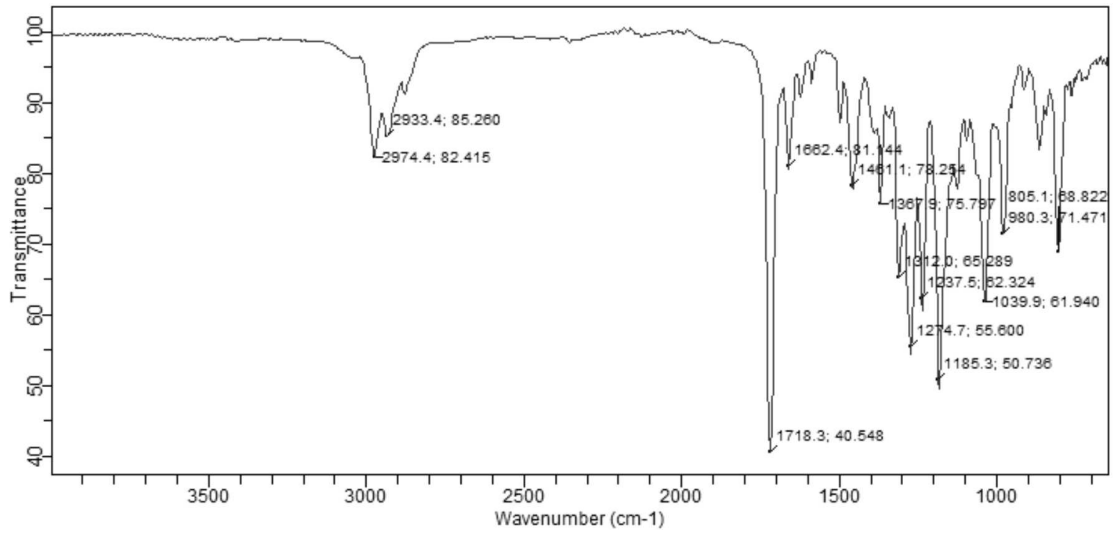

Ethyl (*Z*)-3-(5-methyl-1H-benzo[d][1,2,3]triazol-1-yl)hex-3-enoate (*N*1-isomer) and ethyl (*Z*)-3-(6-methyl-1H-benzo[d][1,2,3]triazol-1-yl)hex-3-enoate (*N*3-isomer) (153an) (^{1}H NMR: 400 MHz, ^{13}C NMR: 101 MHz, $CDCl_3$; IR)

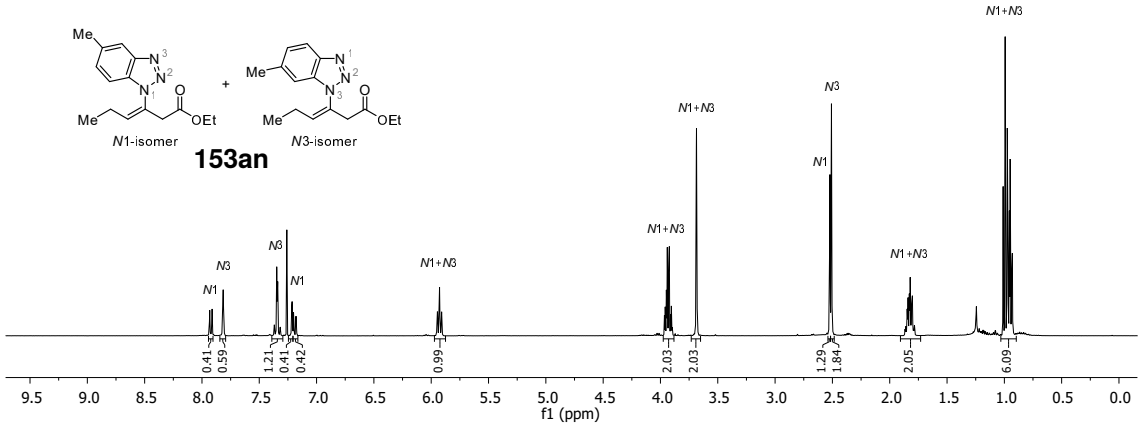

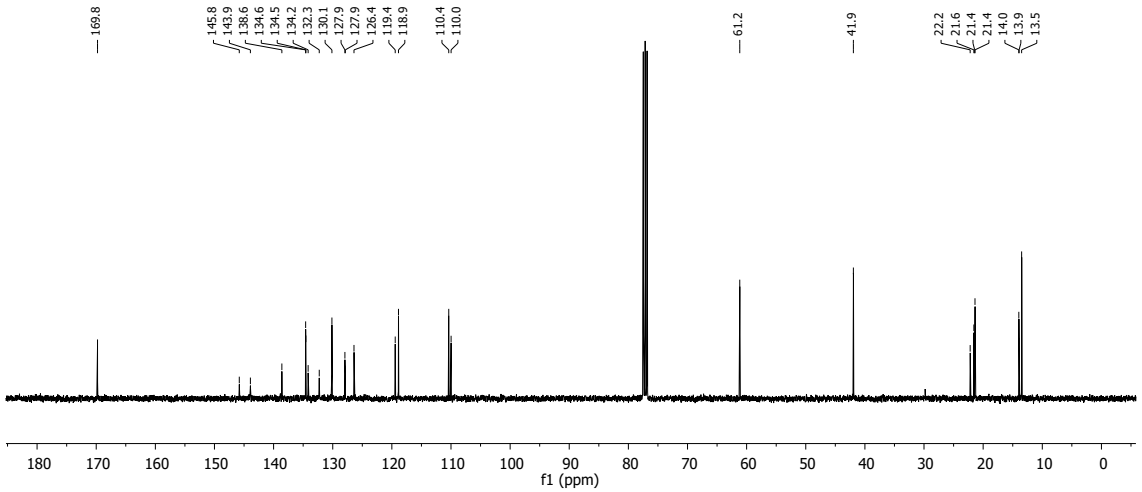

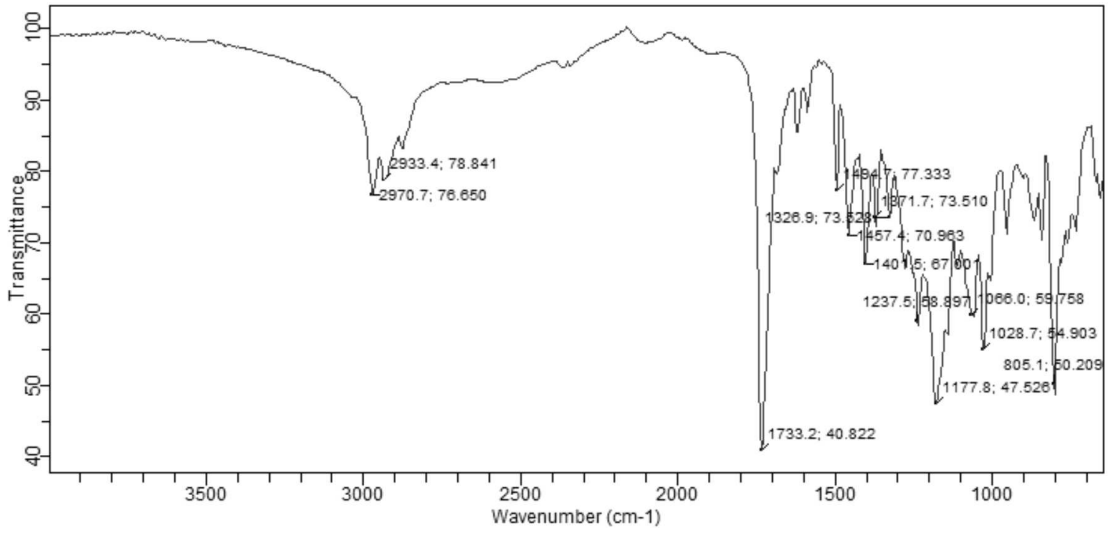

Ethyl (*E*)-4-hydroxyhex-2-enedioate (159) (^{1}H NMR: 300 MHz, ^{13}C NMR: 101 MHz, $CDCl_3$; IR)

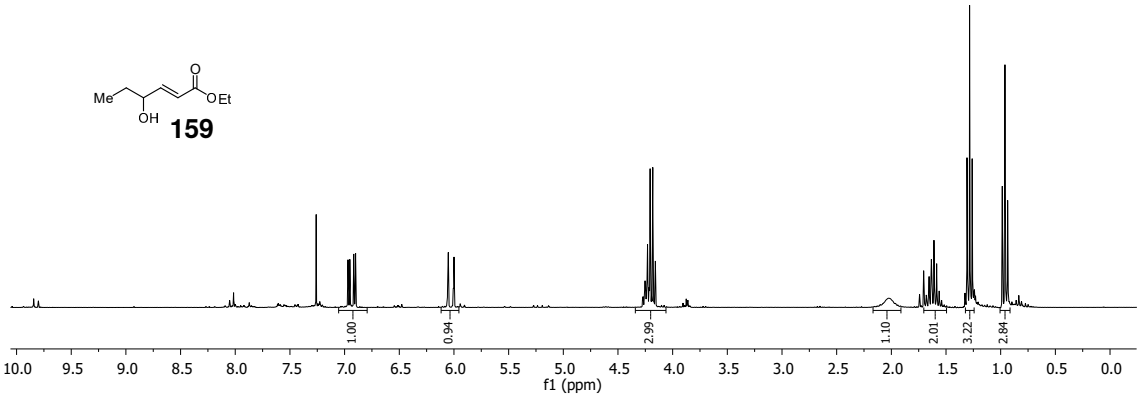

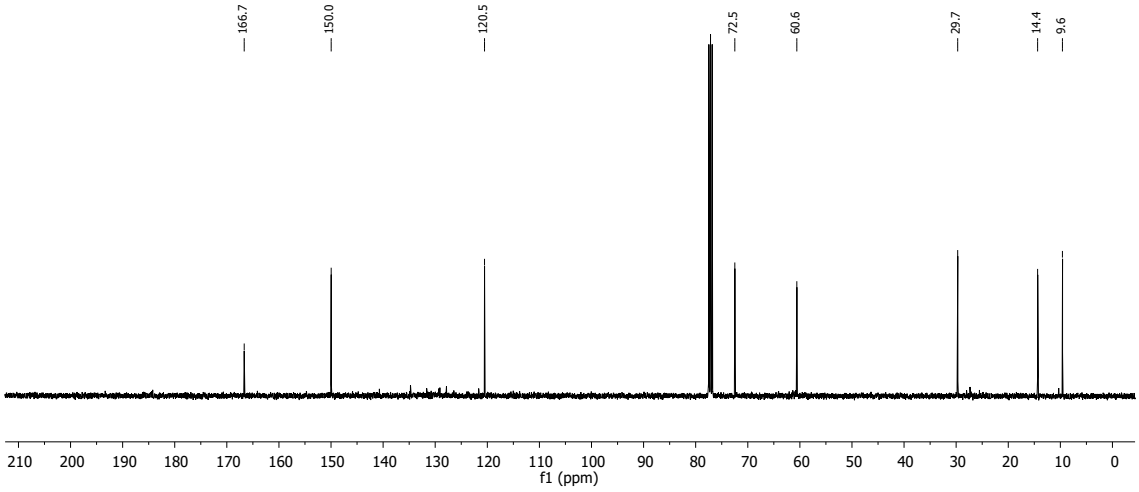

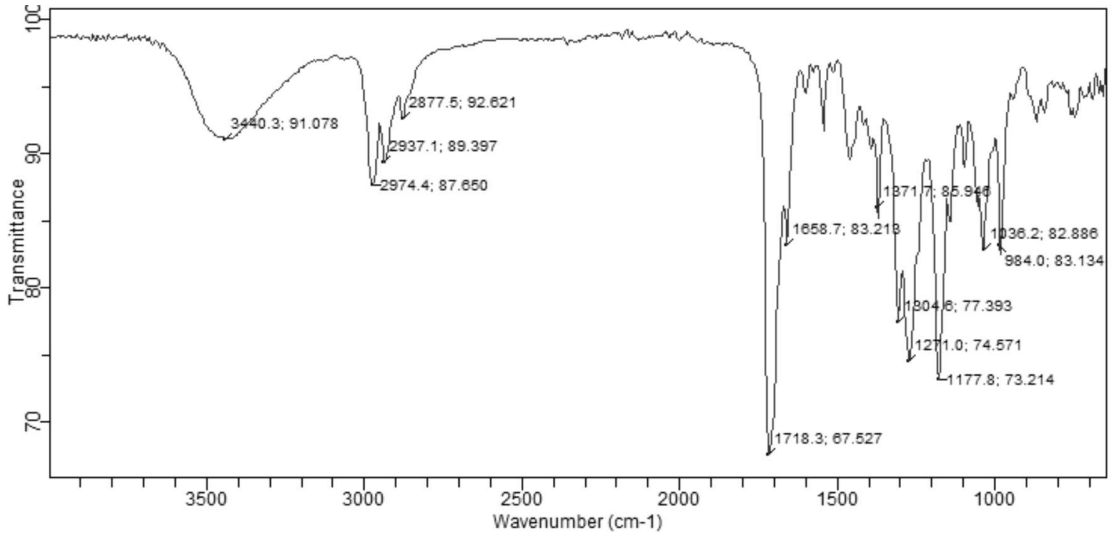

Ethyl (*E*)-4-(5-methyl-1H-tetrazol-1-yl)hex-2-enoate (152ao)) (^{1}H NMR: 300 MHz, ^{13}C NMR: 75 MHz, NOESY, $CDCl_3$; IR)

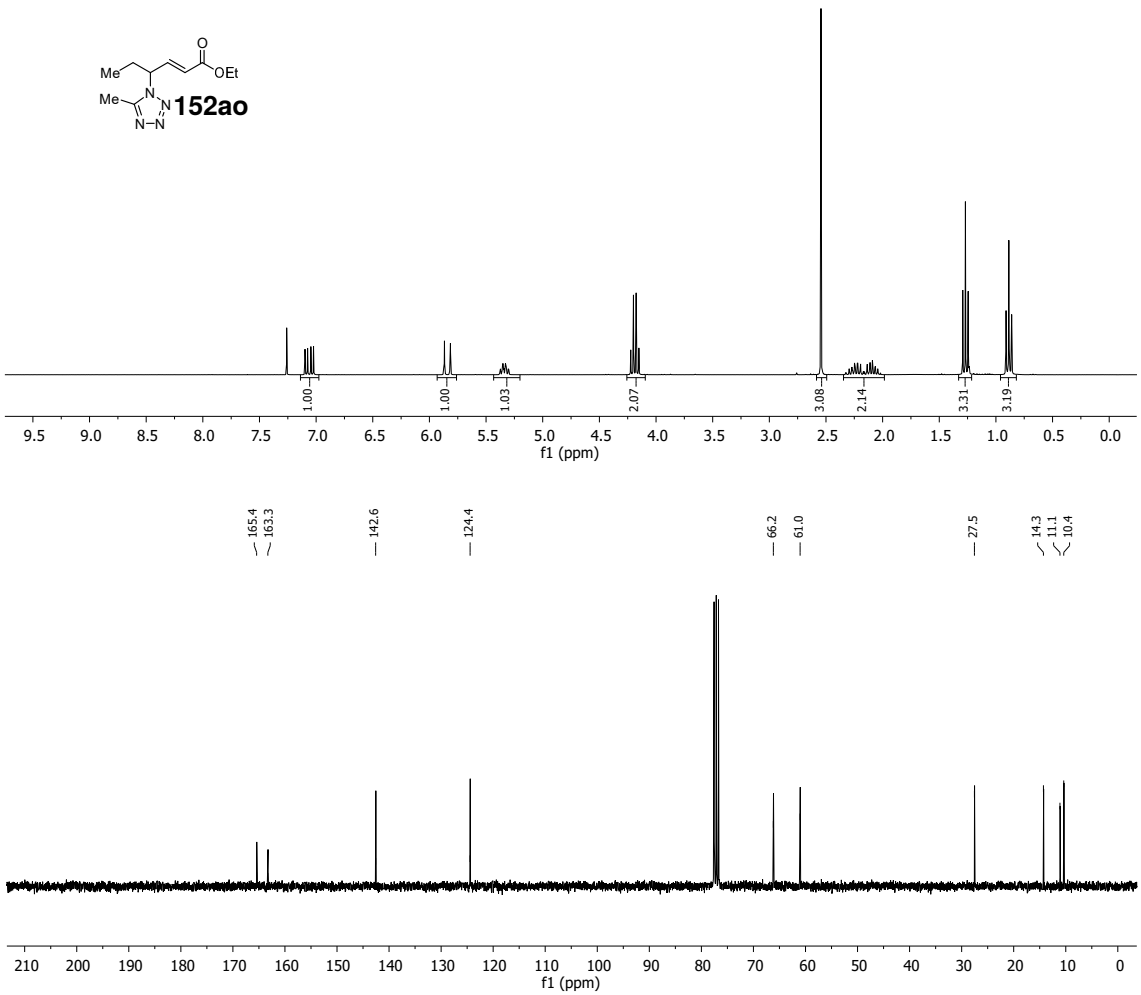

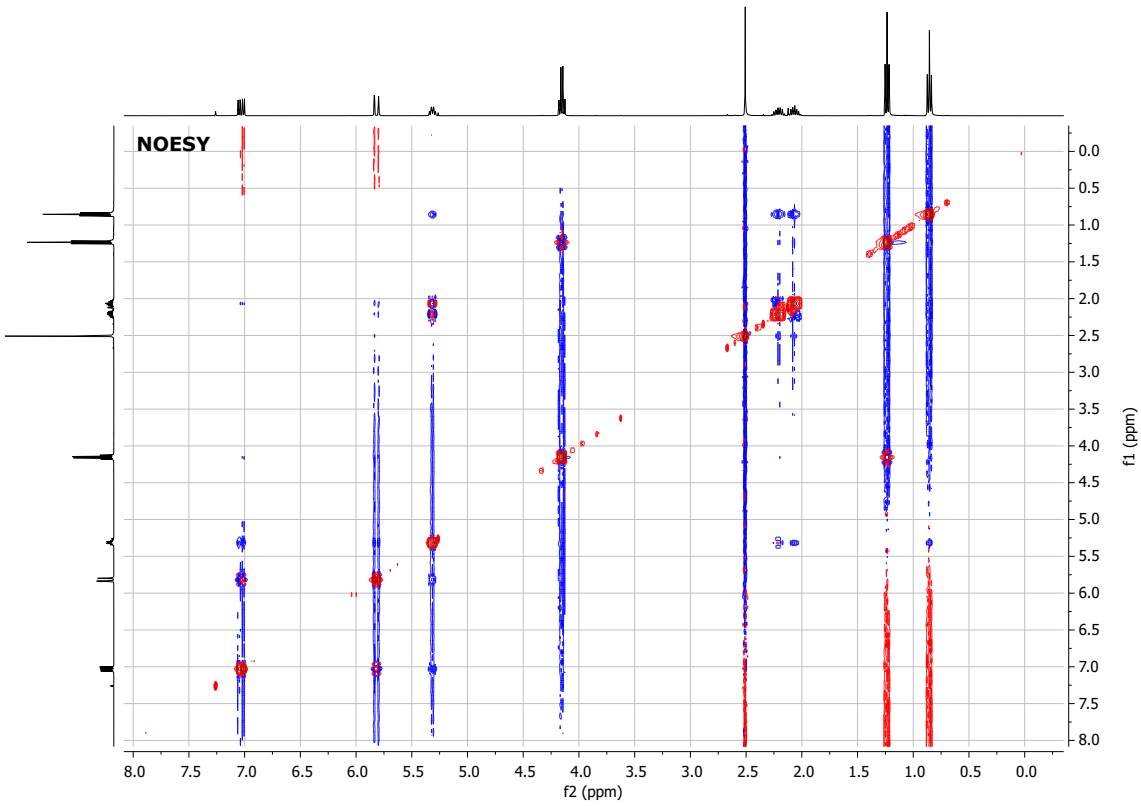
NOESY
f2 (ppm)
f1 (ppm)

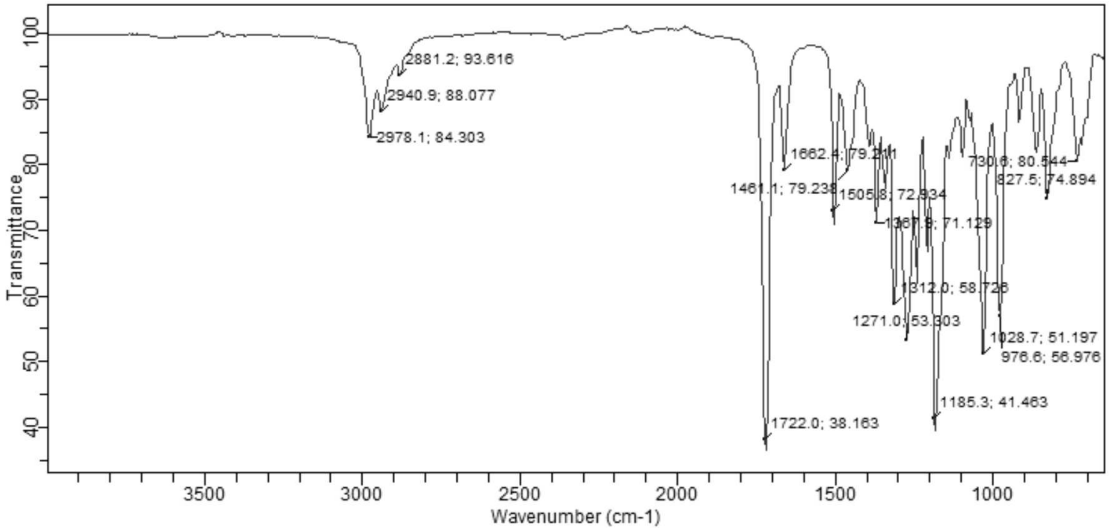
Transmittance
Wavenumber (cm-1)
2881.2; 93.616
2940.9; 88.077
2978.1; 84.303
1722.0; 38.163
1185.3; 41.463
976.6; 56.976

Ethyl (*Z*)-3-(5-methyl-1H-tetrazol-1-yl)hex-3-enoate (153ao) (^{1}H NMR: 400 MHz, ^{13}C NMR: 101 MHz, $CDCl_3$; IR)

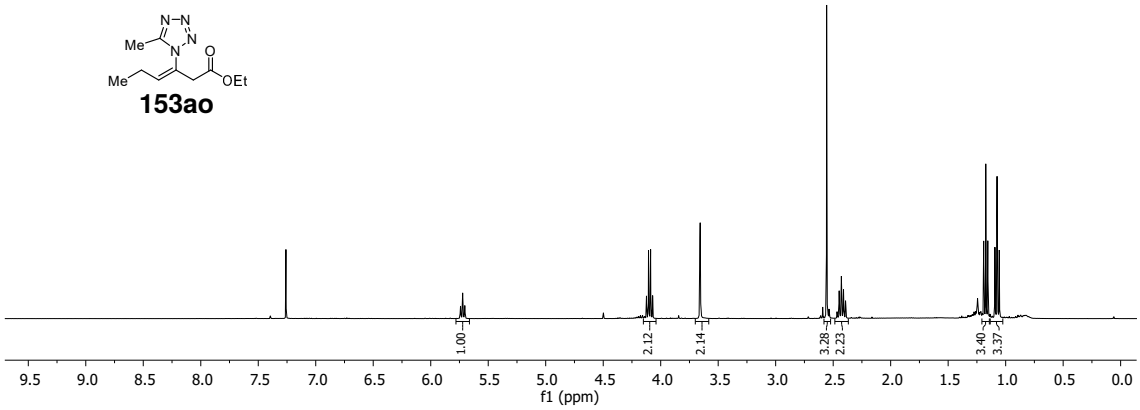

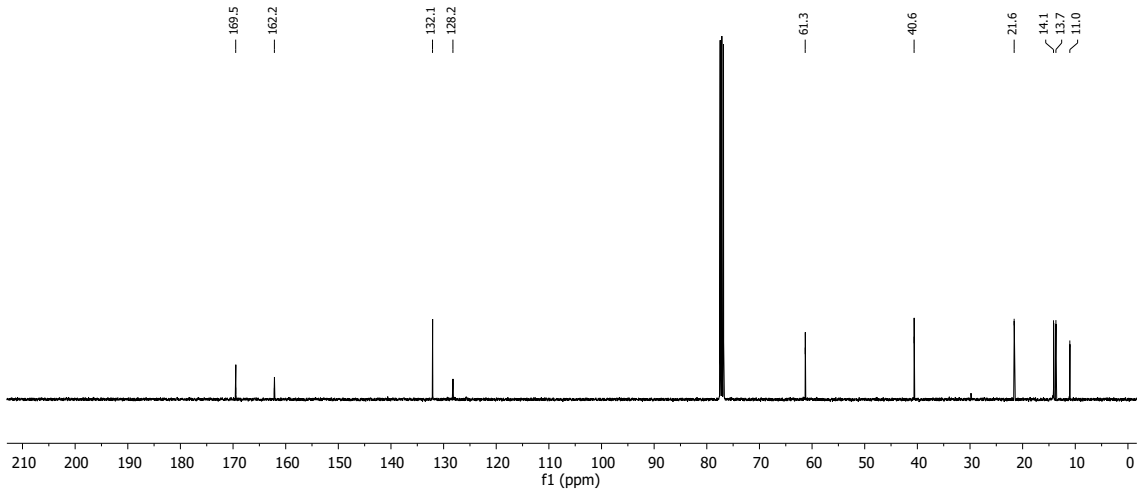

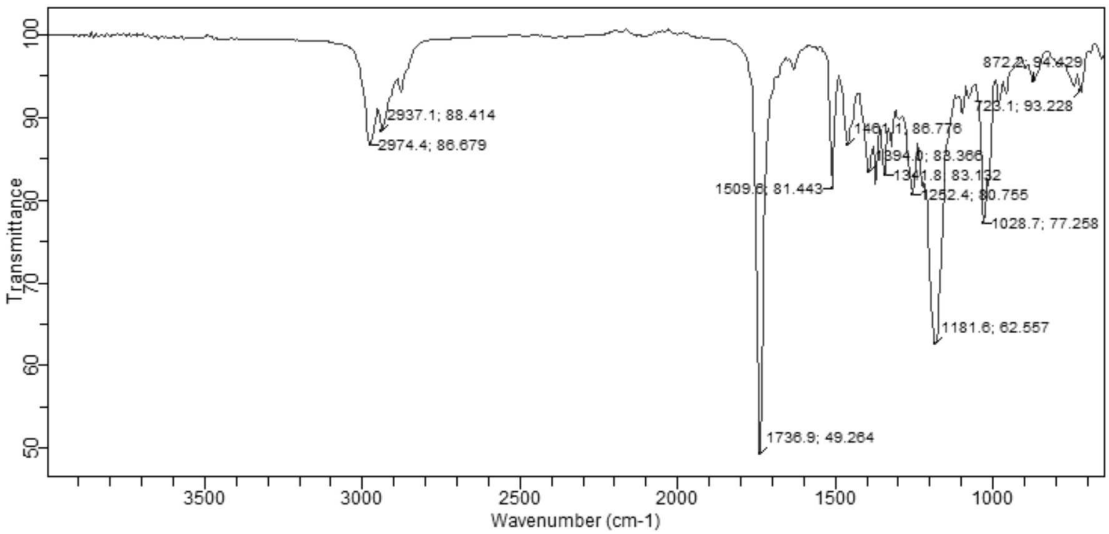

Diethyl (*E*)-4-(1H-pyrazol-1-yl)hex-2-enedioate (152au) (^{1}H NMR: 400 MHz, ^{13}C NMR: 101 MHz, $CDCl_3$; IR)

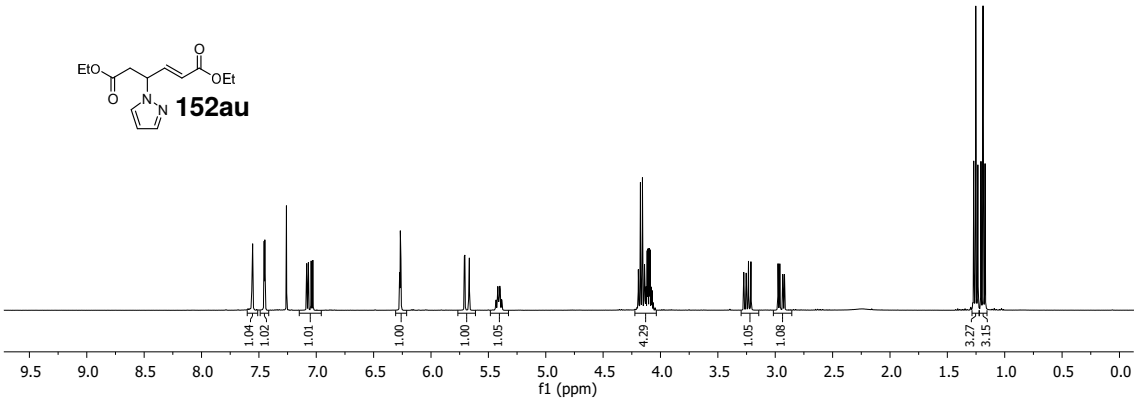

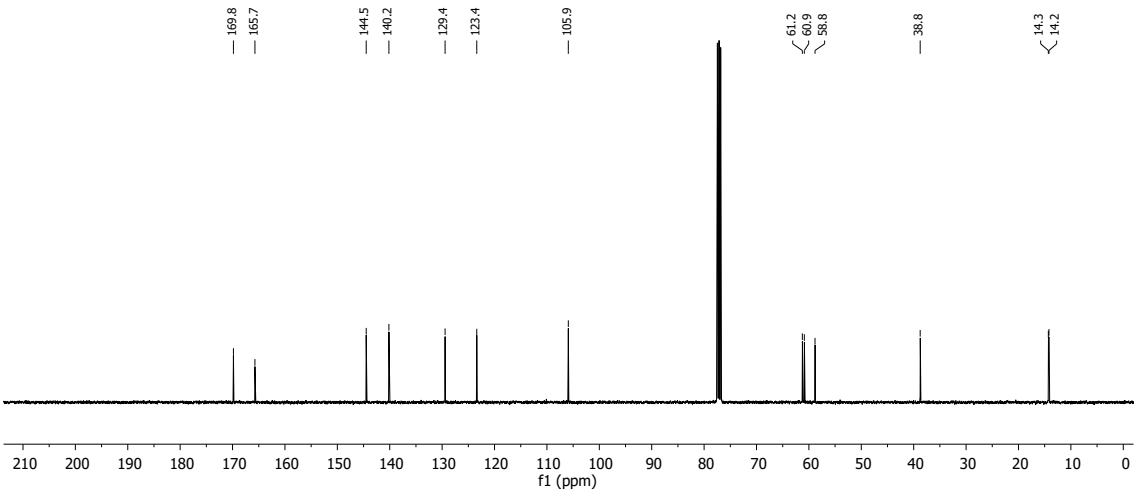

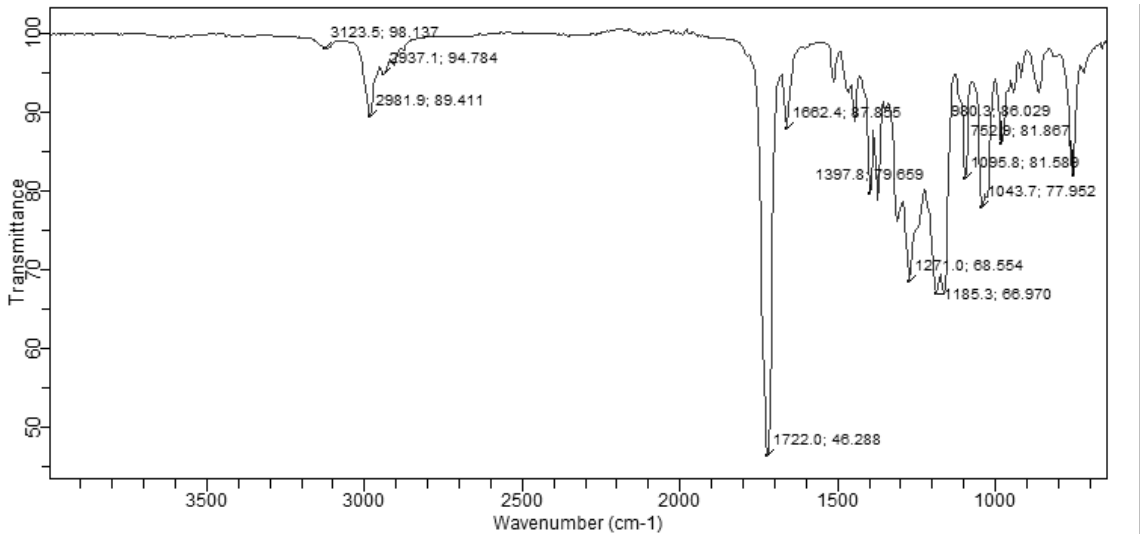

Diethyl (*E*)-4-(4-methyl-1H-pyrazol-1-yl)hex-2-enedioate (152av) (^{1}H NMR: 400 MHz, ^{13}C NMR: 101 MHz, $CDCl_3$; IR)

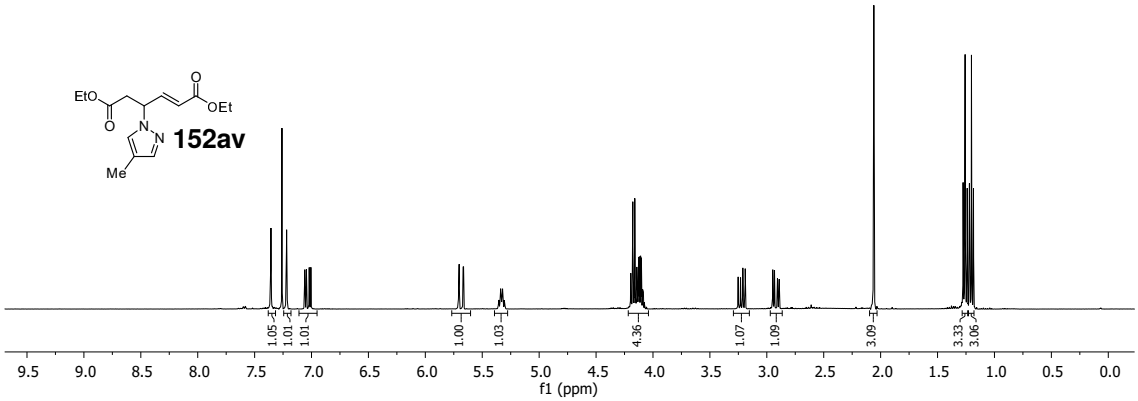

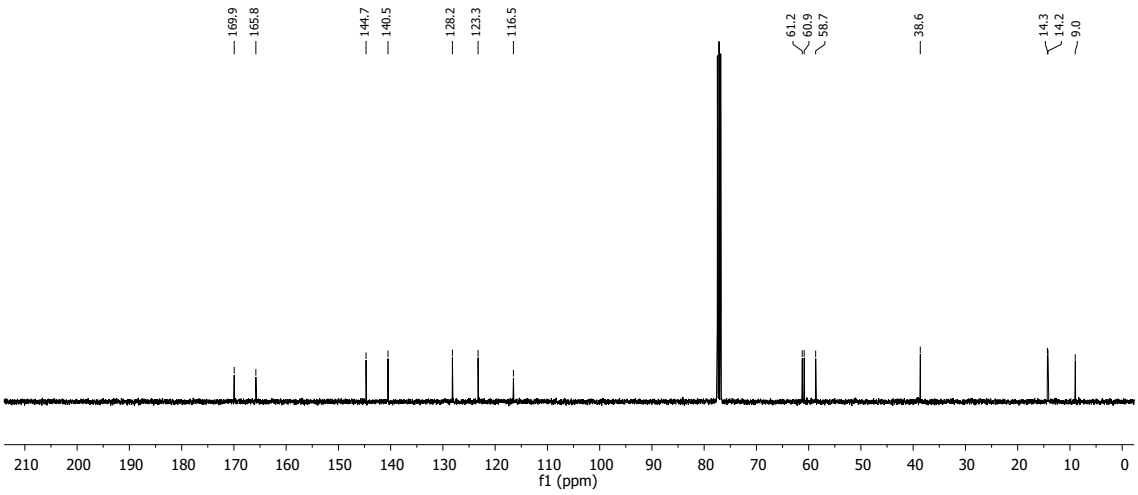

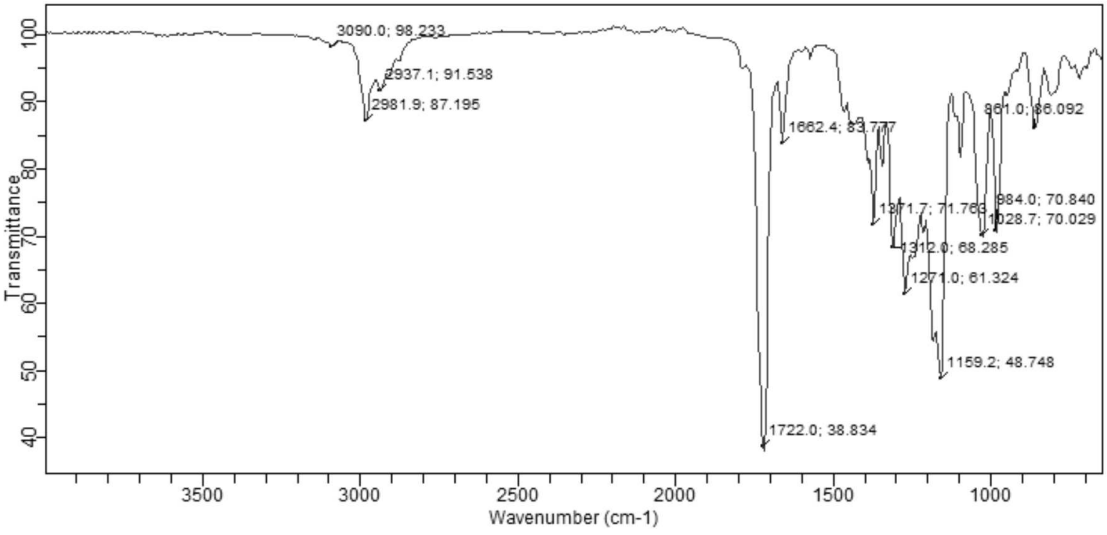

Diethyl (*E*)-4-(4-(trifluoromethyl)-1H-pyrazol-1-yl)hex-2-enedioate (152aw) (^{1}H NMR: 400 MHz, ^{13}C NMR: 101 MHz, ^{19}F NMR: 376 MHz, $CDCl_3$; IR)

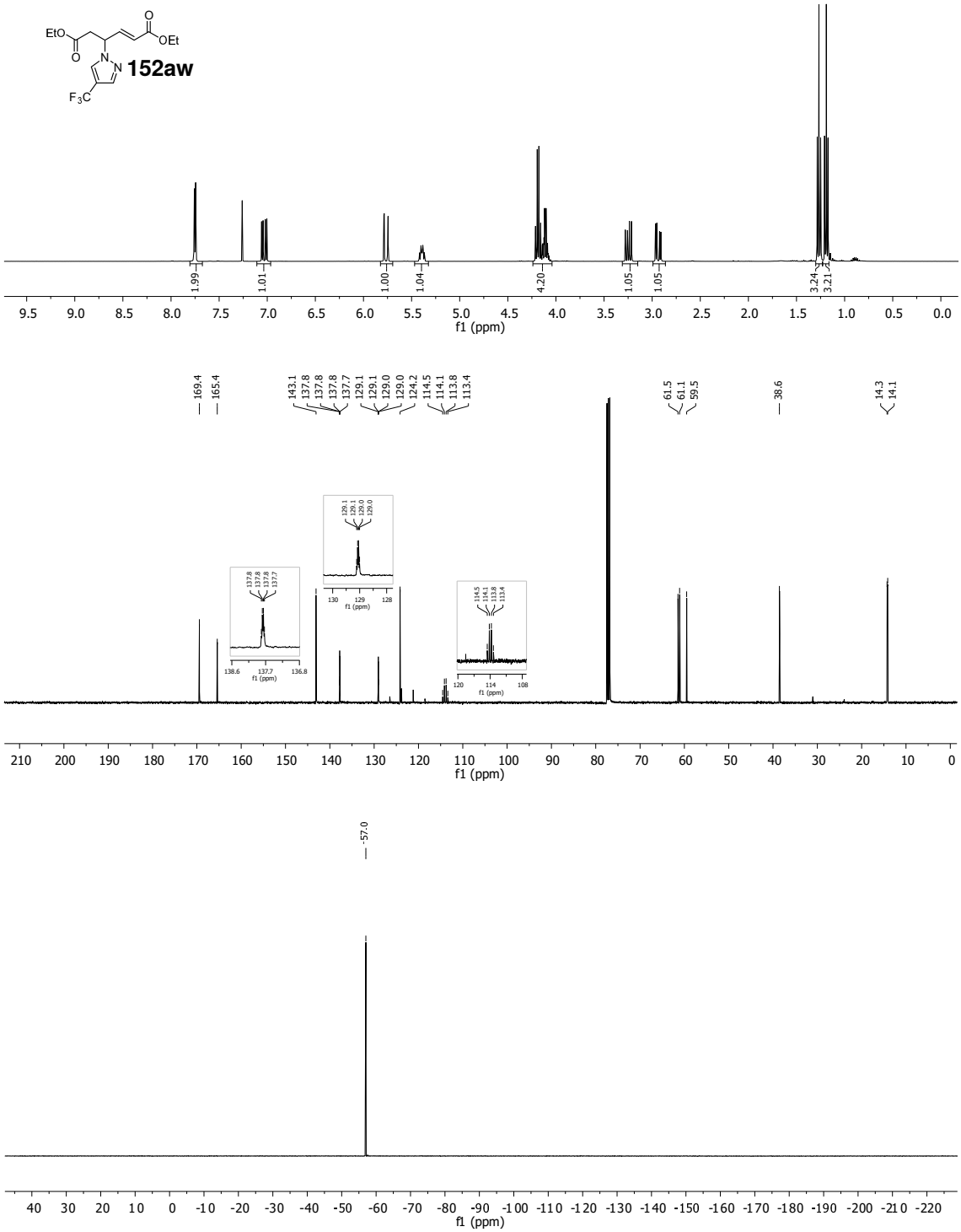

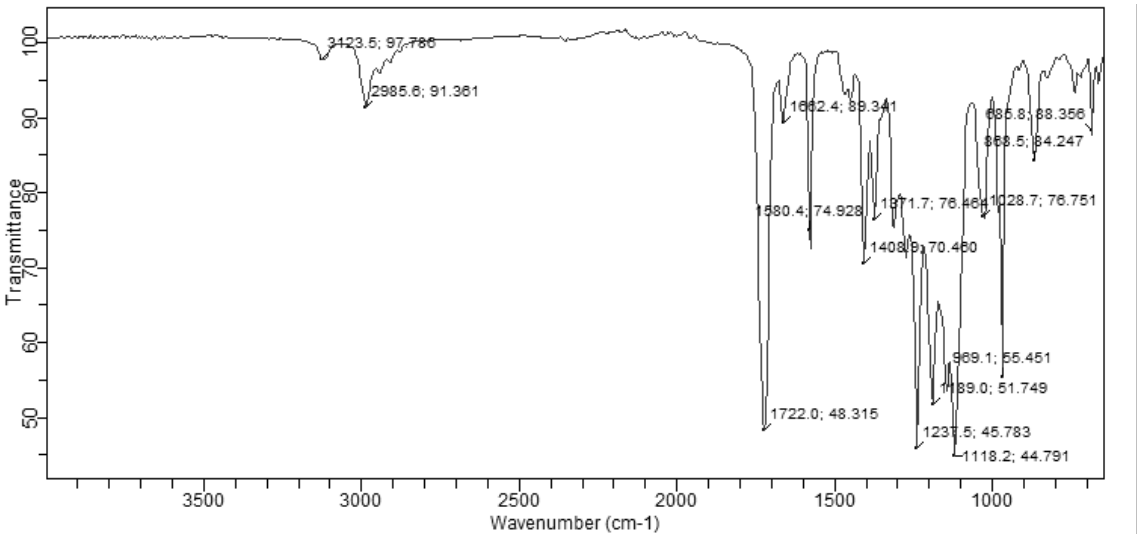
Transmittance
100
90
80
70
60
50
3500
3000
2500
2000
1500
1000
Wavenumber (cm-1)
3123.5; 97.786
2985.6; 91.361
1662.4; 89.341
1580.4; 74.928
1722.0; 48.315
1408.9; 70.460
1371.7; 76.464
1028.7; 76.751
885.8; 88.356
868.5; 84.247
969.1; 55.451
1189.0; 51.749
1237.5; 45.783
1118.2; 44.791

Diethyl (*E*)-4-(5-methyl-2H-tetrazol-2-yl)hex-2-enedioate (152ba) (^{1}H NMR: 400 MHz, ^{13}C NMR: 101 MHz, NOESY, $CDCl_3$; IR)

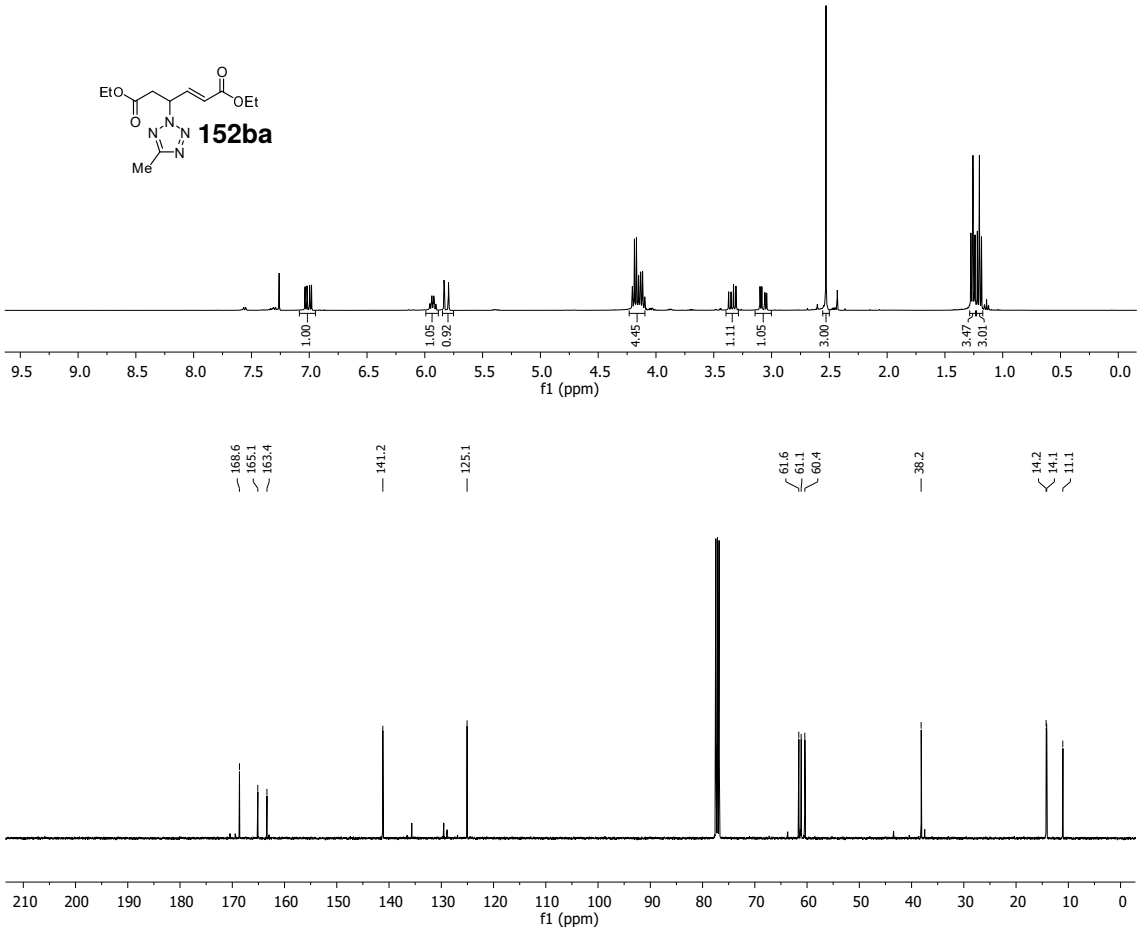

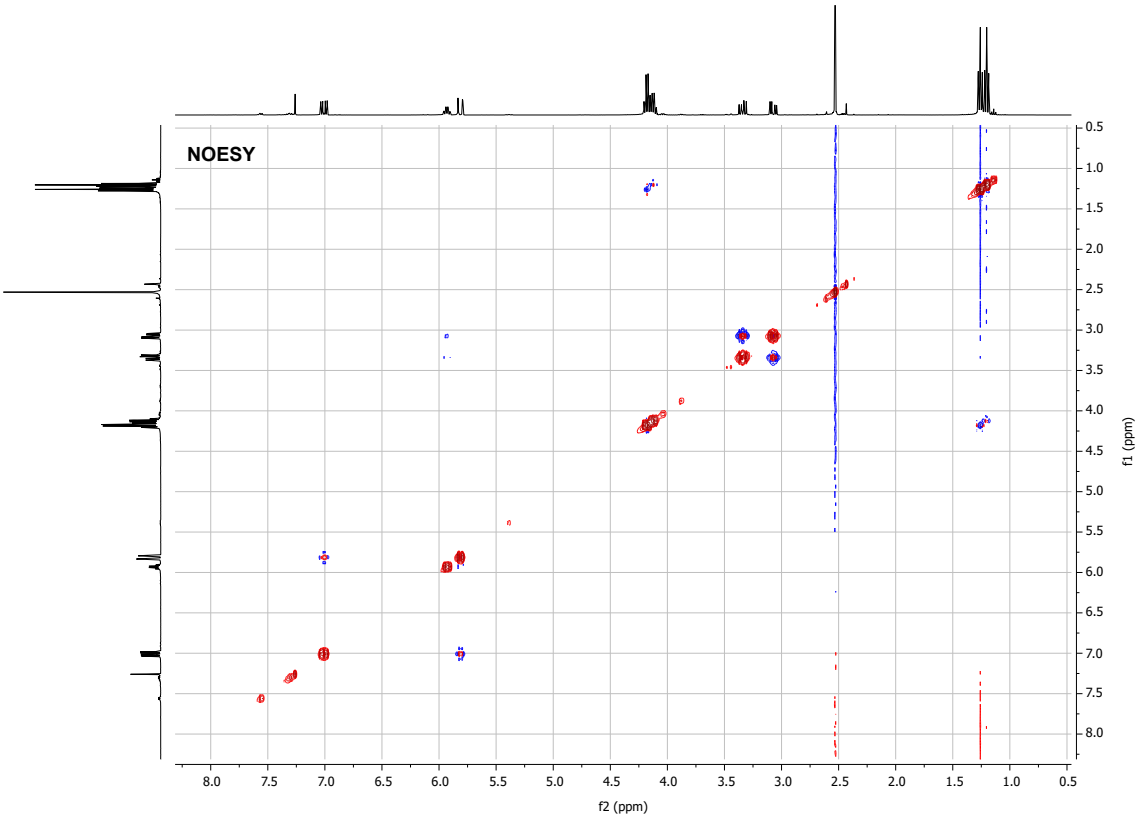
NOESY
f2 (ppm)
f1 (ppm)

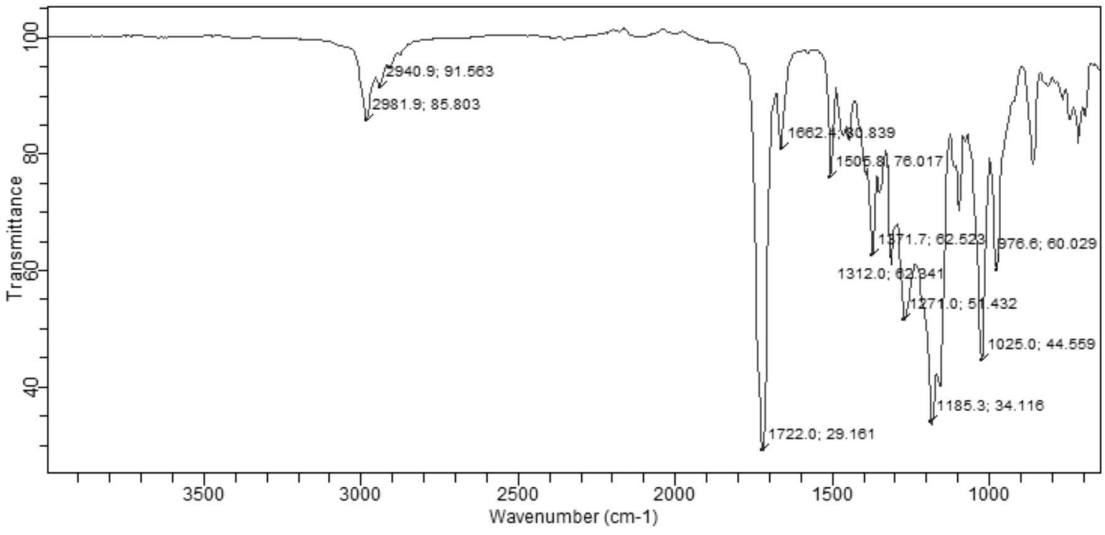
Transmittance
Wavenumber (cm-1)
2940.9; 91.563
2981.9; 85.803
1722.0; 29.161
1185.3; 34.116
1025.0; 44.559
1271.0; 51.432
1312.0; 62.841
1371.7; 62.523
876.6; 60.029

Diethyl (*E*)-4-hydroxyhex-2-enedioate (186) (^{1}H NMR: 400 MHz, ^{13}C NMR: 101 MHz, $CDCl_3$; IR)

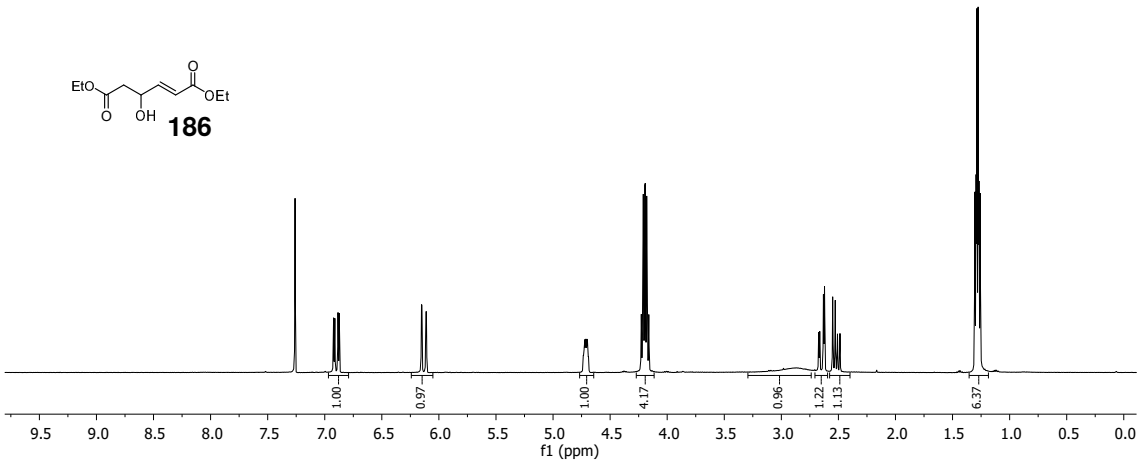

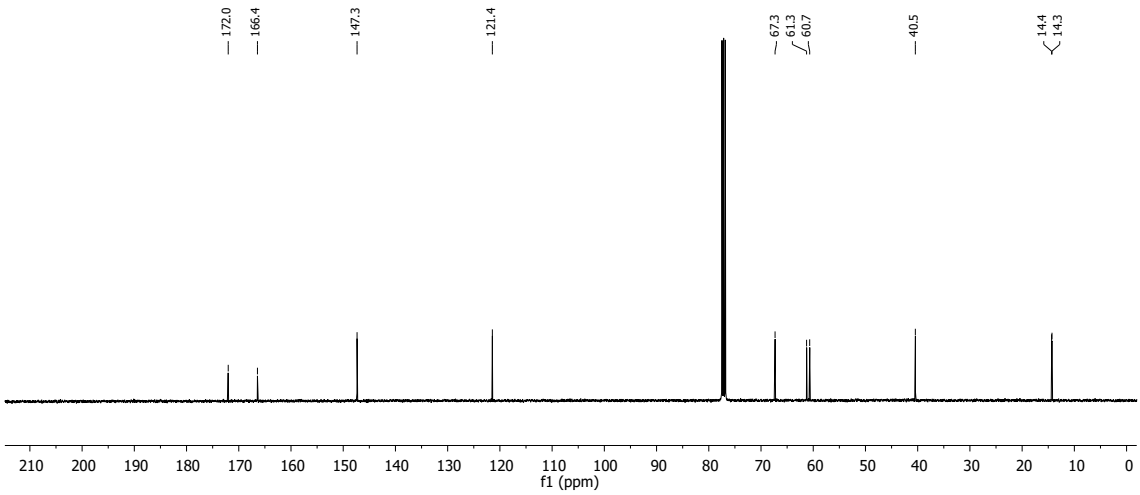

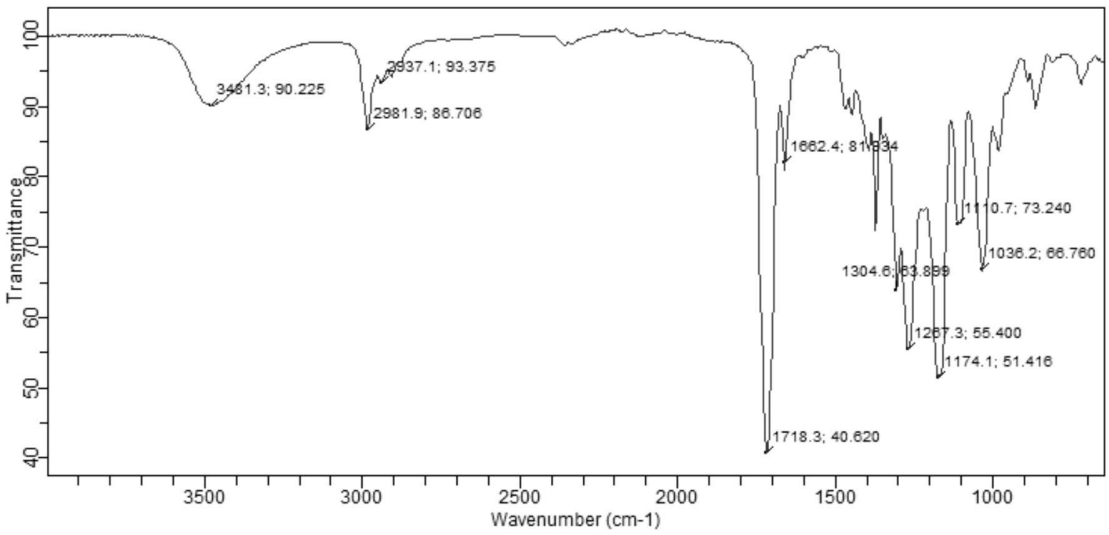

Diethyl (*E*)-4-(5-phenyl-2H-tetrazol-2-yl)hex-2-enedioate (152bb) (^{1}H NMR: 400 MHz, ^{13}C NMR: 101 MHz, NOESY, $CDCl_3$; IR)

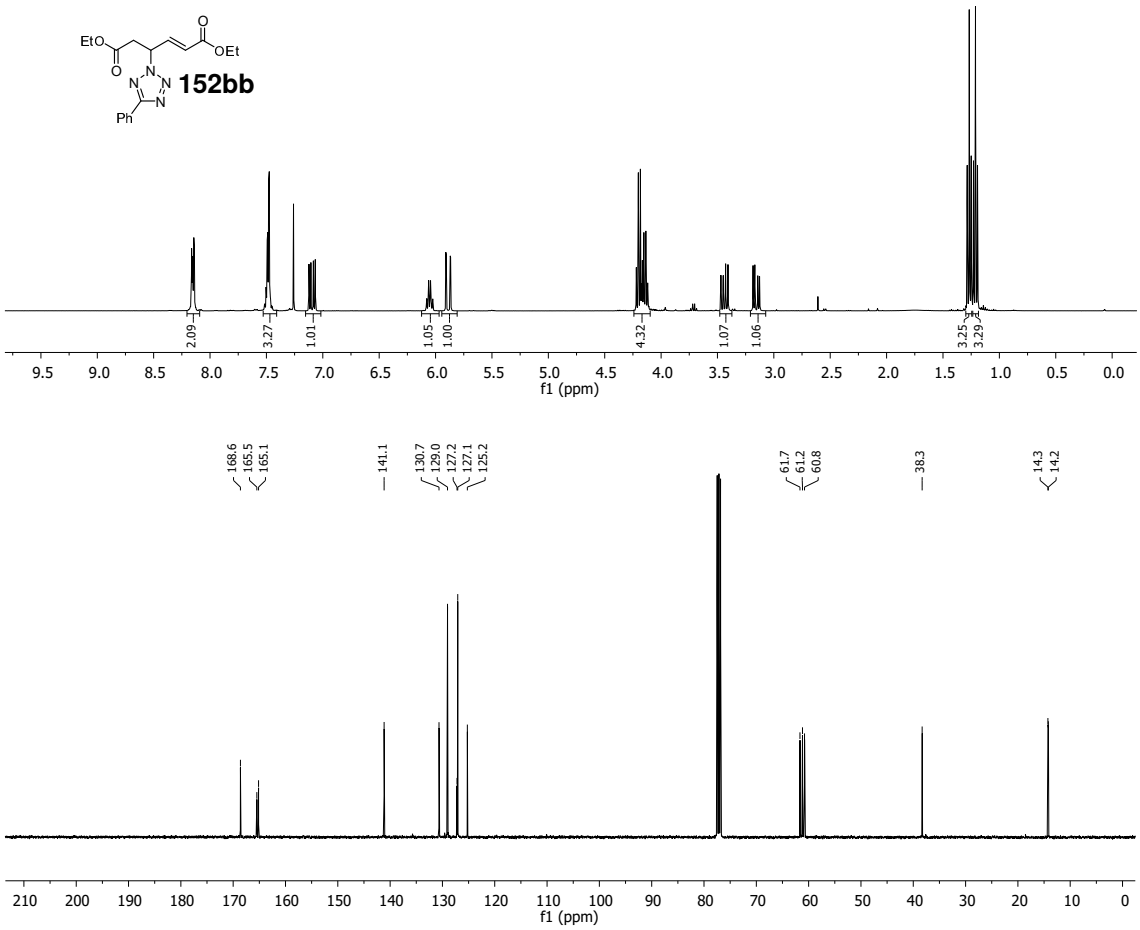

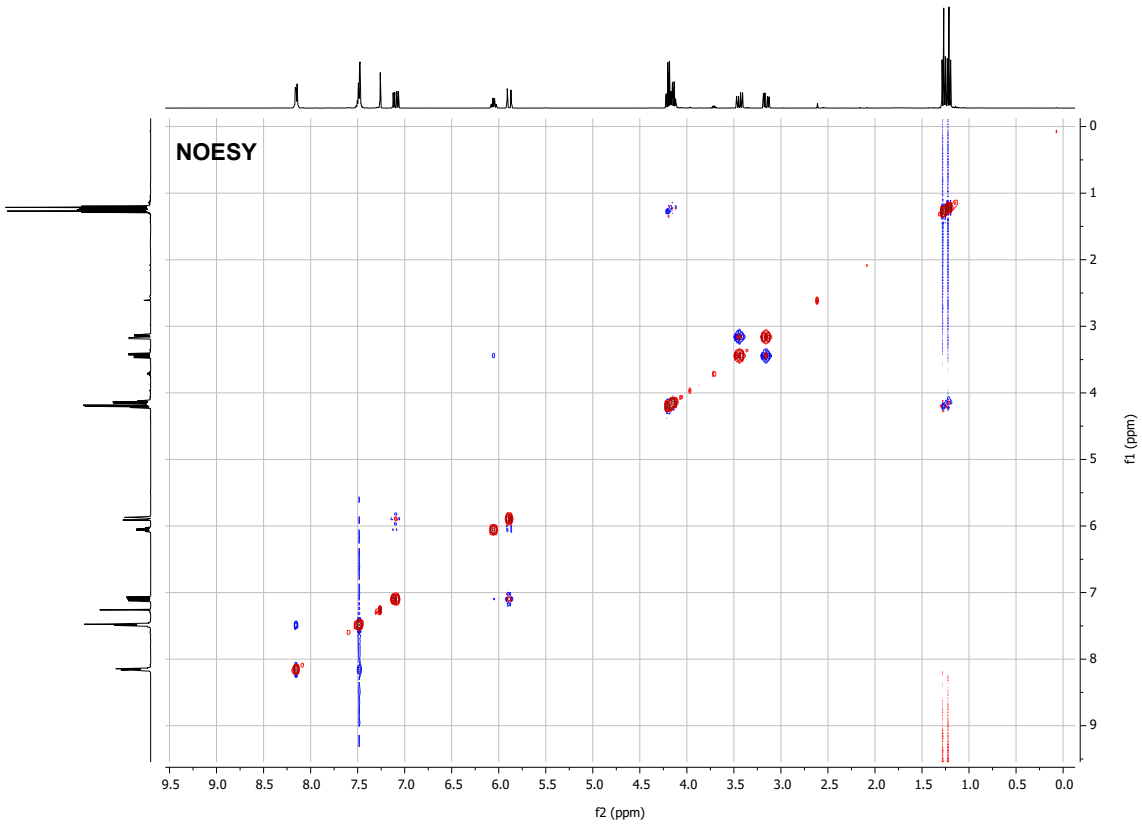
NOESY
f2 (ppm)
f1 (ppm)

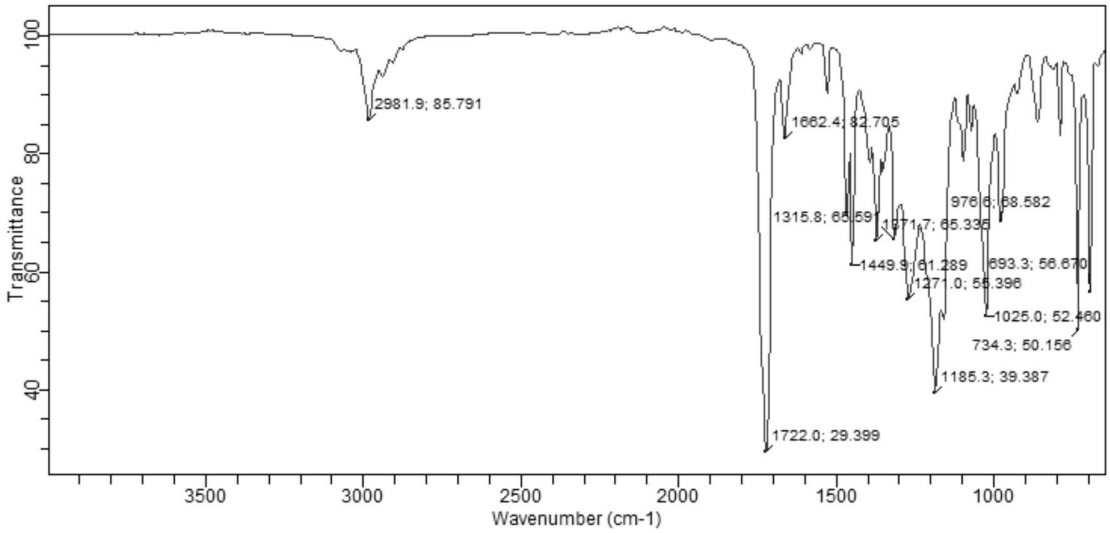
Transmittance
Wavenumber (cm-1)
2981.9; 85.791
1662.4; 82.705
1722.0; 29.399
1185.3; 39.387
1025.0; 52.460
734.3; 50.156

Diethyl (*E*)-4-(5-(p-tolyl)-1H-tetrazol-1-yl)hex-2-enedioate (152bc) (^{1}H NMR: 400 MHz, ^{13}C NMR: 101 MHz, NOESY, $CDCl_3$; IR)

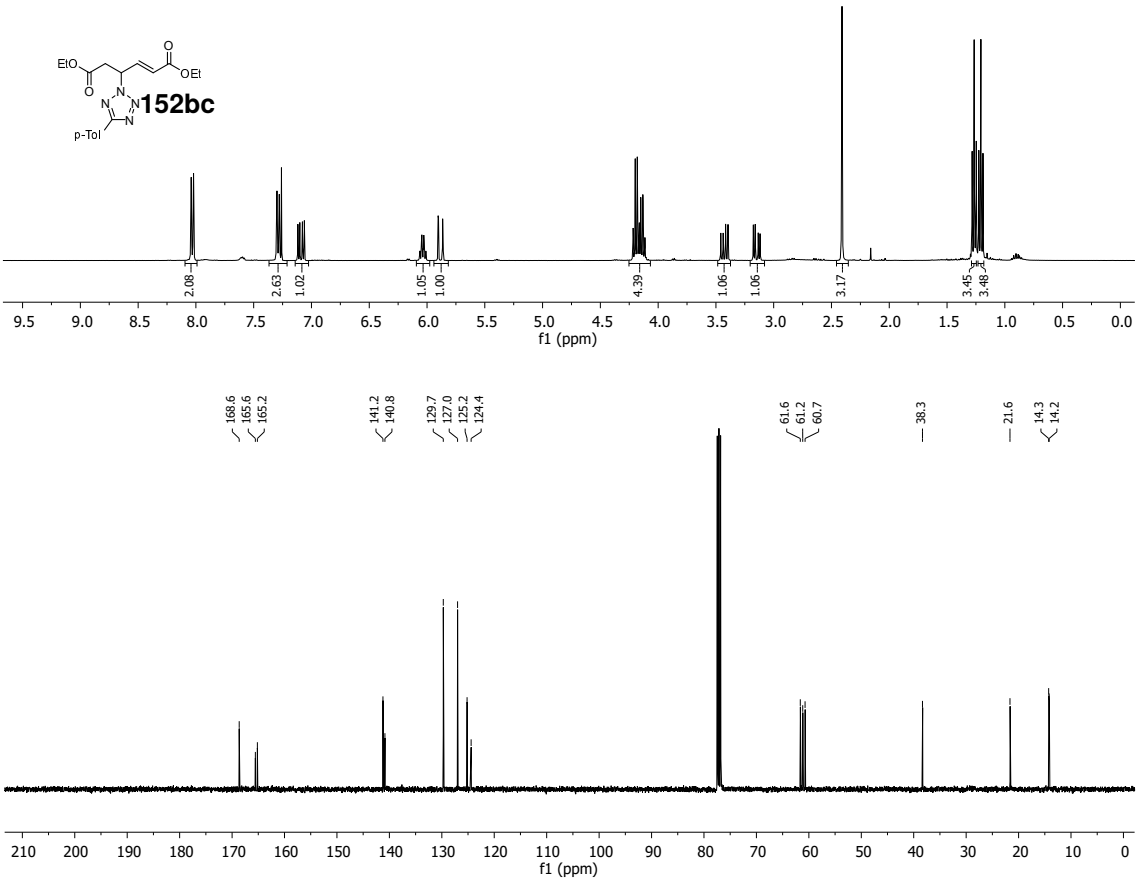

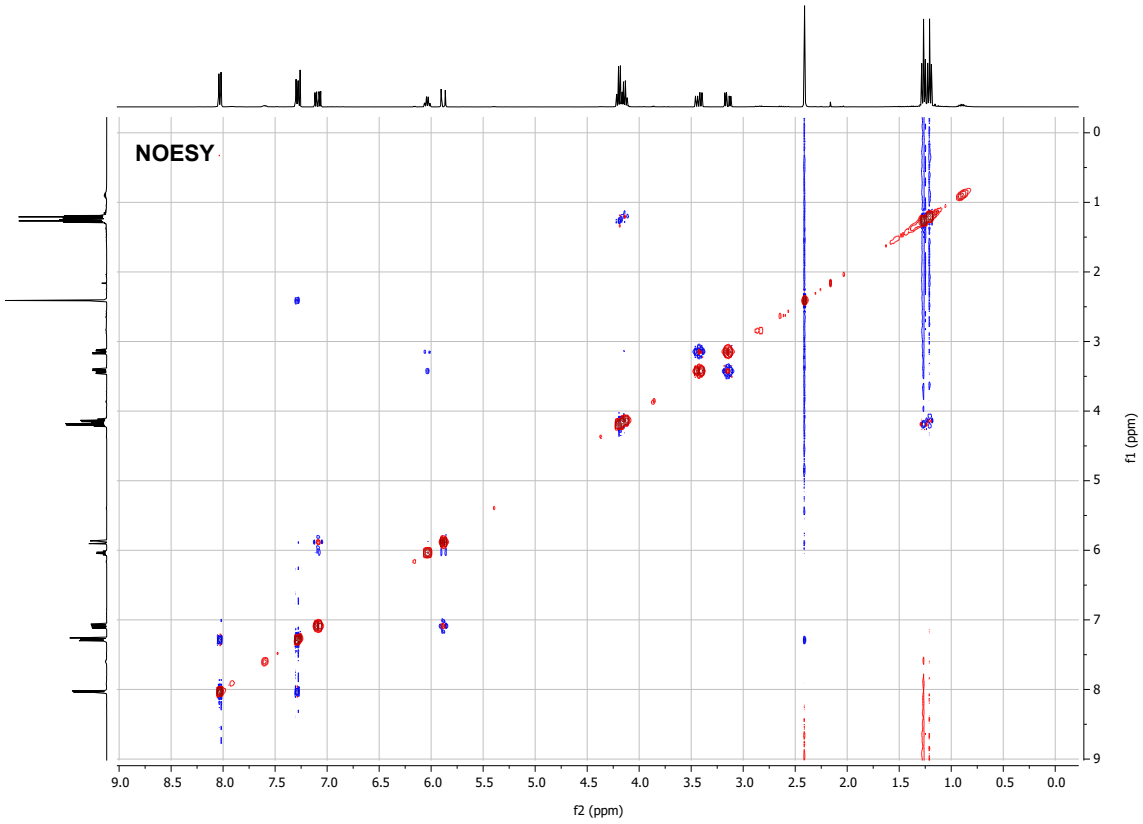
NOESY
f2 (ppm)
f1 (ppm)

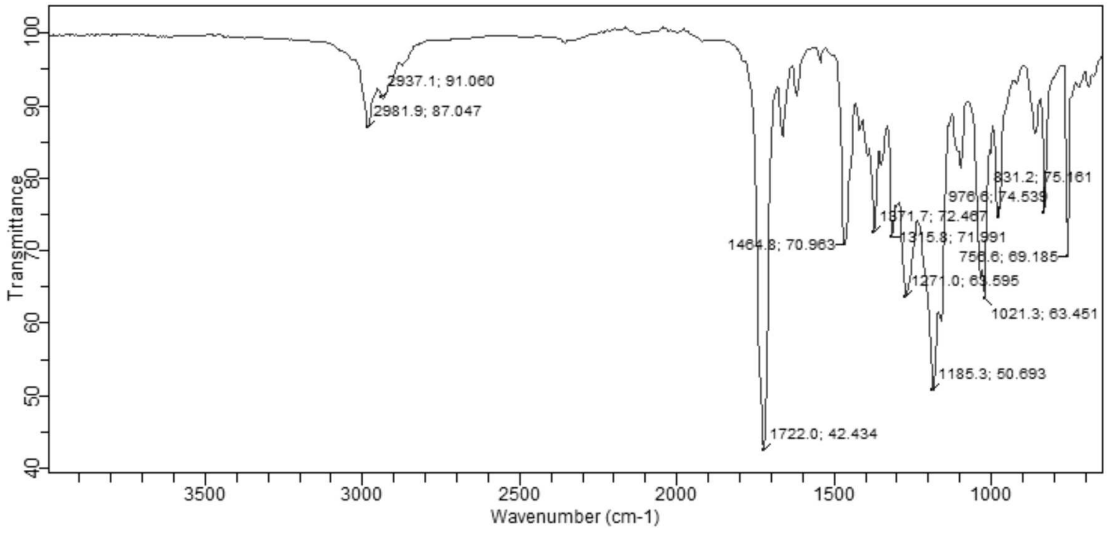
Transmittance
Wavenumber (cm-1)
2937.1; 91.060
2981.9; 87.047
1464.8; 70.963
1722.0; 42.434
1185.3; 50.693
1021.3; 63.451

Diethyl (E)-4-(1H-benzo[d][1,2,3]triazol-1-yl)hex-2-enedioate (152bf) (^{1}H NMR: 400 MHz, ^{13}C NMR: 101 MHz, $CDCl_3$; IR)

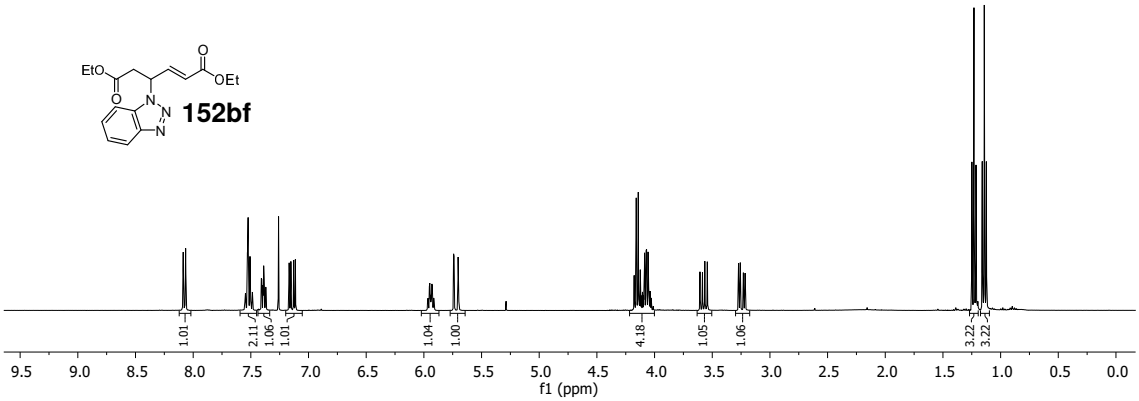

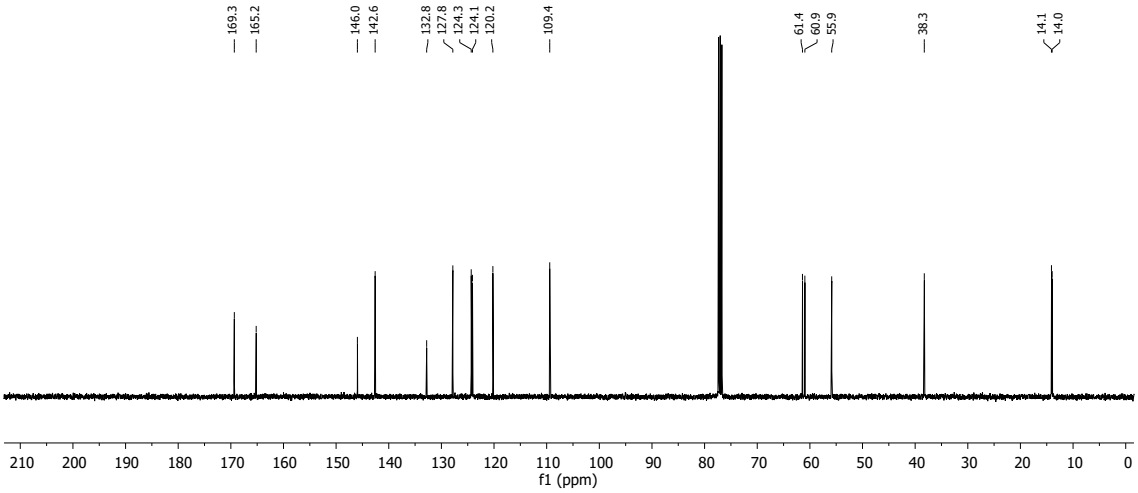

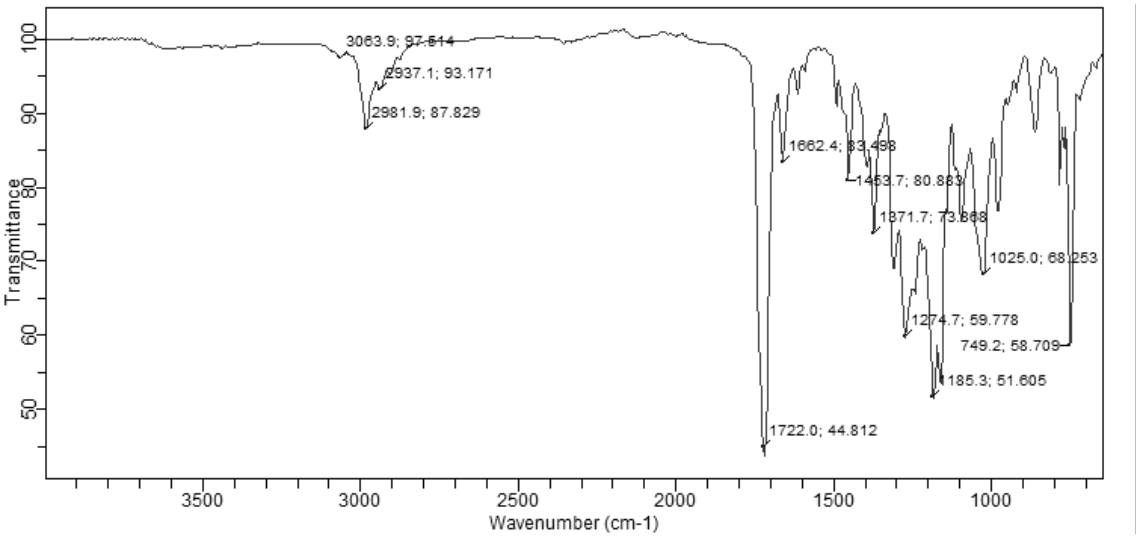

Diethyl (*E*)-4-(2H-benzo[d][1,2,3]triazol-2-yl)hex-2-enedioate (185b) (^{1}H NMR: 400 MHz, ^{13}C NMR: 101 MHz, $CDCl_3$; IR)

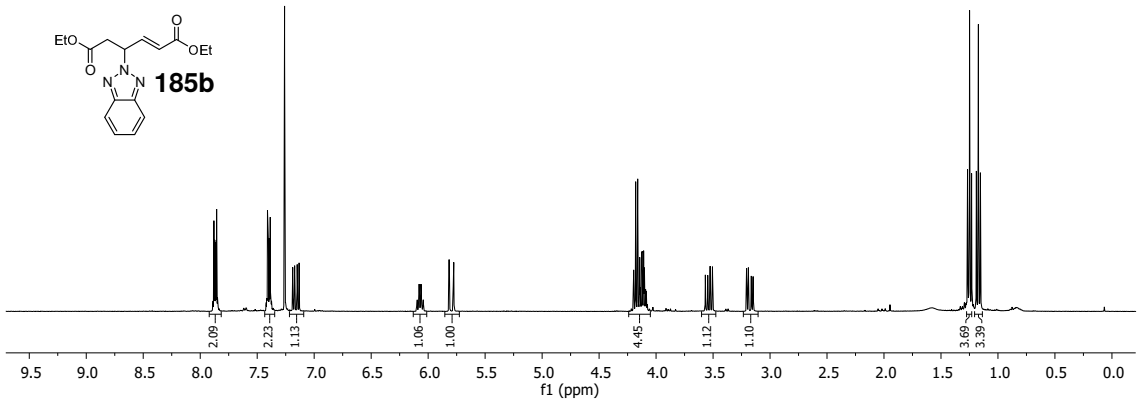

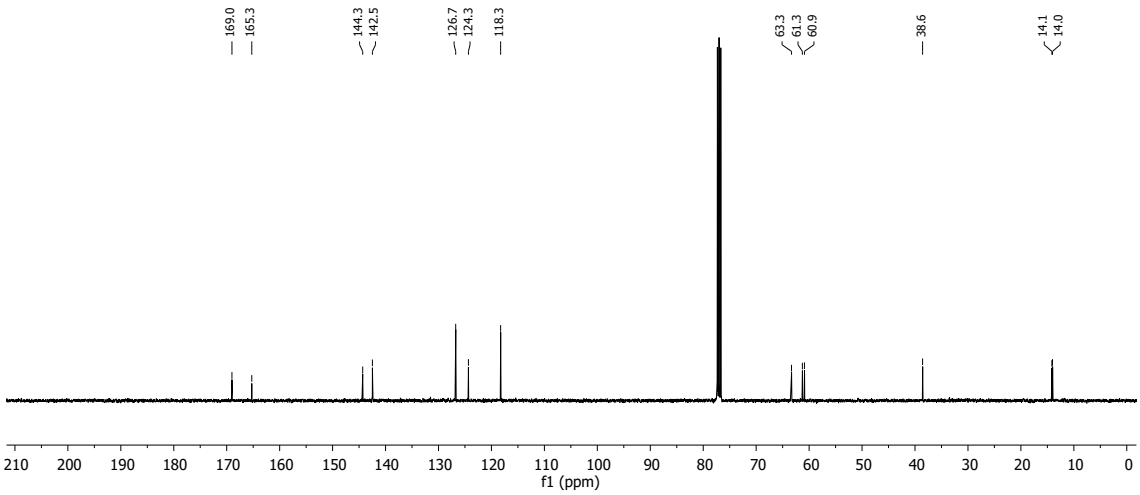

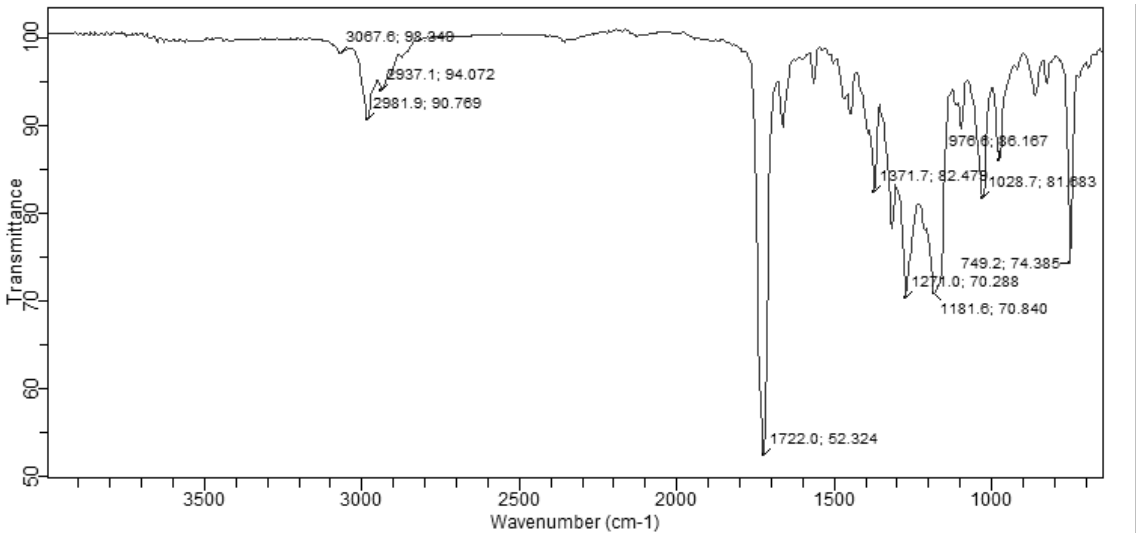

Diethyl (*E*)-4-((1S,3aS,3bR,5aS,10aS,10bS,12aS)-1-hydroxy-1,10a,12a-trimethyl-2,3,3a,3b,4,5,5a,6,10,10a,10b,11,12,12a-tetradecahydrocyclopenta[5,6]naphtho[1,2-f]indazol-8(1H)-yl)hex-2-enedioate (152bg, *N*2-isomer) (^{1}H NMR: 400 MHz, ^{13}C NMR: 101 MHz, NOESY, $CDCl_3$; IR)

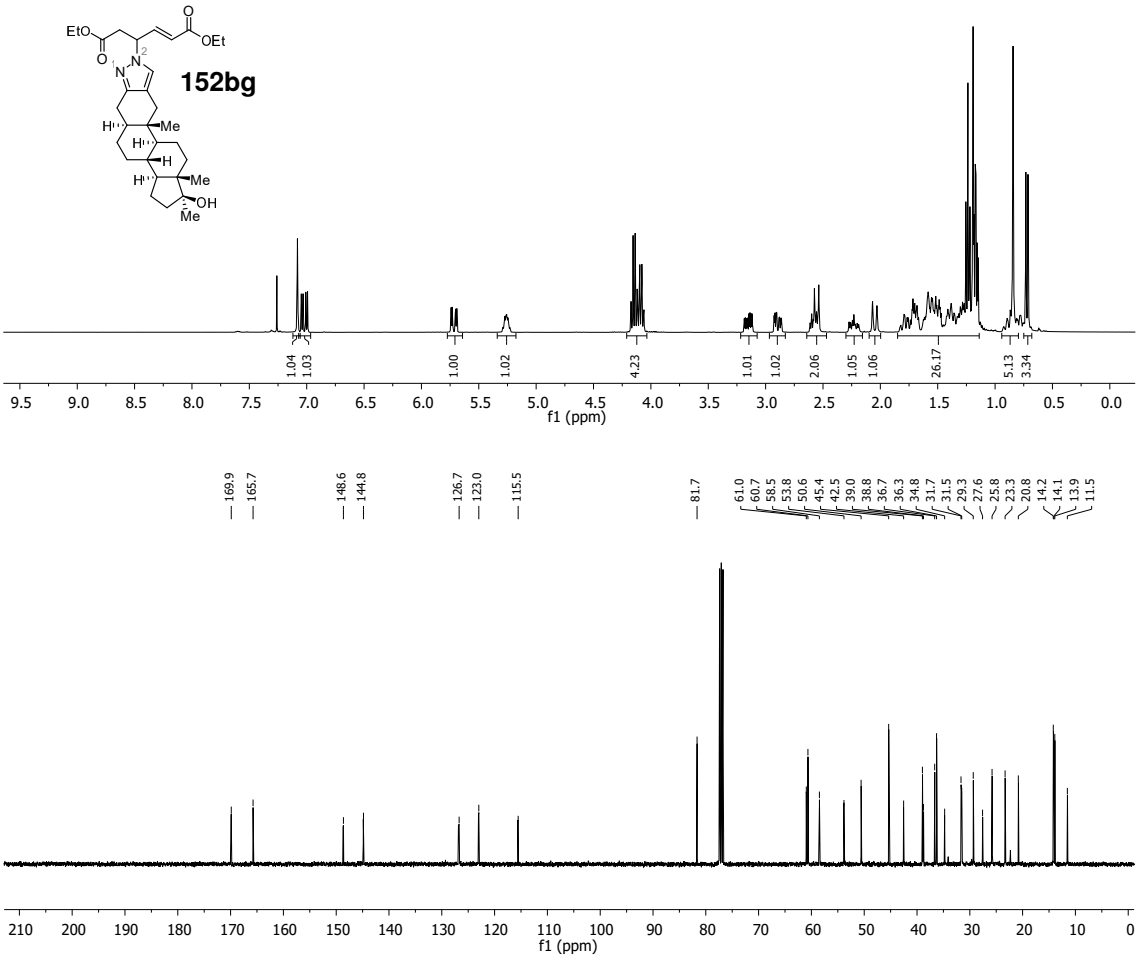

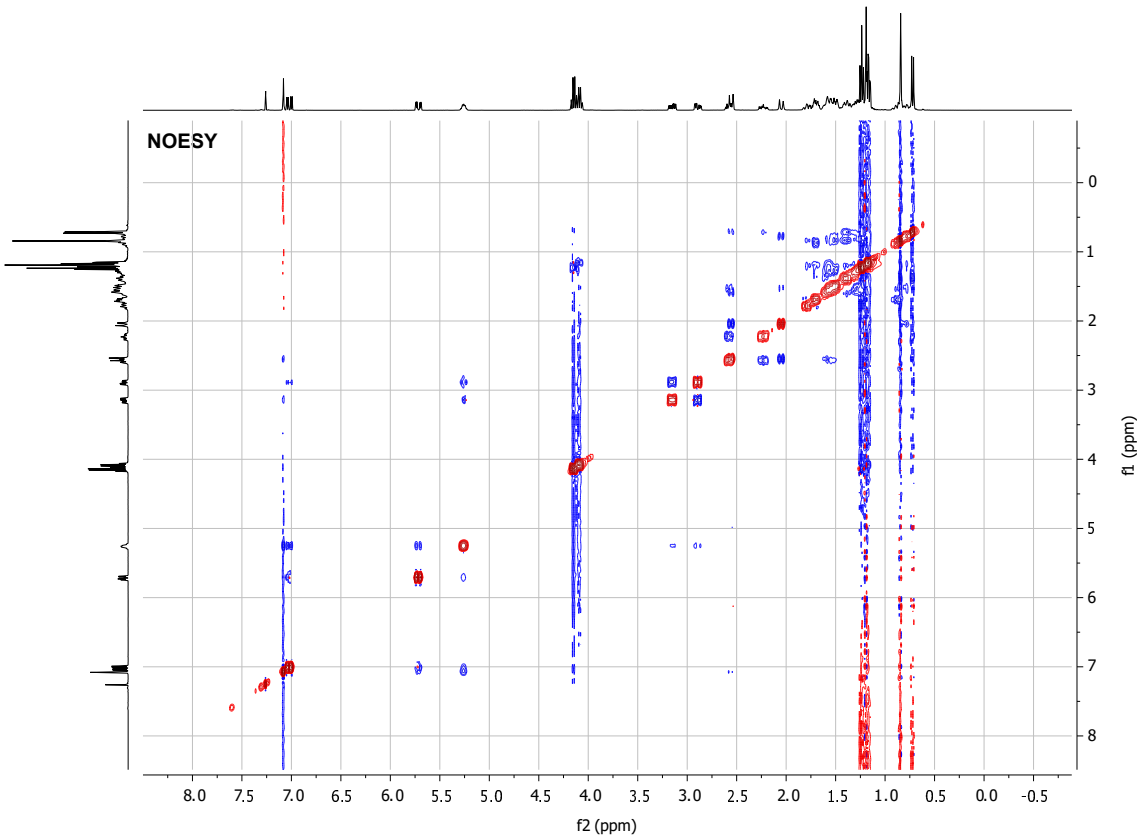
NOESY
f2 (ppm)
f1 (ppm)

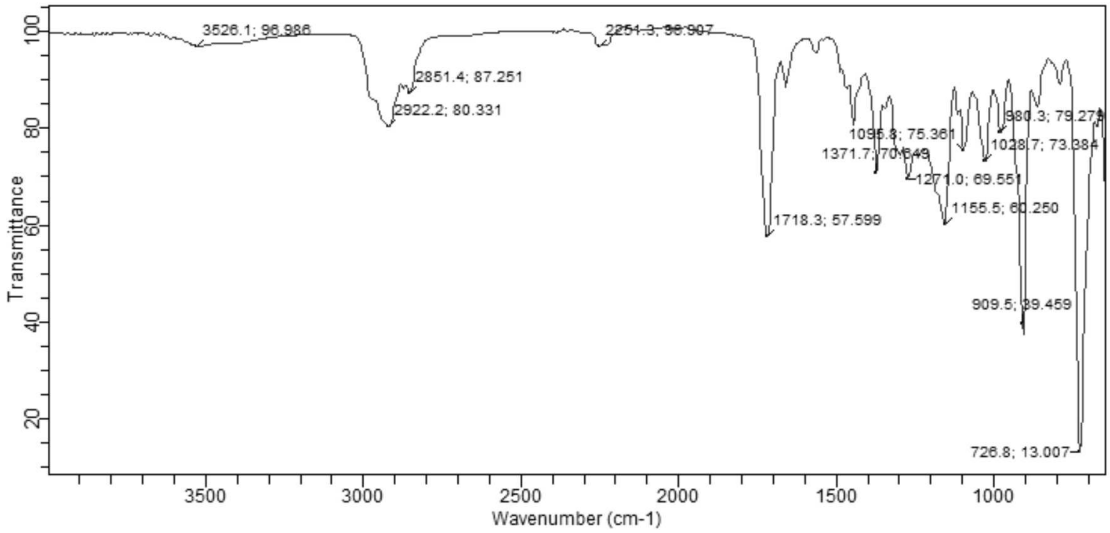
Transmittance
Wavenumber (cm-1)
3526.1; 96.986
2851.4; 87.251
2922.2; 80.331
2251.3; 88.907
1718.3; 57.599
1371.7; 70.649
1271.0; 69.551
1155.5; 60.250
1096.8; 75.361
1028.7; 73.084
980.3; 79.273
909.5; 39.459
726.8; 13.007

Diethyl (*E*)-4-((1S,3aS,3bR,5aS,10aS,10bS,12aS)-1-hydroxy-1,10a,12a-trimethyl-2,3,3a,3b,4,5,5a,6,10,10a,10b,11,12,12a-tetradecahydrocyclopenta[5,6]naphtho[1,2-f]indazol-7(1H)-yl)hex-2-enedioate (152bg, *N*1-isomer) and diethyl (*E*)-4-((1S,3aS,3bR,5aS,10aS,10bS,12aS)-1-hydroxy-1,10a,12a-trimethyl-2,3,3a,3b,4,5,5a,6,10,10a,10b,11,12,12a-tetradecahydrocyclopenta[5,6]naphtho[1,2-f]indazol-8(1H)-yl)hex-2-enedioate (152bg, *N*2-isomer) (^{1}H NMR: 400 MHz, ^{13}C NMR: 101 MHz, NOESY, $CDCl_3$; IR)

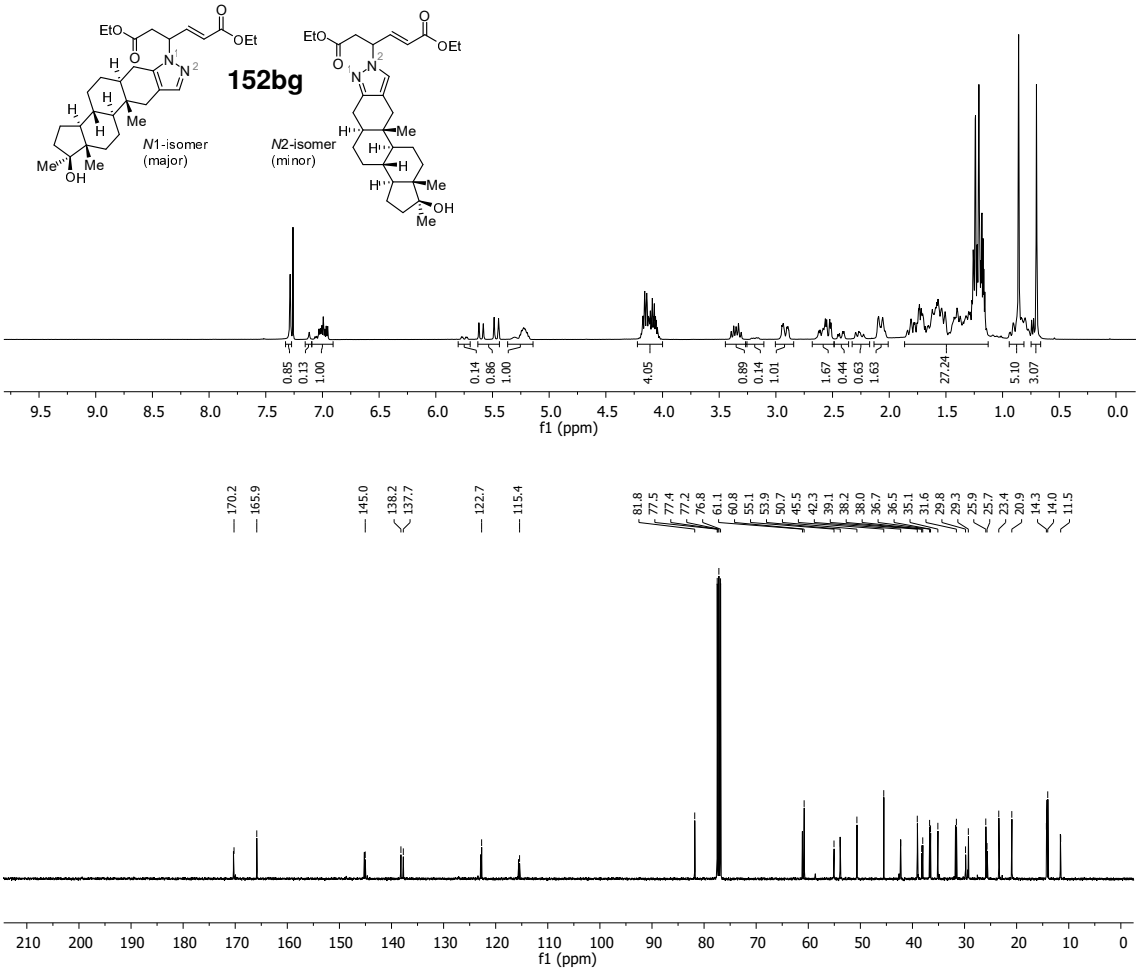

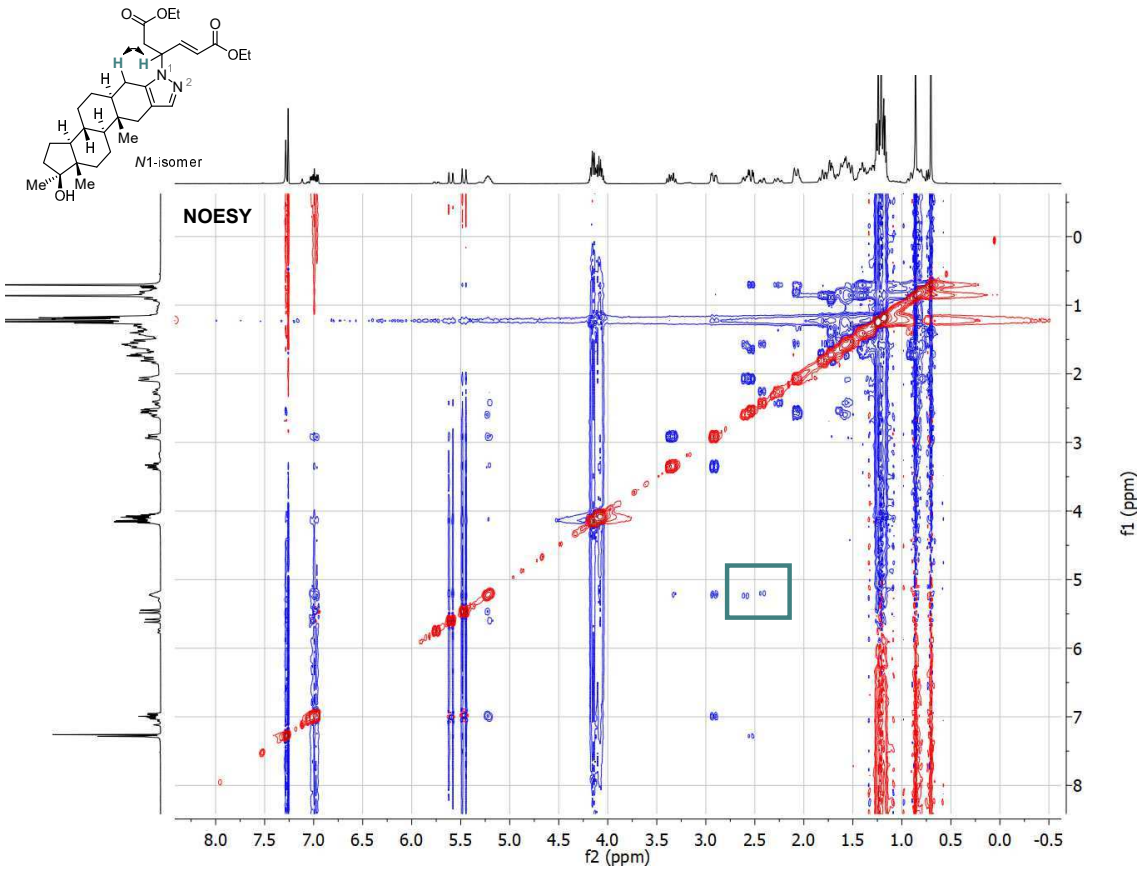
N1-isomer
NOESY
f2 (ppm)
f1 (ppm)

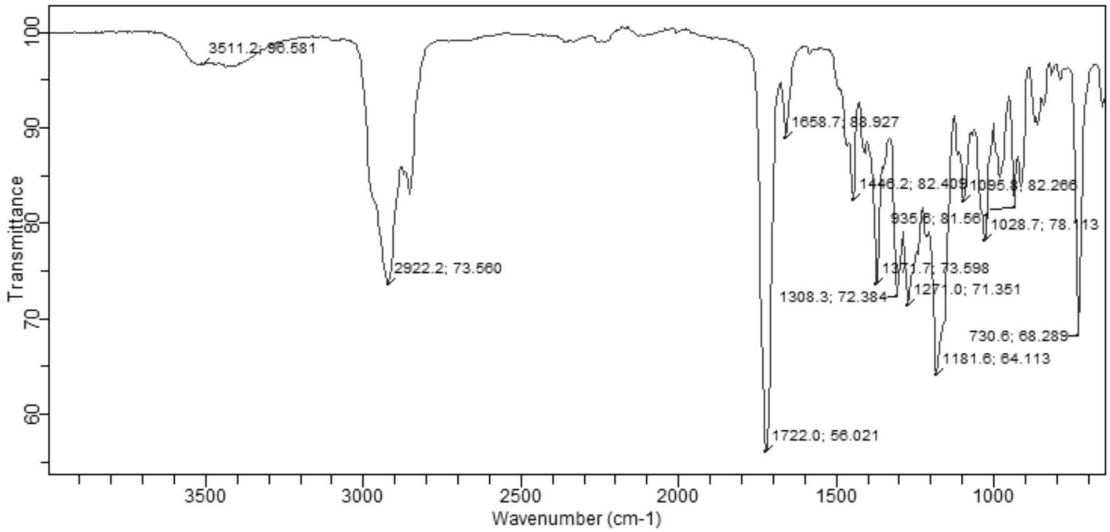
Transmittance
Wavenumber (cm-1)
3511.2; 86.581
2922.2; 73.560
1722.0; 56.021
1658.7; 83.927
1446.2; 82.409
1095.8; 82.266
935.6; 81.561
1028.7; 78.113
1371.7; 73.598
1308.3; 72.384
1271.0; 71.351
730.6; 68.289
1181.6; 64.113

(Z)-1,3,5-tris(4-methoxyphenyl)pent-2-ene-1,5-dione (179) (^{1}H NMR: 400 MHz, ^{13}C NMR: 101 MHz, $CDCl_3$; IR)

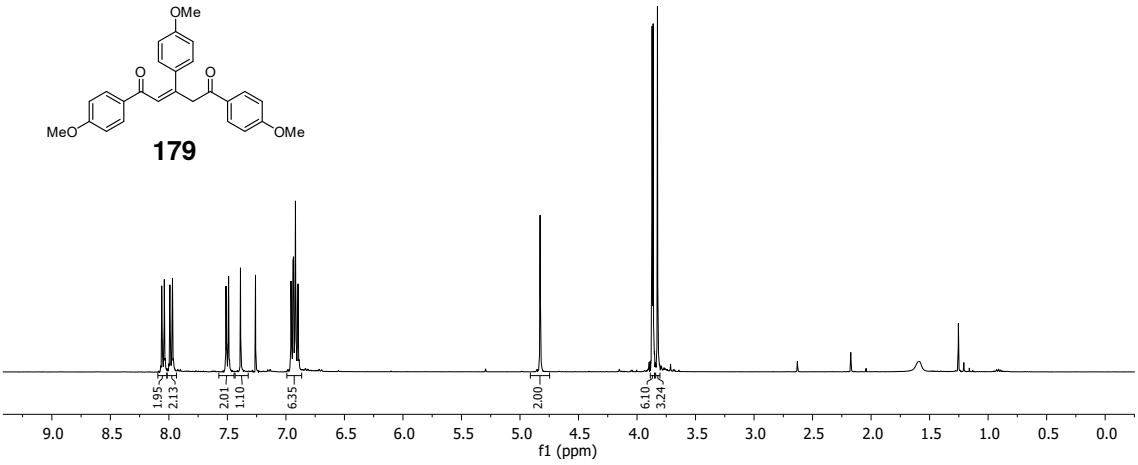

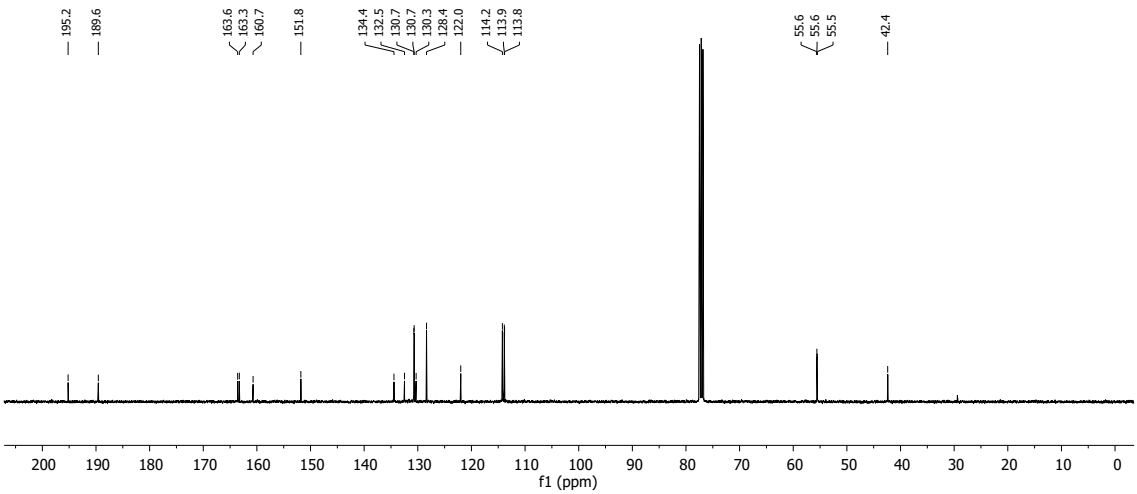

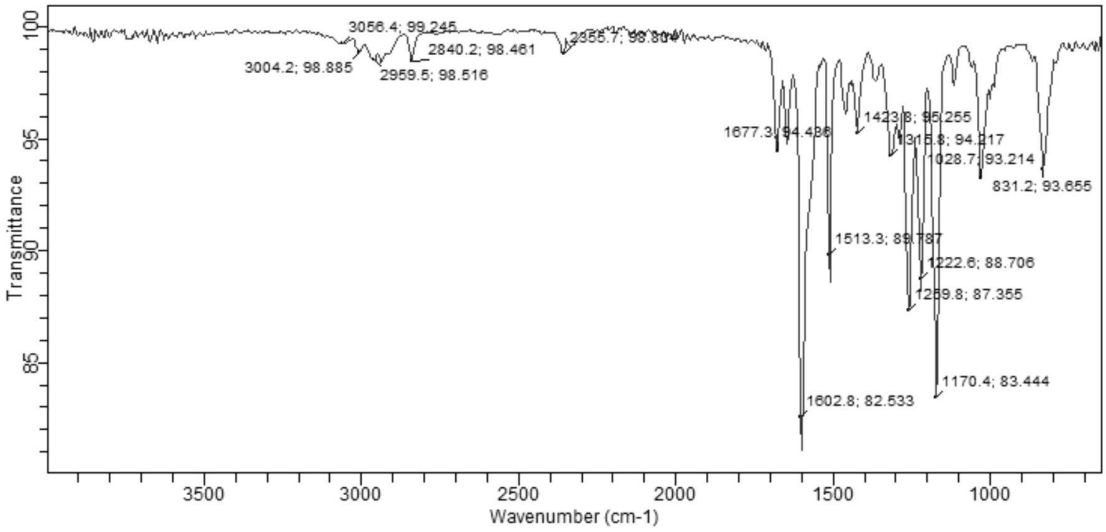

2,4,6-tris(4-methoxyphenyl)pyrylium (2s,11bS)-2,6-bis(2,4,6-triisopropylphenyl)dinaphtho[2,1-d:1',2'-f][1,3,2]dioxaphosphepin-4-olate 4-oxide (180a) (^{1}H NMR: 400 MHz, ^{13}C NMR: 151 MHz, ^{31}P NMR: 162 MHz, $CDCl_3$; IR)

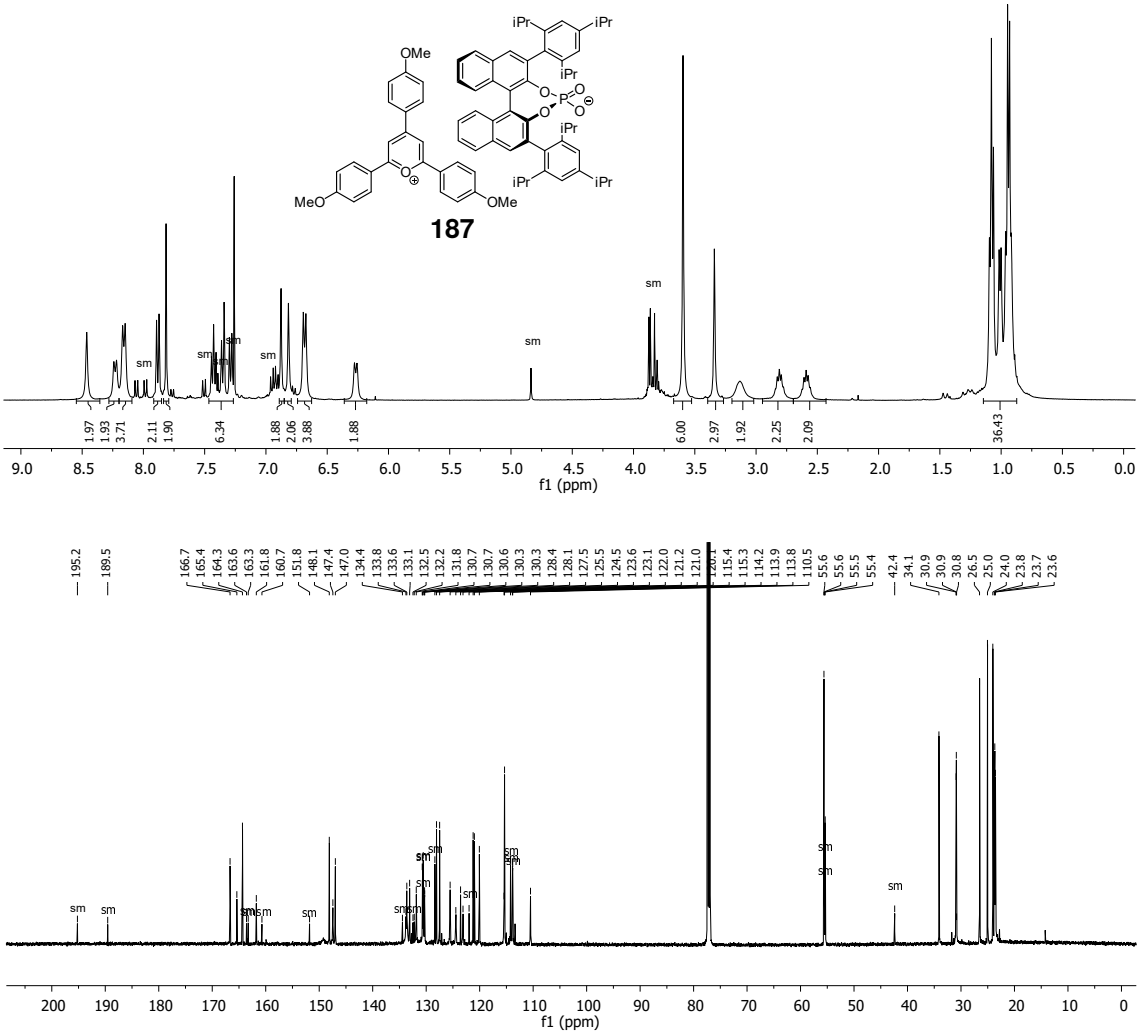

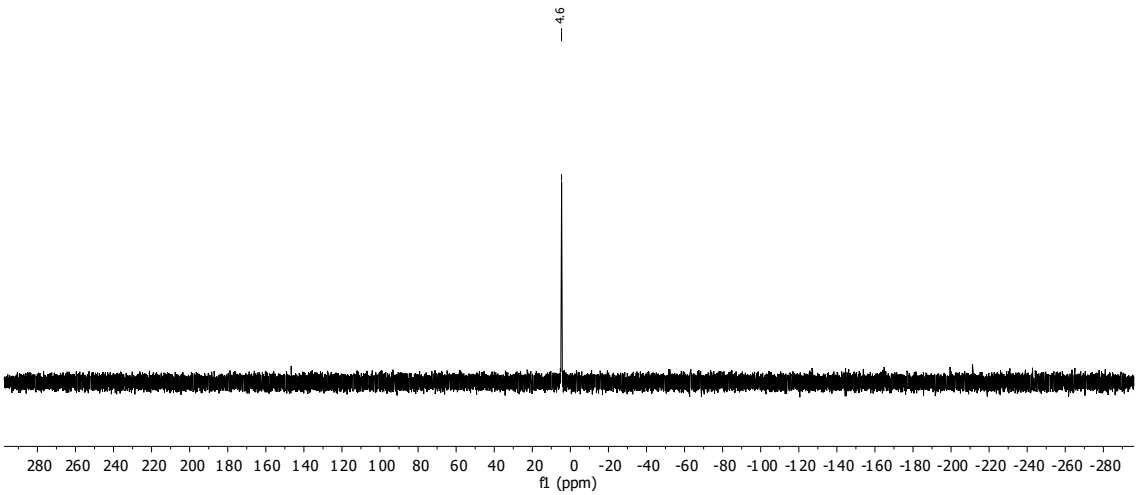
4.6
280 260 240 220 200 180 160 140 120 100 80 60 40 20 0 -20 -40 -60 -80 -100 -120 -140 -160 -180 -200 -220 -240 -260 -280
f1 (ppm)

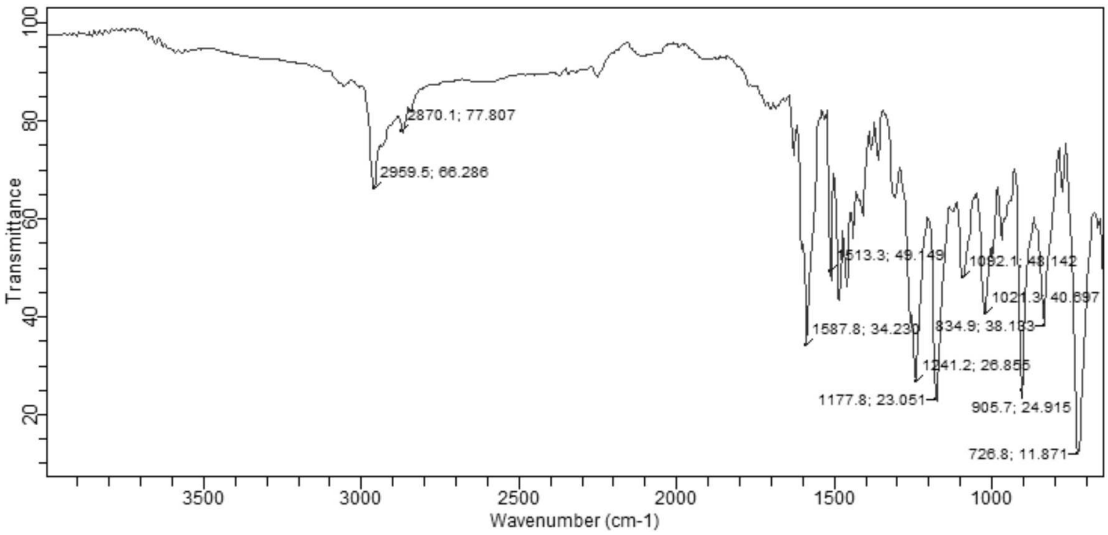
Transmittance
100
80
60
40
20
2870.1; 77.807
2959.5; 66.286
1513.3; 49.149
1092.1; 48.142
1021.3; 40.897
1587.8; 34.230
834.9; 38.183
1241.2; 26.855
1177.8; 23.051
905.7; 24.915
726.8; 11.871
3500
3000
2500
2000
1500
1000
Wavenumber (cm-1)

2,4,6-tris(4-methoxyphenyl)pyrylium (2r,11cS)-2,6-bis(2,4,6-triisopropylphenyl)dinaphtho[2,1-d:1',2'-f][1,3,2]dioxaphosphepin-4-olate 4-oxide (180b) (^{1}H NMR: 400 MHz, ^{13}C NMR: 151 MHz, ^{31}P NMR: 162 MHz, $CDCl_3$; IR)

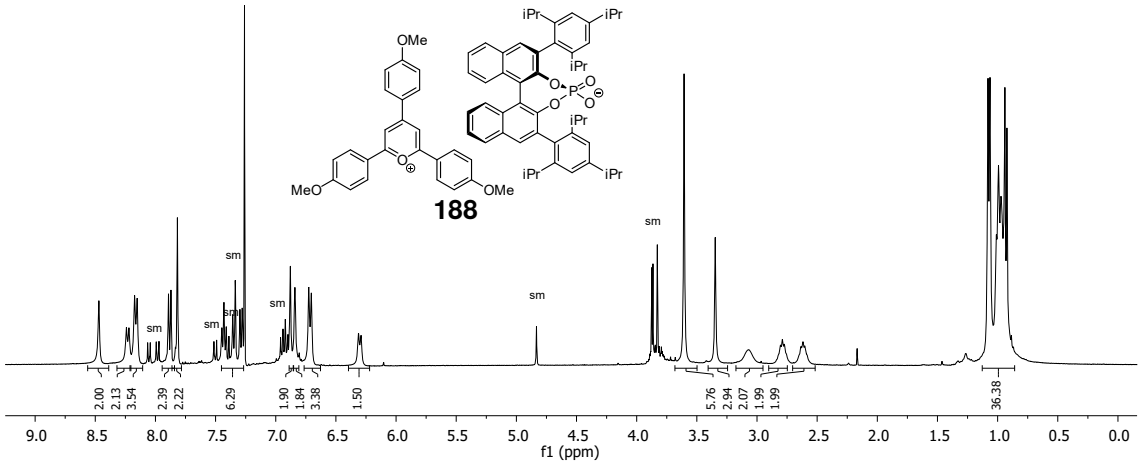

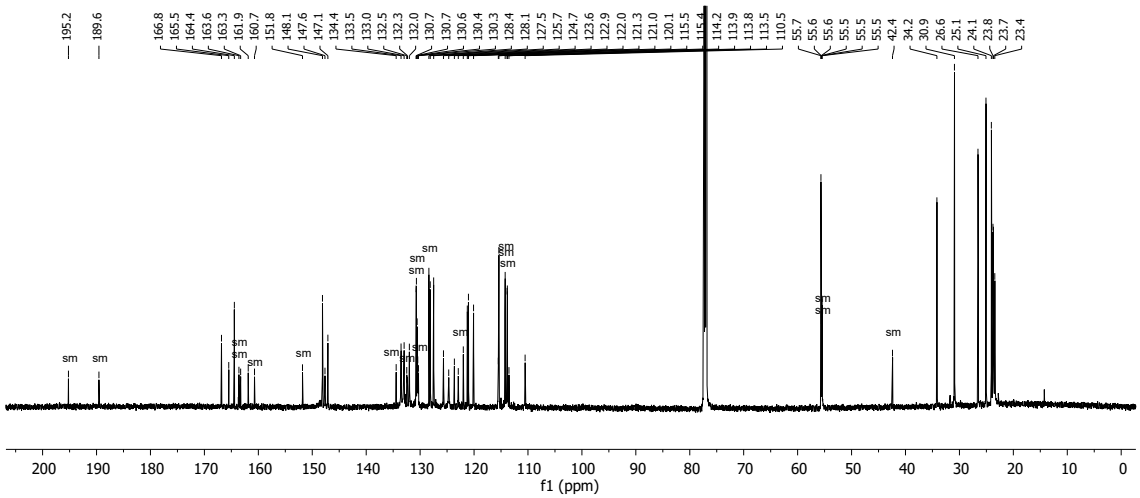

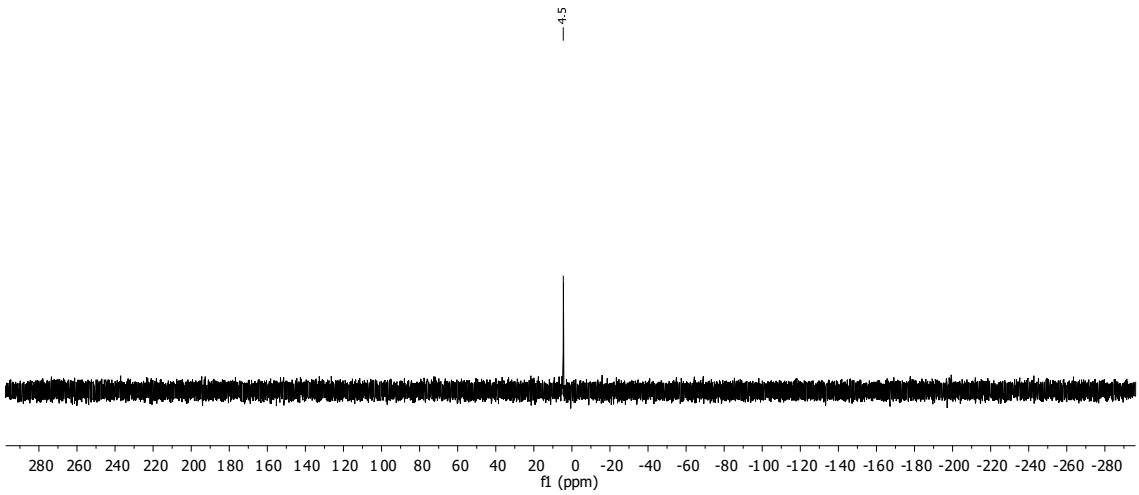
4.5
280 260 240 220 200 180 160 140 120 100 80 60 40 20 0 -20 -40 -60 -80 -100 -120 -140 -160 -180 -200 -220 -240 -260 -280
f1 (ppm)

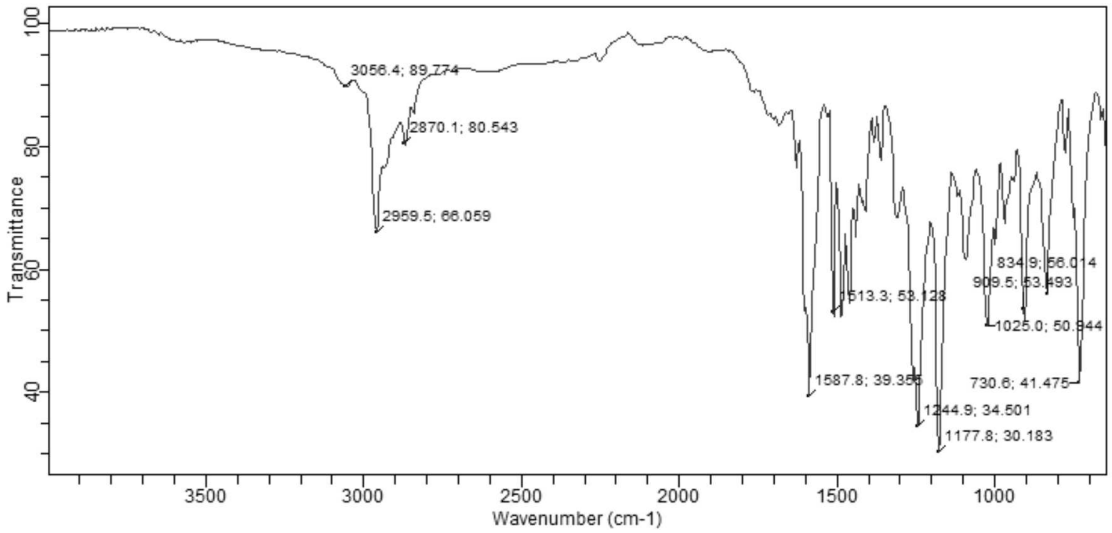
Transmittance
100
80
60
40
3056.4; 89.774
2870.1; 80.543
2959.5; 66.059
1587.8; 39.356
1513.3; 53.128
1244.9; 34.501
1177.8; 30.183
1025.0; 50.944
909.5; 53.493
834.9; 56.014
730.6; 41.475
3500
3000
2500
2000
1500
1000
Wavenumber (cm-1)

2,4,6-tris(4-methoxyphenyl)pyrylium ((1S,4R)-7,7-dimethyl-2-oxobicyclo[2.2.1]heptan- 1-yl)methanesulfonate (180c) (^{1}H NMR: 400 MHz, ^{13}C NMR: 101 MHz, $CDCl_3$; IR)

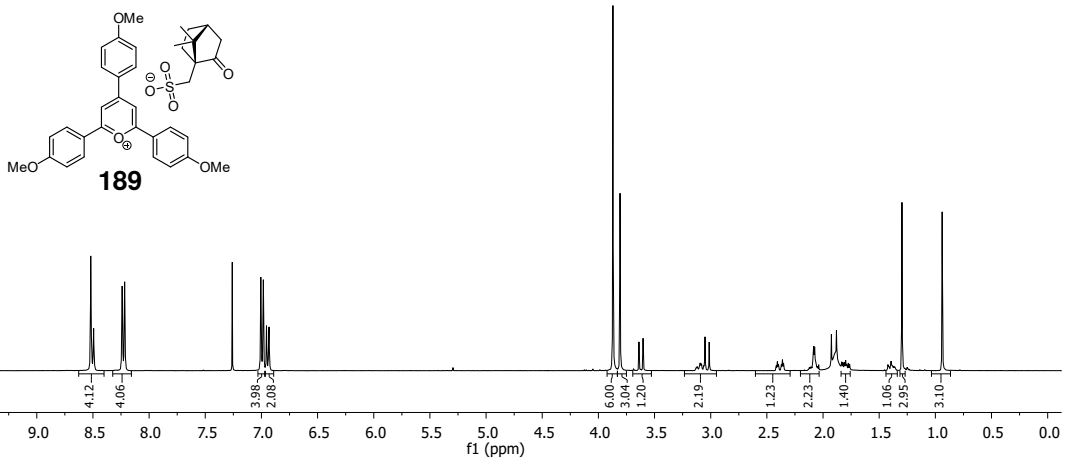

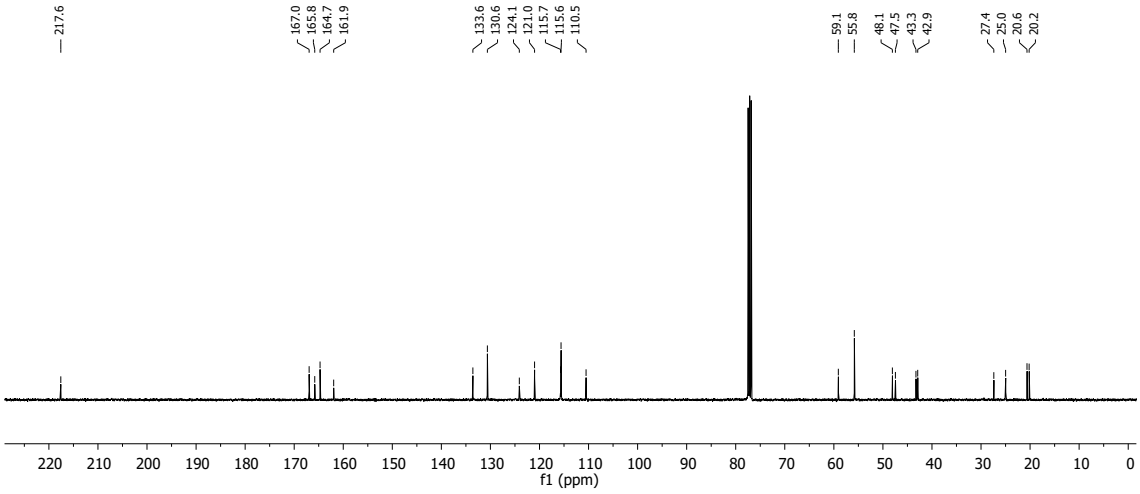

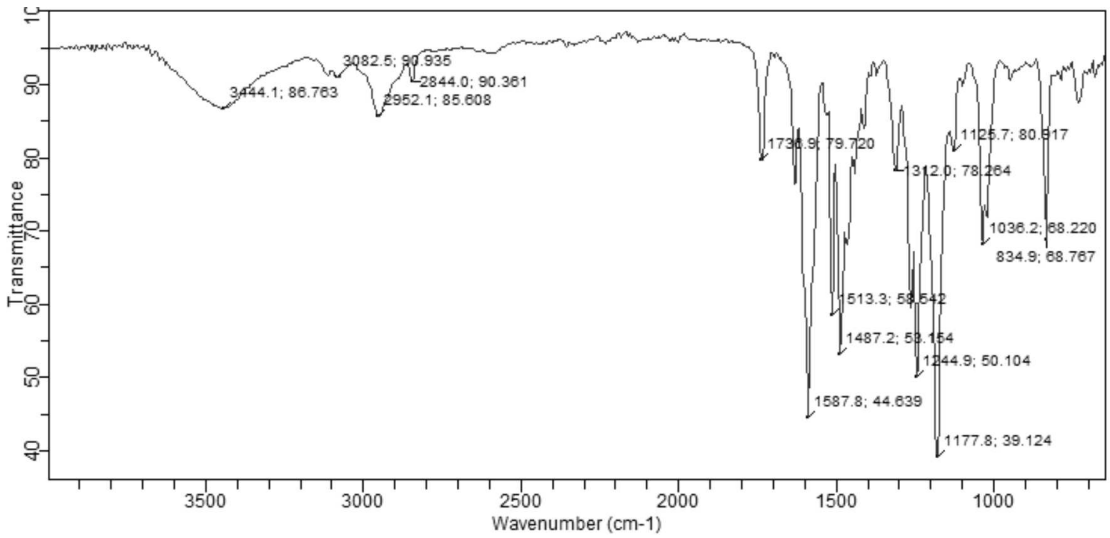
Transmittance
Wavenumber (cm-1)
3500
3000
2500
2000
1500
1000
3444.1; 86.763
3082.5; 90.935
2952.1; 85.608
2844.0; 90.361
1587.8; 44.639
1177.8; 39.124
1036.2; 68.220
834.9; 68.767

2,4,6-tris(4-methoxyphenyl)pyrylium ((1R,4S)-7,7-dimethyl-2-oxobicyclo[2.2.1]heptan- 1-yl)methanesulfonate (180d) (^{1}H NMR: 400 MHz, ^{13}C NMR: 101 MHz, $CDCl_3$; IR)

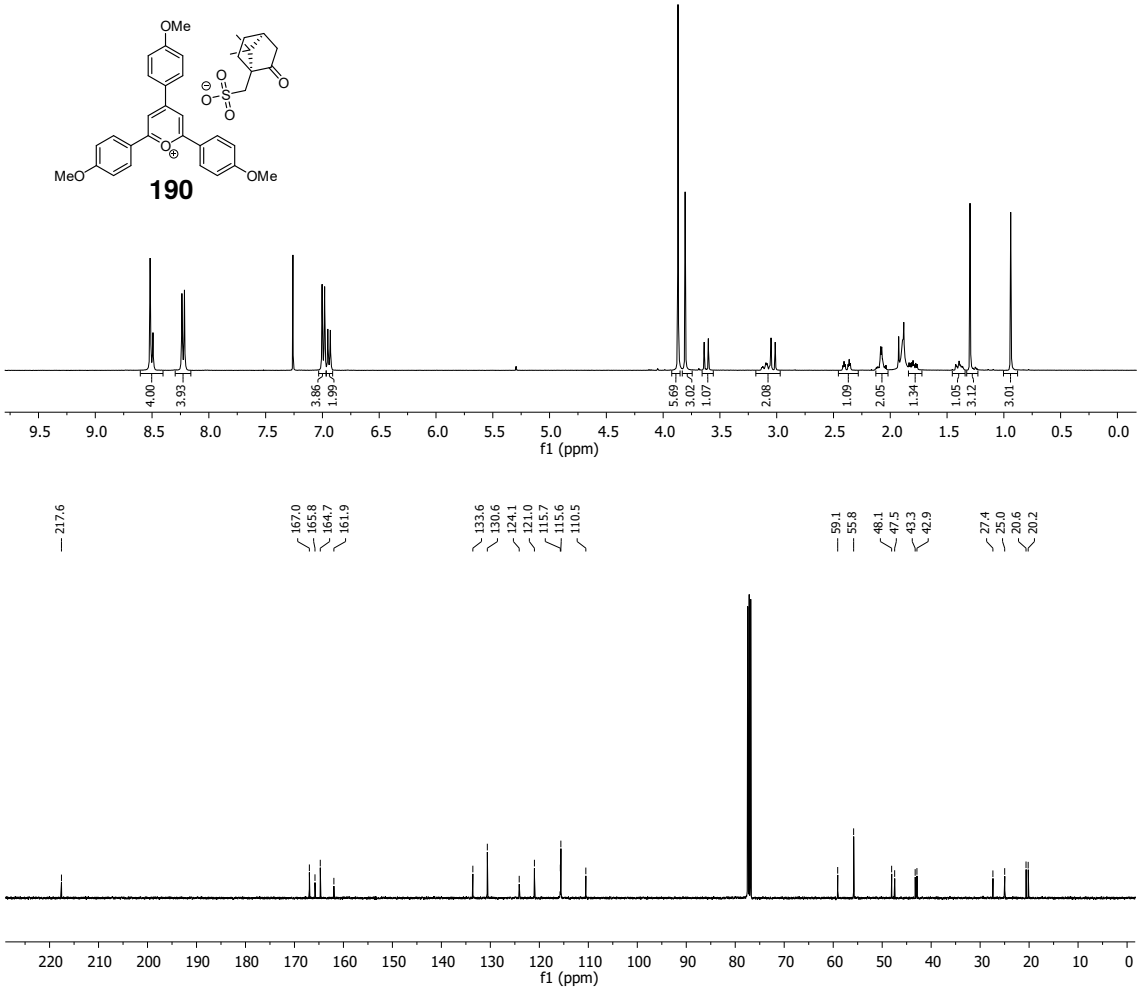

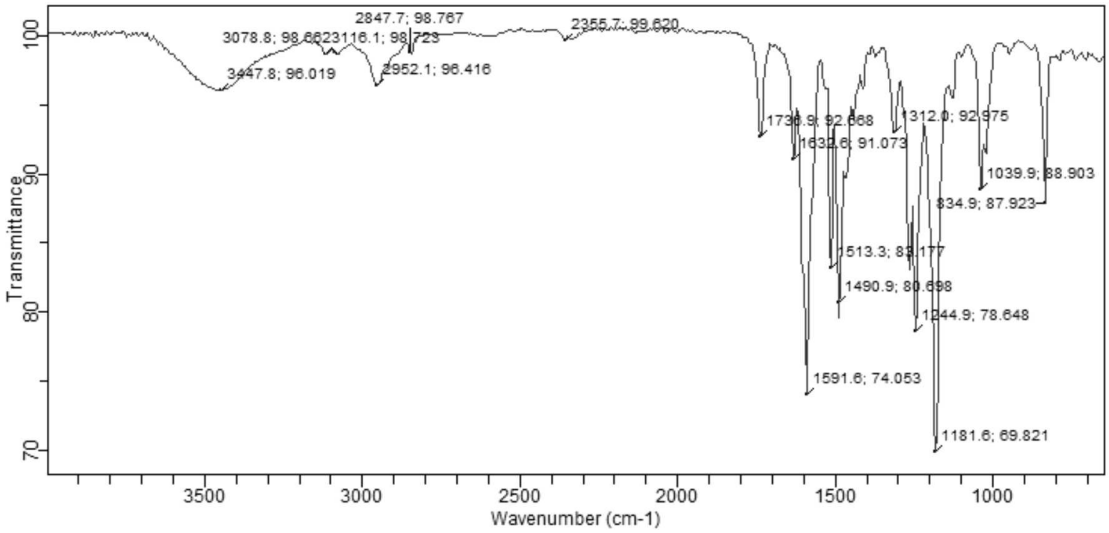
2847.7; 98.767
3078.8; 98.662
3116.1; 98.723
2355.7; 99.620
3447.8; 96.019
2952.1; 96.416
1736.9; 92.668
1312.0; 92.975
1632.6; 91.073
1039.9; 88.903
834.9; 87.923
1513.3; 83.177
1490.9; 80.698
1244.9; 78.648
1591.6; 74.053
1181.6; 69.821
Transmittance
100
90
80
70
3500
3000
2500
2000
1500
1000
Wavenumber (cm-1)

7 References

[1] K. Vollhardt, N. Schore, *Organische Chemie*, 3. Aufl., Wiley-VCH, Weinheim, **2000**.

[2] R. Hili, A. K. Yudin, "Making carbon-nitrogen bonds in biological and chemical synthesis", *Nat. Chem. Biol.* **2006**, *2*, 284–287.

[3] N. A. McGrath, M. Brichacek, J. T. Njardarson, "A Graphical Journey of Innovative Organic Architectures That Have Improved Our Lives", *J. Chem. Educ.* **2010**, *87*, 1348–1349.

[4] A. Breder, "Oxidative Allylic Amination Reactions of Unactivated Olefins - At the Frontiers of Palladium and Selenium Catalysis", *Synlett* **2014**, *25*, 899–904.

[5] E. Vitaku, D. T. Smith, J. T. Njardarson, "Analysis of the Structural Diversity, Substitution Patterns, and Frequency of Nitrogen Heterocycles among U.S. FDA Approved Pharmaceuticals", *J. Med. Chem.* **2014**, *57*, 10257–10274.

[6] R. E. Williams, J. T. Njardarson, Top 200 Small Molecules by Retail Sales in 2022, https://njardarson.lab.arizona.edu/sites/njardarson.lab.arizona.edu/files/NjardarsonGroup2022SmallMoleculeTopPosterV3.pdf, **2022 (accessed 02.11.2023)**.

[7] A. Ricci, *Amino Group Chemistry: From Synthesis to the Life Sciences*, John Wiley & Sons, **2008**.

[8] M. Johannsen, K. A. Jørgensen, "Allylic Amination", *Chem. Rev.* **1998**, *98*, 1689–1708.

[9] T. Hayashi, A. Yamamoto, Y. Ito, E. Nishioka, H. Miura, K. Yanagi, "Asymmetric Synthesis Catalyzed by Chiral Ferrocenylphosphine–Transition-Metal Complexes. 8. Palladium-Catalyzed Asymmetric Allylic Amination", *J. Am. Chem. Soc.* **1989**, *111*, 6301–6311.

[10] K. Burgess, L. T. Liu, B. Pal, "Asymmetric Syntheses of Optically Active α,β-Disubstituted β-Amino Acids", *J. Org. Chem.* **1993**, *58*, 4758–4763.

[11] R. Jumnah, J. M. Williams, A. C. Williams, "Synthesis of N-Protected Amino Esters via Palladium Catalysed Allylic Substitution", *Tetrahedron Lett.* **1993**, *34*, 6619–6622.

[12] Justin F. Bower, Roshan Jumnah, Andrew C. Williams, Jonathan M. J. Williams, "Palladium-catalysed asymmetric allylic substitution: synthesis of α- and β-amino acids", *J. Chem. Soc.* **1997**, *1*, 1411–1420.

[13] B. M. Trost, "Cyclisierungsreaktionen über Palladium-katalysierte allylische Alkylierungen", *Angew. Chem.* **1989**, *101*, 1199–1219.

[14] P. Magnus, J. Lacour, I. Coldham, B. Mugrage, W. B. Bauta, "New Trialkylsilyl Enol Ether Cemistry: α-*N*-Tosylamination of Triisopropylsilyl Enol Ethers", *Tetrahedron* **1995**, *51*, 11087–11110.

[15] B. M. Trost, D. L. Van Vranken, "A General Synthetic Strategy toward Aminocyclopentitol Glycosidase Inhibitors. Application of Palladium Catalysis to the Synthesis of Allosamizoline and Mannostatin A", *J. Am. Chem. Soc.* **1993**, *115*, 444–458.

[16] T. E. Müller, K. C. Hultzsch, M. Yus, F. Foubelo, M. Tada, "Hydroamination: Direct Addition of Amines to Alkenes and Alkynes", *Chem. Rev.* **2008**, *108*, 3795–3892.

[17] R. Blieck, M. Taillefer, F. Monnier, "Metal-Catalyzed Intermolecular Hydrofunctionalization of Allenes: Easy Access to Allylic Structures via the Selective Formation of C-N, C-C, and C-O Bonds", *Chem. Rev.* **2020**, *120*, 13545–13598.

[18] A. F. Abdel-Magid, K. G. Carson, B. D. Harris, C. A. Maryanoff, R. D. Shah, "Reductive Amination of Aldehydes and Ketones with Sodium Triacetoxyborohydride. Studies on Direct and Indirect Reductive Amination Procedures", *J. Org. Chem.* **1996**, *61*, 3849–3862.

[19] J. Clayden, N. Greeves, S. G. Warren, *Organic chemistry*, Second edition, Oxford University Press, Oxford, **2012**.

[20] O.-Y. Lee, K.-L. Law, C.-Y. Ho, D. Yang, "Highly Chemoselective Reductive Amination of Carbonyl Compounds Promoted by $InCl_3$/Et_3SiH/MeOH System", *J. Org. Chem.* **2008**, *73*, 8829–8837.

[21] M. Tajbakhsh, R. Hosseinzadeh, H. Alinezhad, S. Ghahari, A. Heydari, S. Khaksar, "Catalyst-Free One-Pot Reductive Alkylation of Primary and Secondary Amines and N,N-Dimethylation of Amino Acids Using Sodium Borohydride in 2,2,2-Trifluoroethanol", *Synthesis* **2011**, *2011*, 490–496.

[22] I. Sorribes, K. Junge, M. Beller, "Direct Catalytic N-Alkylation of Amines with Carboxylic Acids", *J. Am. Chem. Soc.* **2014**, *136*, 14314–14319.

[23] L. Liu, R. Luo, J. Tong, J. Liao, "Iridium-catalysed reductive allylic amination of α,β-unsaturated aldehydes", *Org. Biomol. Chem.* **2024**, *22*, 585–589.

[24] K. G. Andrews, D. M. Summers, L. J. Donnelly, R. M. Denton, "Catalytic reductive *N*-alkylation of amines using carboxylic acids", *Chem. Commun.* **2016**, *52*, 1855–1858.

[25] Y. Xia, L. Ouyang, J. Liao, X. Yang, R. Luo, "Construction of α-Alkylated Amines by Iridium Complex-Catalyzed One-Step Transfer Hydrogenation of C=C and C=N Bonds", *Synthesis* **2021**, *53*, 1821–1827.

[26] J. Tsuji, H. Takahashi, M. Morikawa, "Organic syntheses by means of noble metal compounds XVII. Reaction of π-allylpalladium chloride with nucleophiles", *Tetrahedron Lett.* **1965**, *6*, 4387–4388.

[27] B. M. Trost, D. L. Van Vranken, "Asymmetric Transition Metal-Catalyzed Allylic Alkylations", *Chem. Rev.* **1996**, *96*, 395–422.

[28] B. M. Trost, E. Keinan, "An Approach to Primary Allylic Amines via Transition-Metal-Catalyzed Reactions. Total Synthesis of (±)-Gabaculine", *J. Org. Chem.* **1979**, *44*, 3451–3457.

[29] Q. Cheng, H.-F. Tu, C. Zheng, J.-P. Qu, G. Helmchen, S.-L. You, "Iridium-Catalyzed Asymmetric Allylic Substitution Reactions", *Chem. Rev.* **2019**, *119*, 1855–1969.

[30] Z.-P. Yang, R. Jiang, C. Zheng, S.-L. You, "Iridium-Catalyzed Intramolecular Asymmetric Allylic Alkylation of Hydroxyquinolines: Simultaneous Weakening of the Aromaticity of Two Consecutive Aromatic Rings", *J. Am. Chem. Soc.* **2018**, *140*, 3114–3119.

[31] P. von Matt, O. Loiseleur, G. Koch, A. Pfaltz, C. Lefeber, T. Feucht, G. Helmchen, "Enantioselective Allylic Amination with Chiral (Phosphino-oxazoline)Pd Catalysts", *Tetrahedron: Asymmetry* **1994**, *5*, 573–584.

[32] A. Togni, U. Burckhardt, V. Gramlich, P. S. Pregosin, R. Salzmann, "Palladium-Catalyzed Asymmetric Allylic Amination Using Ferrocenyl Pyrazole Ligands: Steric Control of η^3-Allyl Configuration and Site-Selective Nucleophilic Attack", *J. Am. Chem. Soc.* **1996**, *118*, 1031–1037.

[33] U. Burckhardt, M. Baumann, G. Trabesinger, V. Gramlich, A. Togni, "A Bimetallic Palladium Catalyst for Asymmetric Allylic Substitution Reactions", *Organometallics* **1997**, *16*, 5252–5259.

[34] R. Grange, E. Clizbe, P. Evans, "Recent Developments in Asymmetric Allylic Amination Reactions", *Synthesis* **2016**, *48*, 2911–2968.

[35] Z.-B. Chen, R.-X. Liu, Z.-H. Li, T.-M. Ding, H.-Y. Bai, Z. Shen, S.-Y. Zhang, "An Axially Chiral Styrene–Phosphine Ligand for Pd-Catalyzed Asymmetric *N*-Alkylation of Indoles", *J. Org. Chem.* **2023**, *88*, 14719–14727.

[36] N. Kvasovs, J. Fang, F. Kliuev, V. Gevorgyan, "Merging of Light/Dark Palladium Catalytic Cycles Enables Multicomponent Tandem Alkyl Heck/Tsuji-Trost Homologative Amination Reaction toward Allylic Amines", *J. Am. Chem. Soc.* **2023**, *145*, 18497–18505.

[37] X. Wang, X. Wang, S. Shu, J. Liu, Q. Liu, T. Wang, Z. Zhang, "N^1-Allylation of Arylhydrazines via a Palladium-Catalyzed Allylic Substitution", *Org. Lett.* **2023**, *25*, 4880–4885.

[38] J. P. Janssen, G. Helmchen, "First Enantioselective Alkylations of Monosubstituted Allylic Acetates Catalyzed by Chiral Iridium Complexes", *Tetrahedron Lett.* **1997**, *38*, 8025–8026.

[39] A. Leitner, C. Shu, J. F. Hartwig, "Effects of Catalyst Activation and Ligand Steric Properties on the Enantioselective Allylation of Amines and Phenoxides", *Org. Lett.* **2005**, *7*, 1093–1096.

[40] J. Qu, G. Helmchen, "Applications of Iridium-Catalyzed Asymmetric Allylic Substitution Reactions in Target-Oriented Synthesis", *Acc. Chem. Res.* **2017**, *50*, 2539–2555.

[41] S. L. Rössler, D. A. Petrone, E. M. Carreira, "Iridium-Catalyzed Asymmetric Synthesis of Functionally Rich Molecules Enabled by (Phosphoramidite,Olefin) Ligands", *Acc. Chem. Res.* **2019**, *52*, 2657–2672.

[42] Z.-T. He, J. F. Hartwig, "Enantioselective α-functionalizations of ketones via allylic substitution of silyl enol ethers", *Nat. Chem.* **2019**, *11*, 177–183.

[43] M. K. Arachchi, R. N. Schaugaard, H. B. Schlegel, H. M. Nguyen, "Scope and Mechanistic Probe into Asymmetric Synthesis of α-Trisubstituted-α-Tertiary Amines by Rhodium Catalysis", *J. Am. Chem. Soc.* **2023**, *145*, 19642–19654.

[44] S. Khan, M. Salman, Y. Wang, J. Zhang, A. Khan, "Green Chemistry Approach toward the Regioselective Synthesis of α,α-Disubstituted Allylic Amines", *J. Org. Chem.* **2023**, *88*, 11992–11999.

[45] S. Khan, J. Zhang, A. Khan, "Molybdenum-Catalyzed Regio- and Enantioselective Amination of Allylic Carbonates: Total Synthesis of (S)-Clopidogrel", *Org. Lett.* **2023**, *26*, 2758–2762.

[46] I. D. G. Watson, A. K. Yudin, "New Insights into the Mechanism of Palladium-Catalyzed Allylic Amination", *J. Am. Chem. Soc.* **2005**, *127*, 17516–17529.

[47] Q. Cheng, J. Chen, S. Lin, T. Ritter, "Allylic Amination of Alkenes with Iminothianthrenes to Afford Alkyl Allylamines", *J. Am. Chem. Soc.* **2020**, *142*, 17287–17293.

[48] S. Wang, Y. Gao, Z. Liu, D. Ren, H. Sun, L. Niu, D. Yang, D. Zhang, X. Liang, R. Shi, X. Qi, A. Lei, "Site-selective amination towards tertiary aliphatic allylamines", *Nat. Catal.* **2022**, *5*, 642–651.

[49] H. Lei, T. Rovis, "A site-selective amination catalyst discriminates between nearly identical C–H bonds of unsymmetrical disubstituted alkenes", *Nat. Chem.* **2020**, *12*, 725–731.

[50] T. Ide, K. Feng, C. F. Dixon, D. Teng, J. R. Clark, W. Han, C. I. Wendell, V. Koch, M. C. White, "Late-Stage Intermolecular Allylic C–H Amination", *J. Am. Chem. Soc.* **2021**, *143*, 14969–14975.

[51] I. R. Hazelden, R. C. Carmona, T. Langer, J. F. Pringle, Paul G.band Bower, "Pyrrolidines and Piperidines by Ligand-Enabled Aza-Heck Cyclizations and Cascades of *N*-(Pentafluorobenzoyloxy)carbamates", *Angew. Chem. Int. Ed.* **2018**, *57*, 5124–5128.

[52] S. Mann, L. Benhamou, T. Sheppard, "Palladium(II)-Catalysed Oxidation of Alkenes", *Synthesis* **2015**, *47*, 3079–3117.

[53] F. Liron, J. Oble, M. M. Lorion, G. Poli, "Direct Allylic Functionalization Through Pd-Catalyzed C–H Activation", *Eur. J. Org. Chem.* **2014**, *2014*, 5863–5883.

[54] R. A. Fernandes, J. L. Nallasivam, "Catalytic allylic functionalization *via* π-allyl palladium chemistry", *Organic & Biomolecular Chemistry* **2019**, *17*, 8647–8672.

[55] S. A. Reed, A. R. Mazzotti, M. C. White, "A Catalytic, Brønsted Base Strategy for Intermolecular Allylic C−H Amination", *J. Am. Chem. Soc.* **2009**, *131*, 11701–11706.

[56] K. Pak Shing Cheung, J. Fang, K. Mukherjee, A. Mihranyan, V. Gevorgyan, "Asymmetric intermolecular allylic C-H amination of alkenes with aliphatic amines", *Science* **2022**, *378*, 1207–1213.

[57] G. Yin, Y. Wu, G. Liu, "Scope and Mechanism of Allylic C–H Amination of Terminal Alkenes by the Palladium/PhI(OPiv)$_2$ Catalyst System: Insights into the Effect of Naphthoquinone", *J. Am. Chem. Soc.* **2010**, *132*, 11978–11987.

[58] Y.-W. Chen, Y. Liu, H.-Y. Lu, G.-Q. Lin, Z.-T. He, "Palladium-catalyzed regio- and enantioselective migratory allylic C(sp^3)-H functionalization", *Nat. Commun.* **2021**, *12*, 1–9.

[59] X. Li, J. Jin, P. Chen, G. Liu, "Catalytic remote hydrohalogenation of internal alkenes", *Nat. Chem.* **2022**, *14*, 425–432.

[60] S. Z. Ali, B. G. Budaitis, D. F. A. Fontaine, A. L. Pace, J. A. Garwin, M. C. White, "Allylic C–H amination cross-coupling furnishes tertiary amines by electrophilic metal catalysis", *Science* **2022**, *376*, 276–283.

[61] K. J. Fraunhoffer, M. C. White, "*syn*-1,2-Amino Alcohols via Diastereoselective Allylic C–H Amination", *J. Am. Chem. Soc.* **2007**, *129*, 7274–7276.

[62] S. A. Reed, M. C. White, "Catalytic Intermolecular Linear Allylic C–H Amination via Heterobimetallic Catalysis", *J. Am. Chem. Soc.* **2008**, *130*, 3316–3318.

[63] G. Liu, G. Yin, L. Wu, "Palladium-Catalyzed Intermolecular Aerobic Oxidative Amination of tTerminal Alkenes: Efficient Synthesis of Linear Allylamine Derivatives", *Angew. Chem. Int. Ed.* **2008**, *47*, 4733–4736.

[64] L. Wu, S. Qiu, G. Liu, "Brønsted Base-Modulated Regioselective Pd-Catalyzed Intramolecular Aerobic Oxidative Amination of Alkenes: Formation of Seven-Membered Amides and Evidence for Allylic C–H Activation", *Org. Lett.* **2009**, *11*, 2707–2710.

[65] G. Liu, S. S. Stahl, "Two-Faced Reactivity of Alkenes: *cis*- versus *trans*-Aminopalladation in Aerobic Pd-Catalyzed Intramolecular Aza-Wacker Reactions", *J. Am. Chem. Soc.* **2007**, *129*, 6328–6335.

[66] K. Muñiz, C. H. Hövelmann, J. Streuff, "Oxidative Diamination of Alkenes with Ureas as Nitrogen Sources: Mechanistic Pathways in the Presence of a High Oxidation State Palladium Catalyst", *J. Am. Chem. Soc.* **2008**, *130*, 763–773.

[67] M. S. Chen, M. C. White, "A Sulfoxide-Promoted, Catalytic Method for the Regioselective Synthesis of Allylic Acetates from Monosubstituted Olefins via C–H Oxidation", *J. Am. Chem. Soc.* **2004**, *126*, 1346–1347.

[68] M. S. Chen, P. Narayanasamy, N. A. Labenz, M. C. White, "Serial Ligand Catalysis: A Highly Selective Allylic C–H Oxidation", *J. Am. Chem. Soc.* **2005**, *127*, 6970–6971.

[69] D. J. Covell, M. C. White, "A Chiral Lewis Acid Strategy for Enantioselective Allylic C–H Oxidation", *Angew. Chem. Int. Ed.* **2008**, *47*, 6448–6451.

[70] J. S. Burman, S. B. Blakey, "Regioselective Intermolecular Allylic C-H Amination of Disubstituted Olefins via Rhodium/π-Allyl Intermediates", *Angew. Chem. Int. Ed.* **2017**, *56*, 13666–13669.

[71] Amaan M. Kazerouni, Quincy A. McKoy, Simon B. Blakey, "Recent advances in oxidative allylic C–H functionalization *via* group IX-metal catalysis", *Chem. Commun.* **2020**, *56*, 13287–13300.

[72] P. Sihag, M. Jeganmohan, "Iridium(III)-Catalyzed Intermolecular Allylic C-H Amidation of Internal Alkenes with Sulfonamides", *J. Org. Chem.* **2019**, *84*, 13053–13064.

[73] S. Sumino, A. Fusano, T. Fukuyama, I. Ryu, "Carbonylation Reactions of Alkyl Iodides through the Interplay of Carbon Radicals and Pd Catalysts", *Acc. Chem. Res.* **2014**, *47*, 1563–1574.

[74] J. Meng, H. Liu, Z. Wu, W. Zhang, "Palladium Catalyzed Aerobic Oxidative Amination of Alkenes", *Asian J. Org. Chem.* **2023**, *12*, e202300172.

[75] M. R. Luzung, C. A. Lewis, P. S. Baran, "Direct, Chemoselective *N*-*tert*-Prenylation of Indoles by C–H Functionalization", *Angew. Chem. Int. Ed.* **2009**, *48*, 7025–7029.

[76] F. Liron, J. Oble, M. M. Lorion, G. Poli, "Direct Allylic Functionalization Through Pd-Catalyzed C–H Activation", *Eur. J. Org. Chem.* **2014**, *2014*, 5863–5883.

[77] E. M. Beccalli, G. Broggini, G. Paladino, A. Penoni, C. Zoni, "Regioselective Formation of Six- and Seven-Membered Ring by Intramolecular Pd-Catalyzed Amination of N-Allyl-anthranilamides", *J. Org. Chem.* **2004**, *69*, 5627–5630.

[78] G. Yang, W. Zhang, "Regioselective Pd-Catalyzed Aerobic Aza-Wacker Cyclization for Preparation of Isoindolinones and Isoquinolin-1(2H)-ones", *Org. Lett.* **2012**, *14*, 268–271.

[79] S. R. Fix, J. L. Brice, S. S. Stahl, "Efficient Intramolecular Oxidative Amination of Olefins through Direct Dioxygen-Coupled Palladium Catalysis", *Angew. Chem. Int. Ed.* **2002**, *41*, 164–166.

[80] A. H. Aebly, T. J. Rainey, "Pd(II)-catalyzed enantioselective intramolecular oxidative amination utilizing (+)-camphorsulfonic acid", *Tetrahedron Lett.* **2017**, *58*, 3795–3799.

[81] X. Kou, Q. Shao, C. Ye, G. Yang, W. Zhang, "Asymmetric Aza-Wacker-Type Cyclization of N-Ts Hydrazine-Tethered Tetrasubstituted Olefins: Synthesis of Pyrazolines Bearing One Quaternary or Two Vicinal Stereocenters", *J. Am. Chem. Soc.* **2018**, *140*, 7587–7597.

[82] A. Sen, K. Takenaka, H. Sasai, "Enantioselective Aza-Wacker-Type Cyclization Promoted by Pd-SPRIX Catalyst", *Org. Lett.* **2018**, *20*, 6827–6831.

[83] A. Bahamonde, B. Al Rifaie, V. Martín-Heras, J. R. Allen, M. S. Sigman, "Enantioselective Markovnikov Addition of Carbamates to Allylic Alcohols for the Construction of α-Secondary and α-Tertiary Amines", *J. Am. Chem. Soc.* **2019**, *141*, 8708–8711.

[84] J. R. Allen, A. Bahamonde, Y. Furukawa, M. S. Sigman, "Enantioselective *N*-Alkylation of Indoles via an Intermolecular Aza-Wacker-Type Reaction", *J. Am. Chem. Soc.* **2019**, *141*, 8670–8674.

[85] D. G. Kohler, S. N. Gockel, J. L. Kennemur, P. J. Waller, K. L. Hull, "Palladium-catalysed *anti*-Markovnikov selective oxidative amination", *Nat. Chem.* **2018**, *10*, 333–340.

[86] X. Qi, D. G. Kohler, K. L. Hull, P. Liu, "Energy Decomposition Analyses Reveal the Origins of Catalyst and Nucleophile Effects on Regioselectivity in Nucleopalladation of Alkenes", *J. Am. Chem. Soc.* **2019**, *141*, 11892–11904.

[87] O. Eisenstein, R. Hoffmann, "Activation of a Coordinated Olefin toward Nucleophilic Attack", *J. Am. Chem. Soc.* **1980**, *102*, 6148–6149.

[88] O. Eisenstein, R. Hoffmann, "Transition-Metal Complexed Olefins: How their Reactivity toward a Nucleophile Relates to Their Electronic Structure", *J. Am. Chem. Soc.* **1981**, *103*, 4308–4320.

[89] J. E. Baeckvall, E. E. Bjoerkman, L. Pettersson, P. Siegbahn, "Reactivity of Coordinated Nucleophiles toward Cis Migration in (π-Olefin)palladium Complexes", *J. Am. Chem. Soc.* **1984**, *106*, 4369–4373.

[90] P. Kočovský, J.-E. Bäckvall, "The *syn*/*anti*-Dichotomy in the Palladium-Catalyzed Addition of Nucleophiles to Alkenes", *Chem. Eur. J.* **2015**, *21*, 36–56.

[91] J. L. Brice, J. E. Harang, V. I. Timokhin, N. R. Anastasi, S. S. Stahl, "Aerobic Oxidative Amination of Unactivated Alkenes Catalyzed by Palladium", *J. Am. Chem. Soc.* **2005**, *127*, 2868–2869.

[92] M. M. Rogers, V. Kotov, J. Chatwichien, S. S. Stahl, "Palladium-Catalyzed Oxidative Amination of Alkenes: Improved Catalyst Reoxidation Enables the Use of Alkene as the Limiting Reagent", *Org. Lett.* **2007**, *9*, 4331–4334.

[93] A. Sen, L. Zhu, S. Takizawa, K. Takenaka, H. Sasai, "Synthesis of Allylamine Derivatives via Intermolecular Aza–Wacker–Type Reaction Promoted by Palladium–SPRIX Catalyst", *Adv. Synth. Catal.* **2020**, *362*, 3558–3563.

[94] R. K. Gabr, T. Hatakeyama, K. Takenaka, S. Takizawa, Y. Okada, M. Nakamura, H. Sasai, "DFT Study of a 5-*endo-trig*-Type Cyclization of 3-Alkenoic Acids by Using Pd-Spiro-bis(isoxazoline) as Catalyst: Importance of the Rigid Spiro Framework for both Selectivity and Reactivity", *Chem. Eur. J.* **2013**, *19*, 9518–9525.

[95] L. Buzzetti, G. E. M. Crisenza, P. Melchiorre, "Mechanistic Studies in Photocatalysis", *Angew. Chem. Int. Ed.* **2019**, *58*, 3730–3747.

[96] M. H. Shaw, J. Twilton, D. W. C. MacMillan, "Photoredox Catalysis in Organic Chemistry", *J. Org. Chem.* **2016**, *81*, 6898–6926.

[97] D. Staveness, I. Bosque, C. R. J. Stephenson, "Free Radical Chemistry Enabled by Visible Light-Induced Electron Transfer", *Acc. Chem. Res.* **2016**, *49*, 2295–2306.

[98] N. L. Reed, G. A. Lutovsky, T. P. Yoon, "Copper-Mediated Radical-Polar Crossover Enables Photocatalytic Oxidative Functionalization of Sterically Bulky Alkenes", *J. Am. Chem. Soc.* **2021**, *143*, 6065–6070.

[99] C.-M. You, C. Huang, S. Tang, P. Xiao, S. Wang, Z. Wei, A. Lei, H. Cai, "*N*-Allylation of Azoles with Hydrogen Evolution Enabled by Visible-Light Photocatalysis", *Org. Lett.* **2023**, *25*, 1722–1726.

[100] S. Ortgies, A. Breder, "Oxidative Alkene Functionalizations via Selenium-π-Acid Catalysis", *ACS Catal.* **2017**, *7*, 5828–5840.

[101] S. E. Denmark, A. Jaunet, "Catalytic, Enantioselective, Intramolecular Carbosulfenylation of Olefins. Preparative and Stereochemical Aspects", *J. Org. Chem.* **2014**, *79*, 140–171.

[102] G. Ciancaleoni, "Lewis Base Activation of Lewis Acid: A Detailed Bond Analysis", *ACS Omega* **2018**, *3*, 16292–16300.

[103] C. Santi, S. Santoro in *Organoselenium Chemistry*, (Ed.: T. Wirth), Wiley-VCH Verlag GmbH & Co. KGaA, Weinheim, **2012**, pp. 1–52.

[104] L. Yang, Y. Liu, W.-X. Fan, D.-H. Tan, Q. Li, H. Wang, "Regiocontrolled allylic functionalization of internal alkene *via* selenium-π-acid catalysis guided by boron substitution", *Chem. Sci.* **2022**, *13*, 6413–6417.

[105] T. Hori, K. B. Sharpless, "Conversion of Allylic Phenylselenides to the Rearranged Allylic Chlorides by *N*-Chlorosuccinimide. Mechanism of Selenium-Catalyzed Allylic Chlorination of β-Pinene", *J. Org. Chem.* **1979**, *44*, 4208–4210.

[106] B. Chabaud, B. Sharpless, "Selenium-Catalyzed Nonradical Chlorination of Olefins with *N*-Chlorosuccinimide", *J. Org. Chem.* **1979**, *44*, 4204–4208.

[107] S. Ortgies, A. Breder, "Selenium-Catalyzed Oxidative C(sp^2)–H Amination of Alkenes Exemplified in the Expedient Synthesis of (Aza-)Indoles", *Org. Lett.* **2015**, *17*, 2748–2751.

[108] Z. Deng, J. Wei, L. Liao, H. Huang, X. Zhao, "Organoselenium-Catalyzed, Hydroxy-Controlled Regio- and Stereoselective Amination of Terminal Alkenes: Efficient Synthesis of 3-Amino Allylic Alcohols", *Org. Lett.* **2015**, *17*, 1834–1837.

[109] X. Zhang, R. Guo, X. Zhao, "Organoselenium-catalyzed synthesis of indoles through intramolecular C–H amination", *Org. Chem. Front.* **2015**, *2*, 1334–1337.

[110] L. Liao, R. Guo, X. Zhao, "Organoselenium-Catalyzed Regioselective C-H Pyridination of 1,3-Dienes and Alkenes", *Angew. Chem. Int. Ed.* **2017**, *56*, 3201–3205.

[111] T. Zheng, J. R. Tabor, Z. L. Stein, F. E. Michael, "Regioselective Metal-Free Aza-Heck Reactions of Terminal Alkenes Catalyzed by Phosphine Selenides", *Org. Lett.* **2018**, *20*, 6975–6978.

[112] X. Wang, Q. Wang, Y. Xue, K. Sun, L. Wu, B. Zhang, "An organoselenium-catalyzed N^1- and N^2-selective aza-Wacker reaction of alkenes with benzotriazoles", *Chem. Commun.* **2020**, *56*, 4436–4439.

[113] M. Iwaoka, S. Tomoda, "Catalytic Conversion of Alkenes into Allylic Ethers and Esters using Diselenides having Internal Tertiary Amines", *J. Chem. Soc. Chem. Commun.* **1992**, 1165–1967.

[114] M. Tiecco, L. Testaferri, M. Tingoli, L. Bagnoli, C. Santi, "Selenium Catalysed Conversion of β,γ-Unsaturated Acids into Butenolides", *Synlett* **1993**, *10*, 798–800.

[115] J. A. Tunge, S. R. Mellegaard, "Selective Selenocatalytic Allylic Chlorination", *Org. Lett.* **2004**, *6*, 1205–1207.

[116] O. Niyomura, M. Cox, T. Wirth, "Electrochemical Generation and Catalytic Use of Selenium Electrophiles", *Synlett* **2006**, 251–254.

[117] D. M. Browne, O. Niyomura, T. Wirth, "Catalytic Use of Selenium Electrophiles in Cyclizations", *Org. Lett.* **2007**, *9*, 3169–3171.

[118] Y. Kawamata, T. Hashimoto, K. Maruoka, "A Chiral Electrophilic Selenium Catalyst for Highly Enantioselective Oxidative Cyclization", *J. Am. Chem. Soc.* **2016**, *138*, 5206–5209.

[119] W. Wei, X. Zhao, "Organoselenium-Catalyzed Cross-Dehydrogenative Coupling of Alkenes and Azlactones", *Org. Lett.* **2022**, *24*, 1780–1785.

[120] R. Guo, J. Huang, H. Huang, X. Zhao, "Organoselenium-Catalyzed Synthesis of Oxygen- and Nitrogen-Containing Heterocycles", *Org. Lett.* **2016**, *18*, 504–507.

[121] Y. Otsuka, Y. Shimazaki, H. Nagaoka, K. Maruoka, T. Hashimoto, "Scalable Synthesis of a Chiral Selenium π-Acid Catalyst and Its Use in Enantioselective Iminolactonization of β,γ-Unsaturated Amides", *Synlett* **2019**, *30*, 1679–1682.

[122] A. J. Cresswell, S. T.-C. Eey, S. E. Denmark, "Catalytic, stereospecific *syn*-dichlorination of alkenes", *Nat. Chem.* **2014**, *7*, 146–152.

[123] B. B. Gilbert, S. T.-C. Eey, P. Ryabchuk, O. Garry, S. E. Denmark, "Organoselenium-Catalyzed Enantioselective *Syn*-Dichlorination of Unbiased Alkenes", *Tetrahedron* **2019**, *75*, 4086–4098.

[124] Z. Tao, B. B. Gilbert, S. E. Denmark, "Catalytic, Enantioselective *syn*-Diamination of Alkenes", *J. Am. Chem. Soc.* **2019**, *141*, 19161–19170.

[125] J. R. Tabor, D. C. Obenschain, F. E. Michael, "Selenophosphoramide-catalyzed diamination and oxyamination of alkenes", *Chem. Sci.* **2020**, *11*, 1677–1682.

[126] E. M. Mumford, B. N. Hemric, S. E. Denmark, "Catalytic, Enantioselective Syn-Oxyamination of Alkenes", *J. Am. Chem. Soc.* **2021**, *143*, 13408–13417.

[127] S. Graf, H. Pesch, T. Appleson, T. Lei, A. Breder, I. Siewert, "Mechanistic Analysis Reveals Key Role of Interchalcogen Multicatalysis in Photo-Aerobic 3-Pyrroline Syntheses by Aza-Wacker Cyclizations", *ChemSusChem* **2024**, e202301518.

[128] M. Wilken, S. Ortgies, A. Breder, I. Siewert, "Mechanistic Studies on the Anodic Functionalization of Alkenes Catalyzed by Diselenides", *ACS Catal.* **2018**, *8*, 10901–10912.

[129] J. Trenner, C. Depken, T. Weber, A. Breder, "Direct Oxidative Allylic and Vinylic Amination of Alkenes through Selenium Catalysis", *Angew. Chem. Int. Ed.* **2013**, *52*, 8952–8956.

[130] Q.-B. Zhang, P.-F. Yuan, L.-L. Kai, K. Liu, Y.-L. Ban, X.-Y. Wang, L.-Z. Wu, Q. Liu, "Preparation of Heterocycles via Visible-Light-Driven Aerobic Selenation of Olefins with Diselenides", *Org. Lett.* **2019**, *21*, 885–889.

[131] H. Li, L. Liao, X. Zhao, "Organoselenium-Catalyzed Aza-Wacker Reactions: Efficient Access to Isoquinolinium Imides and an Isoquinoline N-Oxide", *Synlett* **2019**, *30*, 1688–1692.

[132] D. C. Obenschain, J. R. Tabor, F. E. Michael, "Metal-Free Intermolecular Allylic C–H Amination of Alkenes Using Primary Carbamates", *ACS Catal.* **2023**, *13*, 4369–4375.

[133] J. E. Baldwin, "Rules for Ring Closure", *J. Chem. Soc. Chem. Commun.* **1976**, 734–736.

[134] I. Vilotijevic, T. F. Jamison, "Synthesis of Marine Polycyclic Polyethers *via Endo*-Selective Epoxide-Opening Cascades", *Mar. Drugs* **2010**, *8*, 763–809.

[135] K. Gilmore, R. K. Mohamed, I. V. Alabugin, "The Baldwin rules: revised and extended", *WIREs Comput Mol Sci* **2016**, *6*, 487–514.

[136] J. Ma, L. Dong, J. Yao, A. Lin, H. Yao, "Construction of 2-Azabicyclo[2.2.1]heptenes via Selenium-Catalyzed Intramolecular Oxidative Amination of Cyclopentenes", *Adv. Synth. Catal.* **2023**, *365*, 2043–2048.

[137] G. Pandey, V. J. Rao, U. T. Bhalerao, "Formation of Electrophilic Selenium Species ($PhSe^+$) by Photo-oxidative (Single-electron Transfer) Cleavage of Diphenyl Diselenide", *J. Chem. Soc. Chem. Commun.* **1989**, 416–417.

[138] G. Pandey, B. B. V. S. Sekhar, "In Situ Generation and Utilization of Electrophilic Selenium Species ($PhSe^+$) by Photooxidative (Single Electron transfer) Cleavage of Diphenyl Diselenide (PhSeSePh)", *J. Org. Chem.* **1992**, *57*, 4019–4023.

[139] G. Pandey, B. B. V. S. Sekhar, "Enyne Cyclization *via* Photoinduced Electron Transfer (PET) Generated Electrophilic Selenium Species: a New Carbon–Carbon Bond Formation Strategy", *J. Chem. Soc. Chem. Commun.* **1993**, 780–782.

[140] Q.-B. Zhang, Y.-L. Ban, P.-F. Yuan, S.-J. Peng, J.-G. Fang, L.-Z. Wu, Q. Liu, "Visible-light-mediated aerobic selenation of (hetero)arenes with diselenides", *Green Chem.* **2017**, *19*, 5559–5563.

[141] J. Hua, M. Bian, T. Ma, M. Yang, W. He, Z. Yang, C. Liu, Z. Fang, K. Guo, "The sunlight-promoted aerobic selective cyclization of olefinic amides and diselenides", *Catal. Sci. Technol.* **2021**, *11*, 2299–2305.

[142] J. Park, D. Y. Kim, "Synthesis of selenated γ-lactones via photoredox-catalyzed selenylation and ring closure of alkenoic acids with diselenides", *Bull. Korean Chem. Soc.* **2022**, *43*, 941–945.

[143] S. Protti, M. Fagnoni, "Recent Advances in Light-Induced Selenylation", *ACS Org. Inorg. Au* **2022**, *2*, 455–463.

[144] Y.-H. Wang, Y.-Q. Jiang, Y.-Q. Zhang, Y. Ling, L. Ming, G.-Q. Liu, "Photocatalytic Aerobic Cyclization of *N*-Propargylamides Enabled by Selenium-π-Acid Catalysis", *Chem. Eur. J.* **2023**, *29*, e202300530.

[145] E. S. Conner, K. E. Crocker, R. G. Fernando, F. R. Fronczek, G. G. Stanley, J. R. Ragains, "Visible-Light-Promoted Selenofunctionalization of Alkenes", *Org. Lett.* **2013**, *15*, 5558–5561.

[146] G. Pandey, B. B. V. S. Sekhar, U. T. Bhalerao, "Photoinduced Single Electron Transfer Initiated Heterolytic Carbon–Selenium Bond Dissociation. Sequential One-Pot Selenenylation and Deselenenylation Reaction", *J. Am. Chem. Soc.* **1990**, *112*, 5650–5651.

[147] G. Pandey, B. B. V. Soma Sekhar, "Photoinduced Electron Transfer Initiated Activation of Organoselenium Substrates as Carbocation Equivalents: Sequential One-Pot Selenylation and Deselenylation Reaction", *J. Org. Chem.* **1994**, *59*, 7367–7372.

[148] G. Pandey, R. Sochanchingwung, "Photoinduced Electron Transfer (PET) Promoted Cross-coupling of Organoselenium and Organosilicon Compounds: a New Carbon–Carbon Bond Formation Strategy", *J. Chem. Soc. Chem. Commun.* **1994**, 1945–1946.

[149] G. Pandey, K. S. Sesha Poleswara Rao, K. V. N. Rao, "Photosensitized Electron Transfer Promoted Reductive Activation of Carbon-Selenium Bonds To Generate Carbon-Centered Radicals: Application for Unimolecular Group Transfer Radical Reactions", *J. Org. Chem.* **1996**, *61*, 6799–6804.

[150] S. Ortgies, C. Depken, A. Breder, "Oxidative Allylic Esterification of Alkenes by Cooperative Selenium-Catalysis Using Air as the Sole Oxidant", *Org. Lett.* **2016**, *18*, 2856–2859.

[151] S. Ortgies, R. Rieger, K. Rode, K. Koszinowski, J. Kind, C. M. Thiele, J. Rehbein, A. Breder, "Mechanistic and Synthetic Investigations on the Dual Selenium-π-Acid/Photoredox Catalysis in the Context of the Aerobic Dehydrogenative Lactonization of Alkenoic Acids", *ACS Catal.* **2017**, *7*, 7578–7586.

[152] M. Martiny, E. Steckhan, T. Esch, "Cycloaddition Reactions Initiated by Photochemically Excited Pyrylium Salts", *Chem. Ber.* **1993**, *126*, 1671–1682.

[153] V. V. Pavlishchuk, A. W. Addison, "Conversion constants for redox potentials measured versus different reference electrodes in acetonitrile solutions at 25 °C", *Inorganica Chimica Acta* **2000**, *298*, 97–102.

[154] A. Kunai, J. Harada, J. Izumi, H. Tachihara, K. Sasaki, "Anodic oxidation of diphenyldiselenide in acetonitrile", *Electrochimica Acta* **1983**, *28*, 1361–1366.

[155] K. Rode, M. Palomba, S. Ortgies, R. Rieger, A. Breder, "Aerobic Allylation of Alcohols with Non-Activated Alkenes Enabled by Light-Driven Selenium-π-Acid Catalysis", *Synthesis* **2018**, *50*, 3875–3885.

[156] C. Depken, F. Krätzschmar, R. Rieger, K. Rode, A. Breder, "Photocatalytic Aerobic Phosphatation of Alkenes", *Angew. Chem. Int. Ed.* **2018**, *57*, 2459–2463.

[157] K. A. Müller, C. H. Nagel, A. Breder, "Synthesis of 1,3-Dioxan-2-ones by Photo-Aerobic Selenium-π-Acid Multicatalysis", *Eur. J. Org. Chem.* **2023**, *26*, e2022011.

[158] A. C. Benniston, A. Harriman, P. Li, J. P. Rostron, H. J. van Ramesdonk, M. M. Groeneveld, H. Zhang, J. W. Verhoeven, "Charge Shift and Triplet State Formation in the 9-Mesityl-10-methylacridinium Cation", *J. Am. Chem. Soc.* **2005**, *127*, 16054–16064.

[159] N. A. Romero, D. A. Nicewicz, "Mechanistic Insight into the Photoredox Catalysis of Anti-Markovnikov Alkene Hydrofunctionalization Reactions", *J. Am. Chem. Soc.* **2014**, *136*, 17024–17035.

[160] N. A. Romero, D. A. Nicewicz, "Organic Photoredox Catalysis", *Chem. Rev.* **2016**, *116*, 10075–10166.

[161] J. E. Baldwin, R. C. Thomas, L. I. Kruse, L. Silberman, "Rules for Ring Closure: Ring Formation by Conjugate Addition of Oxygen Nucleophiles", *J. Org. Chem.* **1977**, *42*, 3846–3852.

[162] K. Kai, H. Fujii, R. Ikenaka, M. Akagawa, H. Hayashi, "An acyl-SAM analog as an affinity ligand for identifying quorum sensing signal synthases", *Chem. Commun.* **2014**, *50*, 8586–8589.

[163] L. G. Bonnet, B. M. Kariuki, "Ionic Liquids: Synthesis and Characterisation of Triphenylphosphonium Tosylates", *Eur. J. Inorg. Chem.* **2006**, 437–446.

[164] C. Xu, T. Li, P. Jiang, Y. J. Zhang, "Practical synthesis of phosphonium salts with orthoformates and their application as flame retardants in polycarbonate", *Tetrahedron* **2020**, *76*, 131107.

[165] S. Graf, *Studies Towards Photoaerobic Cycloamination Reactions via Selenium-π-Acid Catalysis: Dissertation*, **2024**.

[166] F. Krätzschmar, M. Kaßel, D. Delony, A. Breder, "Selenium-Catalyzed C(sp^3)–H Acyloxylation: Application in the Expedient Synthesis of Isobenzofuranones", *Chem. Eur. J.* **2015**, *21*, 7030–7034.

[167] T. Lei, S. Graf, C. Schöll, F. Krätzschmar, B. Gregori, T. Appleson, A. Breder, "Asymmetric Photoaerobic Lactonization and Aza-Wacker Cyclization of Alkenes Enabled by Ternary Selenium–Sulfur Multicatalysis", *ACS Catal.* **2023**, *13*, 16240–16248.

[168] T. Lei, T. Appleson, A. Breder, "Intermolecular Aza-Wacker Coupling of Alkenes with Azoles by Photo-Aerobic Selenium-π-Acid Multicatalysis", *ACS Catal.* **2024**, 9586–9593.

[169] T. Lanyon-Hogg, M. Ritzefeld, N. Masumoto, A. I. Magee, H. S. Rzepa, E. W. Tate, "Modulation of Amide Bond Rotamers in 5-Acyl-6,7-dihydrothieno[3,2-*c*]pyridines", *J. Org. Chem.* **2015**, *80*, 4370–4377.

[170] I. Ledneczki, P. Forgo, J. T. Kiss, Á. Molnár, I. Pálinkó, "Conformational behaviour of acetamide derivatives studied by NMR spectroscopic and computational methods", *Journal of Molecular Structure* **2007**, *834-836*, 349–354.

[171] T. T. Nguyen, L. Grigorjeva, O. Daugulis, "Aminoquinoline-directed, cobalt-catalyzed carbonylation of sulfonamide sp^2 C–H bonds", *Chem. Commun.* **2017**, *53*, 5136–5138.

[172] S. Menichetti, C. Biagioli, C. Viglianisi, L. Tofani, L. Lunazzi, M. Mancinelli, A. Mazzanti, "Structure and conformational dynamics of an aromatic sulfonamide: NMR, X-Ray and computational studies", *Arkivoc* **2015**, *2015*, 66–79.

[173] In *Solvents and solvent effects in organic chemistry*, (Eds.: C. Reichardt, T. Welton), Wiley-VCH, Weinheim, **2011**, pp. 425–508.

[174] G. O. Schenck, "Zur Theorie der photosensibilisierten Reaktion mit molekularem Sauerstoff", *Naturwissenschaften* **1948**, *35*, 28–29.

[175] H. Roth, N. Romero, D. Nicewicz, "Experimental and Calculated Electrochemical Potentials of Common Organic Molecules for Applications to Single-Electron Redox Chemistry", *Synlett* **2016**, *27*, 714–723.

[176] T. Erabi, K. Shimizu, S. Hayase, M. Wada, "Anodic Oxidation of Bis (2, 6-dimethoxyphenyl) dichalcogenides in Acetonitrile", *Denki Kagaku oyobi Kogyo Butsuri Kagaku* **1995**, *63*, 960–961.

[177] A. Joshi-Pangu, F. Lévesque, H. G. Roth, S. F. Oliver, L.-C. Campeau, D. Nicewicz, D. A. DiRocco, "Acridinium-Based Photocatalysts: A Sustainable Option in Photoredox Catalysis", *J. Org. Chem.* **2016**, *81*, 7244–7249.

[178] A. U. Meyer, A. L. Berger, B. König, "Metal-free C–H sulfonamidation of pyrroles by visible light photoredox catalysis", *Chem. Commun.* **2016**, *52*, 10918–10921.

[179] C. J. Schürmann, T. L. Teuteberg, A. C. Stückl, P. N. Ruth, F. Hecker, R. Herbst-Irmer, R. A. Mata, D. Stalke, "Trapping X-ray Radiation Damage from Homolytic Se–C Bond Cleavage in BnSeSeBn Crystals (Bn=benzyl, $CH_2C_6H_5$)", *Angew. Chem. Int. Ed.* **2022**, *61*, e202203665.

[180] J. Y. C. Chu, D. G. Marsh, W. H. H. Guenther, "Photochemistry of Organochalcogen Compounds. I. Photolysis of Benzyl Diselenide", *J. Am. Chem. Soc.* **1975**, *97*, 4905–4908.

[181] M. Riener, D. A. Nicewicz, "Synthesis of cyclobutane lignans *via* an organic single electron oxidant–electron relay system", *Chem. Sci.* **2013**, *4*, 2625–2629.

[182] G. Guirado, C. N. Fleming, T. G. Lingenfelter, M. L. Williams, H. Zuilhof, J. P. Dinnocenzo, "Nanosecond Redox Equilibrium Method for Determining Oxidation Potentials in Organic Media", *J. Am. Chem. Soc.* **2004**, *126*, 14086–14094.

[183] E. S. Pysh, N. C. Yang, "Polarographic Oxidation Potentials of Aromatic Compounds", *J. Am. Chem. Soc.* **1963**, *85*, 2124–2130.

[184] M. Hajimohammadi, A. Vaziri Sereshk, C. Schwarzinger, G. Knör, "Suppressing Effect of 2-Nitrobenzaldehyde on Singlet Oxygen Generation, Fatty Acid Photooxidation, and Dye-Sensitizer Degradation", *Antioxidants* **2018**, *7*, https://doi.org/10.3390/antiox7120194.

[185] R. J. Steffan, E. Matelan, M. A. Ashwell, W. J. Moore, W. R. Solvibile, E. Trybulski, C. C. Chadwick, S. Chippari, T. Kenney, A. Eckert, L. Borges-Marcucci, J. C. Keith, Z. Xu, L. Mosyak, D. C. Harnish, "Synthesis and Activity of Substituted 4-(Indazol-3-yl)phenols as Pathway-Selective Estrogen Receptor Ligands Useful in the Treatment of Rheumatoid Arthritis", *J. Med. Chem.* **2004**, *47*, 6435–6438.

[186] A. M. Vinggaard, U. Hass, M. Dalgaard, H. R. Andersen, E. Bonefeld-Jørgensen, S. Christiansen, P. Laier, M. E. Poulsen, "Prochloraz: an imidazole fungicide with multiple mechanisms of action", *International Journal of Andrology* **2006**, *29*, 186–192.

[187] W. Vaccaro, T. Huynh, J. Lloyd, K. Atwal, H. J. Finlay, P. Levesque, M. L. Conder, T. Jenkins-West, H. Shi, L. Sun, "Dihydropyrazolopyrimidine Inhibitors of KV1.5 (IKur)", *Bioorg. Med. Chem. Lett.* **2008**, *18*, 6381–6385.

[188] F. Amblard, J. H. Cho, R. F. Schinazi, "Cu(I)-catalyzed Huisgen azide-alkyne 1,3-dipolar cycloaddition reaction in nucleoside, nucleotide, and oligonucleotide chemistry", *Chem. Rev.* **2009**, *109*, 4207–4220.

[189] J. Lloyd, H. J. Finlay, W. Vacarro, T. Hyunh, A. Kover, R. Bhandaru, L. Yan, K. Atwal, M. L. Conder, T. Jenkins-West, H. Shi, C. Huang, D. Li, H. Sun, P. Levesque, "Pyrrolidine amides of pyrazolodihydropyrimidines as potent and selective $K_V1.5$ blockers", *Bioorg. Med. Chem. Lett.* **2010**, *20*, 1436–1439.

[190] B. C. Monk, A. A. Sagatova, P. Hosseini, Y. N. Ruma, R. K. Wilson, M. V. Keniya, "Fungal Lanosterol 14α-demethylase: A target for next-generation antifungal design", *BBA - Proteins and Proteomics* **2020**, *1868*, 140206.

[191] K. Kang, J. Kim, A. Lee, W. Y. Kim, H. Kim, "Palladium-Catalyzed Dehydrative Cross-Coupling of Allylic Alcohols and *N*-Heterocycles Promoted by a Bicyclic Bridgehead Phosphoramidite Ligand and an Acid Additive", *Org. Lett.* **2016**, *18*, 616–619.

[192] M. T. Zambri, T. R. Hou, M. S. Taylor, "Synergistic Organoboron/Palladium Catalysis for Regioselective N-Allylations of Azoles with Allylic Alcohols", *Org. Lett.* **2022**, *24*, 7617–7621.

[193] J. M. Alonso, M. P. Muñoz, "Platinum and Gold Catalysis: à la Carte Hydroamination of Terminal Activated Allenes with Azoles", *Org. Lett.* **2019**, *21*, 7639–7644.

[194] W.-S. Jiang, D.-W. Ji, W.-S. Zhang, G. Zhang, X.-T. Min, Y.-C. Hu, X.-L. Jiang, Q.-A. Chen, "Orthogonal Regulation of Nucleophilic and Electrophilic Sites in Pd-Catalyzed Regiodivergent Couplings between Indazoles and Isoprene", *Angew. Chem. Int. Ed.* **2021**, *60*, 8321–8328.

[195] S. V. Sieger, I. Lubins, B. Breit, "Hydrofunctionalization of Propadiene – New Life for a Previously Unwanted Product", *ACS Catal.* **2022**, *12*, 11301–11305.

[196] H.-Z. Miao, Y. Liu, Y.-W. Chen, H.-Y. Lu, J. Li, G.-Q. Lin, Z.-T. He, "Stereoselective Pd-Catalyzed Remote Hydroamination of Skipped Dienes with Azoles", *Synlett* **2023**, *34*, 451–456.

[197] Y. Wei, F. Liang, X. Zhang, "N-Bromoimide/DBU Combination as a New Strategy for Intermolecular Allylic Amination", *Org. Lett.* **2013**, *15*, 5186–5189.

[198] Y. Wu, F. Y. Kwong, P. Li, A. S. C. Chan, "An Efficient Oxidative Cross-Coupling Reaction between C–H and N–H Bonds; A Transition-Metal-Free Protocol at Room Temperature", *Synlett* **2013**, *24*, 2009–2013.

[199] J. Sun, Y. Wang, Y. Pan, "Metal-Free Catalytic Approach for Allylic C–H Amination Using *N*-Heterocycles via sp^3 C–H Bond Activation", *J. Org. Chem.* **2015**, *80*, 8945–8950.

[200] S. Saba, J. Rafique, M. S. Franco, A. R. Schneider, L. Espíndola, D. O. Silva, A. L. Braga, "Rose Bengal catalysed photo-induced selenylation of indoles, imidazoles and arenes: a metal free approach", *Org. Biomol. Chem.* **2018**, *16*, 880–885.

[201] Y. Fang, J. Wang, Y. Liu, J. Yan, "An environmentally benign and efficient synthesis of 4–Selanylpyrazoles catalyzed by haloid salts in water", *Appl. Organometal Chem.* **2019**, *33*, e4921.

[202] A. Belladona, R. Cervo, D. Alves, T. Barcellos, R. Cargnelutti, R. Schumacher, "C H functionalization of (hetero)arenes: Direct selanylation mediated by Selectfluor", *Tetrahedron Lett.* **2020**, *61*, 152035.

[203] M. Prein, W. Adam, "The Schenck Ene Reaction: Diastereoselective Oxyfunctionalization with Singlet Oxygen in Synthetic Applications", *Angew. Chem. Int. Ed. Engl.* **1996**, *35*, 477–494.

[204] M. A. Miranda, M. A. Izquierdo, R. Pérez-Ruiz, "Direct Photophysical Evidence for Quenching of the Triplet Excited State of 2,4,6-Triphenyl(thia)pyrylium Salts by 2,3-Diaryloxetanes", *J. Phys. Chem. A* **2003**, *107*, 2478–2482.

[205] A. Gevorgyan, S. Mkrtchyan, T. Grigoryan, V. O. Iaroshenko, "Disilanes as Oxygen Scavengers and Surrogates of Hydrosilanes Suitable for Selective Reduction of Nitroarenes, Phosphine Oxides and other Valuable Substrates", *Org. Chem. Front.* **2017**, *4*, 2437–2444.

[206] J. A. Terrett, M. D. Clift, D. W. C. MacMillan, "Direct β-Alkylation of Aldehydes via Photoredox Organocatalysis", *J. Am. Chem. Soc.* **2014**, *136*, 6858–6861.

[207] H. Zhao, H. P. Caldora, O. Turner, J. J. Douglas, D. Leonori, "A Desaturative Approach for Aromatic Aldehyde Synthesis via Synergistic Enamine, Photoredox and Cobalt Triple Catalysis", *Angew. Chem. Int. Ed.* **2022**, *61*, e202201870.

[208] A. Tolba, A. M. El-Zohry, J. I. Khan, E. Svobodová, J. Chudoba, J. Klíma, K. Lušpai, J. Šturala, R. Cibulka, "Redox-innocent scandium(III) as the sole catalyst in visible light photooxidations", *ChemRxiv* **2024**, doi:10.26434/chemrxiv-2024-m0xw7. This content is a preprint and has not been peer–reviewed.

[209] G. A. Olah, S. C. Narang, "Iodotrimethylsilane—a versatile synthetic reagent", *Tetrahedron* **1982**, *38*, 2225–2277.

[210] G. A. Olah, S. C. Narang, B. B. Gupta, R. Malhotra, "Synthetic Methods and Reactions. 62. Transformations with Chlorotrimethylsilane/Sodium Iodide, a Convenient in Situ Iodotrimethylsilane Reagent", *J. Org. Chem.* **1979**, *44*, 1247–1251.

[211] M. E. Jung, P. L. Ornstein, "A new method for the efficient conversion of alcohols into iodides via treatment with trimethylsilyl iodide", *Tetrahedron Lett.* **1977**, *18*, 2659–2662.

[212] The International Union of Pure and Applied Chemistry, IUPAC - Markownikoff rule (M03707), https://goldbook.iupac.org/terms/view/M03707, **2025 (accessed 12.07.2025)**.

[213] S. E. Denmark, M. G. Edwards, "On the Mechanism of the Selenolactonization Reaction with Selenenyl Halides", *J. Org. Chem.* **2006**, *71*, 7293–7306.

[214] M. Martiny, E. Steckhan, T. Esch, "Cycloaddition Reactions Initiated by Photochemically Excited Pyrylium Salts", *Chemische Berichte* **1993**, *126*, 1671–1682.

[215] N. J. Gesmundo, D. A. Nicewicz, "Cyclization–endoperoxidation cascade reactions of dienes mediated by a pyrylium photoredox catalyst", *Beilstein J. Org. Chem.* **2014**, *10*, 1272–1281.

[216] Hans Reich's Collection. Bordwell pKa Table. https://organicchemistrydata.org/hansreich/resources/pka, **2017 (accessed 22.02.2025)**.

[217] F. G. Bordwell, "Equilibrium acidities in dimethyl sulfoxide solution", *Acc. Chem. Res.* **1988**, *21*, 456–463.

[218] T. Wirth, "Organoselenium Chemistry in Stereoselective Reactions", *Angew. Chem. Int. Ed.* **2000**, *39*, 3740–3749.

[219] S. Lai, X. Liang, Q. Zeng, "Recent Progress in Synthesis and Application of Chiral Organoselenium Compounds", *Chem. Eur. J.* **2024**, *30*, e202304067.

[220] F. Krätzschmar, S. Ortgies, R. Willing, A. Breder, "Rational Design of Chiral Selenium-π-Acid Catalysts", *Catalysts* **2019**, *9*, 153.

[221] L. Hevesi, A. Krief, "Photo-Oxygenation of Selenides–A New Pathway to Selenoxides", *Angew. Chem. Int. Ed. Engl.* **1976**, *15*, 381.

[222] A. Krief, F. Lonez, "Singlet oxygen oxidation of selenides to selenoxides", *Tetrahedron Lett.* **2002**, *43*, 6255–6257.

[223] H. Zhang, S. Lin, E. N. Jacobsen, "Enantioselective Selenocyclization via Dynamic Kinetic Resolution of Seleniranium Ions by Hydrogen-Bond Donor Catalysts", *J. Am. Chem. Soc.* **2014**, *136*, 16485–16488.

[224] S. E. Denmark, D. Kalyani, W. R. Collins, "Preparative and Mechanistic Studies toward the Rational Development of Catalytic, Enantioselective Selenoetherification Reactions", *J. Am. Chem. Soc.* **2010**, *132*, 15752–15765.

[225] T. E. Schirmer, B. König, "Ion-Pairing Catalysis in Stereoselective, Light-Induced Transformations", *J. Am. Chem. Soc.* **2022**, *144*, 19207–19218.

[226] P. D. Morse, T. M. Nguyen, C. L. Cruz, D. A. Nicewicz, "Enantioselective counter-anions in photoredox catalysis: The asymmetric cation radical Diels-Alder reaction", *Tetrahedron* **2018**, *74*, 3266–3272.

[227] S. Das, C. Zhu, D. Demirbas, E. Bill, C. K. De, B. List, "Asymmetric counteranion-directed photoredox catalysis", *Science* **2023**, *379*, 494–499.

[228] S. Park, *H-Bond-Mediated, Photocatalytic Modulation of Nucleofugal Selenium for Semipinacol Rearrangement and its Application in Asymmetric Migratory Tsuji-Wacker Oxidation: Dissertation*, **2025**.

[229] G. R. Fulmer, A. J. M. Miller, N. H. Sherden, H. E. Gottlieb, A. Nudelman, B. M. Stoltz, J. E. Bercaw, K. I. Goldberg, "NMR Chemical Shifts of Trace Impurities: Common Laboratory Solvents, Organics, and Gases in Deuterated Solvents Relevant to the Organometallic Chemist", *Organometallics* **2010**, *29*, 2176–2179.

[230] L. Hintermann, AK Hintermann List of qNMR Standards: Version 1.7, https://www.ch.nat.tum.de/fileadmin/w00bzu/oca/Ressources/AK_Hintermann_List_of_qNMR_Standards.pdf, **2021 (accessed 16.10.2023)**.

[231] P. Gerschel, B. Battistella, D. Siegmund, K. Ray, U.-P. Apfel, "Electrochemical CO_2 Reduction — The Effect of Chalcogenide Exchange in Ni-Isocyclam Complexes", *Organometallics* **2020**, *39*, 1497–1510.

[232] M. Millard, J. D. Gallagher, B. Z. Olenyuk, N. Neamati, "A Selective Mitochondrial-Targeted Chlorambucil with Remarkable Cytotoxicity in Breast and Pancreatic Cancers", *J. Med. Chem.* **2013**, *56*, 9170–9179.

[233] R. An, L. Liao, X. Liu, S. Song, X. Zhao, "Acid-catalyzed oxidative cleavage of S–S and Se–Se bonds with DEAD: efficient access to sulfides and selenides", *Org. Chem. Front.* **2018**, *5*, 3557–3561.

Declaration

Hereby I declare that this presented thesis was conducted and written independently by myself. Wherever contributions from others are involved, all of them are marked clearly, with reference to the literature, license, and acknowledgment of collaborative research.

München, 26.11.2025

_____

Theresa Appleson